Electronic control of electromechanical energy conversion in electrical machines : with some aspects of a theoretical and experimental study of a group of systems with variable electromagnetic slip

ELECTRONIC CONTROL OF ELECTROMECHANICAL ENERGY CONVERSION IN ELECTRICAL MACHINES

J.D. VAN WYK

ELECTRONIC CONTROL OF ELECTROMECHANICAL ENERGY CONVERSION IN ELECTRICAL MACHINES

with some aspects of a theoretical and experimental study of a group of systems with variable electromagnetic slip

PROEFSCHRIFT

TER VERKRIJGING VAN DE GRAAD VAN DOCTOR IN DE TECHNISCHE WETENSCHAPPEN AAN DE TECHNISCHE HOGESCHOOL TE EINDHOVEN OP GEZAG VAN DE RECTOR MAGNIFICUS PROF.DR.IR. A.A.TH.M. VAN TRIER, HOOGLERAAR IN DE AFDELING DER ELEKTROTECHNIEK, VOOR EEN COMMISSIE UIT DE SENAAT TE VERDEDIGEN OP DINSDAG 23 SEPTEMBER 1969 DES NAMIDDAGS TE 4 UUR

DOOR

JACOBUS DANIEL VAN WYK

GEBOREN TE FAURESMITH
(ORANJE VRIJSTAAT, ZUID-AFRIKA)

1969
DRUKKERIJ BRONDER-OFFSET N.V.
ROTTERDAM

DIT PROEFSCHRIFT IS GOEDGEKEURD DOOR DE PROMOTOR
PROF.DR.IR. J.G. NIESTEN

AAN ANKIE

MY LEERMEESTERS

MY OUERS

C O N T E N T S

Summary. 13

Introductory remarks. 17

Chapter 1. Machine-electronics: a study on the development and extent of the subject.

Synopsis. 21
1.1 The different methods to control electrical machines. 21
1.2 Machine-electronic systems in the presented survey. 32
1.2.1 Definitions of power electronics and machine-electronics. 33
1.3 The development of the subject of machine-electronics. 33
1.3.1 The development of the different switching devices. 34
1.3.2 The development of the circuits for the control of electrical power. 34
1.3.3 Development of ideas to control electrical machines. 39
1.3.3.1 Initial attempts.
1.3.3.2 Machines with electronic commutators.
1.3.3.3 Schemes for the control of induction machines without changing the supply frequency.
1.3.3.4 Voltage regulation of direct voltage machines by mutators.
1.3.3.5 Electronic chopper control of direct voltage machines.
1.4 Growth of the subject of machine-electronics. 43

Chapter 2. Systematics of machine-electronic systems.

Synopsis. 46
2.1 The different criteria applicable for classification of machine-electronic systems. 46
2.1.1 The systems to be studied. 46
2.1.2 Review of possibilities for classification. 47
2.2 Power flow in relation to systematics of machine-electronic systems. 50
2.2.1 The physical model to be used in the systematics. 50
2.2.1.1 Particulars concerning the model.
2.2.1.2 Power flow in the model.
2.2.2 Fundamental power flow in the different systems. 56
2.2.3 A classification for machine-electronic systems: a summary of the previous paragraphs. 61
2.2.4 Some hybrid systems. 62
2.3 A more detailed investigation of power flow in the machine-electronic systems. 64
2.3.1 Power flow considerations for Group I systems, class 1 and 2. 65
2.3.2 Power flow considerations for Group II systems, class 1 and 2. 68
2.3.3 Power flow considerations for GroupIII systems, class 1 and 2. 73
2.4 A review of machine-electronic systems. 73
2.4.1 Group I systems: Frequency control of induction and synchronous machines. 76
2.4.2 Group II systems: Stator and rotor control of induction machines. 77
2.4.3 Group III systems: Electronic control of d.v. machines and field control of synchronous machines. 83

Chapter 3. A general theoretical analysis of the electromechanical converter as used in the machine-electronic systems.

Synopsis. 86
3.1 Representation of the effects of the power electronic circuits on the excitation. 86
3.2 Model to be analysed. 87
3.3 Formulation of the equations. 90
3.3.1 The general n-m phase stator-rotor equations. 90
3.3.2 Reduction of the general equations by an instantaneous symmetrical transformation. 95
3.3.3 Complex rotating rotor-stator transformation. 98
3.3.4 Complex rotating stator-rotor transformation. 100
3.3.5 Partitioning of the stator-transformed and rotor-transformed equations. 103
3.3.6 The excitation functions. 106
3.3.7 General solution for stator and rotor currents. 111
3.3.8 Investigation of expressions for current and torque under conditions of periodical switching. 117
3.4 Examination of an equivalent circuit representation. 130
3.5 Remarks regarding some simplifying conditions in the investigated model. 137
3.6 Consideration of some simplified models for the theoretical analysis of the electromechanical transducer used in the machine-electronic system. 144
3.6.1 Electromechanical converters with switching in the rotor to control the current flow angle. 145
3.6.2 Electromechanical converters with switching circuits in the rotor having a current source effect. 147

Chapter 4. Theoretical investigations of some characteristics of Group II and Group IIA machine-electronic systems.

Synopsis. 149
4.1 The systems to be subjected to investigation. 149
4.2 An example of Group II, class 1 machine-electronic systems: control of the stator voltage of an induction machine by variation of the delay of the ignition instant. 151
4.2.1 Investigation of the switching mode, and derivation of the switching commands. 152
4.2.2 The system equations for the semi-four-phase induction machine with stator voltage control by ignition angle delay in the electronic switches. 155
4.2.2.1 Equations for the assumed model.
4.2.2.2 Considerations concerning the excitation functions.
4.2.2.3 The nature of the induced voltages during blocking periods: two approximations.
4.2.2.4 The induced voltage during blocking with all resistances neglected: a third approximation.
4.2.2.5 Transformation of the complete excitation functions.
4.2.3 Solution for the machine currents. 174
4.2.4 The electromagnetic torque for the ignition instant stator controlled induction machine. 181
4.2.5 Calculation of some system characteristics. 185
4.2.5.1 Torque-speed characteristics and transfer functions.

4.2.5.1.1 The angle of natural commutation and the initial conditions for the induced excitation functions.
4.2.5.1.2 The power factor, supply current distortion and effective stator phase current.
4.2.5.2 Results of the theoretical calculations on the system.
4.2.6 Remarks regarding an equivalent circuit representation. 191
4.3 Examples of Group II, class 2 and Group IIA machine-electronic systems. 192
4.3.1 Rotor control of an induction machine by variation of the delay of the instant of current ignition. 192
4.3.1.1 Investigation of the switching modes, and derivation of the switching commands.
4.3.1.2 The equations describing the system.
4.3.1.3 Calculation of some system characteristics.
4.3.2 Rotor control of an induction machine by variation of the instant of current extinction. 200
4.3.2.1 Specification of the switching mode, and derivation of the switching commands.
4.3.2.2 The equations describing the system.
4.3.2.3 Calculation of some system characteristics.
4.3.2.4 A combination of α_r-control and β_r-control to obtain minimum phase shift between fundamental current and induced voltage.
4.3.3 Control of an induction machine by using a high-frequency chopper circuit with a resistive load. 208
4.3.3.1 An investigation of the switching modes and the derivation of the switching commands.
4.3.3.2 Equations for the assumed model of the electronic Leblanc cascade.
4.3.4 Control of an induction machine by feeding back part of the slip power to the supply. 220
4.3.4.1 Investigation of the switching modes, and derivation of the switching commands.
4.3.4.2 Equations describing the assumed model for the electronic Scherbius cascade.
4.3.5 Control of an induction machine by feeding back the slip power to the supply by a compensated inverter. 223
4.3.5.1 Investigation of the switching modes and derivation of the switching commands.
4.3.5.2 Equations describing the model assumed for the electronic Scherbius cascade with reactive power compensation.

Chapter 5. Experimental investigations on Group II and Group II A machine-electronic systems.

Synopsis 229

Part I. Some machine-electronic systems developed for experiments. 229

5.1 A short review of the systems developed for experimental investigations. 229
5.2 The machine-electronic systems developed:structure and functioning. 232
5.2.1 Systems for stator control by variation of the delay of the instant of triggering on a semi-four-phase induction machine. 232
5.2.2 Systems for rotor control by variation of the delay of the instant of triggering on a semi-four-phase induction machine. 234
5.2.2.1 A system for Δt_{α_r}-control.

5.2.2.2 A system for α_r-control.
5.2.3 Systems for rotor control by variation of the delay of the instant of current extinction in a semi-four-phase induction machine. 238
5.2.3.1 A system for t_{β_r}-control.
5.2.4 A system for β_r rotor control of a semi-four-phase induction machine by an electronic Leblanc cascade. 240
5.2.5 A system for electronic recuperation of the slip power (electronic Scherbius cascade) of a semi-four-phase induction machine. 242
5.2.6 A system for electronic recuperation of the slip power - with compensation of the reactive power - of a semi-four-phase induction machine. 244
5.2.7 A system for rotor control of a three-phase machine by variation of the instant of triggering. 246
5.2.8 A system for rotor control of a three-phase induction machine by means of a resistively loaded electronic chopper. 248
5.3 A consideration of some typical general problems encountered during design, development and construction of machine-electronic systems. 248
5.3.1 Forced commutation and its application to electronic chopper circuits. 249
5.3.1.1 Power switches employed to switch-off the rotor current.
5.3.1.2 Consideration of a modified auxiliary commutated power electronic switch.
5.3.1.3 Consideration of an electronic switching circuit for the low-high chopper used for rotor control.
5.3.2 Transmission of triggering commands to power electronic switches. 262
5.3.2.1 Some problems concerning gating of static switches.
5.3.2.2 Model to be analysed.
5.3.2.3 Analysis during the commutation period.
5.3.3 Regarding the application of semiconductor switching elements in power electronic switching circuits. 271

Part II. Experimental investigation of the characteristics of some Group II and Group IIA machine-electronic systems. 274

5.4 A brief review of the experimental investigations. 274
5.5 Concerning the actual experimental set-up. 276
5.6 Some of the experimental measurements conducted on the described systems. 279
5.6.1 Torque-speed characteristics of the systems. 279
5.6.2 Electrical characteristics of some systems. 279
5.6.3 A general discussion of the experimental results - the electromechanical characteristics. 281
5.6.3.1 A system for α_s-control and $\Delta\alpha_s$-control (WHGM).
5.6.3.2 A system for α^s-control and Δt_α^s-control (WHGM).
5.6.3.3 A system for t_β^r-control (WHGM).
5.6.3.4 Systems for β_r rotor control by electronic Leblanc cascade and compensated electronic Scherbius cascade (WHGM).
5.6.3.5 A system for rotor control by electronic Scherbius cascade (WHGM).
5.6.3.6 Considerations concerning harmonic torques in the systems employing the semi-four-phase machine.
5.6.3.7 α_r-control and an electronic Leblanc cascade on a three-phase machine.
5.6.4 A general discussion of the experimental results - the electrical characteristics. 300

5.6.5 A general discussion of the experimental results - the presented oscillograms. 301
5.7 Conclusions. 312

Literature cited. 314

Appendices.

A2 (Concerning chapter 2) 321

A3 (Concerning chapter 3) 332

A4 (Concerning chapter 4) 341

Opsomming. 382

Nawoord by die afsluiting van hierdie werk. 386

SUMMARY

In this dissertation an investigation is conducted into the control of electromechanical energy conversion on power flow principles. An attempt is made to approach the subject as general as feasible, in order to develop a theory for these types of systems. A group of the general systems is selected for further theoretical investigation. Examples of these "machine-electronic" systems have been developed and investigated experimentally in order to establish the validity of the theoretical approaches developed.

It is attempted to illustrate what the extent of the subject of machine-electronics is and how it has evolved through the years, since this is not generally appreciated. Chapter 1 consequently treats methods of power flow control associated with the electromechanical energy conversion process, presents a review of methods for control of this process, reviews the history of machine-electronics and concludes with some information on the extent of the subject.

In Chapter 2 systematics for systems with electronic control of the electromechanical energy conversion process are derived from power flow principles. The systems are divided into three groups that differ fundamentally from each other (Group I, Group II, Group III). It is shown that some machine-electronic systems with a more complicated structure are actually hybrid systems constructed from the different group-elements. Since the systematics are derived on a basis of fundamental power flow it is important to investigate the effects of the different harmonic components of the current circulating in stator and rotor circuit. These currents are generated by the switching action of the power electronic switching circuits used to control the power flow. Existing machine-electronic systems and systems that may possibly be constructed are classified, and the different groups subdivided. This subdivision of the different groups is executed by taking into account the circuit structure and mode of switching of the power electronic circuits. After having divided all the systems into their respective groups the mutual relationship becomes more clear, and one may proceed with a general theoretical approach.

By postulating that the effect of the periodical switched excitation encountered in machine-electronic systems may be simulated in general by a series and parallel switch acting in conjunction with a nonsinusoidal multiphase supply on the machine windings, a general theoretical approach to machine-electronic systems operating in steady state is developed in Chapter 3. The case of an n-m phase electromechanical converter with either stator control or rotor control is investigated by means of the instantaneous symmetrical component transformation and the rotor-stator and stator-rotor rotating complex coordinate transformation. Solution for the machine currents yields the general equations for the instantaneous and mean electromagnetic torque. These expressions are split up into their pulsating, synchronous and asynchronous components. Attention is devoted to a representation of the solved currents in terms of equivalent circuits. The previous investigations have all been conducted on a symmetrical n-m phase machine with arbitrary n-m phase unbalanced excitation. The implications of a symmetrical switched excitation of the machine on currents, electromagnetic torque and equivalent circuit representation are examined.

Chapter 3 is concluded by developing a simplified model for the analysis of some Group II machine-electronic systems from the power flow considerations of chapter 2. These simplified models are used later in chapter 4 to gain insight into the behaviour of some machine-electronic systems from the said group having rotor control.

Since it is impossible to investigate all machine-electronic systems in detail in one volume, chapter 4 presents a selection. The groups of machine-electronic systems having an essentially variable electromagnetic slip have been selected for investigation. To be able to conduct a comparative theoretical and experimental study on these systems, it was selected to investigate stator control by variation of the delay of the instant of current ignition by the general methods of chapter 3. Rotor control by variation of the delay of the instant of current ignition, by variation of the delay of the instant of current extinction, by a resistively loaded electronic chopper circuit, by electronic Scherbius cascade and by a reactive power compensated electronic Scherbius cascade are all investigated by the simplified models developed in Chapter 3 from power flow considerations. In order to illustrate the differences in transfer function arising due to the different structures possible for the information electronic part of a machine-electronic system, several possibilities for deriving the switching commands for the stator circuit from system-related voltages are considered. In the course of the investigations on the stator control system extensive attention is given to the nature of the induced stator phase voltage when the electronic switch is nonconducting. An approximation theory for this problem is developed. Solutions for the currents and torque are found in terms of two components of the stator excitation function of the induction machine. This excitation function is divided into a "supply-derived excitation" acting on the machine windings during conduction of the switches, and an "induced voltage derived excitation" acting on the machine windings during the time that all switches are blocking. An investigation is conducted into the approximation obtained with the induced voltage derived excitation components neglected.

By observing the simplifying assumptions under which the power flow model was constructed, the rotor control systems are investigated. The different possible methods to derive the switching commands for the systems are investigated for each case. For the rotor control systems with delay of current ignition or delay of current extinction, extensive calculations on some mechanical and electrical characteristics are presented. For the other systems, calculations of characteristics are only presented in so far as they convey new insight.

Chapter 5 presents the experimental work conducted on the selected groups of machine-electronic systems. The present study concerns electromechanical energy conversion, and therefore it is not necessary to cover all systems in detail. A brief description of each of the systems is presented with the aid of a simplified block diagram. As all the systems had to be designed and developed prior to the experiments an appreciable part of the experimental work was involved herewith. This is not interesting for the present study, and not presented. However, some of the problems appeared to be of general significance for the entire field of machine electronics. Therefore some aspects of the use of force commutated electronic switches to interrupt inductive currents are presented. Problems encountered during transmission of triggering commands to static switching circuits and the measurements taken to

solve them are also presented. The application of semiconductor switching elements under the conditions sometimes prevailing in the described experimental equipment, necessitated development of special testing facilities to investigate some switching phenomena.

Torque-speed curves as a function of the control parameter, are presented for all the systems investigated in the course of this study. From these curves it is possible to derive the experimental transfer functions. Electrical characteristics for the stator ignition angle controlled induction machine are presented in the form of stator current, rotor current, extinction angle and power factor as a function of control parameter and slip. Space limitations prohibit the presentation of all electrical characteristics of this system and all the rotor control systems at length. Therefore these characteristics are presented very briefly. The novel electrical and mechanical characteristics that may be obtained by, for instance, such an unconventional system as the control of the current extinction angle, are pointed out and compared to the characteristics of the ignition angle control and an uncontrolled induction machine. Harmonic torques observed during the experiments are briefly referred to, and oscillograms are presented to illustrate system behaviour, validity of assumptions and measurements.

The experiments have shown that the theory developed in chapter 3, and extended for stator control in chapter 4, describes the behaviour of the system accurately. The simplified models developed for analysis are suitable for a qualitative insight into the behaviour of the machine-electronic systems. It was concluded that the assumptions made during the analysis proved to be justified under those conditions prevailing when the machine-electronic system is applied as part of an electrical drive.

INTRODUCTORY REMARKS

Rotating electrical machines have a relatively long history compared to some other branches of electrical engineering. For the duration of this historical development schemes have been devised to change the relation between the torque delivered by a particular machine and its mechanical speed. The relationship between these two mechanical variables of the machine, being determined by the electrical parameters of the machine, the parameters of the supply and the type of machine, is of a predestined form for a specific machine operating from one of the normally available supplies. The motivation for the above mentioned search has been the necessity to achieve a range of operating conditions with a given load and a specific driving machine. Practical execution of the theoretical schemes suggested to achieve this end did not always follow so easily, and the eventual widespread practical application of the solutions to the problem was in many instances prevented by the intricate combination of economics, reliability, efficiency, power factor, speed range, regulation, simplicity, ease of control and maintenance, power-to-weight ratio, obsoleteness and many other factors determining the practical future of a solution to a problem in engineering practice.

The past two decades have seen a new stimulus of the search for efficient control of the electromechanical energy conversion process, while more advanced performance of these systems has simultaneously become a requisite. One of the most important stimulating factors has been the continuously expanding automation. The almost universal application of electronic control systems resulted in the requirement of a low power electronic signal as input. The advanced performance requisite is posed by the increasingly narrowing tolerances and increasing system complexity, brought about by the characteristics expected of the processes or systems employing the controlled electrical machine as a prime mover in some or other capacity.

The century of history of the electrical machine has presented a rich array of methods to change the torque-speed relationship of electrical machines, the half-century old electronic method being but one of the solutions to the problem, as is to be illustrated subsequently in this work. Although the other control methods may again bloom to new life some day in the future, availability of an enlarging family of semiconductor switches capable of operating in the complete power spectrum of microwatts to megawatts - at the opportune moment during the past two decades - has decided the search in favour of power electronic control for the present and foreseeable future. The methods of controlling the electromechanical energy conversion process by using power electronics form the basis of this study. This subject has come to be known as machine-electronics.

Due to the previously sketched circumstances, the field of machine-electronics is extensive, and expanding fast in some respects. Yet it is probably correct to remark that our ability to subdivide and specialize, in the process of solving technological problems and finding new applications, is also in this case steadily outranging our ability to unify them and relate them to each other afterwards. Finding this mutual relation is an essential element to aid insight, and promote the engineering art of machine-electronics more and more to the engineering science of machine-electronics. The present investigations were initiated as a first stepping stone on the path of unifying research into the field of the electronic control of the electro-mechanical energy conversion process.

Unifying research sometimes leads to new aspects (in this case new control methods) coming to light, due to a particular field proving not to have been investigated yet, when known aspects are ordered in a systematic classification. Furthermore it may be expected that these types of investigations may clarify how the combination of previously found solutions to the conversion control problem may be combined to define new hybrid solutions to eliminate disadvantages and enhance advantages. Especially in engineering science, where every solution to a problem is in its essence a compromise, this may be an important result. On the other hand, although both these above mentioned aspects have also been found to hold for the investigations described in this dissertation, it is the opinion of the author that merely the possibility that unification of some of the detailed knowledge of the field may result, should be enough stimulation to undertake such research.

It is not the intention to attempt the impossible and present a recipe of how one should proceed at such unifying research. Some remarks concerning the attempt contained in this study will be made in order to explain the background somewhat, since but a fraction of all the investigations can eventually find their way into a final presentation such as the present study.

The almost quite random nature of the literature known on the subject necessitated systematic bibliographical work. From this an extensive bibliography has already been compiled.(79 This accentuated the history the subject has. One quite often encounters the idea that machine-electronics is a modern subject having grown out of the availability of power semiconductor switches. As there is nothing further from the truth, the reader will find that this study not only represents technical matters, but also an amount of pure historical research - of technical interest non the less. This historical research has brought matters to light not previously appreciated.

Paramount to an investigation covering a wide field is a suitable classification of the subject matter. As the classification concerning machine-electronics was non-existent when the investigation started, a systematic classification was devised and is discussed here. It has already been mentioned that this systematic classification resulted in the recognisation of inadequate attention to some matters, having ultimately had practical results in the new approaches to the electromechanical energy conversion control problem. Such a classification necessarily also results in a well documented survey of the field.

An attempt was made to develop a method whereby the characteristics of switched electrical machines are to be calculated. In the power

branch of electrical engineering much importance is attached to a knowledge of the harmonic components of non-sinusoidal voltages and currents. This with regard to design of the electrical machine and other equipment, and the fact that the system is mostly supplied from the national power grid, into which harmonic currents may not be introduced at random. When the machine-electronic systems operate at higher power levels the harmonic components of voltages and currents may result in serious interaction with other electrical equipment, and even cause malfunctioning of the system itself. In these cases it is even more important to be able to know the harmonic components in advance. The above considerations resulted in the method of theoretical analysis being essentially a Fourier method. The calculations are complicated by the fact that the differential equations contain periodically varying coefficients even under constant speed constraints. It is believed that all these problems have been solved satisfactorily, however.

The theoretical characteristics of the power electronic circuits found in the machine-electronic systems also need systematic classification and investigation. Where all the previously investigated aspects were general, a restriction was observed here, however. It is possible to devise a classification for the main groups of power electronic circuits. However, the variety in these circuits prohibits an exhaustive study of the different variants to the same extent that it is possible for the different methods of control of electrical machines, resulting in the said restriction. Consequently the aspects represented here chiefly concerns the circuits employed in the groups of systems investigated experimentally during the course of this research. By combining the knowledge of the behaviour of the switched electromechanical transducer and the power electronic circuits, it then proved feasible to calculate the characteristics of the investigated systems by applying the appropriate constraints.

It is inevitable that when one comes to experimental investigations, they will again have a specialized character. In order to counteract this tendency as much as physically possible, a whole range of systems from one of the classified groups were selected, designed and developed. This tends to impart the character of a comparative practical study to the experimental investigations. This is in itself already valuable. During such investigations it is difficult to decide at what degree of sophistication the development should be discontinued, as the primary objective is not to develop flawless practical systems, but to provide support for the theoretical analysis. Investigation on the realized system will continue to point out the unrealistic assumptions that had been made in designing the system or in developing improvements, as the results are never exactly predictable during these stages. The spiral has to be broken off at some point.

Development of the machine-electronic systems and subsequent experiments stressed that the behaviour of the power semiconductor elements is known insufficiently to allow reliable and optimum design of the systems. Development of extensive dynamic testing facilities had to be incorporated into the research program in order to investigate some effects physically. These investigations, just as the majority of the work on power-electronic circuits, do not have such an intimate relation with the attempt at conducting unifying research on machine-electronics, and are consequently only reported on in the experimental

section in so far as it is important in that constellation.

In conclusion some remarks concerning that part of the machine-electronic system not referred to in the above paragraphs will be made. The switching action of the power electronics is related to current or voltage levels, related to the machine on their part. It will become clear when design of the systems is discussed, that at the power, voltage and distortion levels involved, it is an art on its own to derive this relationship electronically. Often this is responsible for the failure of an otherwise elegant method of control. Delivering the switching command to the different switching elements in the electronic switch itself proves to be yet another specialized art. The binary and linear electronic circuits introduced between these input and output units are of more "normal" character, yet must answer to very stringent requirements on the point of spurious noise immunity. These low-power electronic circuits operate in close proximity to the power switching circuits generating periodic current-time gradients sometimes in excess of a few hundred amperes per microsecond. As one may reasonably expect, the characteristics of all these "information - electronic" circuits are assumed to be ideal during the theoretical analysis of the power-electronic electrical machine subsystem. The same considerations are regarded during the initial design stages - it is only during development that these time consuming problems come into their own.

Interaction between non-ideal characteristics of the power-electronic circuits and the eletromechanical transducer, or vice versa, has as a matter of fact not been anticipated in the idealized theoretical constellation, yet may be expected to occur in practical systems. As a systematic knowledge of these effects is non-existent at present, it appears to be an extremely worth-while subject for future unifying research on the electronic control of the electromechanical energy conversion process.

CHAPTER 1

MACHINE-ELECTRONICS: A STUDY ON THE DEVELOPMENT AND EXTENT OF THE SUBJECT

Synopsis

In this chapter the different possibilities to control the power flow between power source and mechanical load are considered. Of these possibilities the control of the power flow during the electromechnical conversion process is investigated further. A representation of the different fundamental possibilities to achieve control of the power flow during conversion is given. A representative survey of electrical drive systems with control of power flow is drawn up in order to illustrate the relation of machine-electronics to all the other solutions to the investigated problem.

After definition of this subject, an investigation of the development of power-electronic switching devices, power electronic circuit techniques important aspects of machine-electronics and the extent of the subject is presented.

1.1 THE DIFFERENT METHODS TO CONTROL ELECTRICAL MACHINES

The control of electrical machines finds reason for existence in the fact that although a large amount of power or energy is needed in mechanical form to aid and supplement the mechanical power living beings can develop, an appreciable part of this power is transported by electrical methods. The rotating electromechanical converter is probably the most commonly employed transducer to obtain mechanical power from this system. A situation as in fig. 1.1 is the result.

Assume the power characteristics of the mechanical load given. If the existence of a large number of random mechanical loads be accepted, it becomes a logical conclusion that they cannot all be connected to identical transducers - i.e. control of power flow is implied. Let the power flow from generation to load be followed:

Electrical power is obtained from a generating system, where energy is converted from non-electrical to electrical form. Control of power flow at this stage is a possibility. However, considering that it has been electrical practice to centralize power generation as much as possible at power stations and that this station feeds an enormous number of random loads, it follows that this type of power control is not feasible. If it is wished to control the voltage of an electrical system, this must be done locally.

During transmission a loss of power P_{det} in the electrical power transmission system may be found. This suggests another method to control the power flow: changing parameters of the transmission system.

Again due to the centralized nature of the majority of these systems this type of power flow control is only feasible if it is applied locally.

Power then passes the electromechanical converter where it is converted into mechanical power at a loss P_{dem}. This is an obvious possibility to control the power flow. To what extent this is possible is to be investigated subsequently. The converted power now passes in its mechanical form via the mechanical transmission system - with a transmission loss P_{dmt} - to the mechanical load. Changing the loss parameters of this transmission system offers the last possibility to regulate the power flow to the load, as the use of slip couplings (electrical and mechanical) illustrates. Under these conditions the electromechanical energy converter has an aggregate load that is constant. In summary the power flow in the electrical, electromechanical and mechanical systems may then be described by:

$$P_{\sum} - P_{det} = P_{dem} + P_{dmt} + P_{m} \qquad 1.1a$$

and

$$P_{in} - P_{dem} = P_{em} \qquad 1.1b$$

It will now be considered how the mechanical power P_{em} is to be influenced.

In order to investigate the main groups of control methods for power flow control in the electromechanical energy conversion process, consider a general converter as in fig. 1.2. Let it have a stationary "stator" (s) and rotating "rotor" (r), constructed of magnetically active material, and carrying respectively n and m sets of symmetrical windings. The characteristics of the magnetically active material are:

a. The material has no magnetic hysteresis

b. The material has infinite electrical resistance.

The n,m machine "phases" are fed from n,m phase symmetrical supply systems of fundamental frequencies f_s and f_r. Examine the voltage relations of the winding of the k th phase:

$$u_k = R_k i_k + \frac{d\phi_k}{dt} \qquad 1.2a$$

In general the flux linkages with the k th phase may be written as a univalued function of the different machine currents and the angular coordinate:

$$\phi_k = \phi_k(i_1, i_2, i_3, \ldots i_k \ldots, \theta) \qquad 1.3a$$

This has the consequence that the magnetic field energy is also a

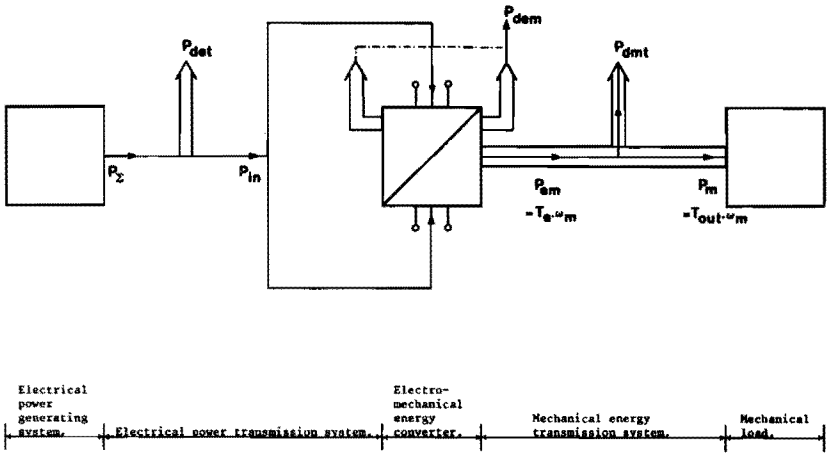

FIG. 1.1 SCHEMATIC REPRESENTATION OF POWER FLOW BETWEEN ELECTRICAL SUPPLY AND MECHANICAL LOAD.

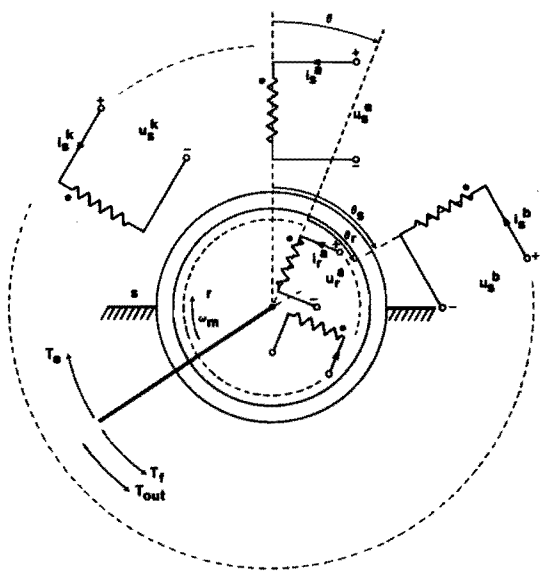

FIG. 1.2 SCHEMATIC REPRESENTATION OF ELECTROMECHANICAL ENERGY CONVERTER OF THE ROTATING TYPE.

univalued function:

$$W_m = W_m\,(i_1,\ i_2,\ i_3\ \ldots\ i_k\ \ldots,\ \theta) \qquad 1.3b$$

For this configuration the instantaneous electromagnetic torque T_e in the air gap is found as (B16

$$T_e = \frac{\partial W_m'}{\partial \theta} \qquad 1.4a$$

with instantaneous electromagnetic power flow:

$$p_{em} = T_e\ \frac{d\theta}{dt} \qquad 1.4b$$

The magnetic coenergy of the system is represented by:

$$W_m' = \sum_{k=1}^{m+n} \int_0^{i_k} \phi_k . di_k \qquad \theta = \text{constant} \qquad 1.5$$

Expression 1.4 indicates that the instantaneous value of the air gap torque may be directly influenced by the flux-linkages. This will influence the instantaneous power flow. Taking into consideration that the flux linkages with the k th phase always contain a "leakage" term $\phi_{k\sigma}(i_k)$ that is in no way active in the electromechanical energy conversion process, relations 1.2a and 1.3a may be modified into:

$$\phi_k = \phi_{k\sigma}(i_k) + \phi_{kh}\,(i_1,\ i_2,\ i_3,\ \ldots.\ i_k\ \ldots.\ \theta) \qquad 1.3c$$

and

$$u_k = R_k i_k + \frac{\partial \phi_{k\sigma}}{\partial i_k} \cdot \frac{di_k}{dt} + \sum_{q=1}^{m+n} \frac{\partial \phi_{kh}}{\partial i_q} \cdot \frac{di_q}{dt} + \frac{\partial \phi_{kh}}{\partial \theta} \cdot \frac{d\theta}{dt} \qquad 1.2b$$

When one assumes that the supply is fundamentally a voltage source, as in 1.2b, and abandons variation of the flux linkage change with current

$$\partial \phi_{kh}/diq \qquad \text{or with angular coordinate}$$

$\partial\phi_{kh}/\partial\theta$

it follows from the voltage equation (1.2) that the magnetic field in the machine may be influenced by changing the current in the k th winding (1.5). Two fundamental possibilities present themselves to achieve this change in current:

(i) alteration of the supply voltage u_k,

(ii) inclusion of an additional curcuit element in series with the machine winding.

This alternative will be examined further. Relation 1.2b indicates that the two voltage drop terms already occurring in the machine winding (both "non-conversion", "non-coupled" voltage drops) without having part in the conversion process may be termed resistive and leakage drop. These two terms may be modified by external circuit elements of resistive, inductive or capacitive character. An extension of this idea is the inclusion of a switching element (periodically varying resistance) to influence the magnitude of the winding current by periodic operation. Depending on the mode of operation, this switch may indirectly give rise to resistive, capacitive or inductive effects.

Alternative (i) clearly constitutes control of a supply parameter (which should be executed locally according to the initial discussion in this chapter). Whether the modification or the resistive voltage drop or leakage drop be classified as control of a supply or a machine parameter is largely a matter of definition.

The first alternative (i) will be referred to as power control through magnetic field change by voltage variation. Alternative (ii) is fundamentally variation of a circuit parameter somewhere between the electrical power source and the active electromechanical converter and is consequently named power control through magnetic field change by circuit parameter variation.

When one is interested in the control of the mean electromechanical power flow, the above mentioned actions should be executed to result in a change in the mean electromagnetic torque:

$$\overline{T_e} = \frac{p}{2\pi} \int_{\theta_o}^{\theta_o + \frac{2\pi}{p}} T_e . d\theta \qquad 1.6a$$

with θ_o arbitrary and p the number of pairs of poles.

It is now furthermore possible to prove that if continuous conversion of electromechanical power is desired, i.e. the mean value of the electromagnetic torque in the air gap must have a value different from zero:

$$\overline{T_e} \neq 0 \qquad 1.6b$$

and the converter operates at constant angular speed ω_m the frequencies of the currents on stator and rotor should be (B16

$$|2\pi\mu_s f_s \pm 2\pi\mu_r f_r| = |p\omega_m| \qquad 1.7$$

where μ_s and μ_r may in general be any real numbers, not necessarily integral. Consider the fundamental harmonic current ($\mu_{sr} = 1$). Keeping the magnetic field in the machine constant means keeping the torque in the machine constant (1.4, 1.5). Adjusting the stator and rotor frequency gives a modified speed of rotation for the air gap field, corresponding to a modified mechanical speed ω_m for continuous electromechanical power conversion. Conversely the frequencies on the rotor or stator may be kept constant, and the number of pairs of poles p changed. This also results in a change in the speed of rotation of the air gap field, and consequently adjustment of mechanical speed. These types of power flow control schemes are to be referred to as power control by variation of velocity of rotation of the magnetic field in the air gap.

In the preceding paragraphs attention has been devoted to obtaining power flow control in the electromechanical energy converter by change of torque or change of speed. As indicated in fig. 1.1, however, the intention is to transfer the electromechanical power to the load. Consider the mechanical equation of motion (complementary to the n + m electrical equations of motion 1.2a):

$$J_r \frac{d^2\theta}{dt^2} + T_f + T_{out} = \frac{\partial W'_m}{\partial \theta} = T_e \qquad 1.8a$$

If the electromechanical converter operates at constant speed ω_m as stated and the kinetic energy reservoir may be neglected in the flow considerations, the electromechanical power flow will be described by:

$$\overline{T}_{out} \cdot \omega_m = \overline{T_e} \cdot \omega_m - \overline{T_f} \cdot \omega_m \qquad 1.8b$$

This indicates that the output power will be effectively controlled by both the measures suggested in the previous paragraphs, and that these measures may be applied separately or simultaneously. This will depend on the characteristics of the load and the performance expected of the system. As an example it may be considered that in conventional practice the variable speed operation (in steady state) of a drive system is obtained by modification of the torque-speed relation of the driving machine, resulting in the equality 1.8b being fulfilled at another speed.

For the further clarification of the power control principles during the conversion process the types of transducers to be found will be classified into two types: synchronous and asynchronous. The definitions

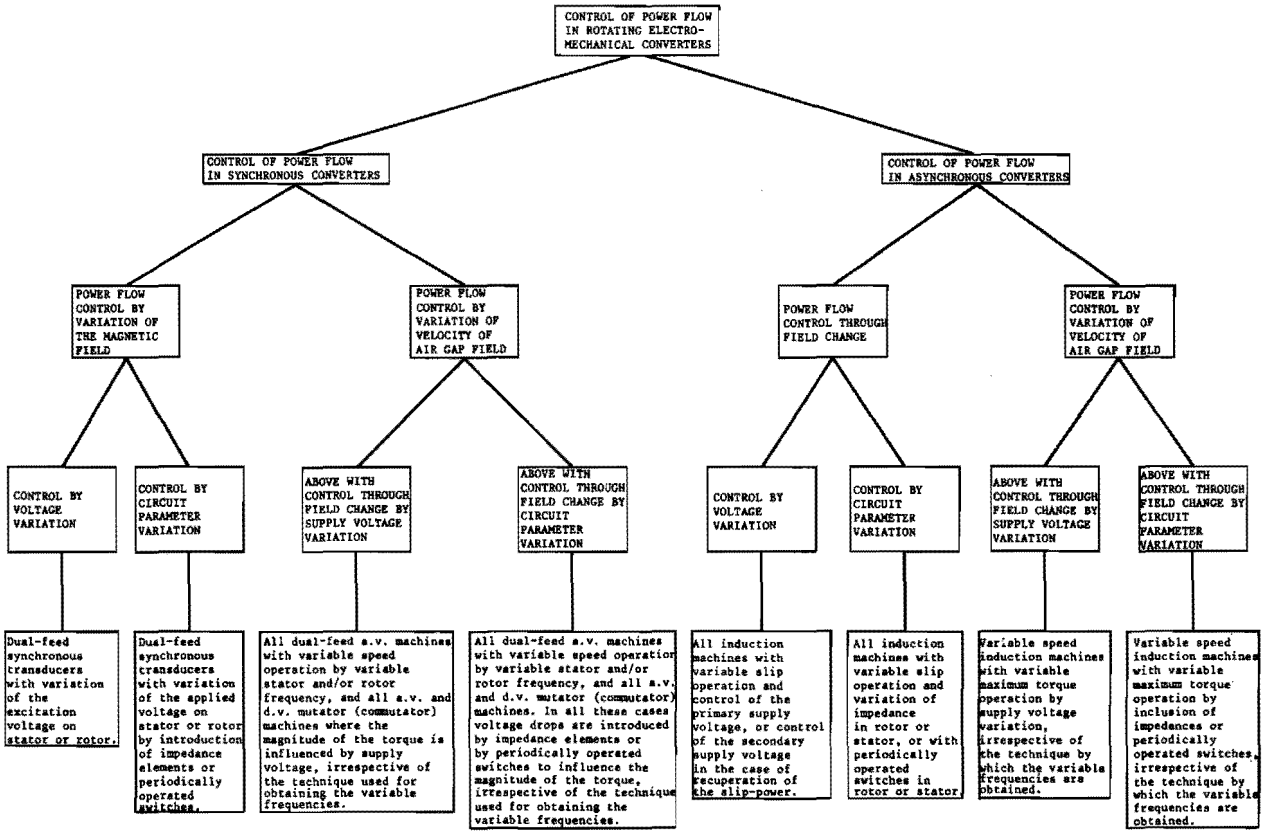
CONTROL OF POWER FLOW IN ROTATING ELECTRO-MECHANICAL CONVERTERS
CONTROL OF POWER FLOW IN SYNCHRONOUS CONVERTERS
CONTROL OF POWER FLOW IN ASYNCHRONOUS CONVERTERS
POWER FLOW CONTROL BY VARIATION OF THE MAGNETIC FIELD
POWER FLOW CONTROL BY VARIATION OF VELOCITY OF AIR GAP FIELD
POWER FLOW CONTROL THROUGH FIELD CHANGE
POWER FLOW CONTROL BY VARIATION OF VELOCITY OF AIR GAP FIELD
CONTROL BY VOLTAGE VARIATION
CONTROL BY CIRCUIT PARAMETER VARIATION
ABOVE WITH CONTROL THROUGH FIELD CHANGE BY SUPPLY VOLTAGE VARIATION
ABOVE WITH CONTROL THROUGH FIELD CHANGE BY CIRCUIT PARAMETER VARIATION
CONTROL BY VOLTAGE VARIATION
CONTROL BY CIRCUIT PARAMETER VARIATION
ABOVE WITH CONTROL THROUGH FIELD CHANGE BY SUPPLY VOLTAGE VARIATION
ABOVE WITH CONTROL THROUGH FIELD CHANGE BY CIRCUIT PARAMETER VARIATION
Dual-feed synchronous transducers with variation of the excitation voltage on stator or rotor.
Dual-feed synchronous transducers with variation of the applied voltage on stator or rotor by introduction of impedance elements or periodically operated switches.
All dual-feed a.v. machines with variable speed operation by variable stator and/or rotor frequency, and all a.v. and d.v. mutator (commutator) machines where the magnitude of the torque is influenced by supply voltage, irrespective of the technique used for obtaining the variable frequencies.
All dual-feed a.v. machines with variable speed operation by variable stator and/or rotor frequency, and all a.v. and d.v. mutator (commutator) machines. In all these cases voltage drops are introduced by impedance elements or by periodically operated switches to influence the magnitude of the torque, irrespective of the technique used for obtaining the variable frequencies.
All induction machines with variable slip operation and control of the primary supply voltage, or control of the secondary supply voltage in the case of recuperation of the slip-power.
All induction machines with variable slip operation and variation of impedance in rotor or stator, or with periodically operated switches in rotor or stator
Variable speed induction machines with variable maximum torque operation by supply voltage variation, irrespective of the technique by which the variable frequencies are obtained.
Variable speed induction machines with variable maximum torque operation by inclusion of impedances or periodically operated switches, irrespective of the technique by which the variable frequencies are obtained.

FIG. 1.3

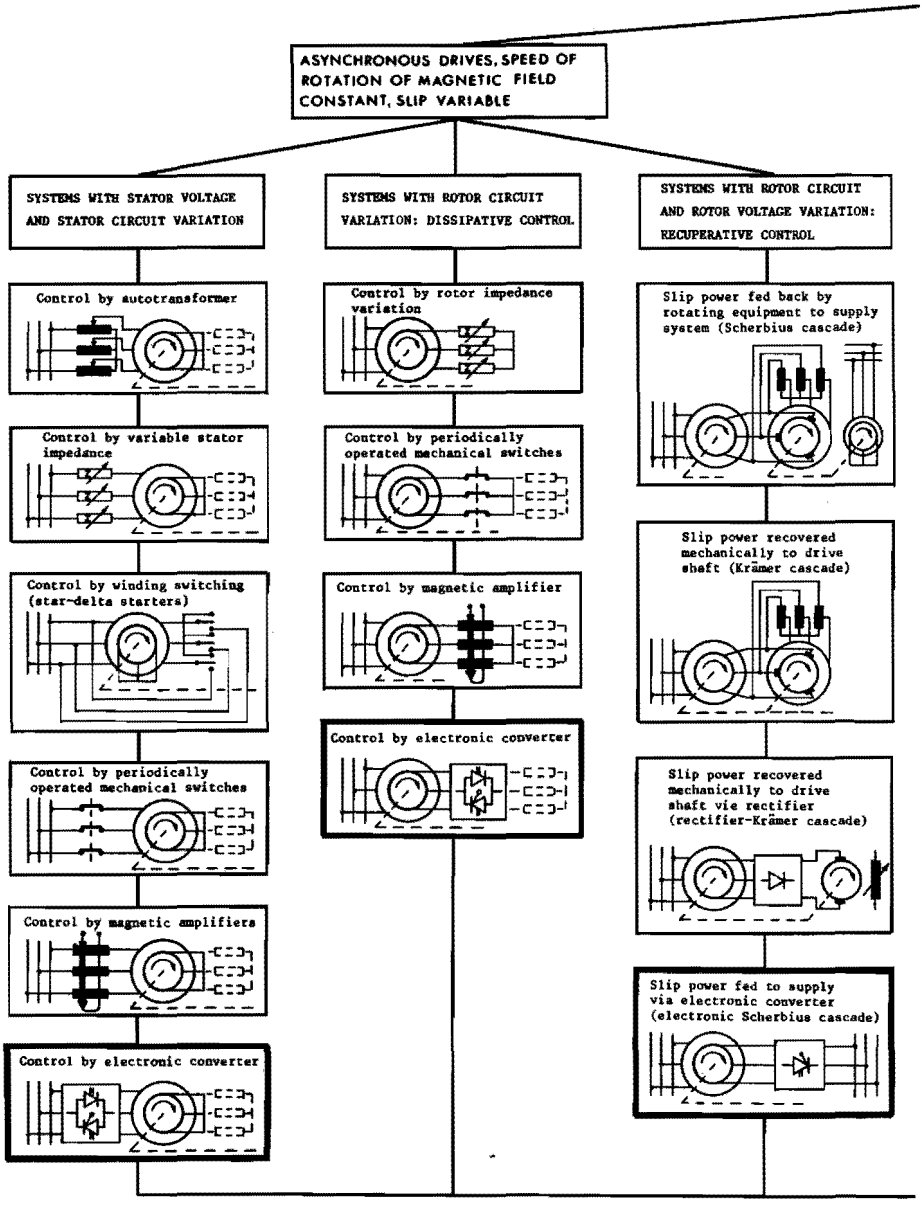

FIG. 1.4 CLASSIFICATION OF SOME ELECTRICAL DRIVE SYSTEMS WITH CONTROL OF POWER FLOW. PART I

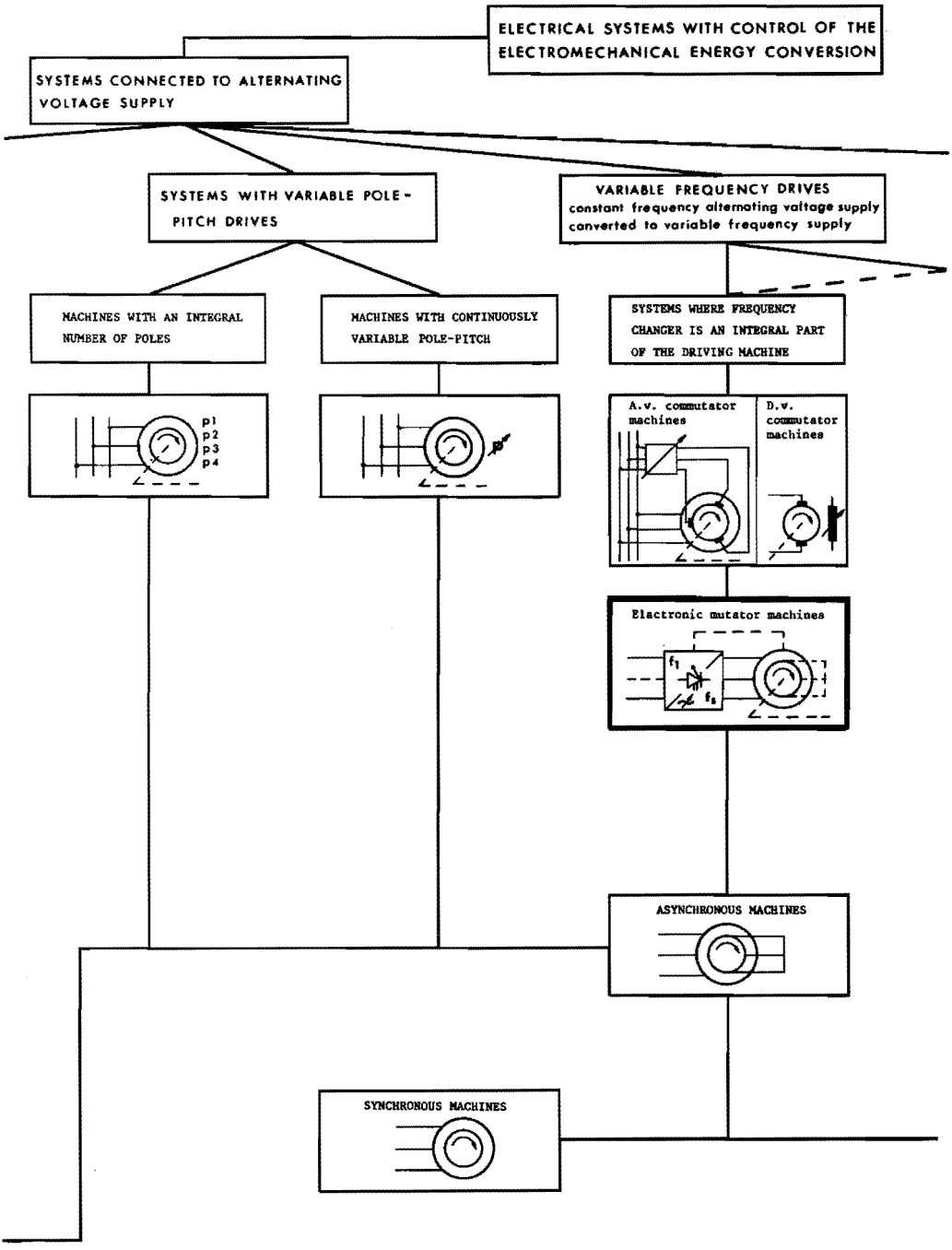

FIG. 1.4 CLASSIFICATION OF SOME ELECTRICAL DRIVE SYSTEMS WITH CONTROL OF POWER FLOW. PART II

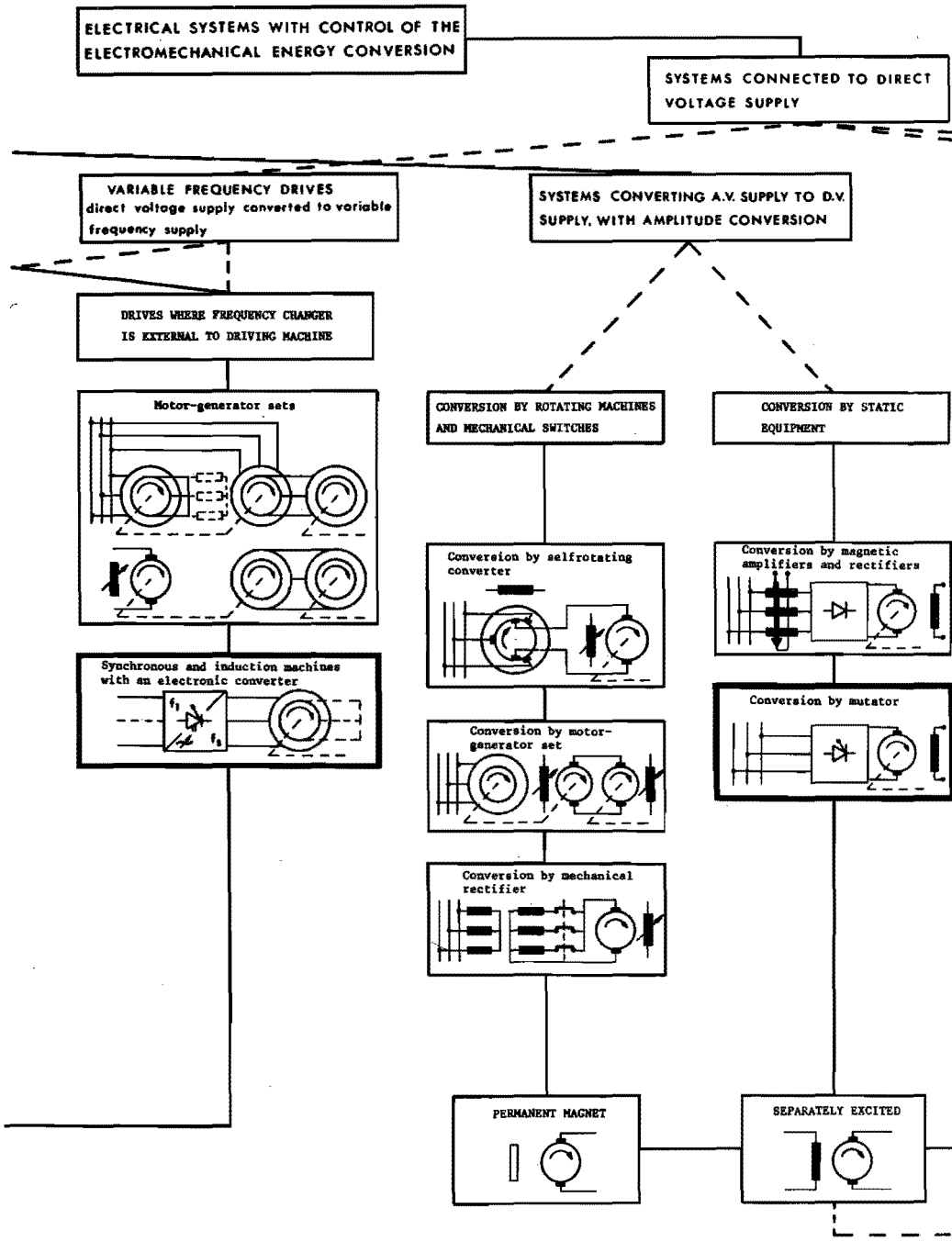

FIG. 1.4 CLASSIFICATION OF SOME ELECTRICAL DRIVE SYSTEMS WITH CONTROL OF POWER FLOW. PART III

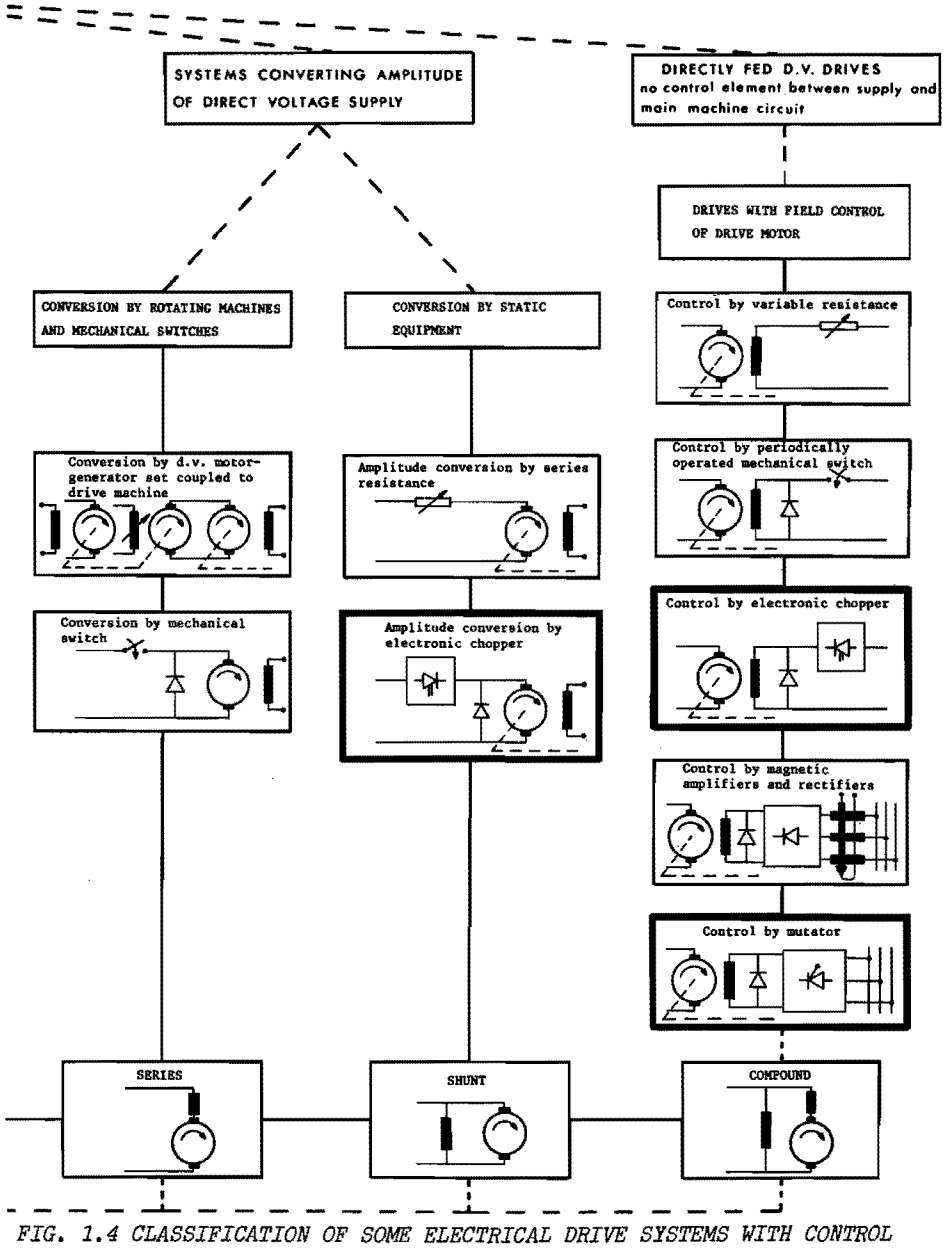

FIG. 1.4 CLASSIFICATION OF SOME ELECTRICAL DRIVE SYSTEMS WITH CONTROL OF POWER FLOW. PART IV

depart from the classical definitions in this field.

Synchronous electromechanical converters are converters in which both the stator and the rotor windings are fed by currents with frequencies determined by external sources, the mechanical speed having a discrete set of values according to rel. 1.7 (All synchronous machines and commutator machines fall into this class. These machines are all dually fed, unless permanent magnets are used to substitute windings carrying a current of frequency zero.)

Asynchronous electromechanical converters are converters in which either the rotor or the stator frequency is determined by an external source, and at least the frequency of the current on the other member is determined solely by electromagnetic induction, related to the mechanical speed according to rel. 1.7 (This category includes induction machines and contrary to conventional practice some dual-feed machines under certain control modes.)

Fig. 1.3 gives an indication of how these fundamental principles may be used to classify the different systems used for the control of electromechanical power conversion. In the above, and in this survey one is able to include the commutator machines in the group of the synchronous converters by viewing this machine as a synchronous machine with a frequency changer, as one is apt to do on inspiration of the generalized machine theory [51] . This general classification does not include all the cross-coupling effects such as converters showing both synchronous and asynchronous effects during their operation, for instance.

A survey of the controlled electrical drives that have been developed through the years, and may be developed, is indicated in fig. 1.4. In order to obtain better correspondence with historical electrical engineering practice, it has been subdivided into alternating and direct voltage supply systems, with the normal machine types also included. The classification of fig. 1.3 has been kept in mind as far as possible. For the remainder the diagram is self explanatory.

1.2 MACHINE-ELECTRONIC SYSTEMS IN THE PRESENTED SURVEY

Examination of fig. 1.4 indicates that an electronic counterpart may be found for most of the control methods - with exception of the change of pole-pitch. This diagram further gives a good impression of what percentage of all solutions to the power flow control problem is electronic in nature. For completeness it must be remarked that some solutions have been omitted, notably systems with cascading of induction machines, induction machines with rotating stators, a complete survey of all a.v. commutator machines and a complete survey of all types of special "rotating converters" (in the classical sense).

It should be noted that all but one of the electronic systems controls the power flow in the main flow path. The family of field-control systems, being the exception, operates at a much lower power level than the machine - but has a correspondingly longer time constant. The most efficient mode for all systems with electronic control of the power flow is a switching mode. In larger systems this becomes a necessity. Needless to say this switching action subjects the electromechanical transducer to harmonic powers it is not called upon to handle under symmetrical sinusoidal excitation, and also introduces them into the power supply system.

In order to continue the investigation of the machine-electronic

systems for the control of electromechanical power conversion, a few concepts to be used hereafter will now be defined.

1.2.1 DEFINITIONS OF POWER ELECTRONICS AND MACINE-ELECTRONICS

Under normal conditions the accent in an electrical system falls on the information processing aspect or on the power processing aspect, quite apart from the power level involved. In the electronic systems used in combination with electrical machines, these two functions are both present. It will be postulated here that the part of the system in which the accent is on information processing be called the information electronics and the other part of the system correspondingly the power electronics. These functions will not be fulfilled by electronic elements operating at different power levels in all practical systems, but for the majority of systems it is customary. The case of micromotors with electronic commutators, is one of the notable exceptions. It is worthwhile to note that diverging power levels for these parts of the system are usually accompanied by correspondingly diverging times of response. The word "machine-electronics" in itself is misleading, since as such it merely means electronics used with a machine, and it is specifically intended to indicate a system consisting of an electronic part and a rotating electromechanical transducer (rotating electrical machine). The use of this word is only justified since it forms a handy acronymn for something that may be specified as a "power-electronic rotating electromechanical transducer" system. From the preceding it is clear that a machine-electronic system consists of two subsystems - the electronics and the rotating electrical machine. With respect to the electronics it may be remarked that mostly the information-electronics is left out of the analysis of the system, and the subsystem electronics becomes the power electronics. As definitions may therefore be considered:

Power electronics
concerns itself with the study of that part of an electronic system in which the accent falls on the processing of power necessary at the output rather than on information. The definition is not coupled to a certain absolute level of power, but is relative.

Machine electronics
concerns itself with the study of systems consisting of power-electronics in conjunction with rotating electromechanical transducers (rotating electrical machines). The machine-electronic system controls power flow during the electromechanical energy conversion process.

1.3 THE DEVELOPMENT OF THE SUBJECT OF MACHINE-ELECTRONICS

The oldest known switch used in the control of electrical machines is the mechanical commutator. This was followed by a mechanical switching arrangement to control the field of generators, the Tirrill controller. Subsequently the gaseous valves showed promise for generating the switching functions necessary to control machines. These devices had some disadvantages and at a time it appeared that the mechanical metallic rectifier (a modified commutator !) was the future promise. Almost simultaneously it was succeeded by a device developing

in parallel - the transductor or magnetic amplifier. The era of the semiconductor switches then dawned - an era from which we, being still concerned in its development, are able to derive but limited historical perspective.

Numerous works have been published and circuit configurations and methods of controlling electrical machines electronically worked out or suggested in the past. It has therefore become extremely difficult to ascertain the origin of most of the circuits and methods of control employed at present in machine-electronics. The aim of this historical introduction is to present the knowledge acquired on these matters in an attempt to clear up some of these aspects.

1.3.1 DEVELOPMENT OF THE DIFFERENT SWITCHING DEVICES

Although the practical application of these devices did not come into being before nearly a quarter of the twentieth century was past, it is interesting to note that the physical principles underlying the behaviour of mercury-arc rectifiers had apparently been recognised in 1882 by *Jemin* and *Meneuvrier* ([B11]). They gave an account of the property of an electric arc established between mercury and carbon electrodes, mentioning that the current will flow in one direction only. In 1889 Fleming investigated the property of unilateral conductivity of the electric arc in air, while between 1894 and 1898 *Sahulka* described the results of indentical investigations pertaining to atmospheric arcs between mercury and iron or carbon electrodes.

All these experiments were conducted under atmospheric conditions. In the years 1890 - 1892 *Arons* made the first vapour lamps by enclosing the arc in an evacuated vessel. Apparently a rectifier based on the unidirectional conduction principle of the mercury-arc emerged around 1900 when *Cooper-Hewitt* took up the manufacture of these lamps on a commercial scale for lighting purposes. During further investigations of his lamps the idea of building a converter for alternating current to direct current cropped up. This conversion equipment was apparently first demonstrated at the turn of the year 1902 - 1903 ([18,59] in public, and aroused considerable interest. The mercury-arc rectifier-family developed from this beginning in all its varieties. Table 1.1 gives an impression of this development and of related devices. It may be said that the development of the mercury-arc rectifier-family did not reach a stage where enormous practical development of circuits was inspired before 1930.

1.3.2 DEVELOPMENT OF THE CIRCUITS FOR THE ELECTRONIC CONTROL OF ELECTRICAL POWER

It is of course impossible to sketch the development of all the power electronic techniques in a few words - therefore only the most important ideas concerning:

(i) power electronic frequency changers,
(ii) d.v. to d.v. transforming circuits (electronic choppers),
(iii) phase control circuits for adjusting output voltage will be traced.

Although in the previous paragraph it has been indicated that the efficient controlled power switches had a gradual development, static frequency conversion dates from 1903 as far as rectification is

concerned. Performing the inverse of this process proved more difficult as a suitable method of controlling the arc-discharge was not available. Before 1906 *Steinmetz* actually built an inverter circuit by using a single-cathode, four anode unit in which the discharge spontaneously switched from anode to anode in predictable order (fig. 1.5a). Switching characteristics of the tube were found to be mostly dependent on the interelectrode distance of the electrodes [45]. It appears reasonable to assume that this characteristic was necessary to start up the circuit, and once a-c loads had been connected to the output natural commutation would aid the process of inversion. This process for the circuit shown depends on the cyclic transfer of the arc in order 1-2-3-4-1. *Prince* developed the later well known parallel inverter in 1925, adding forced commutation to the scheme in 1928. As indicated in fig. 1.5b his first inverter circuit used natural commutation, assisted

Mercury-arc rectifier (glass envelope)	Cooper-Hewitt	1900 [B11]
Mercury-arc rectifier (metal envelope)	Cooper-Hewitt	1908 [10]
	Schäfer	1910 [61]
Controlled mercury-arc rectifier (ignition by high voltage impulse on auxilary electrodes)	Cooper-Hewitt	1903 [B7]
Hot-cathode mercury vapour tube: without grid phanotron, with grid thyratron	Langmuir	1914 [29]
Mechanical field regulator	Tirrill	1902 [71]
Contact rectifier, high current metal contacts	Koch	1901 [36]
	Kesselring	1923 [35]
	Koppelman	1941 [37]
Selenium rectifier	Presser	1925 [56]
Copper-oxide rectifier	Grondahl	1926 [24]
Junction thyristor, p-n-p-n configuration	Shockley	1951 [64]
	Moll/York	1956 [50]
		1957 [B4]
Bidirectional triode switch p-n-p-n-p configuration	Gentry, Scace	1964 [19]
	Flowers	

TABLE 1.1 DEVELOPMENT OF SOME SWITCHING DEVICES USED IN THE CONTROL OF ELECTRICAL MACHINES

by the grids of the thermionic vacuum tubes. It was unable to handle any reactive power, and therefore the synchronous machine in the output circuit was a necessity. The use of 15 kV in order to overcome the disadvantage of the high voltage drop in the vacuum switching elements is interesting. The force commutated circuit of fig. 1.5c was still unable to handle reactive power, but represented a major advance in the characteristic that it was able to work independently of an already existing supply. After the possibility to handle

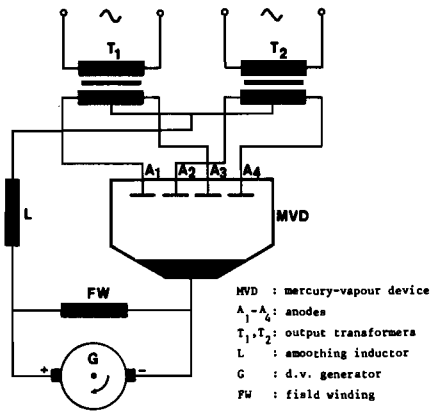

MVD : mercury-vapour device
A_1-A_4: anodes
T_1,T_2: output transformers
L : smoothing inductor
G : d.v. generator
FW : field winding

(a) Stainmetz inverter.

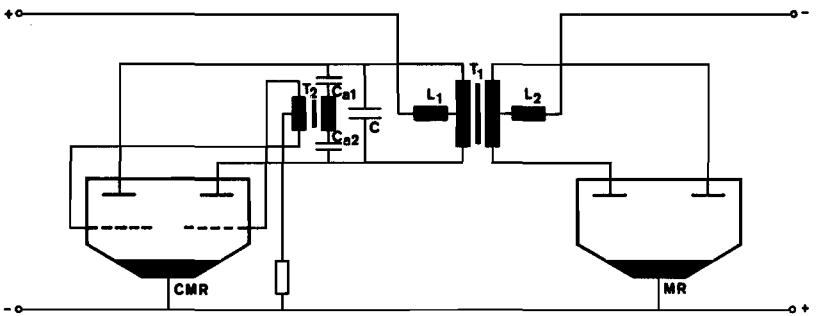

T_1 : inverter transformer
CMR: controlled mercury-arc rectifier
MR : mercury-arc rectifier

T_2 : grid transformer
C : commutation capacitor
C_{a1},C_{a2}: auxiliary capacitors
L_1,L_2 : smoothing inductors

(c) D.v. transforming circuit of Prince with forced commutation.

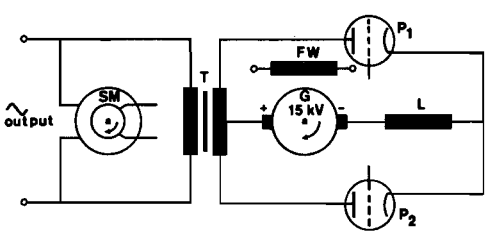

SM : synchronous machine
T : inverter transformer
P_1,P_2: "pliotron" tubes

G : high-voltage d.v. generator
FW: field winding
L : smoothing inductor

(b) The inverter circuit of Prince.

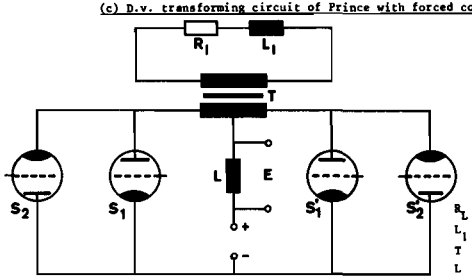

R_L : load resistance
L_1 : load inductance
T : inverter transformer
L : commutation inductor
E : commutation EMF
S_1,S_2,S_1',S_2': gas tubes

(d) Proposed inverter circuit of Petersen with "Petersen" tubes.

FIG. 1.5 INITIAL DEVELOPMENT OF SOME FUNDAMENTAL IDEAS IN POWER-ELECTRONICS.

"Switching tube" inverter circuit	Steinmetz	pre-1906 [45]
"Parallel"-inverter circuit with natural commutation	Prince	1925 [58]
Parallel-inverter circuits with forced commutation	Prince	1928 [57]
Inverter circuits with series configuration	Fitzgerald, Henderson, Sabbah	1929 [30]
Feedback diodes to handle reactive power in inverter circuits	Petersen	1932 [55]
Decoupling diodes for commutation circuits	Umarov	- 1956 [25]
Cycloconverter circuits	Rissik	= 1930 [B11]
Synchronous envelope cycloconverter	Löbl	1932 [46]
Asynchronous envelope cycloconverter	Krämer	pre-1935 [B11]
Continuously variable cycloconverter	Schenkel, von Issendorf	1932 [62]
Direct-voltage chopper circuit	Prince, Hull	1929 [30]
	Tompkins	1932 [72]
Phase control d.v. circuits	Dunoyer, Toulon	1924 [15]
Phase control a.v. circuits (anti-parallel configuration)	Lenz	1933 [44]

TABLE 1.2 DEVELOPMENT OF SOME IMPORTANT POWER-ELECTRONIC CIRCUIT TECHNIQUES

reactive power with these circuits was introduced by *Petersen* in 1932 (fig. 1.5d), and the cycloconverter-family of circuits had been developed, the development of power electronic frequency changers advanced to a considerable degree. This may be observed by studying the histograms of paragraph 1.4. Table 1.2 again presents some aspects of this development.

A direct voltage chopper circuit, or d.v. to d.v. transformer, necessitates the forced commutation of direct current through the electronic switch. Although this art was well understood before 1930, as introduced by *Prince* [57] and *Hull* [30], and treated explicitly by *Tompkins* [72] it was apparently not applied to the control of electro-mechanical transducers until recently.

On the other hand efficient phase control circuits were developed early, and applied with success to the control of d.v. machines and other d.v. loads, and to the control of a.v. loads. Using the idea of control of the discharge of *Cooper-Hewitt*, *Dunoyer* and *Toulon* [15] effectively demonstrated how to obtain regulation at the output of an electronic mutator in 1924. Modifying this idea for current flow in both directions, *Lenz* [44] proposed and tested the antiparallel naturally commutated switch configuration in 1933. This configuration and the previous found extensive application in the control of welding equipment [23].

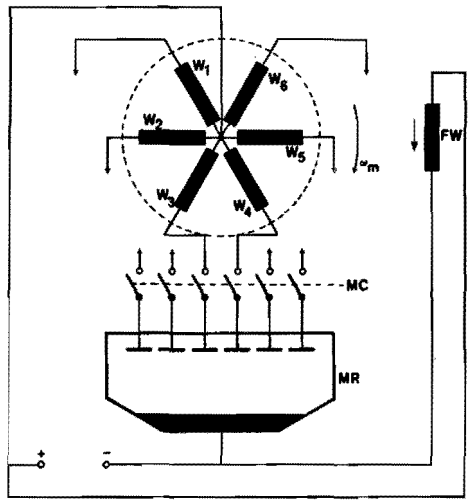

MC: mechanical commutator
MR: mercury-arc rectifier
$W_1 - W_6$ machine armature windings
FW field winding

(a) Illustration of the principle of the "high-voltage" d.v. machine of Bolliger.

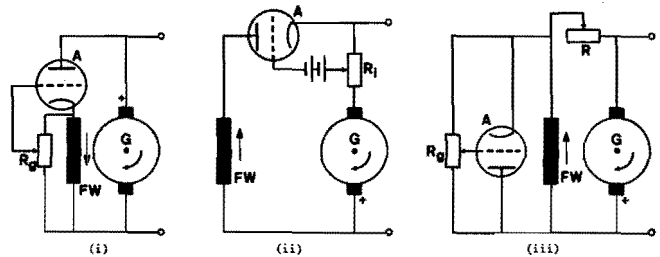

A : "audion"
G : d.v. generator
FW: field winding
R_g: grid resistor
R_i: current resistor

(b) Schemes presented by van der Bijl.

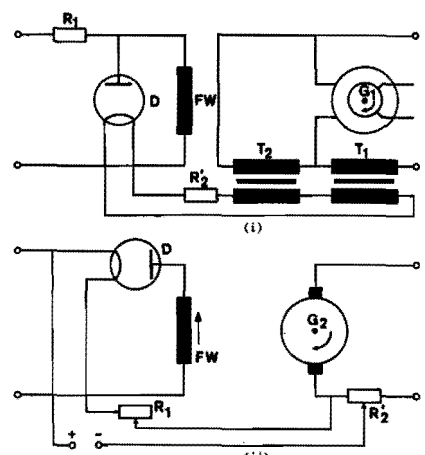

G_1: a.v. generator
G_2: d.v. generator
FW: field winding
D : vacuum diode
T_1: current transformer
T_2: voltage transformer

(c) Original schemes of Voorhoeve for controlling generator voltage.

FIG. 1.6 SOME INITIAL ATTEMPTS AT CONTROLLING ELECTRICAL MACHINES BY ELECTRONIC METHODS.

1.3.3 DEVELOPMENT OF IDEAS TO CONTROL ELECTRICAL MACHINES

Ideas to use electronic elements to control, regulate or augment electrical machines appear to have been put into practice for the first time during the years immediately before and after 1920. It is possible that these contributions may not be characterised as machine-electronics as it is known today, yet it may be considered as the very beginning of the subject.

1.3.3.1 Initial attempts

In the year 1917 *Bolliger* came upon the idea of a "high-voltage" d.v. machine (published 1921) in which the substantial part of the commutator action is executed by a mercury-arc rectifier. To quote Bolliger: "Der Kommutator arbeitet lediglich als ein bei leerlaufenden Phasen kontaktmachender Spannungsschaltapparat, ohne jede Stromwendung unter den Bürsten. Der Gleichrichter hingegen wirkt als ein durch die Betriebsphasenspannungen gesteuerter Stromwendeapparat, ..." (B3 .

From the previous paragraph and from figure 1.6a it may be gathered that by connecting the discharge tube in series with a mechanical switch he was able to obtain the characteristic of a controlled rectifier. This is the more remarkable, since at that stage the controlled mercury-arc rectifier still belonged to the future. The high voltages in the reverse direction and the actual commutation were the responsibilities of the rectifier. This indicates that Bolliger had already fully realised the necessity for a static electronic commutator - but did not yet have the necessary circuit elements. His appropriate comment on his work was: "Einen Anfang zu etwas dass noch nicht ist".

Van der Bijl described control systems for d.v. generator current and voltage in 1920 (B2 , attributing the origin of the ideas to *Wold*. In these systems a vacuum triode ("audion") was connected either in series or in parallel with the field winding of the generator, the essential control element (fig. 1.6).

In the years before 1930 *Voorhoeve* in the Netherlands investigated possibilities to control generator voltages by electronic means. Contrary to the work reported by Van der Bijl, he employed vacuum diodes, the heating current being the variable (fig. 1.6). This was done in the conviction that gas discharge tubes did not yet have the constant characteristics essential for achieving accurate control. Later work by the same group included the use of vacuum triodes, but was overshadowed by the fast developing control schemes with grid controlled mercury-arc rectifiers (65,75.

1.3.3.2 Machines with electronic commutators

Reference has already previously been made to the fact that the electronic switches may be used to perform the same function as the mechanical switches in conjunction with an electrical machine.

One of the initial ideas that sprung from the availability of the controlled mercury-arc rectifier was to build an electronic commutator. This idea grew gradually. It is worth mentioning that in 1913 two steel tank mercury-arc rectifiers were installed in a traction unit of the Pennsylvania Railroad in the U.S.A. This unit, with four motors of 200 h.p., 600 V, completed approximately 20.000 km in normal traction

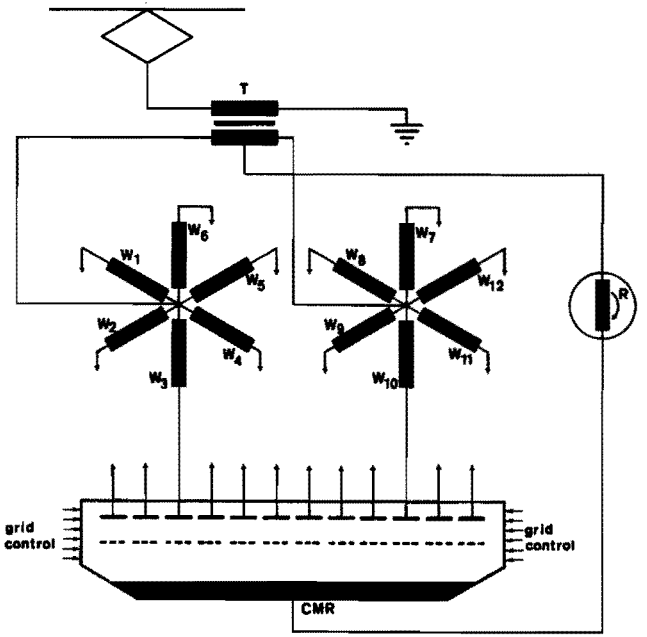

$W_1 - W_{12}$: machine stator windings
R : rotor and field winding
T : transformer
CMR : controlled mercury-arc rectifier

(a) Thyratron-commutator machine proposed by Kern.

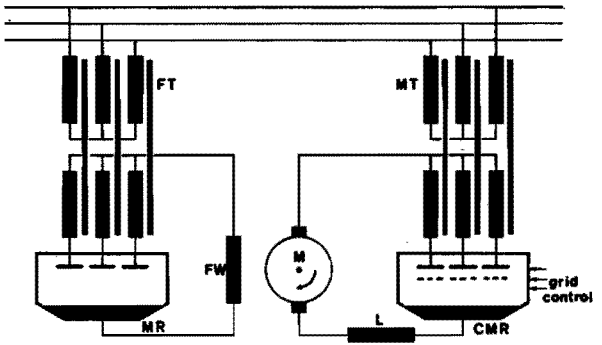

FT: field transformer
MT: main transformer
MR: mercury-arc rectifier
CMR: controlled mercury-arc rectifier
L: smoothing inductor
M: direct voltage motor
FW: field winding

(b) Original scheme for a.v. fed d.v. motor investigated by Schilling.

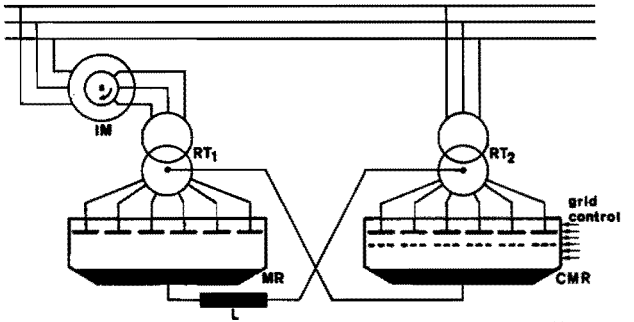

IM : inducrion motor
RT_1, RT_2: rectifier transformers
CMR: controlled mercury-arc rectifier
MR: mercury-arc rectifier
L: smoothing inductor

(c) Electronic Scherbius cascade of Stöhr.

FIG. 1.7 IMPORTANT MACHINE-ELECTRONIC DEVELOPMENTS.

service in the years before 1920 [87]. In this case two frequency conversion processes are to be observed, one of which is still mechanical. The first machine to use a true electronic commutator was the machine of *Kern* - a now famous example [34]. In fact, Kern suggested various configurations, one being shown in fig. 1.7, the first locomotive being built with this system by Brown Boveri around 1930.

In the years before 1940 these types of machines were studied by many workers, and were originally primarily intended for traction purposes [47]. Although it was applied on the European continent and in the U.S.A. to a certain extent [7], the thyratron or controlled mercury-arc commutator motor never attained true widespread practical application, despite considerable enthusiasm (see for instance dicussion of Alexander to Marti [47]). One of the ideas being worked out at present is the use of thyristor frequency changers in conjunction with squirrel-cage induction machines for electric traction purposes [13,14]. This idea is not new - it has been considered in the past, but rejected [67]. The reason for the rejection of this proposal in 1940 was the enormous amount of equipment needed, it being impossible to transport it aboard an ordinary locomotive. Thyristors are relatively small in size and eliminate this problem, as has been illustrated by the present experiments. The main hazards besetting the application of this type of traction at present seem to be economics and reliability.

The interest in electronic commutators - stimulated anew by the thyristor - has apparently stimulated the use of transistors for the same function in small machines. This is the inevitable conclusion, as it was not before 1962 that this type of electronically commutated machine received serious attention [40,5], although switching transistors were available years before.

1.3.3.3 Schemes for control of induction machines without changing the supply frequency

Compared to direct current machines, wound rotor induction machines are relatively cheap and it is therefore interesting to investigate all possibilities to control them. Electronic regulation of the rotor current of these machines has only recently received some worthwhile attention, however.

The first work on electronic rotor control of induction machines concerned electronic Scherbius cascades. The considerations that mercury-arc controlled rectifiers are expensive and have a voltage drop of 15V - 25V during forward conduction confined these investigations to larger machines. *Alexanderson* proposed an electronic Scherbius cascade in 1938 [4]. Working independently, *Stöhr* reported investigations comparing machines with an electronic commutator to the mentioned cascade in 1939 [69]. Later the operation of the electronic Scherbius cascade was extended to the oversynchronous region of operation [68]. Subsequently *Hölters* (1943) [27] also investigated this type of system. To his system the rather unfortunate name of "Asynchronstromrichtermotor" was given. This name has since been used to indicate another type of system, i.e. that of a variable frequency inverter feeding an induction motor, the motor windings being part of the inverter.

Development of silicon rectifiers renewed the interest in systems consisting of wound-rotor induction machines and frequency converters in the rotor [49], while thyristors hold the promise of making this drive economic and compact - also for smaller machines.

The magnetic amplifier was, and still is, applied with good results to stator and rotor control [41], but it is only during the last decade, after the development of the thyristor, that this type of control has received increasing attention in the form of electronic switching of the rotor current, notably in Germany (see for instance [2]). Although the idea of using antiparallel switches to regulate voltage has been existent for a long time it does not seem to have been worked out further for stator control of induction machines. In the years around 1950 the idea of applying phase-control to rotor and stator circuits of induction machines by magnetic amplifiers found wide application [41,31]. Only after 1960 did interest arise in employing this type of control to advantage on the stator of squirrel cage motors by using electronic switches [20]. The appearance of the triac has made this type of drive an attractive proposition in the lower power range (< 10 kW).

1.3.3.4 Voltage regulation of direct voltage machines by mutators

Control of d.v. machines fed by three phase or single-phase a.v. systems drew attention after the introduction of the controlled mercury-arc rectifier in 1928. It was realised that this offers the possibility to regulate the main current in the motor [6], and was apparently first extensively investigated by *Schilling* [63] (See fig. 1.7.) Later attention was devoted to constructing static Ward-Leonard drives in this way. (See for instance [65].) Semiconductor switches increased the possibilities, and it may be expected that the present popularity of this type of semiconductor controlled drive will still continue for a considerable time. In the same way that the thyristor revived the interest in converter locomotives in countries with a.v. traction systems, the controlled mercury-arc rectifier originally initiated design of converter locomotives - the first example being that of Reichel [60].

1.3.3.5 Electronic chopper control of direct voltage machines

Apparently the inventor of armature voltage control of d.v. machines by pulse modulation, the so-called series chopper - was *Blaufuss* in 1940 [8]. The problem was to obtain a mechanical or electronic switch that could be operated reliably and fast enough to achieve this control. It took years before the idea of Blaufuss was taken up again. The first practical realization of this scheme by electronic means appears to be due to *Jones* [33] in the U.S.A. and to *Abraham, Heumann* and *Koppelmann* [1] in Germany, the two groups working independently, and employing thyristors as switches. It is interesting to note that the electronic chopper as employed by these groups was discussed in 1929 by *Hull* in relation to the parallel inverter [30]. These types of power-electronic systems have since developed rapidly - especially with respect to the circuit improvements possible. Electronic choppers regulating series direct voltage machines is one of the most successfull machine-electronics systems at present, finding widespread application for low loss control in traction circuits.

Semi-electronic commutator machine	Bolliger	1917 ([83]
Field-regulation of generators by vacuum triodes	Van der Bijl, Wold	1920 ([82]
Field-regulation of generators by vacuum diodes	Voorhoeve	1928 ([75]
All-electronic commutator machine	Kern	1930 ([34]
Electronic Scherbius cascade	Alexanderson	1938 ([4]
Electronic Ward-Leonard control	Schilling, Bayha	1933 ([63], [6]
Electronic chopper control	Jones	1961 ([33]
	Abraham, Heumann, Koppelmann	1962 ([1]

TABLE 1.3 SOME IMPORTANT DEVELOPMENTS IN MACHINE-ELECTRONICS

1.4 GROWTH OF THE SUBJECT OF MACHINE ELECTRONICS

As a conclusion to this introductory chapter on the development and extent of the subject studied it will be attempted to present some statistical information to indicate the growth. This information has been extracted from a bibliography ([79] that is continuously being renewed, so that it may be taken to be representative. The bibliography includes a selected list of contributions of 2×10^3, the most important selection criteria having been that the contributions should treat theoretical and/or experimental study of problems in machine-electronics and power electronics. It may therefore be concluded that its contents reflects research activity for the most part, and is less influenced by application, fabrication and commercial aspects.

The histogram of fig. 1.8a depicts the time distribution of that part of the contents of the bibliography that concerns power electronic frequency changers and their associated circuit and power system techniques. Time distribution of the contents as far as the investigations on the actual machine-electronic systems are concerned may be found in fig. 1.8b. It should be noted that the histogram of fig. 1.8c indicates the work on power semiconductor switching elements, such as diodes, thyristors, triacs etc. and does not concern any of the circuit techniques associated with applications of these components. These circuit techniques are included in 1.8a.

By studying these histograms one may take note of the fact that activity in the field of power electronics in the period 1930-1940 was of the same order as the present activity in this field. The same does not hold for the activity in the field of machine electronics. To the author's opinion this is the proof of the statement already made that the nature of the gaseous switching elements restricted their application to larger machines, added to the steadily increasing application of electromotive power through the years.

In conclusion, it is clearly evident how the new surge in both branches corresponds to the activity in the field of power semiconductor elements, and that there is all reason to expect this activity to continue even its rate of increase for the near future. In conjunction with the formation presented in the other paragraphs of this chapter these

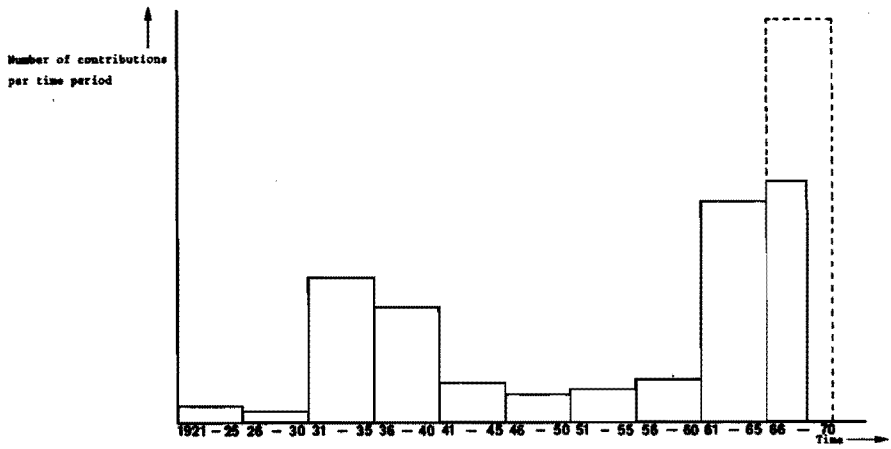

(a) Literature on power-electronic frequency changers.

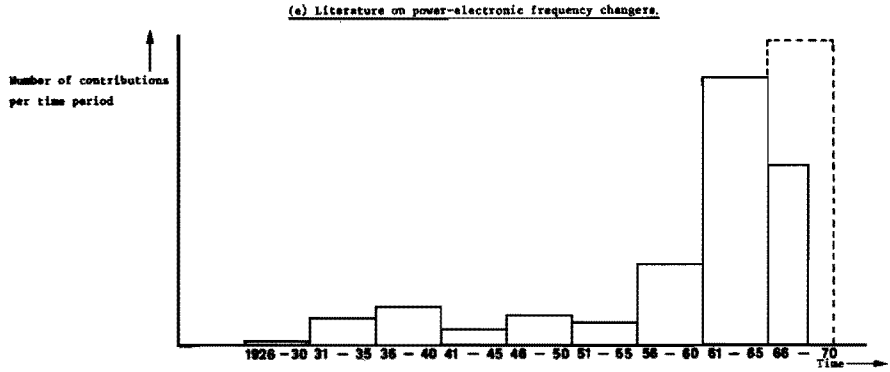

(b) Literature on machine-electronics.

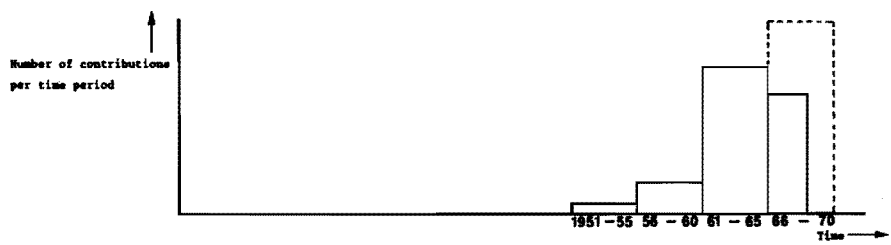

(c) Literature on semiconductor power switching elements.

FIG. 1.8 HISTOGRAMS DEPICTING LITERATURE ACTIVITY IN THE FIELDS OF POWER-ELECTRONICS, MACHINE-ELECTRONICS, AND POWER SEMICONDUCTOR ELEMENTS. (SAME SCALE VERTICAL AND HORIZONTAL)

expectations constitute a motivation for the systematic study to be taken up in the following chapters.

CHAPTER 2

SYSTEMATICS OF MACHINE-ELECTRONIC SYSTEMS

Synopsis

The different possibilities to develop a systematic classification for the machine-electronic systems are briefly investigated and the criterion of power flow in the electromechanical converter selected. The model used for classification purposes is described and three fundamental groups of systems identified according to the power flow in the electromechanical converter. It is found that some groups of hybrid systems may be distinguished, and the possibility for constructing further hybrid systems is pointed out. The stringent constraints regarding harmonic currents in the model are relaxed, and the implications investigated.

The three fundamental groups of systems discerned on theoretical grounds are related to the practical systems by presenting a classified survey of practical machine-electronic systems. Subdivision of the machine-electronic groups according to the switching functions generated by the power-electronic circuits and according to the structure of these circuits, concludes the chapter.

2.1 THE DIFFERENT CRITERIA APPLICABLE FOR CLASSIFICATION OF MACHINE-ELECTRONIC SYSTEMS

2.1.1 *THE SYSTEMS TO BE STUDIED*

For the purpose of the systematic classification to be investigated, let a variable speed drive system as in fig. 2.1 be regarded. The system is defined as being enclosed by boundary B_1 with transfer function [F] so that

$$[x_{out}] = [F] \cdot [x_{in}] \qquad 2.1$$

the input and output vectors $[x_{in}]$ and $[x_{out}]$ being multi-dimensional, as will be treated in the following chapter. For the present the boundary is shifted to B_2 for investigating the machine-electronic systems. This includes information-electronics, power electronics and electro-mechanical energy converter. These functions have been defined in the previous chapter.

The systemactic classification will concentrate on the power flow characteristics, and the information electronic part is excluded. Being energy processing, the machine-electronic systems use switches as

adjustors. By the nature of a switch the proportionality between input command and current flow through the switch disappears once it has been closed. Possibility of control is regained only after the zero-current condition has again been reached, and it may therefore be expected that the systems are discrete-time systems. The transfer functions calculated in the course of this study does not take this into account, but concerns mean values of the relevant electrical and mechanical variables.

Systems characterised by linear differential equations with constant coefficients may be considered time-invariant. As will be clear in the next chapter the equations describing the electromechanical transducer are generally non-linear, but reduce to linear differential equations with time-varying-coefficients under constraints of constant speed of rotation. It will be shown that irrespective of the excitation, these equations may be subjected to coordinate transformations reducing the set of equations to linear differential equations with constant coeffficients. This is the reason that - despite the time-dependence of the general equations - the machine electronic system will be considered as time-invariant.

2.1.2 *REVIEW OF POSSIBILITIES FOR CLASSIFICATION OF THE SYSTEMS*

A systematic study may be conducted from a number of viewpoints. Some of the most obvious alternatives are given below.

.1 Classification according to the type of power supply needed to excite the system.
.2 Classification according to the different types of power-electronic circuits used as adjustors in the system.
.3 Classification according to the parameters in the theoretical torque-speed relationship that are subject to changes due to the control action.
.4 Classification according to the type of electrical machine chosen as output unit for the system.
.5 Classification according to the fundamental power relations in the system.

2.1.2.1

In the past a powerful tradition has grown in electrical engineering with a view to the grouping of electrical drives or electrical machines into the two categories "a.c drives" and "d.c. drives". * This may also be introduced as regards machine-electronic systems, since the systems known at present are either fed from an alternating voltage supply, or from a direct voltage supply. The latter may be obtained from batteries or by rectification and filtering. To a certain extent these criteria have been applied to compile fig. 1.4 - in order to find some correspondence with present practice.

* In fact these drives may better be termed "a.v. drives" and "d.v. drives", since in practice machines are almost always fed from a voltage supply, and not by a current source.

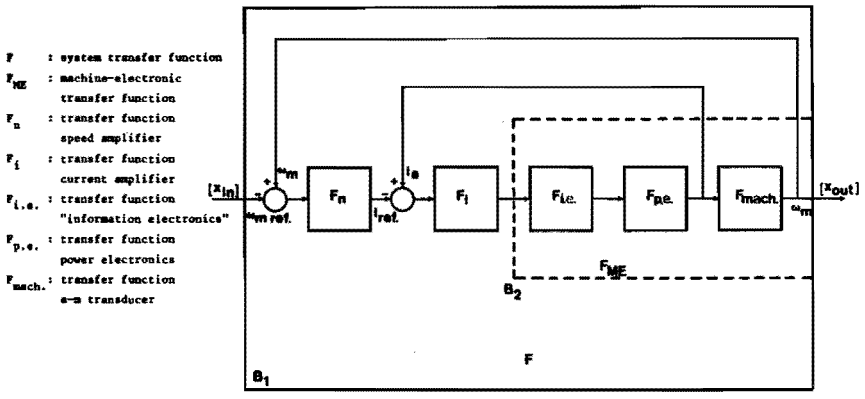

FIG. 2.1 ELECTRICAL VARIABLE SPEED DRIVE AS A GENERAL SYSTEM.

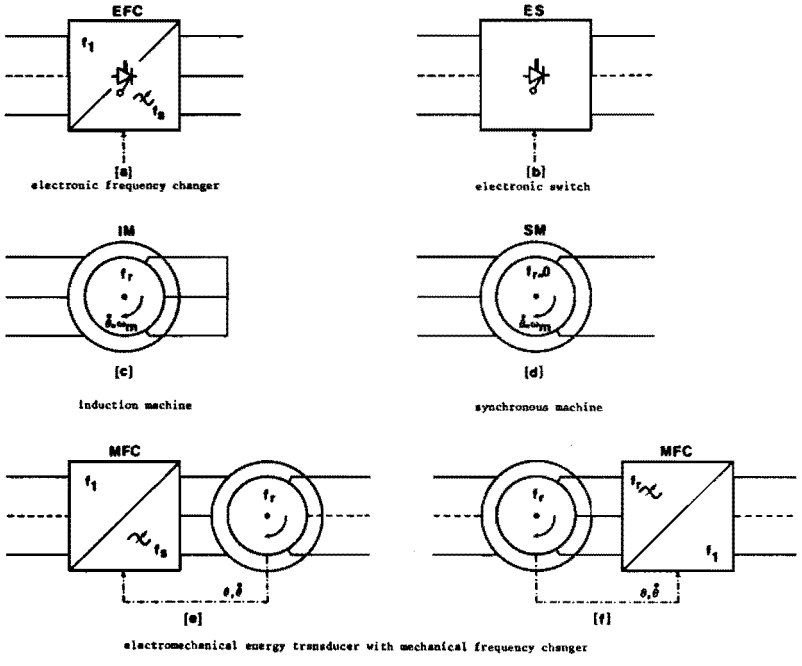

FIG. 2.2 SOME DEFINITIONS CONCERNING THE SYSTEMATICS.

It is felt, however, that such a grouping of the machine-electronic systems will only lead to confusion by placing drives with totally different characteristics in the same category. (Example: an induction machine fed by (a) a cycloconverter, (b) chopped voltage source of fundamental frequency.)

2.1.2.2

Recently some extensive attempts have been made to develop a systematic approach to power electronic circuits by Abraham and Koppelman (and Heumann (, and this may also be employed to systematize the machine-electronics, A classification using details of the power-electronic circuits to distinguish between the different systems will tend to obscure the function of the machine-electronics as part of an electrical drive. As will be evident later this type of classification may be used to advantage for subdivision of the main types of machine-electronic systems, but is not suited to setting up a general classification.

2.1.2.3

Under the assumption that rotating electromechanical transducers operate under steady state conditions, have sinusoidal spatial current distributions on moving and stationary members, have a linear magnetic circuit, and are excited by voltages and currents of simple harmonic type, the torque speed relationship becomes a function of the lumped-elements in the equivalent circuit, and the voltage impressed thereon. When one of these parameters is changed, the torque speed characteristic is influenced and one may therefore speak of systems with R_r, R_s, control - as has become customary in machine practice. This method of classification is not suitable for a general approach to machine-electronic systems. It is not feasible to represent the power control effects by the variation of elements of the equivalent circuit. As will be shown later the switching elements cannot simply be included in the equivalent circuit.

2.1.2.4

The same arguments that plead against a division of machine-electronic systems into a.v. and d.v. categories, also plead against classification according to the output machine. Although such an approach may be useful when it concerns choosing a system for given environmental conditions, it must be dismissed as a possibility for a general classification.

2.1.2.5

Machine-electronic systems may always be considered to be part of an electrical drive, and as such power considerations are of primary importance. When one examines the power flow in the different machine-electronic systems, it becomes apparent that there are groups of systems in which the power electronics influences the flow of power in different ways. Use of this characteristic to set up a classification should aid insight and the validity is not affected by any internal change in the power-electronics. In the following it will be attempted to develop such a classification system.

2.2 POWER FLOW IN RELATION TO SYSTEMATICS OF MACHINE-ELECTRONIC SYSTEMS

2.2.1 *THE PHYSICAL MODEL TO BE USED IN THE SYSTEMATICS*

2.2.1.1 *Particulars concerning the model*

The rotating electromechanical converter is taken to consist of a stator and a rotor, both constructed from magnetically active material and carrying windings as described in paragraph 1.1, chapter 1. For the definitions regarding synchronous and asynchronous transducers one may also refer to the same paragraph.

To distinguish between different methods of electronic control of electromechanical power conversion in the present chapter, it is necessary to define two basic power electronic units: an "electronic switch" (ES) and an "electronic frequency changer" (EFC). In order to appreciate the differences and similarities between these two units, it is necessary to examine the principle of electronic power flow control by switching action.

The machine-electronic system is mostly fed by a fixed power source as already considered in chapter 1. It is usual for this power source to have a voltage of only fundamental frequency (f_1, or $f = 0$ in the case of a d.v. source). Introduction of the (non-linear) switching element - contained in both ES and EFC - converts the single frequency power into a power spectrum. The use made of all these harmonic power components now determines the character of the power electronic unit.

If it is attempted to arrange the switching action and the internal power circuit structure (for instance electrical and magnetical energy reservoirs) in such a way that the component of the output power used corresponds in frequency to the fundamental input power, the arrangement will be termed an electronic switch. In this configuration it is usually attempted to suppress all other power components as much as is feasible. The function of an ES therefore approaches amplitude and phase adjustment of the output voltage and current, as has been stressed in chapter 1 where periodical switching action was seen as an extension of the concept of circuit parameter variation.

When it is attempted to arrange the switching action and internal power circuit structure to obtain a main output power component differing essentially in frequency from the input power, the arrangement is to be termed an electronic frequency changer. The function of an EFC therefore approaches the conversion of input power at a fixed frequency into output power of a different (variable) frequency. In practice it is mostly found that an electronic frequency changer is built up out of an arrangement of electronic switches and electromagnetic energy reservoirs. In the following considerations it will be assumed that the EFC works between the fixed input frequency f_1 and the variable output frequencies f_r or f_s.

Whether the power circuit arrangement functions as ES or EFC, it is inevitable that the output power will still contain voltages of different frequencies. Sometimes these components may be put to use in the electromechanical energy conversion process, and sometimes they are merely dissipative. To investigate the power flow in the different machine-electronic systems, some ideal characteristics will firstly be ascribed to the EFC and ES in paragraph 2.2. These constraints are then to be relaxed afterwards. The ideal characteristics are:

(a) no generation of harmonics or subharmonics other than the desired frequency,
(b) zero internal impedance,
(c) ideal switching without power loss.

These idealized characteristics are specified when used, and do not apply universally for all the subsequent arguments.

Regarding the configurations used, some further remarks are necessary. An electronic frequency changer (EFC, fig. 2.2a) may be naturally commutated or force commutated, both these functions being indicated with the symbol for the switching element. The specific functions of natural and forced commutation are to be discussed in a later chapter. The same remarks may be applied to an electronic switch (ES, fig. 2.2b). It is stated clearly that the switching element symbol bears no relation to the direction of power flow. To be able to construct a commutator machine in the classical sense in the proposed system it is necessary to interpose a mechanical frequency changer between either the stator and the supply or the rotor and the supply (fig. 2.2e and f). In both cases it is necessary to provide a read-out of the rotor angular position, and feed this information to the frequency changer in order to satisfy the angular speed condition. Classical commutator machines are mostly constructed to have configuration (f), since the mechanical frequency changer may then be coupled to the rotor - the stator containing only the field winding. Technically there are advantages in constructing the electronic counter-part of the commutator machine inversely, i.e. with configuration (e). To obtain uniformity the mechanical variant will also be presented in configuration (e) in this work.

In terms of the model it is also to be understood that two supply lines indicate a d.v. system, while triple feed indicates a balanced multiphase voltage system, the voltage of which may either be simple harmonic functions of time or be of a more complex character. This enables direct and alternating voltage commutator machines to be incorporated symbolically into fig. 2.2 (e) or (f).

2.2.1.2 *Power flow in the model*

Consider the rotating electromechanical converter. Let it be a symmetrical machine connected to a symmetrical supply operating in steady state. Therefore:

$$\frac{dW_{kin}}{dt} = 0 = \frac{dW_{em}}{dt} \qquad 2.2$$

with W_{kin} and W_{em} the mechanical and electrical energy contained in the machine respectively. Consider the power balance for the assumed model as shown in fig. 2.3 (:

$$P^{s}_{in} - P^{s}_{de} + P^{r}_{in} = P^{r}_{de} + P_{em} \qquad 2.3a$$

$$P_{em} = P_{dm} + P_{a} \qquad 2.3b$$

Furthermore taking into account that the mechanical angular speed at which output occurs is identical for all harmonic torques,

$$P^s_{in} - P^s_{de} = P^r_{de} - P^r_{in} + \overline{T}_e.\omega_m \qquad 2.4$$

The currents circulating in the stator are supposed to be of general order μ_s (chapter 1). As indicated in appendix A2.1 these components

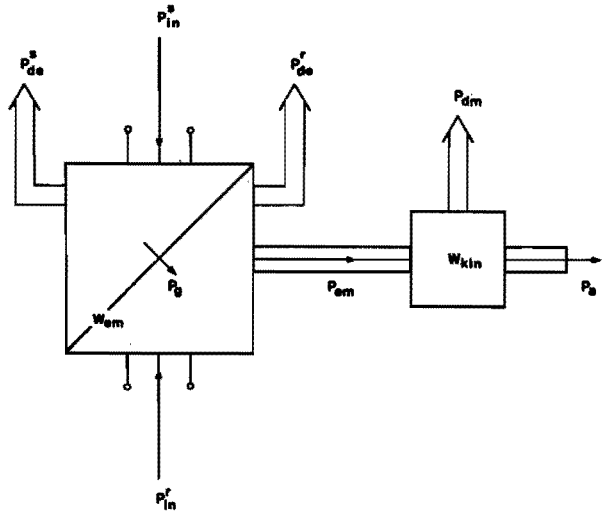

FIG. 2.3 POWER FLOW SCHEME USED IN SYSTEMATIC MODEL.

are divided into components or order ν_s due to the stator excitation and ν_{sr} due to the induction from the rotor. The same considerations apply to division of the rotor harmonics of order μ_r into ν_r and ν_{rs}. Consequently the following components may be discerned for the terms of e.q. 2.4:

$$P^s_{in} = \sum_{\nu_s} P^s_{in(\nu_s)} \quad ; \quad P^r_{in} = \sum_{\nu_r} P^r_{in(\nu_r)}$$

$$P^s_{de} = \sum_{\nu_s,\nu_{sr}} P^s_{de(\nu_s,\nu_{sr})} \quad ; \quad P^r_{de} = \sum_{\nu_r,\nu_{rs}} P^r_{de(\nu_r,\nu_{rs})}$$

$$\overline{T}_e = \sum_{\nu_{sr},\nu_{rs}} \overline{T}_{e(\nu_{sr},\nu_{rs})} + \sum_{\nu_s,\nu_r} \overline{T}_{e(\nu_s,\nu_r)}$$

$$\nu_r,\nu_s \geq 1 \text{ whole}$$

$$\nu_{sr},\nu_{rs} > 0$$

As indicated in appendix A2.1 the torques expected in general from the model studied may be seen as a summation of synchronous torques

$$\overline{T}_{e,(\nu_s,\nu_r)}$$

and asynchronous torques

$$\overline{T}_{e(\nu_{sr},\nu_{rs})}$$

The harmonic asynchronous torques only occur when the stator and rotor excitation by the electronic circuits may not simultaneously be seen as current sources (See fig. 2.5 (a)).

The stator and rotor currents are assumed known. General calculation of these currents for the conditions in the model is to be investigated in a later chapter. If the y^{th} stator phase is fed by a power electronic circuit representing a current source:

$$i^y_s = \sqrt{2} \sum_{\nu_s=1}^{\infty} I^y_{s(\nu_s)} \cos(\nu_s \omega_s t - \psi_{\nu_s}) \qquad 2.5a$$

Similarly for the rotor phase:

$$i^x_r = \sqrt{2} \sum_{\nu_r=1}^{\infty} I^x_{r(\nu_r)} \cos(\nu_r \omega_r t - \psi_{\nu_r}) \qquad 2.5b$$

The general frequency condition has already been mentioned in relation 1.7 for the rotor and stator currents. For the fundamental harmonics in relation to the present model this results in the following angular speed condition

$$\omega_m = \left(\frac{\omega_s}{p} - \frac{\omega_r}{p} \right) \qquad 2.6$$

In chapter 1 it has been stated that the synchronous transducers are always fed on both rotor and stator. For the following discussion the rotor frequency of these transducers will be assumed zero, giving a configuration known in conventional practice as a synchronous machine.

Now consider the general power balance equation 2.4 again. It is indicated in appendix A2.1 that for the assumed model it may be expressed as:

$$\left\{ P^s_{in(1)} - P^s_{de(1)} \right\} + \left\{ \sum_{\nu_s} P^s_{in(\nu_s)} - \sum_{\nu_s,\nu_{sr}} P^s_{de(\nu_s,\nu_{sr})} \right\} =$$

$$\left\{ P^r_{de(1)} - P^r_{in(1)} \right\} + \left\{ \sum_{\nu_r,\nu_{rs}} P^r_{de(\nu_r,\nu_{rs})} - \sum_{\nu_r} P^r_{in(\nu_r)} \right\} +$$

$$\overline{T}_{e(1)} \cdot \omega_m + \left(\sum_{\nu_r \nu_s} \overline{T}_{e(\nu_s,\nu_r)} \right) \omega_m + \left(\sum_{\nu_{rs},\nu_{sr}} \overline{T}_{e(\nu_{rs},\nu_{sr})} \right) \omega_m$$

$$\nu_r, \nu_s > 1$$

$$\nu_{rs}, \nu_{sr} > 0 \qquad 2.7a$$

In principle this power flow equation will now be used to investigate the power flow in the different systems. In the first instance all the harmonic effects will be neglected, and the power flow investigated for the fundamental component.

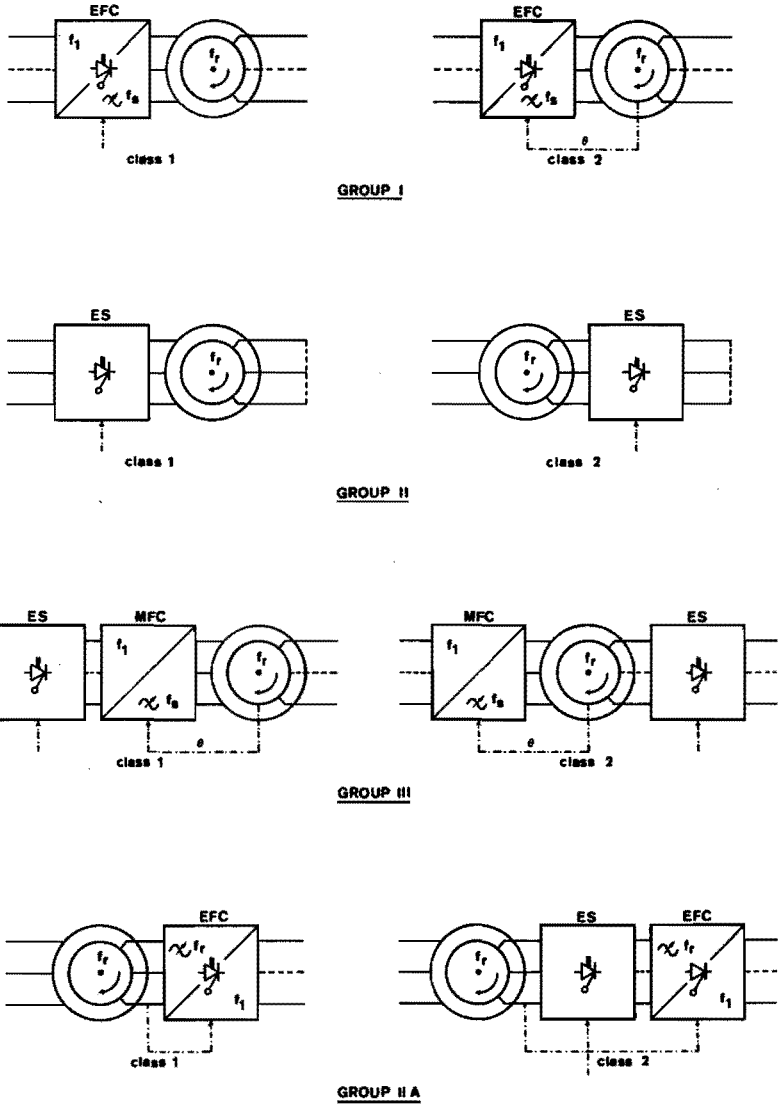

FIG. 2.4 THE FUNDAMENTAL GROUPS OF MACHINE-ELECTRONIC SYSTEMS.

2.2.2 *FUNDAMENTAL POWER FLOW IN THE DIFFERENT SYSTEMS*

When it is assumed that the power flow control is executed in such a way as to eliminate the generation of harmonics, the relations become simply

$$P^s_{in(1)} - P^s_{de(1)} = P^s_{g(1)} = \overline{T}_{e(1)} \cdot \frac{\omega_s}{p} \qquad 2.7b$$

where $P^s_{g(1)}$ is the power flowing across the air gap at the fundamental harmonic frequency. Therefore:

$$P^r_{de(1)} - P^r_{in(1)} = \overline{T}_{e(1)} \cdot \frac{s\omega_s}{p} \qquad 2.7c$$

with

$$s = \frac{\frac{\omega_s}{p} - \omega_m}{\frac{\omega_s}{p}} = \frac{\omega_r}{\omega_s}$$

Fig. 2.4 indicates the fundamental groups of machine-electronic systems that may be distinguished. Considerations will now be given to the characteristics and fundamental power flow:

GROUP I SYSTEMS may be characterised by an electronic frequency changer between the electrical ports on either the rotor or the stator and the fixed power supply system for these ports. In general the remaining electrical ports may either be connected to a constant power supply system, or have a short circuit applied across them. It will be assumed that the EFC will be located on the stator side. Two families of variants exist: class 1 and class 2. The difference between these two classes is that in the latter the rotor position is coupled to the EFC, determining the frequency and phase relationship of the stator voltage explicity by the mechanical speed and rotor position respectively, while in the former the EFC receives an external command. In this case the frequency and phase relationship of the stator voltage may be determined by other considerations than the instantaneous rotor speed and position. Reference to Group I systems may be made as "variable frequency control", but it is more accurate to observe the definition of chapter I: This definition says that the speed of rotation of the fundamental harmonic component of the air gap magnetic field is controlled. The voltage of the EFC is mostly controlled to keep the magnetic field constant, resulting in a constant torque.

Examine the power flow in a *synchronous converter* ($f_r = 0$) operating at speed ω_{mn}, irrespective of its class (1 or 2). Let the load torque be constant (fig. 2.5b), and the frequency changer ideal

$$\overline{T}_{e(1)n} \cdot \frac{\omega_{sn}}{p} = \overline{T}_{e(1)n} \cdot \omega_{mn} \qquad 2.8a$$

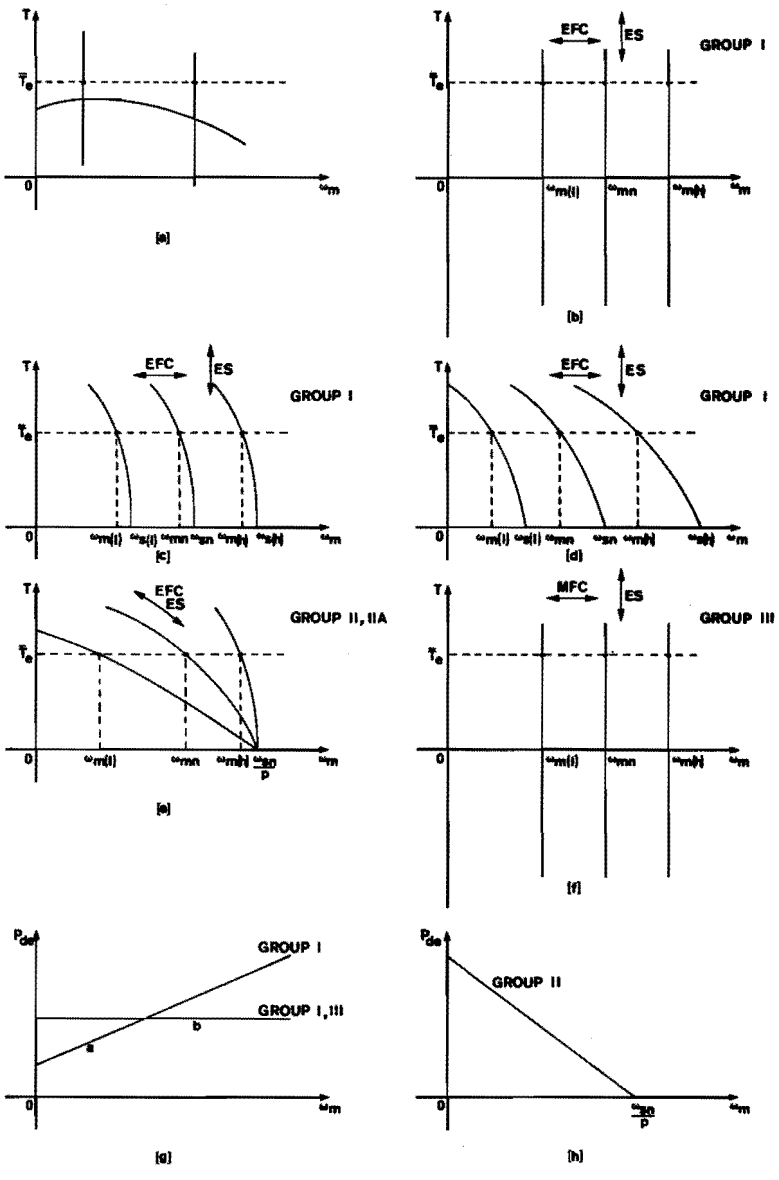

FIG. 2.5 CHARACTERISTICS OF THE DIFFERENT GROUPS OF MACHINE-ELECTRONIC SYSTEMS.

Recuding speed by a factor q

$$\omega_m = \frac{\omega_{mn}}{q} = \frac{\omega_{sn}}{pq} \qquad 2.8b$$

it is evident that the losses should remain constant (fig. 2.5g)

$$p^r_{de(1)} - p^r_{in(1)} = 0 \qquad 2.8c$$

while relation 2.7c indicates that the rotor source only supplies the (constant) excitation dissipation loss. Since the synchronous air gap power is equal to the electromechanical output power the input power is reduced by the same factor as the output power. The same considerations apply for a speed increase. As may be seen from fig. 2.5b there are two modes of power control in this situation. The frequency change of the EFC causes a horizontal translation, but by electronic switching action it is also possible to abtain a vertical shift of the point of operation by expansion of maximum torques in the torque-power-angle diagram.

Next examine the power flow in an *asynchronous converter* operating at speed ω_{mn}, irrespective of its class. Let the load torque be constant (fig. 2.5c and d), and the rotor be short circuited.

$$\left.\begin{aligned} \overline{T}_{e(1)n}\,\frac{\omega_{sn}}{p} &= \overline{T}_{e(1)n}\,\frac{s_n\omega_{sn}}{p} + \overline{T}_{e(1)n}\omega_{mn} \\ \text{and} \qquad p^r_{de(1)} &= \overline{T}_{e(1)n}\,\frac{s_n\omega_{sn}}{p} \end{aligned}\right\} \qquad 2.8d$$

Reduce mechanical speed by a factor q (relation 2.8b). Two cases are to be distinguished, depending on whether the *slip frequency* or the *slip* be taken constant. In the first instance:

$$\left.\begin{aligned} s_n\omega_{sn} &= \text{constant} \\ \omega_s &= \frac{\omega_{sn}}{q} + \omega_{rn}\left(\frac{q-1}{q}\right) = \left(\frac{\omega_{sn}}{q} + \Delta\omega_s\right) \end{aligned}\right\} \qquad 2.8e$$

(see fig. 2.5c), and the second instance:

$$\omega_s = \frac{\omega_{sn}}{q}, \quad s_n = \text{constant} = \frac{\omega_{rn}}{\omega_{sn}} \qquad 2.8f$$

(see fig. 2.5d). Therefore the two relations describing the power flow become:

constant slip frequency:

$$\overline{T}_{e(1)n}\left\{\frac{\omega_{sn}}{qp}+\frac{\Delta\omega_s}{p}\right\}=\overline{T}_{e(1)n}\frac{s_n\omega_{sn}}{p}+\frac{1}{q}\overline{T}_{e(1)n}\cdot\omega_{mn} \qquad 2.8g$$

constant slip:

$$\frac{1}{q}\overline{T}_{e(1)n}\cdot\frac{\omega_{sn}}{p}=\frac{1}{q}\overline{T}_{e(1)n}\cdot\frac{s_n\omega_{sn}}{p}+\overline{T}_{e(1)n}\frac{1}{q}\cdot\omega_{mn} \qquad 2.8h$$

An examination of these last two relations indicates that the first type of system operates at constant rotor loss with decrease of mechanical output. The second type of system has a decreasing rotor loss with decreasing mechanical speed. In the former instance the EFC does not reduce the fundamental synchronous air gap power directly proportional to the reduction in output power, while this direct proportionality exists in the latter instance. Conversely it may be remarked that when the mechanical output power is increased (fig. 2.5c, d) the dissipation loss remains constant in the first, but increases in the second case. These loss characteristics are represented by curve b and curve a of fig. 2.5g respectively. As in the case of the synchronous transducer it is also possible to obtain an increased torque at a specific speed by increasing the magnetic field in the air gap by electronic switching action.

In summary, one notices that in all the electromechanical power converters employed in Group I systems, the EFC changes the synchronous power flow across the air gap in the same sense as the change in output power. Dependence of the dissipative power loss on the speed is a function of the constraint applied to the rotor frequency, but the power loss never increases with decreasing speed. The torque-speed curve is mainly subjected to a horizontal translation due to the action of the EFC (fig. 2.5b, c, d).

GROUP II SYSTEMS may be characterised by an electronic switch inserted between the electrical ports on either rotor or stator and the electrical supply system, as indicated in fig. 2.4. In group I systems no essential difference was made between inclusion of the power-electronic switch in rotor or stator, but in group II systems this difference is essential. Although these systems operate with a switching circuit, it is assumed that the fundamental stator, respectively rotor, frequency remains constant, while the slip is variable.

Asynchronous operation of the electromechanical converter necessitates a variable frequency rotor supply. This is a complication, and it will be assumed that in group II systems the rotor electrical ports have a short circuit applied across them when the ES is in the stator, (class 1) or that the rotor supply input terminals have a short circuit

applied across them when the ES is located in the rotor (class 2).

During operation at a mechanical speed ω_{mn} relation 2.8d describes the power balance. At present no difference will be made between the effects that rotor or stator control have on the torque speed characteristics (fig. 2.5e). It will be assumed that the control by the power switch is executed in such a way that no harmonics are introduced into rotor or stator. Let the mechanical speed now be reduced by the factor q

$$\overline{T}_{e(1)n} \cdot \frac{\omega_{sn}}{p} = \overline{T}_{e(1)n} \cdot \frac{s.\omega_{sn}}{p} + \overline{T}_{e(1)n} \frac{\omega_{mn}}{q} \qquad 2.9a$$

with

$$P^{r}_{de(1)} = \frac{s.\omega_{sn}}{p} \cdot \overline{T}_{e(1)n} \qquad 2.9b$$

and

$$s = \frac{s_n + \overline{q - 1}}{q} \qquad 2.9c$$

An examination of these relations indicates that the electrical power dissipation in the rotor will increase linearly with decreasing speed as depicted in fig. 2.5h. The power electronic switching circuit does not adjust the synchronous fundamental power flow across the air gap when the mechanical output is reduced, but merely causes a change in the torque-speed relation for constant stator frequency. The torque-speed curve "rotates" around the point of synchronous operation of the fundamental machine in the torque-speed plane.

GROUP III SYSTEMS may be characterised by an electronic switch operated in conjunction with a mechanical frequency changer (fig. 2.4). Two different approaches are possible: the power switch may be connected in series with the mechanical frequency changer (MFC) in the stator, or it may be interposed between the power supply system to the rotor and the electrical ports on the rotor. The group of electromechanical converters with MFC - known in conventional practice as commutator machines- may be supplied with either d.v. or a.v. to rotor and stator.

Relations 2.8a and 2.8c describes power flow in case of a change of mechanical speed. As may be deduced from fig. 2.5f the change of power flow concerned with this action is the responsibility of the MFC. The fact that the rotor supply consequently only covers the rotor loss is the reason that this supply is termed "field-supply", and the associated control by ES: field control (Group III, class 2). As may be seen by inspection of fig. 2.7, Group III systems are at present in practice exclusively operated with direct voltage excitation of the rotor and direct voltage input to the MFC. The electromechanical converter is never operated in the asynchronous mode.

Again with reference to relation 2.8a the effect of the electronic switching

in class 1 or class 2 will be examined. These relations will be valid when it is assumed that the mechanical frequency changer is ideal to such an extent that the switching harmonics introduced by the electronic switch at its input do not influence its output. In practice this will mostly not be the case, so that one may expect a continuously changing harmonic power balnce resulting from the beat frequencies of the ES and the MFC. This effect will be neglected for the present. It will furthermore be assumed that the MFC is ideal. The effect of the switching on the power flow then reduces to a decrease of the amplitude of the fundamental supply. No control is exerted on the MFC. This should alter the flux-linkage conditions in the machine in such a way that the fundamental torque is reduced. Inclusion of the ES in the rotor circuit will have the same effect. According to 2.8c the rotor power loss will also decrease in this case. For a constant load torque $\bar{T}_e$ as in fig. 2.5f the loss characteristics of fig. 2.5g curve (b) applies.

In summary it may be concluded that in Group III machine-electronic systems power flow is controlled by changing the magnitude of the fundamental air gap torque by a power electronic switching circuit on either rotor or stator. The possibility of variable speed operation is due to the inclusion of a mechanical frequency changer in the system. If the variable speed operation is not desired, the frequency changer may be omitted.

2.2.3 *A CLASSIFICATION FOR MACHINE-ELECTRONIC SYSTEMS: A SUMMARY OF THE PREVIOUS PARAGRAPHS*

In the previous paragraph the power flow conditions in the transducers have been examined, and it became evident that the power flow of the fundamental harmonic component is not subjected to the same effects in the different groups of systems. In all the forementioned cases the function of the power-electronics was then defined according to the influence on the fundamental power flow in an ideal situation. This results in the following definitions:

GROUP I MACHINE-ELECTRONIC SYSTEMS are those systems in which the power flow across the air gap of the electromechanical converter at a constant load torque is controlled by changing the velocity of rotation of the fundamental air gap field by means of an EFC. Due to this characteristic of the system it is capable of delivering this torque at different mechanical speeds with either constant electrical power loss or power loss increasing with speed, depending on whether constant slip frequency of constant slip is observed. The magnitude of the electromagnetic torque in the machine may also be influenced by switching action in the EFC. Group I machine-electronic systems may be divided into class 1 and class 2 systems. In the former, frequency of the output voltage of the EFC is determined by external requirements (externally directed systems) and in the latter the frequency and the phase of the output voltage of the EFC is determined by rotor speed and position (self-directed systems). All these systems may in principle use either synchronous or asynchronous electromechanical converters.

GROUP II MACHINE-ELECTRONIC SYSTEMS are those systems in which the power flow across the air gap of the electromechanical converter at constant load torque is not affected by the power-electronics for the

fundamental harmonic. The control of output power is obtained by the modification of the torque-speed relationship as a result of the presence of the ES to such an extent that the electromechanical converter operates at variable slip with constant stator frequency. The constant fundamental power flow across the air gap implies that this system is unable to deliver the same mechanical torque at various mechanical speeds with the same electrical power loss during conversion. The power loss increases with decreasing speed (increasing slip). Group II machine electronic systems may be divided into class 1 and class 2 systems. In the former the electronic switch acts on the stator windings, and in the latter on the rotor windings. Variable slip neccessitates the use of asynchronous electromechanical converters in these systems.

GROUP III MACHINE-ELECTRONIC SYSTEMS are systems with power flow control by alteration of the magnitude of the fundamental component of the electromagnetic torque with an electronic switch. In order to operate at variable speed the system contains a self-directed mechanical frequency changer to adapt the velocity of rotation of the fundamental field component in the air gap to the mechanical speed. The system is therefore in principle capable of operating at a constant power loss with variable speed and constant load torque. Whereas both the functions of changing the magnitude of the air gap torque and the velocity of rotation was concentrated in the EFC in Group I systems, these functions are respectively fulfilled by the ES and the MFC in Group III systems. Group III machine-electronic systems may be subdivided into class 1 and class 2 systems. In the former the ES is located in series with the MFC in the stator, and in the latter the ES is introduced between the rotor windings and rotor supply. When no variable speed operation is desired, but merely a control of power flow by variation of the magnitude of the fundamental electromagnetic torque, the MFC may be omitted in either case.

2.2.4 *SOME HYBRID SYSTEMS*

With reference to the groups of systems depicted in fig. 2.4, and discussed in the previous paragraphs, possibilities for some hybrid systems now present themselves.

During discussion of Group II machine-electronic systems it was obvious that the systems have increasing loss with decreasing speed (fig. 2.5h). If an EFC of Group I systems is now introduced between the rotor and the supply of Group II, class 1 systems, or between the rotor ES and the supply of class 2 systems, a possibility arises of feeding some of the asynchronous rotor power to the supply. It proves possible to control the power flow sufficiently by the EFC in the rotor, so that the ES in either rotor or stator becomes unnecessary. There are reasons for retaining the ES in series with the EFC in some systems, although these reasons do not concern power flow considerations, but considerations such as power factor and system response time. As these considerations are not included in the present chapter, note is only to be taken of the existence of these systems.

This leads to the hybrid *GROUP IIA MACHINE-ELECTRONIC SYSTEMS* of fig. 2.4. Class 1 systems are derived from Group II class 1 or 2 by the said elimination of the electronic switches, and class 2 systems still retain the ES for reasons subsequently to become clear.

Examine the power flow in Group IIA hybrid systems: Let the load

torque be constant (fig. 2.5e). Concerning power flow the two variants, class 1 and class 2, will be identical. The power switches and frequency changers are assumed to be ideal, generating no harmonics other than the fundamental and having no dissipative power loss. Power flow is described by relation 2.8d. Let the speed be decreased by a factor q according to 2.8b. Relation 2.9a now describes the power flow, with:

$$P^{r}_{de(1)} = P^{r}_{in(1)} + \overline{T}_{e(1)} \cdot \frac{s.\omega_{sn}}{p} \qquad 2.10$$

If the EFC is now arranged to absorb power from the rotor the possibility arises to modify the loss characteristics as a function of speed (fig. 2.5)

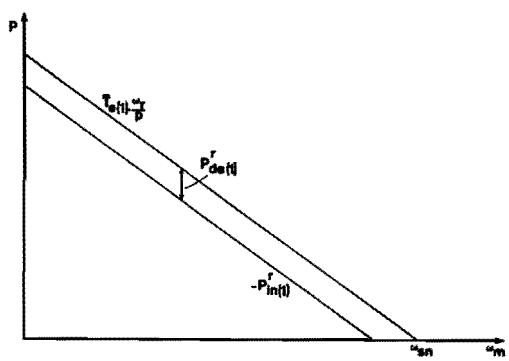

FIG. 2.5i LOSS CHARACTERISTICS FOR HYBRID GROUP IIA MACHINE-ELECTRONIC SYSTEMS.

The electromechanical converter still operates in an asynchronous mode, for the power flow across the air gap is still occuring due to induction effects (see definition, chapter 1). It is to be noted that although an EFC is employed, systems of Group IIA differs from Group I regarding the influence of the power electronic circuit on the power flow. In Group IIA systems it is employed to feed back the excess rotor power whereas it is employed to adapt the air gap power in Group I. Since a high efficiency is usually desired, it will be attempted to keep the rotor dissipation as low and constant as possible over the speed range.

A brief remark on a possibility of a hybrid system in Group III concerns simultaneous stator and rotor control by an ES. In fig. 2.4 it

may be seen that the ES either controls the power flow in the main path or to the field. If the field supply is taken from the main power supply, between the ES and the MFC, a new hybrid system results, with the said simultaneous control (fig. 2.6a).

As an illustration of all the further hybrid systems that may be constructed from the systematics discussed, the system of fig. 2.6b may be taken. Main power flow control is achieved by the EFC, while vernier adjustment of speed is possible by an ES in the rotor, thus obtaining a *hybrid system Group I-II*, class 1-1. There are many more possibilities for constructing hybrid systems, but seeing that these systems have not been investigated during the course of this study, and may not yet be encountered in practice, this discussion will not be extended.

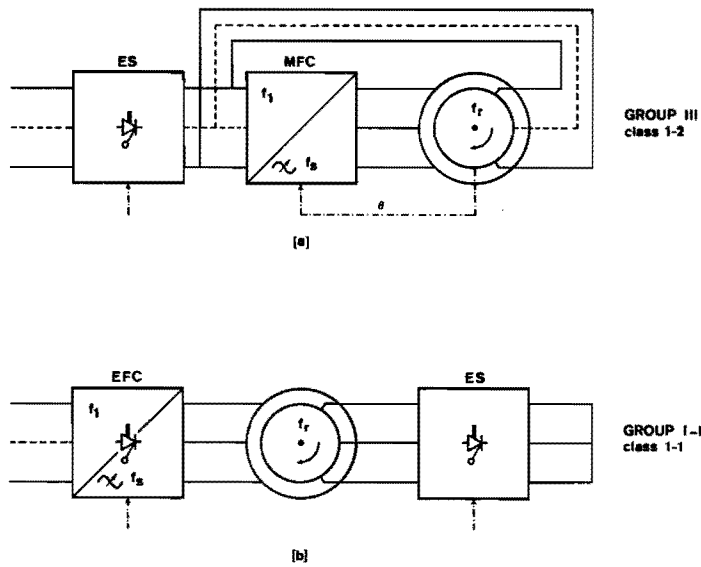

FIG. 2.6 ILLUSTRATION OF SOME HYBRID MACHINE-ELECTRONIC SYSTEMS DERIVED FROM THE FUNDAMENTAL SYSTEMS.

2.3 A MORE DETAILED INVESTIGATION OF POWER FLOW IN THE MACHINE-ELECTRONIC SYSTEMS

The power flow equation 2.7a contains information concerning the harmonic components. Although these components have been neglected in the previous paragraph in order to state the control principles, practical machine-electronic systems are influenced by their presence to such an extent that it is necessary to take their influence into

account. This will be done in subsequent chapters. Power flow considerations will be necessary to develop some aspects of the theory and will therefore be examined in more detail in the following paragraphs. During these investigations the power electronics will be taken to operate with negligible dissipative power loss. As these systems are all used in variable speed drives, the power flow will be investigated for a change in speed represented by reducing the mechanical speed by a factor q as beore. Conditions prior to this speed change will be referred to as nominal (n), in agreement with the previous paragraphs.

2.3.1 *POWER FLOW CONSIDERATIONS FOR GROUP I SYSTEMS, CLASS 1 AND 2*

If the EFC is not taken to be ideal, the stator supply contains harmonics. Firstly assume the rotor to be excited by a *direct voltage ($f_r = 0$) source* having zero impedance for harmonic currents. The fundamental torque is *synchronous* in nature; the harmonic torques are *asynchronous* since the stator current source contains harmonics of order ν_s. As indicated in appendix A2.1 the power flow becomes:

$$\overline{T}_{e(1)n} \cdot \frac{\omega_{sn}}{p} + \sum_{\nu_s} \overline{T}_{e(\nu_{rs})n} \frac{(-1)^{c_{s\nu_s}} \omega_{sn}}{p} =$$

$$\overline{T}_{e(1)n} \cdot \omega_{mn} + \sum_{\nu_{rs}} \overline{T}_{e(\nu_{rs})n} \frac{s_{\nu rsn} (-1)^{c_{s\nu_s}} \omega_{sn}}{p}$$

$$+ \left(\sum_{\nu_{rs}} \overline{T}_{e(\nu_{rs})n} \right) \cdot \omega_{mn} \qquad 2.11a$$

Reduction of the mechanical speed by a factor q - according to relation 2.8b - does not alter the harmonic slip $s_{\nu rs}$ of the currents induced into the rotor by the stator magnetic field (see equation A2.8f). The power balance consequently becomes:

$$\frac{1}{q} \overline{T}_{e(1)} \cdot \frac{\omega_{sn}}{p} + \frac{1}{q} \sum_{\nu_s} \overline{T}_{e(\nu_{rs})} \frac{(-1)^{c_{s\nu_s}} \omega_{sn}}{p} =$$

$$\frac{1}{q} \overline{T}_{e(1)} \cdot \omega_{mn} + \frac{1}{q} \sum_{\nu_s} T_{e(\nu_{rs})} \frac{s_{\nu rs} (-1)^{c_{s\nu_s}} \omega_{sn}}{p}$$

$$+\frac{1}{q}\cdot\sum_{\nu_{rs}}\overline{T}_{e(\nu_{rs})} \qquad 2.11b$$

It is evident that the fundamental power flow is reduced by the reduction factor of the speed when the fundamental torque is constant, as already seen previously.

Relation A2.8f indicates that in the present case it is always valid that

$$s_{\nu rs} > 0 \qquad 2.11c$$

For the following discussion it will furthermore be considered that the converter operates in the region appreciably removed from the locked rotor point. In general the harmonic asynchronous torques may be either positive or negative. The stator is fed by a current source, and consequently the maximum harmonic torques will be constant. Although the harmonic slip now remains constant with a change in fundamental harmonic speed, or equivalently with a change in mechanical speed, the harmonic torques may still be subject to change, since the rotor harmonic frequencies will be subjected to change. The expression for the harmonic slip indicates that for the range of operation specified by 2.11c and 2.11d, the harmonic slip approaches unity for the higher harmonics, so that it may be expected that the harmonic torques do not change appreciably, and at least not by an order of magnitude.

If the argument is accepted that in this way the sum of the harmonic torques remains approximately constant, it may be concluded that for these systems the harmonic power output also changes approximately proportional to the change in mechanical speed. It is to be noted that it cannot be predicted whether the individual synchronous harmonic powers and the individual harmonic power losses will increase or decrease with the change in mechanical speed, as it depends on the direction of rotation of the harmonic fields in the air gap, and consequently on the number of machine phases and the order of the harmonic.

When the rotor of the converter *has no external supply, but a short circuit* is applied across the rotor electrical ports, the power relation 2.7a becomes (see appendix A2.1)(induction machine):

$$\overline{T}_{e(1)n}\cdot\frac{\omega_{sn}}{p}+\sum_{\nu_s}\overline{T}_{e(\nu_{rs})n}\frac{(-1)^{c_{s_\nu}}\omega_{s\,sn}}{p}=$$

$$\overline{T}_{e(1)n}\cdot\frac{s_n\omega_{sn}}{p}+\overline{T}_{e(1)n}\cdot\omega_{mn}$$

$$+ \sum_{\nu_s} \bar{T}_{e(\nu_{rs})n} \frac{s_{\nu rsn}(-1)^{c s_{\nu_s}} \omega_{sn}}{p} +$$

$$\left(\sum_{\nu_{rs}} \bar{T}_{e(\nu_{rs})n} \right) \cdot \omega_{mn} \qquad 2.12a$$

where the fundamental torque is now *asynchronous* in nature. In 2.8e and 2.8f it is stated that the reduction in mechanical speed by a factor q results in different conditions for constant slip frequency control and constant slip control. In the first instance the harmonic slip at ω_m becomes:

$$s_{\nu rs} = s_{\nu rsn} + \Delta s_{\nu rs}$$

for

$$\frac{q\Delta\omega_s}{\omega_{sn}} << 1 : \quad \Delta s_{\nu rs} \simeq \left\{ \frac{q.\Delta\omega_s}{(-1)^{c s_{\nu_s}} \omega_{sn}} \cdot \frac{p\omega_{mn}}{\omega_{sn}} \right\} \qquad 2.12b$$

with

$$\Delta\omega_s = \omega_{rn} \left(\frac{q-1}{q}\right)$$

In the second instance the harmonic slip (rel. A2.8f) $s_{\nu rs}$ remains constant and the fundamental frequency is reduced by the speed reduction factor. For the power flow under the different conditions the following power balances may be set up.

Constant slip frequency:

$$\bar{T}_{e(1)} \left\{ \frac{\omega_{sn}}{qp} + \frac{\Delta\omega_s}{p} \right\} + \sum_{\nu_s} \bar{T}_{e(\nu_{rs})} (-1)^{c s_{\nu_s}} \left\{ \frac{\omega_{sn}}{qp} + \frac{\Delta\omega_s}{p} \right\} = \bar{T}_{e(1)} \cdot \frac{s_n \omega_{sn}}{p} +$$

$$\bar{T}_{e(1)} \cdot \frac{\omega_{mn}}{q} + \sum_{\nu_s} \bar{T}_{e(\nu_{rs})} \cdot s_{\nu rs} (-1)^{c s_{\nu_s}} \left\{ \frac{\omega_{sn}}{qp} + \frac{\Delta\omega_s}{p} \right\} + \sum_{\nu_{rs}} \bar{T}_{e(\nu_{rs})} \frac{\omega_{mn}}{q} \qquad 2.12c$$

constant slip:

$$\frac{1}{q}\,T_{e(1)}\cdot\frac{\omega_{sn}}{p}+\frac{1}{q}\sum_{\nu_s}\overline{T}_{e(\nu_{rs})}\,(-1)^{c_s}\cdot\frac{\nu_s\omega_{sn}}{p}=\frac{1}{q}\,\overline{T}_{e(1)}\cdot\frac{s_n\omega_{sn}}{p}+$$

$$\frac{1}{q}\,\overline{T}_{e(1)}\cdot\omega_{mn}+\frac{1}{q}\sum_{\nu_s}\overline{T}_{e(\nu_{rs})}\,\frac{s_{\nu rsn}(-1)^{c_s}\nu_s\omega_{sn}}{p}+\sum_{\nu_{rs}}\overline{T}_{e(\nu_{rs})}\,\frac{\omega_{mn}}{q}\qquad 2.12d$$

Equation 2.12c indicates that when the conditions for a constant fundamental torque are fulfilled, fundamental input power decreases less than fundamental output power due to the constant fundamental rotor loss. When the slip is constant, the input power, rotor loss and output power for the fundamental frequency decrease by the same factor. Operation for both cases is assumed to be in the motoring/ dissipator region.

$$s > 0 \qquad 2.12e$$

The harmonic mechanical output power in 2.12c and 2.12d decreases with the same factor as the fundamental output power when the harmonic torques may be assumed constant and the locked rotor point is not approached. In practice these torques will not be absolutely constant, but since the harmonic slip approaches unity, these torques should not change appreciably. Corresponding to the situation in the controlled synchronous transducer, whether the individual harmonic power inputs and power losses increases or decreases agian depends on the number of phasesand order of the harmonics. These powers will change by the factor of speed reduction only in the case of control with constant slip.

2.3.2 *POWER FLOW CONSIDERATIONS FOR GROUP II SYSTEMS, CLASS 1 AND 2*

It may be expected that the assumption of negligible harmonics in the stator supply or the rotor supply during electronic switching is unrealistic. A considerable difference in harmonic power flow between class 1 and class 2 systems is found. This in contrary to the assumption of paragraph 2.2.2 that the stator and rotor switching affects the torque - speed characteristics indentically. Class 1 and class 2 systems will now be examined in succession.

Consider a *system of Group II, class 1* operating at constant angular speed ω_{mn}. The power flow is described by a relation similar to 2.12a. Let the mechanical speed be reduced by a factor q as previously. The balance becomes:

$$\overline{T}_{e(1)}\cdot\frac{\omega_{sn}}{p}+\sum_{\nu_s}\overline{T}_{e(\nu_{rs})}\,\frac{(-1)^{c_s}\nu_s\omega_{sn}}{p}=$$

$$\overline{T}_{e(1)} \cdot \frac{s\omega_{sn}}{p} + \overline{T}_{e(1)} \cdot \frac{\omega_{mn}}{q}$$

$$+ \sum_{\nu_s} \overline{T}_{e(\nu_{rs})} \cdot s_{\nu rs} \quad \frac{(-1)^{c_{s_{\nu_s}}} \omega_{sn}}{p}$$

$$+ \sum_{\nu_{rs}} \overline{T}_{e(\nu_{rs})} \quad \frac{\omega_{mn}}{q} \qquad 2.13a$$

with

$$s_{\nu rs} = s_{\nu rsn} + \frac{\overline{q-1}\, p\omega_{mn}}{q(-1)^{c_{s_{\nu_s}}} \omega_{sn}} \qquad 2.13b$$

Let the operation of the converter be in the region

$$0 < \omega_m < \frac{\omega_{sn}}{p} \quad \text{or} \quad 1 < s < 0$$

It is assumed that operation occurs at constant load torque:

$$\left(\overline{T}_{e(1)} + \sum_{\nu_{rs}} \overline{T}_{e(\nu_{rs})}\right) = \left(\overline{T}_{e(1)n} + \sum_{\nu_{rs}} \overline{T}_{e(\nu_{rs})n}\right) \qquad 2.13c$$

The synchronous speeds of fundamental and harmonic rotating magnetic fields in the air gap of the machine do not change, being respectively

$$\omega_{m(1)}^{syn} = \frac{\omega_{sn}}{p}$$

and

$$\omega_{m\nu rs}^{syn} = \frac{(-1)^{c_{s_{\nu_s}}} \omega_{sn}}{p} \qquad 2.13c$$

The last expression corresponds with fundamental slip

$$s_o^{\nu rs} = 1 - (-1)^{c_{s_{\nu_s}}}$$

In the case op Group I systems the approximation was used that the higher harmonic slips approach unity. The same approximation will be used in the present case. From 2.13b it may be seen that for the higher harmonics the contribution of the change in mechanical speed to the change in harmonic slip becomes negligible.

In order to comment on the change in mechanical output powers and power losses the individual torque components should be considered. In the next paragraph, where a review of machine-electronic systems will be presented, it will become evident that in some systems of Group II, class 1, current control is incorporated and as such the harmonic frequency spectrum of the stator current may be assumed constant for a constant value of the control parameter over the speed range. Since a change in speed will normally entail a change in control parameter, it cannnot be stated that the harmonic frequency spectrum will remain constant with a change in speed. When no current control is used, the change in harmonic content for a constant control parameter with speed defies general description, so that for the speed change at constant torque operation no general conclusion can be reached.

When some restrictions corresponding to practical situations are applied, it is still possible to reach some conclusions regarding the power flow. The system will be mostly designed so that the contributions of the fundamental torque (2.13c) to the output torque is an order of magnitude larger than the contribution of the harmonic torques. The change of the contribution of the harmonic torques is now restricted by the fact that the harmonic slip approaches unity, and is subjected to a neglegible change by the change in speed when one applies the same considerations as has been applied in the case of systems of Group I in this respect. The change in harmonic dissipation will consequently also be small.

The fundamental slip 2.9c is subject to a much larger change, and as the fundamental synchronous speed remains constant, relation 2.13a indicates that the dissipation in the rotor increases linearly with decreasing speed at (approximately) constant fundamental torque. The constant harmonic synchronous speeds (2.13d) also results in approximately constant total harmonic input power.

As before no general indication can be given as to the decrease or increase of the individual harmonic input powers, power losses and output powers with the change in speed, as the direction of rotation and action of torques are dependent on harmonic order and number of machine phases.

Let the power flow in a transducer in a system of *Group II, class 2* now be investigated. The ES is in the rotor circuit, and therefore the rotor current may be taken to contain harmonics of order ν_r. By combining the relations A2.10e and A2.10g derived in appendix A2.1, the power flow equation in this case may be written for nominal operation at speed ω_{mn} as:

$$\overline{T}_{e(1)n}\cdot\frac{\omega_{sn}}{p}+\sum_{\nu_r}\overline{T}_{e(\nu_{sr})n}\cdot\frac{(-1)^{\overline{c_r+1}}\,\nu_r\cdot s_n\omega_{sn}}{p}=\overline{T}_{e(1)n}\cdot\frac{s_n\cdot\omega_{sn}}{p}+$$

$$+ \overline{T}_{e(1)n} \cdot \omega_{mn} + \sum_{\nu_r} \overline{T}_{e(\nu_{sr})n} \cdot \frac{(-1)^{\overline{c_r+1}} \nu_r s_n \omega_{sn}}{p} +$$

$$+ \left(\sum_{\nu_{sr}} \overline{T}_{e(\nu_{sr})n} \right) \omega_{mn} \qquad 2.14a$$

Again assuming that the mechanical speed is changed according to 2.8b, the new situation is described by:

$$\overline{T}_{e(1)} \cdot \frac{\omega_{sn}}{p} + \sum_{\nu_r} \overline{T}_{e(\nu_{sr})} \frac{(-1)^{\overline{c_r+1}} \nu_r \cdot s\omega_{sn}}{p} = \overline{T}_{e(1)} \cdot \frac{s\omega_{sn}}{p} +$$

$$+ \overline{T}_{e(1)} \cdot \frac{\omega_{mn}}{q} + \sum_{\nu_r} \overline{T}_{e(\nu_{sr})} \cdot s_{\nu sr} \cdot \frac{(-1)^{\overline{c_r+1}} \nu_r s\omega_{sn}}{p} +$$

$$+ \left(\sum_{\nu_{sr}} \overline{T}_{e(\nu_{sr})} \right) \frac{\omega_{mn}}{q} \qquad 2.14b$$

In fig. 2.5e operation at constant torque has been taken as normative for the investigations, Therefore

$$\left(\overline{T}_{e(1)} + \sum_{\nu_{sr}} \overline{T}_{e(\nu_{sr})} \right) = \left(\overline{T}_{e(1)n} + \sum_{\nu_{sr}} \overline{T}_{e(\nu_{sr})n} \right) \qquad 2.14c$$

The general situation now differs from the situation with stator switching with respect to the synchronous speed of the harmonic fields arising due to the rotor switching. With stator harmonics or order ν_s it was possible to establish that the harmonic synchronous speed does not fall into the region $0 < s < 1$. The harmonic synchronous speed in the present case is (see relation A2.10b):

$$\omega_{m\nu sr}^{syn} = \frac{(-1)^{\overline{c_r+1}}\,\nu_r s\omega_{sn}}{p} \qquad 2.14d$$

This corresponds with a certain mechanical speed of the fundamental machine. At this mechanical speed the fundamental slip is:

$$s_o^{\nu sr} = \frac{1}{1-(-1)^{c_r}.\nu_r} \qquad 2.14e$$

This indicates that the region where the harmonic asynchronous torques will pass through their synchronous speed may be characterised by the following ranges for the fundamental slip, with the harmonic magnetic fields rotating with ($c_r = 2$) or against ($c_r = 1$) the direction of rotation of the fundamental rotor field:

$$\left.\begin{aligned} c_r = 2, \quad 1 < \nu_r < \infty \;:\; -1 < s_o^{\nu sr} < 0 \\ c_r = 1, \quad 1 < \nu_r < \infty \;:\; 0.5 < s_o^{\nu sr} < 0 \end{aligned}\right\} \qquad 2.14f$$

It may therefore be expected that some of the harmonic induced currents will have a synchronous speed in the motoring region of the fundamental machine. It may then be estimated that there is a probability that the harmonic torques change by an order of magnitude with a change in speed, in contrast to what has been experienced in previous cases.

The fundamental slip s at low speed still follows from 2.9c, but the harmonic slip is described by:

$$s_{\nu sr} = s_{\nu srn} + \frac{\omega_{mn}.p}{(-1)^{c_r}\nu_r s_n \omega_{sn}} \left(\frac{s_n - qs}{qs}\right) \qquad 2.14g$$

Similar to class 1 systems of Group II the fundamental power loss in the rotor will increase with a decrease in speed. If the fundamental torque component may be assumed constant this increase will be linear and the synchronous power flow across the air gap may be taken as constant for this component. Examination of the terms representing the synchronous power flow for the harmonic components indicates that this does not hold for these components, as the "synchronous speed" for these components continuously changes.

It may therefore be concluded that no general statement concerning the harmonic power flow can be made with the conditions known at present.

This problem is investigated further for a simplified model in appendix A2.1.5, while attention is also devoted to the case where the rotor electrical ports are connected to a voltage supply of rotor frequency. These problems will again receive attention in subsequent chapters.

2.3.3 *POWER FLOW CONSIDERATIONS FOR GROUP III SYSTEMS, CLASS 1 AND 2*

As pointed out in paragraph 2.2, the electromechanical transducer in these systems operates conventionally as a synchronous machine ($f_r = 0$). As such the MFC may not be considered to be ideal, and equation 2.11a, with the successive considerations, applies to these systems when the MFC is fed from a well-filtered source of direct voltage. It is worthwhile to point out some problems that may arise in these systems, but due to the limitations in the scope of the present work they will not be treated here.

When the ES in series with the MFC gives rise to harmonic currents of arbitrary order, it may be expected that the harmonic currents arising due to the interaction of the two switches, and having beat frequencies of f_{ES} and f_{MFC}, may in general give rise to synchronous and asynchronous torques (appendix A2.1, relation A2.5b) which may upset the power balance and power loss in the transducer considerably. It is to be noted that the fundamental frequency f_{ES} varies continuously in some systems (d.v. choppers), while the harmonic content of the switched current also changes due to the change in waveform. Where hybrid systems of Group IIIA, class 1-2 are used, the rotor currents also contain these beat effects.

2.4 A REVIEW OF MACHINE-ELECTRONIC SYSTEMS

The possibilities for a systematic classification have already been investigated. Out of all the possibilities the criterion of power flow was selected, and the power flow subsequently investigated for groups of systems. According to this power flow the different fundamental groups of systems have been defined and the possibility of constructing hybrid systems having additional advantages has been pointed out. No mention about the "internal structure" of the power-electronic circuits (ES and EFC), their modes of operation or their interrelation has been made. These characteristics will be extremely inportant as far as a more detailed investigation into power flow, harmonics and system characteristics is concerned. This will be done in subsequent chapters.

A classification of practical machine-electronic systems may be found in fig. 2.7. It is the intention of the figure to relate the abstract models constructed in this chapter to practical realisable systems. As yet no circuit detail is presented. With regard to these systems, and those to be presented in future it may be remarked that the representation of the power switching elements by thyristors or mercury-arc rectifiers is in no way intended to restrict the work to these systems. All the models examined, and still to be examined, relate in the first instance to electronic switching, and is therefore universally applicable. Only in second instance are the nature of the switches taken into account. As the experimental work concerns higher power applications, the power electronic switching elements inevitably have thyratron-like characteristics.

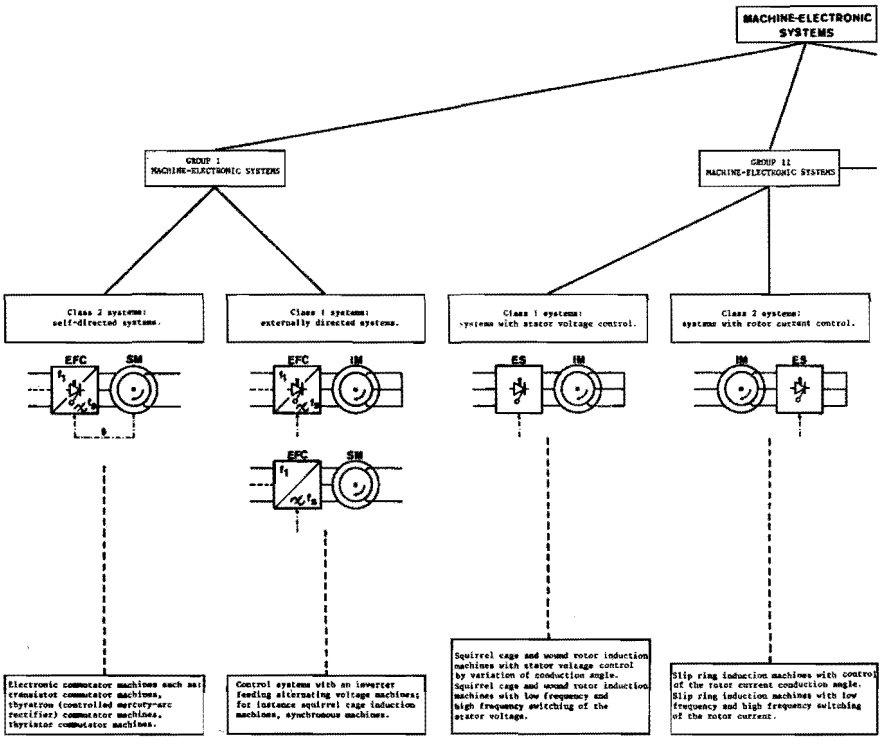
MACHINE-ELECTRONIC SYSTEMS
GROUP I
MACHINE-ELECTRONIC SYSTEMS
GROUP II
MACHINE-ELECTRONIC SYSTEMS
Class 2 systems:
self-directed systems.
Class 1 systems:
externally directed systems.
Class 1 systems:
systems with stator voltage control.
Class 2 systems:
systems with rotor current control.
EFC
SM
EFC
IM
EFC
SM
ES
IM
IM
ES
Electronic commutator machines such as:
transistor commutator machines,
thyratron (controlled mercury-arc rectifier) commutator machines,
thyristor commutator machines.
Control systems with an inverter feeding alternating voltage machines; for instance squirrel cage induction machines, synchronous machines.
Squirrel cage and wound rotor induction machines with stator voltage control by variation of conduction angle.
Squirrel cage and wound rotor induction machines with low frequency and high frequency switching of the stator voltage.
Slip ring induction machines with control of the rotor current conduction angle.
Slip ring induction machines with low frequency and high frequency switching of the rotor current.

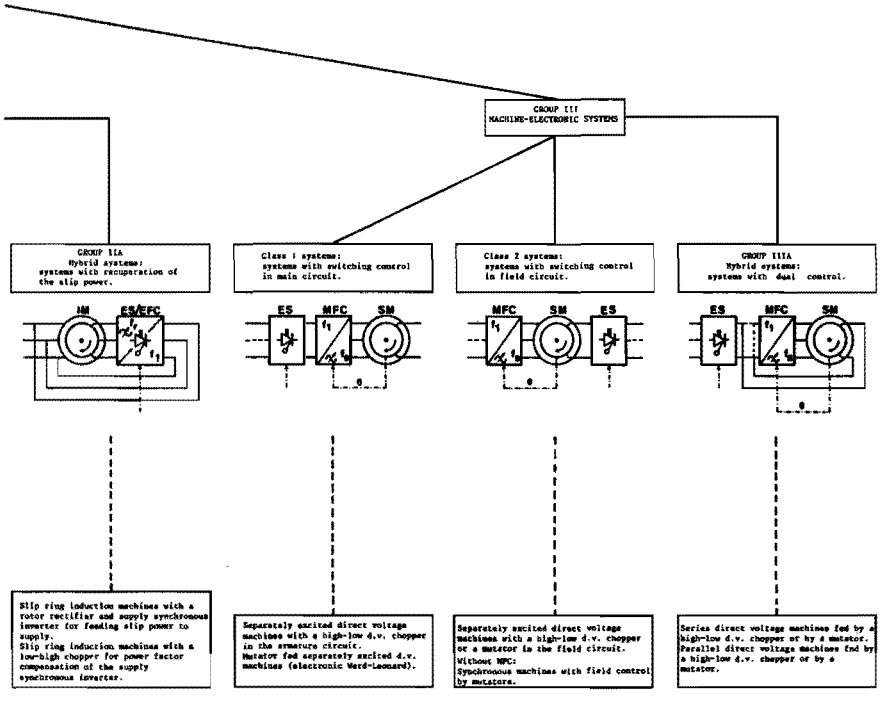

FIG. 2.7 A CLASSIFICATION OF PRACTICAL MACHINE-ELECTRONIC SYSTEMS.

Brief reference to the structure of machine-electronic systems of the three fundamental groups will be made in order to be able to distinguish the different variants.

2.4.1 *GROUP I SYSTEMS: FREQUENCY CONTROL OF INDUCTION AND SYNCHRONOUS MACHINES*

The control of induction and synchronous machines over a wide frequency range requires an adjustment of the amplitude of the output voltage of the fundamental frequency of the inverter in order to prevent saturation of the magnetic circuits of the electrical machine. Of these converters or inverters a wide variety may be found in practice; the details are the same for class 1 or class 2 systems. It is worth pointing out the main types to be found:

First divide the circuits into two types (see fig. 2.8), depending on the nature of the commutation employed to reduce the current through the electronic switches in the converter to zero. Two cases will be considered.

(i) *Natural commutation*: The current through the switch becomes zero as a consequence of the circuit voltages always present in the circuit due to either the supply system or the load.

(ii) *Forced commutation*: The current through the switch becomes zero as a consequence of a voltage introduced at a certain time into the circuit. This voltage may be in parallel or in series with the conducting element.

In practice it is found that circuits employing natural commutation have a series configuration (see fig. 2.81) (example: all supply-synchronous converters or mutators) and most circuits with forced commutation use the parallel configuration (see fig. 2.8k) (example: d.c. choppers of the high-low type or parallel inverters).

In each of these two classes different systems may be distinguished, depending on how the voltage-adjustment of the fundamental frequency is carried out. It is important to distinguish between all these arts, as each will influence the machine in a characteristic way. With regard to the representation of the output voltage waveforms in fig. 2.8 it should be noted that these waveforms are depicted for resistive loads of the force commutated converters. This has been done in order not to complicate the classification by the different influences that inductive and active effects in the machine have on the performance of the power electronic circuits. With an electrical machine as load the waveforms will depart from the given functions in a way determined by the internal structure of the power-electronic circuit.

FORCED COMMUTATION CONVERTERS (fig. 2.8a, b, c)

The normal alternating voltage supply is first converted by a rectifier, and when necessary passed through an intermediary energy reservoir with inductance and/or capacitance. The direct voltage is then again converted to the necessary m-phase, variable frequency output by the force-commutated inverter.

Regulation of the fundamental output voltage with frequency (approximately proportional to frequency) may be obtained by including an autotransformer or induction regulator in either the input or the output circuit (fig. 2.8a (i),(ii)). This technique will keep the frequency distribution of the output voltage constant and change the

amplitude of the peak voltages. Correspondingly the different harmonic frequencies remain constant in relation to the fundamental harmonic. It is also possible to adjust the intermediary direct voltage by using a controlled mutator as first stage (fig. 2.8b). The same considerations as previously mentioned apply for the voltage harmonics at the output (assuming that the filtering is effective).

When the output voltage is composed of a series of pulses, as indicated in fig. 2.8c, it is possible to obtain regulation of the output voltage by pulse-width modulation pwm or pulse-frequecy modulation pfm. The amplitude of the pulses remains constant. Consequently the frequency spectrum relative to the fundamental output voltage will change drastically with frequency. An advantage is the possibility of obtaining good simulation of any desired current waveform by employing two-level current control, with the desired waveform as the input (i_{o1}, i_{o2}). The current harmonics then reduce to a low percentage at the chopping frequency when appropriate freewheeling and feedback diodes are included.

NATURAL COMMUTATION CONVERTERS

This type of converter (fig. 2.8d) may actually also be seen as a subsynchronous mutator. By repetitive triggering of either the anti-parallel branches for equal periods an output voltage with positive or negative mean value may be obtained. Changing this repetitive triggering period changes the output frequency. In the simplest system the elements in the mutator are gated "on" during the conduction period, the input or output voltage being regulated by means of autotransformers or induction regulators (synchronous cyclo-converters). However, when employing a delay of the triggering angle of each individual element to regulate the output voltage, voltage control with frequency similar to the methods in fig. 2.8c may be used (variable ratio asynchronous cycloconverters (fig. 2.8d iii)). The difference between the different types are mostly not reflected in the circuit configuration - the configuration of fig. 2.8i or 2.8j may be used for all variants basically. The only exception is the fixed ratio asynchronous cycloconverter family, where an extra commutating harmonic transformer is introduced in the output.

Differences amongst the force commutated converters may further be found in the ways in which the power switches are arranged in the forced commutation part. Basically most of these complicated arrangements may be broken down into a number of the centre-tapped circuits (fig. 2.8e and 2.8g) - depending on whether d.v. source or output transformer is centre-tapped - or the bridge-type circuits (fig. 2.8f and 2.8h). Actual commutation circuits to obtain the desired voltages are responsible for the enormous variety of inverter circuits found in practice. This is important to the extent that these details have to be taken into account when calculating the influence of the switching on the electrical machine, and often affect the circuit economy and reliability.

2.4.2 *GROUP II-SYSTEMS.*
STATOR AND ROTOR CONTROL OF INDUCTION MACHINES (fig. 2.9)

Basically the stator and rotor control systems may be divided according to the frequency of operation of the switches used to

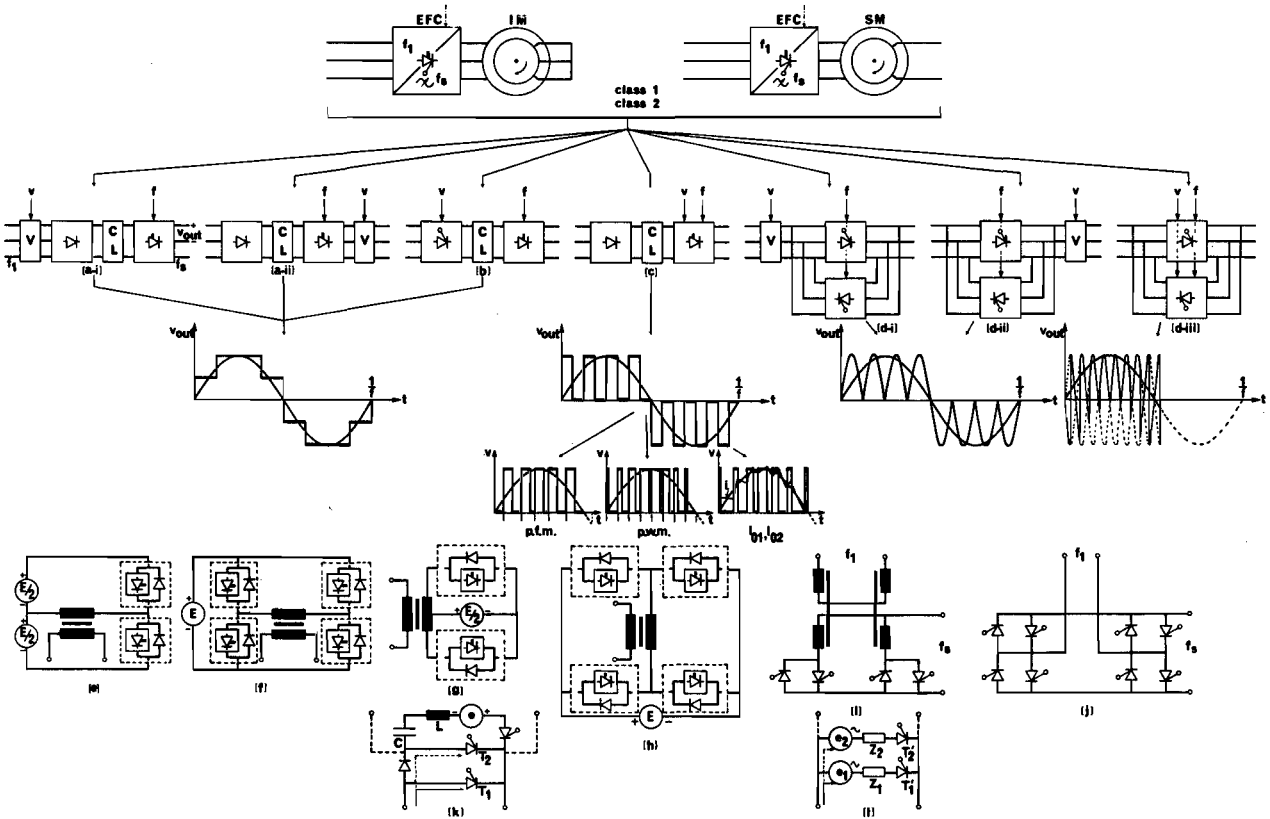
EFC
IM
EFC
SM
clase 1
clase 2
(a-i)
(a-ii)
(b)
(c)
(d-i)
(d-ii)
(d-iii)
p.f.m.
p.w.m.
(e)
(f)
(g)
(h)
(i)
(j)
(k)
(l)

FIG. 2.8

LEGEND TO FIG. 2.8

EFC	:	Electronic frequency changer
IM	:	Induction machine
SM	:	Synchronous machine
f_1 and f_s	:	Respectively fixed supply frequency and variable stator frequency
C, L	:	Filter circuit or commutation circuit
V	:	Unit for voltage adjustment, such as an induction regulator or autotransformer
v, f	:	Information input for voltage and frequency variation
v_{out}	:	Instantaneous output voltage with a resistive or inactive load, as applicable
pwm	:	Pulse width modulation
pfm	:	Pulse frequency modulation
i_{o1}, i_{o2}	:	Symbol for two level current control
E	:	D.v. source for inverter building block, centre-tapped to give a voltage E/2 as applicable
e	:	Instantaneous voltage for parallel commutation
e_1, e_2	:	Instantaneous voltages for series commutation
(a)	:	Fundamental methods of adjusting voltages with frequency by autotransformer, induction regulator in input or output
(b)	:	Voltage adjustment by control of the input mutator
(c)	:	Voltage adjustment by pulse modulation of the inverter waveform
(d) (i) (ii):		Main methods of adjusting input or output voltages of cycloconverters by autotransformers or induction regulators in input or output (Fixed ratio cyclo-converters
(d) (iii):		Voltage adjustment by ignition angle control (Continuous ratio cycloconverters)
(e), (f):		Principal building blocks for multiphase inverter circuits with centre-tapped supply or with bridge circuits
(g), (h):		Principal building blocks for multiphase inverter circuits with centre-tapped output transformer, or a bridge configuration essentially similar to (f)
(i), (j):		Principal building blocks for fixed ratio and continuously variable cycloconverter circuits
(k), (l):		Principal methods of commutation in forced and naturally commutated circuits

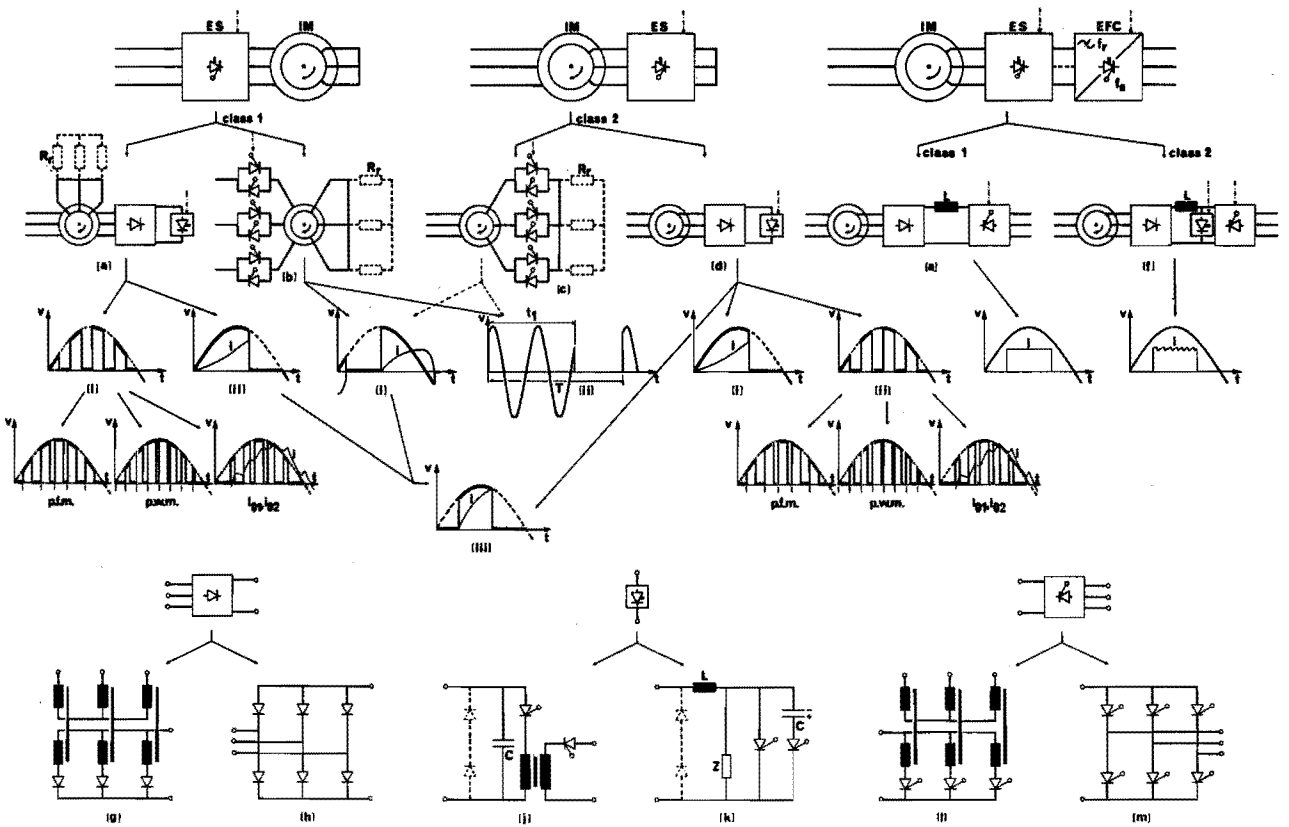

FIG. 2.9

LEGEND TO FIG. 2.9

EFC	:	Electronic frequency changer
ES	:	Electronic switch
f_s	:	Fixed stator supply frequency
f^s	:	Variable rotor frequency
R^r	:	Rotor resistor
L	:	Smoothing inductor
C	:	Commutation capacitor
V	:	Instantaneous part of the stator phase excitation derived from the supply voltage, or instantaneous part of the induced rotor voltage applied to the shorted rotor circuit, as applicable
pfm	:	Pulse frequency modulation
pwm	:	Pulse width modulation
i_{o1}, i_{o2}	:	Symbol indicating two level current control
i^{o1}	:	Instantaneous stator or rotor phase current, as applicable.
(a) (i)	:	Stator control by "high-frequency" switching
(a) (ii)	:	Stator control by extinction-angle variation
(b) (i)	:	Stator control by ignition-angle variation
(a)-(b) (iii)	:	A combination of (a)(ii) and (b)(i) gives full conduction angle control in the stator circuit
(b) (ii)	:	Stator control by low frequency pulse train switching
(c) (i)	:	Rotor control by ignition angle variation
(c) (ii)	:	Rotor control by low frequency pulse train switching
(d) (i)	:	Rotor control by extinction angle variation
(c)-(d) (iii)	:	Combination of (c)(i) and (d)(i) again leads to rotor control by conduction angle variation
(d) (ii)	:	Rotor control by "high frequency" switching.
(e)	:	Rotor control by recuperation of the slip power through a classical electronic Scherbius cascade
(f)	:	Rotor control by recuperation of the slip power through a power factor compensated electronic Sherbius cascade
(g) (h)	:	Principle methods of constructing uncontrolled mutators
(j), (k)	:	Principle methods of constructing direct voltage choppers
(l), (m)	:	Principle methods of constructing controlled mutators

influence the torque-speed characteristic. In both stator and rotor circuits the following switching modes will be distinguished:

(i) Switching frequency much higher than the stator/rotor frequency,
(ii) Switching freqency equal to the stator/rotor frequency,
(iii) Switching frequency much lower than the stator/rotor frequency.

It is not usual to choose the switching frequency of the same order as the stator/rotor frequency. In such a case the beat frequencies will affect the machine-behaviour adversely, and therefore it is normally attempted to avoid this drawback in systems operating with modes (i) and (iii). Systems with *switching frequency much higher than the rotor or stator frequency* have forced commutation. In order to avoid using 2 m antiparallel switching circuits for an m-phase machine, a bridge-rectifier circuit is inserted between the stator windings and the star point, or the slipring voltage is first fed to a rectifier (fig. 2.9a (i) and fig. 2.9d (ii). The output of this rectifier is then shorted by a forced commutation or d.v. "chopper" circuit. Analogous to the previous example of such a pulse system in the inverter category, the stator voltage/rotor current may be regulated by a pulse width modulation(pwm), a pulse frequency modulation(pfm), or a two-level control of current (i_{o1}, i_{o2}). In none of these cases will the harmonic components be constant. It is to be noted that as soon as the high frequency switching circuit is cascaded with a rectifier, the influence on the machine changes as the switching character is now that of switching at rotor/stator frequency, with the high frequency superposed. Normally it is attempted to obtain quasi-continuous flow of current in the machine windings by incorporation of freewheeling switching elements and impedances in the switch. Under these conditions the behaviour approaches that of stator/rotor frequency switching as far as the machine is concerned. Influence of the high switching frequency on power electronic aspects remains to the same extent as previously.

Switching frequency equal to the stator/rotor frequency. In this case one may distinguish between three methods of conducting-angle control, each with its own merits. The angle of stator/rotor current extinction may be regulated (fig. 2.9a (ii) and fig. 2.9d (i)), or the angle of current ignition may be regulated (fig. 2.9b (i) and fig. 2.9c (i)). In both cases of extinction control the basic circuit configuration is the same as for the high-frequency control. The differences in commutation will be pointed out subsequently. The antiparallel configuration of the switching elements for the ignition angle control is indicated in both fig. 2.9b and 2.9c. A rectifier with switching of its output as in a and d cannot be employed as the possibility exists that current flow will extend beyond

$$\pi \left(\frac{m + 2}{2m}\right)$$

The extinction angle control will tend to add capacitive influence to the fundamental harmonic frequency, and the ignition-angle control inductive influence. Combination of these two types (fig. 2.9a (iii) or fig. 2.9d (iii)) leads to control of the power factor of the machine-electronic system, and may be used for optimization in a specific situation.

Switching frequency much lower than the stator/rotor frequency. The circuits operate with natural commutation identical to the ignition angle control in the previous case. For both cases the circuit configurations may be chosen identical (fig. 2.9b (ii) and 2.9c (ii)). This extremely simple method of control functions by changing the on-off ratio of the switches per switching cycle, i.e. t_1/T. The natural commutation has the consequence that the control range is not continuous, but proceeds in discrete steps determined by the fundamental frequency of the rotor/stator.

Systems feeding back the slip power to the supply have a hybrid nature as already stressed previously. With reference to fig. 2.4 these systems consist of either a frequency changer (class 1) or an electronic switch and a frequency changer inserted between the rotor and the rotor supply voltage (class 2). Fig. 2.9e indicates that the frequency changer consists of an uncontrolled and controlled mutator as rectifier and supply synchronous inverter in cascade. When it is taken into account that the rectifier switches at rotor frequency, and the supply synchronous inverter at supply frequency, it may be expected that the further hybridization of the system by including the electronic switch can only be worthwhile when the switch operates at a frequency appreciable higher than the rotor frequency (fig. 2.9f). These systems will exhibit characteristics commensurate with the switching at rotor frequency. Superposed on this influence on the rotating electromechanical converter will be the effect of the supply synchronous inverter (mutator) and the "high" switching frequency of the power switch.

Further diversity in systems for stator/rotor control of induction machines at a frequency much higher than, or equal to, the stator/rotor frequency may be found due to the forced commutation methods employed. Some systems, especially those for extinction angle control, employ a d.v. forced-commutator chopper at the output of a rectifier or mutator circuit (fig. 2.9a, d). With parallel commutation this will give rise to short-circuit currents through the diodes, and it is essential to employ series-commutation (fig. 2.9j).

On the other hand other systems (current control) employ an impedance in parallel to the chopper, with a large inductor to decouple the chopper from the rectifier, and keep the current constant. In these cases a chopper with parallel forced commutation may be used (fig. 2.9k). Further differences that may be found in the arrangement of the rest of the commutating circuits will be treated later (circuit details for obtaining correct charge polarity and voltage on the commutating capacitor etc.).

2.4.3 *GROUP III SYSTEMS: ELECTRONIC CONTROL OF D.V. MACHINES AND FIELD CONTROL OF SYNCHRONOUS MACHINES*

As indicated in fig. 2.10a, b the armature voltage or field voltage of the d.v. machine may be controlled by an electronic converter. This converter may be a mutator or a high-low d.v. chopper. A third possibility may be found by combining (a) and (b) obtaining a series machine regulated by either of these means (hybrid Group IIIA). This type of control is extremely important for all traction purposes.

Control of d.v. machines by mutator employs a circuit with natural (series) commutation. The circuit configuration may be of an m-phase neutral point form, or of m-phase bridge-form (fig. 2.9g, h, l, m). A freewheel-diode may be included in the output, and control of the output voltage is obtained by adjustment of the current ignition angle in

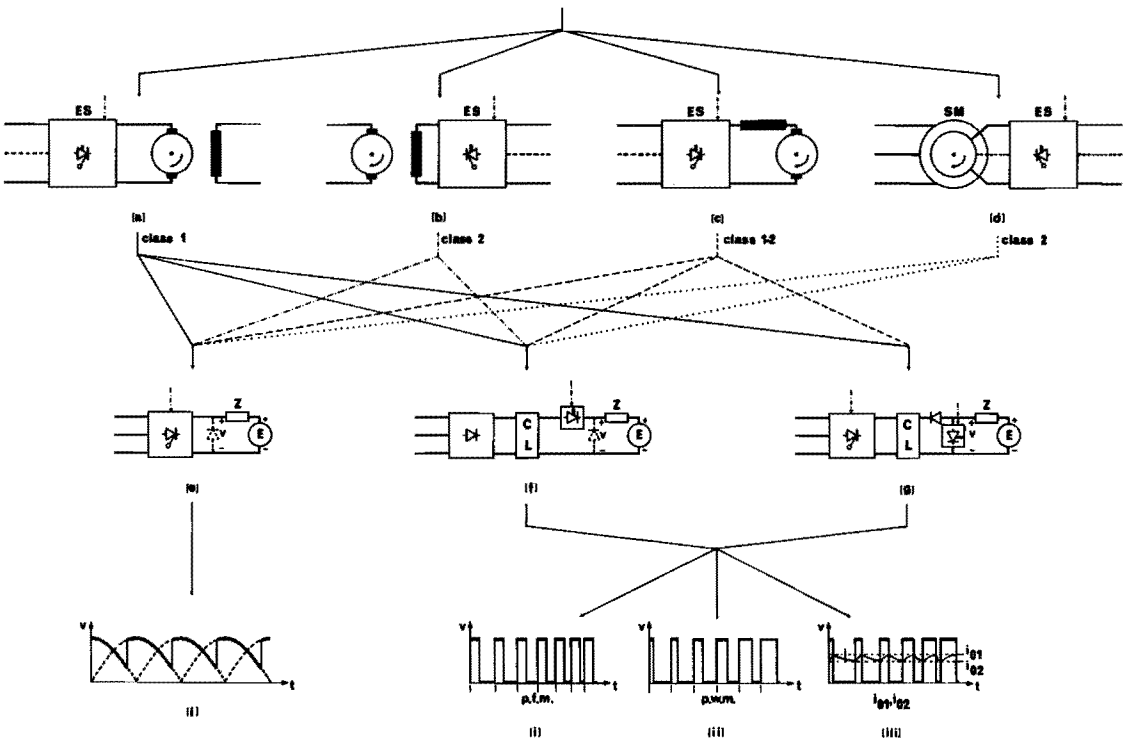
ES
ES
ES
SM
ES
(a)
(b)
(c)
(d)
class 1
class 2
class 1-2
class 2
Z
C
L
E
(e)
(f)
(g)
(i)
p.f.m.
p.w.m.
(ii)
(iii)
(iii)

FIG 2.10

each branch (fig. 2.10e (i)). This will adjust the mean output voltage from positive through zero to negative values. The output current is unidirectional, indicating that the direction of power flow through the mutator may change. It is one of the important advantages of these types of circuits when employed in electronic armature and series control that recuperative braking is possible.

Control of d.v. machines by d.v. high-low chopper uses a circuit with forced commutation - mostly of the parallel type, as no parallel discharge path to the element to be commutated exists. The system may incorporate an m-phase rectifier and intermediary L-C circuit as shown in fig. 2.10f. The methods of control possible are analogous to all the previously discussed pulse systems: pulse-width modulation, pulse-frequency modulation, and a combination by using a two level current control. Recuperative braking is not possible with this system: power flow is confined to one direction. When recuperative breaking of the d.v. machine is desired, a low-high chopper as indicated in fig. 2.10g must be added to the system. The rectifier circuit must become a mutator in order to absorb the reversed power flow. Failing this, the L-C circuit may be replaced by a resistor to enable electrical braking, With a d.v. source available from lead batteries in battery traction vehicles the system becomes simpler, the rectifier/mutator and the filter circuit being unnecessary.

Field control of synchronous machines by either a high-low chopper circuit or a mutator circuit is a possibility indicated in the combination of fig. 2.10d, e and f. While the natural commutation in the mutator circuit limits the electronic speed of response to the appropriate part of a cycle of the a.v. feeding the circuit, the corresponding speed of response of a high-low chopper circuit can be much higher. In practice circuits of the mutator type are mostly employed.

LEGEND TO FIG. 2.10

ES	:	Electronic switch
SM	:	Synchronous machine
v	:	Instantaneous voltage applied to controlled tranducers
C, L	:	Filter circuits for d.c. current
Z	:	Internal impedance of transducer to be controlled
E	:	Induced e.m.f. of transducer if applicable
(a)	:	Armature control of a d.v. machine with the ES in series with the MFC
(b)	:	Field control of a d.v. machine with the ES and MFC respectively on stationary and rotating members
(c)	:	Hybrid control system with the ES influencing both the armature through the MFC and the field (Series control by electronic converter)
(d)	:	Field control without an MFC: excitation-control of a synchronous machine
(e)	:	Principle of mutator control for (a), (b), (c) and (d)
(f)	:	Principle of high-low chopper control for (a), (b), (c) and (d)
(g)	:	Principle of recuperative control for (a) and (c)

CHAPTER 3

A GENERAL THEORETICAL ANALYSIS OF THE ELECTROMECHANICAL CONVERTER AS USED IN THE MACHINE-ELECTRONIC SYSTEMS

Synopsis

In machine-electronic systems the excitation of the electromechanical converter is determined by electronic switching in the stator or rotor. The effect of this switching may be reduced to the action of one series and one parallel switch per phase, both idealized. Under some constraints regarding construction, materials and switching mode, the general problem of an n-m phase converter switched in either stator or rotor, as used in Group I, II or III machine-electronic systems, and having unbalanced excitation on the different phases, is investigated. After determination and transformation of the general excitation functions the case of a converter switched in the stator circuit is examined further. Expressions for the instantaneous symmetrical component transforms of all (n-2) and (m-2) zero torque currents and four conversion currents on the stator and rotor respectively, are found. The instantaneous electromagnetic torque is calculated from the expressions for the conversion currents. Attention is given to representing the transformed voltages and currents in an equivalent circuit.

It is shown that the investigated model simplifies somewhat under conditions of balanced excitation. The results are linked with the harmonic magnetic fields rotating with and against the direction of rotation of the fundamental magnetic field, as investigated for the power flow problem in the previous chapter.

Two simplified models that may be applied to a range of systems from Group II with rotor control are investigated and found suitable for approximate calculation of system characteristics.

3.1 REPRESENTATION OF THE EFFECTS OF THE POWER ELECTRONIC CIRCUITS ON THE EXCITATION.

If it is possible to reduce the influence of the power electronic circuits to the action of idealized switches and known supply systems, combining to form an excitation function, the problem may be approached as a general switching problem and the solution will consequently gain in generality.

Every "winding phase" of the electromechanical transducer will be connected in some or other way to the power supply through a power

electronic circuit. The construction and disposition of the windings are for the present considered to be arbitrary. Constraints here-on will be imposed in the following paragraph (3.2). As will be evident from the previous chapter the different windings of an electrical machine in any of the systems may be considered to be excited by:

(1) EFC,
(2) ES,
(3) ES in series with MFC,
(4) MFC.

In the review of machine-electronic systems in paragraph 2.4 brief reference was made to the internal structure of the power electronic circuits. From the internal structure of an EFC one may deduce that its effect on the winding excitation in case (1) may be represented by a multiphase system and switches in series and /or parallel with the windings. In general the voltages of this equivalent multiphase system will not be simple harmonic functions of time, but it is always possible to express these voltages as an infinite series when the EFC operates in the steady state. In the next paragraph (3.2) it will be evident that the switching action is constrained in such a manner that the composite effect of the equivalent multiphase system and the switching action on the windings - comprising the part of the winding excitation derived from an external supply - can be expressed as a Fourier series.

Let the excitation in case (2) be investigated. The electronic switches have as input a known voltage from a given supply system that may be expressed mathematically. If the switching is suitably constrained, The same type of expression as in case (1) can be derived for the supply-derived part of the winding excitation function.

When such an ES is in series with a MFC as in case (3) it will be assumed that because the mechanical frequency changer generates a "multiphase" voltage system, it is possible to represent the effect of the ES by switches in series and/or parallel to the machine windings fed by the said multiphase system. This results in the same situation as in (1). The switching effects of the MFC itself may also be incorporated in the series/parallel switch, giving the possibility to include (4) in the description.

It therefore becomes possible to obtain a mathematical expression for the excitation function derived from an external supply in the case of all Group I, Group II, Group III and hybrid groups of machine-electronic systems with steady state operation of the electronic switching circuits, the electronic frequency changers and the mechanical frequency changers.

The results of the present chapter may therefore be considered valid for all machine electronic systems when the conditions of paragraph 3.2 are fulfilled. In general these results are applicable to all systems for control of electromechanical power conversion whenever a mathematical expression for the total excitation function can be derived, and apply to all the switched systems for control of electromechanical power conversion depicted in fig. 1.4, under the constraints of paragraph 3.2.

3.2 MODEL TO BE ANALYSED.

In order to compile the differential equations describing the behaviour of the rotating electromechanical energy transducer and still

retain a possibility of solving these equations, certain restrictions have to be placed on the construction of the machine, the materials utilized in this construction and the effects that will be taken into account.

3.2.1 *CONSTRUCTION*: a. The electrical windings carried on the rotor and stator of the machine are included in the magnetic circuit in such a way that the magnetic field is not disturbed by their presence if unexcited.

b. The windings are arranged in such a manner that the radial component of the magnetic field in the air gap may be represented by a simple harmonic function of the circumferential coordinate.

c. The machine phases on stator, rotor respectively are all symmetrical in resistance and arrangement.

d. The structures are of double cylindrical nature, and the air gap between rotor and stator bodies is constant, being negligible when compared to the radius of the rotor or stator bore.

e. No permanent magnets are included in the system.

3.2.2 *MATERIALS USED*:a. The magnetic material employed to construct the machine is of such a nature that the magnetic fluxes in the machine are in every state univalued. (no hysteresis flux).

b. The material is free from magnetic energy loss and has an infinite electrical resistance.

c. The magnetic material does not saturate magnetically, and the permeability is of such an order that compared to that of the air gap, it may be taken to approach infinity.

3.2.3 *EFFECTS NEGLECTED*: a. Axial end effects in the stator and rotor windings, and their influence on machine-performance are neglected.

b. The electromagnetic field energy of the electrical machine is taken to be only determined by the magnetic field. The influence of the electrical energy of the distributed winding capacitances are therefore not taken into account.

3.2.4 *THE SWITCHING AND EXCITATION*:

a. It will be assumed that the n stator phases and m rotor phases are connected to a multiphase grid $[u^n_{sg}]$, $[u^m_{rg}]$ respectively through (n + m) electronic switching circuits. This indicates that the stator and rotor applied voltage will not be considered to be simple harmonic functions of time.

b. The only restrictions placed on the operation of the electronic switching circuits are:

(i) The switching functions developed by the n, m electronic subsystems respectively are identical for stator, rotor circuits

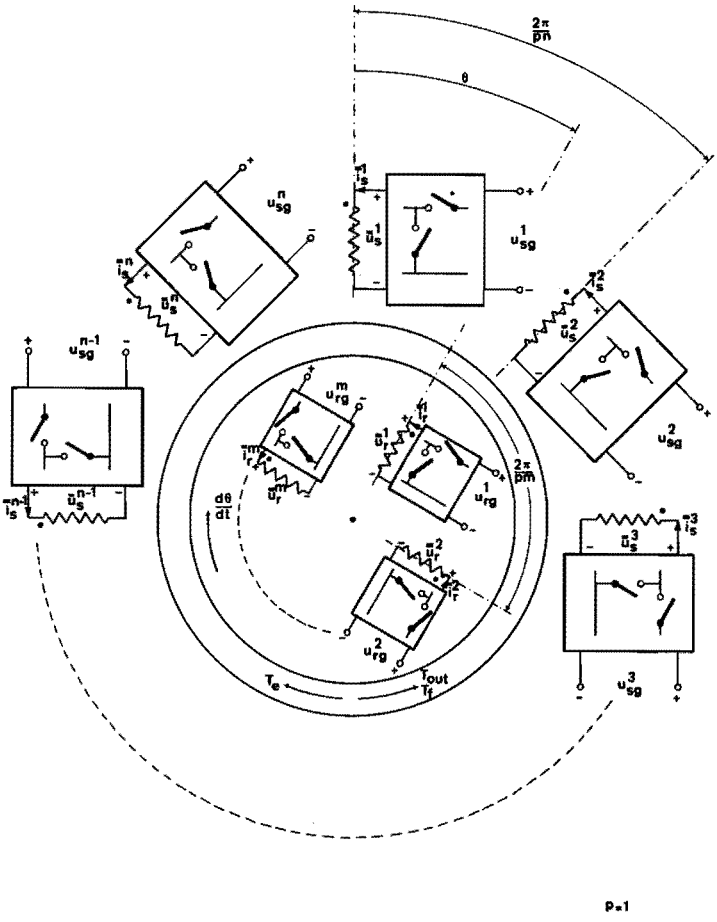

FIG 3.1 DIAGRAMMATIC REPRESENTATION OF N-M PHASE DOUBLE CYLINDRICAL ROTATING ELECTROMECHANICAL ENERGY CONVERTER WITH SWITCHED EXCITATION IN ROTOR AND STATOR CIRCUITS.

respectively in relation to the corresponding phase relation of the supply grid.
(ii) To a first approximation the switch characteristics are assumed to be ideal, i.e. no voltage drop during conduction, infinite resistance when blocking, zero switching time and no power loss during switching.

3.3 FORMULATION OF THE EQUATIONS

In this paragraph the equations will be given for an electromechanical converter having an arrangement as described in the previous paragraph, with n stator phases and m rotor phases. The compiled equations are then simplified by an instantaneous symmetrical component transformation. In order to eliminate angular dependence of the mutual coupling terms, the equations are subjected to a complex rotating transformation. For systems with stator control a Ku rotor-stator transformation is employed, while for systems with rotor control it is indicated that a Ku stator-rotor transformation is desirable. After partitioning the equations into groups active in producing electromechanical energy conversion due to mutual coupling and groups without any contribution in the said process due to the absence of any mutual coupling, the appropriate excitation functions are derived. Solution of the current then allows calculation of the instantaneous electromagnetic torque of the n-m phase converter.

3.3.1 *THE GENERAL N-M PHASE STATOR-ROTOR EQUATIONS*

Keeping the previous assumptions in mind, a machine with an n-phase stator and m-phase rotor, both with p pairs of poles, will be considered. The transducer has n electrical stator ports, m electrical rotor ports and one mechanical port on the rotor. The (m + n + 1) differential equations describing its behaviour are:[B16]

$$\begin{bmatrix} u_s^n \end{bmatrix} = \begin{bmatrix} R_s^n \end{bmatrix} \cdot \begin{bmatrix} i_s^n \end{bmatrix} + \frac{d}{dt} \begin{bmatrix} \begin{bmatrix} L_{ss}^{nn} \end{bmatrix} & 0 \\ 0 & \begin{bmatrix} L_{sr}^{nm} \end{bmatrix} \end{bmatrix} \cdot \begin{bmatrix} \begin{bmatrix} i_s^n \end{bmatrix} \\ \begin{bmatrix} i_r^m \end{bmatrix} \end{bmatrix} \qquad 3.1$$

$$\begin{bmatrix} u_r^m \end{bmatrix} = \begin{bmatrix} R_r^m \end{bmatrix} \cdot \begin{bmatrix} i_r^m \end{bmatrix} + \frac{d}{dt} \begin{bmatrix} \begin{bmatrix} L_{rr}^{mm} \end{bmatrix} & 0 \\ 0 & \begin{bmatrix} L_{rs}^{mn} \end{bmatrix} \end{bmatrix} \cdot \begin{bmatrix} \begin{bmatrix} i_r^m \end{bmatrix} \\ \begin{bmatrix} i_s^n \end{bmatrix} \end{bmatrix} \qquad 3.2$$

$$J_r \frac{d^2\theta}{dt^2} + T_f + T_{out} = \frac{1}{2}\left\{\left[i_s^n\right]_t \cdot \frac{\partial}{\partial\theta}\left[L_{sr}^{nm}\right] \cdot \left[i_r^m\right] + \left[i_r^m\right]_t \frac{\partial}{\partial\theta}\left[L_{rs}^{mn}\right] \cdot \left[i_s^n\right]\right\} \qquad 3.3$$

where the following elements will be employed for the matrices:

$$\left[u_s^n\right] = \begin{bmatrix} u_s^1 \\ u_s^2 \\ u_s^3 \\ \vdots \\ u_s^{n-1} \\ u_s^n \end{bmatrix}, \left[u_r^m\right] = \begin{bmatrix} u_r^1 \\ u_r^2 \\ u_r^3 \\ \vdots \\ u_r^{m-1} \\ u_r^m \end{bmatrix}, \left[i_s^n\right] = \begin{bmatrix} i_s^1 \\ i_s^2 \\ i_s^3 \\ \vdots \\ i_s^{n-1} \\ i_s^n \end{bmatrix}, \left[i_r^m\right] = \begin{bmatrix} i_r^1 \\ i_r^2 \\ i_r^3 \\ \vdots \\ i_r^{m-1} \\ i_r^m \end{bmatrix}, \left[R_s^n\right] = R_s \cdot \left[1_u^n\right], \left[R_r^m\right] = R_r \cdot \left[1_u^m\right]$$

$$\left[L_{ss}^{nn}\right] = \begin{bmatrix} L_{ss}^{1,1} & L_{ss}^{1,2} & L_{ss}^{1,3} & \cdots & L_{ss}^{1,n-1} & L_{ss}^{1,n} \\ L_{ss}^{2,1} & L_{ss}^{2,2} & L_{ss}^{2,3} & & & L_{ss}^{2,n} \\ L_{ss}^{3,1} & L_{ss}^{3,2} & L_{ss}^{3,3} & & & L_{ss}^{3,n} \\ \vdots & \vdots & \ddots & & & \\ L_{ss}^{n-1,1} & L_{ss}^{n-1,2} & & & & \\ L_{ss}^{n,1} & L_{ss}^{n,2} & L_{ss}^{n,3} & \cdots & L_{ss}^{n,n-1} & L_{ss}^{nn} \end{bmatrix},$$

$$\left[L_{rr}^{mm}\right] = \begin{bmatrix} L_{rr}^{1,1} & L_{rr}^{1,2} & L_{rr}^{1,3} & \cdots & L_{rr}^{1,m-1} & L_{rr}^{1,m} \\ L_{rr}^{2,1} & L_{rr}^{2,2} & L_{rr}^{2,3} & & & L_{rr}^{2,m} \\ L_{rr}^{3,1} & L_{rr}^{3,2} & L_{rr}^{3,3} & & & L_{rr}^{3,m} \\ \vdots & \vdots & & \ddots & & \\ L_{rr}^{m-1,1} & L_{rr}^{m-1,2} & & & & \\ L_{rr}^{m,1} & L_{rr}^{m,2} & L_{rr}^{m,3} & \cdots & L_{rr}^{m,m-1} & L_{rr}^{mm} \end{bmatrix}$$

$$\left[L_{sr}^{nm}\right] = \begin{bmatrix} L_{sr}^{1,1} & L_{sr}^{1,2} & L_{sr}^{1,3} & \cdots & L_{sr}^{1,m-1} & L_{sr}^{1,m} \\ L_{sr}^{2,1} & L_{sr}^{2,2} & L_{sr}^{2,3} & & & L_{sr}^{2,m} \\ L_{sr}^{3,1} & L_{sr}^{3,2} & L_{sr}^{3,3} & & & L_{sr}^{3,m} \\ \vdots & \vdots & & \ddots & & \\ L_{sr}^{n-1,1} & L_{sr}^{n-1,2} & L_{sr}^{n-1,3} & & & \\ L_{sr}^{n,1} & L_{sr}^{n,2} & L_{sr}^{n,3} & \cdots & L_{sr}^{n,m-1} & L_{sr}^{nm} \end{bmatrix}$$

$$\left[L_{rs}^{mn}\right] = \begin{bmatrix} L_{rs}^{1,1} & L_{rs}^{1,2} & L_{rs}^{1,3} & \cdots & L_{rs}^{1,n-1} & L_{rs}^{1,n} \\ L_{rs}^{2,1} & L_{rs}^{2,2} & L_{rs}^{2,3} & & & L_{rs}^{2,n} \\ L_{rs}^{3,1} & L_{rs}^{3,2} & L_{rs}^{3,3} & & & L_{rs}^{3,n} \\ \vdots & \vdots & & \ddots & & \\ L_{rs}^{m-1,1} & L_{rs}^{m-1,2} & L_{rs}^{m-1,3} & & & \\ L_{rs}^{m,1} & L_{rs}^{m,2} & L_{rs}^{m,3} & \cdots & L_{rs}^{m,n-1} & L_{rs}^{mn} \end{bmatrix}$$

Taking the winding symmetries in the machine into account, it may be proved that for the vth and wth phase on either rotor or stator

$$L_{ss,rr}^{v,(v-k)} = L_{ss,rr}^{v,(v+k)} \quad , \quad L_{ss,rr}^{v,(w-k)} = L_{ss,rr}^{(v+k),w} \tag{3.4}$$

Furthermore the same considerations for the mutual inductances of the windings lead to

$$L_{rs}^{wv} = L_{sr}^{vw} = M_{sr} \cos p(\theta + \frac{2\pi}{pm} \cdot \overline{w-1} - \frac{2\pi}{pn} \cdot \overline{v-1}) \tag{3.5}$$

This will result in the simplification of equations 3.1, 3.2, 3.3 into

$$\begin{bmatrix} [u_s^n] \\ [u_r^m] \end{bmatrix} = \begin{bmatrix} [R_s^n] & 0 \\ 0 & [R_r^m] \end{bmatrix} \begin{bmatrix} [i_s^n] \\ [i_r^m] \end{bmatrix} + \frac{d}{dt} \begin{bmatrix} [L_{ss}^{nn}] & [L_{sr}^{nm}] \\ [L_{rs}^{mn}] & [L_{rr}^{mm}] \end{bmatrix} \cdot \begin{bmatrix} [i_s^n] \\ [i_r^m] \end{bmatrix} \tag{3.6}$$

$$J_r \frac{d^2\theta}{dt^2} + T_f + T_{out} = \tfrac{1}{2} \left\{ \begin{bmatrix} [i_s^n]_t & [i_r^m]_t \end{bmatrix} \cdot \frac{\partial}{\partial\theta} \begin{bmatrix} 0 & [L_{sr}^{nm}] \\ [L_{rs}^{mn}] & 0 \end{bmatrix} \cdot \begin{bmatrix} [i_s^n] \\ [i_r^m] \end{bmatrix} \right\} \tag{3.7}$$

where the inductance matrices have all been simplified to the following form in which the symmetry is circulant:

$$[L_{ss}^{nn}] = \begin{bmatrix} L_{ss}^{1,1} & L_{ss}^{1,2} & L_{ss}^{1,3} & \cdots & L_{ss}^{1,3} & \cdots & L_{ss}^{1,2} \\ L_{ss}^{1,2} & L_{ss}^{1,1} & L_{ss}^{1,2} & \cdots & \cdots & \cdots & L_{ss}^{1,3} \\ L_{ss}^{1,3} & L_{ss}^{1,2} & L_{ss}^{1,1} & \cdots & \cdots & \cdots & L_{ss}^{1,4} \\ \vdots & \vdots & \vdots & & & & \\ L_{ss}^{1,3} & L_{ss}^{1,4} & \cdots & \cdots & \cdots & & \\ L_{ss}^{1,2} & L_{ss}^{1,3} & L_{ss}^{1,4} & \cdots & L_{ss}^{1,2} & & L_{ss}^{1,1} \end{bmatrix} ,$$

$$\left[L_{rr}^{mm}\right] = \begin{bmatrix} L_{rr}^{1,1} & L_{rr}^{1,2} & L_{rr}^{1,3} & \cdots & L_{rr}^{1,3} & L_{rr}^{1,2} \\ L_{rr}^{1,2} & L_{rr}^{1,1} & L_{rr}^{1,2} & \cdots & \vdots & L_{rr}^{1,3} \\ L_{rr}^{1,3} & L_{rr}^{1,2} & L_{rr}^{1,1} & \cdots & \vdots & L_{rr}^{1,4} \\ \vdots & \vdots & \vdots & \ddots & \vdots & \vdots \\ L_{rr}^{1,3} & L_{rr}^{1,4} & \vdots & \cdots & \vdots & \vdots \\ L_{rr}^{1,2} & L_{rr}^{1,3} & L_{rr}^{1,4} & \cdots & L_{rr}^{1,2} & L_{rr}^{1,1} \end{bmatrix}$$

$$\left[L_{sr}^{nm}\right] = M_{sr} \cdot$$

$$\begin{bmatrix} \cos p\,\theta & \cos p(\theta + \frac{2\pi}{pm}) & \cdots & \cos p(\theta + \overline{m-1}\,\frac{2\pi}{pm}) \\ \cos p(\theta - \frac{2\pi}{pn}) & \cos p(\theta + \frac{2\pi}{pm} - \frac{2\pi}{pn}) & \cdots & \cos p(\theta + \overline{m-1}\,\frac{2\pi}{pm} - \frac{2\pi}{pn}) \\ \cos p(\theta - \frac{4\pi}{pn}) & \cos p(\theta + \frac{2\pi}{pm} - \frac{4\pi}{pn}) & \cdots & \cos p(\theta + \overline{m-1}\,\frac{2\pi}{pm} - \frac{4\pi}{pn}) \\ \vdots & \vdots & & \vdots \\ \cos p(\theta - \overline{n-1}\,\frac{2\pi}{pn}) & \cos p(\theta + \frac{2\pi}{pm} - \overline{n-1}\,\frac{2\pi}{pn}) & \cdots & \cos p(\theta + \overline{m-1}\,\frac{2\pi}{pm} - n\text{-}1\,\frac{2\pi}{pn}) \end{bmatrix}$$

$$\left[L_{rs}^{mn}\right] = M_{sr} \cdot$$

$$\begin{bmatrix} \cos p\,\theta & \cos p(\theta - \frac{2\pi}{pn}) & \cdots & \cos p(\theta - \overline{n-1}\,\frac{2\pi}{pn}) \\ \cos p(\theta + \frac{2\pi}{pm}) & \cos p(\theta + \frac{2\pi}{pm} - \frac{2\pi}{pn}) & \cdots & \cos p(\theta + \frac{2\pi}{pm} - \overline{n-1}\,\frac{2\pi}{pn}) \\ \cos p(\theta + \frac{4\pi}{pm}) & \cos p(\theta + \frac{4\pi}{pm} - \frac{2\pi}{pn}) & \cdots & \\ \vdots & \vdots & & \\ \cos p(\theta + \overline{m-1}\,\frac{2\pi}{pm}) & \cos p(\theta + \overline{m-1}\,\frac{2\pi}{pm} - \frac{2\pi}{pn}) & \cdots & \cos p(\theta + \frac{2\pi}{pm}\,\overline{m-1} - \overline{n-1}\,\frac{2\pi}{pn}) \end{bmatrix}$$

3.3.2 *REDUCTION OF THE GENERAL EQUATIONS BY AN INSTANTANEOUS SYMMETRICAL TRANSFORMATION*

It may be shown that these equations may be considerably simplified by employing the symmetrical component complex transformation([B16], as this will lead to a diagonalisation of the parameter matrices. Under use of the power-invariant transformation([B16].

$$\begin{bmatrix} [i_s^n] \\ [i_r^m] \end{bmatrix} = \begin{bmatrix} [S_s^n] & 0 \\ 0 & [S_r^m] \end{bmatrix} \begin{bmatrix} [\dot{i}_s^n]' \\ [\dot{i}_r^m]' \end{bmatrix} \qquad 3.8a$$

$$\begin{bmatrix} [u_s^n] \\ [u_r^m] \end{bmatrix} = \begin{bmatrix} [S_s^n] & 0 \\ 0 & [S_r^m] \end{bmatrix} \begin{bmatrix} [\dot{u}_s^n]' \\ [\dot{u}_r^m]' \end{bmatrix}$$

with

$$[S_m^n]_{sr} = \frac{1}{\sqrt{n_m}}$$

$$\begin{bmatrix} 1 & 1 & 1 & \cdots & 1 & 1 \\ 1 & z_{sr}^{-1} & z_{sr}^{-2} & \cdots & z_{sr}^{-(\frac{n}{m}-2)} & z_{sr}^{-(\frac{n}{m}-1)} \\ 1 & z_{sr}^{-2} & z_{sr}^{-4} & \cdots & z_{sr}^{-2(\frac{n}{m}-2)} & z_{sr}^{-2(\frac{n}{m}-1)} \\ \vdots & \vdots & \vdots & \ddots & \vdots & \vdots \\ 1 & z_{sr}^{-(\frac{n}{m}-2)} & z_{sr}^{-2(\frac{n}{m}-2)} & \cdots & z_{sr}^{-(\frac{n}{m}-2)(\frac{n}{m}-2)} & z_{sr}^{-(\frac{n}{m}-2)(\frac{n}{m}-1)} \\ 1 & z_{sr}^{-(\frac{n}{m}-1)} & z_{sr}^{-2(\frac{n}{m}-1)} & \cdots & z_{sr}^{-(\frac{n}{m}-2)(\frac{n}{m}-1)} & z_{sr}^{-(\frac{n}{m}-1)(\frac{n}{m}-1)} \end{bmatrix} \qquad 3.8b$$

the complex numbers z_s and z_r being

$$z_s = \exp(j\,\frac{2\pi}{n})$$

$$z_r = \exp(j\,\frac{2\pi}{m})$$

the equations 3.6 and 3.7 may be written as

$$\begin{bmatrix} [\dot{u}_s^n]' \\ [\dot{u}_r^m]' \end{bmatrix} = \begin{bmatrix} [R_s^n]' & 0 \\ 0 & [R_r^m]' \end{bmatrix} \begin{bmatrix} [i_s^n]' \\ [i_r^m]' \end{bmatrix} + \frac{d}{dt} \begin{bmatrix} [L_{ss}^{nn}]' & [L_{sr}^{nm}]' \\ [L_{rs}^{mn}]' & [L_{rr}^{mm}]' \end{bmatrix} \begin{bmatrix} [i_s^n]' \\ [i_r^m]' \end{bmatrix} \qquad 3.9a$$

and

$$J_r \frac{d^2\theta}{dt^2} + T_f + T_{out} = \tfrac{1}{2} \left\{ \begin{bmatrix} [i_s^n]'^* & [i_r^m]'^* \end{bmatrix}_t \cdot \frac{\partial}{\partial\theta} \begin{bmatrix} 0 & [L_{sr}^{nm}]' \\ [L_{rs}^{mn}]' & 0 \end{bmatrix} \begin{bmatrix} [i_s^n]' \\ [i_r^m]' \end{bmatrix} \right\} \qquad 3.9b$$

with

$$\begin{bmatrix} [R_s^n]' \\ [R_r^m]' \end{bmatrix} = \begin{bmatrix} \left([S_s^n]\right)^{-1} [R_s^n] [S_s^n] \\ \left([S_r^m]\right)^{-1} [R_r^m] [S_r^m] \end{bmatrix} = \begin{bmatrix} [R_s] [I_u^n] \\ [R_r] [I_u^n] \end{bmatrix} \qquad 3.10a$$

$$\begin{bmatrix} L_{rr}^{nn} \\ L_{ss}^{mm} \end{bmatrix}' = \left([S_r^n]\right)^{-1} \cdot \begin{bmatrix} L_{ss}^{nn} \\ L_{rr}^{mm} \end{bmatrix} [S_r^n] = \begin{bmatrix} L_{sr}^{1} & 0 & 0 \text{----} 0 \\ 0 & L_{sr}^{2} & 0 \text{----} 0 \\ 0 & 0 & L_{sr}^{3} \text{----} 0 \\ \vdots & \vdots & \vdots \quad \ddots \quad \vdots \\ 0 & 0 & 0 \text{---} L_{sr}^{m} \end{bmatrix}, L_{sr}^{y} = \sum_{v=1}^{\frac{n}{m}} (z_s)^{(y-1)(v-1)} L_{ss}^{1,v} \qquad 3.10b$$

with y=1,2....m or n.

$$\begin{bmatrix} nm \\ mn \\ L_{sr} \\ rs \end{bmatrix}' = \left(\begin{bmatrix} n \\ S^{m} \\ s \\ r \end{bmatrix} \right)^{-1} \begin{bmatrix} nm \\ mn \\ L_{sr} \\ rs \end{bmatrix} \begin{bmatrix} m \\ S^{n} \\ r \\ s \end{bmatrix} = \sqrt{nm} \frac{M_{sr}}{2}$$

$$\begin{array}{c} \begin{matrix} \overset{m}{n} \rightarrow & & \\ \end{matrix} \\ \begin{bmatrix} 0 & 0 & 0 \cdots\cdots 0 \\ 0 & \exp+jp\theta & 0 \cdots\cdots 0 \\ 0 & 0 & 0 \cdots\cdots 0 \\ \vdots & \vdots & \ddots \\ 0 & 0 & 0 \cdots\cdots \exp+jp\theta \end{bmatrix} \end{array} \begin{matrix} n \\ m \end{matrix} \downarrow \qquad 3.10c$$

This now indicates that the (n+m+1) non-linear differential equations have been reduced to (n+m-4) linear, independent equations that may be solved in terms of the transformed currents and four non-linear equations. The above parameters clearly indicate, however, that only the four non-linear equations remaining will yield the necessary coupling between electrical and mechanical ports. This concerns two transformed stator currents and two transformed rotor currents, to be called $\dot{i}_s^{2,t}$, $\dot{i}_s^{n,t}$, $\dot{i}_r^{2,t}$ and $\dot{i}_r^{m,t}$ respectively. Combining the parameter matrices into one impedance matrix, it is possible to write the voltage relations as:(The currents giving a zero contribution to the torque are written as $\dot{i}_s^{y,z}$ and $\dot{i}_r^{x,z}$).

$$\begin{bmatrix} \dot{u}_s^{1,z} \\ \dot{u}_s^{2,t} \\ \dot{u}_s^{3,z} \\ \vdots \\ \dot{u}_s^{(n-1),z} \\ \dot{u}_s^{n,t} \\ \dot{u}_r^{1,z} \\ \dot{u}_r^{2,t} \\ \dot{u}_r^{3,z} \\ \vdots \\ \dot{u}_r^{(m-1),z} \\ \dot{u}_r^{m,t} \end{bmatrix} = \left[\begin{array}{ccccc|ccccc} R_s + DL_s^1 & 0 & 0 \cdots\cdots 0 & 0 & 0 & 0 & 0 & 0 \cdots 0 & 0 \\ 0 & R_s + DL_s^2 & 0 \cdots\cdots 0 & 0 & 0 & D\sqrt{\frac{nm}{4}}M_{sr}\exp jp\theta & 0 & 0 \cdots 0 & 0 \\ 0 & 0 & R_s + DL_s^3 \cdots 0 & 0 & 0 & 0 & 0 & 0 \cdots 0 & 0 \\ \vdots & \vdots & \ddots R_s + DL_s^{(n-1)} & \vdots & \vdots & \vdots & \vdots & \ddots & \vdots \\ 0 & 0 & 0 \cdots\cdots 0 & R_s + DL_s^n & 0 & 0 & 0 & 0 \cdots 0 & D\sqrt{\frac{nm}{4}}M_{sr}\exp -jp\theta \\ \hline 0 & 0 & 0 \cdots\cdots 0 & 0 & R_r + DL_r^1 & 0 & 0 & 0 \cdots 0 & 0 \\ 0 & D\sqrt{\frac{nm}{4}}M_{sr}\exp -jp\theta & 0 \cdots\cdots 0 & 0 & 0 & R_r + DL_r^2 & 0 & 0 \cdots 0 & 0 \\ 0 & 0 & 0 \cdots\cdots 0 & 0 & 0 & 0 & R_r + DL_r^3 \cdots 0 & 0 \\ \vdots & \vdots & \ddots & \vdots & \vdots & \vdots & \ddots R_r + DL_r^{(m-1)} & 0 \\ 0 & 0 & 0 \cdots\cdots 0 & D\sqrt{\frac{nm}{4}}M_{sr}\exp jp\theta & 0 & 0 & 0 & 0 & R_r + DL_r^m \end{array}\right] \begin{bmatrix} \dot{i}_s^{1,z} \\ \dot{i}_s^{2,t} \\ \dot{i}_s^{3,z} \\ \vdots \\ \dot{i}_s^{(n-1),z} \\ \dot{i}_s^{n,t} \\ \dot{i}_r^{1,z} \\ \dot{i}_r^{2,t} \\ \dot{i}_r^{3,z} \\ \vdots \\ \dot{i}_r^{(m-1),z} \\ \dot{i}_r^{m,t} \end{bmatrix} \qquad 3.11$$

with the differential operator $D = \frac{d}{dt}$

3.3.3 *COMPLEX ROTATING ROTOR-STATOR TRANSFORMATION:*

With reference to fig. 3.1 it will now be useful to regard with some attention the nature of the systems in which the electromechanical component is to be employed. It is extremely rare in practice to encounter systems with simultaneous switching in rotor and stator circuits. The switches are mostly incorporated in either rotor or stator. In cases where switching circuits are incorporated in both stator and rotor supply, they are usually intended for operating in a different speed range of the machine, so that they are by design not supposed to operate simultaneously. With switching elements incorporated in either rotor or stator, the complementary electrical ports may be assumed to be excited by voltages that are simple harmonic functions of time. Capitalizing on this knowledge, when the switching elements are contained in the stator circuits, equation 3.11 will be transformed by the Ku-transformation-to eliminate the angular dependence of the mutual coupling terms-to the stator frequency. Therefore:(Bl6

$$\begin{bmatrix} [1^n_u] & 0 \\ 0 & [K_s]^{-1} \end{bmatrix} \cdot \begin{bmatrix} [\dot{u}^n_s]' \\ [\dot{u}^m_r]' \end{bmatrix} = \begin{bmatrix} [1^n_u] & 0 \\ 0 & [K_s]^{-1} \end{bmatrix} \cdot \left\{ \begin{bmatrix} [R^n_s]' & 0 \\ 0 & [R^m_r]' \end{bmatrix} + D \begin{bmatrix} [L^{nn}_{ss}]' & [L^{nm}_{sr}]' \\ [L^{mn}_{rs}]' & [L^{mm}_{rr}]' \end{bmatrix} \right\} \begin{bmatrix} [1^n_u] & 0 \\ 0 & [K_s] \end{bmatrix} \begin{bmatrix} [i^n_s]^{ks} \\ [i^m_r]^{ks} \end{bmatrix} \qquad 3.12a$$

with

$$[K_s] = \begin{bmatrix} (1)^1 & 0 & 0 & \cdots & 0 \\ 0 & \exp -jp\theta & 0 & \cdots & 0 \\ 0 & 0 & (1)^3 & \cdots & 0 \\ 0 & 0 & 0 & (1)^4 \ddots & 0 \\ \vdots & \vdots & \vdots & \ddots & \vdots \\ 0 & 0 & 0 & 0 \; (1)^{m-1} & 0 \\ 0 & 0 & 0 & 0 \quad 0 & \exp jp\theta \end{bmatrix} \qquad 3.12b$$

The voltage equations are transformed into

$$\begin{bmatrix} [\dot{u}^n_s]^{ks} \\ [\dot{u}^m_r]^{ks} \end{bmatrix} = \begin{bmatrix} [R^n_s]^{ks} & 0 \\ 0 & [R^m_r]^{ks} \end{bmatrix} \begin{bmatrix} [i^n_s]^{ks} \\ [i^m_r]^{ks} \end{bmatrix} + \begin{bmatrix} [L^{nn}_{ss}]^{ks}_D & [L^{nm}_{sr}]^{ks}_D \\ [L^{mn}_{rs}]^{ks}_D & [L^{mm}_{rr}]^{ks}_D \end{bmatrix} \cdot \begin{bmatrix} [i^n_s]^{ks} \\ [i^m_r]^{ks} \end{bmatrix} \qquad 3.13a$$

with the new parameters defined as

$[R^n_s]^{ks} = [R^n_s]'$, and $[R^m_r]^{ks} = [R^m_r]'$, the latter being defined in

equation 3.10

$$\left[L_{ss}^{nn}\right]_D^{ks} = \begin{bmatrix} L_s^1.D & 0 & 0 \cdots\cdots 0 \\ 0 & L_s^2.D & 0 \cdots\cdots 0 \\ 0 & 0 & L_s^3.D \cdots 0 \\ \vdots & \vdots & \vdots \quad \ddots \quad \vdots \\ 0 & 0 & 0 \cdots\cdots L_s^n.D \end{bmatrix} \qquad 3.13b$$

$$\left[L_{sr}^{nm}\right]_D^{ks} = \sqrt{\frac{nm}{4}} M_{sr} \begin{bmatrix} 0 & 0 & 0 \cdots\cdots 0 \\ 0 & D & 0 \cdots\cdots 0 \\ 0 & 0 & 0 \cdots\cdots 0 \\ \vdots & \vdots & \vdots \quad \ddots \quad \vdots \\ 0 & 0 & 0 \cdots\cdots D \end{bmatrix} \qquad 3.13c$$

$$\left[L_{rs}^{mn}\right]_D^{ks} = \sqrt{\frac{nm}{4}} M_{sr} \begin{bmatrix} 0 & 0 & 0 \cdots\cdots 0 \\ 0 & (D-jpD\theta) & 0 \cdots\cdots 0 \\ 0 & 0 & 0 \cdots\cdots 0 \\ \vdots & \vdots & \vdots \quad \ddots \quad \vdots \\ 0 & 0 & 0 \cdots (D+jpD\theta) \end{bmatrix} \qquad 3.13d$$

$$\left[L_{rr}^{mm}\right]_D^{ks} = \begin{bmatrix} L_r^1.D & 0 & 0 \cdots\cdots 0 \\ 0 & L_r^2(D-jpD\theta) & 0 \cdots\cdots 0 \\ 0 & 0 & L_r^3.D \\ \vdots & \vdots & \ddots \\ 0 & 0 & 0 \cdots L_r^m (D+jpD\theta) \end{bmatrix} \qquad 3.13e$$

From 3.10a the expression for the electromagnetic torque becomes, when taking the transformations of 3.12 into account:

$$T_e = \tfrac{1}{2} \left\{ \left[i_s^{n*} \right]_t^{ks} \left[i_r^{m*} \right]_t^{ks} \cdot \begin{array}{|c|c|} \hline 0 & \left[L_{sr}^{nm}\right]_{D_\theta}^{ks} \\ \hline \left[L_{rs}^{mn}\right]^{ks} & 0 \\ \hline \end{array} \cdot \begin{array}{|c|} \hline \left[i_s^{n} \right]^{ks} \\ \hline \left[i_r^{m} \right]^{ks} \\ \hline \end{array} \right\} \qquad 3.14a$$

In these matrices $D_\theta = \frac{\partial}{\partial\theta}$ and

$$\left[L_{sr}^{nm}\right]_{D\theta}^{ks} = M_{sr}\cdot\sqrt{\frac{nm}{4}}\begin{bmatrix} 0 & 0 & 0 & \cdots & 0 \\ 0 & D_\theta & 0 & \cdots & 0 \\ 0 & 0 & \ddots & & \vdots \\ \vdots & \vdots & & \ddots & \vdots \\ 0 & 0 & 0 & \cdots & D_\theta \end{bmatrix} \qquad 3.14b$$

$$\left[L_{rs}^{mn}\right]^{ks} = M_{sr}\cdot\sqrt{\frac{nm}{4}}\begin{bmatrix} 0 & 0 & 0 & \cdots & 0 \\ 0 & -jp & 0 & \cdots & 0 \\ 0 & 0 & \ddots & & \vdots \\ \vdots & \vdots & & \ddots & \vdots \\ 0 & 0 & 0 & & jp \end{bmatrix} \qquad 3.14c$$

3.3.4 *COMPLEX ROTATING STATOR-ROTOR TRANSFORMATION.*

Complementary to the statement made in the introduction to paragraph 3.3.3, systems may also be found in which the stator circuits are excited by a multiphase system of voltages that are simple harmonic functions of time, and the switching elements are incorporated into the rotor. If it is considered that the complex voltages obtained from the instantaneous symmetrical transformation (eq. 3.9a) require the transformation of the switching functions, it is obvious that to avoid the additional frequency tranformation of the switching functions, it is attractive to transform the whole system by a complex rotating transformation to the frequency at which the switching action is taking place, as has already been done in the case of the stator switched systems. This same philosophy now inspires the transformation of the equations from the stationary reference frame of the stator to the rotating reference frame of the rotor. Again taking eq. 3.11 as basis, the following transformation is to be performed:

$$\begin{bmatrix} [K_r]^{-1} & 0 \\ 0 & [1_u^m] \end{bmatrix}\begin{bmatrix} [\dot{u}_s^n]' \\ [\dot{u}_r^m]' \end{bmatrix} = \begin{bmatrix} [K_r] & 0 \\ 0 & [1_u^m] \end{bmatrix}\left\{\begin{bmatrix} [R_s^n]' & 0 \\ 0 & [R_r^m]' \end{bmatrix} + D\begin{bmatrix} [L_{ss}^{nn}]' & [L^{nm}]' \\ [L_{rs}^{mn}]' & [L_{rr}^{mm}]' \end{bmatrix}\right\}\cdot \begin{bmatrix} [K_r] & 0 \\ 0 & [1_u^m] \end{bmatrix}\cdot\begin{bmatrix} [\dot{i}_s^n]^{kr} \\ [\dot{i}_r^m]^{kr} \end{bmatrix} \qquad 3.15a$$

where

$$\left(\left[K_r\right]\right)^{-1} = \begin{bmatrix} 1^1 & 0 & 0 & 0 & \cdots & 0 \\ 0 & \exp(-jp\theta) & 0 & 0 & \cdots & 0 \\ 0 & 0 & (1)^3 & 0 & \cdots & 0 \\ 0 & 0 & 0 & (1)^4 & \cdots & 0 \\ \vdots & \vdots & \vdots & \ddots & \ddots & \vdots \\ 0 & 0 & 0 & (1)^{\overline{m-1}} & & 0 \\ 0 & 0 & 0 & 0 & & \exp jp\theta \end{bmatrix} \qquad 3.15b$$

The resulting transformed parameter-matrices and the voltage equations may then be shown to be:

$$\begin{bmatrix} \dot{u}_s^n \\ \dot{u}_r^m \end{bmatrix}^{kr} = \left\{ \begin{bmatrix} R_s^n & 0 \\ 0 & R_r^m \end{bmatrix}^{kr} + \begin{bmatrix} L_{ss}^{nn} & L_{sr}^{nm} \\ L_{rs}^{mn} & L_{rr}^{mm} \end{bmatrix}_D^{kr} \right\} \begin{bmatrix} \dot{i}_s^n \\ \dot{i}_r^m \end{bmatrix}^{kr} \qquad 3.16a$$

$$\left[R_s^n\right]^{kr} = \left[R_s^n\right]^{ks} \; ; \; \left[R_r^m\right]^{kr} = \left[R_r^m\right]^{ks} \qquad 3.16b$$

$$\left[L_{ss}^{nn}\right]_D^{kr} = \begin{bmatrix} L_s^1.D & 0 & 0 & \cdots & 0 \\ 0 & L_s^2(D+jp\theta) & 0 & \cdots & 0 \\ 0 & 0 & L_s^3.D & \ddots & \vdots \\ \vdots & \vdots & \ddots & \ddots & \\ 0 & 0 & 0 & \cdots & L_s^n(D-jp\theta) \end{bmatrix} \qquad 3.16c$$

$$\left[L_{sr}^{nm}\right]_D^{kr} = \sqrt{\frac{nm}{4}}\, M_{sr} \begin{bmatrix} 0 & 0 & 0 & \cdots & 0 \\ 0 & (D+jpD\theta) & 0 & \cdots & 0 \\ 0 & 0 & 0 & \ddots & \vdots \\ \vdots & \vdots & \vdots & \ddots & \\ 0 & 0 & 0 & \cdots & (D-jpD\theta) \end{bmatrix} \qquad 3.16d$$

$$\left[L_{rs}^{mn}\right]_{D}^{kr} = \sqrt{\frac{nm}{4}}\, M_{sr} \begin{bmatrix} 0 & 0 & 0 & \cdots & 0 \\ 0 & D & 0 & \cdots & 0 \\ 0 & 0 & 0 & \cdots & 0 \\ \vdots & \vdots & \vdots & \ddots & \vdots \\ 0 & 0 & 0 & \cdots & D \end{bmatrix} \qquad 3.16e$$

$$\left[L_{rr}^{mm}\right]_{D}^{kr} = D \cdot \left[L_{rr}^{mm}\right]' \qquad 3.16f$$

It is useful to note the transformed torque equation now as:

$$T_e = \tfrac{1}{2} \left\{ \begin{bmatrix} \left[i_s^{n*}\right]^{kr} & \left[i_r^{m*}\right]^{kr} \end{bmatrix}_t \cdot \begin{bmatrix} 0 & \left[L_{sr}^{nm}\right]^{kr} \\ \left[L_{rs}^{mn}\right]_{D_\theta}^{kr} & 0 \end{bmatrix} \cdot \begin{bmatrix} \left[i_s^{n}\right] \\ \left[i_r^{m}\right]^{kr} \end{bmatrix} \right\} \qquad 3.17a$$

specifying the parameters as:

$$\left[L_{sr}^{nm}\right]^{kr} = \sqrt{\frac{nm}{4}}\, M_{sr} \begin{bmatrix} 0 & 0 & 0 & \cdots & 0 \\ 0 & jp & 0 & \cdots & 0 \\ 0 & 0 & 0 & \cdots & 0 \\ \vdots & \vdots & \vdots & \ddots & \vdots \\ 0 & 0 & 0 & \cdots & -jp \end{bmatrix} \qquad 3.17b$$

$$\left[L_{rs}^{mn}\right]_{D_\theta}^{kr} = \sqrt{\frac{nm}{4}}\, M_{sr} \begin{bmatrix} 0 & 0 & 0 & \cdots & 0 \\ 0 & D_\theta & 0 & \cdots & 0 \\ 0 & 0 & 0 & \cdots & 0 \\ \vdots & \vdots & \vdots & \ddots & \vdots \\ 0 & 0 & 0 & \cdots & D_\theta \end{bmatrix} \qquad 3.17c$$

When equation 3.17a is evaluated, the torque expression 3.10a for the complex transformed stator and rotor currents becomes

$$J_r \frac{d^2\theta}{dt^2} + T_f + T_{out} = jpM_{sr}\sqrt{\frac{nm}{4}} \left\{ i_s^{2,t*} i_r^{2,t} \exp(jp\theta) - i_r^{2,t*} i_s^{2,t} \exp(-jp\theta) \right\} \qquad 3.18a$$

and from 3.14a it is obtained that

$$J_r \frac{d^2\theta}{dt^2} + T_f + T_{out} = jpM_{sr}\sqrt{\frac{nm}{4}}\left\{\dot{i}_s^{n,t}\dot{i}_r^{2,t}\exp(jp\theta) - \dot{i}_s^{2,t}\dot{i}_r^{m,t}\exp(-jp\theta)\right\} \quad 3.18b$$

By employing the characteristics of the instantaneous symmetrical component transformation that(

$$\dot{i}_s^{2,t^*} = \dot{i}_s^{n,t};\ \dot{i}_s^{n,t^*} = \dot{i}_s^{2,t};\ \dot{i}_r^{2,t^*} = \dot{i}_r^{m,t};\ \dot{i}_r^{m,t^*} = \dot{i}_r^{2,t} \quad 3.18c$$

it may be shown that these two expressions are identical.

3.3.5 *PARTITIONING OF THE STATOR-TRANSFORMED AND ROTOR-TRANSFORMED EQUATIONS.*

It has already been noted that after diagonalization by the instantaneous symmetrical component transformation, the problem of the switched n-m phase transducer has been reduced to an equivalent two phase problem as far as the electromechanical energy conversion is concerned. This is clearly reflected in the (n-2)stator, and (m-2) rotor, voltage-current equations that give no indication of coupling between rotor and stator. As there is consequently no contribution to the electromagnetic torque to be expected from these equations, they will be referred to as the zero equations. The remaining two stator equations and two rotor equations represent the energy-conversion process. Whereas the (n+m-4) zero equations are of linear differential form, the 4 conversion equations contain angular-dependent terms due to the angular dependence of the inductance terms. Although the complex rotating transformations have removed this angular dependence, these conversion equations will contain speed terms, and it is therefore desirable to solve them separately.

By adding the resistance and inductance matrices of 3.13a the stator-transformed zero equations are rewritten as:

$$\begin{bmatrix} \left[\dot{u}_s^{n-2,z}\right]^{ks} \\ \left[\dot{u}_r^{m-2,z}\right]^{ks} \end{bmatrix} = \begin{bmatrix} \left[Z_s^{n-2,z}\right]^{ks} & 0 \\ 0 & \left[Z_r^{m-2,z}\right]^{ks} \end{bmatrix} \cdot \begin{bmatrix} \left[\dot{i}_s^{n-2,z}\right]^{ks} \\ \left[\dot{i}_r^{m-2,z}\right]^{ks} \end{bmatrix} \quad 3.19a$$

with

$$\left[\dot{u}_s^{n-2,z}\right]^{ks} = \begin{bmatrix} \dot{u}_s^{1,z} \\ \dot{u}_s^{3,z} \\ \dot{u}_s^{4,z} \\ \vdots \\ \dot{u}_s^{n-1,z} \end{bmatrix}; \left[\dot{u}_r^{m-2,z}\right] = \begin{bmatrix} \dot{u}_r^{1,z} \\ \dot{u}_r^{3,z} \\ \dot{u}_r^{4,z} \\ \vdots \\ \dot{u}_r^{m-1,z} \end{bmatrix}; \left[\dot{i}_s^{n-2,z}\right] = \begin{bmatrix} \dot{i}_s^{1,z} \\ \dot{i}_s^{3,z} \\ \dot{i}_s^{4,z} \\ \vdots \\ \dot{i}_s^{n-1,z} \end{bmatrix}; \left[\dot{i}_r^{m-2,z}\right] = \begin{bmatrix} \dot{i}_r^{1,z} \\ \dot{i}_r^{3,z} \\ \dot{i}_r^{4,z} \\ \vdots \\ \dot{i}_r^{m-1,z} \end{bmatrix} \qquad 3.19b$$

$$\left[Z_s^{n-2,z}\right]^{ks} = \begin{bmatrix} R_s+L_s^1D & 0 & 0 \cdots 0 \\ 0 & R_s+L_s^3D & 0 \cdots 0 \\ 0 & 0 & R_s+L_s^4D \cdots 0 \\ \vdots & \vdots & \ddots \quad \vdots \\ 0 & 0 & 0 \cdots R_s+L_s^{n-1}D \end{bmatrix} \qquad 3.19c$$

$$\left[Z_r^{m-2,z}\right]^{ks} = \begin{bmatrix} R_r+L_r^1D & 0 & 0 \cdots 0 \\ 0 & R_r+L_r^3D & 0 \cdots 0 \\ 0 & 0 & R_r+L_r^4D \cdots 0 \\ \vdots & \vdots & \ddots \quad \vdots \\ 0 & 0 & 0 \cdots R_r+L_r^{m-1}D \end{bmatrix} \qquad 3.19d$$

The currents contributing to the electromagnetic torque are contained in:

$$\begin{bmatrix} \left[\dot{u}_s^t\right]^{ks} \\ \left[\dot{u}_r^t\right]^{ks} \end{bmatrix} = \begin{bmatrix} \left[Z_s^t\right]^{ks} & \left[Z_{sr}^t\right]^{ks} \\ \left[Z_{rs}^t\right]^{ks} & \left[Z_r^t\right]^{ks} \end{bmatrix} \cdot \begin{bmatrix} \left[\dot{i}_s^t\right]^{ks} \\ \left[\dot{i}_r^t\right]^{ks} \end{bmatrix} \qquad 3.20a$$

further

$$\begin{bmatrix} \dot{u}_s^t \\ \dot{u}_r^t \end{bmatrix}^{ks} = \begin{bmatrix} \dot{u}_s^{2,t} \\ \dot{u}_s^{n,t} \\ \dot{u}_r^{2,t}\exp(jp\theta) \\ \dot{u}_r^{m,t}\exp(-jp\theta) \end{bmatrix}; \begin{bmatrix} \dot{i}_s^t \\ \dot{i}_r^t \end{bmatrix}^{ks} = \begin{bmatrix} \dot{i}_s^{2,t} \\ \dot{i}_s^{n,t} \\ \dot{i}_r^{2,t}\exp(jp\theta) \\ \dot{i}_r^{m,t}\exp(-jp\theta) \end{bmatrix} \qquad 3.20b$$

and

$$\begin{bmatrix} Z^t \end{bmatrix}^{ks} = \left[\begin{array}{cc:cc} R_s+L_s^2D & 0 & \sqrt{\frac{nm}{4}}M_{sr}D & 0 \\ 0 & R_s+L_s^nD & 0 & \sqrt{\frac{nm}{4}}M_{sr}D \\ \hdashline M_{sr}\sqrt{\frac{nm}{4}}(D-jpD\theta) & 0 & R_r+L_r^2(D-jpD\theta) & 0 \\ 0 & M_{sr}\sqrt{\frac{nm}{4}}(D+jpD\theta) & 0 & R_r+L_r^m(D+jpD\theta) \end{array}\right] \qquad 3.20c$$

$$= \begin{bmatrix} \begin{bmatrix} Z_s^t \end{bmatrix}^{ks} & \begin{bmatrix} Z_{sr}^t \end{bmatrix}^{ks} \\ \begin{bmatrix} Z_{rs}^t \end{bmatrix}^{ks} & \begin{bmatrix} Z_r^t \end{bmatrix}^{ks} \end{bmatrix}$$

Performing the same partitioning on the equations describing the system under a Ku-transformation from the stator to the rotor, it may be shown that in the equations

$$\begin{bmatrix} \begin{bmatrix} \dot{u}_s^{n-2,z} \end{bmatrix}^{kr} \\ \begin{bmatrix} \dot{u}_r^{m-2,z} \end{bmatrix}^{kr} \end{bmatrix} = \begin{bmatrix} \begin{bmatrix} Z_s^{n-2,z} \end{bmatrix}^{kr} & 0 \\ 0 & \begin{bmatrix} Z_r^{m-2,z} \end{bmatrix}^{kr} \end{bmatrix} \cdot \begin{bmatrix} \begin{bmatrix} \dot{i}_s^{n-2,z} \end{bmatrix}^{kr} \\ \begin{bmatrix} \dot{i}_r^{m-2,z} \end{bmatrix}^{kr} \end{bmatrix} \qquad 3.21a$$

$$\begin{bmatrix} \dot{u}_s^{n-2,z} \end{bmatrix}^{kr} = \begin{bmatrix} \dot{u}_s^{n-2,z} \end{bmatrix}^{ks}; \begin{bmatrix} \dot{u}_r^{m-2,z} \end{bmatrix}^{kr} = \begin{bmatrix} \dot{u}_r^{m-2,z} \end{bmatrix}^{ks};$$

$$\begin{bmatrix} \dot{i}_s^{n-2,z} \end{bmatrix}^{kr} = \begin{bmatrix} \dot{i}_s^{n-2,z} \end{bmatrix}^{ks}; \begin{bmatrix} \dot{i}_r^{m-2,z} \end{bmatrix}^{kr} = \begin{bmatrix} \dot{i}_r^{m-2,z} \end{bmatrix}^{ks} \qquad 3.21b$$

$$\begin{bmatrix} Z_s^{n-2,z} \end{bmatrix}^{kr} = \begin{bmatrix} Z_s^{n-2} \end{bmatrix}^{ks}; \begin{bmatrix} Z_r^{m-2,z} \end{bmatrix}^{kr} = \begin{bmatrix} Z_r^{m-2,z} \end{bmatrix}^{ks} \qquad 3.21c$$

so that these zero equations will not be developed further. Analogous to the conversion equations resulting from the rotor-stator Ku-transformation, the conversion equations resulting from the stator-rotor Ku-transformation become:

$$\begin{bmatrix} \dot{u}_s^t \end{bmatrix}^{kr} = \begin{bmatrix} Z_s^t \end{bmatrix}^{kr} \begin{bmatrix} \dot{i}_s^t \end{bmatrix}^{kr} + \begin{bmatrix} Z_{sr}^t \end{bmatrix}^{kr} \begin{bmatrix} \dot{i}_r^t \end{bmatrix}^{kr} \qquad 3.22a$$

$$\begin{bmatrix} \dot{u}_r^t \end{bmatrix}^{kr} = \begin{bmatrix} Z_{rs}^t \end{bmatrix}^{kr} \begin{bmatrix} \dot{i}_s^t \end{bmatrix}^{kr} + \begin{bmatrix} Z_r^t \end{bmatrix}^{kr} \begin{bmatrix} \dot{i}_r^t \end{bmatrix}^{kr}$$

where

$$\begin{bmatrix} \dot{u}_{sr}^t \end{bmatrix}^{kr} = \begin{bmatrix} \dot{u}_s^{2,t} \exp(-jp\theta) \\ \dot{u}_s^{n,t} \exp(jp\theta) \\ \dot{u}_r^{2,t} \\ \dot{u}_r^{m,t} \end{bmatrix} ; \quad \begin{bmatrix} \dot{i}_{sr}^t \end{bmatrix}^{kr} = \begin{bmatrix} \dot{i}_s^{2,t} \exp(-jp\theta) \\ \dot{i}_s^{n,t} \exp(jp\theta) \\ \dot{i}_r^{2,t} \\ \dot{i}_r^{m,t} \end{bmatrix} \qquad 3.22b$$

$$\begin{bmatrix} Z^t \end{bmatrix}^{kr} = \left[\begin{array}{cc:cc} R_s+L_s^2(D+jpD\theta) & 0 & \sqrt{\frac{nm}{4}}M_{sr}(D+jpD\theta) & 0 \\ 0 & R_s+L_s^n(D-jpD\theta) & 0 & \sqrt{\frac{nm}{4}}M_{sr}(D-jpD\theta) \\ \hdashline \sqrt{\frac{nm}{4}}M_{sr}D & 0 & R_r+L_r^2D & 0 \\ 0 & \sqrt{\frac{nm}{4}}M_{sr}D & 0 & R_r+L_r^mD \end{array}\right] \qquad 3.22c$$

$$= \begin{bmatrix} Z_s^t \end{bmatrix}^{kr} \begin{bmatrix} Z_{sr}^t \end{bmatrix}^{kr} \\ \begin{bmatrix} Z_{rs}^t \end{bmatrix}^{kr} \begin{bmatrix} Z_r^t \end{bmatrix}^{kr}$$

3.3.6 *THE EXCITATION FUNCTIONS.*

Before solution of either the zero equations (3.19a, 3.21a) or the two sets of conversion equations (3.20a, 3.22a) is possible, the as yet undefined excitation functions have to be determined.

It was previously stated that of the two vectors $\left[u^{n}_{s}\right]$ and $\left[u^{m}_{r}\right]$ comprising the voltage excitation functions of the electromechanical converter, only one set at a time will be determined by switching. The remaining electrical ports are assumed to be excited by a multiphase system having voltages that are simple harmonic functions of time. As the electronic switches are for the present analysis considered to be ideal, all voltage changes caused by switching are instantaneous. The switching mode is taken to be strictly periodic, with switching function:

$$S(t) = \sum_{k=0}^{\infty} \left\{ S_u(t - \overline{t_{on} + k\,\tau_{sw}}) - S_u(t - \overline{t_{off} + k\,\tau_{sw}}) \right\} \qquad 3.23$$

where S_u is the unit step function and t_{on} and t_{off} the times of switching on and off respectively and τ_{sw} the period of the switching function.

The stator or rotor electrical ports will then be excited by the multiphase system:

$$\left[u^{n}_{m}{}^{sg}_{r}\right] = \frac{1}{\sqrt{2}} \left\{ \dot{U}^{x}_{s}{}_{r} \exp j(\omega_{s}{}_{r} t - \overline{x-1}\Delta_{s}{}_{r}) + \dot{U}^{x*}_{s}{}_{r} \exp -j(\omega_{s}{}_{r} t - \overline{x-1}\Delta_{s}{}_{r}) \right\} \qquad 3.24a$$

with

$$x: 1,2,3 \qquad \overline{n}_{m},\ \Delta_{s} = \frac{2\pi}{n},\ \Delta_{r} = \frac{2\pi}{m},\ \dot{U}^{x}_{s}{}_{r} = U^{x}_{s}{}_{r} \exp -j\theta^{x}_{s}{}_{r} \qquad 3.24b$$

Rearrangement gives:

$$\left[u^{n}_{m}{}^{sg}_{r}\right] = \frac{1}{\sqrt{2}} \left(\begin{bmatrix} 1.\dot{U}^{1}_{s}{}_{r} \\ (z_{s}{}_{r})^{-1}\dot{U}^{2}_{s}{}_{r} \\ (z_{s}{}_{r})^{-2}\dot{U}^{3}_{s}{}_{r} \\ \vdots \\ (z_{s}{}_{r})^{-\overline{n-2}\,\overline{m-1}}\dot{U}_{s}{}_{r} \\ (z_{s}{}_{r})^{-\overline{n-1}\,\overline{m}}\dot{U}_{s}{}_{r} \end{bmatrix} \exp j\omega_{s}{}_{r} t + \begin{bmatrix} 1.\dot{U}^{1*}_{s}{}_{r} \\ (z_{s}{}_{r})U^{2*}_{s}{}_{r} \\ (z_{s}{}_{r})^{2}U^{3*}_{s}{}_{r} \\ \vdots \\ (z_{s}{}_{r})^{\overline{n-2}\,\overline{m-1}*}U_{s}{}_{r} \\ (z_{s}{}_{r})^{\overline{n-1}\,\overline{m}*}\dot{U}_{s}{}_{r} \end{bmatrix} \exp -j\omega_{s}{}_{r} t \right) \qquad 3.24c$$

Due to the fact that the switching is constrained to be periodic, the voltages on the electrical machine ports that are controlled may be expressed in a Fourier series (in an exponential form). Taking phase "1" on the stator as normative, it is found that:

$$\underline{\underline{u}}^{1}_{s}(t) = \frac{1}{\sqrt{2}} \sum_{\nu_s=0}^{\infty} \left\{ \underline{\dot{U}}^{1}_{s\nu} \exp j\nu_s \omega_s t + \underline{\dot{U}}^{1*}_{s\nu} \exp -j\nu_s \omega_s t \right\}$$

the ν_s-th effective harmonic voltage component being $\overline{\overline{U}}_{s\nu}$ in the switched circuit. When the electromechanical transducer is fed by a true alternating voltage system in the steady state the direct voltage components will be assumed to be eliminated. In normal a.v. systems the percentage of even harmonics is negligible. Switching action by power electronic means may actually introduce even harmonics into the excitation function of the machine. However, as it is normally attempted to reduce the harmonic content as much as possible, and elimination of even harmonics may be obtained by the simple measure of a half-wave symmetric switched excitation, only odd harmonics will be considered in the following calculations. The number of cases where this does not apply is very limited, while the criterion is certainly fulfilled by all the systems to be investigated in chapters 4 and 5. Consequently it is possible that:

$$\nu = (2h + 1), (h=0 \quad \infty)$$

Taking the corresponding phase shift into account for the different phases, it is possible to represent the vectors $\left[\underline{\underline{u}}^{n}_{m\,s_r}\right]$ as:

$$\begin{bmatrix} \underline{\underline{u}}^{1}_{s_r} \\ \underline{\underline{u}}^{2}_{s_r} \\ \underline{\underline{u}}^{3}_{s_r} \\ \vdots \\ \underline{\underline{u}}^{n}_{m\,s_r} \end{bmatrix} = \frac{1}{\sqrt{2}} \sum_{h=0}^{\infty} \begin{bmatrix} \left\{ z_{s_r} \right\}^{-\overline{2h+1}} & \underline{\dot{U}}^{1}_{s_r}\,\overline{2h+1} \\ \left\{ (z_{s_r})^2 \right\}^{-\overline{2h+1}} & \underline{\dot{U}}^{2}_{s_r}\,\overline{2h+1} \\ \vdots & \vdots \\ \left\{ (z_{s_r})^{\overline{m-1}} \right\}^{-\overline{2h+1}} & \underline{\dot{U}}^{n}_{m\,s_r}\,\overline{2h+1} \end{bmatrix} \exp j(\overline{2h+1}\,\omega_{s_r} t) +$$

3.25

$$+ \begin{bmatrix} & \dot{\bar{\bar{U}}}^{1*}_{s\,r\ \overline{2h+1}} \\ \left\{z_{s\,r}\right\}^{\overline{2h+1}} & \dot{\bar{\bar{U}}}^{2*}_{s\,r\ \overline{2h+1}} \\ \left\{(z_{s\,r})^{2}\right\}^{\overline{2h+1}} & \dot{\bar{\bar{U}}}^{3*}_{s\,r\ \overline{2h+1}} \\ \vdots & \vdots \\ \left\{(z_{s\,r})^{\overline{m-1}}\right\}^{\overline{2h+1}} & \dot{\bar{\bar{U}}}^{n*}_{m\,s\,r\ \overline{2h+1}} \end{bmatrix} \exp -j(\overline{2h+1}\ \omega_{s\,r}t) \qquad 3.25$$

$$\dot{\bar{\bar{U}}}^{x}_{s\,r\ \overline{2h+1}} = \dot{\bar{\bar{U}}}^{x}_{s\,r\ \overline{2h+1}} \exp -j\theta_{s\,r\ \overline{2h+1}} \quad , \text{ with the general harmonic}$$

voltage component given by: $$\dot{\bar{\bar{U}}}^{x}_{s\,r\ \overline{2h+1}} = \frac{\sqrt{2}}{\pi}\int_{0}^{\pi}\left\{\bar{\bar{u}}^{x}_{s\,r}(\omega_{s\,r}t)\exp -j(\overline{2h+1}\ \omega_{s\,r}t)\right\}d(\omega_{s\,r}t)$$

Taking into account the instantaneous symmetrical component transformation, and employing relation 3.8b, the vectors $\left[\dot{\bar{\bar{u}}}^{n}_{m\,s\,r}\right]'$ are obtained, i.e.

$$\begin{bmatrix} \dot{\bar{\bar{u}}}^{1,z}_{s\,r} \\ \dot{\bar{\bar{u}}}^{2,t}_{s\,r} \\ \dot{\bar{\bar{u}}}^{3,z}_{s\,r} \\ \vdots \\ \dot{\bar{\bar{u}}}^{\overline{n}-1,z}_{m\,s\,r} \\ \dot{\bar{\bar{u}}}^{n,t}_{m\,s\,r} \end{bmatrix} = \frac{1}{\sqrt{2\overset{n}{m}}} \sum_{x=1}^{\overset{n}{m}} \sum_{h=0}^{\infty} \begin{bmatrix} \left\{(z_{s\,r})^{\overline{x-1}}\right\}^{-2\overline{h+1}} \\ \left\{(z_{s\,r})^{\overline{x-1}}\right\}^{1-2\overline{h+1}} \\ \left\{(z_{s\,r})^{\overline{x-1}}\right\}^{2-2\overline{h+1}} \\ \vdots \\ \left\{(z_{s\,r})^{\overline{x-1}}\right\}^{(\overline{m-2}-2\overline{h+1})} \\ \left\{(z_{s\,r})^{\overline{x-1}}\right\}^{(\overline{m-1}-2\overline{h+1})} \end{bmatrix} \dot{\bar{\bar{U}}}^{x}_{s\,r\ \overline{2h+1}} \exp j(\overline{2h+1}\ \omega_{s\,r}t) +$$

$$+\begin{bmatrix} \left\{(z_{sr})^{\overline{x-1}}\right\}^{\overline{2h+1}} \\ \left\{(z_{sr})^{\overline{x-1}}\right\}^{1+\overline{2h+1}} \\ \left\{(z_{sr})^{\overline{x-1}}\right\}^{2+\overline{2h+1}} \\ \vdots \\ \left\{(z_{sr})^{\overline{x-1}}\right\}^{(\overline{\frac{n}{m}-2}+\overline{2h+1})} \\ \left\{(z_{sr})^{\overline{x-1}}\right\}^{(\overline{\frac{n}{m}-1}+\overline{2h+1})} \end{bmatrix} \dot{\underline{U}}^{x*}_{sr\,\overline{2h+1}} \exp -j(\overline{2h+1}\ \omega_{sr} t) \Bigg) \qquad 3.26$$

In the case that no switching occurs, the instantaneous symmetrical component voltages, found from 3.8b and 3.24, will reduce to:

$$\begin{bmatrix} u^{\bullet 1,z}_{sr} \\ u^{\bullet 2,t}_{sr} \\ u^{\bullet 3,z}_{sr} \\ \vdots \\ u^{\bullet \frac{n}{m}-1,z}_{sr} \\ u^{\bullet \frac{n}{m},t}_{sr} \end{bmatrix} = \frac{1}{\sqrt{2\frac{n}{m}}} \sum_{x=1}^{\frac{n}{m}} \begin{bmatrix} (z_{sr})^{-\overline{x-1}} \\ 1 \\ (z_{sr})^{\overline{x-1}} \\ \vdots \\ (z_{sr})^{(\overline{\frac{n}{m}-3}).\overline{x-1}} \\ (z_{sr})^{(\overline{\frac{n}{m}-2}).\overline{x-1}} \end{bmatrix} \dot{U}^{x}_{sr} \exp j\omega_{sr} t \ + \qquad 3.27$$

$$+ \left[\begin{array}{c} (z_{sr})^{\overline{x-1}} \\ (z_{sr})^{\overline{2x-1}} \\ (z_{sr})^{\overline{3x-1}} \\ \vdots \\ (z_{sr})^{\overline{\frac{n}{m}-1}.\overline{x-1}} \\ (z_{sr})^{\overline{\frac{n}{m}}\,\overline{x-1}} \end{array} \right] \hat{U}_{sr}^{x\#} \exp -j\omega_r t_s \Bigg) \qquad 3.27$$

It is clearly to be noted that the general coefficients $(\bar{\bar{U}}_{sr}^{x}{}_{\overline{2h+1}})$ are to be determined from the known product of the switching function S(t) and the supply vector $\left[u_{sr}^{\frac{m}{n}} g \right]$, and the induced excitation in the x-th phase. This gives an indication under which conditions one may expect to solve the equations by expressing the excitation function on the controlled electrical ports of the machine as a complex Fourier series. This will only be successful under constraints of constant speed, and constant switching frequency. As soon as speed changes are allowed it will not be possible to express the induced voltage on the controlled ports explicitly as a function of time.

3.3.7 *GENERAL SOLUTIONS FOR STATOR AND ROTOR CURRENTS.*

In multiphase electrical power systems it is universally attempted to supply a voltage being a simple harmonic function of time, and to observe this restriction also as far as possible for the currents. It is therefore extremely important to know the harmonic power drawn from the supply by electronically controlled electrical machines. From the viewpoint of interference of machine-electronic systems with other equipment (telecommunications for instance) and with its own functioning, the harmonic frequency spectra of the currents and voltages are also important. Furthermore the electrical machine designer prefers accurate prediction of the harmonic content of the currents and voltages in the machine, in order to adapt the design to the detrimental effects caused by the inevitable deviation of the materials and construction from the ideal conditions set out in section 3.2.

These arguments serve to illustrate that in the systems at present under investigation it is important to know the Fourier-components of current and voltage. This section will be devoted to solve for the currents directly in terms of these components by employing the excitation functions of the previous section.

The (n+m-4) zero equations for stator and rotor may be solved for the steady-state currents when the input voltages are known. This can only be done under a constraint of constant mechanical angular speed (in spite of the absence of terms indicating a coupling between rotor and stator in these equations), for those zero equations related to the controlled electrical ports.

Before it is possible to obtain the currents in the case of the 4 conversion equations the inverse operational impedance matrix must be derived. The impedance matrix for the conversion equations contains variable elements in terms of the mechanical angular speed. In order to be able to determine the steady-state currents as a sum of their respective Fourier components the constraint will be applied that

$$\frac{d\theta}{dt} = \text{constant} = \omega_m \qquad 3.28a$$

Therefore the speed-dependent terms of relations 3.20c and 3.22c become

$$(D \pm jpD\theta) = (D \pm jp\omega_m) \qquad 3.28b$$

Now consider the zero currents in the circuits not related to the controlled electrical ports. For these circuits the yth transformed current may be found from relations 3.19, 3.21 and 3.24 as:

$$i^{y,z}_{s_r} = \frac{1}{\sqrt{2^{n}_{m}}} \sum_{x=1}^{\overline{n \atop m-1}} \left(\left\{ (z_{s_r})^{\overline{y-2}^{x-1}} \right\} I^{z\ xy}_{s_r} \exp j\omega_{s_r} t + \left\{ (z_{s_r})^{\overline{y}^{x-1}} \right\} I^{z,xy*}_{s_r} \exp -j\omega_{s_r} t \right) \qquad 3.29a$$

where $y = (1,3,4, \text{----} \overline{n \atop m-1})$

$$I^{z,xy}_{s_r} = U^{x}_{s_r} \left((R_{s_r})^2 + (\omega_{s_r} L^{y}_{s})^2 \right)^{-\frac{1}{2}} \exp -j(\theta_{s_r} + \psi^{y}_{s_r}) \qquad 3.29b$$

$$\tan \psi^{y}_{s_r} = \frac{(\omega_{s_r} L^{y}_{s})}{(R_{s_r})} \qquad 3.29c$$

The zero-currents in the remaining n-2, or m-2 equations related to the controlled ports are then represented by:

$$\dot{I}^{y,z}_{s\,r} = \frac{1}{\sqrt{2\overline{m}^{n}}} \sum_{x=1}^{n} \sum_{h=0}^{\infty} \left(\left\{ (z_{s\,r})^{\overline{x-1}} \right\}^{\overline{y-1}-\overline{2h+1}} \dot{I}^{z,xy}_{s\,r\;\overline{2h+1}} \exp j(\overline{2h+1}\ \omega_{s\,r} t) + \right.$$

$$\left. + \left\{ (z_{s\,r})^{\overline{x-1}} \right\}^{\overline{y-1}+\overline{2h+1}} \dot{I}^{z,xy*}_{s\,r\;\overline{2h+1}} \exp -j(\overline{2h+1}\ \omega_{s\,r} t) \right) \qquad 3.30a$$

$$y = (1,3,4\ \text{------}\ \overline{n-1})$$

$$\dot{I}^{z,xy}_{s\,r\;2h+1} = \bar{U}^{x}_{s\,r\;\overline{2h+1}} \left((R_{s\,r})^2 + (\overline{2h+1}\ \omega_{s\,r} L^{y}_{s\,r})^2 \right)^{-\frac{1}{2}} \exp -j \left(\theta_{s\,r\;\overline{2h+1}} + \psi^{y}_{s\,r\;2h+1} \right) \qquad 3.30b$$

$$\tan \psi^{y}_{s\,r\;\overline{2h+1}} = \frac{(\overline{2h+1}\ \omega_{s\,r} L^{y}_{s\,r})}{(R_{s\,r})} \qquad 3.30c$$

when taking into account the above relations and relation 3.26.

To obtain the conversion currents it will be necessary to distinguish between stator-controlled and rotor-controlled transducers. Consider the stator-controlled transducers. From 3.20:

$$\left[\dot{i}^{t}_{s\,r} \right]^{ks} = \left(\left[Z^{t} \right]^{ks} \right)^{-1} \left[\dot{u}^{t}_{s\,r} \right]^{ks} \qquad 3.31$$

Consider eq. 3.20c; from the definitions of $L^{2}_{s\,r}$ and $L^{m}_{n\;s\,r}$ follows

$$L^{2}_{s\,r} = \sum_{v=1}^{n} (z_{s\,r})^{-\overline{v-1}} L_{ss\,rr}\,av = \sum_{v=1}^{n} (z_{s\,r})^{-\overline{n-1}.\overline{v-1}} L_{ss\,rr}\,av = L^{m}_{n\;s\,r} = L_{s\,r} \qquad 3.32$$

Therefore :

$$\left[Z^t\right]^{ks} = \begin{bmatrix} Z_{sD} & 0 & \sqrt{\frac{nm}{4}}M_{sr}D & 0 \\ 0 & Z_{sD} & 0 & \sqrt{\frac{nm}{4}}M_{sr}D \\ \sqrt{\frac{nm}{4}}M_{sr}(D-jp\omega_m) & 0 & Z_{rD}^{-} & 0 \\ 0 & \sqrt{\frac{nm}{4}}M_{sr}(D+jp\omega_m) & 0 & Z_{rD}^{+} \end{bmatrix} \qquad 3.33a$$

the elements being specified by:

$$\left.\begin{aligned} Z_{sD} &= (R_s + L_s D) \\ Z_{rD}^{\mp} &= R_r + L_r(D \mp jp\omega_m) \end{aligned}\right\} \qquad 3.33b$$

Taking $\left[Z^t\right]_t^{ks}$, and calculating the appropriate cofactors, the inverse matrix is as in. 3.34. The currents in the conversion equations as transformed to the stator is then expressed in terms of this operational admittance matrix, taking into account that the stator excitation will be influenced by switching.

$$\left(\left[Z^t\right]^{ks}\right)^{-1} = \begin{bmatrix} \frac{1}{Z_D^{ks-}} & 0 & -\frac{\sqrt{\frac{nm}{4}}M_{sr}D}{Z_{rD}^{-}Z_D^{ks-}} & 0 \\ 0 & \frac{1}{Z_D^{ks+}} & 0 & -\frac{\sqrt{\frac{nm}{4}}M_{sr}D}{Z_{rD}^{+}Z_D^{ks+}} \\ -\frac{\sqrt{\frac{nm}{4}}M_{sr}(D-jp\omega_m)}{Z_{rD}^{-}Z_D^{ks-}} & 0 & \frac{Z_{sD}}{Z_{rD}^{-}Z_D^{ks-}} & 0 \\ 0 & -\frac{\sqrt{\frac{nm}{4}}M_{sr}(D+jp\omega_m)}{Z_{rD}^{+}Z_D^{ks+}} & 0 & \frac{Z_{sD}}{Z_{rD}^{+}Z_D^{ks+}} \end{bmatrix} \qquad 3.34a$$

The impedance $Z_D^{ks\mp}$ is represented by

$$Z_D^{ks\mp} = \left\{ Z_{sD} - \frac{\frac{nm}{4}(M_{sr})^2 D(D \mp jp\omega_m)}{Z_{rD}^{\mp}} \right\} \qquad 3.34b$$

Since

$$\theta = \int_0^t \theta dt + \theta_o = (\omega_m t + \theta_o) \qquad 3.35$$

from relation 3.28a, the final solutions for the stator and rotor currents in the stator-controlled system (rotor-stator transformed) upon expanding eq. 3.31 are:

$$\dot{\underline{i}}_s^{2\bar{n},t} = \frac{\dot{\underline{u}}_s^{2\bar{n},t}}{Z_D^{ks\mp}} - \frac{\sqrt{\frac{nm}{4}} M_{sr} D}{Z_{rD}^{\mp} Z_D^{ks\mp}} \cdot \dot{u}_r^{n\bar{m},t} \exp \mp j(p\overline{\omega_m t + \theta_o}) \qquad 3.36a$$

$$\dot{i}_r^{2\bar{m},t} \exp \mp j(p\overline{\omega_m t + \theta_o}) = -\frac{\sqrt{\frac{nm}{4}} M_{sr}(D \mp jp\omega_m)}{Z_{rD}^{\mp} Z_D^{ks\mp}} \cdot \dot{\underline{u}}_s^{2\bar{n},t} +$$

$$+ \frac{Z_{sD}}{Z_{rD}^{\mp} Z_D^{ks\mp}} \cdot \dot{u}_r^{2\bar{m},t} \exp \mp j(p\overline{\omega_m t + \theta_o}) \qquad 3.36b$$

Formulation of explicit expressions is to be undertaken in the next paragraph. The true stator and rotor currents may then be found from the inverse transformation of 3.29a, 3.30a, 3.36a and 3.36b if necessary.

Now turning our attention to the equations transformed to the rotor, an analogous expression for the conversion currents as in the previous case is obtained.

$$\left[\dot{i}_{sr}^{t}\right]^{kr} = \left(\left[Z^{t}\right]^{kr}\right)^{-1} \cdot \left[\dot{u}_{sr}^{t}\right]^{kr} \qquad 3.37$$

By noting the equivalence of inductances in the relation 3.22c according to eq. 3.32 it is obtained that:

$$\left[Z^t\right]^{kr} = \begin{bmatrix} Z^+_{sD} & 0 & \sqrt{\frac{nm}{4}}M_{sr}(D+jp\omega_m) & 0 \\ 0 & Z^-_{sD} & 0 & \sqrt{\frac{nm}{4}}M_{sr}(D-jp\omega_m) \\ \sqrt{\frac{nm}{4}}M_{sr}D & 0 & Z_{rD} & 0 \\ 0 & \sqrt{\frac{nm}{4}}M_{sr}D & 0 & Z_{rD} \end{bmatrix} \qquad 3.38a$$

$$\left.\begin{aligned} \text{with } Z_{rD} &= (R_r + L_r D) \\ Z^{\mp}_{sD} &= R_s + L_s(D \mp jp\omega_m) \end{aligned}\right\} \qquad 3.38b$$

From $\left[Z^t\right]^{kr}_t$ and the appropriate cofactors the inverse is calculated as:

$$\left(\left[Z^t\right]^{kr}\right)^{-1} = \begin{bmatrix} \frac{Z_{rD}}{Z^+_{sD}Z^{kr+}_D} & 0 & -\frac{\sqrt{\frac{nm}{4}}M_{sr}(D+jp\omega_m)}{Z^+_{sD}Z^{kr+}_D} & 0 \\ 0 & \frac{Z_{rD}}{Z^-_{sD}Z^{kr-}_D} & 0 & -\frac{\sqrt{\frac{nm}{4}}M_{sr}(D-jp\omega_m)}{Z^-_{sD}Z^{kr-}_D} \\ -\frac{\sqrt{\frac{nm}{4}}M_{sr}D}{Z^+_{sD}Z^{kr+}_D} & 0 & \frac{1}{Z^{kr+}_D} & 0 \\ 0 & -\frac{\sqrt{\frac{nm}{4}}M_{sr}D}{Z^-_{sD}Z^{kr-}_D} & 0 & \frac{1}{Z^{kr-}_D} \end{bmatrix} \qquad 3.39a$$

$$Z^{kr\mp}_D = \left\{ Z_{rD} - \frac{\frac{nm}{4}(M_{sr})^2 D(D\mp jp\omega_m)}{Z^{\mp}_{sD}} \right\} \qquad 3.39b$$

It is now possible to expand eq. 3.37, and to obtain the stator and rotor currents for the rotor-controlled system (stator-rotor transformed) as:

$$\dot{\underline{i}}^{2}_{s}{}^{\underline{n},t}\exp\underline{+}j(p\overline{\omega_m t + \theta_o}) = \frac{Z_{rD}}{\underline{+}\,Z_{sD}Z_D^{kr\underline{+}}}\,\dot{\underline{u}}^{2}_{s}{}^{\underline{n},t}\exp\underline{+}j(p\overline{\omega_m t + \theta_o}) -$$

$$-\frac{\sqrt{\frac{nm}{4}}M_{sr}(D\underline{+}jp\omega_m)}{\underline{+}\,Z_{sD}Z_D^{kr\underline{+}}}\;\dot{\underline{u}}^{2}_{r}{}^{\underline{m},t} \qquad 3.40a$$

and

$$\dot{\underline{i}}^{2}_{r}{}^{\underline{m},t} = -\frac{\sqrt{\frac{nm}{4}}M_{sr}D}{\underline{+}\,Z_{sD}Z_D^{kr\underline{+}}}\cdot\dot{\underline{u}}^{2}_{s}{}^{\underline{n},t}\exp\underline{+}j(p\overline{\omega_m t + \theta_o}) + \frac{\dot{\underline{u}}^{2}_{r}{}^{\underline{m},t}}{Z_D^{kr\underline{+}}} \qquad 3.40b$$

Formulation of explicit expressions is to be undertaken in the next paragraph. The rotor and stator currents may be found from the inverse transformation of 3.29a, 3.30a and 3.40a and 3.40b if necessary.

3.3.8 *INVESTIGATION OF EXPRESSIONS FOR CURRENT AND TORQUE UNDER CONDITIONS OF PERIODICAL SWITCHING.*

Relations for the currents in terms of the excitation functions and transformed operational winding impedances are now known. By employing symmetry characteristics of the excitation function and evaluating the actual transformed impedances it is possible to obtain exact expressions for the currents, and consequently arrive at an explicit expression for instantaneous and mean electromagnetic torque. These calculations for the case of stator-switched electromechanical transducers will now be pursued in the present paragraph.

As already stated in the course of this chapter the equations for the electromechanical converter under control by stator switching are all referred to the stator coordinate system. The general relations have been obtained (3.36a and 3.36b), and will now be examined in more detail.

From rel. 3.26 the instantaneous symmetrical component voltages for the switched stator circuits are:

$$\begin{bmatrix} \dot{\underline{u}}^{2}_{s}{}^{2,t} \\ \\ \dot{\underline{u}}^{2}_{s}{}^{\underline{n},t} \end{bmatrix} = \frac{1}{\sqrt{2n}}\sum_{x=1}^{n}\sum_{h=0}^{\infty}\begin{bmatrix} \left\{(z_s)^{\overline{x-1}}\right\}^{1-\overline{2h+1}} \\ \\ \left\{(z_s)^{\overline{x-1}}\right\}^{\overline{n-1}-\overline{2h+1}} \end{bmatrix}\dot{\underline{U}}^{x}_{s}\;\frac{}{2h+1}\exp j(\overline{2h+1}\;\omega_s t) + \qquad 3.41a$$

$$+\left[\begin{array}{c}\left\{(z_s)^{\overline{x-1}}\right\}^{1+\overline{2h+1}}\\ \\ \left\{(z_s)^{\overline{x-1}}\right\}^{\overline{n-1}+\overline{2h+1}}\end{array}\right]\dot{\underline{\underline{U}}}^{x*}_{s}\,\frac{}{2h+1}\exp -j(\overline{2h+1}\ \omega_s t)\Bigg\}$$

The rotor circuits are not switched and consequently the instantaneous symmetrical voltage components reduce to:

$$\left[\begin{array}{c}\dot{u}^{2,t}_{r}\\ \\ \dot{u}^{m,t}_{r}\end{array}\right]=\frac{1}{\sqrt{2m}}\sum_{x=1}^{m}\Bigg\{\left[\begin{array}{c}1\\ \\ (z_r)^{\overline{m-2}.\overline{x-1}}\end{array}\right]\dot{U}^{x}_{r}\exp j\omega_r t+$$

3.41b

$$+\left[\begin{array}{c}(z_r)^{2\overline{x-1}}\\ \\ (z_r)^{m\overline{x-1}}\end{array}\right].\ \dot{U}^{x*}_{r}\exp -j\omega_r t\Bigg\}$$

It has already been noted that a characteristic of the Fortescue transformation is that the first and second sequence ("positive" and "negative" sequence) components, concerned with the conversion equations, are complex conjugates (rel. 3.18c). Performing the Ku-transformation on the rotor voltages and taking the complex relationship into account, the two previous equations change to:

$$\begin{bmatrix} \dot{\bar{u}}_{s}^{2,t} \\ \\ \\ \dot{\bar{u}}_{s}^{n,t} \end{bmatrix} =$$

3.41c

$$= \frac{1}{\sqrt{2n}} \sum_{x=1}^{n} \sum_{h=0}^{\infty} \begin{bmatrix} \dot{\bar{V}}_{s}^{xp} \frac{}{\sqrt{2h+1}} \exp j(\sqrt{2h+1}\ \omega_s t) + \dot{\bar{V}}_{s}^{xn*} \frac{}{\sqrt{2h+1}} \exp -j(\sqrt{2h+1}\ \omega_s t) \\ \\ \dot{\bar{V}}_{s}^{xn} \frac{}{\sqrt{2h+1}} \exp j(\sqrt{2h+1}\ \omega_s t) + \dot{\bar{V}}_{s}^{xp*} \frac{}{\sqrt{2h+1}} \exp -j(\sqrt{2h+1}\ \omega_s t) \end{bmatrix}$$

and

$$\begin{bmatrix} \dot{u}_{r}^{2,t\ ks} \\ \\ \\ \dot{u}_{r}^{m,t\ ks} \end{bmatrix} =$$

3.41d

$$= \frac{1}{\sqrt{2m}} \sum_{x=1}^{m} \begin{bmatrix} \dot{V}_{r}^{xp} \exp j(\omega_s t + p\theta_o) + \dot{V}_{r}^{xn*} \exp -j(\sqrt{\omega_s - 2p\omega_m}\, t - p\theta_o) \\ \\ \dot{V}_{r}^{xn} \exp j(\sqrt{\omega_s - 2p\omega_m}\, t - p\theta_o) + \dot{V}_{r}^{xp*} \exp -j(\omega_s t + p\theta_o) \end{bmatrix}$$

(See appendix A3.1)

If the conversion currents in the stator are expressed as:

$$\begin{bmatrix} \dot{\underline{i}}^{2,t}_{s} \\ \\ \dot{\underline{i}}^{n,t}_{s} \end{bmatrix} = \begin{bmatrix} \dot{\underline{i}}^{2,t}_{ss}(\underline{u}^{2,t}_{s}) + \dot{i}^{2,t}_{sr}(u^{2,t\ ks}_{r}) \\ \\ \dot{\underline{i}}^{n,t}_{ss}(\underline{u}^{n,t}_{s}) + \dot{i}^{n,t}_{sr}(u^{m,t\ ks}_{r}) \end{bmatrix} \qquad 3.42a$$

it may be shown (see appendix A3.1) that these currents have the form:

$$\begin{bmatrix} \dot{\underline{i}}^{2,t}_{s} \\ \\ \dot{\underline{i}}^{n,t}_{s} \end{bmatrix} = \frac{1}{\sqrt{2n}} \sum_{x=1}^{n} \sum_{h=0}^{\infty} \begin{bmatrix} \dot{\underline{I}}^{xp}_{s\ \overline{2h+1}} \exp j(\overline{2h+1}\ \omega_s t) + \dot{\underline{I}}^{xn*}_{s\ \overline{2h+1}} \exp -j(\overline{2h+1}\ \omega_s t) \\ \\ \dot{\underline{I}}^{xn}_{s\ \overline{2h+1}} \exp j(\overline{2h+1}\ \omega_s t) + \dot{\underline{I}}^{xp*}_{s\ \overline{2h+1}} \exp -j(\overline{2h+1}\ \omega_s t) \end{bmatrix}$$

$$+ \frac{1}{\sqrt{2m}} \sum_{x=1}^{m} \begin{bmatrix} \dot{I}^{xp}_{sr} \exp j\omega_s t + \dot{I}^{xn*}_{sr} \exp -j(\overline{\omega_s - 2p\omega_m} t) \\ \\ \dot{I}^{xn}_{sr} \exp j(\overline{\omega_s - 2p\omega_m} t) + \dot{I}^{xp*}_{sr} \exp -j\omega_s t \end{bmatrix} \qquad 3.42b$$

with the components due to stator excitation being

$$\dot{\underline{I}}^{xp}_{s\ \overline{2h+1}} = \frac{\dot{\underline{V}}^{xp}_{s\ \overline{2h+1}}}{\left\{ R^{p}_{s\ \overline{2h+1}} + j\ X^{p}_{s\ \overline{2h+1}} \right\}} = \frac{\dot{\underline{V}}^{xp}_{s\ \overline{2h+1}}}{\dot{Z}^{p}_{s\ \overline{2h+1}}}$$

$$R^{p}_{s\ \overline{2h+1}} = \left[R_s + \frac{\overline{2h+s}.\overline{2h+1}\ R_r.nm\ X^2_M}{4(R^2_r + \overline{2h+s}^2\ X^2_r)} \right] \qquad 3.42c$$

$$X^{p}_{s\ 2h+1} = \overline{2h+1} \left[X_s - \frac{\overline{2h+s}^2\ X_r\ nm\ X^2_M}{4(R^2_r + \overline{2h+s}^2\ X^2_r)} \right]$$

where $X_s = 2\pi f_s L_s$; $X_r = 2\pi f_s L_r$; $X_M = 2\pi f_s M_{sr}$

$$\dot{\underline{I}}^{xn}_{s\ \overline{2h+1}} = \frac{\bar{\bar{V}}^{xn}_{s\ \overline{2h+1}}}{\left\{R^{n}_{s\ \overline{2h+1}} + j\ X^{n}_{s\ \overline{2h+1}}\right\}} = \frac{\bar{\bar{V}}^{xn}_{s\ \overline{2h+1}}}{\dot{Z}^{n}_{s\ \overline{2h+1}}}$$

$$R^{n}_{s\ \overline{2h+1}} = \left[R_s + \frac{\overline{2h+1}.\overline{2h+2-s}\ R_r.nm\ X_M^2}{4(R_r^2 + \overline{2h+2-s}^2\ X_r^2}\right] \qquad 3.42c$$

$$X^{n}_{s\ \overline{2h+1}} = \overline{2h+1}\left[X_s - \frac{\overline{2h+2-s}^2\ X_r\ nm\ X_M^2}{4(R_r^2 + \overline{2h+2-s}^2\ X_r^2}\right]$$

The components due to the rotor excitation are correspondingly:

$$\dot{I}^{xp}_{sr} = -\frac{\dot{V}^{xp}_{r}\exp jp\theta_o}{\left\{R^{p}_{sr} - j\ X^{p}_{sr}\right\}} = -\frac{\dot{V}^{xp}_{r}\exp jp\theta_o}{\dot{Z}^{p}_{sr}}$$

$$\dot{I}^{xn}_{sr} = \frac{\dot{V}^{xn}_{r}\exp - jp\theta_o}{\left\{R^{n}_{sr} - j\ X^{n}_{sr}\right\}} = \frac{\dot{V}^{xn}_{r}\exp - jp\theta_o}{\dot{Z}^{n}_{sr}}$$

with

$$R^{p}_{sr} = \left(\sqrt{\frac{nm}{4}}\ X_M\right)^{-1}\ (sR_sX_r + R_rX_s) \qquad 3.42d$$

$$X^{p}_{sr} = \left(\sqrt{\frac{nm}{4}}\ X_M\right)^{-1}\left[R_sR_r + s\left(\frac{nmX_M^2}{4} - X_rX_s\right)\right]$$

and

$$R^{n}_{sr} = \left(\sqrt{\frac{nm}{4}}\ \overline{1-2s}\ X_M\right)^{-1}\ (sR_sX_r - \overline{1-2s}\ R_rX_s)$$

$$X^{n}_{sr} = \left(\sqrt{\frac{nm}{4}}\ \overline{1-2s}\ X_M\right)^{-1}\left[R_sR_r + 5.\overline{1-2s}\left(\frac{nmX_M^2}{4} - X_rX_s\right)\right]$$

Similarly the stator-transformed rotor conversion currents are:

$$\begin{bmatrix} \dot{i}_r^{2,t\ ks} \\ \\ \\ \dot{i}_r^{m,t\ ks} \end{bmatrix} = \begin{bmatrix} \underline{\dot{I}}_{rs}^{2,t\ ks}(\underline{u}_s^{2,t}) + i_{rr}^{2,t\ ks}(u_r^{2,t\ ks}) \\ \\ \\ \underline{\dot{I}}_{rs}^{m,t\ ks}(\underline{u}_s^{n,t}) + i_{rr}^{m,t\ ks}(u_r^{m,t\ ks}) \end{bmatrix} \qquad 3.43a$$

As indicated in appendix A3.1 these currents are now to be expressed as:

$$\begin{bmatrix} \dot{i}_r^{2,t\ ks} \\ \\ \\ \dot{i}_r^{m,t\ ks} \end{bmatrix} = \frac{1}{\sqrt{2n}} \sum_{x=1}^{n} \sum_{h=0}^{\infty} \begin{bmatrix} \dot{I}_r^{xp} \frac{}{\sqrt{2h+1}} \exp j(\overline{2h+1}\ \omega_s t) + \dot{I}_r^{xn*} \frac{}{\sqrt{2h+1}} \exp -j(\overline{2h+1}\ \omega_s t) \\ \\ \\ \dot{I}_r^{xn} \frac{}{\sqrt{2h+1}} \exp j(\overline{2h+1}\ \omega_s t) + \dot{I}_r^{xp*} \frac{}{\sqrt{2h+1}} \exp -j(\overline{2h+1}\ \omega_s t) \end{bmatrix}$$

$$3.43b$$

$$+ \frac{1}{\sqrt{2m}} \sum_{x=1}^{m} \begin{bmatrix} \dot{I}_{rr}^{xp} \exp j\omega_s t + \dot{I}_{rr}^{xn*} \exp -j(\overline{\omega_s - 2p\omega_m}\ t) \\ \\ \\ \dot{I}_{rr}^{xn} \exp j(\overline{\omega_s - 2p\omega_m}\ t) + \dot{I}_{rr}^{xp*} \exp -j\omega_s t \end{bmatrix}$$

where the complex amplitudes for the currents due to stator excitation are:

$$\dot{I}^{xp}_{r\ \overline{2h+1}} = -\frac{\dot{\hat{V}}^{xp}_{s\ \overline{2h+1}}}{\dot{Z}^{p}_{sr\ \overline{2h+1}}}$$

with

$$Z^{p}_{sr\ \overline{2h+1}} = (\overline{2h+s}\sqrt{\frac{nm}{4}}\,X_M)^{-1}\left[\overline{2h+s}\,X_r - jR_r\right].\,\dot{Z}^{p}_{s\ \overline{2h+1}}$$

$$\dot{I}^{xn}_{r\ \overline{2h+1}} = \frac{\dot{\hat{V}}^{xn}_{s\ \overline{2h+1}}}{\dot{Z}^{n}_{sr\ \overline{2h+1}}}$$

$$\dot{Z}^{n}_{sr\ \overline{2h+1}} = (\overline{2h+2-s}\sqrt{\frac{nm}{4}}\,X_M)^{-1}\left[\overline{2h+2-s}\,X_r - jR_r\right].\,\dot{Z}^{n}_{s\ \overline{2h+1}}$$

3.43c

Correspondingly the components resulting from rotor excitation may be given by:

$$\dot{I}^{xp}_{rr} = \frac{\dot{V}^{xp}_{r}\exp jp\theta_o}{\left\{R^{p}_{rr} + j\,X^{p}_{rr}\right\}} = \frac{\dot{V}^{xp}_{r}\exp jp\theta_o}{\dot{Z}^{p}_{rr}}$$

$$R^{p}_{rr} = \left[R_r + \frac{sR_s\ nm\ X_M^2}{4(R_s^2 + X_s^2)}\right];\quad X^{p}_{rr} = \left[sX_r - \frac{sX_s\ nm\ X_M^2}{4(R_s^2 + X_s^2)}\right]$$

3.43d

and

$$\dot{I}^{xn}_{rr} = \frac{\dot{V}^{xn}_{r}\exp -jp\theta_o}{\left\{R^{n}_{rr} + j\,X^{n}_{rr}\right\}} = \frac{\dot{V}^{xn}_{r}\exp -jp\theta_o}{\dot{Z}^{n}_{rr}}$$

$$R^{n}_{rr} = R_r - \frac{s.\overline{1-2s}\ R_s\ nm\ X_M^2}{4(R_s^2 + \overline{1-2s}^2\ X_s^2}$$

$$X^{n}_{rr} = sX_r - \frac{s.\overline{1-2s}^2\ X_s\ nm\ X_M^2}{4(R_s^2 + \overline{1-2s}^2\ X_s^2)}$$

Since the components of all the instantaneous symmetrical component currents in rotor and stator are now known, it is possible to investigate the relation for the electromagnetic torque further for steady state operation of the electromechanical energy transducer. By substitution of equation 3.42b and equation 3.43b into relation 3.17a the instantaneous electromagnetic torque is obtained as: (see Appendix A3.1)

$$T_e = jp\sqrt{\frac{nm}{4}}\,M_{sr}\left[\left\{\frac{1}{2n}\sum_{y=1}^{n}\sum_{x=1}^{n}\sum_{h=0}^{\infty}\left(\dot{\bar{I}}^{yn}_{s\ \overline{2h+1}}.\dot{I}^{xp}_{r\ \overline{2h+1}}\exp j2(\overline{2h+1}\ \omega_s t)\right.\right.\right.$$

$$\left.\left.\left.+\ \dot{\bar{I}}^{yn}_{s\ \overline{2h+1}}.\dot{I}^{xn*}_{r\ \overline{2h+1}}+\dot{\bar{I}}^{yp*}_{s\ \overline{2h+1}}.\dot{I}^{xp}_{r\ \overline{2h+1}}+\dot{\bar{I}}^{yp*}_{s\ \overline{2h+1}}-\dot{I}^{xn*}_{r\ \overline{2h+1}}\exp -j2(\overline{2h+1}\ \omega_s t)\right)\right.$$

$$+\frac{1}{2\sqrt{nm}}\sum_{y=1}^{n}\sum_{x=1}^{m}\sum_{h=0}^{\infty}\left(\dot{\bar{I}}^{yn}_{s\ \overline{2h+1}}.\dot{I}^{xp}_{rr}\exp j2(\overline{h+1}\ \omega_s t)+\right.$$

$$+\ \dot{\bar{I}}^{yn}_{s\ \overline{2h+1}}.\dot{I}^{xn*}_{rr}\exp j2(\overline{h+1-s}\ \omega_s t)$$

$$\left.+\ \dot{\bar{I}}^{yp*}_{s\ \overline{2h+1}}.\dot{I}^{xp}_{rr}\exp -j2h\omega_s t+\dot{\bar{I}}^{yp*}_{s\ \overline{2h+1}}\dot{I}^{xn*}_{rr}\exp -j2(\overline{h+s}\omega_s t)\right)$$

$$+\frac{1}{2\sqrt{mn}}\sum_{y=1}^{m}\sum_{x=1}^{n}\sum_{h=0}^{\infty}\left(\dot{I}^{yn}_{sr}.\dot{I}^{xp}_{r\ \overline{2h+1}}\exp j2(\overline{h+s}\omega_s t)+\right.$$

$$+\ \dot{I}^{yn}_{sr}.\dot{I}^{xn*}_{r\ \overline{2h+1}}\exp -j2(\overline{h+1-s}\omega_s t)$$

$$\left.+\ \dot{I}^{yp*}_{sr}.\dot{I}^{xp}_{r\ \overline{2h+1}}\exp j2h\omega_s t+\dot{I}^{yp*}_{sr}.\dot{I}^{xn*}_{r\ \overline{2h+1}}\exp -j2(\overline{h+1}\ \omega_s t)\right)$$

$$+\frac{1}{2m}\sum_{y=1}^{m}\sum_{x=1}^{m}\left(\dot{I}^{yn}_{sr}.\dot{I}^{xp}_{rr}\exp j2s\omega_s t + \dot{I}^{yn}_{sr}.\dot{I}^{xn*}_{rr}\right.$$

$$\left.+\dot{I}^{yp*}_{sr}.\dot{I}^{xp}_{rr} - \dot{I}^{yp*}_{sr}.\dot{I}^{xn*}_{rr}\exp -j2s\omega_s t\right)\Bigg\}$$

$$-\Bigg\{\frac{1}{2n}\sum_{y=1}^{n}\sum_{x=1}^{n}\sum_{h=0}^{\infty}\left(\dot{\bar{I}}^{yp}_{s\ \overline{2h+1}}.\dot{I}^{xn}_{r\ \overline{2h+1}}\exp j2(\overline{2h+1}\ \omega_s t)+\dot{\bar{I}}^{yp}_{s\ \overline{2h+1}}.\dot{I}^{xp*}_{r\ \overline{2h+1}}\right.$$

$$\left.+\dot{\bar{I}}^{yn*}_{s\ \overline{2h+1}}.\dot{I}^{xn}_{r\ \overline{2h+1}} + \dot{\bar{I}}^{yn*}_{s\ \overline{2h+1}}.\dot{I}^{xp*}_{r\ \overline{2h+1}}\exp -j2(\overline{2h+1}\ \omega_s t)\right)$$

$$+\frac{1}{2\sqrt{nm}}\sum_{y=1}^{n}\sum_{x=1}^{m}\sum_{h=0}^{\infty}\left(\dot{\bar{I}}^{yp}_{s\ \overline{2h+1}}.\dot{I}^{xn}_{rr}\exp j2(\overline{h+s}\omega_s t) +\right.$$

$$+\dot{\bar{I}}^{yp}_{s\ \overline{2h+1}}.\dot{I}^{xp*}_{rr}\exp j2h\omega_s t$$

$$\left.+\dot{\bar{I}}^{yn*}_{s\ \overline{2h+1}}.\dot{I}^{xn}_{rr}\exp -j2(\overline{h+1-s}\omega_s t) + \dot{\bar{I}}^{yn*}_{s\ \overline{2h+1}}\dot{I}^{xp*}_{rr}\exp -j2(\overline{h+1}\ \omega_s t)\right)$$

$$+\frac{1}{2\sqrt{mn}}\sum_{y=1}^{m}\sum_{x=1}^{n}\sum_{h=0}^{\infty}\Bigg(\dot{I}_{sr}^{yp}.\dot{I}_{r}^{xn}\frac{}{\sqrt{2h+1}}\exp j2(\sqrt{h+1}\ \omega_s t)+$$

$$+\dot{I}_{sr}^{yp}\dot{I}_{r}^{xp*}\frac{}{\sqrt{2h+1}}\exp -j2h\omega_s t$$

$$+\dot{I}_{sr}^{yn*}.\dot{I}_{r}^{xn}\frac{}{\sqrt{2h+1}}\exp j2(\sqrt{h+1-s}\omega_s t)+\dot{I}_{sr}^{yn*}.\dot{I}_{r}^{xp*}\frac{}{\sqrt{2h+1}}\exp -j2(\sqrt{h+s}\omega_s t)\Bigg)$$

$$+\frac{1}{2m}\sum_{y=1}^{m}\sum_{x=1}^{m}\Bigg(\dot{I}_{sr}^{yp}.\dot{I}_{rr}^{xn}\exp j2s\omega_s t+\dot{I}_{sr}^{yp}.\dot{I}_{rr}^{xp*}$$

$$+\dot{I}_{sr}^{yn*}.\dot{I}_{rr}^{xn}+\dot{I}_{sr}^{yn*}.\dot{I}_{rr}^{xp*}\exp -j2s\omega_s t\Bigg)\Bigg\}\Bigg] \qquad 3.44a$$

In this expression for the electromagnetic torque the products of the different current components of relation 3.17a may be distinguished. It may now be shown that this expression is equivalent to the following relation in which the complex-conjugate nature of the positive and negative sequence current components has been taken into account. (Refer to appendix A3.1)

$$T_e =$$

$$-\Bigg\{\frac{p}{2}\sqrt{\frac{m}{n}}M_{sr}\sum_{y=1}^{n}\sum_{x=1}^{n}\sum_{h=0}^{\infty}\Bigg(Im\Big\{\Big[\dot{I}_{s}^{yn}\frac{}{\sqrt{2h+1}}.\dot{I}_{r}^{xp}\frac{}{\sqrt{2h+1}}-\dot{I}_{s}^{yp}\frac{}{\sqrt{2h+1}}.\dot{I}_{r}^{xn}\frac{}{\sqrt{2h+1}}\Big]$$

$$\exp j2(\sqrt{2h+1}\ \omega_s t)\Big\}$$

$$+ Im\left\{\dot{\bar{I}}^{yn}_{s\ \overline{2h+1}} . \dot{I}^{xn*}_{r\ \overline{2h+1}}\right\} + Im\left\{\dot{\bar{I}}^{yp*}_{s\ \overline{2h+1}} . \dot{I}^{xp}_{r\ \overline{2h+1}}\right\}\Bigg)$$

$$+ \frac{pM_{sr}}{2} \sum_{y=1}^{n} \sum_{x=1}^{m} \sum_{h=0}^{\infty} \Bigg(Im\left\{\left[\dot{\bar{I}}^{yn}_{s\ \overline{2h+1}} . \dot{I}^{xp}_{rr} - \dot{I}^{yn}_{r\ \overline{2h+1}} . \dot{I}^{xp}_{sr}\right] \right.$$

$$\left. \exp j2(\overline{h+1}\ \omega_s t)\right\}$$

$$+ Im\left\{\left[\dot{\bar{I}}^{yn}_{s\ \overline{2h+1}} . \dot{I}^{xn*}_{rr} - \dot{I}^{yn}_{r\ \overline{2h+1}} . \dot{I}^{xn*}_{sr}\right] \exp j2(\overline{h+1-s}\omega_s t)\right\}$$

$$+ Im\left\{\left[\dot{\bar{I}}^{yp*}_{s\ \overline{2h+1}} . \dot{I}^{xp}_{rr} - \dot{I}^{yp*}_{r\ \overline{2h+1}} . \dot{I}^{xp}_{sr}\right] \exp -j2h\omega_s t\right\}$$

$$+ Im\left\{\left[\dot{\bar{I}}^{yp*}_{s\ \overline{2h+1}} . \dot{I}^{xn*}_{rr} - \dot{I}^{yp*}_{r\ \overline{2h+1}} . \dot{I}^{xn*}_{sr}\right] \exp -j2(\overline{h+s}\omega_s t)\right\}\Bigg)$$

$$+ \frac{p}{2}\sqrt{\frac{n}{m}}\, M_{sr} \sum_{x=1}^{m} \sum_{x=1}^{m} \Bigg(Im\left\{\left[\dot{I}^{yn}_{sr} . \dot{I}^{xp}_{rr} - \dot{I}^{yp}_{sr} . \dot{I}^{xn}_{rr}\right] \exp j2s\omega_s t\right\}$$

$$+ Im\left\{\dot{I}^{yn}_{sr} . \dot{I}^{xn*}_{rr}\right\} + Im\left\{\dot{I}^{yp*}_{sr} . \dot{I}^{xp}_{rr}\right\}\Bigg)\Bigg\} \qquad 3.44b$$

Inspection of this relation for the torque indicates that the torque may be considered to consist of synchronous, asynchronous and pulsating components. The pulsating components has not been encountered in the simplified power flow considerations of the previous chapter. The instantaneous electromagnetic torque is now represented by:

$$T_e = \sum_{h=0}^{\infty} T^{puls.sr}_{e(2h+1)}(2\overline{2h+1}\,\omega_s t) + \sum_{h=0}^{\infty} T^{puls.rs}_{e(2h+1)}(\overline{2h+1}\,\omega_s t)$$

$$+ \sum_{h=1}^{\infty} T^{puls.rs}_{e(2h+1)}(2h\omega_s t)$$

$$+ \sum_{h=0}^{\infty} T^{syn.}_{e(2h+1)}(\overline{2h+1-s}\omega_s t) + \sum_{h=0}^{\infty} T^{syn.}_{e(2h+1)}(\overline{2h+s}\omega_s t) + T^{syn.}_{e(1)}(2s\omega_s t)$$

$$+ \sum_{h=0}^{\infty} T^{asyn.sr}_{e(2h+1)} + T^{asyn.rs}_{e(1)h=0} + T^{asyn.rs}_{e(1)} \qquad 3.44c$$

where all the different torque components are defined in appendix A3.1.

If one is now interested in the mean value of the electromagnetic torque important for the continuous conversion of electrical into mechanical energy, examine relation 3.44c. The pulsating components of torque will not contribute to the mean value, and these components appear to have a frequency of pulsation independent of the speed of the machine. The synchronous torques will only contribute to the mean torque at certain speeds, while the asynchronous components are time independent, and will contribute at all speeds, barring their synchronous speeds. From relation 3.44b consequently follows:

$$T_e = -\left\{ \frac{p}{2}\sqrt{\frac{m}{n}}\, M_{sr} \sum_{y=1}^{n} \sum_{x=1}^{n} \sum_{h=0}^{\infty} \left(Im \left\{ \underline{\dot{I}}^{yn}_{s\,\overline{2h+1}} \cdot \dot{I}^{xn*}_{r\,\overline{2h+1}} \right\} \right.\right.$$

$$\left.\left. + Im \left\{ \underline{\dot{I}}^{yp*}_{s\,\overline{2h+1}} \cdot \dot{I}^{xp}_{r\,\overline{2h+1}} \right\} \right)$$

$$+\frac{pM_{sr}}{2}\sum_{y=1}^{n}\sum_{x=1}^{m}\sum_{h=0}^{\infty}\Bigg(Im\Big\{\Big[\dot{\bar{I}}^{yn}_{s\ \overline{2h+1}}.\dot{I}^{xn*}_{rr}-\dot{I}^{yn}_{r\ \overline{2h+1}}.\dot{\bar{I}}^{xn}_{sr}\Big]\Big\}$$

$$\text{for } s=(h+1)$$

$$+Im\Big\{\Big[\dot{\bar{I}}^{yp*}_{s\ \overline{2h+1}}.\dot{I}^{xn*}_{rr}-\dot{I}^{yp*}_{r\ \overline{2h+1}}.\dot{I}^{xn*}_{sr}\Big]\Big\}\Bigg)$$

$$\text{for } s=-h$$

$$+\frac{p}{2}\sqrt{\frac{n}{m}}M_{sr}\sum_{x=1}^{m}\sum_{x=1}^{m}\Bigg(Im\Big\{\Big[\dot{I}^{yn}_{sr}.\dot{I}^{xp}_{rr}-\dot{I}^{yp}_{sr}.\dot{I}^{xn}_{rr}\Big]\Big\}$$

$$\text{for } s=0$$

$$+Im\Big\{\dot{I}^{yn}_{sr}.\dot{I}^{xn*}_{rr}\Big\}+Im\Big\{\dot{I}^{yp*}_{sr}.\dot{I}^{xp}_{rr}\Big\}\Big)\Bigg\} \qquad 3.45a$$

or equivalently:

$$T_e=\sum_{h=0}^{\infty}T^{syn.}_{e(2h+1)}+\sum_{h=0}^{\infty}T^{syn.}_{e(2h+1)}+T^{syn.}_{e(1)}$$

$$\text{for } s=h+1 \qquad \text{for } s=-h \qquad \text{for } s=0$$

$$+\sum_{h=0}^{\infty}T^{asyn.sr}_{e(2h+1)}+T^{asyn.rs}_{e(1)h=0}+T^{asyn.rs}_{e(1)} \qquad 3.45b$$

3.4 EXAMINATION OF AN EQUIVALENT CIRCUIT REPRESENTATION.

In the previous paragraphs of this chapter a method has been developed to calculate currents and torques in an n-m-phase rotating electromechanical converter subjected to switching action on sets of windings. It was found that it is possible to obtain exact expressions for currents and torques caused by all harmonic components of the excitation function. This general solution also covers unbalanced conditions of excitation as far as amplitudes of the excitation components are concerned. Investigation of the characteristics of switched transducers found in the literature may be devided into two main classes. Either the system is simulated on an analogue computer (For the case of induction machines see for instance([20],[39]), or an attempt is made to calculate the performance in terms of the normal equivalent circuit of the transducer under sinusoidal excitation (for instance([3],[66]). When the method developed in this chapter is valid (that is under steady state conditions), it is evident that simulation with an analogue computer is in principle not necessary although it may be considered feasible for other reasons. In order to be able to evaluate the validity of the attempts to use the conventional equivalent circuit, it will now be investigated to what extent it is possible to represent the calculations in terms of equivalent circuits. Attention will be turned to the case of a transducer subjected to control by stator switching.

The instantaneous symmetrical component currents under the Ku rotor-stator transformation are given in relations 3.29, 3.30, 3.36a and 3.36b. The partitioned stator and rotor equations of relations 3.19 and 3.20 have indicated that the voltages are related to the currents by an operational impedance matrix in each case. The diagonal matrices with respectively (n-2) and (m-2) rows and columns may be represented by a series of (n-2), (m-2) independent equivalent circuits. These circuits are to be termed "operational impedance" equivalent circuits. Correspondingly the 4 by 4 operational impedance matrix relating the conversion currents and voltages may be represented by a four mesh "operational impedance" equivalent circuit. All these equivalent circuits necessary to describe the electrical behaviour of the switched n-m phase electromechanical transducer are given in fig. 3.2.

The transformed rotor and stator conversion currents of relations 3.36a and 3.36b are calculated by superposition , as an inspection of relation 3.42a and 3.43a, and of appendix A3.1.1 suffices to illustrate. These superposition components are shown in the equivalent circuits of fig. 3.3. It may be shown by a simple calculation that the impedances of these circuits correspond to the appropriate elements of the operational impedance matrix.

As soon as the transformed voltages impressed on the "operational impedance" equivalent circuits of figs. 3.2 and 3.3 are expressed as a known function of time, the impedance elements in the equivalent circuits of fig. 3.4 and 3.5 are specified. With reference to the zero equivalent circuits of fig. 3.4 and fig. 3.5 and the relations 3.30, 3.29

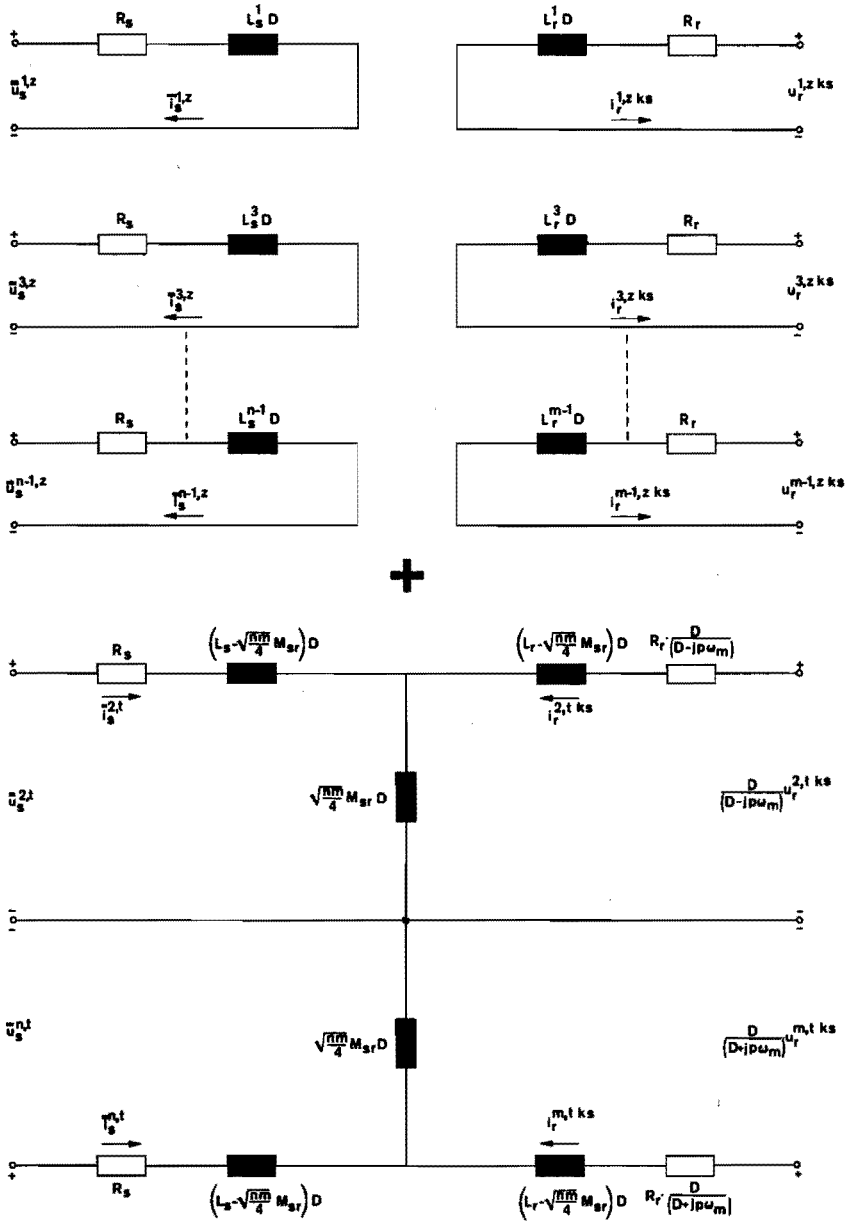

FIG. 3.2 REPRESENTATION OF THE SWITCHED N-M PHASE ELECTROMECHANICAL TRANSDUCER BY "OPERATIONAL IMPEDANCE" EQUIVALENT CIRCUITS.

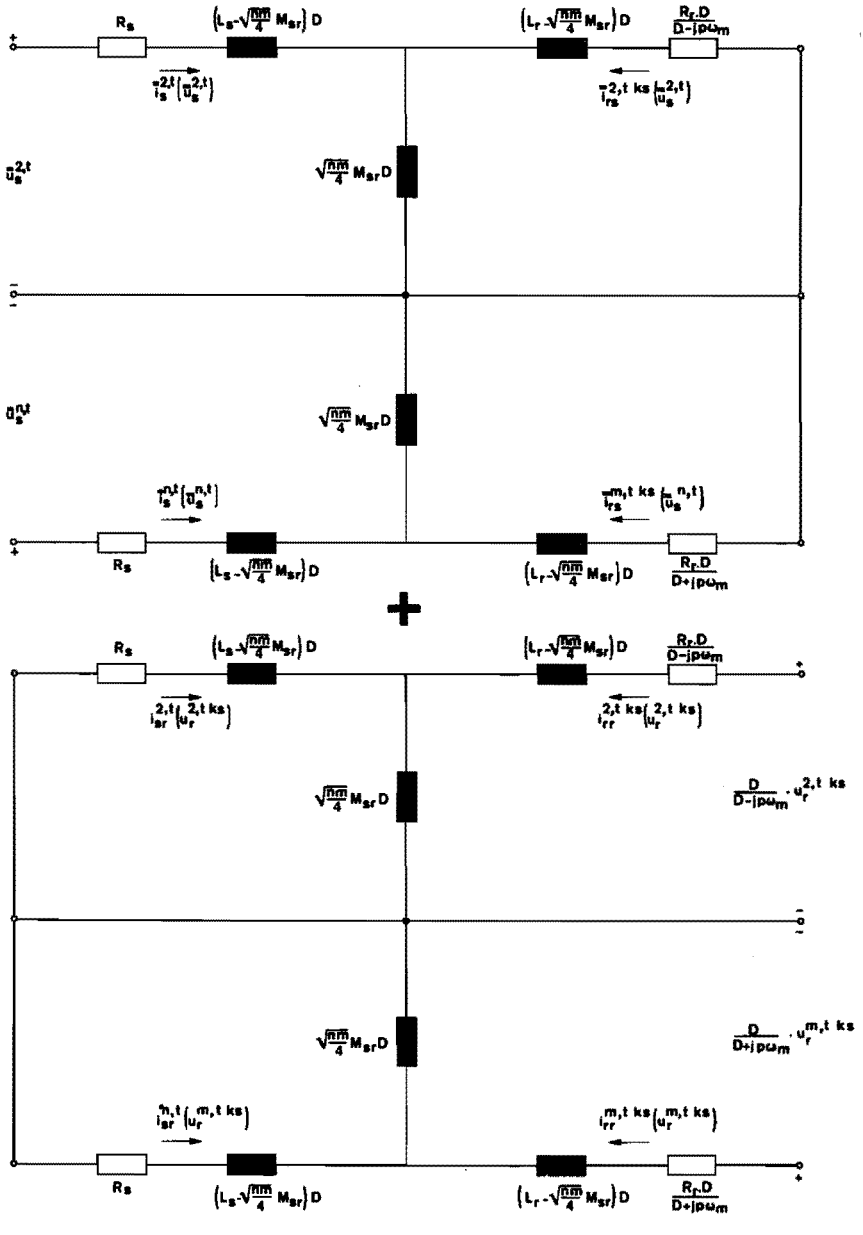

FIG. 3.3 THE DIFFERENT COMPONENTS OF THE TRANSFORMED STATOR AND ROTOR CONVERSION CURRENTS OF THE SWITCHED N-M PHASE ELECTROMECHANICAL CONVERTER IN TERMS OF THE "OPERATIONAL IMPEDANCE" EQUIVALENT CIRCUIT.

$$\begin{bmatrix} \dot{\underline{\underline{V}}}^{zx1}_{s\ \overline{2h+1}} \\ \dot{\underline{\underline{V}}}^{zx3}_{s\ \overline{2h+1}} \\ \dot{\underline{\underline{V}}}^{z,x\overline{n-1}}_{s\ \overline{2h+1}} \end{bmatrix} = \begin{bmatrix} \left\{(z_s)^{\overline{x-1}}\right\}^{-\overline{2h+1}} \\ \left\{(z_s)^{\overline{x-1}}\right\}^{2-\overline{2h+1}} \\ \left\{(z_s)^{\overline{x-1}}\right\}^{\overline{n-2}-\overline{2h+1}} \end{bmatrix} \dot{\underline{\underline{U}}}^{x}_{s\ \overline{2h+1}} \qquad 3.46a$$

$$\begin{bmatrix} \dot{V}^{z,x1}_{r} \\ \dot{V}^{z,x3}_{r} \\ \dot{V}^{z,x\overline{m-1}}_{r} \end{bmatrix} = \begin{bmatrix} (z_r)^{-\overline{x-1}} \\ (z_r)^{\overline{x-1}} \\ (z_r)^{\overline{m-3}\cdot\overline{x-1}} \end{bmatrix} \dot{U}^{x}_{r} \qquad 3.46b$$

The zero torque-currents of relations 3.30 and 3.29 may then be calculated from the components found from the (n-2) and (m-2) stator and rotor symmetrical component zero equivalent circuits.

Regarding the two four mesh equivalent circuits of fig. 3.4 and fig. 3.5 for the complex amplitudes of the instantaneous symmetrical component transforms of stator and rotor currents due to the switched stator voltage and due to the rotor excitation respectively, the appropriate terminal voltages have already been defined in relations 3.41c and 3.41d. For the circuit concerning the conversion currents in fig. 3.4(a) a simple calculation proves that for the input impedance between terminals 1 and 0, the following holds:

$$\left.\begin{aligned} \dot{Z}_{10} &= \dot{Z}^{p}_{s\ \overline{2h+1}} \\ \text{Similarly:} \qquad & \\ \dot{Z}_{20} &= \dot{Z}^{n}_{s\ \overline{2h+1}} \end{aligned}\right\} \qquad 3.46c$$

resulting in calculation of the currents as in 3.42c. From the same

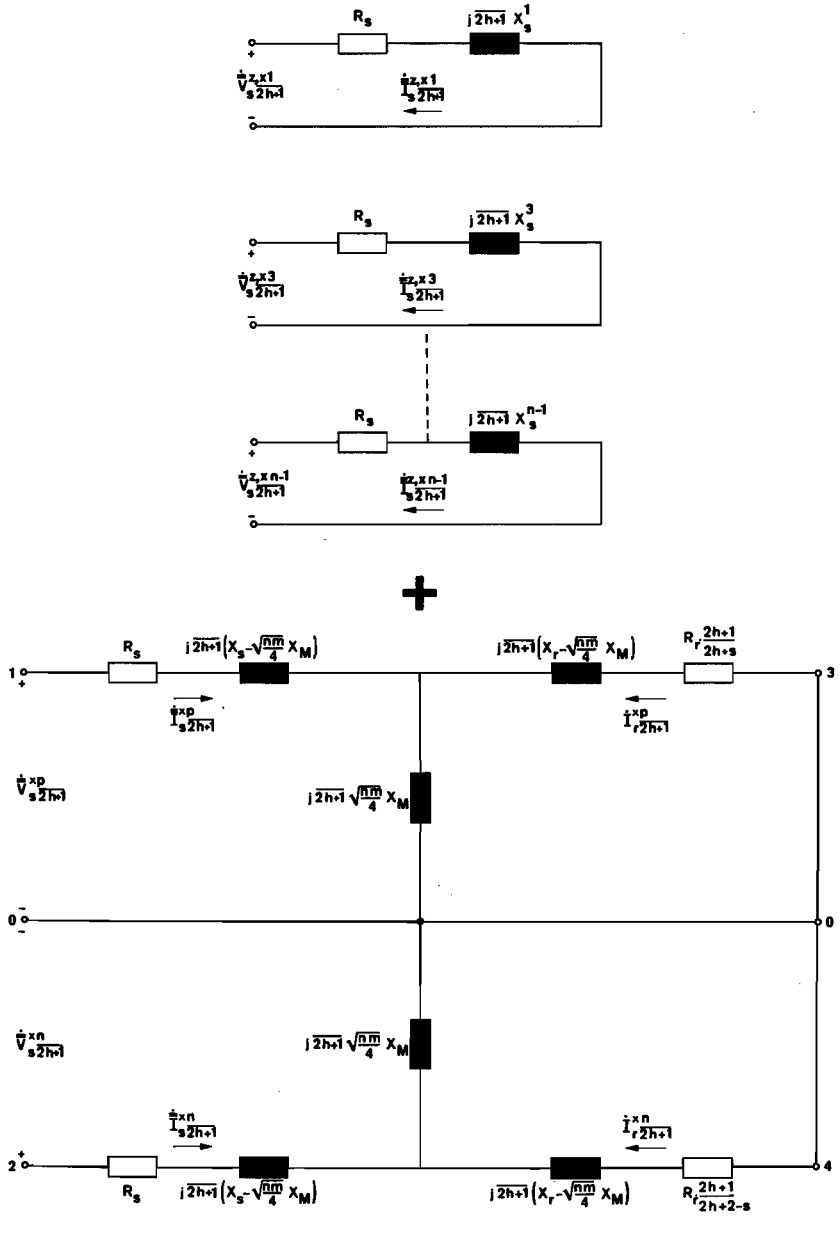

FIG. 3.4 EQUIVALENT CIRCUITS FOR CALCULATING THE COMPLEX AMPLITUDES OF THE HARMONIC COMPONENTS OF THE TRANSFORMED ZERO AND CONVERSION CURRENTS IN THE CONVERTER DUE TO THE SWITCHED EXCITATION.

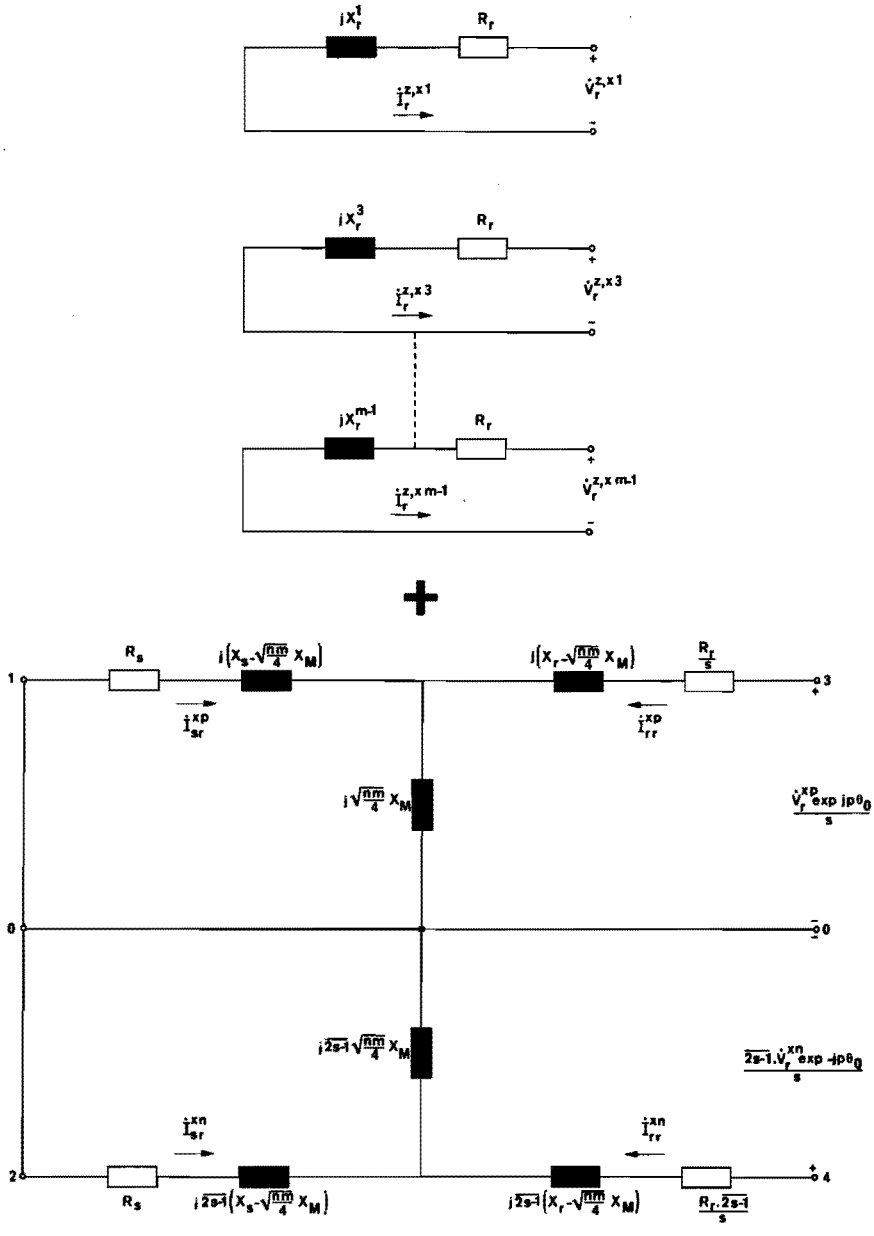

FIG. 3.5 EQUIVALENT CIRCUITS FOR CALCULATING THE COMPLEX AMPLITUDES OF THE COMPONENTS OF THE TRANSFORMED ZERO AND CONVERSION CURRENTS DUE TO ROTOR EXCITATION.

equivalent circuit it also follows that

$$-\dot{I}^{xp}_{r\ \overline{2h+1}} = \frac{j\overline{2h+1}\sqrt{\frac{nm}{4}}\,X_M}{\left\{R_r \cdot \frac{2h+1}{2h+s} + j\overline{2h+1}X_r\right\}} \cdot \dot{\bar{I}}^{xp}_{s\ \overline{2h+1}}$$

or

$$\dot{Z}^{p}_{sr\ \overline{2h+1}} = \frac{\left\{R_r \cdot \frac{2h+1}{2h+s} + j\overline{2h+1}X_r\right\}}{j\overline{2h+1}\sqrt{\frac{nm}{4}}\,X_M} \cdot \dot{Z}_{10} \qquad 3.46d$$

In exactly the same way it follows that:

$$\dot{Z}^{n}_{sr\ \overline{2h+1}} = \frac{\left\{R_r \cdot \frac{2h+1}{sh+2-s} + j\overline{2h+1}X_r\right\}}{j\ 2h+1\sqrt{\frac{nm}{4}}\,X_M} \cdot \dot{Z}_{20} \qquad 3.46e$$

Relations 3.46d and 3.46e result in calculation of the rotor transformed currents according to 3.43c.

From the equivalent circuit of fig. 3.5(b) a similar reasoning leads to the calculation of the rotor and stator currents due to the general unswitched rotor excitation as given in 3.42d and 3.43d. Due to the similarity with the previous proofs this will not be repeated. It will be considered proven that the equivalent circuits of figures 3.4 and 3.5 represent the necessary steps for calculation of all the complex amplitudes in the previous transformed model of the switched machine. The case of a rotor switched, stator fed machine has not been presented beyond the general solutions for the currents after stator-rotor transformation (paragraph 3.3.7) and expansion in terms of the operational impedance matrix (relations 3.40a and 3.40b) in the present chapter. However, a corresponding situation regarding an equivalent circuit representation is found. Therefore the conclusions drawn regarding validity of attempts to use the equivalent circuit for sinusoidal excitation to estimate behaviour under switched conditions will be considered valid for both stator and rotor switched systems.

The "normal" equivalent circuit for a multiphase induction machine will be taken as example, since the further theoretical and experimental investigations in chapters 4 and 5 will concern Group II machine-electronic systems. The circuits obtained for an n-m phase machine with a short circuit applied to the m rotor electrical ports resemble the circuits of fig. 3.4 for only the fundamental harmonic component in rotor and stator. It should be noted that these currents, and the voltages impressed on the equivalent circuit *are not the actual machine currents or machine terminal voltages.* As the excitation and currents are all simple harmonic functions of time, and is in conventional practice mostly represented by "vectors" or

"phasors", this difference is normally not in evidence. When the machine excitation functions, and consequently the currents, contain harmonic components, the difference becomes apparent, as the transformations employed do not have the same influence on all harmonic components.

This leads to the conclusion that attempts to investigate the characteristics of a switched electromechanical converter by applying the switched voltages to the equivalent circuit[66] or by incorporating the switches into the equivalent circuit[43] are incorrect and may only lead to reasonable results when the percentage of harmonic voltages in the excitation function is low[77] . In a following paragraph (3.6) some investigations into the possibility to represent switched machines by a more simplified model than hitherto used are to be conducted.

3.5 REMARKS REGARDING SOME SIMPLIFYING CONDITIONS IN THE INVESTIGATED MODEL.

During the previous calculations of the characteristics of a switched electromechanical transducer possible asymmetrical effects of the supply systems were incorporated in the conditions of assumption. It was furthermore assumed that all odd harmonic components are represented in the instantaneous symmetrical component transforms of the stator and rotor currents used to calculate the torque. Some simplifying conditions will now be investigated. Let the rotor excitation in the case of a stator-switched electromechanical transducer be examined.

The instantaneous symmetrical component transforms of the rotor excitation functions are given in rel. 3.41d, with the elements specified in relation A3.1b. With reference to rel. 3.24b that specifies the different phase voltages, let

$$\dot{U}_r^x = \dot{U}_r^1 = \dot{U}_r^2 = \dot{U}_r^3 = ... = \dot{U}_r \qquad 3.47a$$

Therefore:

$$\dot{V}_r^p = \sum_{x=1}^{m} \dot{U}_r^x = m.\dot{U}_r \qquad 3.47b$$

and

$$\dot{V}_r^n = \dot{U}_r \sum_{x=1}^{m} \left\{ (\underline{z}_r)^{\overline{m-2-x-1}} \right\} \equiv 0 \qquad 3.47c$$

In this balanced case the rotor excitation consequently becomes, after transformation:

$$\begin{bmatrix} \dot{u}^{2,t}_{r} \\ \\ \dot{u}^{m,t}_{r} \end{bmatrix} = \sqrt{\frac{m}{2}} \begin{bmatrix} \dot{U}_r \ \exp j\omega_r t \\ \\ \dot{U}_r^{*} \exp -j\omega_r t \end{bmatrix} \qquad 3.47d$$

Consequently

$$\begin{bmatrix} \dot{u}^{2,t\ ks}_{r} \\ \\ \dot{u}^{m,t\ ks}_{r} \end{bmatrix} = \sqrt{\frac{m}{2}} \begin{bmatrix} \dot{U}_r \ \exp j(\omega_s t + p\theta_o) \\ \\ \dot{U}_r^{*} \exp -j(\omega_s t + p\theta_o) \end{bmatrix} \qquad 3.47e$$

Let the instantaneous symmetrical component transforms of the stator excitation functions now be examined when all phases have balanced excitation, i.e.:

$$\underset{s\ \overline{2h+1}}{\bar{\bar{\dot{U}}}^{x}} = \underset{s\ \overline{2h+1}}{\bar{\bar{\dot{U}}}^{1}} = \underset{s\ \overline{2h+1}}{\bar{\bar{\dot{U}}}^{2}} = \underset{s\ \overline{2h+1}}{\bar{\bar{\dot{U}}}^{3}} = \underset{s\ \overline{2h+1}}{\bar{\bar{\dot{U}}}} \qquad 3.48a$$

The complex amplitude of the instantaneous symmetrical component transforms of the positive sequence voltage is (from rel. A3.1a and rel. 3.41c)

$$\underset{s\ \overline{2h+1}}{\dot{\bar{V}}^{p}} = \underset{s\ \overline{2h+1}}{\dot{\bar{U}}} \sum_{x=1}^{n} \left\{ \left(z_s^{\ \overline{x-1}} \right)^{-2h} \right\} \qquad 3.48b$$

$$h = 0,\ 1,\ 2,\ 3,\ 4,\ \ldots\ \infty$$

It may now be shown that:

$$\sum_{x=1}^{n} \left\{ \left(z_s^{\ \overline{x-1}} \right)^{-2h} \right\} = n$$

for all $h = nk$, $\qquad k = 0,\ 1,\ 2,\ 3,\ \ldots\ \infty$

For all other h,

$$\sum_{x=1}^{n} \left\{ \left(z_s^{\overline{x-1}} \right)^{-2h} \right\} = 0$$

This indicates that the transforms are different from zero for harmonics of the order

$$\nu = (2nk + 1) \qquad 3.48c$$

Therefore, from relation 3.48b

$$\dot{\overline{V}}^{p}_{s\ \overline{2nk+1}} = n. \dot{\overline{U}}_{s\ \overline{2nk+1}} \qquad 3.48d$$

$$k = 0, 1, 2, 3, - - - - \infty$$

Examination of the conditions for the negative sequence component voltage indicates that:

$$\dot{\overline{V}}^{n}_{s\ \overline{2h+1}} = \dot{\overline{U}}_{s\ \overline{2h+1}} \sum_{x=1}^{n} \left\{ \left(z_s^{\overline{x-1}} \right)^{\overline{n-1}-\overline{2h+1}} \right\} \qquad 3.48e$$

when relations A3.1a and 3.41c are taken into account. In this summation

$$\sum_{x=1}^{n} \left\{ \left(z_s^{\overline{x-1}} \right)^{n-\overline{2h+2}} \right\} = n$$

for all $h = gn-1 \qquad g = 1, 2, 3, - - - - - \infty$

For all other h

$$\sum_{x=1}^{n} \left\{ \left(z_s^{\overline{x-1}} \right)^{n-\overline{2h+2}} \right\} = 0$$

These transforms are different from zero for harmonics of order

$$\nu = (2ng - 1) \qquad 3.48f$$

and relation 3.48e is to be noted as:

$$\dot{\bar{\bar{V}}}^{n}_{s\ 2\overline{ng-1}} = n.\dot{\bar{\bar{U}}}_{2\overline{ng-1}}$$

Again taking h as representing zero and all positive numbers

$$(2nk+1) \equiv (2nh+1) \quad ; \quad (2ng-1) \equiv (2nh+\overline{2n-1}) \qquad 3.48g$$

$$h = 0,\ 1,\ 2,\ \text{-------}\ \infty$$

The instantaneous symmetrical component transforms of the stator excitation are consequently represented by:

$$\begin{bmatrix} \dot{\bar{\bar{u}}}^{2,t}_{s} \\ \\ \dot{\bar{\bar{u}}}^{n,t}_{s} \end{bmatrix} = \sqrt{\frac{n}{2}} \sum_{h=0}^{\infty} \left\{ \begin{bmatrix} \dot{\bar{\bar{U}}}_{s\ \overline{2nh+1}}\ \exp j(\overline{2nh+1}\omega_s t) \\ \\ \dot{\bar{\bar{U}}}_{s\ \overline{2nh+\overline{2n-1}}}\ \exp j(\overline{2nh+\overline{2n-1}}\omega_s t) \end{bmatrix} + \right.$$

$$\left. + \begin{bmatrix} \dot{\bar{\bar{U}}}^{*}_{s\ \overline{2nh+\overline{2n-1}}}\ \exp{-j}(\overline{2nh+\overline{2n-1}}\omega_s t) \\ \\ \dot{\bar{\bar{U}}}^{*}_{s\ \overline{2nh+1}}\ \exp{-j}(\overline{2nh+1}\omega_s t) \end{bmatrix} \right\} \qquad 3.48h$$

In these expressions for the excitation function transforms it has now been indicated that in the case of balanced excitation the harmonic spectrums of the respective terms are reduced in contrast to the general unbalanced case where all uneven harmonics occur. During computation this may lead to a considerable reduction in labour. It will be found in chapter 4 that for semi-four-phase systems:

$$\left.\begin{aligned} (2nh+1) &\equiv (4h+1) \\ (2nh+\overline{2n-1}) &\equiv (4h+3) \end{aligned}\right\} \qquad 3.48i$$

Correspondingly for three phase systems:

$$\left.\begin{aligned} (2nh+1) &\equiv (6h+1) \\ (2nh+\overline{2n-1}) &\equiv (6h+5) \end{aligned}\right\} \qquad 3.48j$$

Reference to the equivalent circuits of figs. 3.4 and 3.5 shows that if only the conversion currents are taken into account, and the rotor excitation is reduced to zero, the equivalent circuit of fig. 3.6 may be set up. In this circuit it may now be shown how the electrical effects of the series of magnetic fields rotating with and against the stator fundamental magnetic field, as investigated in the power flow model in appendix A2, have been separated.

For stator harmonic fields arising due to switching in the stator the harmonic slip is rewritten from rel. A2.8f as:

$$s_{\nu rs} = \frac{(-1)^{c_s \nu_s} - \overline{1-s}}{(-1)^{c_s \nu_s}} \qquad 3.49a$$

$$c_s = 1,2$$

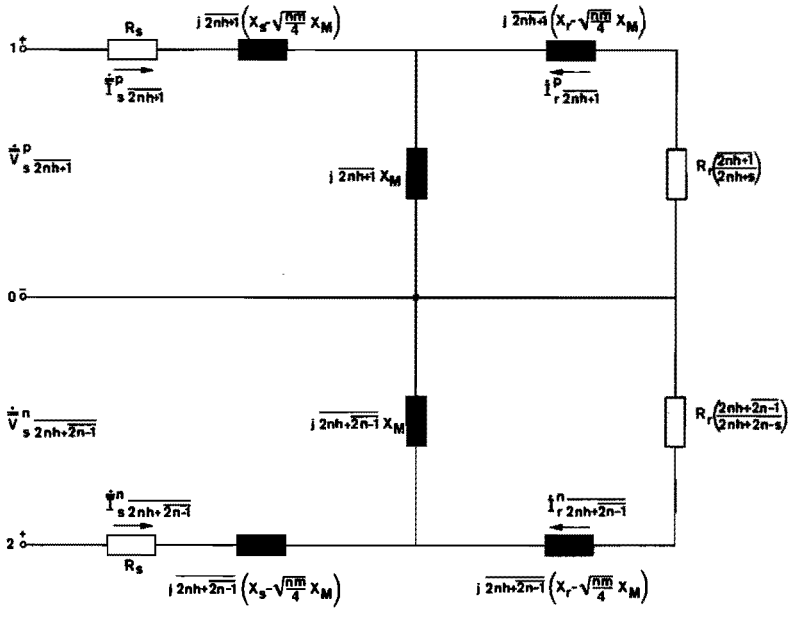

FIG. 3.6 EQUIVALENT CIRCUIT FOR THE POSITIVE AND NEGATIVE SEQUENCE COMPONENTS OF A STATOR SWITCHED CONVERTER WITH BALANCED EXCITATION.

For the harmonic fields rotating with the fundamental field a slip

$$s^{+}_{\nu rs} = \frac{\nu_s - 1 + s}{\nu_s} \qquad 3.49b$$

is obtained, while the slip

$$s^{-}_{\nu rs} = \frac{\nu_s + 1 - s}{\nu_s} \qquad 3.49c$$

is associated with the fields rotating against the direction of rotation of the fundamental field. Taking note of the fact that in fig. 3.6

$$R_r\left(\frac{2nh+1}{2nh+s}\right) = \frac{R_r}{s^{+}_{\nu rs}} \quad ; \quad R_r\left(\frac{2nh+\overline{2n-1}}{2nh+2n-s}\right) = \frac{R_r}{s^{-}_{\nu rs}} \qquad 3.49d$$

it may be seen that the equivalent circuit between terminals 1 and 0 clearly represents the effects of the harmonic fields rotating with the fundamental field, while the circuit between 2 and 0 represents the effects of the harmonic fields rotating against the fundamental field.

If the case of a three phase converter is examined, rel. 3.48j states that in combination with the above, harmonics of order 7, 13, 19, 25 etc. will rotate with, and harmonics of order 5, 11, 17, 23 etc. will rotate against the fundamental harmonic field. This corresponds with results to be found in the literature regarding three phase machines[32]

In conclusion to these remarks concerning some simplifying conditions of the assumed model, the influence of the excitation conditions on the different torque components are to be examined. Let the influence of the rotor excitation be examined first.

As discussed, the multiphase rotor excitation is balanced. With reference to rel. 3.44b and 3.44c the following torque components will be zero:

1) synchronous torques due to interaction of fields arising from unbalanced excitation and harmonic fields

$$\underline{\dot{V}}^{n}_{r} \equiv 0 \equiv \underline{\dot{I}}^{n}_{rr} \equiv \underline{\dot{I}}^{n*}_{sr} \equiv \underline{\dot{I}}^{n*}_{rr} \equiv \underline{\dot{I}}^{n}_{sr}$$

$$\therefore \sum_{h=0}^{\infty} T^{syn}_{e(2h+1)} \; (\overline{2h+1}-s\omega_s t) \equiv 0$$

$$\sum_{h=0}^{\infty} T^{syn}_{e(2h+1)} \; (\overline{2h+s}\omega_s t) \equiv 0 \qquad \left.\right\} \; 3.50a$$

2) synchronous torques due to the unbalanced excitation regarding the fundamental harmonic stator and rotor fields

$$T^{syn}_{e(1)} \; (2s\omega_s t) \equiv 0 \qquad 3.50b$$

When the rotor excitation derived from an external supply is reduced to zero, the torque expression will be simplified further, since the following conditions will hold, with reference to relation 3.44b and 3.44c

$$\dot{V}^p_r \equiv 0 \equiv \dot{I}^p_{rr} \equiv \dot{I}^{p*}_{rr} \equiv \dot{I}^p_{sr} \equiv \dot{I}^{p*}_{sr}$$

Therefore the following"pulsating"torques will disappear:

$$\sum_{h=0}^{\infty} T^{puls.rs}_{e(2h+1)} \; (\overline{2h+1}\omega_s t) \equiv 0$$

$$\sum_{h=1}^{\infty} T^{puls.rs}_{e(2h+1)} \; (2h\omega_s t) \equiv 0 \qquad \left.\right\} \; 3.50c$$

The above conditions will simultaneously result in the elimination of all asynchronous components arising from the rotor excitation

3.50d

$$\left.\begin{aligned} T^{asyn}_{e(1)h=0} &\equiv 0 \\ T^{asyn.rs}_{e(1)} &\equiv 0 \end{aligned}\right\} \qquad 3.50d$$

In relation 3.48h it has been shown that in the balanced case not all the harmonic components exist in the instantaneous symmetrical component transforms, so that it may also be expected that the spectrum of harmonic pulsating and asynchronous torques due to stator-rotor interaction will be reduced in the balanced case. This will be further investigated in the application of the theory to a stator control system in chapter 4.

3.6 CONSIDERATION OF SOME SIMPLIFIED MODELS FOR THE THEORETICAL ANALYSIS OF THE ELECTROMECHANICAL TRANSDUCER USED IN THE MACHINE-ELECTRONIC SYSTEM.

Up to the present consideration has been given to a model as general as possible for the switched electromechanical transducer. It has been illustrated that under some constraints this model may be applied to all machine-electronic systems discussed under Group I, Group II and Group III in chapter 2. Application of this model to the analysis of a stator controlled semi-four-phase machine in chapter 4 will indicate that the computational procedures concerned can be quite involved. By way of comparison it has therefore been decided to develop a range of simpler models for some systems to be analysed. It will be realized that the less general such a model is, the more it becomes necessary to develop additional models for other systems. This increases the amount of specialized work, and forces one to make a selection in the presentation.

It has been selected to present some models that may be used to analyse rotor-controlled induction machines in the present paragraph. These models are also used in chapter 4 for actual system investigations, and fit into the general intention of an experimental investigation of examples from all classes of Group II and Group IIA systems. As a basis for this simplified model the power flow investigations of chapter 2 will be used.

In appendix 2.1.5 a simplified power flow model for systems with rotor harmonics of order $\nu_r = \overline{2h+1}$ was investigated. It will be supposed that the most general case is investigated, i.e. the rotor electrical ports are fed by a voltage source. From relation A2.12f the electromagnetic torque is found as:

$$\bar{T}_{e(1)} = \frac{p}{s\omega_s}\left(\sum_{h=0}^{\infty} P^r_{de(2h+1)} - P^r_{in(1)}\right) \qquad 3.51a$$

At a given slip it is therefore necessary to know the total rotor dissipation and input power to calculate the mean electromagnetic torque. Since the rotor source voltages and the rotor winding resistances are known, it becomes a matter of obtaining the different rotor current components.

In general it is possible to classify the rotor control systems into two groups as far as the solution for the current is concerned. These two alternatives are now to be examined in succession.

3.6.1 *ELECTROMECHANICAL CONVERTERS WITH SWITCHING IN THE ROTOR TO CONTROL THE CURRENT FLOW ANGLE.*

In the discussion of Group II systems in paragraph 2.4.2 it was illustrated that in some variants the angle of rotor current flow per period is changed to achieve power flow control. In these systems the switching rhythm is equal to twice the rotor frequency, and it will be assumed (in accordance with appendix A2.1.5) that the stator of the converter is fed by a "flux source" while the rotor voltage sources are zero. This has as a consequence a constant fundamental rotating field causing an induced e.m.f. in each phase that is a simple harmonic function of time. Referring to fig. 3.1 it can be seen that the effect of the stator of the machine has now been entirely replaced by the constant rotating field. The torque is now given by:

$$\overline{T}_{e(1)} = \frac{p}{s\omega_s} \cdot \sum_{h=0}^{\infty} P^{r}_{de(2h+1)} \qquad 3.51b$$

The induced rotor e.m.f. in the xth phase is:

$$e_r^x = s.\sqrt{2}\,E_{ro}\,\sin(\omega_r t - \overline{x-1}\,\Delta_r)$$

$$\Delta_r = \frac{2\pi}{m}$$

In the following it will now be assumed that the transducer is a semi-four-phase machine. The voltage equations during the conduction period in the "a" and "b" phases are:

$$\left[e_r^{a,b}\right] = \frac{d}{dt}\left[L_r^{a,b}\right] \cdot \left[i_r^{a,b}\right] + \left[R_r^{a,b}\right]\left[i_r^{a,b}\right]\Bigg|_{\alpha_a\alpha_b}^{\beta_a\beta_b} \qquad 3.51c$$

with $\left[e_r^{a,b}\right] = \begin{bmatrix} e_r^a \\ e_r^b \end{bmatrix}$, $\left[i_r^{a,b}\right] = \begin{bmatrix} i_r^a \\ i_r^b \end{bmatrix}$

Due to the spatial arrangement of the windings of the transducer mutual influences may be neglected, and as has been done previously all windings are assumed to be identical. Therefore

$$\left[L_r^{a,b}\right] = \begin{bmatrix} L_{r\sigma} & 0 \\ 0 & L_{r\sigma} \end{bmatrix} \quad ; \quad \left[R_r^{a,b}\right] = \begin{bmatrix} R_r & 0 \\ 0 & R_r \end{bmatrix} \qquad 3.51d$$

with $L_{r\sigma}$ the leakage inductance per phase. In order to determine the current it will now suffice to consider only one phase, say phase "a". Solution of equation 3.51c during conduction results in:

$$i_r^a = \frac{s\sqrt{2}\,E_{ro}}{\sqrt{R_r^2 + \omega_r^2 L_{r\sigma}^2}} \left\{ \sin(\omega_r t - \psi_r) - \sin(\alpha - \psi_r)\exp-(\omega_r t - \alpha)\cot\psi_r \right\}_{\alpha_a}^{\beta_a} \qquad 3.52$$

with $\psi_r = \arctan\left(\frac{\omega_r L_{r\sigma}}{R_r}\right)$

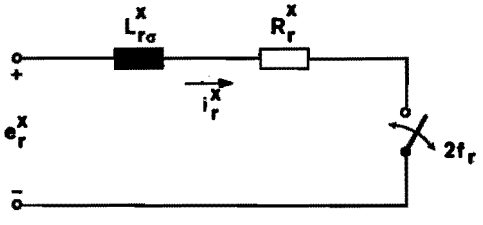

[a]

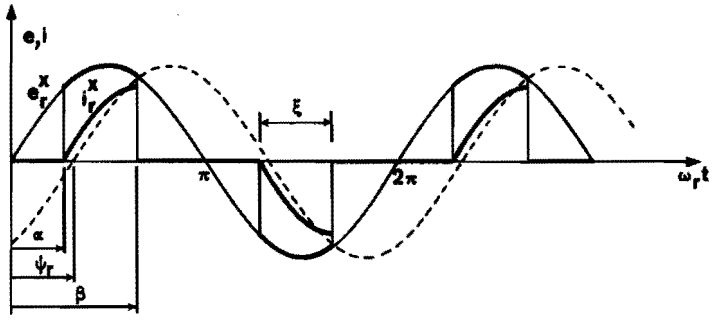

[b]

FIG. 3.7 EQUIVALENT CIRCUIT AND WAVEFORM DEFINITIONS FOR SIMPLIFIED MODEL OF ROTOR-SWITCHED ELECTROMECHANICAL TRANSDUCER.

By using relation 3.51b it may now be shown (see appendix A3.3) that the mean electromagnetic torque may be calculated from:

$$\overline{T}_{e(1)} = \frac{2p\, E_{r\sigma}^2}{\omega\pi_s \sqrt{\frac{R_r^2}{s^2} + \omega_s^2 L_{r\sigma}^2}} \left\{ \frac{\sin(2\alpha - \psi_r) - \sin(2\beta - \psi_r) + \xi \cos\psi_r}{2} + \right.$$

$$+ \frac{2 \sin(\alpha - \psi_r)}{\operatorname{cosec}^2 \psi_r} \left[(\cot\psi_r \sin\beta + \cos\beta)\exp - \xi\cot\psi_r - \right.$$

$$\left. \left. - (\cot\psi_r \sin\alpha + \cos\alpha) \right] \right\} \qquad 3.53$$

At each value of the slip the known harmonic current spectrum now not only enables one to calculate the torque, but also the power factor, effective rotor current and supply distortion caused by the harmonic currents. Investigation of the current flowing in the supply necessitates relaxation of the constraint that the rotating magnetic field is constant, and consequently introduces some errors.

3.6.2 *ELECTROMECHANICAL CONVERTERS WITH SWITCHING CIRCUITS IN THE ROTOR HAVING A CURRENT SOURCE EFFECT.*

Again referring to the discussion of Group II and Group IIA systems presented in paragraph 2.4.2, the feasibility of the model to be investigated will be illustrated. In systems of Group IIA, class 1, for recuperation of the slip power, a large inductance is included in the output of the rotor rectifier (fig. 2.9). This tends to keep the current at the output constant, and at the input to the rotor the power electronic system acts as a current source. The same considerations apply to systems of Group IIA, class 2. In systems of Group II class 2 where switching at a frequency much higher than the rotor frequency is used for control in the rotor circuit, a rotor rectifier is mostly used (see fig. 2.9). Inclusion of an inductor between the chopper and the rectifier combined with a two level current control system results in a current source presented to the rotor input. Any influences that commutation effects in the power electronic circuits may have on the current harmonic distribution is neglected for the present.

With reference to rel. 2.5b the current in the xth rotor phase is then known as:

$$\bar{\bar{i}}^{x}_{r} = \sqrt{2} \sum_{h=0}^{\infty} \bar{\bar{I}}^{x}_{r\ \overline{2h+1}} \cos(\overline{2h+1}\omega_r t - \psi_{r\ \overline{2h+1}}) \qquad 3.54$$

Now it has been stated in appendix A2.1.5 that the source connected to the rotor electrical ports supplies only fundamental power. If the electronic switching circuits mentioned above are seen as current sources for the rotor, the constraint of fundamental power delivered by the rotor sources must be relaxed. The power balance for the rotor electrical power consequently becomes:

$$\bar{T}_{e(1)} \cdot \frac{s\omega_s}{p} = \sum_{h=0}^{\infty} \left(P^{r}_{de(2h+1)} - P^{r}_{in(2h+1)} \right) \qquad 3.55$$

From the known particulars of the electronic switching circuit the harmonic power input $P^{r}_{in(2h+1)}$ may be considered known, as will be evident in chapters 4 and 5. The electromagnetic torque is then consequently found from:

$$\bar{T}_{e(1)} = \frac{p}{s\omega_s} \left\{ m.R_r \sum_{h=0}^{\infty} \left(I_{r\ \overline{2h+1}} \right)^2 - \sum_{h=0}^{\infty} P^{r}_{in(2h+1)} \right\} \qquad 3.56$$

It is now again possible to calculate the torque, power factor and effective rotor current at any point in that part of the torque-slip plane included by the maximum torque-slip characteristic. Since the harmonic content of the rotor current is now known, the harmonic distortion of the stator supply current may be estimated. Although the calculation of the harmonic currents flowing in the stator circuit necessitates relaxation of the assumption of a constant rotating magnetic field, no error is introduced, as the amplitudes of the harmonics derived from the rotor current source may in first approximation be supposed to be independent of the induced rotor voltage wave-form.

CHAPTER 4

THEORETICAL INVESTIGATIONS OF SOME CHARACTERISTICS OF GROUP II AND GROUP IIA MACHINE-ELECTRONIC SYSTEMS

Synopsis

In this chapter the theoretical investigations are restricted to the group of machine-electronic systems that are to be investigated experimentally. The switching mode for each system is investigated, and attention given to the contribution of the information-electronics to the steady state transfer function. For the purpose of these aforementioned investigations the information-electronics and power electronics are idealized.

The investigations conducted comprise an example of the application of the generalized theory for switched electromechanical transducers as developed in the previous chapter to a stator controlled induction-machine, and application of some simplified methods of analysis for rotor control systems.

The stator controlled machine-electronic system belongs to Group II, class 1 and is controlled by delay of the instant of triggering of the electronic switches. The rotor controlled systems fall into Group II, class 2 and Group IIA and comprise rotor control by delay of the instant of triggering of the electronic switches, rotor control by delay of the instant of current extinction of the electronic switches, an electronic Leblanc cascade, an electronic Scherbius cascade and a compensated electronic Scherbius cascade.

In the parallel usage of these two approaches it is attempted to reflect the philosophy that the approaches lying between these two alternatives are mostly restricted in utility, and do not necessarily aid insight.

It is attempted to present calculated characteristics for each system investigated that may subsequently be compared with the experimental results of the next chapter on Group II machine-electronic systems.

4.1 THE SYSTEMS TO BE SUBJECTED TO INVESTIGATION

In this chapter Group II and Group IIA machine-electronic systems are to be investigated as an example of general investigations of the characteristics of machine-electronic systems. The systems to be treated are chosen to have as a field of application the low, medium and high

power range of electrical drives, in order to achieve a representative study.

Examples of Group II machine-electronic systems that are to be investigated in this chapter are:

(1) control of the stator voltage by delay of the ignition instant of the electronic switches in the stator circuit;
(2) control of the rotor current by delay of the ignition instant of the electronic switches in the rotor circuit;
(3) control of the rotor current by variation of the extinction instant of the electronic switches in the rotor circuit; (In this case the ignition angle will be taken as constant.)
(4) control of the rotor current by employing a chopper circuit with a resistive load in the rotor circuit;
(5) control of the rotor current by recuperation of the slip power to the supply system via an inverter;
(6) control of the rotor current by recuperation of the slip power to the supply system via an inverter with power factor compensation with an electronic chopper circuit.

It may be stated that system (1) finds its application in the low and medium power range. Systems cited in case (2) find application chiefly in the medium power range, with some applications in the lower and higher ranges. An example of this type of control applied to a Ward Leonard Ilgner set in the high power range will be given in the experimental work. Systems of the type investigated in (3) are novel, and have neither been investigated nor proposed previously as far as known at present. These experiments are a direct result of the systematic investigation indicating the feasibility and simultaneously the lack of such types of investigations. Although it is disputable whether the specific system investigated will be applied in practice, the results obtained will certainly stimulate the application of similar ideas in other systems. This will be discussed at some length later however.

Systems with recuperation of the slip power, and consequently all systems of Group IIA, have as a field of application the medium and high power ranges. The systematic classification and investigation of the machine-electronic systems have also indicated that the majority of the examples known and used at present pay little attention to the power factor and harmonics presented to the supply system. In chapter 1 it was illustrated that machine-electronics is not a new subject, but due to the factors mentioned in chapter 1, application was restricted in the past. At present the situation is changing, and the total power capacity of the systems already installed is increasing rapidly. This is steadily increasing the importance of the amount of reactive power and the harmonic currents drawn from the supply. Direct harmonic compensation has not yet been investigated for machine-electronic systems. The power factor problem stimulated the development of systems cited in (3) and supplied the incentive to investigate compensated power recuperation systems such as (6).

Up to the present no attention has been paid to the influence the information-electronic part of the system has on the characteristics. For the purposes of classification only the power flow in the electromechanical converter was taken into account. Under a specific set of operating conditions, when the electromechanical converter operates

at a certain speed, delivering a specific load torque, the power factor, machine and electronic switch currents and harmonic components of all the currents are not influenced by the information electronic system as long as it has been designed to operate satisfactorily under these conditions. However, as soon as one is interested in the characteristics for open or closed loop application of this control system, the characteristics of the information electronics become important. In this chapter attention will be devoted to the influence an ideal information electronic subsystem will have on the transfer characteristics of the machine-electronic system.

A word about the theoretical models to be used in all these investigations is in order. In chapter 3 an extensive analysis as well as a simplified approach were developed. Whereas the extensive analysis may be applied to all machine-electronic systems with the correct constraints, the simplified analysis was specifically investigated with induction machines with rotor control in mind. The extensive analysis will be applied to the systems with control of the stator voltage by delay of the ignition angle of the electronic switches, whereas a simplified approach will be used for all the rotor control systems to be investigated. In the stator control system with ignition angle delay the nature of the electronic switching circuit - in principle two antiparallel thyristors - is so simple that it is not necessary to account for their presence by a further investigation of the model. The same considerations hold for the ignition angle delay of the rotor current to a certain degree. In all the other systems to be investigated, however, the characteristics of the electronic switches have to be taken into account in the analysis in order to be able to find correspondence with the experimental investigations later.

Lastly it must be remarked that to correspond with the majority of subsequent experimental investigations, the electromechanical converter to be used in the analysis of the present chapter will be a semi-four-phase induction machine.

4.2 AN EXAMPLE OF GROUP II CLASS 1 MACHINE-ELECTRONIC SYSTEMS: CONTROL OF THE STATOR VOLTAGE OF AN INDUCTION MACHINE BY VARIATION OF THE IGNITION ANGLE.

As has been explained in the previous paragraph, attention will now be devoted to the theoretical investigation, under the idealized conditions of chapter 3, of the control of the applied stator voltage by delay of the triggering instant of the electronic switches in the stator circuits. The current reduces to zero during each cycle by natural commutation, and correspondingly the switching rhythm is at the stator frequency. By employing the complex-Fourier approach of chapter 3, it is possible to obtain expressions for the stator currents of a semi-four-phase induction machine.The known values of these currents as a function of the delay angle of the control system enables one to obtain torque-speed characteristics, transfer function, harmonic current distortion and power factor for the proposed system.

4.2.1 *INVESTIGATION OF THE SWITCHING MODE, AND DERIVATION OF THE SWITCHING COMMANDS.*

The switching function is zero up to a time t_{α_s} after the line zero voltage condition. The different possible stable asymmetrical conditions due to triggering (80 will be examined later. It will now only be assumed that:

$$\left.\begin{array}{c} \psi_s \leqslant \alpha_s \leqslant \pi \\ \text{resulting in} \quad \alpha_s \leqslant \gamma_s \leqslant \psi_s + \pi \\ \xi_s \leqslant \pi \end{array}\right\} \qquad 4.1$$

where ψ_s is the steady state phase angle between voltage and current in the unswitched condition.

The information for operating the switches must be derived in some or other way from voltages related to the system. Fundamentally there are three possibilities, namely, u^x_{sg}, u_e and $\bar{u}^x_s$. It is furthermore also dependent on the principle chosen for the input unit of the information electronics subsystem. Two methods for operating this function block present themselves. Let the applied voltage be

$$u^x_{sg} = \sqrt{2}U_{sg} \sin(\omega_s t - \overline{x-1}\ \frac{2\pi}{n}) \qquad 4.2$$

and the induced voltage across the machine winding when the electronic switch is nonconducting be:

$$t_{\overline{\gamma_s - \pi}} < t < t \quad : \qquad e^x_s = e^x_s\ (t, \alpha_s, s) \qquad 4.3$$

therefore

$$t_{\overline{\gamma_s - \pi}} < t < t_{\gamma_s} \quad : \qquad \bar{u}^x_s = e^x_s\ (t, \alpha_s, s) \qquad 4.4a$$

and

$$t_{\alpha_s} < t < t_{\gamma_s} \quad : \qquad \bar{u}^x_s = u^x_{sg} \qquad 4.4b$$

In the ideal case

$$t_{\overline{\gamma_s - \pi}} < t < t_{\alpha_s} \qquad u_e = u^x_{sg} - e^x_s\ (t, \alpha_s, s) \qquad 4.5$$

$$t_{\alpha_s} < t < t_{\gamma_s} \qquad u_e = +U_e$$

where U_e is a small constant positive voltage drop of the order of 1 volt.

In the first instance consider that the voltage zero condition at the input of the information-electronics subsystem is detected, and the derivation of the triggering command related to this instant. Three types of control will result

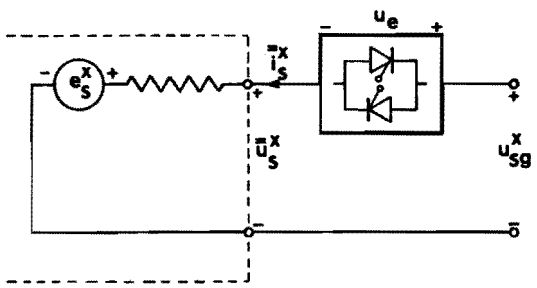

FIG. 4.1(a) VOLTAGE AND CURRENT DEFINITIONS FOR A STATOR PHASE WITH VOLTAGE CONTROL BY DELAY OF THE INSTANT OF CONTROL IGNITION.

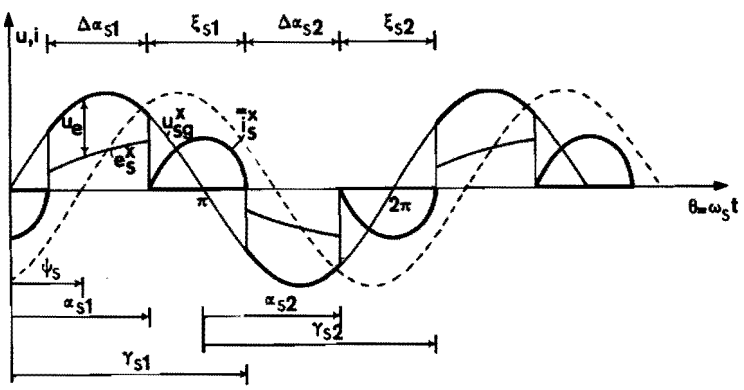

FIG. 4.1(b) WAVEFORM DEFINITIONS CONCERNING THE STATOR VOLTAGE CONTROL BY DELAY OF THE IGNITION ANGLE IN THE STATOR.

(i) *Input* u_{sg}^{x} : zero conditions are detected at

$$\omega_s t = h\pi \quad , \quad (h = 0, \pm 1 - - - - \infty) \qquad 4.6$$

If the triggering instant is now obtained by introducing a constant delay, the operating conditions are specified by

$$\text{or} \qquad \begin{matrix} t_{\alpha_s} = \text{constant} \\ \alpha_s = \text{constant} \end{matrix} \qquad 4.7$$

This type of control will be referred to as "constant ignition angle delay" or " α_s -control".

(ii) *Input* $u_s^{=x}$. Since relation 4.1 specifies α_s, γ_s and ξ_s zero conditions of the input voltage will be detected at the instants given by relation 4.6. However, since e_s^x may exhibit a zero voltage condition in the interval $(t_{\alpha_s} - t_{\overline{\gamma_s - \pi}})$, a possibility exists for introducing this additional information into the information-electronic subsystem input. Whereas the first zero voltage condition is specified explicitly, the last is dependent on slip, ignition angle and operating conditions. Design of the information electronics will then need to eliminate this second condition. The triggering angle will then also be specified by relation 4.7 in this case.

(iii) *Input* u_e. Zero voltage conditions will be detected at

$$\omega_s t = \overline{\gamma_s - h\pi} \quad (h = 0, \pm 1, \pm 2 - - - \pm \infty) \qquad 4.8a$$

With a constant delay after the detection of the above condition, operation is now specified by:

$$\text{or} \qquad \begin{matrix} (t_{\alpha_s} - t_{\overline{\gamma_s - \pi}}) = \text{constant} \\ \Delta\alpha_s = (\alpha_s - \overline{\gamma_s - \pi}) = \text{constant} \end{matrix} \qquad 4.8b$$

To this type of control will be referred as "ignition delay with constant blocking angle", or " $\Delta\alpha_s$-control".

In the second instance the angle of triggering may be determined by integration of the system-related input voltage up to a pre-set limit. As will be discussed later, there are various practical reasons that impart considerable elegance to this method (see chapter 5). Again three types of control will result:

(i) *Input* u_{sg}^{x}. The operating conditions are specified by:

$$\int_0^{t_{\alpha_s}} u_{sg}^{x} \, dt = \text{constant} \qquad 4.9$$

which reduces to relation 4.7 after evaluation with an input unit started at t = 0.

With a continuously integrating input unit the conditions are:

$$\int_{t_{\alpha_s - \pi}}^{t_{\alpha_s}} u_{sg}^{x}\, dt = \text{constant} \qquad 4.10$$

making it unsuitable for control since the information contains no zero voltage reference.

(ii) *Input* $\bar{u}_s^x$. With integration initiated at the zero condition, the operation is constrained to:

$$\int_{0}^{t_{\gamma_s - \pi}} u_{sg}^{x}\, dt + \int_{t_{\gamma_s - \pi}}^{t_{\alpha_s}} e_s^x\,(t, \alpha_s, s)\, dt = \text{constant} \qquad 4.11$$

Considering the implicit dependence of e_s^x on the operating conditions, one is not likely to employ this method.

(iii) *Input* u_e. The input voltage is nearly zero during conducting of the switch, therefore

$$\int_{0}^{t_{\gamma_s - \pi}} u_e\, dt + \int_{t_{\gamma_s - \pi}}^{t_{\alpha_s}} u_{sg}^{x}\, dt - \int_{t_{\gamma_s - \pi}}^{t_{\alpha_s}} e_s^x(t, \alpha_s, s)\, dt = \text{constant} \qquad 4.12$$

This method will suffer from the same drawbacks as the previous proposed integration of the applied winding voltage.

Considerations regarding the practical execution of the systems have confined the investigated types to constant ignition angle delay (α_s-control) and ignition delay with constant blocking angle ($\Delta\alpha_s$-control). In the following paragraphs attention will be given to the transfer functions of these two variants. As the calculation of harmonic distortion, power factor or torque is general, the results do not suffer from a limited applicability, however.

4.2.2 *THE SYSTEM EQUATIONS FOR THE SEMI-FOUR PHASE INDUCTION MACHINE WITH STATOR VOLTAGE CONTROL BY IGNITION ANGLE DELAY IN THE ELECTRONIC SWITCHES.*

4.2.2.1 *Equations for the assumed model.*

The general relations developed for an n-m phase induction machine under switched excitation on the stator side will now be applied to the

specific case of a semi-four-phase machine with the previously explained ignition delay, switched at the stator frequency.

Consider an electromechanical transducer with four phases on rotor and stator, corresponding voltages and currents being:

$$\left[u_s^n\right]=\begin{bmatrix} u_s^a \\ u_s^b \\ u_s^c \\ u_s^d \end{bmatrix} \quad ; \quad \left[u_r^n\right]=\begin{bmatrix} u_r^a \\ u_r^b \\ u_r^c \\ u_r^d \end{bmatrix} \quad ; \quad \left[i_s^n\right]=\begin{bmatrix} i_s^a \\ i_s^b \\ i_s^c \\ i_s^d \end{bmatrix} \quad ; \quad \left[i_r^n\right]=\begin{bmatrix} i_r^a \\ i_r^b \\ i_r^c \\ i_r^d \end{bmatrix} \quad - - - -$$

4.13

From relation 3.8a

$$z_r = z_s = \exp\left(j\frac{\pi}{2}\right)$$

giving an instantaneous symmetrical component transformation matrix for the Fortescue transformation:

$$\left[\$_s^n\right] = \left[\$_r^n\right]=\frac{1}{2}\begin{bmatrix} 1 & 1 & 1 & 1 \\ 1 & -j & -1 & j \\ 1 & -1 & 1 & -1 \\ 1 & j & -1 & -j \end{bmatrix} \quad - - - - - \qquad 4.14$$

From relations 4.13 and 4.14, in accordance with relation 4.9, it may be shown that under semi-balanced constraints on this system, i.e. for

$$\left.\begin{aligned} u_s^a &= -u_s^c \quad ; \quad u_s^b = -u_s^d \\ i_s^a &= -i_s^c \quad ; \quad i_s^b = -i_s^d \end{aligned}\right\} \quad - - - - - - - \qquad 4.15$$

The voltages and currents under the instantaneous symmetrical component transformation become:

$$\begin{bmatrix} \dot{u},i^{1,z} \\ \dot{u},i^{2,t} \\ \dot{u},i^{3,z} \\ \dot{u},i^{4,t} \end{bmatrix}_{s/r} = \begin{bmatrix} 0 & 0 \\ 1 & j \\ 0 & 0 \\ 1 & -j \end{bmatrix} \cdot \begin{bmatrix} u,i^{a} \\ u,i^{b} \end{bmatrix}_{s/r} \qquad 4.16$$

This proves that the zero-torque voltages and currents do not occur in the above semi-balanced four phase system, which may be represented by its equivalent semi-four-phase system

$$\begin{bmatrix} u^{a,b}_{s/r} , i^{a,b}_{s/r} \end{bmatrix} \qquad 4.16a$$

It is worthwhile noting that even in the case of this semi-four-phase system being unbalanced, the representation will be complete, and the zero-torque equations will remain zero. In the following analysis this representation will be employed, and will have general validity. The semi-four-phase machine and electronic system are both represented schematically in fig. 4.2(a). Referring to this model, the voltage-current equations are noted as:

$$\begin{bmatrix} u^{a}_{s} \\ u^{b}_{s} \\ \hline 0 \\ 0 \end{bmatrix} = \left[\begin{array}{cc:cc} R_s + DL_s & 0 & D\{M_{sr}\cos p\omega_m t\} & D\{M_{sr}\cos p(\omega_m t + \frac{\pi}{2p})\} \\ 0 & R_s + DL_s & D\{M_{sr}\cos p(\omega_m t - \frac{\pi}{2p})\} & D\{M_{sr}\cos p\omega_m t\} \\ \hdashline D\{M_{sr}\cos p\omega_m t\} & D\{M_{sr}\cos p(\omega_m t - \frac{\pi}{2p})\} & R_r + DL_r & \\ D\{M_{sr}\cos p(\omega_m t + \frac{\pi}{2p})\} & D\{M_{sr}\cos p\omega_m t\} & & R_r + DL_r \end{array}\right] \begin{bmatrix} i^{a}_{s} \\ i^{b}_{s} \\ \hline i^{a}_{r} \\ i^{b}_{r} \end{bmatrix} \qquad 4.17$$

under assumption that the mechanical speed is constant, and equal to ω_m.

Therefore: $\theta = \omega_m t$ ($\theta_o = 0$). Furthermore $L_s = L_{s,h} + L_{s\sigma}$, $L_r = L_{r,h} + L_{r\sigma}$

4.2.2.2 *Considerations concerning the excitation functions.*

Following the procedure of chapter 3, and taking the previous arguments into account, the transformation matrix for the Fortescue transformation now becomes

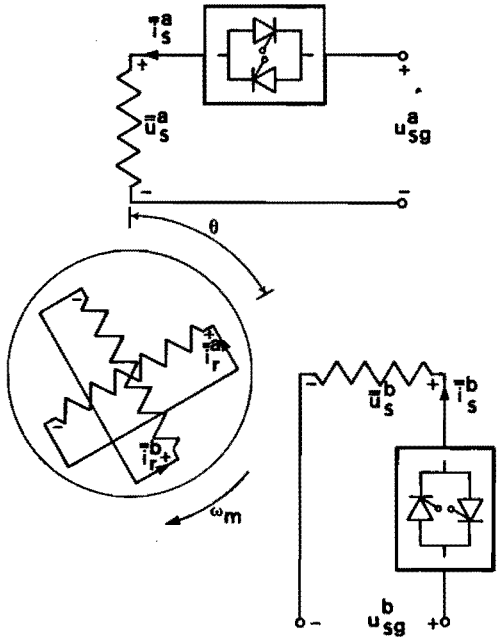

FIG. 4.2(a) DEFINITIONS PERTAINING TO THE ANALYSED SEMI-FOUR-PHASE INDUCTION MACHINE MODEL.

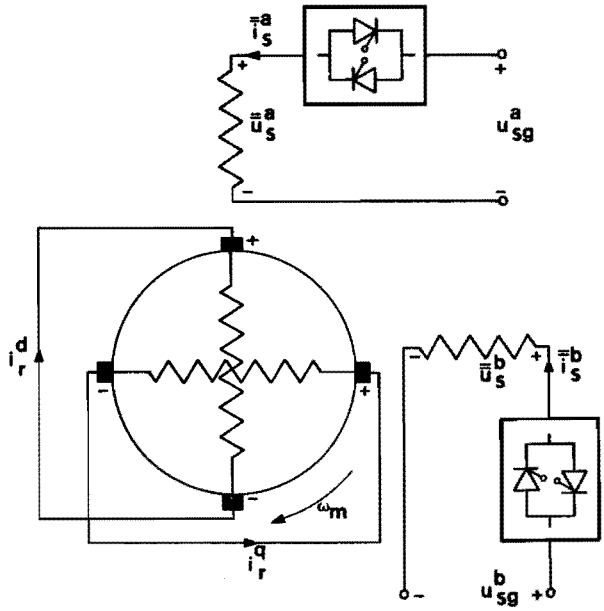

FIG. 4.2(b) CONTROLLED INDUCTION MACHINE MODEL UNDER PARK-TRANSFORMATION.

$$\left[S^{2}_{s/r}\right] = \frac{1}{\sqrt{2}}\begin{bmatrix} 1 & 1 \\ -j & j \end{bmatrix}, \left(\left[S^{2}_{s/r}\right]\right)^{-1} = \begin{bmatrix} 1 & j \\ 1 & -j \end{bmatrix} \quad -- \quad 4.18a$$

giving

$$\begin{bmatrix} \left[\dot{u},\dot{i}\right]^{2,t}_{s/r} \\ \left[\dot{u},\dot{i}\right]^{4,t}_{s/r} \end{bmatrix} = \frac{1}{\sqrt{2}}\begin{bmatrix} \left[u,i\right]^{a}_{s/r} + j\left[u,i\right]^{b}_{s/r} \\ \left[u,i\right]^{a}_{s/r} - j\left[u,i\right]^{b}_{s/r} \end{bmatrix} = \begin{bmatrix} \left[\dot{u},\dot{i}\right]^{(+)}_{s/r} \\ \left[\dot{u},\dot{i}\right]^{(-)}_{s/r} \end{bmatrix} \quad --- \quad 4.18b$$

With reference to figures 4.2(a), 4.3 and relations 4.3 to 4.5 the excitation functions for the two stator phases may be expressed as:

$$\left.\begin{aligned} \bar{\bar{u}}^{a}_{s}(t) &= \bar{\bar{u}}^{a}_{sg}(t) + \bar{\bar{e}}^{a}_{s}(t) \\ \bar{\bar{u}}^{b}_{s}(t) &= \bar{\bar{u}}^{b}_{sg}(t) + \bar{\bar{e}}^{b}_{s}(t) \end{aligned}\right\} \quad ------ \quad 4.19a$$

The waveforms contain only odd harmonics. The switched parts of the supply voltages are:

$$\begin{bmatrix} \bar{\bar{u}}^{a}_{sg}(t) \\ \bar{\bar{u}}^{b}_{sg}(t) \end{bmatrix} = \frac{1}{\sqrt{2}} \sum_{h=0}^{\infty} \left(\begin{bmatrix} (j)^{\overline{2h+1}} \\ 1 \end{bmatrix} \dot{\bar{\bar{U}}}_{sg\ \overline{2h+1}} \exp j(\overline{2h+1}\ \omega_s t) + \right.$$

$$\left. + \begin{bmatrix} (-j)^{\overline{2h+1}} \\ 1 \end{bmatrix} \dot{\bar{\bar{U}}}^{*}_{sg\ \overline{2h+1}} \exp -j(\overline{2h+1}\ \omega_s t) \right) \quad 4.19b$$

with

$$\dot{\bar{\bar{U}}}_{sg\ \overline{2h+1}} = \frac{U_{sg}}{\pi} \left\{ (2h)^{-1} \left(\exp -j\overline{2h\gamma_s} - \exp -j\overline{2h\alpha_s}\right) - \right.$$

$$\left. (\overline{2h+1})^{-1} \left(\exp -j\overline{2h+1\gamma_s} - \exp -j\overline{2h+1\alpha_s}\right) \right\} \quad 4.19c$$

and

$$\hat{\underline{U}}_{sg1} = -\frac{U_{sg}}{\pi}\left\{ j\xi_s + \tfrac{1}{2}(\exp -j2\gamma_s - \exp -j2\alpha_s)\right\} \qquad 4.19d$$

as indicated in A4.1 along with the alternative expressions.

In order to find the full excitation function, the induced voltage during the time interval $(\alpha_s - \overline{\gamma_s - \pi})$, (non-conducting period of the electronic switches), must be estimated. Inspection of the expected voltage and current relationships as a function of time (fig. 4.3) indicates that it may be expected to find two modes of operation as far as the determination of the induced voltage is concerned. During the following investigation of the induced voltage phase "b" will be taken as normative and phase "a" as complementary.

4.2.2.3 *The nature of the induced voltages during blocking periods: two approximations.*

MODE I (See fig. 4.3a,b)

During the time that the switch is nonconducting in the normative phase, the current in the complementary phase is zero (first blocking period) starts its conduction cycle (second blocking period), and again reduces to zero before the normative phase again resumes its conduction (third blocking period). For this mode therefore:

$$(\alpha_s - \tfrac{\pi}{2}) > \gamma_s - \pi \qquad 4.20a$$

$$\left.\begin{array}{l} \bar{i}_s^a = 0 \\ \bar{i}_s^b = 0 \end{array}\right\} \quad \text{for} \quad (\gamma_s - \pi) < \omega_s t < (\alpha_s - \tfrac{\pi}{2})$$

$$\left.\begin{array}{l} \bar{i}_s^a = i_s^a(t) \\ \bar{i}_s^b = 0 \end{array}\right\} \quad \text{for} \quad (\alpha_s - \tfrac{\pi}{2}) < \omega_s t < (\gamma_s - \tfrac{\pi}{2}) \qquad \text{- - - -} \quad 4.20b$$

$$\left.\begin{array}{l} \bar{i}_s^a = 0 \\ \bar{i}_s^b = 0 \end{array}\right\} \quad \text{for} \quad (\gamma_s - \tfrac{\pi}{2}) < \omega_s t < \alpha_s$$

MODE II (See fig. 4.3c,d)

For this mode the current conduction in the complementary phase overlaps the non-conducting period of the normative phase completely. Therefore

$$(\gamma_s - \pi) \geq (\alpha_s - \tfrac{\pi}{2}) \qquad \text{- - - -} \quad 4.21a$$

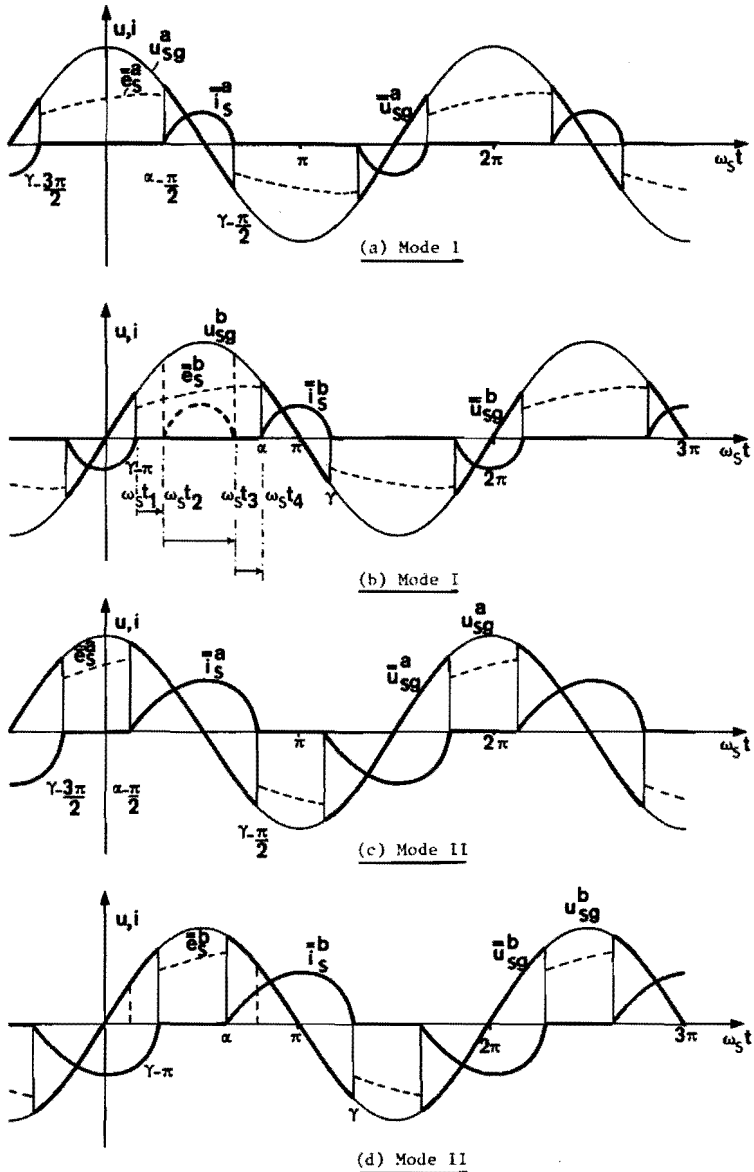

FIG. 4.3 WAVEFORMS RELEVANT TO THE STATOR CONTROL WITH IGNITION DELAY.

$$\left.\begin{aligned} i_s^a &= i_s^a(t) \\ i_s^b &= 0 \end{aligned}\right\} \quad \gamma_s - \pi < \omega_s t < \alpha_s \qquad \text{- - - -} \qquad 4.21b$$

The induced voltage under operation according to mode I will now be examined.

This case is treated fairly extensively in Appendix A4.2. Consider the situation during the first blocking period. Phases "b" and "a" both block, and the rotor currents will decay exponentially in each phase. As no coupling (magnetic) exists between the two phases first order equations are expected. During the second blocking period; at $t = t_2$, phase "a" starts to conduct. The situation is reminiscent of a two phase synchronous machine where a short circuit has been applied to both rotor circuits, and the field is switched on to an arbitrary supply. As these types of problems may mostly be simplified considerably by employing a d-q transformation for the rotor variables, the same line of attack will be followed here, and the model of the machine as shown in fig. 4.2(b) is obtained.

Let the direct-axis current, and voltage of the rotor circuit i_r^d u_r^d, and the quadrature-axis current and voltage i_r^q, u_r^q of the rotor circuit, respectively be defined as:

$$\begin{bmatrix} i, u_r^d \\ i, u_r^q \end{bmatrix} = \begin{bmatrix} \cos p\omega_m t & -\sin p\omega_m t \\ \sin p\omega_m t & \cos p\omega_m t \end{bmatrix} \begin{bmatrix} i, u_r^a \\ i, u_r^b \end{bmatrix} \qquad 4.22$$

Define i_{s2}^a as the transient current that will flow in the complementary phase, ("a"), during the second blocking period. Taking into account that the current in the normative phase will be zero, and that the rotor circuits have an external short circuit, the transformation results in:

$$\begin{bmatrix} u_{s2}^a \\ e_{s2}^b \\ 0 \\ 0 \end{bmatrix} = \begin{bmatrix} R_s + L_s D & M_{sr} D & 0 \\ 0 & 0 & M_{sr} D \\ M_{sr} D & R_r + L_r D & p\omega_m L_r \\ -p\omega_m L_r & -p\omega_m L_r & R_r + L_r D \end{bmatrix} \begin{bmatrix} i_{s2}^a \\ i_{r2}^d \\ i_{r2}^q \end{bmatrix} \qquad 4.23$$

where i_{r2}^d and i_{r2}^q refer specifically to the direct and quadrature axis currents during the second blocking period. Examination of relation 4.23 and fig. 4.2(b) indicates that the change in flux linkages in

the quadrature-axis of the now obtained model always represents induced e.m.f. in the phase b during blocking. This suggests treating the whole problem of determining the induced e.m.f. in the blocking phase with this model, as may be found in the treatment of Appendix A4.2. Considering this treatment, the induced e.m.f. in phase "b" during the first blocking period may now be shown to be

$$e_{s1}^{bi} = M_{sr} \exp -t' \tau_r^{-1} \left\{ (\overline{1-s}\ \omega_s I_r^a(t_1) - I_r^b(t_1)\ \tau_r^{-1}) \cos \overline{1-s}\ \omega_s t \right.$$

$$\left. - (\overline{1-s}\ \omega_s I_r^b(t_1) + I_r^a(t_1)\ \tau_r^{-1}) \sin \overline{1-s}\ \omega_s t \right\} \quad ---- \quad 4.24$$

where $I_r^a(t_1)$ and $I_r^b(t_1)$ are the initial values of the rotor currents in the "a" and "b" phases of the semi-four-phase machine model, and the time

$$t' = (t - \frac{\gamma_s - \pi}{\omega_s})$$

The induced e.m.f. in phase "b" during the second blocking period will now be examined.

The characteristic equation for 4.23 may be calculated in terms of the rotor and stator time constants and the slip as:

$$\lambda^3 + \left\{ \frac{\tau_s^{-1}\tau_s^{-1}}{\sigma} + \tau_r^{-1} \right\} \lambda^2 + \left\{ \frac{\tau_r^{-1} + 2\tau_s^{-1}}{\tau_r \sigma} + \overline{1-s}^2\ \omega_s^2 \right\} \lambda$$

$$+ \left\{ \frac{\tau_r^{-2} + \overline{1-s}^2\ \omega_s^2}{\tau_s \sigma} \right\} = 0 \quad ---- \quad 4.25$$

Although this equation may be solved accurately numerically, little information pertaining to the influence of variation of slip on the flux linkages, and consequently the induced voltage, can be extracted from these solutions. With finite rotor and stator time constants it is possible to divide the slip scale into three regions, defined by the approximations used for the characteristic equation in these regions.

If

$$\sigma^{-1}\ \omega_s^{-2} (\tau_r^{-2} + 2\tau_s^{-1}\ \tau_r^{-1}) \ll \overline{1-s}^2 \qquad 4.26a$$

certain coefficients of rel. 4.24 may be simplified. On the other hand, when

$$\tau_r^{-2}\ \omega_s^{-2} \gg \overline{1-s}^2 \qquad 4.26b$$

another approximation will arise. Defining the boundary slip as the slip where the inequality changes to an equation, the corresponding boundary slips will be:

$$s_{fa} = 1 \pm \left\{ \sigma^{-1}\, \omega_s^{-2} (\tau_r^{-2} + 2\, \tau_s^{-1}\, \tau_r^{-1}) \right\}^{\frac{1}{2}} \qquad 4.26c$$

for the first approximation and

$$s_{sa} = 1 \pm \omega_s^{-1}\, \tau_r^{-1} \qquad 4.26d$$

for the second approximation, as is shown in appendix A4. It is to be noted that in the slip range

$$s = \pm \left\{ \sigma^{-1}\, \omega_s^{-2} (\tau_r^{-2} + 2\tau_s^{-1}\, \tau_r^{-1}) \right\}^{\frac{1}{2}} \mp \omega_s^{-1}\, \tau_r^{-1} \qquad 4.26e$$

no approximation is valid, and for numerical solution the accurate equation must be used.

Before attempting to formulate the dependence of the induced e.m.f. on slip, one additional simplication will be made. If the dependence of the relative resistive voltage drop in the stator on machine power is investigated, it is found that its decrease is inverseley proportional to more than the square-root of the relative increase in power ([B13]. As the stator leakage inductance decreases less, it may be expected that the electrical stator time constant will only increase with machine size. Neglecting the influence of the stator time constant will furthermore not alter the problem fundamentally, nor change the order of the system when the stator resistance is supposed to be negligible. It should furthermore be noted that under conditions of very large stator time constant, the slip range separating the two different approximation regions approaches minimum span. (see fig. 4.3.1)

Solving 4.23 under these constraints for the quadrature axis current, it may be shown that under first approximation the induced e.m.f. is represented by:

$$e_{s2}^{bi} = M_{sr} \Big[\exp -t''\tau_e^{-1} \Big\{ (\omega_e I_{riii}^{qi} - \tau_e^{-1}\, I_{rii}^{qi}) \cos \omega_e t'' - (\omega_e\, I_{riii}^{qi} + \tau_e^{-1}\, I_{rii}^{qi}) \sin \omega_e t'' \Big\} - \omega_s \sqrt{2}\, I_{r2}^{qi} \sin(\omega_s t + \phi_2^{qi}) \Big] \qquad ---- \qquad 4.27a$$

with

$$t'' = \left(t - \frac{2\alpha_s - \pi}{2\omega_s}\right)$$

and

$$\tau_e = (2\sigma .\ \overline{1+\sigma}^{-1})\tau_r \ ; \ \omega_e = (\overline{1-s}^2\, \omega_s^2 - 4\sigma^{-2}\tau_r^{-2}\, \overline{1+\sigma}^2)^{\frac{1}{2}} \qquad 4.27b$$

and the constants as specified in appendix A4.2.

For a given machine with given rotor time constant, the eigenfrequency of the induced e.m.f. will be a function of the slip, and when the slip becomes either large or small, this frequency will approach the mechanical angular speed, transferred to the electrical side, or simply the "mechanical frequency" $\overline{1-s}\omega_s$. On the other hand, as pointed out in appendix A4.2, when the slip approached the boundary slip for the first approximation (i.e. the machine reduces speed in either direction of rotation), the eigenfrequency departs from the mechanical frequency at a rate in excess of that at which the boundary slip is approached. Depending on machine size (i.e. on machine resistances and leakage coefficients) the eigenfrequency may become so low that the eigenfrequency of the induced e.m.f. is transformed in a damping term at slips closer to one.

Solution of the set 4.23 for i_r^q under the constraints of the second approximation - slip around unity - results in a non-oscillating expression for the induced e.m.f., as already anticipated in the above argumentation. e_s^b now becomes:

$$e_{s2}^{bii} = -M_{sr}\left\{\tau_{e-}^{-1} I_{rii}^{qii} \exp -t''.\ \tau_{e-}^{-1} + \tau_{e+}^{-1} I_{riii}^{qii} \exp t''.\tau_{e+}^{-1} + \omega_s \sqrt{2}\ I_{r2}^{qii} \sin(\omega_s t + \phi_2^{qii})\right\} \quad - - - - \quad 4.28a$$

with

$$\tau_{e\pm}^{-1} = \left\{\tau_e^{-1} \pm \tau_r^{-1}\left(\frac{\overline{1+\sigma^2}}{2\sigma^2} - \sigma^{-1}\right)^{\frac{1}{2}}\right\} \quad - - - - \quad 4.28b$$

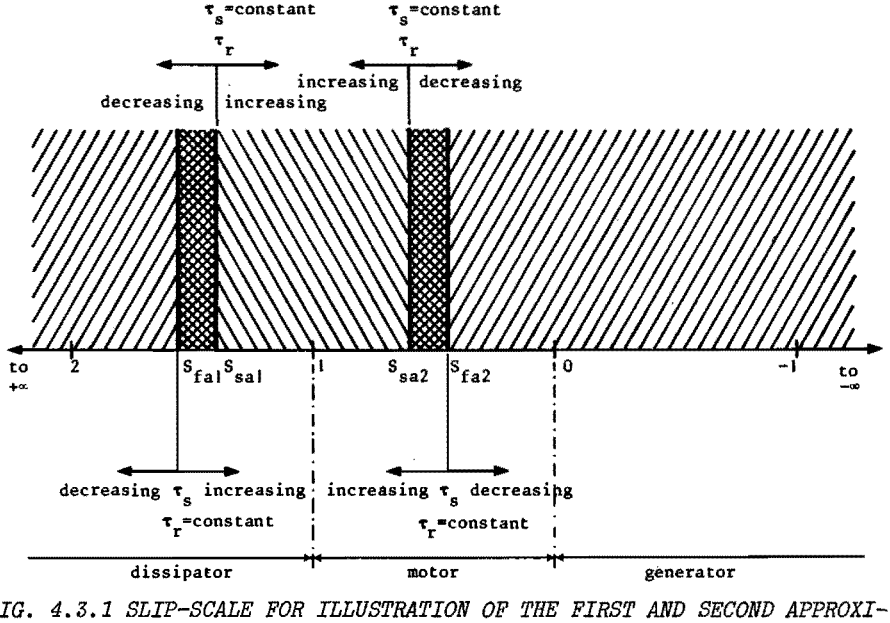

FIG. 4.3.1 SLIP-SCALE FOR ILLUSTRATION OF THE FIRST AND SECOND APPROXIMATIONS TO THE SOLTUIONS OF THE CHARACTERISTIC EQUATION DURING THE SECOND BLOCKING PERIOD.

and t" as defined previously. It may be observed that the amplitude of the transient component at a specific slip is now only a function of the equivalent time constants. Slip must still be taken into account, although it does not appear explicitly in 4.28. The constants are still found to be slip dependent. (See appendix A4.2)

Referring to the values of the constants of the first approximation:

$$(I^{qi}_{rii}\ ,\ I^{qi}_{riii}\ \text{ and the sustained component } I^{qi}_{r2})$$

and the second approximation:

$$(I^{qii}_{rii}\ ,\ I^{qii}_{riii}\ \text{ and the sustained component } I^{qii}_{r2})$$

and the boundary slips, some limiting situations will now be examined. It has been mentioned that when the stator time constant tends to very large values, the boundary slips for both approximations become separated by a minimum value

$$s_{fa\ 1,2} - s_{sa\ 1,2} = \pm\, \omega_s^{-1}\, \tau_r^{-1}\, (\sigma^{-\frac{1}{2}} - 1) \qquad 4.29$$

(refer to fig. 4.3.1 and to appendix A4.2).

With the rotor time constant increasing, the boundary slips move towards the stationary condition of the machine, extending the region where the induced e.m.f. shows an eigenoscillation. The expressions for the first approximation may not be investigated for the limiting condition of unity slip, however, due to the constraint of rel. 4.26a, unless the rotor time constant also approaches the limiting condition of a very large value. This is not interesting in practice. The expressions for the first approximation will be investigated later in this chapter for the limiting condition of extremely large rotor time constant at a value of slip different from unity, to indicate that they correspond with the third approximation, where all resistances will be neglected.

The second approximation is valid as zero mechanical speed is approached. At zero speed the values of the appropriate constants from 4.28a will be:

$$\left.\begin{aligned} I^{qii}_{rii} &= \frac{\tau_{e-}}{\tau_r}\left\{1 - \frac{\tau_{e+}(\tau_{e-} - \tau_r)}{\tau_r\,(\tau_{e-} - \tau_{e+})}\right\}\, i^{qii}_{r2}\ (t=t_2) \\ I^{qii}_{riii} &= \left\{\frac{\tau^2_{e+}\,(\tau_{e-} - \tau_r)}{\tau^2_r\,(\tau_{e-} - \tau_{e+})}\right\}\, i^{qii}_{r2}\qquad (t=t_2) \\ I^{qii}_{r2} &= 0 \end{aligned}\right\} \qquad 4.30$$

where the initial value of the quadrature current at the start of conduction in the complementary phase can be determined from relation A4.20a, appendix A4.2 as:

$$\omega_m=0 : i_{r2}^{qi}(t=t_2)=i_{r2}^{qii}(t=t_2)=i_{ri}^{qi}(t=t_2)=I_r^b(t_1)\exp-\tau_r^{-1}\left(\frac{2\alpha_s-2\gamma_s+\pi}{2\omega_s}\right) \qquad 4.31$$

Referring this to the relation for the induced voltage (4.28a), and taking fig. 4.2(a) and (b) into account, it may be deduced that in the steady stationary state $I_r^b(t_1) = 0$, so that in the stationary condition an induced voltage across the normative phase can only appear when the flux linkages in the quadrature axis are still decaying toward zero. In steady stationary condition this voltage will be zero.

During the third blocking period a similar situation as in the first blocking period arises - only the initial conditions differ. The induced e.m.f. in the normative phase is therefore of the same form as in rel. 4.24, i.e.:

$$e_{s3}^{bi} = M_{sr} \exp -t''' \tau_r^{-1} \left\{ \left(\overline{1-s}\, \omega_s I_{rii}^{qI} - \tau_r^{-1} I_{ri}^{qI} \right) \cos \overline{1-s}\omega_s t''' - \left(\overline{1-s}\, \omega_s I_{ri}^{qI} + \tau_r^{-1} I_{rii}^{qI} \right) \sin \overline{1-s}\, \omega_s t''' \right\} \quad - - - \; 4.32$$

with

$$t''' = (t - \frac{2\gamma_s - \pi}{2\omega_s})$$

As pointed out in appendix A4.2, the constants in the above expression may be determined by calculating the initial conditions either by the first or the second approximation during the second blocking period. In effect this results in two expressions for $e_{s3}^{bi,ii}$, which are not investigated further, as they have the same properties.

Reviewing the expressions obtained thus far for the induced voltage in the normative phase, and taking the complex expressions for the different constants into account, it may be seen that the Fourier coefficients, and consequently the currents calculated according to the methods of chapter 3, will be extremely complicated. Mostly the time that the induced voltage has to be taken into account will be less than a quarter period of the supply frequency, and the question arises whether it is not feasible to investigate an approximation that assumes the rotor time constant to be very large. This will also aid the insight into the problem by simplifying the expressions. The role of the rotor time constant can be accurately estimated by afterwards comparing the third with the first and second approximations.

4.2.2.4 *The induced voltage during blocking with all resistances neglected.*

From relation 4.29 it is evident that under the constraints that the stator and rotor resistances are assumed zero

$$s_{fa\ 1,2} = s_{sa\ 1,2} \qquad 4.33a$$

so that the difference between first and second approximations disappears, while the boundary slip according to 4.26c and 4.26d becomes:

$$s_{fa} = s_{sa} = 1 \qquad 4.33b$$

The approximation investigated therefore describes the whole slip scale, with exception of unity slip, which isalimiting condition. (refer to fig. 4.3.1)

Consider the first blocking period:

The equations for the four circuits of fig. 4.2(b) are:

$$t_1 < t < t_2 \quad \begin{bmatrix} e_{s1}^{aii} \\ e_{s1}^{bii} \\ 0 \\ 0 \end{bmatrix} = \begin{bmatrix} M_{sr}D & 0 \\ 0 & M_{sr}D \\ L_rD & \overline{1-s}\,\omega_s L_r \\ -\overline{1-s}\,\omega_s L_r & L_rD \end{bmatrix} \cdot \begin{bmatrix} i_{r1}^{dii} \\ i_{r1}^{qii} \end{bmatrix} \qquad 4.34$$

resulting in a second order characteristic equation, giving an oscillatory solution for i_r^q and i_r^d, consequently for the induced e.m.f. in phase "b" from 4.34 and A4.31d

$$t_1<t<t_2 : e_{s1}^{bii} = M_{sr}Di_{r1}^{qii} = \overline{1-s}\omega_s M_{sr}\left\{I_r^a(t_1)\cos\overline{1-s}\omega_s t - I_r^b(t_1)\sin\overline{1-s}\omega_s t\right\} \qquad 4.35a$$

It may be seen that the induced e.m.f. is proportional to the mechanical frequency, and that the eigenfrequency there of - as found previously for the first approximation - now corresponds to the mechanical frequency. This is concurrent with relation 4.27b.

Now consider the second blocking period. The descriptive equations are:

$$t_2<t<t_3 \quad \begin{bmatrix} u_{s2}^{a} \\ e_{s2}^{biii} \\ 0 \\ 0 \end{bmatrix} = \begin{bmatrix} L_sD & M_{sr}D & 0 \\ 0 & 0 & M_{sr}D \\ M_{sr}D & L_rD & \overline{1-s}\omega_s L_r \\ -\overline{1-s}\omega_s M_{sr} & -\overline{1-s}\omega_s L_r & L_rD \end{bmatrix} \begin{bmatrix} i_{s2}^{aiii} \\ i_{r2}^{diii} \\ i_{r2}^{qiii} \end{bmatrix} \qquad 4.36$$

For the solutions of the characteristic equation describing this third order system one may state categorically that the solution contains one d.c term and two oscillating terms at the same eigenfrequency than before (due to the positive, real nature of the coefficients), plus a sustained supply frequency term. As proved in appendix A4.2 the d.c term as well as the sustained supply frequency term of the

quadrature current has zero amplitude. From 4.36 and A4.34b the corresponding induced voltage is:

$$t_2<t<t_3 \quad e_{s2}^{biii} = M_{sr} Di_{r2}^{qiii} = \overline{1-s}\omega_s M_{sr}\left\{I_r^a(t_1)\cos\overline{1-s}\omega_s t - I_r^b(t_1)\sin\overline{1-s}\omega_s t\right\} \qquad 4.35b$$

This induced voltage corresponds to that previously found for the first blocking period, and is a continuation thereof.

As indicated in the appendix A4.2, the same equations and solutions for the direct and quadrature-axis currents and induced e.m.f. are found in the third blocking period. For the induced e.m.f. during the whole blocking period it is therefore found that:

$$t_1 < t < t_4 : e_s^b \simeq e_{s1}^{bii} + e_{s2}^{biii} + e_{s3}^{biii}$$

$$= \overline{1-s}\ \omega_s M_{sr}\left\{I_r^a(t_1)\cos\overline{1-s}\omega_s t - I_r^b(t_1)\sin\overline{1-s}\omega_s t\right\} \qquad 4.35c$$

A few words concerning the limiting conditions of the first approximation of paragraph 4.2.2.3 are in order. This has already been anticipated in the named paragraph. The last part of appendix A4.2 indicates what the limiting values of the quadrature current of the approximation concerned are. As remarked earlier, approximation one passes over into approximation three (all resistance neglected) in the limit, while the second approximation disappears (only valid at unity slip). The limits of the equations calculated in A4.2 prove this statement. Furthermore it may be seen that with the rotor resistance tending to zero, or the rotor time constant tending to a very large value, the coupling between the normative phase and the complementary phase due to rotation disappears: the component of the induced e.m.f. having a supply frequency disappears. In this state the limiting condition also illustrates that the influence of switching the complementary phase on and off during conduction of the normative phase disappears. The induced e.m.f. continues its oscillation at an eigenfrequency corresponding to the mechanical frequency, with amplitude determined solely by the initial conditions at the instant the electronic switch in the normative phase commences to block. Depending on the electrical time constants of the machine circuits, these views have to be adjusted according to the investigation of the previous pages.

Up to the present attention has been devoted to describing the induced e.m.f. during the blocking period of the normative phase under conditions where no overlapping of conduction with the complementary phase occurs. With reference to fig. 4.3(c) and (d) it may be seen that during operation according to mode II the "a" phase conducts during the entire blocking interval of phase "b". The system is again described by the simultaneous set of rel. 4.36, although the initial conditions in the solutions will differ from the initial conditions for mode I. In the following investigations it will be assumed that the induced e.m.f. under operating conditions according to mode II may be represented by the same type of expression as used for mode I.

Seeing that the induced voltage is now known, the expression may be noted in its Fourier components as follows:

$$\begin{bmatrix} \overline{\overline{e}}^{a}_{s}(t) \\ \overline{\overline{e}}^{b}_{s}(t) \end{bmatrix} = \frac{\overline{1-s}}{\sqrt{2}} \sum_{h=0}^{\infty} \left(\begin{bmatrix} (j)^{\overline{2h+1}} \\ 1 \end{bmatrix} \dot{\overline{\overline{E}}}_{s\overline{2h+1}} \exp j(\overline{2h+1}\omega_s t) + \right.$$

$$\left. + \begin{bmatrix} (-j)^{\overline{2h+1}} \\ 1 \end{bmatrix} \dot{\overline{\overline{E}}}^{*}_{s\overline{2h+1}} \exp -j(\overline{2h+1}\omega_s t) \right) \qquad 4.37a$$

with

$$\dot{\overline{\overline{E}}}_{s\overline{2h+1}} = \frac{jE^{ba}_{sr}}{\pi} \left\{ \frac{\exp -j(2h+2-s)\,\alpha_s - \exp -j(2h+2-s)\,(\gamma_s - \pi)}{(2h+2-s)} + \right.$$

$$\left. + \frac{\exp -j(2h+s)\alpha_s - \exp -j(2h+s)\,(\gamma_s - \pi)}{(2h+s)} \right\}$$

$$+ \frac{E^{bb}_{sr}}{\pi} \left\{ \frac{\exp -j(2h+2-s)\alpha_s - \exp -j(2h+2-s)\,(\gamma_s - \pi)}{(2h+2-s)} + \right.$$

$$\left. - \frac{\exp -j(2h+s)\alpha_s - \exp -j(2h+s)\,(\gamma_s - \pi)}{(2h+s)} \right\} \qquad 4.37b$$

and

$$\begin{bmatrix} \sqrt{2}\, E^{ba}_{sr} \\ \sqrt{2}\, E^{bb}_{sr} \end{bmatrix} = \omega_s M_{sr} \begin{bmatrix} I^{a}_{r}(t_1) \\ I^{b}_{r}(t_1) \end{bmatrix} \qquad 4.37c$$

as indicated along with alternative expressions in appendix A4.3. This may now be substituted in 4.19a to obtain the complete excitation functions for the present case.

4.2.2.5 *Transformation of the complete excitation functions.*

By using relation 4.18b and 4.19a the symmetrical component stator voltages now become:

$$\begin{bmatrix} \dot{\overline{\overline{u}}}^{(+)}_{s} \\ \dot{\overline{\overline{u}}}^{(-)}_{s} \end{bmatrix} = \frac{1}{\sqrt{2}} \begin{bmatrix} 1 & j \\ 1 & -j \end{bmatrix} \begin{bmatrix} \overline{\overline{u}}^{a}_{sg}(t) + \overline{\overline{e}}^{a}_{s}(t) \\ \overline{\overline{u}}^{b}_{sg}(t) + \overline{\overline{e}}^{b}_{s}(t) \end{bmatrix}$$

The complete set of voltages will be:

$$\begin{bmatrix} \dot{\bar{\bar{u}}}_s^{(+)} \\ \dot{\bar{\bar{u}}}_s^{(-)} \\ \dot{u}_r^{(+)} \\ \dot{u}_r^{(-)} \end{bmatrix} = \frac{1}{\sqrt{2}} \begin{bmatrix} \bar{\bar{u}}_{sg}^{a}(t) + j\bar{\bar{u}}_{sg}^{b}(t) + \bar{\bar{e}}_s^{a}(t) + j\bar{\bar{e}}_s^{b}(t) \\ \bar{\bar{u}}_{sg}^{a}(t) - j\bar{\bar{u}}_{sg}^{b}(t) + \bar{\bar{e}}_s^{a}(t) - j\bar{\bar{e}}_s^{b}(t) \\ 0 \\ 0 \end{bmatrix}$$

Substitution of the components from relations 4.19b and 4.37a indicates that not all the harmonic components will exist in the instantaneous symmetrical component voltage transforms. The relation simplifies into an expression containing only the $\overline{4h+1}$ st and $\overline{4h+3}$ rd components as follows:

$$\begin{bmatrix} \dot{\bar{\bar{u}}}_s^{(+)} \\ \dot{\bar{\bar{u}}}_s^{(-)} \end{bmatrix} = \sum_{h=0}^{\infty} \left\{ \begin{array}{l} j\left\{ (\dot{\bar{\bar{U}}}_{sg\overline{4h+1}} + \overline{1-s}\,\dot{\bar{\bar{E}}}_{s\overline{4h+1}}) \exp j(\overline{4h+1}\omega_s t) + \right. \\ \left. + (\dot{\bar{\bar{U}}}^{*}_{sg\overline{4h+3}} + \overline{1-s}\,\dot{\bar{\bar{E}}}^{*}_{s\,\overline{4h+3}}) \exp -j(\overline{4h+3}\omega_s t) \right\} \\ -j\left\{ (\dot{\bar{\bar{U}}}_{sg\overline{4h+3}} + \overline{1-s}\,\dot{\bar{\bar{E}}}_{s\overline{4h+3}}) \exp j(\overline{4h+3}\omega_s t) + \right. \\ \left. + (\dot{\bar{\bar{U}}}^{*}_{sg\overline{4h+1}} + \overline{1-s}\,\dot{\bar{\bar{E}}}^{*}_{s\,\overline{4h+1}}) \exp -j(\overline{4h+1}\omega_s t) \right\} \end{array} \right\} \quad 4.38a$$

In the relation the harmonic components will have the following values:
The switched supply components:

$$\dot{\bar{\bar{U}}}_{sg\overline{4h+1}} = U_{sg}\left\{ \left(A^{U}_{s\overline{4h+1}} \right)^2 + \left(B^{U}_{s\overline{4h+1}} \right)^2 \right\}^{\frac{1}{2}} \exp -j\phi^{U}_{s\overline{4h+1}}$$

$$\phi^{U}_{s\overline{4h+1}} = \arctan \left\{ \frac{B^{U}_{s\overline{4h+1}}}{A^{U}_{s\overline{4h+1}}} \right\}$$

where

$$A^{U}_{s\overline{4h+1}} = \frac{1}{\pi}\left(\frac{\cos 4h\gamma_s - \cos 4h\alpha_s}{4h} - \frac{\cos \overline{4h+2}\gamma_s - \cos \overline{4h+2}\alpha_s}{4h+2} \right)$$

$$B^{U}_{s\overline{4h+1}} = \frac{1}{\pi}\left(\frac{\sin 4h\gamma_s - \sin 4h\alpha_s}{4h} - \frac{\sin \overline{4h+2}\gamma_s - \sin \overline{4h+2}\alpha_s}{4h+2} \right)$$

for h=0:

$$A^{U}_{s1} = \frac{1}{\pi}\left(-\frac{\cos 2\gamma_s - \cos 2\alpha_s}{2}\right)$$

$$B^{U}_{s1} = \frac{1}{\pi}\left(\xi_s - \frac{\sin 2\gamma_s - \sin 2\alpha_s}{2}\right) \quad ; \quad \xi_s = (\gamma_s - \alpha_s)$$

Furthermore

$$\dot{\bar{\bar{U}}}_{sg\overline{4h+3}} = U_{sg}\left\{\left(A^{U}_{s\overline{4h+3}}\right)^2 + \left(B^{U}_{s\overline{4h+3}}\right)^2\right\}^{\frac{1}{2}} \exp -j\phi^{U}_{s\overline{4h+3}}$$

$$\phi^{U}_{s\overline{4h+3}} = \arctan\left\{\frac{B^{U}_{s\overline{4h+3}}}{A^{U}_{s\overline{4h+3}}}\right\} \qquad 4.38b$$

$$A^{U}_{s\overline{4h+3}} = \frac{1}{\pi}\left(\frac{\cos\overline{4h+2}\gamma_s - \cos\overline{4h+2}\alpha_s}{4h+2} - \frac{\cos\overline{4h+4}\gamma_s - \cos\overline{4h+4}\alpha_s}{4h+4}\right)$$

$$B^{U}_{s\overline{4h+3}} = \frac{1}{\pi}\left(\frac{\sin\overline{4h+2}\gamma_s - \sin\overline{4h+2}\alpha_s}{4h+2} - \frac{\sin\overline{4h+4}\gamma_s - \sin\overline{4h+4}\alpha_s}{4h+4}\right)$$

The switched "induced voltage" components:

$$\dot{\bar{\bar{E}}}_{s\overline{4h+1}} = \bar{\bar{E}}_{s\overline{4h+1}} \cdot \exp -j\phi^{E}_{s\overline{4h+1}}$$

$$\bar{\bar{E}}_{s\overline{4h+1}} = \left\{\left(E^{ba}_{sr}\, A^{Ea}_{s\overline{4h+1}} + E^{bb}_{sr}\, A^{Eb}_{s\overline{4h+1}}\right)^2 + \left(E^{ba}_{sr}\, B^{Ea}_{s\overline{4h+1}} + E^{bb}_{sr}\, B^{Eb}_{s\overline{4h+1}}\right)^2\right\}^{\frac{1}{2}}$$

$$\phi^{E}_{s\overline{4h+1}} = \arctan\left\{\frac{E^{ba}_{sr}\, B^{Ea}_{s\overline{4h+1}} + E^{bb}_{sr}\, B^{Eb}_{s\overline{4h+1}}}{E^{ba}_{sr}\, A^{Ea}_{s\overline{4h+1}} + E^{bb}_{sr}\, A^{Eb}_{s\overline{4h+1}}}\right\}$$

where

$$A^{Ea}_{s\overline{4h+1}} = \frac{1}{\pi}\left\{\frac{\sin(\overline{4h+2-s}\alpha_s) - \sin(\overline{4h+2-s}.\overline{\gamma_s-\pi})}{4h+2-s} + \right.$$

$$\left. + \frac{\sin(\overline{4h+s}\alpha_s) - \sin(\overline{4h+s}.\overline{\gamma_s-\pi})}{4h+s}\right\}$$

$$B^{Ea}_{s\overline{4h+1}} = \frac{1}{\pi}\left\{\frac{\cos(\overline{4h+2-s}.\overline{\gamma_s-\pi}) - \cos(\overline{4h+2-s}\alpha_s)}{4h+2-s} + \right.$$

$$+ \frac{\cos\left(\overline{4h+s}.\overline{\gamma_s - \pi}\right) - \cos\left(\overline{4h+s}\alpha_s\right)}{4h+s}\Bigg\}$$

$$A^{Eb}_{\overline{s4h+1}} = \frac{1}{\pi}\left\{\frac{\cos\left(\overline{4h+2-s}\alpha_s\right) - \cos\left(\overline{4h+2-s}.\overline{\gamma_s - \pi}\right)}{4h+2-s} + \right.$$

$$\left. - \frac{\cos\left(\overline{4h+s}\alpha_s\right) - \cos\left(\overline{4h+s}.\overline{\gamma_s - \pi}\right)}{4h+s}\right\}$$

$$B^{Eb}_{\overline{s4h+1}} = \frac{1}{\pi}\left\{\frac{\sin\left(\overline{4h+2-s}\alpha_s\right) - \sin\left(\overline{4h+2-s}.\overline{\gamma_s - \pi}\right)}{4h+2-s} - \right.$$

$$\left. - \frac{\sin\left(\overline{4h+s}\alpha_s\right) - \sin\left(\overline{4h+s}.\overline{\gamma_s - \pi}\right)}{4h+s}\right\} \qquad 4.38c$$

Similarly it may be found that:

$$\dot{\bar{E}}_{\overline{s4h+3}} = \bar{\bar{E}}_{\overline{s4h+3}} \exp -j\phi^{E}_{\overline{s4h+3}}$$

$$\bar{\bar{E}}_{\overline{s4h+3}} = \left\{\left(E^{ba}_{sr} A^{Ea}_{\overline{s4h+3}} + E^{bb}_{sr} A^{Eb}_{\overline{4h+3}}\right)^2 + \left(E^{ba}_{sr} B^{Ea}_{\overline{s4h+3}} + E^{bb}_{sr} B^{Eb}_{\overline{s4h+3}}\right)^2\right\}^{\frac{1}{2}}$$

$$\phi^{E}_{s4h+3} = \arctan\left\{\frac{E^{ba}_{sr} B^{Ea}_{\overline{s4h+3}} + E^{bb}_{sr} B^{Eb}_{\overline{s4h+3}}}{E^{ba}_{sr} A^{Ea}_{\overline{s4h+3}} + E^{bb}_{sr} A^{Eb}_{\overline{s4h+3}}}\right\}$$

where

$$A^{Ea}_{\overline{s4h+3}} = \frac{1}{\pi}\left\{\frac{\sin\left(\overline{4h+4-s}\alpha_s\right) - \sin\left(\overline{4h+4-s}.\overline{\gamma_s - \pi}\right)}{4h+4-s} + \right.$$

$$\left. + \frac{\sin\left(\overline{4h+2+s}\alpha_s\right) - \sin\left(\overline{4h+2+s}.\overline{\gamma_s - \pi}\right)}{4h+2+s}\right\}$$

$$B^{Ea}_{\overline{s4h+3}} = \frac{1}{\pi}\left\{\frac{\cos\left(\overline{4h+4-s}.\overline{\gamma_s - \pi}\right) - \cos\left(\overline{4h+4-s}\alpha_s\right)}{4h+4-s} + \right.$$

$$\left. + \frac{\cos\left(\overline{4h+2+s}.\overline{\gamma_s - \pi}\right) - \cos\left(\overline{4h+2+s}\alpha_s\right)}{4h+2+s}\right\}$$

$$A^{Eb}_{\overline{s4h+3}} = \frac{1}{\pi}\left\{\frac{\cos\left(\overline{4h+4-s}\alpha_s\right) - \cos\left(\overline{4h+4-s}.\overline{\gamma_s - \pi}\right)}{4h+4-s} + \right.$$

$$- \frac{\cos(\overline{4h+2+s}\alpha_s) - \cos(\overline{4h+2+s}.\overline{\gamma_s - \pi}}{4h+2+s} \Bigg\}$$

$$B\frac{Eb}{s4h+3} = \frac{1}{\pi} \left\{ \frac{\sin(\overline{4h+4-s}\alpha_s) - \sin(\overline{4h+4-s}.\overline{\gamma_s - \pi})}{4h+4-s} + \right.$$

$$\left. - \frac{\sin(\overline{4h+2+s}\alpha_s) - \sin(\overline{4h+2+s}.\overline{\gamma_s - \pi})}{4h+2+s} \right\} \qquad 4.38d$$

Before the currents can be found it must be considered that the instantaneous symmetrical voltage-current equations are still subjected to the Ku rotor-stator transformation to relate all equations to the stator reference frame. However, as the rotor voltages are zero, and this transformation does not affect the stator conversion voltages, the above expressions may be employed to calculate the rotor and stator currents.

4.2.3 *SOLUTION FOR THE MACHINE CURRENTS.*

The currents now have to be solved from the set of relations 4.17. The transformed equations, after having applied the instantaneous symmetrical component transformation and the complex rotating rotor-stator transformation succesively as in chapter 3, become:

$$\begin{bmatrix} \dot{\bar{u}}_s^{(+)} \end{bmatrix}_{ks} \Big| \begin{bmatrix} 0 \end{bmatrix} = \begin{bmatrix} Z_s^t \end{bmatrix}_{ks} \Big| \begin{bmatrix} Z_{sr}^t \end{bmatrix}_{ks} \Big/ \begin{bmatrix} Z_{rs}^t \end{bmatrix}_{ks} \Big| \begin{bmatrix} Z_r^t \end{bmatrix}_{ks} \cdot \begin{bmatrix} \dot{\bar{i}}_s^{(+)} \end{bmatrix}_{ks} \Big| \begin{bmatrix} \dot{i}_r^{(+)} \end{bmatrix}_{ks} \qquad 4.39a$$

from relations 3.12 and 3.20a, with the symmetrical transformation as specified in paragraph 4.2.2.2, and the complex rotating transformation given by:

$$\begin{bmatrix} K_s \end{bmatrix} = \begin{bmatrix} \exp -jp\omega_m t & 0 \\ 0 & \exp jp\omega_m t \end{bmatrix} \qquad 4.39b$$

The currents are now specified by:

$$\begin{bmatrix} \dot{i}_{s_r}^{(+)} \end{bmatrix}_{ks} = \begin{bmatrix} \dot{\bar{i}}_s^{(+)} \\ \dot{\bar{i}}_s^{(-)} \\ \dot{i}_r^{(+)} \exp jp\omega_m t \\ \dot{i}_r^{(-)} \exp -jp\omega_m t \end{bmatrix} = \begin{bmatrix} \dot{\bar{i}}_s^{(+)} \\ \dot{\bar{i}}_s^{(-)} \\ \dot{i}_r^{(+),ks} \\ \dot{i}_r^{(-),ks} \end{bmatrix} \qquad 4.39c$$

and the composite impedance matrix by:

$$\left[Z^t\right]_{ks} = \left[\begin{array}{cc|cc} R_s+L_sD & 0 & M_{sr}D & 0 \\ 0 & R_s+L_sD & 0 & M_{sr}D \\ \hline M_{sr}(D-jp\omega_m) & 0 & R_r+L_r(D-jp\omega_m) & 0 \\ 0 & M_{sr}(D+jp\omega_m) & 0 & R_r+L_r(D+jp\omega_m) \end{array}\right] \qquad 4.39d$$

while the zero torque currents all have zero amplitude, as has already been proved earlier in this chapter.

Calculating the inverse impedance matrix, the following result is obtained:

$$\left(\left[Z^t\right]_{ks}\right)^{-1} = \left[\begin{array}{cccc} \frac{1}{Z_D^{ks-}} & 0 & -\frac{M_{sr}D}{Z_{rD}^{-}Z_D^{ks-}} & 0 \\ 0 & \frac{1}{Z_D^{ks+}} & 0 & -\frac{M_{sr}D}{Z_{rD}^{+}Z_D^{ks+}} \\ -\frac{M_{sr}(D-jp\omega_m)}{Z_{rD}^{-}Z_D^{ks-}} & 0 & \frac{Z_{sD}}{Z_{rD}^{-}Z_D^{ks-}} & 0 \\ 0 & -\frac{M_{sr}(D+jp\omega_m)}{Z_{rD}^{+}Z_D^{ks+}} & 0 & \frac{Z_sD}{Z_{rD}^{+}Z_D^{ks+}} \end{array}\right] \qquad 4.40a$$

where

$$\left.\begin{aligned} Z_{sD} &= R_s + L_sD \\ Z_{rD}^{\mp} &= R_r + L_r(D \mp jp\omega_m) \\ Z_D^{ks\mp} &= \left\{Z_{sD} - \frac{M_{sr}^2D(D \mp jp\omega_m)}{Z_{rD}^{\mp}}\right\} \end{aligned}\right\} \qquad 4.40b$$

giving the currents as:

$$\begin{bmatrix} \dot{\underline{i}}_s^{(+)} \\ \dot{\underline{i}}_r \end{bmatrix}_{ks} = \left(\begin{bmatrix} Z^t \end{bmatrix}_{ks} \right)^{-1} \cdot \begin{bmatrix} \begin{bmatrix} \dot{\underline{u}}_s^{(+)} \end{bmatrix}_{ks} \\ 0 \end{bmatrix}$$

Expanding:

$$\dot{\underline{i}}_s^{(+)} = \frac{1}{Z_{D\,ks-}} \cdot \dot{\underline{u}}_s^{(+)} \qquad 4.41a$$

$$\dot{\underline{i}}_s^{(-)} = \frac{1}{Z_{D\,ks+}} \cdot \dot{\underline{u}}_s^{(-)} \qquad 4.41b$$

$$\dot{i}_r^{(+)} \exp\, jp\omega_m = - \frac{M_{sr}(D - jp\omega_m)}{Z_{rD}^{-}\, Z_{D}^{ks-}} \cdot \dot{\underline{u}}_s^{(+)} \qquad 4.41c$$

$$\dot{i}_r^{(-)} \exp -jp\omega_m = - \frac{M_{sr}(D + jp\omega_m)}{Z_{rD}^{+}\, Z_{D}^{ks+}} \cdot \dot{\underline{u}}_s^{(-)} \qquad 4.41d$$

since the transformed rotor voltages of equations 3.3b are still zero.

The "positive sequence" and "negative sequence" stator currents, being the complex conjugate of one another, will be expressed as follows:

$$\begin{bmatrix} \dot{\underline{i}}_s^{(+)} \\ \dot{\underline{i}}_s^{(-)} \end{bmatrix} = \sum_{h=0}^{\infty} \begin{pmatrix} \dot{\underline{I}}^{p}_{s4h+1} \exp j(\overline{4h+1}\,\omega_s t) + \dot{\underline{I}}^{n*}_{s4h+1} \exp -j(\overline{4h+3}\,\omega_s t) \\ \dot{\underline{I}}^{n}_{s4h+3} \exp j(\overline{4h+3}\,\omega_s t) + \dot{\underline{I}}^{p*}_{s4h+1} \exp -j(\overline{4h+1}\,\omega_s t) \end{pmatrix} \qquad 4.42a$$

In these expressions the values of the harmonic components may be found from:

$$\dot{\underline{I}}^{p}_{s4h+1} = \frac{j(\dot{\underline{U}}_{sg\,4h+1} + \overline{1-s}\ \dot{\underline{E}}_{s4h+1})}{Z_{s4h+1}} =$$

$$= j\ \underline{I}^{U}_{s4h+1} \exp -j\ \psi^{U}_{s4h+1} + j\ \overline{1-s}\ \underline{I}^{E}_{s4h+1} \exp -j\ \psi^{E}_{s4h+1}\ ;$$

$$\bar{\bar{I}}^{U}_{s\overline{4h+1}} = \frac{\bar{\bar{U}}_{sg\overline{4h+1}}}{Z_{s\overline{4h+1}}} \quad ; \quad \bar{\bar{I}}^{E}_{s\overline{4h+1}} = \frac{\bar{\bar{E}}_{s\overline{4h+1}}}{Z_{s\overline{4h+1}}}$$

$$\psi^{U}_{s\overline{4h+1}} = \left(\phi^{U}_{s\overline{4h+1}} + \phi^{Z}_{s\overline{4h+1}}\right) \qquad \psi^{E}_{s\overline{4h+1}} = \left(\phi^{E}_{s\overline{4h+1}} + \phi^{Z}_{s\overline{4h+1}}\right)$$

$$\dot{Z}_{s\overline{4h+1}} = \left\{\left(R_{s\overline{4h+1}}\right)^2 + \left(X_{s\overline{4h+1}}\right)^2\right\}^{\frac{1}{2}} \exp j\phi^{Z}_{s\overline{4h+1}}$$

$$\phi^{Z}_{s\overline{4h+1}} = \arctan\left\{\frac{X_{s\overline{4h+1}}}{R_{s\overline{4h+1}}}\right\}$$

$$R_{s\overline{4h+1}} = \left\{R_s + \frac{\overline{4h+1}.\overline{4h+s}.X_M^2 R_r}{R_r^2 + \overline{4h+s}^2 X_r^2}\right\}$$

$$X_{s\overline{4h+1}} = \overline{4h+1}\left\{X_s - \frac{\overline{4h+s}^2 X_r X_M^2}{R_r^2 + \overline{4h+s}^2 X_r^2}\right\}$$

Similarly for the $\overline{4h+3}$ rd terms:

$$\dot{\bar{\bar{I}}}^{U}_{s\overline{4h+3}} = \frac{-j(\dot{\bar{\bar{U}}}_{sg\overline{4h+3}} + \overline{1-s}\dot{\bar{\bar{E}}}_{s\overline{4h+3}}}{\dot{Z}_{s\overline{4h+3}}} =$$

$$= -j\ \bar{\bar{I}}^{U}_{s\overline{4h+3}} \exp -j\psi^{U}_{s\overline{4h+3}} - j\ \overline{1-s}\bar{\bar{I}}^{E}_{s\overline{4h+3}} \exp -j\psi^{E}_{s\overline{4h+3}}$$

$$\bar{\bar{I}}^{U}_{s\overline{4h+3}} = \frac{\bar{\bar{U}}_{sg\overline{4h+3}}}{Z_{s\overline{4h+3}}} \quad ; \quad I^{E}_{s\overline{4h+3}} = \frac{\bar{\bar{E}}_{s\overline{4h+3}}}{Z_{s\overline{4h+3}}} \quad ; \quad \psi^{U}_{s\overline{4h+3}} = \left(\phi^{U}_{s\overline{4h+3}} + \phi^{Z}_{\overline{4h+3}}\right)$$

$$\phi^{Z}_{s\overline{4h+3}} = \arctan\left(\frac{X_{s\overline{4h+3}}}{R_{s\overline{4h+3}}}\right); \quad \psi^{E}_{s\overline{4h+3}} = \left(\phi^{E}_{s\overline{4h+3}} + \phi^{Z}_{\overline{4h+3}}\right)$$

$$\dot{Z}_{s\overline{4h+3}} = \left\{\left(R_{s\overline{4h+3}}\right)^2 + \left(X_{s\overline{4h+3}}\right)^2\right\}^{\frac{1}{2}} \exp j\phi^{Z}_{s\overline{4h+3}}$$

$$R_{s\overline{4h+3}} = \left\{ R_s + \frac{\overline{4h+3}.\overline{4h+4-s}X_M^2 R_r}{R_r^2 + \overline{4h+4-s}^2 X_r^2} \right\} ; \quad X_{s\overline{4h+3}} = \overline{4h+3}\left\{ X_s - \frac{\overline{4h+4-s}^2 X_M^2 X_r}{R_r^2 + \overline{4h+4-s}^2 X_r^2} \right\}$$

4.42b

As already remarked, the rotor excitation in the present case is zero, and the investigations of chapter 3 now indicate that the transformed rotor currents will be of the same frequency as the stator currents. Therefore:

$$\begin{bmatrix} \dot{i}_r^{(+);ks} \\ \dot{i}_r^{(-);ks} \end{bmatrix} = \sum_{h=0}^{\infty} \begin{Bmatrix} \dot{I}^p_{r\overline{4h+1}} \exp j(\overline{4h+1}\omega_s t) + \dot{I}^{n*}_{r\overline{4h+3}} \exp -j(\overline{4h+3}\omega_s t) \\ \dot{I}^n_{r\overline{4h+3}} \exp j(\overline{4h+3}\omega_s t) + \dot{I}^{p*}_{r\overline{4h+1}} \exp -j(\overline{4h+1}\omega_s t) \end{Bmatrix}$$

4.43a

Analogous to the expressions for the stator currents the expressions for the harmonic components of the rotor currents ultimately reduce to:

$$\dot{I}^p_{r\overline{4h+1}} = -j\, I^U_{r\overline{4h+1}} \exp -j\psi^U_{sr\overline{4h+1}} - j\,\overline{1-s}\, I^E_{r\overline{4h+1}} \exp -j\psi^E_{sr\overline{4h+1}}$$

$$I^U_{r\overline{4h+1}} = \frac{\underline{\underline{U}}_{sg\overline{4h+1}}}{Z_{sr\overline{4h+1}}} \quad ; \quad I^E_{r\overline{4h+1}} = \frac{\underline{\underline{E}}_{s\overline{4h+1}}}{Z_{sr\overline{4h+1}}}$$

$$\psi^U_{sr\overline{4h+1}} = \left(\phi^U_{s\overline{4h+1}} + \phi^Z_{sr\overline{4h+1}} \right) ; \quad \psi^E_{sr} = \left(\phi^E_{s\overline{4h+1}} + \phi^Z_{sr\overline{4h+1}} \right)$$

$$Z_{sr\overline{4h+1}} = \left\{ \left(\frac{X_r}{X_M} \right)^2 + \left(\frac{R_r}{\overline{4h+s}X_M} \right)^2 \right\}^{\frac{1}{2}} . Z_{s\overline{4h+1}}$$

$$\phi^Z_{sr\overline{4h+1}} = \left(\phi^Z_{s\overline{4h+1}} - \phi^M_{sr\overline{4h+1}} \right) \quad ; \quad \phi^M_{sr\overline{4h+1}} = \arctan \left(\frac{R_r}{\overline{4h+s}X_r} \right)$$

and

$$\dot{I}^n_{r\overline{4h+3}} = j\, I^U_{r\overline{4h+3}} \exp -j\, \psi^U_{sr\overline{4h+3}} + j\,\overline{1-s}\, I^E_{r\overline{4h+3}} \exp -j\, \psi^E_{sr\overline{4h+3}}$$

4.43b

with

$$I^U_{r\overline{4h+3}} = \frac{\underline{\underline{U}}_{sg\overline{4h+3}}}{Z_{sr\overline{4h+3}}} \quad ; \quad I^E_{r\overline{4h+3}} = \frac{\underline{\underline{E}}_{s\overline{4h+3}}}{Z_{sr\overline{4h+3}}}$$

$$\psi^{U}_{sr\overline{4h+3}} = \left(\phi^{U}_{s\overline{4h+3}} + \phi^{Z}_{sr\overline{4h+3}}\right) \quad ; \quad \psi^{E}_{sr\overline{4h+3}} = \left(\phi^{E}_{s\overline{4h+3}} + \phi^{Z}_{sr\overline{4h+3}}\right)$$

$$Z_{sr\overline{4h+3}} = \left\{\left(\frac{X_r}{X_M}\right)^2 + \left(\frac{R_r}{\overline{4h+4-s}X_M}\right)^2\right\}^{\frac{1}{2}} . Z_{s\overline{4h+3}}$$

$$\phi^{Z}_{sr\overline{4h+3}} = \phi^{Z}_{s\overline{4h+3}} - \phi^{M}_{sr\overline{4h+3}} \quad ; \quad \phi^{M}_{sr\overline{4h+3}} = \arctan\left(\frac{R_r}{\overline{4h+4-s}X_r}\right) \qquad 4.43c$$

In all these expressions it is valid that

$$X_s = 2\pi f_s L_s \quad ; \quad X_r = 2\pi f_s L_r \quad ; \quad X_M = 2\pi f_s M_{sr} \qquad 4.43d$$

Since the instantaneous symmetrical current transforms are now known for both "positive sequence" and "negative sequence" currents in the stator, the true stator phase currents may be found. From relation 4.18a it follows that:

$$\begin{bmatrix} \overline{\overline{i}}^{a}_{s}(t) \\ \overline{\overline{i}}^{b}_{s}(t) \end{bmatrix} = \frac{1}{\sqrt{2}} \begin{bmatrix} 1 & 1 \\ -j & j \end{bmatrix} \begin{bmatrix} \overline{\overline{i}}^{(+)}_{s} \\ \overline{\overline{i}}^{(-)}_{s} \end{bmatrix} \qquad 4.44a$$

By substitution of the values of relations 4.42 and rearrangement, the phase currents are found as:

$$\begin{bmatrix} \overline{\overline{i}}^{a}_{s}(t) \\ \overline{\overline{i}}^{b}_{s}(t) \end{bmatrix} =$$

$$\frac{1}{\sqrt{2}} \sum_{h=0}^{\infty} \begin{bmatrix} j \\ 1 \end{bmatrix} \left(\overline{\overline{I}}^{U}_{s\overline{4h+1}} \exp -j\psi^{U}_{s\overline{4h+1}} + \overline{1-s}\,\overline{\overline{I}}^{E}_{s\overline{4h+1}} \exp -j\psi^{E}_{s\overline{4h+1}} \right) \exp j\overline{4h+1}\omega_s t$$

$$+ \begin{bmatrix} -j \\ 1 \end{bmatrix} \left(\overline{\overline{I}}^{U}_{s\overline{4h+1}} \exp\, j\psi^{U}_{s\overline{4h+1}} + \overline{1-s}\,\overline{\overline{I}}^{E}_{s\overline{4h+1}} \exp\, j\psi^{E}_{s\overline{4h+1}} \right) \exp -j\overline{4h+1}\omega_s t$$

$$+\begin{bmatrix}-j\\1\end{bmatrix}\left(\bar{\bar{I}}^{U}_{s4h+3}\exp -j\psi^{U}_{s4h+3}+\overline{1-s}\;\bar{\bar{I}}^{E}_{s4h+3}\exp -j\psi^{E}_{s4h+3}\right)\exp\, j\overline{4h+3}\omega_s t$$

$$+\begin{bmatrix}j\\1\end{bmatrix}\left(\bar{\bar{I}}^{U}_{s4h+3}\exp\, j\psi^{U}_{s4h+3}+\overline{1-s}\;I^{E}_{s4h+3}\exp\, j\psi^{E}_{s4h+3}\right)\exp -j\overline{4h+3}\omega_s t \qquad 4.44b$$

Expansion of the exponential functions results in the alternative trigonometrical form

$$\begin{bmatrix}\bar{\bar{i}}^{a}_{s}(t)\\ \bar{\bar{i}}^{b}_{s}(t)\end{bmatrix}=\sqrt{2}\sum_{h=0}^{\infty}\left(\bar{\bar{I}}^{U}_{s4h+1}\begin{bmatrix}-\sin\\ \cos\end{bmatrix}\left(\overline{4h+1}\omega_s t-\psi^{U}_{s4h+1}\right)+\bar{\bar{I}}^{U}_{s4h+3}\begin{bmatrix}\sin\\ \cos\end{bmatrix}\left(\overline{4h+3}\omega_s t-\psi^{U}_{s4h+3}\right)\right.$$

$$+\overline{1-s}\left\{\bar{\bar{I}}^{E}_{s4h+1}\cdot\begin{bmatrix}-\sin\\ \cos\end{bmatrix}\left(\overline{4h+1}\omega_s t-\psi^{E}_{s4h+1}\right)+\right.$$

$$\left.\left.+\bar{\bar{I}}^{E}_{s4h+3}\begin{bmatrix}\sin\\ \cos\end{bmatrix}\left(\overline{4h+3}\omega_s t.\psi^{E}_{s4h+3}\right)\right\}\right) \qquad 4.44c$$

The instantaneous symmetrical component transforms calculated for the rotor currents may be found from the relations 4.43, after the inverse Ku-transformation of relation 4.39b as:

$$\begin{bmatrix}\overset{\bullet}{i}^{(+)}_{r}\\ \overset{\bullet}{i}^{(-)}_{r}\end{bmatrix}=\sum_{h=0}^{\infty}\begin{bmatrix}-j\left(\dot{\bar{I}}^{U}_{r4h+1}+\overline{1-s}\;\dot{\bar{I}}^{E}_{r4h+1}\right)\exp\, j(\overline{4h+s}\omega_s t)+\\ \qquad -j\left(\dot{\bar{I}}^{U*}_{r4h+3}+\overline{1-s}\;\dot{\bar{I}}^{E*}_{r4h+3}\right)\exp -j(\overline{4h+4-s}\omega_s t)\\ j\left(\dot{\bar{I}}^{U}_{r4h+3}+\overline{1-s}\;\dot{\bar{I}}^{E}_{r4h+3}\right)\exp\, j(\overline{4h+4-s}\omega_s t)+\\ \qquad +j\left(\dot{\bar{I}}^{U*}_{r4h+1}+\overline{1-s}\;\dot{\bar{I}}^{E*}_{r4h+1}\right)\exp -j(\overline{4h+s}\omega_s t)\end{bmatrix} \qquad 4.45a$$

Taking into account that

$$\begin{bmatrix} i_r^a(t) \\ i_r^b(t) \end{bmatrix} = \frac{1}{\sqrt{2}} \begin{bmatrix} 1 & 1 \\ -j & j \end{bmatrix} \begin{bmatrix} \overset{*}{i}_r^{(+)} \\ \overset{*}{i}_r^{(-)} \end{bmatrix} \qquad 4.45b$$

the rotor phase currents may eventually be reduced to the following trigonometric form:

$$\begin{bmatrix} i_r^a(t) \\ i_r^b(t) \end{bmatrix} = \sqrt{2} \sum_{h=0}^{\infty} \left(I^U_{r\overline{4h+1}} \begin{bmatrix} \sin \\ -\cos \end{bmatrix} \left(\overline{4h+s}\omega_s t - \psi^U_{sr\overline{4h+1}} \right) + \right.$$

$$+ \quad I^U_{r\overline{4h+3}} \begin{bmatrix} -\sin \\ -\cos \end{bmatrix} \left(\overline{4h+4-s}\omega_s t - \psi^U_{sr\overline{4h+3}} \right) +$$

$$+ \overline{1-s} \left\{ I^E_{r\overline{4h+1}} \begin{bmatrix} \sin \\ -\cos \end{bmatrix} \left(\overline{4h+s}\omega_s t - \psi^E_{sr\overline{4h+1}} \right) + \right.$$

$$\left. \left. + I^E_{r\overline{4h+3}} \begin{bmatrix} -\sin \\ -\cos \end{bmatrix} \left(\overline{4h+4-s}\omega_s t - \psi^E_{sr\overline{4h+3}} \right) \right\} \right) \qquad 4.45c$$

4.2.4 *THE ELECTROMAGNETIC TORQUE FOR THE IGNITION ANGLE STATOR CONTROLLED INDUCTION MACHINE.*

The electromagnetic torque as a function of time, and the mean value of the electromagnetic torque, may now be evaluated when one considers the known currents. From chapter 3 the torque of the semi-four-phase induction machine under consideration is noted as:

$$T_e = jpM_{sr} \left\{ \overset{*}{\bar{i}}_s^{(-)} \cdot \overset{*}{i}_r^{(+)} \exp j(\overline{1-s}\omega_s t) - \overset{*}{\bar{i}}_s^{(+)} \cdot \overset{*}{i}_r^{(-)} \exp -j(\overline{1-s}\omega_s t) \right\} \qquad 4.46a$$

By noting the expressions for the instantaneous symmetrical component and complex rotating transforms of the stator and rotor currents respectively, as represented in relations 4.4 2 and 4.4 3, the electromagnetic torque may be expressed after multiplication and rearrange-

ment as:

$$T_e = jpM_{sr} \sum_{h=0}^{\infty} \Bigg\{ \left(\dot{\bar{I}}^{p*}_{s\overline{4h+1}} . \dot{I}^{p}_{r\overline{4h+1}} - \dot{\bar{I}}^{p}_{s\overline{4h+1}} . \dot{I}^{p*}_{r\overline{4h+1}} \right) +$$

$$+ \left(\dot{\bar{I}}^{n}_{s\overline{4h+3}} . \dot{I}^{n*}_{r\overline{4h+3}} - \dot{\bar{I}}^{n*}_{s\overline{4h+3}} . \dot{I}^{n}_{r\overline{4h+3}} \right)$$

$$+ \left(\dot{\bar{I}}^{n}_{s\overline{4h+3}} . \dot{I}^{p}_{r\overline{4h+1}} \exp j\overline{8h+4}\omega_s t - \dot{\bar{I}}^{n*}_{s\overline{4h+3}} . \dot{I}^{p*}_{r\overline{4h+1}} \exp -j\overline{8h+4}\omega_s t \right)$$

$$+ \left(\dot{\bar{I}}^{p*}_{s\overline{4h+1}} . \dot{I}^{n*}_{r\overline{4h+3}} \exp -j\overline{8h+4}\omega_s t - \dot{\bar{I}}^{p}_{s\overline{4h+1}} . \dot{I}^{n}_{r\overline{4h+3}} \exp j\overline{8h+4}\omega_s t \right) \Bigg\}$$

or

4.46b

$$T_e = \sum_{h=0}^{\infty} T^{asyn.sr}_{e(\overline{4h+1}),(\overline{4h+3})} + \sum_{h=0}^{\infty} T^{puls.sr}_{e(\overline{8h+4})} \qquad 4.46c$$

Comparison of relation 4.46c with the torque relations 3.44a and 3.44c indicates that in the present case the only effective torque components remaining are the asynchronous stator-rotor components for the fundamental frequency and all the harmonic frequencies. As the rotor is not excited in the present case, all the rotor-stator asynchronous torques, all the synchronous torques and rotor-stator pulsating torques have zero amplitude. The only pulsating torque remaining is again the stator-rotor component with a frequency equal to the sum of the corresponding harmonic frequencies.

Taking into account the complex conjugate nature of the different parts of the torque expression, the components may be expressed as:

$$T^{asyn.sr}_{e(4h+1),(4h+3)} = -2pM_{sr} \left(Im\left\{ \dot{\bar{I}}^{p*}_{s\overline{4h+1}} . \dot{I}^{p}_{r\overline{4h+1}} \right\} + Im\left\{ \dot{\bar{I}}^{n}_{s\overline{4h+3}} . \dot{I}^{n*}_{r\overline{4h+3}} \right\} \right) \qquad 4.46d$$

$$T^{puls.sr}_{e(\overline{8h+4})} = -2pM_{sr} \left(Im\left\{ \dot{\bar{I}}^{n}_{s\overline{4h+3}} . \dot{I}^{p}_{r\overline{4h+1}} \exp j\overline{8h+4}\omega_s t \right\} + Im\left\{ \dot{\bar{I}}^{p*}_{s\overline{4h+1}} . \dot{I}^{n*}_{r\overline{4h+3}} \exp -j\overline{8h+4}\omega_s t \right\} \right) \qquad 4.46e$$

Concerning the above expressions for the electromagnetic torque of the stator controlled semi-four-phase induction machine a remark concerning the currents will be made. In the relations 4.4.2 and 4.4 3 a distinction was made between the components of the current transforms calculated with aid of two different excitation functions. The excitation function on its part was divided into a set of Fourier components due to the supply voltage switched on to the machine windings

and a set of components due to applying a voltage exactly equivalent to the induced voltage, to the winding during the time that the non linear switching circuit had disconnected the machine from the supply. This division gave rise to the "supply-voltage components" and "induced voltage components" of the current transform as referred to above.

This division was executed with the purpose of investigating the effect of neglecting the "induced"components in the calculations, in order to estimate the magnitude of these effects, since they complicate calculations considerably. Concurrent with this philosophy, the torque equation 4.46b is written in terms of these two series of current components. Taking 4.46d and 4.46e into account it may be shown that the expression reduces to:

$$
\begin{aligned}
T_e = 2pM_{sr}\sum_{h=0}^{\infty}\Bigg\{\Bigg[
&\bar{\bar{I}}^{U}_{s4h+1}\cdot I^{U}_{r4h+1}\sin\left(\psi^{U}_{s4h+1}-\psi^{U}_{sr4h+1}\right)\\
&+\overline{1-s}\;\bar{\bar{I}}^{E}_{s4h+1}\cdot I^{U}_{r4h+1}\sin\left(\psi^{E}_{s4h+1}-\psi^{U}_{sr4h+1}\right)\\
&+\overline{1-s}\;\bar{\bar{I}}^{U}_{s4h+1}\cdot I^{E}_{r4h+1}\sin\left(\psi^{U}_{s4h+1}-\psi^{E}_{sr4h+1}\right)\\
&+\overline{1-s}^{2}\bar{\bar{I}}^{E}_{s4h+1}\cdot I^{E}_{r4h+1}\sin\left(\psi^{E}_{s4h+1}-\psi^{E}_{sr4h+1}\right)\\
&-\bar{\bar{I}}^{U}_{s4h+3}\cdot I^{U}_{r4h+3}\sin\left(\psi^{U}_{s4h+3}-\psi^{U}_{sr4h+3}\right)\\
&-\overline{1-s}\;\bar{\bar{I}}^{E}_{s4h+3}\cdot I^{U}_{r4h+3}\sin\left(\psi^{E}_{s4h+3}-\psi^{U}_{sr4h+3}\right)\\
&-\overline{1-s}\;\bar{\bar{I}}^{U}_{s4h+3}\cdot I^{E}_{r4h+3}\sin\left(\psi^{U}_{s4h+3}-\psi^{E}_{sr4h+3}\right)\\
&-\overline{1-s}^{2}\bar{\bar{I}}^{E}_{s4h+3}\cdot I^{E}_{r4h+3}\sin\psi\left(E_{s4h+3}-\psi^{E}_{sr4h+3}\right)\Bigg]\\
&+\Bigg[\bar{\bar{I}}^{U}_{s4h+3}\cdot I^{U}_{r4h+1}\sin\left(\overline{8h+4}\,\omega_s t-\psi^{U}_{s4h+3}-\psi^{U}_{sr4h+1}\right)\\
&+\overline{1-s}\;\bar{\bar{I}}^{E}_{s4h+3}\cdot I^{U}_{r4h+1}\sin\left(\overline{8h+4}\,\omega_s t-\psi^{E}_{s4h+3}-\psi^{U}_{sr4h+1}\right)\\
&+\overline{1-s}\;\bar{\bar{I}}^{U}_{s4h+3}\cdot I^{E}_{r4h+1}\sin\left(\overline{8h+4}\,\omega_s t-\psi^{U}_{s4h+3}-\psi^{E}_{sr4h+1}\right)
\end{aligned}
$$

$$+ \overline{1-s^2}\,\bar{\bar{I}}^{E}_{s4h+3}.I^{E}_{r4h+1}\sin\left(\overline{8h+4}\,\omega_s t - \psi^{E}_{s4h+3} - \psi^{E}_{sr4h+1}\right)$$

$$- \bar{\bar{I}}^{U}_{s4h+1}.I^{U}_{r4h+3}\sin\left(\overline{8h+4}\,\omega_s t - \psi^{U}_{s4h+1} - \psi^{U}_{sr4h+1}\right)$$

$$- \overline{1-s}\,\bar{\bar{I}}^{E}_{s4h+1}.I^{U}_{r4h+3}\sin\left(\overline{8h+4}\,\omega_s t - \psi^{E}_{s4h+1} - \psi^{U}_{sr4h+3}\right)$$

$$- \overline{1-s}\,\bar{\bar{I}}^{U}_{s4h+1}.I^{E}_{r4h+3}\sin\left(\overline{8h+4}\,\omega_s t - \psi^{U}_{s4h+1} - \psi^{E}_{sr4h+3}\right)$$

$$- \overline{1-s^2}\,\bar{\bar{I}}^{E}_{s4h+1}.I^{E}_{r4h+3}\sin\left(\overline{8h+4}\,\omega_s t - \psi^{E}_{s4h+1} - \psi^{E}_{sr4h+3}\right)$$

$$= \sum_{h=0}^{\infty} T^{asyn.sr}_{e(4h+1),(4h+3)} + \sum_{h=0}^{\infty} T^{puls.sr}_{e(8h+4)} \qquad 4.46d$$

For the continuous conversion of electromechanical energy the mean torque must be found from relation 4.46d, and results in:

$$\bar{T}_e = \sum_{h=0}^{\infty} T^{asyn.sr}_{e(4h+1),(4h+3)} \qquad 4.46a$$

The above expression will now be examined in order to determine the mean electromagnetic torque in the case of continuous current flow. In this situation

$$(\gamma_s - \pi) = \alpha_s = \psi_s \qquad 4.47a$$

From rel. 4.38e it may be seen directly that

$$A^{Ea}_{s4h+1} \equiv B^{Ea}_{s4h+1} \equiv A^{Eb}_{s4h+1} \equiv B^{Eb}_{s4h+1} \equiv 0 \equiv \bar{\bar{E}}_{s4h+1}$$

From rel. 4.38d

$$A^{Ea}_{s4h+3} \equiv B^{Ea}_{s4h+3} \equiv A^{Eb}_{s4h+3} \equiv B^{Eb}_{s4h+3} \equiv 0 \equiv \bar{\bar{E}}_{s4h+3}$$

In 4.46a all components containing currents due to the "induced-excitation function" reduce to zero. For $h \neq 0$, it may be shown from 4.38b that:

$$A^{U}_{s4h+1} \equiv B^{U}_{s4h+1} \equiv A^{U}_{s4h+3} \equiv B^{U}_{s4h+3} \equiv 0 \equiv \bar{\bar{U}}_{s4h+1} \equiv \bar{\bar{U}}_{s4h+3}$$

since 4h is an integral multiple of 2. For h=0,

$$A^U_{s1} \equiv 0 \quad ; \quad B^U_{s1} \equiv 1$$

From 4.46a it is then deduced that

$$\overline{T}_e = 2pM_{sr} \overline{I}^U_{s1} : I^U_{r1} \sin\left(\psi^U_{s1} - \psi^U_{sr1}\right) \qquad 4.47b$$

with the constants as defined in rel. 4.42b. Alternatively this relation may be written in terms of the parameters characterising the normal equivalent circuit of a balanced induction-machine under sinusoidal excitation as:

$$T_e = p.2.U^2_{sg} \frac{\frac{R_r}{s}}{\omega_s \left[\left(\frac{R_r}{s}.\frac{R_s}{X_M} - \frac{\sigma X_s X_r}{X_M}\right)^2 + \left(\frac{R_r}{s}.\frac{X_s}{X_M} + \frac{R_s X_r}{X_M}\right)^2\right]}$$

which may be shown to be equivalent to the expression of the torque of a symmetrical balanced multiphase machine normally found in the literature (B13

4.2.5 *CALCULATION OF SOME SYSTEM CHARACTERISTICS FOR THE STATOR CONTROL BY VARIATION OF THE IGNITION ANGLE OF THE ELECTRONIC SWITCHES.*

In this paragraph attention is to be devoted to the calculation of some system characteristics to indicate the application of the theory treated in the previous paragraphs concerning the stator-controlled semi-four-phase machine. The torque-speed characteristics from which the appropriate transfer function - describing change of torque with change in ignition angle at a given speed - may be deduced, are subsequently to be investigated experimentally for two variants of ignition delay, i.e. α_s-control and $\Delta\alpha_s$control. The power factor, as well as the effective current drawn from the supply, are important in power applications. The same may be said of the harmonic distortion of the supply current.

4.2.5.1 *Torque-speed characteristics and transfer functions.*

In the previous paragraph comment was given relating to the division of the electromagnetic torque into a series of components due to the "supply excitation function" and a series of components due to the "induced excitation function".

From relation 4.46d it may be seen that of all the terms constituting the electromagnetic torque, those arising from an interaction between "supply-excitation currents" and "induced-excitation currents" contain a term proportional to speed, i.e. $\overline{1-s}$. The terms arising from an interaction between components of currents entirely due to the "induced excitation function" are proportional to the square of the

speed, or to $\overline{1-s}^2$. This already seems to indicate that at low speeds all the induced-excitation currents may be neglected to a good approximation. However, one should also consider the dependence of the amplitude of the coefficients of the series representing this excitation; i.e. $E_{s\overline{4h+1}}$, and $E_{s\overline{4h+3}}$, as well as their respective phase angles, on the variation of the ignition angle α_s and the angle of natural commutation γ_s. In order to proceed with this investigation it will now be necessary to consider the determination of the angle of natural commutation γ_s and the initial conditions determining the induced voltage conditions.

4.2.5.1.1 The angle of natural commutation and the initial conditions for the induced-excitation function.

The stator phase currents derived in expression 4.44c may be employed to determine the angle of natural commutation when the converter operates at low speed and the terms containing the induced e.m.f. may be neglected. Selecting the current in phase b:
at $\omega_s t = \gamma_s$

$$i_s^b(\omega_s t=\gamma_s) \equiv 0 \equiv \sqrt{2}\sum_{h=0}^{\infty}\left\{\bar{\bar{I}}^U_{s\overline{4h+1}}(\alpha_s,\gamma_s,s)\cos\left[\overline{4h+1}\gamma_s-\psi^U_{s\overline{4h+1}}(\alpha_s,\gamma_s,s)\right]\right.$$
$$\left. + \bar{\bar{I}}^U_{s\overline{4h+3}}(\alpha_s,\gamma_s,s)\cos\left[\overline{4h+3}\gamma_s-\psi^U_{s\overline{4h+3}}(\alpha_s,\gamma_s,s)\right]\right\} \qquad 4.48a$$

At a given slip and a given delay angle the above equation may be solved iteratively to obtain the angle of natural current extinction

When the "induced excitation function" is taken into account, more equations will be necessary, as the initial conditions of the induced voltage are still unknown. In paragraph 4.2.2.4 the initial conditions of the induced e.m.f. of the machine in phase b was investigated. Using the condition that

$$i_s^b(\omega_s t = \overline{\gamma_s-\pi}) \equiv 0 \qquad 4.48b$$

and the equations for the rotor currents 4.45c, it is possible to derive the following set of equations. (See appendix A4.4)

$$\begin{bmatrix} \left\{X_M I_r^{aU}(\alpha_s,\gamma_s,s)\right\} & \left\{\overline{1-s}X_M Y_r^{aEa}(\alpha_s,\gamma_s,s)-\sqrt{2}\right\} & \left\{\overline{1-s}X_M Y_r^{aEb}(\alpha_s,\gamma_s,s)\right\} \\ \left\{X_M I_r^{bU}(\alpha_s,\gamma_s,s)\right\} & \left\{\overline{1-s}X_M Y_r^{bEa}(\alpha_s,\gamma_s,s)\right\} & \left\{\overline{1-s}X_M Y_r^{bEb}(\alpha_s,\gamma_s,s)-\sqrt{2}\right\} \\ \left\{I_s^{bU}(\alpha_s,\gamma_s,s)\right\} & \left\{\overline{1-s}Y_s^{bEa}(\alpha_s,\gamma_s,s)\right\} & \left\{\overline{1-s}Y_s^{bEb}(\alpha_s,\gamma_s,s)\right\} \end{bmatrix} \cdot \begin{bmatrix} 1 \\ E_{sr}^{ba} \\ E_{sr}^{bb} \end{bmatrix} \equiv 0$$

4.48c

The expressions for the infinite series $I_r^{aU}(\alpha_s,\gamma_s,s)$; $I_r^{bU}(\alpha_s,\gamma_s,s)$; $I_s^{bU}(\alpha_s,\gamma_s,s)$; $Y_r^{aEa}(\alpha_s,\gamma_s,s)$; $Y_r^{bEa}(\alpha_s,\gamma_s,s)$; $Y_s^{bEa}(\alpha_s,\gamma_s,s)$; $Y_r^{aEb}(\alpha_s,\gamma_s,s)$; $Y_r^{bEb}(\alpha_s,\gamma_s,s)$ and $Y_s^{bEb}(\alpha_s,\gamma_s,s)$ are specified in appendix A4.4. The equations now express the relation between the angle of ignition delay α_s, the angle of natural commutation γ_s, the slip s, and the initial conditions of the induced voltage E_{sr}^{ba} and E_{sr}^{bb} at the time when it is known that the phase current in phase "b" undergoes natural commutation as specified in 4.48b. By elimination it is now possible to obtain an expression relating only the triggering angle, angle of current extinction and the slip of the machine to each other:

$$\frac{\left(\frac{X_M I_r^{aU}(\alpha_s,\gamma_s,s)}{\overline{1-sX_M Y_r^{aEb}(\alpha_s,\gamma_s,s)}} - \frac{X_M I_r^{bU}(\alpha_s,\gamma_s,s)}{\overline{1-sX_M Y_r^{bEb}(\alpha_s,\gamma_s,s)-\sqrt{2}}}\right)}{\left(\frac{\overline{1-sX_M Y_r^{aEa}(\alpha_s,\gamma_s,s)-\sqrt{2}}}{\overline{1-sX_M Y_r^{aEb}(\alpha_s,\gamma_s,s)}} - \frac{\overline{1-sX_M Y_r^{bEa}(\alpha_s,\gamma_s,s)}}{\overline{1-sX_M Y_r^{bEb}(\alpha_s,\gamma_s,s)-\sqrt{2}}}\right)} +$$

$$- \frac{\left(\frac{X_M I_r^{bU}(\alpha_s,\gamma_s,s)}{\overline{1-sX_M Y_r^{bEb}(\alpha_s,\gamma_s,s)-\sqrt{2}}} - \frac{I_s^{bU}(\alpha_s,\gamma_s,s)}{\overline{1-sY_s^{bEb}(\alpha_s,\gamma_s,s)}}\right)}{\left(\frac{\overline{1-sX_M Y_r^{bEa}(\alpha_s,\gamma_s,s)}}{\overline{1-sX_M Y_r^{bEb}(\alpha_s,\gamma_s,s)-\sqrt{2}}} - \frac{Y_s^{bEa}(\alpha_s,\gamma_s,s)}{Y_s^{bEb}(\alpha_s,\gamma_s,s)}\right)} \equiv 0 \qquad 4.48d$$

From the above relation it will now be possible to solve by iterative computation at a constant value of triggering delay and slip for the value of the extinction angle γ_s that satisfies the relation.

Manipulation of the same set of equations gives values for the initial conditions of the induced e.m.f. in phase "b" as:

$$E_{sr}^{ba} = \frac{\left(\frac{X_M I_r^{bU}(\alpha_s,\gamma_s,s)}{\overline{1-sX_M Y_r^{bEb}(\alpha_s,\gamma_s,s)-\sqrt{2}}} - \frac{X_M I_r^{aU}(\alpha_s,\gamma_s,s)}{\overline{1-sX_M Y_r^{aEb}(\alpha_s,\gamma_s,s)}}\right)}{\left(\frac{\overline{1-sX_M Y_r^{aEa}(\alpha_s,\gamma_s,s)-\sqrt{2}}}{\overline{1-sX_M Y_r^{aEb}(\alpha_s,\gamma_s,s)}} - \frac{\overline{1-sX_M Y_r^{bEa}(\alpha_s,\gamma_s,s)}}{\overline{1-sX_M Y_r^{bEb}(\alpha_s,\gamma_s,s)-\sqrt{2}}}\right)} \qquad 4.49a$$

$$E^{bb}_{sr}=\frac{\left(\dfrac{I_s^{bU}(\alpha_s,\gamma_s,s)}{\overline{1-s}Y_s^{bEa}(\alpha_s,\gamma_s,s)} - \dfrac{X_M I_r^{aU}(\alpha_s,\gamma_s,s)}{\overline{1-s}X_M Y_r^{aEa}(\alpha_s,\gamma_s,s) -\sqrt{2}}\right)}{\left(\dfrac{\overline{1-s}X_M Y_r(\alpha_s,\gamma_s,s)}{\overline{1-s}X_M Y_r^{aEa}(\alpha_s,\gamma_s,s)-\sqrt{2}} - \dfrac{Y_s^{bEb}(\alpha_s,\gamma_s,s)}{Y_s^{bEa}(\alpha_s,\gamma_s,s)}\right)} \qquad 4.49b$$

In principle it may now be considered that it has been shown that the angle of current commutation in the phases, and the initial conditions of the induced voltage are all calculable to an arbitrary degree of accuracy. Exact expressions have been obtained, and these have to be solved by iteration.

4.2.5.1.2 The power factor, supply current distortion and effective stator phase current.

In the present case it has been assumed that the supply voltage is derived from a symmetrical semi-four-phase supply system having voltages that are a simple harmonic function of time. Again selecting the "b" phase as normative the input power will be given by:

$$P_{in}^{sb} = U_{sg}\,\bar{\bar{I}}_{s1}\cos\psi_{(U_{sg}^{b},\bar{\bar{I}}_{s1}^{b})} \qquad 4.50a$$

In terms of relations 4.38 and 4.42 the r.m.s. value of the fundamental stator current is:

$$\bar{\bar{I}}_{s1} = \frac{\left[\left\{U_{sg}A_{s1}^{U}+\overline{1-s}(E_{sr}^{ba}A_{s1}^{Ea}+E_{sr}^{bb}A_{s1}^{Eb})\right\}^2 + \left\{U_{sg}B_{s1}^{U}+\overline{1-s}(E_{sr}^{ba}B_{s1}^{Ea}+E_{sr}^{bb}B_{s1}^{Eb})\right\}^2\right]^{\frac{1}{2}}}{\left\{(R_{s1})^2 + X_{s1}^2\right\}^{\frac{1}{2}}} \qquad 4.50b$$

The power factor of the circuit is correspondingly:

$$P.F. = \cos\psi_{(U_{sg}^{b},\bar{\bar{I}}_{s1}^{b})} \cdot \frac{\bar{\bar{I}}_{s1}}{\bar{\bar{I}}_{s}} = \left\{\cos\left(\frac{\pi}{2} - \phi_{s1}^{UE} - \phi_{s1}^{Z}\right)\right\} \cdot \frac{\bar{\bar{I}}_{s1}}{\bar{\bar{I}}_{s}} \qquad 4.50c$$

with ϕ_{s1}^{Z} defined in 4.42b and

$$\phi_{s1}^{UE} = \arctan\left\{\frac{U_{sg}B_{s1}^{U} + \overline{1-s}\,(E_{sr}^{ba}B_{s1}^{Ea} + E_{sr}^{bb}B_{s1}^{Eb})}{U_{sg}A_{s1}^{U} + \overline{1-s}\,(E_{sr}^{ba}A_{s1}^{Ea} + E_{sr}^{bb}A_{s1}^{Eb})}\right\} \qquad 4.50d$$

From rel. 4.44c the amplitude of the different harmonic components in the frequency spectrum follows, leading to the following expression

for the r.m.s. value of the stator current drawn from the supply.

$$\underline{\underline{I}}_s = \sqrt{\sum_{h=0}^{\infty}\left\{\left(\frac{\underline{\underline{U}}}{\underline{I}_{s4h+1}}\right)^2 + \left(\frac{\underline{\underline{U}}}{\underline{I}_{s4h+3}}\right)^2 + \left(\frac{\sqrt{1-s}\,\underline{\underline{E}}}{\underline{I}_{s4h+1}}\right)^2 + \left(\frac{\sqrt{1-s}\,\underline{\underline{E}}}{\underline{I}_{s4h+3}}\right)^2\right\}} \qquad 4.50e$$

4.2.5.2 *Results of the theoretical calculations on the system with stator control by ignition angle delay.*

In fig. 4.3.2 some of the results of the calculations performed for the discussed system are displayed graphically.

The following values of the parameter α_s have been taken for the curves:

(a) and (b):

1. $\alpha_s = 45^o$
2. $\alpha_s = 54^o$
3. $\alpha_s = 63^o$
4. $\alpha_s = 72^o$
5. $\alpha_s = 81^o$
6. $\alpha_s = 90^o$
7. $\alpha_s = 99^o$
8. $\alpha_s = 108^o$
9. $\alpha_s = 117^o$
10. $\alpha_s = 126^o$

(c):

1. $\alpha_s = 54^o$
2. $\alpha_s = 63^o$
3. $\alpha_s = 72^o$
4. $\alpha_s = 90^o$
5. $\alpha_s = 108^o$
6. $\alpha_s = 126^o$
7. $\alpha_s = 144^o$

(d):

1. $\alpha_s = 45^o$
2. $\alpha_s = 54^o$
3. $\alpha_s = 63^o$
4. $\alpha_s = 72^o$
5. $\alpha_s = 90^o$
6. $\alpha_s = 108^o$
7. $\alpha_s = 126^o$
8. $\alpha_s = 144^o$

(e), (f), (g)

1. $\alpha_s = 54^o$
2. $\alpha_s = 72^o$
3. $\alpha_s = 90^o$
4. $\alpha_s = 108^o$
5. $\alpha_s = 126^o$
6. $\alpha_s = 144^o$

The calculations for these curves have been executed by neglecting the components contributed by the "induced excitation" function. With reference to fig. 4.3 it may be seen that in fact a model is then applied where the stator windings of the machine are short circuited during the "blocking"period of the electronic switch, i.e. from $t_{\gamma_s-\pi}$ to t_{α_s}. Comparison with practical results later should point out discrepancies.

The general tendency of the torque-speed curves may be seen from (a) and (b) , where (b) actually represents an "expanded" form of that part of (a) at slips smaller than the slip of maximum torque. It may be expected that at high values of slip the model will provide a reasonable approximation to practical behaviour. The control parameter α_s may only be decreased up to the value where $\alpha_s = \psi_s$.Hereafter either halfwaving will occur, or the normal uncontrolled current will be drawn, depending on the type of triggering employed.

Calculation of the effective rotor and stator current and power factor has been done for both high and low resistance cases, but is only presented for a low resistance in fig. 4.3.2. Here the departure of the model with "induced excitation" components neglected from the actual situation may be appreciated. Inspect the curves for the power factor. The fact that the power factor becomes negative at low slip indicates the discrepancy with the true model, and is caused by the current flowing during the short circuit period from $t_{\gamma_s-\pi}$ to t_{α_s}.

It is known that *Takeuchi* [70,84] has calculated the characteristics of a single phase induction machine with high resistance rotor by what may be termed as a special case of the general theory developed in chapter 3. He comes to the conclusion that the induced e.m.f. may be neglected under all circumstances, but seeing the above discrepancy this view cannot be supported. This will be discussed further in chapter 5.

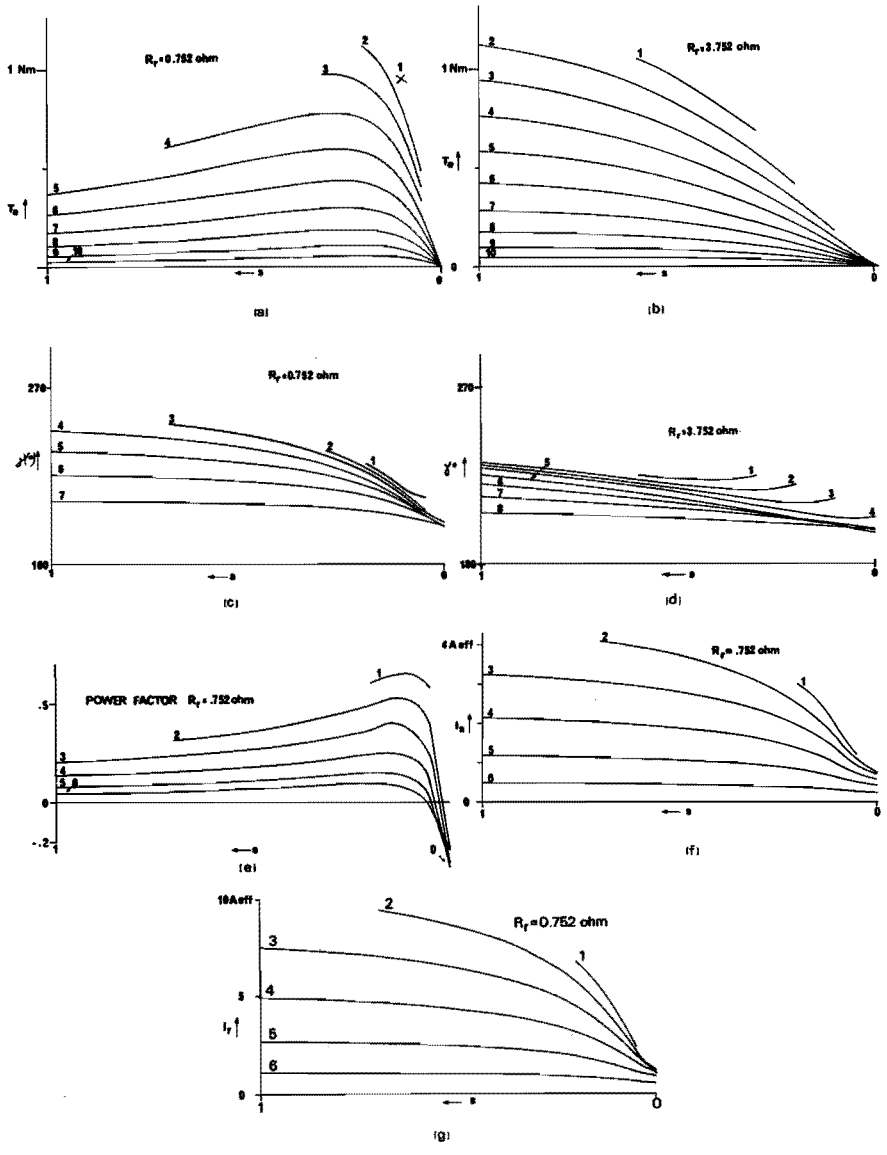

FIG. 4.3.2 RESULTS OF THEORETICAL CALCULATIONS ON AN α_s-CONTROL SYSTEM.

4.2.6 *REMARKS REGARDING AN EQUIVALENT CIRCUIT REPRESENTATION.*

In chapter 3 some attention was devoted to representing the complex amplitudes of the instantaneous symmetrical component transforms of stator and rotor current in an equivalent circuit. All the harmonic components were included in the representation, that was intended to be general. It has been indicated in this chapter that due to the conditions in the semi-four-phase voltage system the simplifying conditions may be introduced that only the $\overline{4h+1}$ st and $\overline{4h+3}$ rd components exist for the first terms of the "instantaneous positive sequence" and "instantaneous negative sequence" components respectively. This situation is represented in fig. 4.4.

In the same way as previously it may be shown that the complex amplitudes of the harmonic components of the instantaneous symmetrical component transforms of the stator and rotor currents calculated from relation 4.41a to 4.41d are represented by the equivalent circuit. In paragraph 4.2.2 it has been indicated that no zero components of voltage and current occur in the semi-four-phase system, and consequently these circuits are not found in fig. 4.4. Due to the more complicated nature of the transforms in the case of the n-m phase transducer treated in chapter 3 the difference between the complex coefficients of the Fourier series of the phase terminal voltage and the transformed voltages impressed on the equivalent circuit is not so evident as in fig. 4.4. The complex conjugate nature of these voltages may be noted from the said figure.

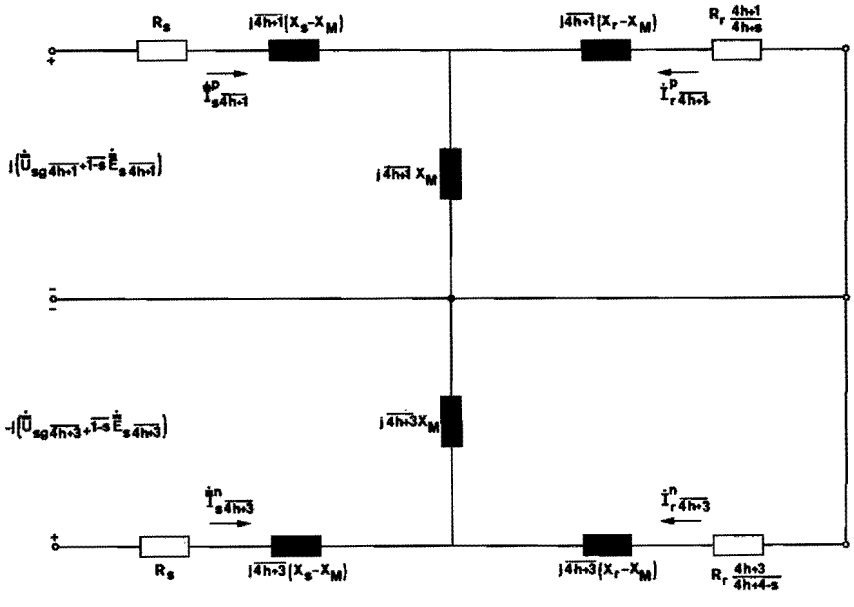

FIG. 4.4 EQUIVALENT CIRCUIT FOR CALCULATING THE COMPLEX AMPLITUDES OF THE HARMONIC COMPONENTS OF THE INSTANTANEOUS SYMMETRICAL COMPONENT TRANSFORMS OF ROTOR AND STATOR CURRENTS IN THE SEMI-FOUR-PHASE INDUCTION MACHINE.

4.3 EXAMPLES OF GROUP II, CLASS 2, MACHINE-ELECTRONIC SYSTEMS AND GROUP IIA, MACHINE-ELECTRONIC SYSTEMS.

The investigations of the previous paragraph on a machine-electronic system with conduction angle control of the stator voltage were executed by means of the general approach developed in chapter 3. In the same chapter it was also pointed out that some systems may be investigated with a much more simplified model. The proposed models concerned the rotor control of induction machines in particular, and referred only to characteristics of the electro-mechanical converter as subjected to switching effects. In the present investigation these models are extended to include the effects of the information and power electronics associated with each particular system in the same way as done previously for the more extended calculations on the ignition angle control of the stator.

4.3.1 *ROTOR CONTROL OF AN INDUCTION MACHINE BY VARIATION OF THE DELAY OF THE INSTANT OF CURRENT IGNITION.*

The first method to be investigated was classified under systems of Group II, class 2, as may be seen by reference to fig. 2.9c (i). In this type of control an antiparallel electronic switch in every rotor phase controls the current flow angle. Natural commutation is employed, and consequently the triggering angles of the switches are to be delayed. The rotor is not fed by external voltage or current sources, and the machine operates as an asynchronous electro-mechanical converter according to the definition of chapter 1. For the purpose of the present investigations the induced rotor voltage per phase will be assumed a simple harmonic function of time as in the discussions of paragraph 3.6. Before giving attention to the equations describing the currents and torques the switching modes to be expected will be examined.

4.3.1.1 *Investigations of the switching modes, and derivation of the switching commands.*

It has been stated that natural commutation is employed. This results in the maximum effective current being equal to the steady-state, uncontrolled current of the machine, and the switching mode may be described by:

$$\left.\begin{aligned} \psi_r \leq \alpha_r &\leq \pi \\ \alpha_r \leq \gamma_r &\leq (\psi_r + \pi) \\ \xi_r &\leq \pi \end{aligned}\right\} \qquad 4.51$$

when the phase angle between steady state current and the induced voltage is described by ψ_r. The information for operating the electronic switches must be related to the time scale of the system, and should be derived from some or other circuit voltage. With reference to fig.

4.5(a) it will be evident that the only external voltage available in the present case will be the voltage across the electronic switching elements. As will be shown in chapter 5 it proves possible to simulate the induced rotor voltage in some or other way, so that it will be assumed for the present that this voltage is also existing for derivation of the switching commands.

Consider the possibility to obtain an electronic delay. This will involve a discrete counting process, or in the limit, an integration process starting at some point in the voltage cycle. For the purpose of this investigation integration will be considered, and the reference or starting point taken as the zero voltage condition. Now the actual input voltage to the information electronic system may be integrated, or an integration of a specific voltage to be determined by other considerations may be initiated, both starting at the zero condition of the voltage. This second voltage that may be integrated will be chosen as a direct voltage. In both cases variation of the triggering angle will be obtained by setting a variable level at which readout of the integrator occurs, causing an output pulse to be delivered.

It will now in succession be examined what type of characteristics may be expected from the information electronics when the process is related to the system voltages by integration of the input voltage and by integration of a constant voltage.

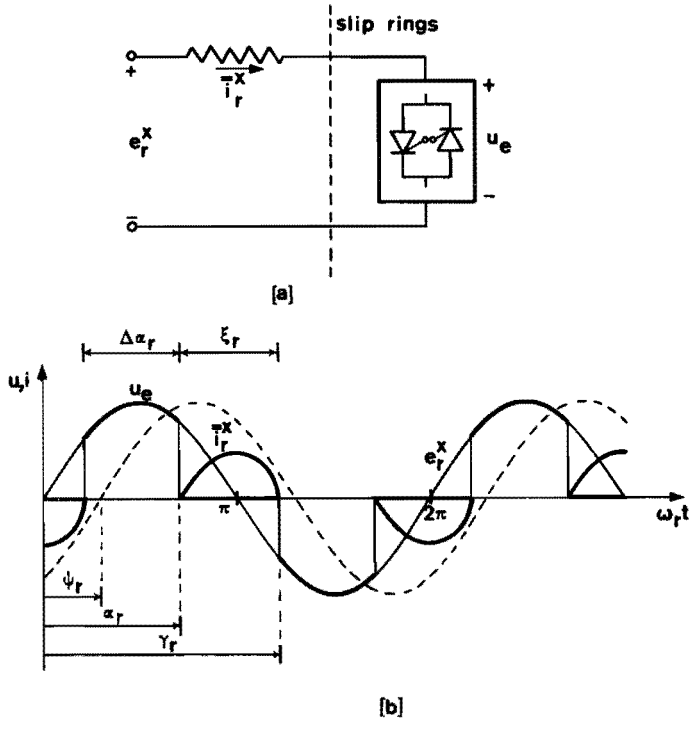

FIG. 4.5 VOLTAGE, CURRENT AND WAVEFORM DEFINITIONS CONCERNING THE ROTOR CONTROL BY IGNITION DELAY.

The induced e.m.f. in the rotor windings will be taken to be represented by:

$$0 < t < t_{\pi} \qquad e_r^x = s\sqrt{2}\,E_{r0}\,\sin(\omega_r t + \overline{x-1}.\frac{\pi}{2}) \qquad 4.52a$$

$$x = 1,2$$

It will be taken that the voltage across the electronic switch (see fig. 4.5a) is described by:

$$\left.\begin{aligned} t_{\overline{\gamma_r - \pi}} < t < t_{\alpha_r} \qquad & u_e = e_r^x \\ t_{\alpha_r} < t < t_{\gamma_r} \qquad & u_e = U_e \end{aligned}\right\} \qquad 4.52b$$

If the input voltage to the information electronics is now integrated, it may be expected to encounter the following situations when the process is always started at a zero voltage condition:

(i) *Input voltage* e_r^x, *voltage integrated:* The read-out conditions are specified by:

$$\int_0^{t_{\alpha_{re}}} e_r^x\,dt = \frac{\sqrt{2}\,E_{r0}}{\omega_s}\,(1 - \cos\alpha_{re}) = \text{constant} \qquad 4.53a$$

This implies that:

$$\alpha_{re} = \arccos\left\{1 - \frac{\omega_s}{\sqrt{2}\,E_{r0}} \int_0^{\frac{\alpha_{re}}{\omega_r}} e_r^x\,dt\right\} \qquad 4.53b$$

which will be constant and independent of the slip. This will be referred to as rotor control with constant ignition delay or as "α_r - control"

(ii) *Input voltage* u_e, *voltage integrated:* The operating conditions of the electronic switches will now be specified by:

$$\int_{t_{\overline{\gamma_{ru} - \pi}}}^{t_{\alpha_{ru}}} u_e\,dt = \frac{\sqrt{2}\,E_{r0}}{\omega_s}\,(\cos\overline{\gamma_{ru} - \pi} - \cos\alpha_{ru}) = \text{constant} \qquad 4.54a$$

The angle of triggering of the electronic switch will consequently be given by:

$$\alpha_{ru} = \arccos\left\{\cos\overline{\gamma_{ru}-\pi} - \frac{\omega_s}{\sqrt{2}\,E_{r0}} \int_{\left(\frac{\gamma_{ru}-\pi}{\omega_r}\right)}^{\frac{\alpha_r}{\omega_r}} u_e\,dt\right\} \qquad 4.54b$$

This relation indicates that the triggering angle is now also dependent on γ_{ru}. This type of control will be referred to as constant integral delay. A comparison of the limiting conditions of the triggering angle as derived by rel. 4.53b and 4.54b illustrates an important difference. The minimum value of α_{re} is

$$\alpha_{re,min} = o$$

consequently 4.55a

$$\alpha_{re,min} \leq \psi_r$$

In contrast

$$\alpha_{ru,min} = \psi_r \qquad 4.55b$$

As will be evident later in chapter 5, rel. 4.55a implies a possibility of instability, unless the ignition angle is deliberately limited to comply with rel. 4.55b.

If the zero voltage condition of the input voltage is now detected, and an integration of a constant voltage initiated, the following conditions are found:

(i) *Input voltage e_r^{α}, zero voltage detection:*

The zero voltage conditions are detected at

$$\omega_r t = g\pi \qquad (g = 0,1,2 - - - - \infty) \qquad 4.56a$$

With a constant voltage of integration, and a preset read-out level, the delay time will be constant.

$$\alpha_{ret} = t_{de} \cdot s\omega_s \qquad 4.56b$$

Since the delay angle is now dependent on the slip, a different type of characteristics from the previous alternative will be obtained, and again it may be stated that

$$\alpha_{ret,min} \leq \psi_r \qquad 4.56c$$

so that measures to avoid instability must be taken in an operative system. In the following work this type of control will be titled rotor control with constant triggering delay time, or t_{α_r}-control.

(ii) *Input voltage u_e, zero voltage detection.*

The zero voltage conditions are detected at

$$\omega_r t = \overline{\gamma_r + g\pi} \qquad (g = 0,\pm1,\pm2 - - - - \infty) \qquad 4.57a$$

As before the integration process results in a constant delay after the times defined by rel. 4.57a, i.e.

$$t_{\alpha_r} - t_{\gamma_r - \pi} = \text{constant} = t_{du} \qquad 4.57b$$

or alternatively

$$\alpha_{rut} = (\gamma_r + s\omega_s t_{du} - \pi) \qquad 4.57c$$

The delay angle is not only dependent on the slip, but also a function of the angle of natural commutation γ_r. From these conditions it may be deduced that

$$\alpha_{rut,min} = \psi_r \qquad 4.57d$$

and the system will not tend to the half-waving instability encountered in the previous case. This type of control will be referred to as rotor control with constant differential triggering delay or Δt_{α_r}-control.

After having examined the different alternatives for derivation of the switching commands it is worthwhile to devote some attention to their practical value. The slip-dependent delay angle of the t_{α_r}-control and the Δt_{α_r} control will prove to be an important disadvantage. From rel. 4.56b it follows that for the t_{α_r}-control the delay angle decreases linearly with slip, so that it may be expected that with a low rotor resistance the system will not be useful due to the sharp increase of the torque with slip. For the t_{α_r}-control rel. 4.57c indicates that although the extinction angle is included in the relation, the same type of characteristic must be expected.

4.3.1.2 *The equations describing the system.*

In paragraph 3.6 it was indicated how approximate characteristics may be calculated for rotor-controlled machine-electronic systems by using a simplified model. In the present case the current reduces to zero by natural commutation, and consequently the relation for the current will be:

$$\bar{i}_{r\alpha} = \frac{s\sqrt{2}\,E_{r0}}{\sqrt{R_r^2+\omega_r^2 L_{r\sigma}^2}} \left\{ \sin(\omega_r t-\psi_r) + \sin(\alpha_r-\psi_r)\, \exp-(\omega_r t-\alpha_r)\cot\psi_r \right\} \Bigg|_{\alpha_r}^{\gamma_r}$$

4.58a

where the angle of natural commutation γ_r must be found iteratively from:

$$\sin(\gamma_r-\psi_r) = \sin(\alpha_r-\psi_r)\, \exp-(\gamma_r-\alpha_r)\, \cot\,\psi_r \qquad 4.58b$$

The mean electromagnetic torque calculated by means of the rotor losses is now expressed as

$$\bar{T}_{e(l)} = \frac{2p\,E_{r0}^2}{\pi\omega_s\sqrt{\frac{R_r^2}{s^2}+\omega_s^2 L_{r\sigma}^2}}\left\{\xi_r\cos\psi_r + \frac{\sin(2\alpha_r-\psi_r)-\sin(2\gamma_r-\psi_r)}{2} + \right.$$

$$\left. + \frac{2\sin(\alpha_r-\psi_r)}{\operatorname{cosec}^2\psi_r}\left[(\cot\psi_r\sin\gamma_r+\cos\gamma_r)\exp-\xi_r\cot\psi_r-(\cot\psi_r\sin\alpha_r+\cos\alpha_r)\right]\right\} \qquad 4.58c$$

By the necessary modification the different harmonic components of the rotor current are to be calculated from rel. A3.8a and A3.8b. The effective rotor current is to be found from:

$$\bar{\bar{I}}_{r\alpha} = \frac{I_r^2}{\pi}\left\{(\gamma_r-\alpha_r) + \frac{\sin2(\alpha_r-\psi_r) - \sin2(\gamma_r-\psi_r)}{2} + \right.$$

$$- 4\sin\psi_r\sin(\alpha_r-\psi_r)(\sin\alpha_r-\sin\gamma_r\exp-\xi_r\cot\psi_r)$$

$$\left. + \frac{\cos2(\alpha_r-\psi_r)-1}{2\cot\psi_r}\left(\exp-2\xi_r\cot\psi_r-1\right)\right\} \qquad 4.58d$$

For calculations of the thermal effects in the semiconductor switches the mean current is just as important as the effective current. This mean current is found from:

$$\bar{\bar{I}}_{r\alpha\ \mathrm{mean}} = \frac{\sqrt{2}\,I_r}{\pi}\left\{\cos(\alpha_r-\psi_r)-\cos(\gamma_r-\psi_r) + \frac{\sin(\alpha_r-\psi_r)}{\cot\psi_r}\left(\exp-\xi_r\cot\psi_r-1\right)\right\} \qquad 4.58e$$

The rotor current contains harmonics, and the power factor of the system will differ from the power factor at which fundamental harmonic power is delivered to the circuit. From the definition of power factor for the case of fundamental and harmonic powers it follows that:

$$(P.F.)_{r\alpha} = \frac{\bar{\bar{I}}_{r1\alpha}}{\bar{\bar{I}}_{r\alpha}}\cos\psi_{r(e_r i_{r1})} \qquad 4.58f$$

4.3.1.3 *Calculation of some system characteristics.*

Fig. 4.6 indicates some calculations performed on an α_r-control system with the simplified model. The values of the control parameter are as indicated in the figure, while the calculation has been performed for the case of a high resistance rotor and a low resistance rotor.

Before numerical calculation can be carried out, the question arises what values to assign to the resistance and leakage inductance of the model. In the present case it has been stated that the "constant flux" model postulated in chapter 3 is also valid in the uncontrolled case. Consequently these values are defined in relation to the measured torque-speed curve of the machine to be used under uncontrolled conditions. This leads to values of

$$E_r = 39 \text{ V}$$
$$R_r = 0.995\Omega/\text{phase}$$
$$L_{r\sigma} = 14.4 \text{ mH/phase}$$

The case of a high resistance rotor was investigated by adding an external resistor of 3Ω/phase.

Examining the curves for the torque as a function of speed and control parameter, it is evident that the controlled operation at a certain α_r is only possible up to

$$\alpha_r = \psi_r$$

as found analogously for the stator ignition-angle control system. It may be seen how this effect is also found in the region of slip smaller than the slip of maximum torque. It does not appear that the slip of maximum torque shows such an unpleasant dependence upon control parameter as with the systems having t_{α_r}-control or Δt_{α_r}-control. This will later be verified, experimentally.

That the current is decreased in the higher resistance case may be seen from a comparison of figures (b) and (f), while it is also immediately obvious how the power factor of the controlled high-resistance machine is improved.

As may be expected the harmonic content of the rotor current will decrease due to the harmonic content and according to the theoretical expressions it should always be lower than the cosine of the phase angle between induced rotor e.m.f. and fundamental phase current. This is illustrated in fig. 4.6(c) and (d) or (g) and (h). The increase in harmonic content of the rotor current with a decrease in slip is also evident. This reduces the power factor in the same sense.

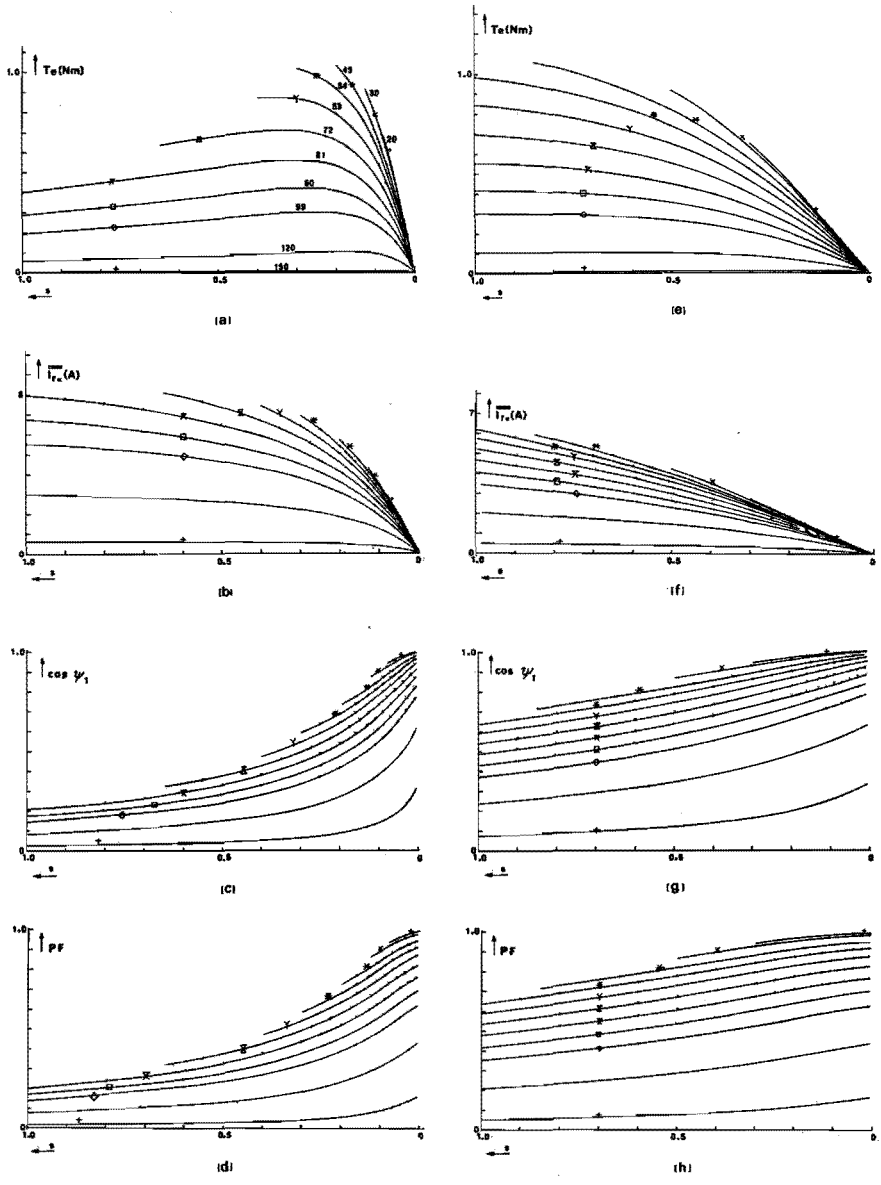

FIG. 4.6 EXAMPLES OF SOME CALCULATED CHARACTERISTICS FOR A MACHINE-ELECTRONIC SYSTEM WITH α_r-CONTROL.
α_r=150° (+); =120° (−); = 99° (◇); = 90° (□); = 81° (⧗); = 72° (⧖); = 63° (Y); = 54° (✱); = 45° (✳); = 30° (×); = 20° (+).

4.3.2 *ROTOR CONTROL OF AN INDUCTION MACHINE BY VARIATION OF THE INSTANT OF CURRENT EXTINCTION.*

In the classification system developed the method to be described in this paragraph was classified under systems of group II, class 2. It is basically represented in fig. 2.9d (i). Further detail regarding the power electronic circuits will be represented in chapter 5, part I. It was previously stated that this type of control was suggested as a logical augmentation of the already existing rotor control methods discerned in the classification system. Due to the natural commutation employed in the system for control of the rotor current by variation of the ignition instant the power factor is low. In contrast it may be suggested to keep the instant of "switching on" constant, and vary the instant of "switching off". This should improve the power factor over the whole range of operating conditions. It will later be evident that other improvements of performance are simultaneously introduced. It should be realized, however, that the system complexity is considerably increased by the forced commutation.

Similar to the systems with variation of the instant of triggering, the present investigations concern an electromechanical converter with short-circuited rotor. Applying the definition of chapter 1, it is evident that the machine will operate as an asynchronous converter. The assumption that the induced rotor e.m.f. is a simple harmonic function of time remains valid.

It has been stressed in chapter 2, that an advantage of a classification system is that the possible combinations of ideas become clearer. In the present case this may for instance be illustrated by variation of both the instant of triggering and the instant of extinction. If the current flow angle is kept constant, the current conduction may be timed to optimize some or other system characteristic, as for instance minimize harmonic generation, minimize current, or maximize power factor. The last case will be investigated as an extension of the system with extinction angle control.

4.3.2.1 *Specification of the switching mode, and derivation of the switching commands.*

As specified the conduction of the electronic switch is initiated at the zero voltage condition of the induced e.m.f., and the current is reduced to zero by forced commutation at a variable instant. This forced commutation process cannot be expected to occur instantaneously, since the model assumed for these calculations (see paragraph 3.6) includes the leakage inductance of the machine phases. Consequently the time taken for switching off is determined by the allowable circuit voltages. For the present it will be assumed that this commutation time

$$t_{com}^{\beta_r} << \frac{1}{2f_r} \qquad 4.59a$$

and consequently the contribution of the rotor current flowing during this time to the system characteristics (torque, power factor, effec-

tive current etc.) will be neglected. The calculations will be performed as if the rotor phase current reduces to zero at the instant of commutation. Consequently the following specifications for the switching mode will be used:

$$\left.\begin{aligned} \alpha_r &= 0 \\ 0 \leqslant \beta_r &\leqslant \pi \\ 0 \leqslant \xi_r &\leqslant \pi \end{aligned}\right\} \qquad 4.59b$$

Assuming a simulated induced rotor e.m.f. to be still available, relation 4.52a remains valid. Taking the voltage across the electronic switch to be described by:

$$\left.\begin{aligned} 0 < t < t_{\beta_r} \qquad & u_e = U_e \\ t_{\beta_r} < t < t_\pi \qquad & u_e = e_r^x \end{aligned}\right\} \qquad 4.59c$$

the two alternatives of either integrating the actual input voltage to the information electronics, or detecting the zero voltage condition will again be considered. The following alternatives then receive attention.

(i) *Input voltage e_r^x, voltage integrated:*

Therefore:

$$\int_0^{t_{\beta_{re}}} e_r^x \, dt = \frac{\sqrt{2}\, E_{r0}}{\omega_s} (1 - \cos \beta_{re}) = \text{constant} \qquad 4.60a$$

The extinction angle will be constant, and independent of slip:

$$\beta_{re} = \arccos \left\{ 1 - \frac{\omega_s}{\sqrt{2}\, E_{r0}} \int_0^{\frac{\beta_{re}}{\omega_r}} e_r^x \, dt \right\} \qquad 4.60b$$

This type of control has been named: "rotor control with constant extinction angle delay" or β_r-control.

(ii) *Input voltage u_e, voltage integrated*

$$\int_0^{t_{\beta_{ru}}} u_e \, dt = \frac{U_e \beta_{ru}}{s\omega_s} = \text{constant} \qquad 4.61a$$

In this case the extinction angle will be slip dependent

$$\beta_{ru} = \left\{ \frac{s.\omega_s}{U_e} \int_0^{\frac{\beta_{ru}}{\omega_r}} u_e \, dt \right\} \qquad 4.61b$$

The voltage across the electronic switch during conduction has been assumed to be constant, and in analogy to the integration of a constant voltage initiated at the zero voltage condition of e_r^x, the delay time before current extinction is accomplished will be constant.

When controlling the instant of triggering, the natural commutation causes the voltage across the electronic switch to pass zero after the induced voltage. This is responsible for the difference in control characteristics between rotor control with constant triggering delay time and rotor control with differential triggering delay. In the present instance the zero voltage conditions of the induced e.m.f. and the electronic switch voltage are coincident. These conditions occur at instants described by relation 4.56a.

Consider the case of *zero voltage detection* initiating integration of a constant voltage. With a preset read-out level, the delay time will be constant.

$$\beta_{rt} = t_d.s\omega_s \qquad 4.62$$

This type of control will be termed "rotor control with constant instant of current extinction" or t_{β_r}-control. With none of the methods inspected so far it may be expected to find the half-waving instability that is possible with"constant ignition angle delay control" and with "constant triggering delay time control".

Relation 4.62 indicates that it may be expected that rotor control with constant instant of current extinction will have characteristics where the torque decreases with the slip.

4.3.2.2 *The equations describing the system.*

With reference to relation 3.52 the current is described under the present conditions by:

$$\bar{i}_{r\beta} = \frac{s\sqrt{2}\,E_{r0}}{\sqrt{R_r^2+\omega_r^2 L_{r\sigma}^2}} \left\{ \sin(\omega_r t-\psi_r)+\sin\psi_r \exp-\omega_r t \cot\psi_r \right\} \Bigg|_0^{\beta_r} \qquad 4.63$$

where the commutation angle β_r is now known explicitly. Consequently the mean electromagnetic torque becomes:

$$\bar{T}_{e(1)} = \frac{2pE_{r0}^2}{\pi\omega_s\sqrt{\frac{R_r^2}{s^2}+\omega_s^2 L_{r\sigma}^2}} \left\{ \beta_r\cos\psi_r - \frac{\sin(2\beta_r-\psi_r)+\sin\psi_r}{2} \right.$$

$$\left. - \frac{2\sin\psi_r}{\operatorname{cosec}^2\psi_r} \left[(\cot\psi_r\sin\beta_r+\cos\beta_r)\exp-\beta_r\cot\psi_r - 1 \right] \right\} \qquad 4.64$$

The different components of current are to be found from rel. A3.8a and A3.8b, while the effective current becomes:

$$\bar{\bar{I}}_{r\beta}^2 = \frac{I_r^2}{\pi}\left\{ \beta_r - \frac{\sin2\psi_r+\sin2(\beta_r-\psi_r)}{2} - 4\sin^2\psi_r\sin\beta_r\exp-\beta_r\cot\psi_r \right.$$

$$\left. + \frac{\cos2\psi_r-1}{2\cot\psi_r}\left(\exp-2\beta_r\cot\psi_r - 1\right) \right\} \qquad 4.65a$$

For calculation of heating effects in the electronic switches the mean current is just as important as the effective current, and therefore the mean current may be found from:

$$\bar{\bar{I}}_{r\beta\ \text{mean}} = \frac{\sqrt{2}\,I_r}{\pi}\left\{ \cos\psi_r-\cos(\beta-\psi_r)-\frac{\sin^2\psi_r}{\cos\psi_r}(\exp-\beta\cot\psi_r - 1)\right\} 4.65b$$

The rotor current contains harmonics, and therefore the power factor of the system is again expressed in terms of all fundamental and harmonic powers as:

$$(P.F.)_{r\beta} = \frac{\bar{\bar{I}}_{r1\beta}}{\bar{\bar{I}}_{r\beta}} \cdot \cos\psi_{r(e_r i_{r1})} \qquad 4.66$$

with $\bar{\bar{I}}_{r1}$ as specified in appendix A3.3 under the conditions that $\alpha_r=0$.

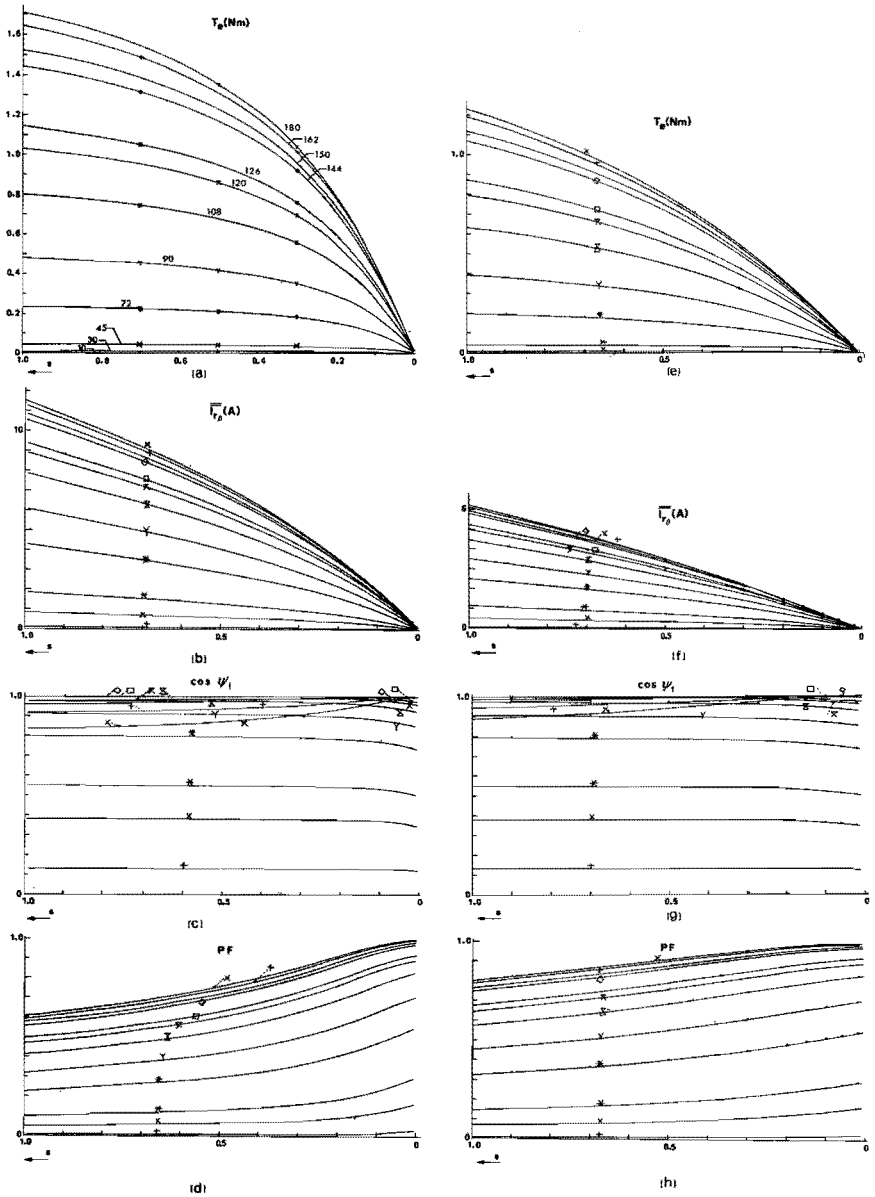

FIG. 4.7 EXAMPLES OF SOME CALCULATED CHARACTERISTICS FOR A MACHINE-ELECTRONIC SYSTEM WITH β_r-CONTROL.
β_r=180° (X); = 162° (+); = 144° (◇); = 126° (□); = 120° (⧓); = 108° (⧖); = 90° (Y); = 72° (✱); = 45° (✱); = 30° (X); = 10° (+).

4.3.2.3 *Calculation of some system characteristics.*

The theoretical results of calculations on systems with β_r-control and t_{β_r}-control are shown in figures 4.7 and 4.8 respectively. The values of the parameters are again given in the appropriate figure. As in previous cases a low and a high resistance rotor were used for calculations.

Determining the values of the circuit parameters of the simplified model with which to perform the calculations has been discussed in the case of α_r-control. The same procedure was employed. In the present case, however, the presence of the power-electronic switch was taken into account to some extent. From the experimental results it will subsequently become clear how the power-electronic switch necessary to interrupt the rotor current affects the steady state torque-speed relationship . Taking the experimentally measured torque-speed relation in uncontrolled condition - with the power-electronic switch present in the rotor - as starting point, the parameters were determined as:

$$E_r = 39\ V$$
$$R_r = 2.04\Omega/\text{phase}$$
$$L_{r\sigma} = 17.5\ \text{mH/phase}$$

The inductive effects are mainly caused by the series commutating transformer of the power switch.

Comparison of figures 4.7 and 4.8 immediately indicates the difference between the β_r-control and t_{β_r}-control. It may be seen how the current flow angle decreases with decreasing slip in the latter case. Whereas the (capacitive) phase shift between induced rotor voltage and fundamental harmonic current remains nearly constant in the case of β_r-control, it may be seen how the angle becomes more capacitive with decreasing slip in the case of t_{β_r}-control.

The difference in both cases (β_r-control and t_{β_r}-control) between low and high rotor resistance is evident. Since the "current surge effect" will be lower in the last case, the maximum torque at standstill, and current, will be lower.

Finally an inspection of these sets of figures, and comparison with fig. 4.6 of α_r-control suffices to illustrate the most novel characteristics of these systems - the increased torque capability and improved (capacitive) power factor. It may again be seen what the influence of the harmonics on the power factor is for the different systems.

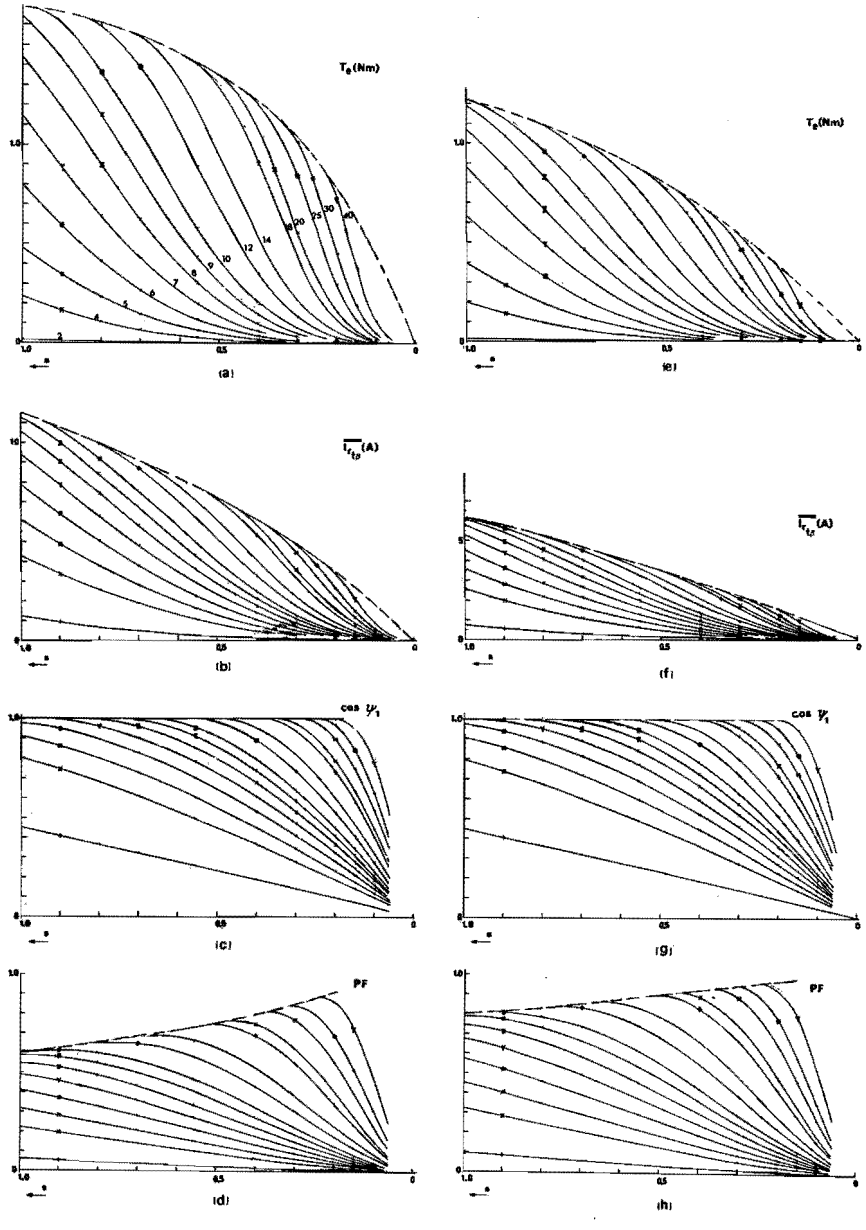

FIG. 4.8 EXAMPLES OF SOME CALCULATED CHARACTERISTICS FOR A MACHINE-ELECTRONIC SYSTEM WITH t_β -CONTROL.

t_β =2ms(+); = 4(×); = 5(✱); = 6(✱); = 7(Y); = 8(✱); = 9(✱); = 10(□); = 12(◇); = 14(−); = 18(+); = 20(×); = 25(×); = 30(✱); = 40(Y).

4.3.2.4 *A combination of α_r-control and β_r-control to obtain minimum phase shift between fundamental current and induced voltage.*

It has been pointed out that different criteria may be applied to attempt an optimization of the rotor control by switching at rotor frequency. If the current flow angle is now kept constant, the ignition and extinction angles are related by:

$$\beta_r = \xi_{r0} + \alpha_r \qquad 4.66$$

Accepting the criterion of minimum phase shift between the fundamental harmonic current and the induced rotor voltage, it is to be calculated for what α_r

$$\frac{d}{d\alpha_r} (\cos \psi_{r1}) \equiv 0 \qquad 4.67$$

where the harmonic phase angle has already been specified in appendix A3.3. It is shown in appendix A4.5 what the necessary values of the coefficients are to perform the calculation of rel. 4.6 7.

An example of the torque-speed relation that may be expected from this method is shown in fig. 4.9. The calculation has been performed for a machine with an open circuit rotor voltage of 200 V at stand-still, and equivalent parameters for the simplified model as specified.

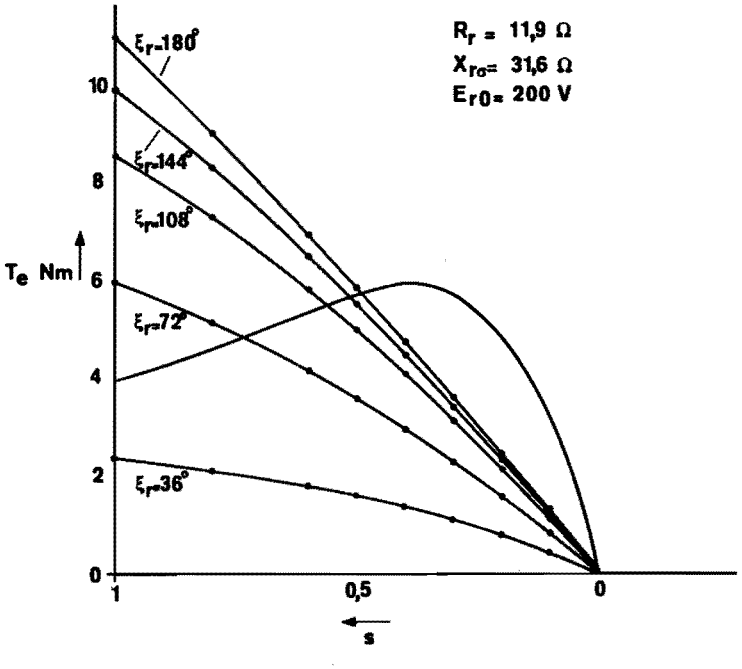

FIG. 4.9 AN EXAMPLE OF TORQUE-SPEED CURVES THAT MAY BE OBTAINED WITH CONSTANT CURRENT FLOW ANGLE AND MINIMUM FUNDAMENTAL PHASE SHIFT

4.3.3 *CONTROL OF AN INDUCTION MACHINE BY USING A HIGH FREQUENCY CHOPPER CIRCUIT WITH A RESISTIVE LOAD.*

The machine electronic system to be investigated in this paragraph has been discussed in principle in paragraph 2.4.2, where it was classified under systems of Group II, class 2 (See fig. 2.9d (ii)). In principle a switching frequency much higher than the rotor frequency of the machine is used. The schematic circuit diagram of fig. 2.9d must be extended before a representative investigation into the system characteristics can be conducted.

When a high switching frequency in stator or rotor circuit is used for the control of the power flow in an electrical machine, it will normally be attempted to keep the machine current continuous by the inclusion of either freewheeling switching elements or impedance elements in parallel to the electronic switching circuit. Such a lay-out of the system will not only decrease the high frequency loss in the electrical machine, but also decrease the switching losses in the power electronic circuits caused by the forced commutation of the currents in the inductive machine circuits. When this type of control is applied to the rotor of an induction machine the only possibility remaining is that of an alternative current path in parallel with the power electronic switch. The arrangement is indicated schematically in fig. 4.10(a) for a semi-four-phase machine. It is, however, an open question whether this arrangement will ever be followed for a practical system. One of the chief objections would be the necessity of constructing two anti-parallel force commutated chopper circuits. Furthermore the minimum switching frequency will be limited by the leakage inductance of the machine, and it could be necessary to increase the inductance by including an extra inductor in series with the parallel combination of switch and impedance.

An arrangement that will be followed in an actual system is shown in fig. 4.10(b). Inclusion of the rectifier has now reduced the number of necessary forced commutation switches. An inductor is included in the output of the rectifier since the said machine leakage inductance is not sufficient to assure that the current flow will be continuous under all conditions. In paragraph 2.4.2 it was already remarked that the rectifier-chopper cascade will tend to impart some characteristics of a system with control by switching at rotor frequency to the arrangement, whilst the high switching frequency effects will be superposed thereon. Seeing that the characteristics of systems built to the configuration of fig. 4.10(a) or (b) respectively will differ so much, only the last alternative is to receive attention in this section. It should be kept in mind, however, that the investigations on the switching modes of the high frequency chopper circuit conducted may be applied for the most part to both configurations.

Finally, consideration must be given to the parallel impedance Z. When the conduction through the electronic switching circuit is interrupted, the current must revert to the parallel path immediately. This excludes inductive elements in this impedance. It should therefore consist of resistive and/or capacitive elements. The alternative with a parallel resistor will be concerned in the next paragraphs.

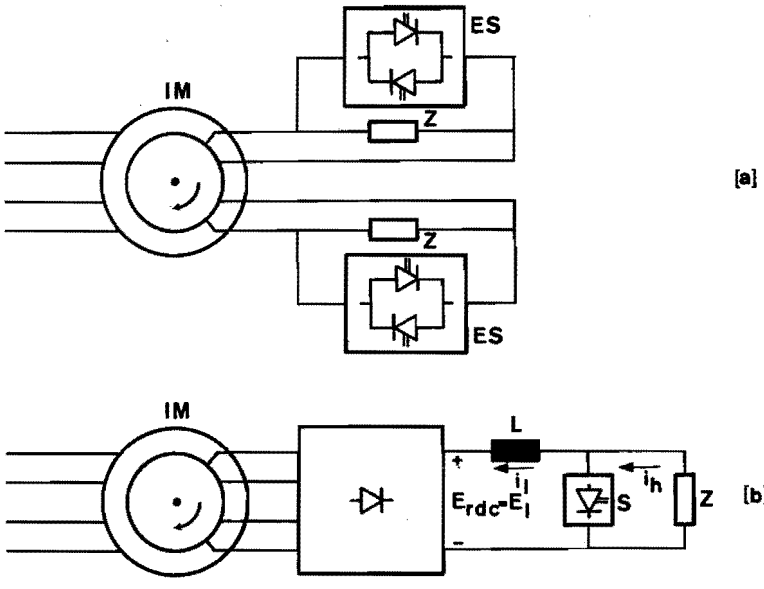

FIG. 4.10 SCHEMATIC ARRANGEMENT OF ALTERNATIVE METHODS OF ROTOR CONTROL BY HIGH-FREQUENCY SWITCHING.

Seeing that this type of control is dissipative as compared to the systems for recuperation of the slip power, but still uses what may be termed an electronically controlled counter e.m.f., it is suggested that it is named an electronic Leblanc-cascade in analogy with the electronic Scherbius cascade.

4.3.3.1 *An investigation of the switching modes and the derivation of the switching commands.*

From the previous discussion it will be clear that attention must be given to the switching mode of the chopper at a frequency much higher than the rotor frequency, and to the switching due to the rectifier. In correspondence with previous investigation the switching will be assumed to be instantaneous in all circuits, and no attention will be devoted to the influence of the internal structure of the power electronic circuits on the system behaviour. These matters will be considered in the experimental chapter.

Let the switching modes in the high-frequency chopper circuit first be considered. For this purpose consider the schematic diagrams and waveform definitions of fig. 4.11. These definitions have been set up to be complementary to other work being done on machine-electronic systems, and therefore it will be found that the actual system currents

are negative. Basically two types of chopper circuits are distinguished: high-low choppers and low-high choppers. The former is responsible for the transport and control of power from a higher to a lower voltage (E_h to E_l, also chosen to correspond with previously agreed conventions outside the scope of this work. The low voltage inevitably corresponds with the induced e.m.f. of an electrical machine) and the latter for the transport and control of power from a lower to a higher voltage. In high-low choppers the switching element exerting control on the power flow is in series with the main power flow path, while in the low-high choppers the controlling switch is located at quadrature with the main power flow path. For the control of power flow in the rotor circuits of induction machine choppers of the low-high type will now be considered further.

In fig. 4.11a a schematic representation of the high low chopper is given. The necessary circuit structure is shown in fig. 4.11b. With reference to the waveform it may be seen that τ_t is the time during which power transport occurs, while during τ_z power transport between low and high voltage sources iz ero. The values of the input current i_l are i_t and i_z during the respective times. In order to obtain some simplification of the relations the following will be considered valid:

$$R_l \equiv 0 \qquad E_h \equiv 0 \qquad \text{4.68a}$$

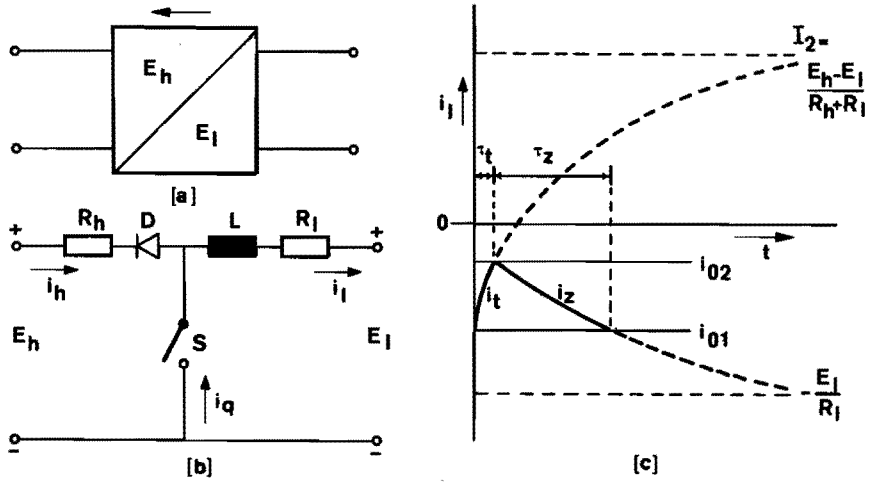

FIG. 4.11 FUNDAMENTAL DEFINITIONS REGARDING LOW-HIGH CHOPPER CIRCUITS FOR POWER TRANSPORT.

The last circumstance is brought about by the resistive load of the chopper as already specified, while the former is an idealization of the rotor, since it is valid that

$$R_r << R_h \qquad 4.68b$$

As indicated in fig. 2.9d (ii) the chopper is a typical pulse system, and the power flow may for instance be controlled by one of the following modes:

(i) pulse width modulation,
(ii) pulse frequency modulation,
(iii) two level current control, which is a combination of (i) and (ii) as far as repetition frequency and on-off ratio is concerned.

For the present systems the investigations are to be restricted to the last type of control. Regarding the characteristics to be presented certain restrictions will also be observed, since it is at present only desired to know those particulars that will affect the energy conversion in the first instance.

It is indicated in appendix A4.6.1 that:

a. the mean chopper current drawn from the low voltage ports ($\bar{\bar{I}}_{1\ mean}$);
b. the mean chopper current delivered at the high voltage ports ($\bar{\bar{I}}_{h\ mean}$);
c. the effective chopper current drawn from the low voltage ports ($\bar{\bar{I}}_1$);
d. the effective chopper current delivered at the high-voltage ports ($\bar{\bar{I}}_h$);

may be represented by the following set of equations for a chopper with resistive load when rel. 4.68a is valid:

$$\bar{\bar{I}}_{1\ mean} = i_{01}\left[\frac{n_R^2 \ln\left(\frac{1-n_R}{k_R-n_R}\right) + \frac{1}{2}(1-k_R^2) + (1-k_R)n_R}{n_R \ln\left(\frac{1-n_R}{k_R-n_R}\right) + \overline{1-k_R}}\right] \qquad 4.69a$$

$$\bar{\bar{I}}_{h\ mean} = i_{01}\left[\frac{n_R^2 \ln\left(\frac{1-n_R}{k_R-n_R}\right) + (1-k_R)n_R}{n_R \ln\left(\frac{1-n_R}{k_R-n_R}\right) + \overline{1-k_R}}\right] \qquad 4.69b$$

$$\bar{\bar{I}}_1^2 = i_{01}^2\left\{\frac{n_R^3 \ln\left(\frac{1-n_R}{k_R-n_R}\right) + (1-k_R)\left[\frac{n_R}{2}(2n_R+1+k_R)+\frac{1}{3}(3k_R+\overline{1-k_R}^2)\right]}{n_R \ln\left(\frac{1-n_R}{k_R-n_R}\right) + \overline{1-k_R}}\right\} \qquad 4.69c$$

$$\bar{I}_h^2 = i_{02}^2 \left[\frac{n_R^3 \ln\left(\frac{1-n_R}{k_R-n_R}\right) + \frac{n_R}{2}(1-k_R)(2n_R+1+k_R)}{n_R \ln\left(\frac{1-n_R}{k_R-n_R}\right) + \overline{1-k_R}} \right] \qquad 4.69d$$

The parameters n_R and k_R are limited by the following considerations:

$$0 < k_R < 1$$
$$0 < n_R < k_R \qquad 4.69e$$

At $k_R=1$ no chopper operation is found, since the two current levels are equal, whilst $k_R=0$ is a limiting condition due to the accompanying fact that for this condition (see defining relations A4.50) either $i_{01} \to \infty$, or $i_{02} \to 0$. The second part of the inequality 4.69e is found from the consideration that for operation of the chopper

$$i_{02} < I_2 \qquad 4.69f$$

Any of the equations 4.69a to d may now be used to investigate the stable region of chopper operation. As will be seen subsequently the power transported to the resistance R_h is of primary importance. Where the chopper circuit is at present used for controlling an induction machine, the variation of this power with the induced voltage (with E_1, and consequently with the slip) is of primary importance.

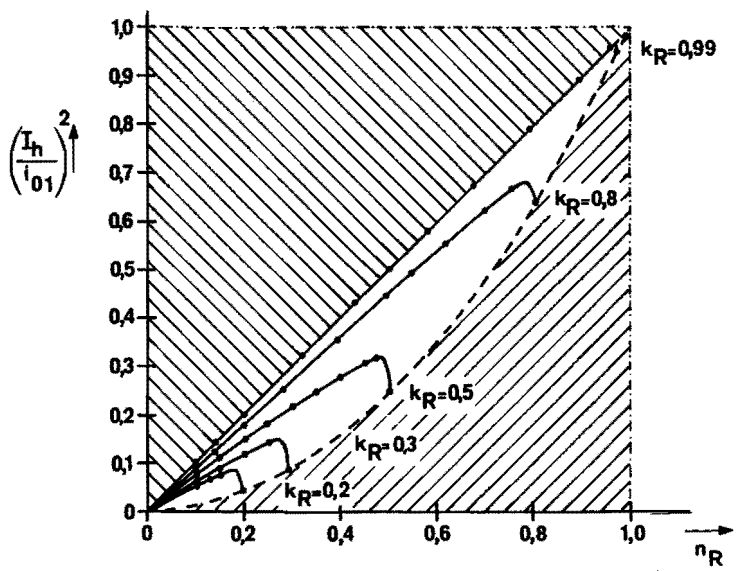

FIG. 4.12 CHARACTERISTICS OF A RESISTIVELY LOADED CHOPPER CIRCUIT.

In fig. 4.12 results of calculation of these normalized quantities for different values of the current ratio k_R by digital computer are presented. In the case of constant maximum chopper current i_{01} the said figure represents the power transport as a function of machine slip. The upper limit of the stability region is given by the maximum attainable current ratio k_R, and the lower limit by the maximum attainable value of n_R. This parameter is actually a measure of the ratio by which the low voltage is transformed upwards at the instant of opening the chopper switch. (see rel. A4.48) From fig. 4.12(a) it may be seen how the operating region of the chopper circuit increases when the current ratio is increased.

In the above considerations attention has been paid to the switching modes and stability region of the low-high electronic chopper circuit used. The presence of the rectification circuit will be considered in more detail in the following recuperative system (electronic Scherbius cascade). For the present purposes it will suffice to state that the chopper frequency is considered to be much higher than the rotor frequency, and the output current of the bridge rectifier consequently nearly constant. With the instantaneous switching of the electronic circuits as assumed (neglecting the effect of rotor leakage impedance and resistance on rectifier commutation) the rotor current will have the basic waveform shown in fig. 4.14e.

Attention will now be turned to the derivation of the switching commands. The two level current control will result in a certain mean output current of the rectifier, as explained above. The relation between this mean current and the machine torque will be examined in the next paragraph. By what means this a.c. current is to be adjusted will now be investigated. Two methods have been examined with a view to feasibility for eventual technical realization. It is feasible to change the difference

$$\Delta i = i_{01} - i_{02} \qquad 4.70a$$

while the current ratio k_R remains constant, or to change the current ratio while the difference remains constant. The switching commands are then derived in such a way that

$$\bar{\bar{I}}_{1\ \text{mean}} = f(k_R)_{\Delta i\ =\ \text{constant}} \qquad 4.70b$$

or that

$$\bar{\bar{I}}_{1\ \text{mean}} = f(\Delta i)_{k_R\ =\ \text{constant}} \qquad 4.70c$$

For the system subsequently to be used for experimental investigations these two relations were then investigated by digital computer. With reference to the relations 4.69 a to d for the currents it may be seen that when the chopper circuit is applied in the rotor of an induction machine the low voltage becomes slip-dependent, so that relations 4.70b and 4.70c can be expressed as:

$$\bar{\bar{I}}_{1\ \text{mean}} = f\left[k_R,\ E_1(s)\right]_{\Delta i\ =\ \text{constant}} \qquad 4.70d$$

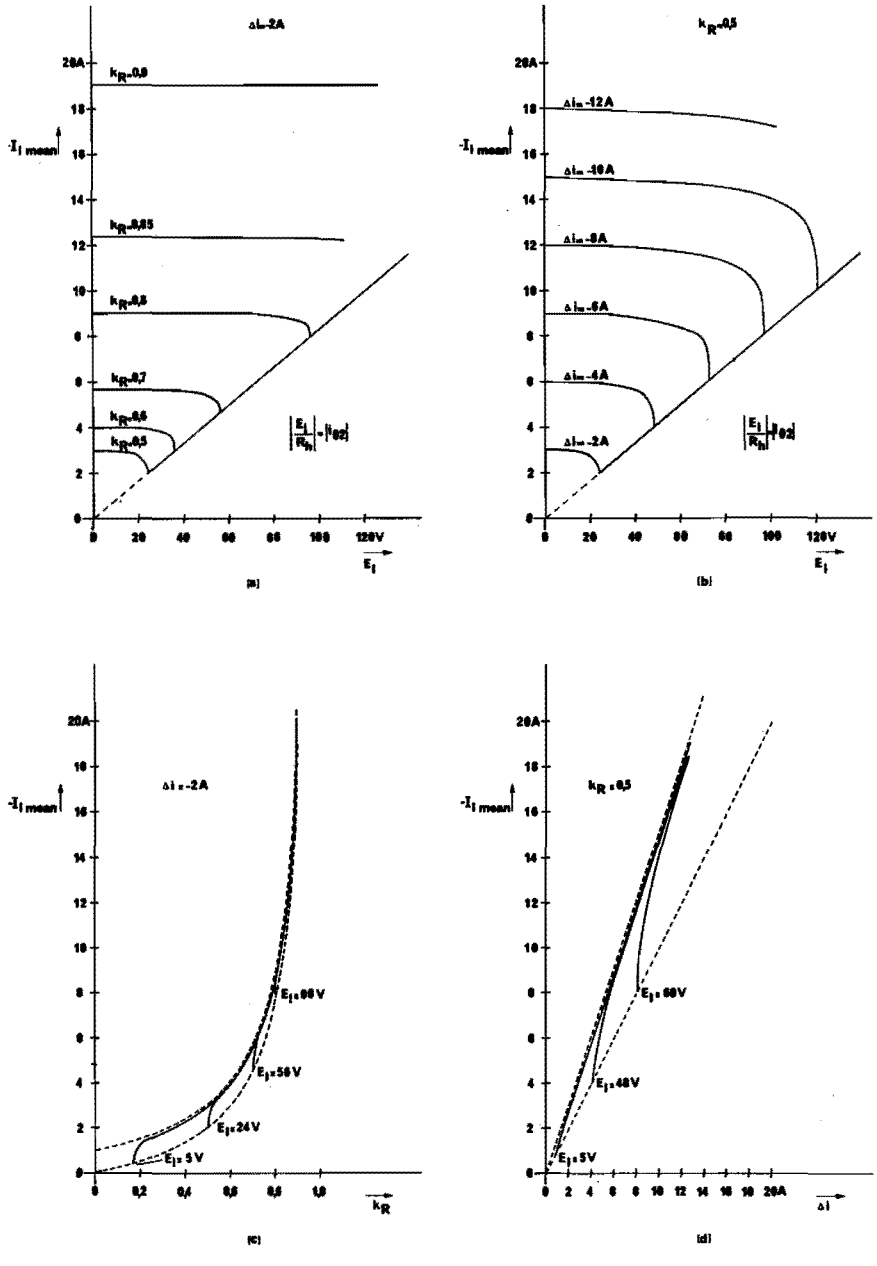

FIG. 4.13 TRANSFER CHARACTERISTICS OF A RESISTIVELY LOADED CHOPPER CIRCUIT.

$$\bar{\bar{I}}_{1\ mean} = f\left[\Delta i,\ E_1(s)\right]_{k_R = \text{constant}} \qquad 4.70c$$

For the calculations $R_h = 12\Omega$, and the low voltage varies from zero to 100 V. These values have been chosen with a view to the possible operation of the Westinghouse Generalized machine in the regio s=0 to s=2, and the rotor resistance value of the machine. The reasons for the choice of these values will become clear in chapter 5.

The relation between the mean input current to the chopper and the induced e.m.f. is shown in fig. 4.13(a) and 4.13(b) for the conditions of 4.70(d) and (e) respectively. With increasing voltage chopper operation is discontinued at the point where

$$\left|\frac{E_1}{R_h}\right| \geq \left|i_{02}\right|$$

These curves indicate that only certain combinations of E_1, Δi and k_R enable chopper operation. In fig. 4.13(c) and (d) the same information is presented, but for a constant value of Δi and k_R that is realistic for the subsequent experimental investigations.
These two sets of curves illustrate clearly that for a decreasing induced rotor voltage the relation between Δi and the mean chopper input current at a constant current ratio becomes increasingly linear, while for a decreasing rotor voltage the relation between the current ratio k_R and the mean current for a constant current difference Δi, becomes increasingly nonlinear. This is a very important observation when it is considered to include the system in a closed loop, and will again be referred to in chapter 5.

4.3.3.2 *Equations for the assumed model of the electronic Leblanc cascade.*

Before examining equations for the electronic Leblanc cascade in this paragraph, a set of general equations valid for all three the rotor control systems with known rotor current will be deduced. Refer to fig. 4.14(a). This figure represents a per phase power equivalent circuit for such a system where the effect of the electronic switching on the rotor may be seen as the action of a current source. The equivalent power-electronic circuit resistance is described by R_e, and the equivalent power electronic circuit voltage by V_e. In the present case the power-electronic circuits have been assumed to be ideal, but even if this is not the case it may be shown that the power characteristics of the circuit may be characterised by these two parameters. The per phase smoothing inductance is L', while it is assumed that the d.c. current I_{dc} contains a negligible percentage of a.c. components. The corresponding waveform for the rotor current with an m_b-phase rectifier bridge is shown in fig. 4.14e.

Taking the relation between the effective rotor current and the rectifier output current into account, the circuit may be transformed to that of fig. 4.14b, when the smoothing inductor and the leakage inductance are omitted. These inductances do not affect the power flow,

and by the previous assumptions the influence of the leakage inductance on the commutation is negligible. This is an important step in the simplification, as the omission of commutation influences results in frequency independence of the circuit transformation. Inspection of fig. 4.14(b) indicates that the non-linear rectifier has no further influence on the power flow, with the result that fig. 4.14(c) may be drawn.

With reference to the power flow models of chapter 2, and paragraph 3.6 the power flow for negligible stator resistance will be:

$$P^{s}_{in(1)} = \sum_{h=0}^{\infty} P^{r}_{de(2h+1)} - \sum_{h=0}^{\infty} P^{r}_{in(2h+1)} + \overline{T}_{e(1)} \cdot \omega_m \qquad 4.72a$$

Consequently

$$\sum_{h=0}^{\infty} P^{r}_{de(2h+1)} - \sum_{h=0}^{\infty} P^{r}_{in(2h+1)} = \overline{T}_{e(1)} \cdot \frac{s\omega_s}{P} \qquad 4.72b$$

From the equivalent circuit of fig. 4.14a, b or c the electromagnetic torque may be found as:

$$\overline{T}_{e(1)} = \frac{m.p}{s\omega_s} \left\{ I_r^2 \left(R_r + \frac{m_b}{2m} R_e \right) + I_r \sqrt{\frac{m_b}{2m^2}} V_e \right\} \qquad 4.73$$

The rotor electrical power input per phase may be written as:

$$E_r . I_r . (P.F.)_r = \frac{1}{m} \left\{ \sum_{h=0}^{\infty} \left(P^{r}_{de(2h+1)} - P^{r}_{in(2h+1)} \right) \right\} \qquad 4.74a$$

Consequently the rotor power factor will be:

$$(P.F.)_r = \left\{ \frac{I_r}{E_r} \left(R_r + \frac{m_b}{2m} R_e \right) + \sqrt{\frac{m_b}{2m^2}} \frac{V_e}{E_r} \right\} \qquad 4.74b$$

It is now important to note that when $V_e \neq 0$, the model is restricted to a slip region where the mean rectified rotor voltage is equal to the mean equivalent electronic circuit voltage. Under the present assumptions, with the rotor e.m.f. being a simple harmonic function of time, the limit is given by:

$$\frac{2\sqrt{2}\, sE_{r0}}{\pi} \left[m_b \sin\left(\frac{\pi}{m_b} \right) \right] = V_e$$

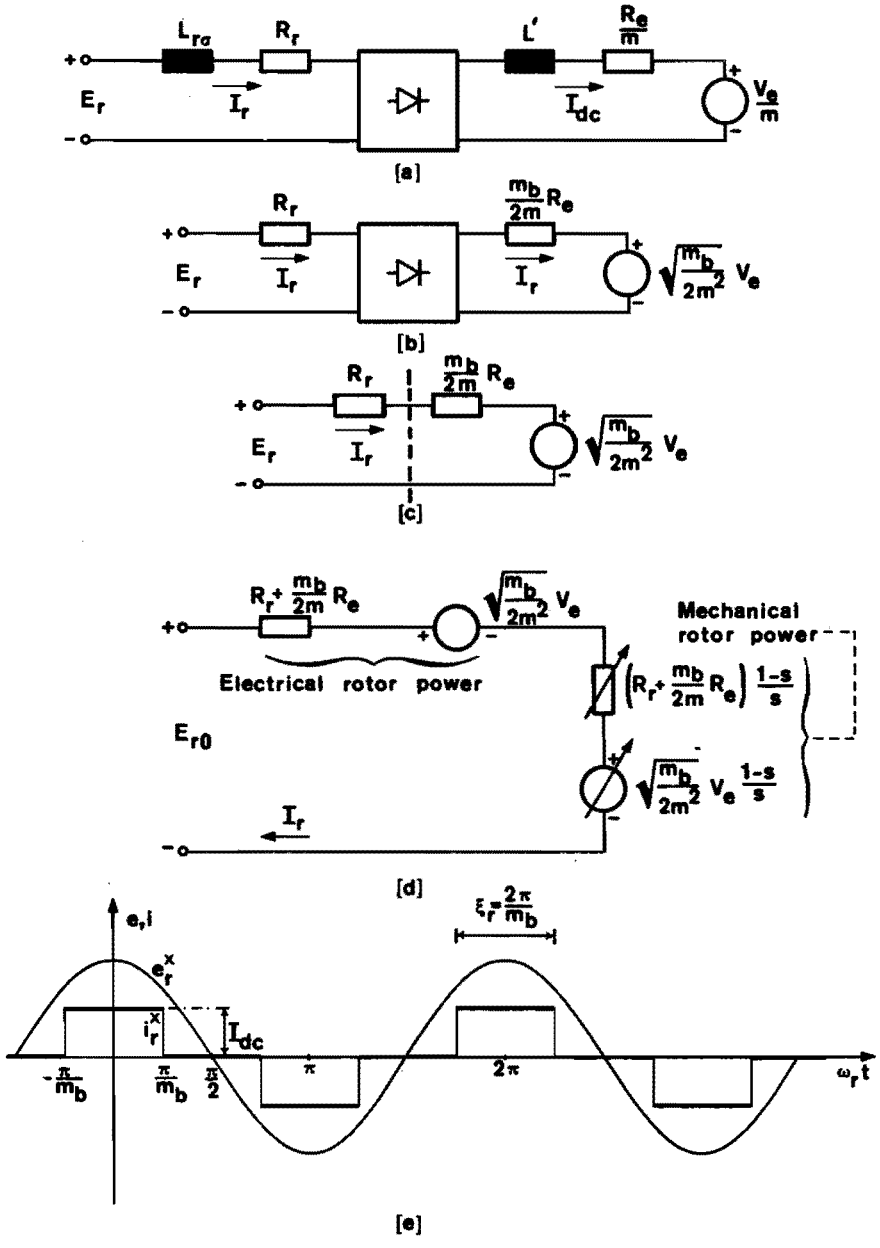

FIG. 4.14 SCHEMATIC DIAGRAMS, EQUIVALENT CIRCUITS AND WAVEFORM DEFINITIONS FOR ROTOR CONTROL SYSTEMS WITH KNOWN ROTOR CURRENT.

or

$$s_{min} = \frac{\pi V_e}{\left[2\sqrt{2}\, E_{r0}\, m_b \sin\left(\frac{\pi}{m_b}\right)\right]} \qquad 4.75$$

For the present case the harmonic rotor current is related to the effective rotor current by:

$$\bar{\bar{I}}_{r\,\overline{2h+1}} = \left[\frac{2\sqrt{m_b}\sin\left(\frac{\overline{2h+1}\,\pi}{m_b}\right)}{\overline{2h+1}\,\pi}\right] \bar{\bar{I}}_r \qquad 4.76a$$

with

$$\bar{\bar{I}}_r = \sqrt{\frac{2}{m_b}}\; I_{dc} \qquad 4.76b$$

It follows from the current waveform that the fundamental waveform is in phase with the induced rotor e.m.f., yet the power factor of the circuit will still depart from unity, since it may be written from rel. 4.74a as:

$$(P.F.)_r = \frac{\bar{\bar{I}}_{r1}}{I_r} = \frac{\sqrt{4m_b}\sin\frac{\pi}{m_b}}{\pi} \qquad 4.77$$

Having examined these general relations for the three types of cascades to be investigated, attention will now be turned to the electronic Leblanc cascade. In order to analyse its behaviour in terms of the above equations it will be necessary to state that

$$\left.\begin{aligned} f_{chop} &>> f_r \\ I_{dc} &\approx |i_{02}| >> \Delta i \end{aligned}\right\} \qquad 4.78$$

It will be pointed out in chapter 5 how these assumptions corresponds with the experimental situation. Additionally it will then become clear that when the conditions of rel. 4.78 are not fulfilled, the system becomes almost useless as an electrical drive.

When the semiconductor elements employed to construct the switches are considered to be ideal (no voltage drop) it may be stated that

$$V_e \equiv 0 \qquad 4.79a$$

$$\therefore \bar{T}_{e(1)} = \frac{m.p}{s\omega_s} \cdot \left\{ I_r^2 \left(R_r + \frac{m_b}{2m} R_e \right) \right\} \qquad 4.79b$$

Alternatively, from rel. 4.72b and rel. 4.74a

$$T_{e(1)} = \frac{m.p}{\omega_s}\, E_{r0} \cdot I_r \cdot \left\{ \frac{\sqrt{4m_b}\sin\left(\frac{\pi}{m_b}\right)}{\pi} \right\} \qquad 4.79c$$

The equivalent resistance of the power-electronic circuit, R_e, varies over the speed range due to the action of the electronic chopper circuit. It has been shown in appendix A4.6.1 that the time of power transport from low voltage to high voltage side and the time of zero power transport both depend on the current ratio k_R and the voltage transformation ratio n_R. During the operation of the electronic chopper circuit in the rotor control system under discussion it has previously been pointed out that there are three parameters to be varied in order to cover that part of the torque-speed plane included by the normal torque-speed curve of the machine in the motoring region. These parameters are the said current ratio k_R and current difference Δi and the slip dependent rectified induced rotor voltage E_1. Writing the transport and short-circuiting times of the chopper in terms of these parameters, it is obtained that:

$$\tau_t = \tau_h \ln \left[\frac{\frac{\Delta i . R_h}{1-k_R} + E_1}{\frac{k_R . \Delta i \, R_h}{1-k_R} + E_1} \right] \qquad 4.80a$$

and

$$\tau_z = \tau_h \left(- \frac{\Delta i \, R_h}{E_1} \right) \qquad 4.80b$$

During the experiments either Δi or k_R will be kept constant over the speed range of the machine, as has already been done in the curves of fig. 4.13. To arrive at a series of curves for experimental purposes, the variable parameter (either Δi or k_R) is assigned a range of values, and the torque-speed curve between standstill and synchronous speed recorded. It will be evident from rel. 4.80a that with decreasing E_1 the time of energy transport will decrease, while rel. 4.80b indicates that the time of zero transport will increase. Since

$$f_{chop} = \frac{1}{\tau_t + \tau_z} \qquad 4.81$$

it may be shown that when the chopper is on the border of its stability region at zero mechanical speed of the machine, the chopping frequency will pass through a maximum before synchronous speed is attained. This will later also be proved experimentally.

The slip dependence of the equivalent electronic resistance R_e due to the above variation in switching periods may be deduced from rel. 4.79b and rel. 4.79c as:

$$R_e = \left\{ s.R_{app}. \frac{4m}{m_b} \sin \left(\frac{\pi}{m_b} \right) - R_r . \frac{2m}{m_b} \right\} \qquad 4.82a$$

with

$$R_{app} = \frac{E_{r0}}{I_r} \quad , \qquad 4.82b$$

the apparent rotor resistance at zero mechanical speed. For a specific torque-speed curve as shown in chapter 5, with both k_R and Δi constant, rel. 4.78 indicates that the rotor current remains constant over the speed range. From rel. 4.79c it follows that the torque should also be constant, while rel. 4.82a indicates that when the apparent rotor resistance at standstill is much larger than the rotor resistance of the machine, the electronic rotor resistance varies directly proportional to the slip.

4.3.4 *CONTROL OF AN INDUCTION MACHINE BY FEEDING BACK PART OF THE SLIP POWER TO THE SUPPLY SYSTEM THROUGH AN ELECTRONIC FREQUENCY CHANGER.*

With reference to fig. 2.9e it may be seen that this type of system has been classified in Group IIA, class 1. In principle the electronic frequency changer consists of two mutator circuits (see fig. 4.15). The first is an uncontrolled mutator used as a rectifier for the rotor induced voltage, and the second is a controlled mutator used as a supply synchronous inverter. The inductor included between these two mutators is important for the efficient functioning of the system. However, as this is well known, it will not be considered further[69] In the following it will be assumed that this inductor is sufficiently large to keep the output current of the rectifier approximately constant.

4.3.4.1 *Investigation of the switching modes, and derivation of the switching commands.*

The switching mode of the rectifier circuit is determined by the induced rotor voltage, resulting in the waveforms indicated in fig. 4.14. This is the reason why the electromechanical converter employed in these types of systems may be included in the definition given of asynchronous electromechanical converters in chapter 1. The effects of the rotor harmonics caused by the switching action, and examined in chapter 2, allows the present system to be investigated under the same assumptions as the electronic Leblanc cascade. The switching of the rotor rectifier will now be of such a nature that:

$$\xi_r = \frac{2\pi}{m_b} \qquad 4.83a$$

For the supply-synchronous inverter:

$$\xi_i = \frac{2\pi}{m_i} \qquad 4.83b$$

where m_i is the "phase-number" of the inverter circuit.
The commutation in the supply synchronous inverter is retarded by an angle α_i with respect to the natural commutation instant. This natural commutation instant is defined with all influences of supply impedances neglected. The commutation action has been covered well in the literature, and will not be analysed further [B10 B11 B15]

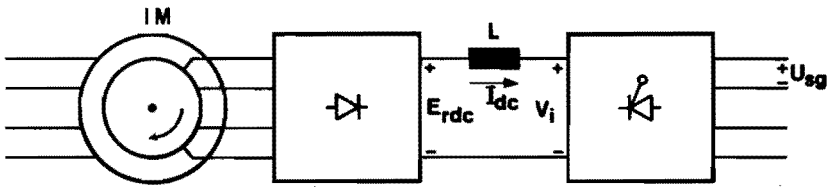

FIG. 4.15 SCHEMATIC DIAGRAM OF ELECTRONIC SCHERBIUS CASCADE.

In the present case it is then found that the mean output voltage presented by the inverter to the d.c. circuit is:

$$V_i = 2\sqrt{2}\, U_{sg} \cdot \frac{m_i}{\pi} \sin\left(\frac{\pi}{m_i}\right) \cos \alpha_i \qquad 4.84$$

In order to achieve this the switching commands initiating the commutation process at angle α_i must be derived so that:

$$\frac{\pi}{2} < \alpha_i < \pi \qquad 4.85$$

with the angle of conduction retardation again referred to the point of natural commutation without control of the mutator elements.

4.3.4.2 *Equations describing the model assumed for the electronic Scherbius cascade.*

The equations developed in paragraph 4.3.3.2 for the general case of an electronic cascade with known rotor current will be modified to cover the present system. Due to the constraints placed on the commutation of the rectifier and the value of the inductance of the smoothing inductor, the rotor current of the machine is still described by rel. 4.76a (see also fig. 4.14). Since the rotor resistance and the electronic circuit resistance may not be neglected for power flow considerations, the electromagnetic torque is given by:

$$\overline{T}_{e(1)} = \frac{mp}{\omega_s} \left\{ I_r \left(\frac{R_r}{s} + \frac{m_b}{2m} \frac{R_e}{s} \right) + \sqrt{\frac{m_b}{2m^2}} \frac{V_{d0}}{s} \cos \alpha_i \right\} I_r \qquad 4.86$$

with

$$V_{d0} = 2\sqrt{2}\, U_{sg} \frac{m_i}{\pi} \sin\left(\frac{\pi}{m_i}\right)$$

It should be noted that in contrast with the electronic Leblanc cascade the value of the equivalent electronic resistance is now constant, and is kept as low as possible in order to achieve maximum recuperation. The power factor of the rotor circuit is still described by equation 4.77. However, since the inverter is decoupled from the rotor by the d.c. intermediary circuit, it will present a different power factor to the supply system. It may be shown that the fundamental harmonic current drawn by the inverter from the supply, experiences a phase shift equal to the triggering delay angle of the inverter [B10.1]. The power factor consequently becomes:

$$(P.F.)_i = \frac{2\sqrt{m_i} \sin\left(\frac{\pi}{m_i}\right)}{\pi} \cos \alpha_i \qquad 4.87$$

It may be seen that the power factor in the present case will be lower than the power factor of the rotor circuit, and when it is considered that the induced rotor voltage must be somewhat in excess of the inverter back e.m.f., it is evident that near synchronous speed the inverter power factor becomes very low. When the rotor resistance of the machine is negligible in comparison with the electronic circuit resistance an expression for either the rotor current or the inverter delay angle may be obtained as:

$$I_r \simeq s. \frac{\sqrt{2}\, E_{rd0}}{\sqrt{m_b}\, R_e} - \frac{\sqrt{2}\, V_{d0}}{\sqrt{m_b}\, R_e} \cos \alpha_i \qquad 4.88$$

or

$$\cos \alpha_i \simeq s. \frac{m_b}{m_i} \frac{E_{r0}}{U_{sg}} \frac{\sin\left(\frac{\pi}{m_b}\right)}{\sin\left(\frac{\pi}{m_i}\right)} - \frac{I_r . \sqrt{m_b}\, R_e}{\sqrt{2}\, V_{d0}} \qquad 4.89$$

with

$$E_{rd0} = 2\sqrt{2}\, E_{r0} \left(\frac{m_b}{\pi}\right) \sin\left(\frac{\pi}{m_b}\right)$$

From relation 4.89 it may be noted that in the ideal case when the rotor resistance and the electronic circuit resistance is negligible, the inverter delay angle should vary directly proportional to the slip. Consideration of relation 4.86 indicates that when the inverter back e.m.f.

is small in relation to the resistive voltage drop in the rotor, the system will approach the operation of a normal induction motor, the behaviour being determined by the magnitude of the resistance. When the inverter back e.m.f. becomes appreciably larger than this resistive voltage drop due to either a decrease of current or a change in α_i, the system will develop an electromagnetic torque that is proportional to the rotor current.

4.3.5 *CONTROL OF AN INDUCTION MACHINE BY FEEDING BACK THE SLIP POWER TO THE SUPPLY SYSTEM BY MEANS OF A CHOPPER-COMPENSATED SUPPLY SYNCHRONOUS INVERTER.*

The system to be investigated in this paragraph may be referred to as an electronic Scherbius cascade with power factor compensation, or reactive power compensation, by means of a low-high chopper circuit. As follows from the previous paragraphs, the power factor deterioration of a "classical" electronic Scherbius cascade is caused by:

(i) generation of higher harmonic currents in the rotor circuit, by the mutator used as rectifier
(ii) generation of higher harmonic currents by the mutator used as supply synchronous inverter to feed back part of the slip power to the supply
(iii) commutation delay angle α_i different from π radians during operation of the supply synchronous inverter due to variation of the slip voltage of the induction machine.

The study of the electronic Leblanc cascade with a low-high chopper has indicated that the circuit can function as an efficient transformer of a low, variable direct voltage, constant current input into high, constant direct voltage, variable current with two level current control applied to the chopper. From the characteristics it may be deduced that the output current is variable, but the output voltage constant for a given Δi and k_R. It will now be clear that under such circumstances the inverter circuit feeding back the slip power to the supply system could operate at a constant commutation delay angle. The chopper circuit may be chosen in such a way that this commutation delay angle may have its optimum value. In the following paragraphs the consequences of including a low-high chopper circuit for "reactive power compensation" of the supply synchronous inverter will be examined. This should eliminate the power factor deterioration of the system due reason (iii). It will be evident that the other causes for power factor deterioration are due to the system configuration, and cannot be improved upon without taking other measures that are not to be discussed here.

4.3.5.1 *Investigation of the switching modes and derivation of the switching commands.*

Attention will in the first instance be focused on the low-high chopper circuit. Refer to fig. 4.11. This circuit will be assumed to work between the two direct voltage sources E_l and E_h, where E_l is associated with the rectified induced rotor e.m.f. and E_h with the supply synchronous inverter back e.m.f. As in the previous cases it

will be assumed that the influence of the commutation in the rectifier bridge on the chopper circuit is negligible. This means that the rotor resistance and leakage reactance may be added to the impedance of the low voltage side of the chopper circuit shown in fig. 4.11.

Fundamentally the chopper circuit remains a pulse system, and as such control of power flow between low voltage and high voltage sources may be effected by more than one method of operation of the switch. As previously only the two level current control will be considered. To characterise the power transport, the mean and effective currents at the low voltage input and the corresponding currents at the high voltage output should be known. It is shown in appendix A4.6.2 how these currents are to be calculated from the differential equations describing the circuit behaviour during the time that switch S (see fig. 4.11a) is either conducting or nonconducting. The expressions for the currents are:

$$\bar{\bar{I}}_{l\ mean} = \frac{i_{02}}{n_E}\left[\frac{(1-q)\ \ln\left(\frac{n_E+q-1}{k_E n_E+q-1}\right) - q\ \ln\left(\frac{k_E n_E+q}{n_E+q}\right)}{\ln\left(\frac{k_E n_E+q}{n_E+q}\right) + \ln\left(\frac{n_E+q-1}{k_E n_E+q-1}\right)}\right] \qquad 4.90a$$

$$\bar{\bar{I}}_{h\ mean} = \frac{i_{02}}{n_E}\left[\frac{(1-q)\ \ln\left(\frac{n_E+q-1}{k_E n_E+q-1}\right) - n_E\ (k_E-1)}{\ln\left(\frac{k_E n_E+q}{n_E+q}\right) + \ln\left(\frac{n_E+q-1}{k_E n_E+q-1}\right)}\right] \qquad 4.90b$$

$$\bar{\bar{I}}_l^2 = \frac{i_{02}^2}{n_E^2}\left[\frac{(q-1)^2\ \ln\left(\frac{n_E+q-1}{k_E n_E+q-1}\right) - n_E(k_E-1) + q^2 \ln\left(\frac{k_E n_E+q}{n_E+q}\right)}{\ln\left(\frac{k_E n_E+q}{n_E+q}\right) + \ln\left(\frac{n_E+q-1}{k_E n_E+q-1}\right)}\right] \qquad 4.90c$$

$$\bar{\bar{I}}_h^2 = \frac{i_{02}^2}{n_E^2}\left[\frac{(q-1)^2\ \ln\left(\frac{n_E+q-1}{k_E n_E+q-1}\right) - n_E(1-q)(k_E-1) + \tfrac{1}{2}n_E^2(1-k_E^2)}{\ln\left(\frac{k_E n_E+q}{n_E+q}\right) + \ln\left(\frac{n_E+q-1}{k_E n_E+q-1}\right)}\right] \qquad 4.90d$$

with the parameters in these equations defined as:

$$\left.\begin{aligned} &\text{voltage transformation ratio} && : q = \frac{E_1}{E_h} \\ &\text{current ratio} && : k_E = \frac{i_{01}}{i_{02}} \\ &\text{normalized resistive voltage drop:} && n_E = \frac{i_{02} \cdot R_1}{E_h} \end{aligned}\right\} \quad 4.90e$$

In obtaining these expressions it has been assumed that the equivalent resistance, of the high-voltage side of the chopper is negligible in comparison with the equivalent resistance of the low voltage side. Where the rotor resistance is added to the electronic circuit resistance at the low voltage side in the present case, the simplification appears to be justified. The parameters defined in relation 4.90c are limited as follows:

$$\left.\begin{aligned} &0 < q \leqslant (1-n_E) \\ &1 < k_E < \infty \\ &-\frac{q}{k_E} < n_E < 0 \end{aligned}\right\} \quad 4.90f$$

At q=0 no chopper operation occurs. When the voltage transformation ratio is increased, the chopper discontinues operation when the current during the power transport period does not reach the level i_{02} any more, as represented by the first condition. Although the current ratio may vary theoretically as indicated large values of k_E will be eliminated in practical systems, due to the enormous increase of the a.c. components superposed on the d.c. current. In the present case it will be attempted to keep the current difference as small as possible (see relation 4.78).

Any of the equations 4.90a to 4.90d may now be used to investigate the stable region of chopper operation. Since it will be attempted to use this chopper circuit as a d.c. transformer of constant current, variable voltage at the low voltage (rotor) input into constant voltage, variable current at the high voltage (inverter) output, it is clear that as far as the behaviour of the electrical machine is concerned, the mean input current will be an important quantity. Therefore the results of some of the calculations presented in fig. 4.16 display the normalized mean input current as a function of the voltage transformation ratio. This choice of independent variable must also be explained. During the operation of the chopper in the rotor circuit the chopper will be expected to work into a constant high voltage. (This voltage is derived from the d.v. of a supply synchronous inverter operating at a constant delay angle. The mean voltage will consequently be constant). The input voltage will vary with the slip of the induction machine and consequently fig. 4.16 displays input current as a function of slip. As in the case of the electronic Leblanc cascade the mean rectifier output current will prove to be proportional to the

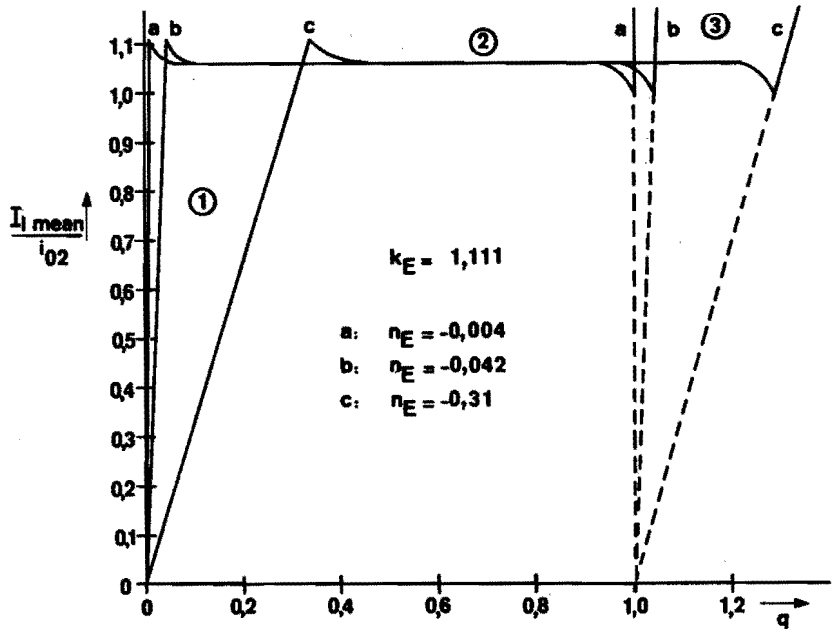

FIG. 4.16 TRANSFER CHARACTERISTICS OF A LOW-HIGH CHOPPER CIRCUIT.

torque, so that the abovementioned curves actually refer to torque-slip curves. (The same as for fig. 4.13)

Brief attention will be devoted to the stability regions defined in figure 4.16. Through the part 1 of each curve the low voltage is so low that the level i_{01} is not reached any more, S conducts continuously and no chopper operation occurs. Therefore no chopper operation occurs for

$$q \leqslant -k_E\, n_E \qquad 4.91a$$

Through part 2 of the curves the chopper circuit is operating. This operation is discontinued when the voltage transformation ratio increases to the point where the current level i_{02} is not reached any more, and S remains continuously in the nonconducting state. With rel. 4.90f and 4.91a the stable operating region for the chopper circuit with variation of the voltage transformation ratio is then

$$-k_E n_E < q < 1-n_E \qquad 4.91b$$

The difference between the maximum and minimum values of voltage transformation ratio still giving operation is

$$q_{max} - q_{min} = 1 + |n_E|\ (1-k_E) \qquad 4.91c$$

It may therefore be concluded that when the current ratio k_E increases, the regio of stable chopper operation will decrease. With an increasing absolute normalized voltage drop n_E the region of stable chopper also decreases. These considerations give the stable region of operation of the low-high chopper circuit, as a function of slip, in the rotor of an induction machine.

The derivation of the switching commands will now be examined. It has been chosen to vary the same quantities that functioned as variables in the chopper with resistance load used in the electronic Leblanc cascade. Therefore it will be necessary to keep either the current difference constant, or the current ratio constant. The input current drawn from the rotor rectifier will then be

$$\bar{\bar{I}}_{1\ mean} = f\left[k_E,\ E_1(s)\right]_{\Delta i\ =\ constant} \qquad 4.92a$$

or

$$\bar{\bar{I}}_{1\ mean} = f\left[\Delta i,\ E_1(s)\right]_{k_E\ =\ constant} \qquad 4.92b$$

Seeing that these considerations lead to the same type of results already examined and presented in paragraph 4.3.3.1, the investigations will not be presented in further detail here. In the experimental work it will be pointed out that exactly the same information-electronic system was employed to operate the low-high chopper between two voltage sources.

4.3.5.2 *Equations describing the model assumed for the electronic Scherbius cascade with reactive power compensation.*

The general equations of paragraph 4.3.3.2 will be valid for the present variant of the electronic Scherbius cascade. In deducing the said equations, it was remarked that when the equivalent electronic circuit voltage V_e is present, the model has a limited range of application. In the present case this does not apply, since the voltage V_e as seen at the input terminals to the chopper circuit is a slip dependent quantity similar to the electronic circuit resistance seen at the input terminals to the chopper circuit in the case of the electronic Leblanc cascade.

The assumptions that the chopping frequency is much higher than the rotor frequency and that the current difference Δi is negligible in comparison with the mean rectifier output current (see relation 4.78) are still valid in the present case. Neglecting the commutation influences in the rectifier circuit results in the rotor current components being written as in rel. 4.77. By using the models of fig. 4.14 it is possible to evaluate the results of the switching of the rectifier on the electromagnetic torque as represented in rel. 4.73. These equations will not be repeated here.

However, the present modification to the electronic Scherbius cascade has been suggested in order to be able to improve the power factor of the system. The rotor current waveform is the same as previously, so that the rotor power factor will still be given by rel. 4.77. The inverter circuit is decoupled by the d.c. intermediary circuit and may have a different power factor. Assuming the inverter back e.m.f. constant and the chopper output voltage constant it is obtained in the

ideal case that:

$$V_i = E_h = V_{d0} \cos \alpha_i \ , \qquad 4.93a$$

where V_{d0} represents the idealized no-load back e.m.f. of the inverter as defined in rel. 4.86. Since this output voltage of the chopper is constant, the power factor of the supply synchronous inverter as presented to the alternating supply system is:

$$(P.F.)_{i\ comp.} = \left(\frac{2\sqrt{m_i} \sin\left(\frac{\pi}{m_i}\right)}{\pi} \right) \cdot \left(\frac{E_h}{V_{d0}} \right) \qquad 4.93b$$

The first factor in the expression presents the effects of the harmonic generation by the inverter and is a given value for the present configuration. The second term may approach unity as a maximum value. However, mostly the supply synchronous inverter is operated at a back e.m.f. below the maximum value to eliminate commutation problems, and consequently the last term will be somewhat less than unity. In contrast to the power factor of the supply-synchronous inverter as given in rel. 4.87 it may be stated that for the compensated inverter:

$$(P.F.)_{i\ comp.} = \text{constant} \geqslant (P.F.)_i \qquad 4.93c$$

over the whole slip range in which the induction machine is operated.

Some remarks regarding the assumptions concerning E_l, E_h, V_i and E_{rdc} are now in order. It has been assumed in all calculations that the rectified rotor e.m.f E_{rdc} is constant and equal to E_l. In the practical systems to be investigated

$$m_b \geqslant 3 \qquad 4.94$$

so that this approximation is reasonable. The maximum variation that may occur in the instantaneous back e.m.f. of the supply synchronous inverter is almost independent of the number of inverter phases, and equal to an appreciable percentage of the difference between maximum positive and negative instantaneous values of the supply phase voltage. The assumption that this voltage is constant as far as calculation of the chopper characteristics is concerned, will be seen to be justified by the inclusion of an energy reservoir between these two power electronic circuits as represented in the experimental section.

CHAPTER 5

EXPERIMENTAL INVESTIGATIONS ON GROUP II AND GROUP IIA MACHINE-ELECTRONIC SYSTEMS.

Synopsis.

In this chapter an account of the experimental investigations conducted on the variable slip category of machine-electronic systems is given. The chapter is divided into two parts. Part I concerns aspects of the synthesis of the systems to be used for experimental investigations and Part II concerns the actual investigations and the results obtained.

Part I supplies a short description of the functioning of each system with the aid of a simplified block diagram. Some typical problems encountered in the course of the work are treated. These problems have been chosen to be representative for the type of problem usually occurring in the course of the development of a machine-electronic system. Attention is devoted successively to the development of some of the power electronic switching circuits, to the problems occurring in transmission of triggering commands and in application of the semiconductor power switches. In all these cases the measures taken to solve the problems are explained.

Part II presents the actual experimental set-up for determining some of the system characteristics, and presents the results of the measurements. The theoretical and experimental results are compared, and the chapter is concluded with an evaluation of the experimental investigations.

PART I

SOME MACHINE-ELECTRONIC SYSTEMS OF GROUP II AND GROUP IIA DEVELOPED FOR EXPERIMENTAL PURPOSES.

5.1 A SHORT REVIEW OF THE SYSTEMS DEVELOPED FOR EXPERIMENTAL INVESTIGATIONS.

In the introductory paragraph to the previous chapter it was mentioned that the investigated systems were specially chosen to cover the whole power spectrum of controlled electrical drives. It will be evident that

when conducting experimental investigations on a laboratory scale the power range is restricted. The main group of systems investigated were developed for a Westinghouse Generalized Machine used as an induction machine. Although this confines the investigations to a low power level, the instrumentation facilities and flexibility of the equipment is an important advantage. This furthermore opens the possibility of a comparative experimental study of different systems using one electromechanical converter. As pointed out in the introduction to this work this is in itself very valuable and as far as known at present such a study has not previously been undertaken. The investigations reported on in this chapter by no means exhaust the possibilities of the experimental complex developed.

It is concievable that the low power and semi-four-phase configuration of the Westinghouse Generalized Machine may lead to some peculiarities in system behaviour. For this reason two systems were developed to be used for the rotor control of a 3kW three-phase induction machine. Experimental results should then indicate to what extent the higher power systems do not duplicate the characteristics of the semi-four-phase systems.

In the systems developed, in correspondence with chapter 4, were the following:

(1) Westinghouse Generalized Machine (WHGM). System for power control by variation of the triggering instant of the antiparallel electronic switches in the semi-four-phase stator circuit (α_s-control and $\Delta\alpha_s$-control)

(2) WHGM. System for power control by variation of the instant of triggering of the antiparallel electronic switches in the semi-four-phase rotor circuit (α_r-control and Δt_{α_r}-control)

(3) WHGM. System for power control by variation of the instant of current extinction in the semi-four-phase rotor circuit with the instant of triggering constant.(Rotor t_β-control)

(4) WHGM. System for power control by variation of the rotor current through a rectifier and resistance-loaded electronic chopper circuit.(Electronic Leblanc cascade)

(5) WHGM. System for power control by feeding back part of the slip power in the rotor of the induction machine to the supply system via an electronic frequency changer.(Electronic Scherbius cascade)

(6) WHGM. System for power control by feeding back part of the rotor slip power to the supply system via an EFC compensated for a low power factor by an electronic chopper circuit. (Compensated electronic Scherbius cascade)

(7) Three-phase 3kW induction machine. System for power control by variation of the conduction angle of the electronic switches in the rotor circuit by delaying the instant of triggering. Executed as an α-control system. The controlled machine is the prime mover in a Ward Leonard Ilgner Set.

(8) Three-phase 3kW induction machine. System for power control through an electronic Leblanc cascade. The controlled induction machine is the prime mover in a Ward Leonard Ilgner set.

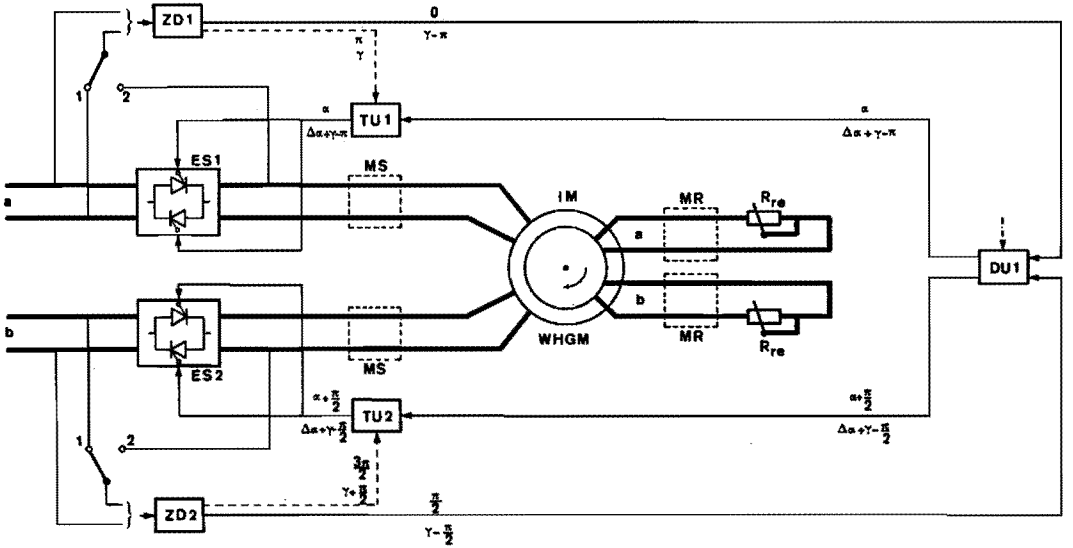

FIG. 5.1 BLOCK DIAGRAM : STATOR α_s AND $\Delta\alpha_s$ CONTROL (WHGM).

In the abovementioned cases more than one variant of each system was usually investigated, as will be evident from the experimental detail. In some cases the systems 1-6 were also tried on three-phase or single phase induction motors, but these experiments will not be covered in the present survey. The larger part of the experimental work concerned the development of systems functioning reliably to such a degree that reproducible measurements were possible. In the course of this work it was necessary to investigate some fundamental characteristics of the information-electronic circuits and the power-electronic circuits and suggest some novel improvements. Investigation of the switching characteristics of semiconductor switching elements brought to light some phenomena not generally appreciated.

5.2 THE MACHINE-ELECTRONIC SYSTEMS DEVELOPED: STRUCTURE AND FUNCTIONING.

In this section a short explanation of the lay-out of each system will be given with reference to a simplified block diagram. The interval structure of each of the function blocks will be discussed as far as it is connected with the characteristics of the system. With the exception of the chopper-controlled systems, the systems contain no closed control loop. The chopper-controlled systems incorporate a two level current control.

5.2.1 *SYSTEMS FOR STATOR CONTROL BY VARIATION OF THE DELAY OF THE INSTANT OF TRIGGERING ON A SEMI-FOUR-PHASE MACHINE.*

As indicated in fig. 5.1 the input voltage to the zero voltage detectors (ZD1, ZD2) may be taken from the supply system (position 1) or from the voltage across the electronic switches (position 2). From the discussion of paragraph 4.2.1 it follows that in the first instance α_s-control will be the result, while in the second instance $\Delta\alpha_s$-control is obtained. ZD1 and ZD2 deliver output pulses at $g\pi$, or $\gamma+g\pi$ and $\frac{1}{2}\pi(2g+1)$, or $\gamma+\frac{1}{2}(2g+1)$. These output pulses are fed to a two-phase delay unit DU1 that delivers the output pulses accurately at $(\alpha+g\pi)$ or $\Delta\alpha+(\gamma+g\pi)$ and $\alpha+\frac{1}{2}\pi(2g+1)$ or $\Delta\alpha+\gamma+\frac{1}{2}\pi(2g+1)$ to the respective output triggering units TU1 and TU2. As the discussion of paragraph 4.2.1 has indicated, it is at present not important for the α_s-control whether the supply voltage zero condition is used to start the integration of a constant voltage. For the $\Delta\alpha_s$-control the only practical possibility in the present set-up is to detect the zero voltage condition of the voltage across the switches and then start the integration of a constant voltage. To achieve this the delay unit DU1 consists in principle of two parallel, identical channels, comprising a pulse shaping circuit, an integrating circuit and a comparator.

The output units deliver the triggering signals at a suitable power level and voltage isolation level to the electronic switches. In principle these units need only deliver a pulse-type signal for a duration of the order of the switching time of the semiconductor switches. A blocking-oscillator with monopulse output will therefore be suitable. However, it will subsequently become clear that the type of signal the triggering unit delivers is very important to eliminate stable asymetrical switching modes. These considerations lead to the use of output

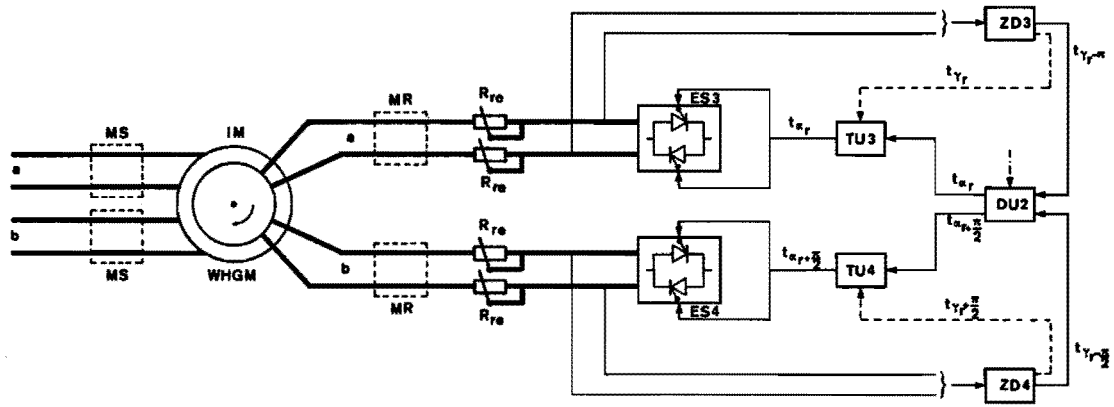

FIG. 5.2 BLOCK DIAGRAM : ROTOR Δt_α CONTROL (WHGM).

units delivering a pulse train of duration $(\pi-\alpha)$ radians. Switch-off signals are derived from ZD1, ZD2.

The number of output channels of TU1, TU2 as determined by the type of switching element used in the power-electronic switches ES1 and ES2. With thyristor units two output channels per output unit is required. Use of triacs simplifies the requirements, due to the fact that the triac has bilateral conductivity, but singular triggering polarity. The switches are naturally commutated as a matter of course. Filter networks in parallel to the electronic switches are used to protect them for certain types of transients. When employing alternative 2 ($\Delta\alpha_s$-control) the distortion of the assumed waveform of the voltage across the semiconductor switch (see fig. 4.1(b)) must be taken into account in the design.

It is worth noting that the triggering requirements for α_s-control are more stringent than for $\Delta\alpha_s$-control due to the absence of the possibility of stable half-waving in the latter case. Monopulse triggering is possible. For both systems integration in a closed loop is possible by using the electrical input to DU1.

5.2.2 *SYSTEMS FOR ROTOR CONTROL BY VARIATION OF THE DELAY OF THE INSTANT OF TRIGGERING ON A SEMI-FOUR-PHASE MACHINE.*

5.2.2.1 *A system for Δt_{α_r}-control.*

The simplified block diagram of the system as realized experimentally is shown in fig. 5.2. This type of system may be termed Δt_{α_r}-control as discussed in paragraph 4.3.1. As indicated in the said diagram the two zero detectors ZD3 and ZD4 read out the zero voltage conditions of the voltage across the electronic switches at instants

$$t_{\gamma_r-\pi} + \tfrac{1}{2}gT \quad \text{and} \quad t_{\gamma_r-\frac{\pi}{2}} + \tfrac{1}{2}gT$$

respectively. The output pulses of the zero detectors are fed to the two phase delay unit DU2. In principle this unit again consists of two separate, identical channels each having a pulseforming part, an integrating stage and a comparator stage. However, the design have to be such that it can work accurately over a wide frequency range of perhaps 1000:1 due to the variation of the rotor frequency. The output signals at times

$$t_{\alpha_r} + \tfrac{1}{2}gT \quad \text{and} \quad t_{\alpha_r+\frac{\pi}{2}} + \tfrac{1}{2}gT$$

excite the trigger units TU3 and TU4. It is again worthwhile to give some attention to the necessary output signal of the units. In steady state it is impossible for halfwaving instabilities to arise due to a variation of the triggering angle, and a single triggering pulse will be sufficient. However, conditions during dynamic operation and starting-up have indicated that it is desirable to have a pulse train as output.

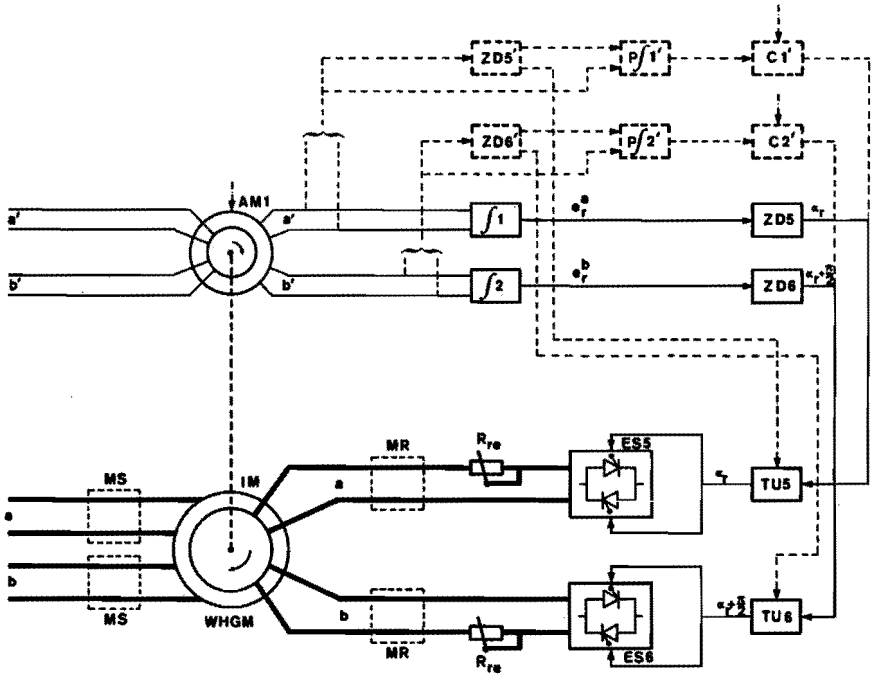

FIG. 5.3 BLOCK DIAGRAM : ROTOR α-CONTROL (WHGM).

Furthermore operation of this system at low slips has indicated that due to the low rotor voltage and large amplitudes of tooth ripples, operation with a pulse train is necessary. In order to supply the electronic switches with a suitable signal when the variable rotor frequency is taken into account, TU3 and TU4 must receive additional signals at

$$t_{\gamma_r} + \tfrac{1}{2}gT \quad \text{and} \quad t_{\gamma_r + \frac{\pi}{2}} + \tfrac{1}{2}gT$$

as shown in fig. 5.2.

From the same figure it is further evident that the power electronic switches ES3 and ES4 are included in each of the rotor phases of the Westinghouse Generalized Machine WHGM used as an induction machine. An antiparallel configuration has been used, and not the alternative of a four-diodebridge with a thyristor switching its output. Input to DU2 is either manual or electrical.

5.2.2.2. *A system for α_r-control.*

As pointed out in chapter 4 it is necessary to have a simulated induced rotor e.m.f. available to obtain a system shown in fig. 5.3 this induced e.m.f. is obtained from a small two-pole auxiliary machine AM mounted on the same shaft as the main machine. It is necessary to know the zero voltage condition of the induced rotor voltage accurately over the whole speed range to be able to maintain the angle of triggering delay constant. Subsequently it will become clear that the tooth harmonics of practical machines introduce a large uncertainty in the detection of the zero voltage position of the induced rotor voltage e.m.f. In order to eliminate this as far as possible the phase voltage of AM is integrated in the integrating units $\int 1$ and $\int 2$. The phase shift α_r between the zero voltage condition of the actual machine rotor e.m.f. and the switching instant may be introduced for experimental purposes by a mechanical phase shift of $\frac{\alpha_r}{p}$ of AM.

The zero detectors ZD5 and ZD6 consequently read out their output information at

$$(\alpha_r + g\pi) \quad \text{and} \quad \alpha_r + (\tfrac{2g+1}{2})\pi$$

Since relation 4.55a indicates that halfwaving may occur in the α_r-control system it is desirable to have a pulse train output from TU5 and TU6.

In the above described lay-out the constant phase shift has been obtained mechanically. This is satisfactory for steady state experimental work. When it is desired to have an electrical input in order to incorporate the system into a variable speed drive, for instance, then the alternative system shown by broken lines has been developed. No mechanical phase shift between AM and the main drive motor exists. The phase voltage of the auxiliary machine is again integrated by periodic integrating units $P\int 1'$ and $P\int 2'$. The integrators are reset by the output information of ZD5' and ZD6' at

$$g\pi \quad \text{and} \quad (\tfrac{2g+1}{2})\pi$$

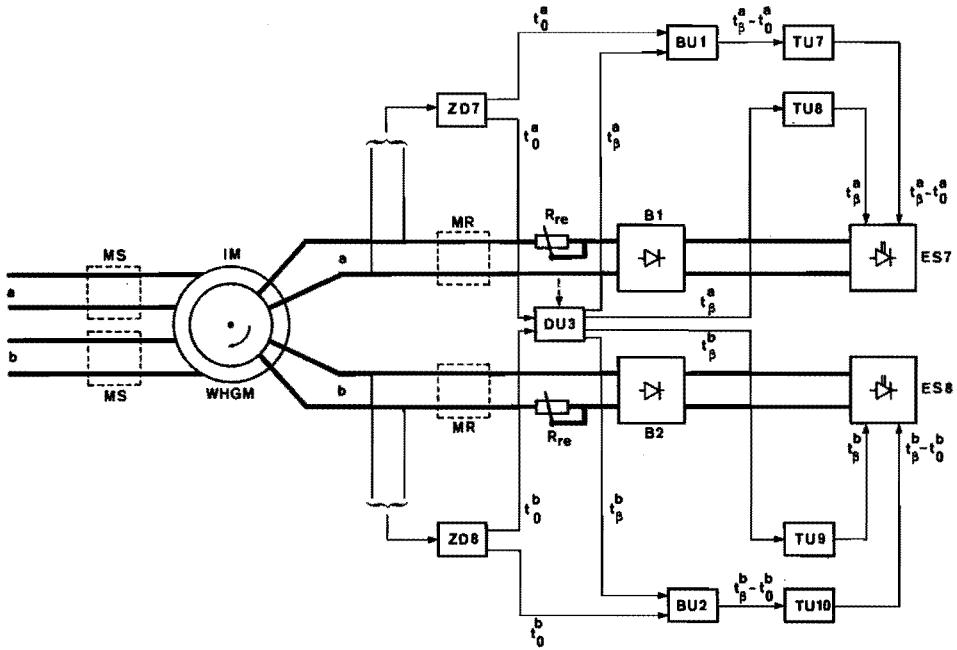

FIG. 5.4 BLOCK DIAGRAM : ROTOR t_β CONTROL (WHGM).

The comparators C1' and C2' then read out the triggering delay angle at their preset read-out level. Since the slip dependence of the amplitude of the induced rotor e.m.f. is eliminated by the integration process, the delay angle will be maintained constant in the entire speed range of the main machine. The same considerations as previously stated apply to the output of the triggering units TU5 and TU6 for this system. If it is desired to have repeated triggering signals of duration $(\pi-\alpha_r)$, TU5 and TU6 should be informed from ZD5' and ZD6' as shown by the broken lines, Switching commands of duration ξ_r may only be obtained by reading out the zero voltage across the switches by additional detectors arranged as in the Δt_{α_r} system of fig. 5.2.

The power electronic switches ES5 and ES6 are identical to the switches in fig. 5.2.

5.2.3 *SYSTEMS FOR ROTOR CONTROL BY VARIATION OF THE DELAY OF THE INSTANT OF CURRENT EXTINCTION IN A SEMI-FOUR-PHASE MACHINE.*

5.2.3.1 *A system for t_{β_r}-control.*

Fig. 5.4 represents a simplified block diagram of the system developed to measure the characteristics of this type of system. The zero voltage condition of the induced rotor e.m.f. can only be read out, when the maximum value of the current flow angle is such that the phase current will be zero at the instant the induced e.m.f. becomes zero (See rel. 4.59b). The system is laid out so that

$$t_0 + \Delta t < t_\beta < t_\pi - \Delta t$$

and

$$\alpha = t_0 + \Delta t$$

where $\Delta t \simeq 100$ μsec. This has the pleasant consequence that it is explicitly known that the electronic switch is nonconducting at the zero voltage condition of the induced rotor e.m.f.

It may therefore be stated that ZD7 and ZD8 read out at

$$(t_0^a + \tfrac{1}{2}gT) \quad \text{and} \quad (t_0^b + \tfrac{1}{2}gT)$$

The output is used to excite bistable units BU1 and BU2, and to start the delay process in the delay unit DU3. This unit is of a two-phase or dual channel lay-out of the same type as DU2 used in system 3. The output of DU3 resets the bistable units. Output information from BU1 and BU2 controls the output of the triggering units TU7 and TU10. Whereas monopulse operation is obtained from the first two output circuits it should be noted that the last two deliver an output of duration β_r/ω_r

In order to avoid using two antiparallel force commutated switches for each phase two bridge rectifiers B1 and B2 are included. The possibility to use a single-four-phase bridge rectifier also exist. However, as this restricts the maximum current flow angle per rotor phase the configuration of fig. 5.4 was chosen for investigation. The force commutated electronic switching circuits ES7 and ES8 are employed to short circuit the two phases at Δt after the zero voltage condition. The choppers commutate the rotor phase currents to zero at a variable instant.

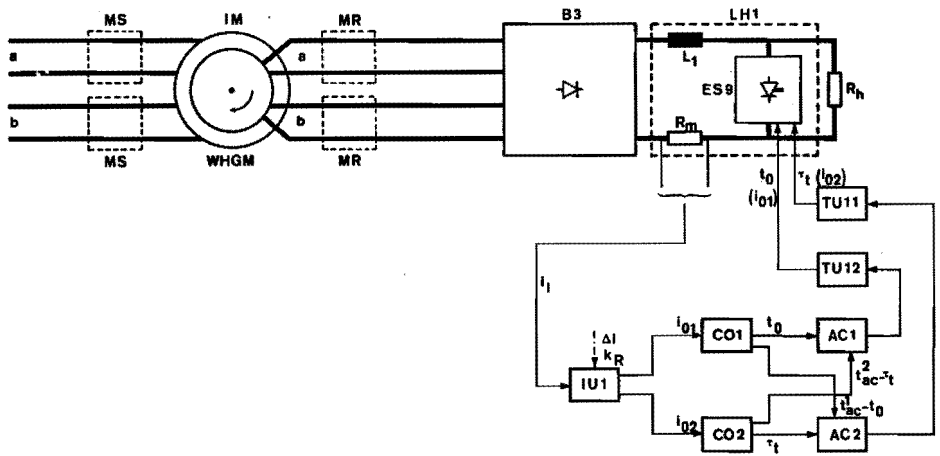

FIG. 5.5 BLOCK DIAGRAM : ELECTRONIC LEBLANC CASCADE (WHGM).

The electronic switches ES7 and ES8 consist of a main circuit for conduction and an auxiliary circuit for commutation. The main circuits should receive triggering commands of extended duration due to holding current requirements of the thyristors used, and are consequently excited by the output units TU7 and TU10. In the auxiliary circuit the triggering commands are used to excite a thyristor included in an oscillatory circuit with a charged capacitor where monopulse triggering is sufficient. Output units TU8 and TU9 are used for this function.
The development and functioning of the chopper circuits will be investigated subsequently. At present it is sufficient to remark that the chopper circuit should be capable of absorbing the energy contained in the leakage inductances of the rotor circuits. This energy transport process will necessarily take time, and therefore instantaneous commutation of the current to zero will not occur. It will later become clear that for a given machine the voltage rating of the semiconductor elements in B1, B2 and ES7, ES8 chiefly determine the duration of the process of commutating the rotor current to zero. In order to fulfill all the requirements a chopper circuit with forced series commutation was developed.

As in previous cases the input to DU3 may be manual or electrical, and it is again important that this unit maintains the similarity between the two channels over the entire frequency range of the rotor.

5.2.4 *SYSTEM 7. A SYSTEM FOR ROTOR CONTROL OF A SEMI-FOUR-PHASE INDUCTION MACHINE BY MEANS OF A RESISTIVELY LOADED ELECTRONIC CHOPPER CIRCUIT. (ELECTRONIC LEBLANC CASCADE).*

Fig. 5.5 represents the abovementioned system. The current i_1 is measured across the shunt R_m as shown.

The input unit IU1 maintains either the current difference Δi or the current ratio k_R constant (see also paragraph 4.3.3.1) and translates the true current into two signals i_{01} and i_{02} operating different comparators. As soon as the current exceeds i_{01}, CO1 is activated and as soon as it is lower than i_{02}, CO2 is activated. It is possible to achieve the same result with a single comparator with variable hysteresis, as will be shown later. The described configuration was chosen for flexibility reasons.

The chopper current measured at R_m contains various high frequency switching transients due to the action of the power semiconductors in the force-commutated chopper. In order to suppress the effects of these transients on the chopper behaviour the anticoincidence circuits AC1 and AC2 are necessary to eliminate the possibility of conduction and extinction commands being coincident. At time t_0 AC2 is inhibited for a time t_{ac}, while the same occurs with AC1 at time τ_t. This eliminates any output from TU11 during time

$$t_0 \quad \text{to} \quad (t_0 + t_{ac})$$

and from TU12 during time

$$\tau_t \quad \text{to} \quad (\tau_t + t_{ac})$$

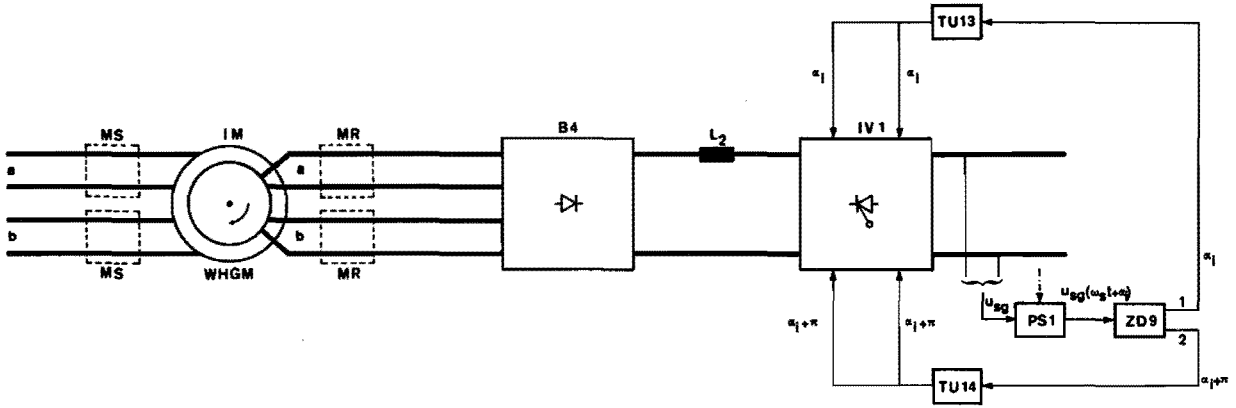

FIG. 5.6 BLOCK DIAGRAM : ELECTRONIC SCHERBIUS CASCADE (WHGM).

Power circuit configuration and initial conditions are such that it is sufficient to employ monopulse triggering for both the conduction and extinction commands.

From fig. 5.5 it is evident that the bridge rectifier used is a full four phase arrangement. The chopper circuit may be seen to be decoupled from the bridge circuit by the smoothing inductor L_1, while with reference to the calculations concerning this type of chopper performed in chapter 4 it follows that $R_h = 12\Omega$. Consequently no low-impedance discharge path in parallel to the main switching element of the chopper exists, enabling one to choose a parallel-commutated circuit configuration for ES9. This circuit will be discussed later.

The induction machine (WHGM) used in these types of systems should preferably have as low a rotor resistance as possible, since it is the objective to transport all the slip power to R_h via the low-high chopper circuit. All the experimental results were consequently recorded with the external rotor resistors R_{re} equal to zero.

5.2.5 *SYSTEM 8. A SYSTEM FOR ELECTRONIC RECUPERATION OF THE SLIP POWER THROUGH A SUPPLY-SYNCHRONOUS INVERTER (ELECTRONIC SCHERBIUS CASCADE) ON A SEMI-FOUR-PHASE INDUCTION MACHINE.*

In the systematic classification it was pointed out that the hybrid group IIA systems employs an electronic frequency changer in the rotor circuit to convert the variable frequency rotor voltage to the supply frequency in order to be able to transport mean power different from zero from the rotor to the supply system. A simplified block diagram of such a system is shown in fig. 5.6.

The supply voltage is transformed down and shifted in phase by an electronic phase shifting circuit PS1. The output voltage of PS1 feeds the zero voltage detector ZD9. Positive going (output 1) and negative going (output 2) zero crossings are separated, and at instants

$$(\alpha_i + 2g\pi)$$

and

$$(\alpha_i + \overline{2g+1}\pi)$$

the triggering units TU13 and TU14 respectively are excited. These triggering units have two output channels each, delivering an output to diametrically opposed thyristors in the inverter IV1. Although the stability of a supply-synchronous inverter necessitates a triggering signal of extended duration in some regions of operation, units TU13 and TU14 have been lain out for monopulse triggering. The inverter circuit will not be operated in the said regions of possible instability.

The rectifier bridge B4 has been constructed to allow the use of one full four phase bridge, or two two phase bridges (as in system 6, fig. 5.4). The supply synchronous inverter IV1 may be used to feed back the slip power as one full four phase inverter, two two phase inverters, or as one two phase inverter feeding back all the slip power of B4. These combinations have been designed into the system in order to be able to investigate the influence of the different current flow angles in rotor and supply circuits resulting from the different

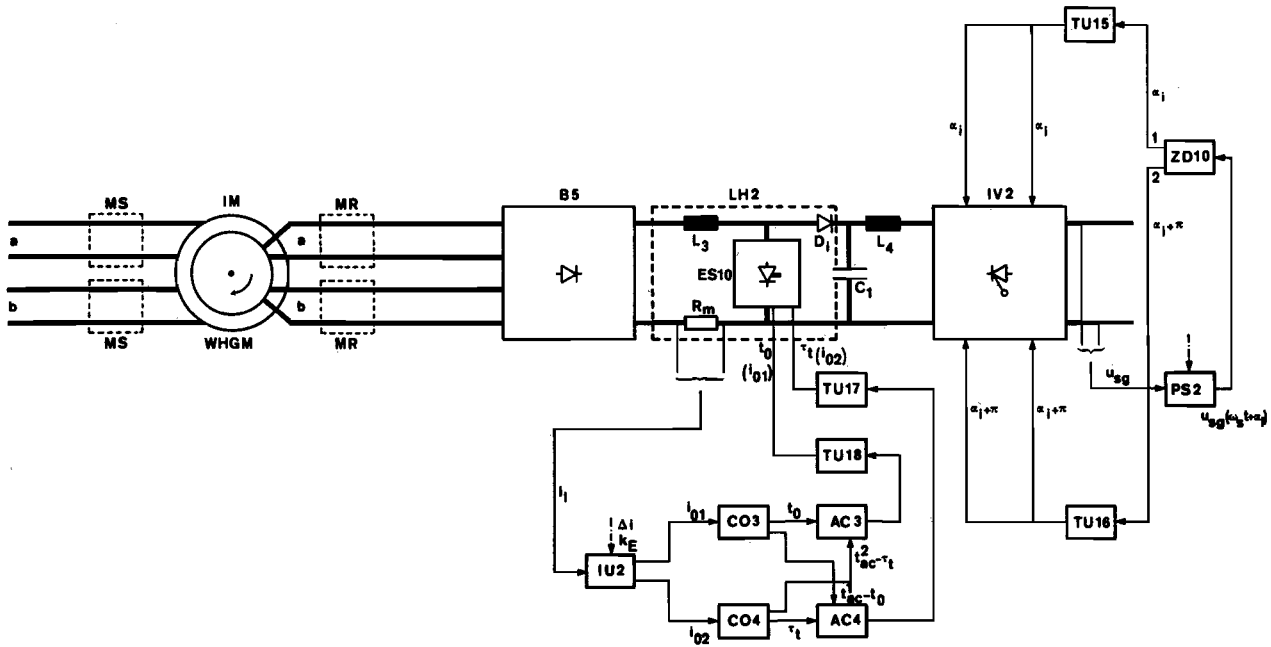

FIG. 5.7 BLOCK DIAGRAM : COMPENSATED ELECTRONIC SCHERBIUS CASCADE (WHGM).

combinations.

From fig. 5.6 and the above description it is clear that the combination of B4 and IV1 constitutes the electronic frequency changer referred to. As pointed out in chapter 4 the presence of a smoothing inductor L_2 of sufficient value is important, since this maintains the direct current in the intermediary circuit constant. If this is not the case the inverter current will flow in short pulses, and the power factor will decrease. In order to obtain as much recuperation as possible the rotor and electronic circuit resistances are kept to a minimum ($R_{re} = 0$).

5.2.6 *SYSTEM 9. A SYSTEM FOR ELECTRONIC RECUPERATION OF THE SLIP POWER OF A SEMI-FOUR-PHASE MACHINE WITH POWER FACTOR COMPENSATION BY A LOW-HIGH ELECTRONIC CHOPPER CIRCUIT.*

The system shown in the simplified block diagram of fig. 5.7 may also be termed a power-factor compensated electronic Scherbius cascade. What has been explained in chapter 4 will be briefly recapitulated: Due to the variable slip voltage of an induction machine, the angle of natural commutation retardation α_i must be decreased as the synchronous speed of the asynchronous machine is approached. This reduces the power factor. If the inverter could work into a constant voltage of correct magnitude at the d.v. side, this objection would be eliminated. By introducing the low-high electronic chopper circuit LH2 between the rectifier bridge B5 and supply synchronous inverter IV2 this is accomplished. The chopper circuit is equipped with current control maintaining an approximately constant input current with time. Power flow considerations then dictate that the output current becomes variable in this case.

The current is measured and the chopper circuit actuated by an information-electronic subsystem exactly similar to that of system 7, fig. 5.5. Comparison of the information-electronic subsystem necessary for operation of the inverter circuit IV2 in fig. 5.7 with that of fig. 5.6 (system 8) also suffices to establish the similarity . No further attention will be devoted to this part of the system at present.

In the compensated electronic Scherbius cascade shown in fig. 5.7 the bridge rectifier circuit B5 is a full four-phase bridge, while the inverter circuit IV2 has been chosen as a two-phase bridge for simplicity. With the equipment developed it is possible to arrange IV2 as two separate two-phase bridges or as one full four-phase bridge.

The output current of LH2 will be a pulsating current with frequency of pulsation equal to the chopping frequency. This would have the flow of pulsating supply currents of a high frequency as a result. This is in general undesirable . Furthermore this would necessitate synchronising of the triggering outputs of TU15 and TU16 to the sequence of TU17 and TU18, or delivering an extended output by TU15 and TU16 of duration equal to half a period of the supply frequency. A solution eliminating both these objections is the introduction of an additional energy reservoir circuit C_1L_4. The supply current will now be continuous, and the output voltage of the low-high chopper LH2 constant, while the information electronic subsystems for LH2 and IV2 remain unaltered.

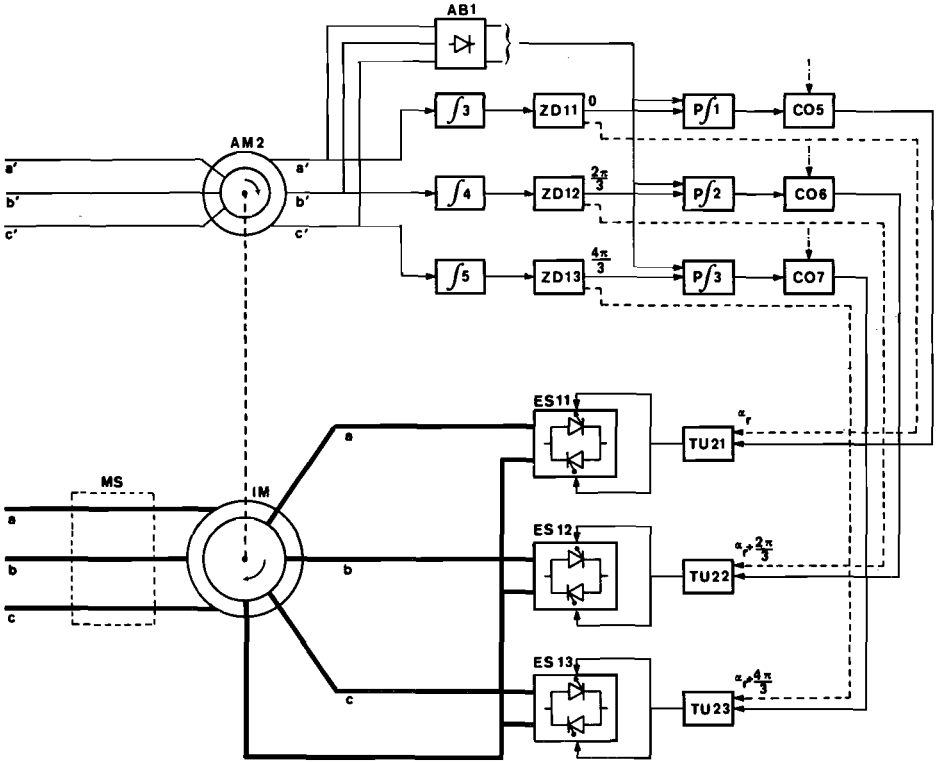

FIG. 5.8 BLOCK DIAGRAM : ROTOR α-CONTROL FOR WARD LEONARD ILGNER SYSTEM (THREE-PHASE MACHINE).

5.2.7 *SYSTEM 10. A SYSTEM FOR ROTOR CONTROL OF A THREE PHASE MACHINE BY VARIATION OF THE INSTANT OF TRIGGERING.*

The feasibility of developing some of the investigated systems for a three-phase machine of higher power than the semi-four-phase machine used as the electromechanical converter in the previously described systems has already been discussed. Although several modifications of the information-electronic system has been investigated and developed, only the constant α_r-control will be described, as represented in the block diagram of fig. 5.8.

It has been pointed out previously that due to tooth harmonics zero voltage detection in asynchronous machines is a hazardous problem at low values of slip. In system 10 use has again been made of an auxiliary machine AM2 to simulate the induced e.m.f. of the main machine. In paragraph 5.2.2.2 two alternatives were described for realizing a rotor control system with constant α_r-control. The present system differs from these systems and is more complex due to the following reasons: It will subsequently become clear that the induction machine to be controlled is intended to be the prime mover in a Ward Leonard Ilgner set that has been scaled down from an actual existing unit. It was therefore attempted to develop an electronic system that would answer to the accuracy and reliability requirements one is liable to encounter at the power level where the system is to be applied.

The induced rotor voltage of the auxiliary machine AM2 is integrated in the units $\int 3$, $\int 4$ and $\int 5$. At instants

$$(0 + g\pi) \; ; \; \frac{1}{3}(2 + 3g)\pi \; ; \; \frac{1}{3}(4 + 3g)\pi$$

the zero detectors ZD11, ZD12, ZD13 read out, resetting the periodic integrating units P$\int$1, P$\int$2, P$\int$3 and the triggering units TU21, TU22, TU23. The periodic integrators start integrating a slip-dependent direct voltage. This voltage is obtained by rectifying the induced rotor voltage of the machine AM2 in bridge AB1 and is directly proportional to slip.

At instants

$$(\alpha_r + g\pi) \; ; \; \alpha_r + \frac{\pi}{3}(2 + 3g) \; ; \; \alpha_r + \frac{\pi}{3}(4 + 3g)$$

the comparators CO5, CO6 and CO7 read out and start the output units TU21, TU22 and TU23. Due to the possibility for generating half-wave instability the triggering units employ an extended triggering signal of duration

$$(\pi - \alpha_r)$$

This signal is delivered to the thyristors in the antiparallel power switches every half period, as indicated, irrespective of which thyristor of a pair is to commence conduction.

The power switches ES7, ES8 and ES9 have been inserted to short-circuit the phases to the neutral. This has been done in order to be able to observe the influence of all the uneven harmonic components in the experimental determination of the torque-speed curve. The primary of the three phase machine is connected in star.

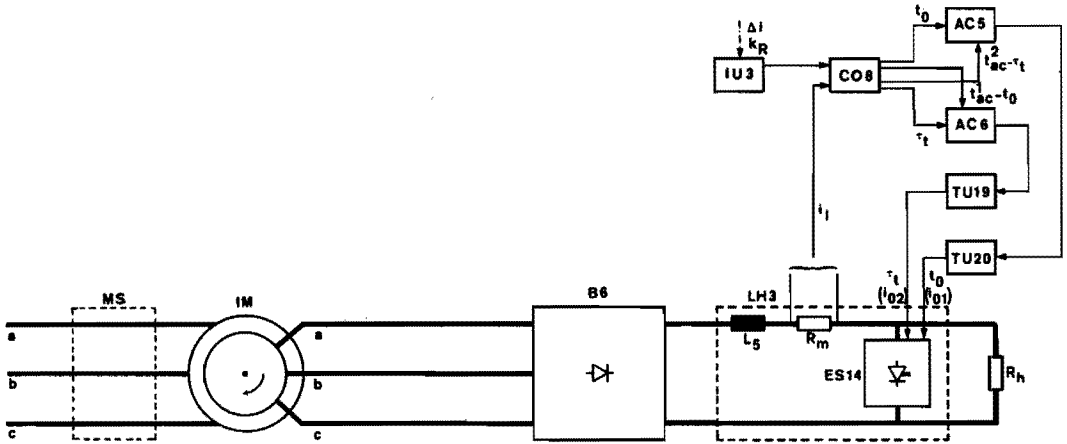

FIG. 5.9 BLOCK DIAGRAM : ELECTRONIC LEBLANC CASCADE FOR WARD LEONARD ILGNER SYSTEM (THREE-PHASE MACHINE).

5.2.8 *SYSTEM 11. A SYSTEM FOR ROTOR CONTROL OF A THREE-PHASE INDUCTION MACHINE BY MEANS OF A RESISTIVELY LOADED ELECTRONIC CHOPPER CIRCUIT.*

The electronic Leblanc cascade depicted in the simplified block diagram of fig. 5.9 has been developed for the same three phase machine that was used in system 10. The system has been lain out with two level current control of the low-high resistance loaded electronic chopper LH3. The information-electronic system differs from the previously discussed configuration for systems 7 and 9.

The input current to the low-high chopper LH3 is measured at R_m. Depending on whether it is chosen to operate with constant current difference Δi or with a constant current ratio k_R, the input unit IU3 translates the command into a signal compared with the current i_1 in the comparator CO8. When the current reaches the maximum value i_{02} at t_0 the anticoincidence circuit AC5 is activated and AC6 inhibited for the time:

$$t_0 \quad \text{to} \quad (t_0 + t_{ac})$$

The output unit TU20 is activated at t_0 and delivers a monopulse triggering signal to the force commutated electronic switch ES14. This signal initiates commutation, the chopper CH5 discontinues conduction and the current i_1 decreases (see also paragraph 4.3.3.). When the current reaches the lower value i_{02} at τ_t the comparator reads out again, AC6 and TU19 are activated and AC5 inhibited for the time

$$\tau_t \quad \text{to} \quad (\tau_t + t_{ac})$$

Unit TU19 delivers a monopulse triggering signal to the main conduction-circuit of switch ES14, resistance R_h is shorted and the current increases again; by using the anticoincidence circuits it is again prevented that the switching transients generated by the switching power semiconductor elements in ES14 cause switching disorders of the system.

The rectifier B6 is a full three-phase bridge, while the force commutated electronic power switch ES14 has been developed with a parallel commutation circuit configuration for the same reasons stated in the discussion of system 7. The two circuits ES14 and ES9 are of the same configuration and differ only in the power level involved.

5.3 A CONSIDERATION OF SOME TYPICAL GENERAL PROBLEMS ENCOUNTERED DURING DESIGN, DEVELOPMENT AND CONSTRUCTION OF MACHINE-ELECTRONIC SYSTEMS.

In the previous paragraph a brief indication of the systems developed for experimental purposes has been given. This work does not pretend to be a general treatise on the analysis and synthesis of electrical drives but concentrates on some aspects of the electronic control of the electromechanical energy conversion process. It is therefore understandable that the systems have been explained only up to the point where the experimental results concerning the electromechanical energy conversion process can be appreciated.

Similar considerations may be advanced regarding the design, development and construction of the systems. It is neither feasible nor appropriate to present all these problems in this volume, the more so since they concern a few examples of one group of machine-electronic systems. However, during the synthesis of these systems some problems were investigated that proved to be of a general nature in the whole field of machine-electronics and power electronics. As such the investigations into these problems and the results obtained (or solutions suggested) may then be regarded as general to a certain extent and will receive brief attention. The problems that will be considered in the course of the subsequent paragraphs are:

(i) Forced commutation and its application to electronic chopper circuits.
(ii) Transmission of triggering commands to power-electronic switches.
(iii) Application of semiconductor power switching elements in power electronic switching circuits.

5.3.1 *FORCED COMMUTATION AND ITS APPLICATION TO ELECTRONIC CHOPPER CIRCUITS.*

The function of forced commutation has been defined and given some attention at the end of chapter 2. It is now desired to examine the consequences and the application to the commutation of the rotor current of an induction machine. This commutation action may actually be divided into two types, as far as the application to the rotor circuit of an induction machine is concerned. In the electronic switch used in the extinction angle control (fig. 5.4, ES7 and ES8) the rotor current is reduced to zero during switching. When the electronic switch is employed in a low-high chopper circuit, the current continues to flow, and is merely transferred to another circuit branch. This difference means that in the first instance all energy contained in the leakage inductances of the windings feeding the electronic switch must be stored in the electronic switch. In the second instance the problem is not severe when the alternative current path does not contain any large inductances.

Storage of leakage energy is only one problem affecting the operation and structure of chopper circuits. Another problem is the strong dependence of the available commutation time on the current that is to be switched. These two aspects will both be examined in the following discussion.

5.3.1.1 *Power switches employed to switch-off the rotor current: consideration of some possibilities.*

Power switches employed to switch-off current in machine-electronic systems frequently suffer from the problem of storing the magnetic energy contained in the leakage inductances of the system. Since the current is zero during the off-period, it is logical to store the energy capacitively, and to attempt to employ the stored energy to good effect during the following conductive cycle. In the power switch employed to switch the rotor current of an induction machine off, the energy stored in the leakage inductance is transferred to the power

switch. Sometimes it is not possible to transfer this energy to the mechanical load, and the only possible way to employ it is for commutation purposes.

The power switch at present under discussion is employed to short circuit the rotor windings of one phase during part of a period. One of the methods that presents itself to commutate the current in such a situation is to connect a correctly charged capacitor in the circuit, as indicated in fig. 5.10a where it has been assumed that the electrical machine may be represented by an equivalent induced rotor e.m.f e_r and equivalent inductance L_{re} and resistance R_{re}. In order to short circuit the rotor completely it is important that two antiparallel thyristors T_{m1} and T_{m2} be employed as main elements. For the time being the method of obtaining correctly charged capacitors will be discussed.

On triggering the commutation thyristors T_c, the current I_o at the instant of commutation will transfer from T_{m1}, T_{m2} to T_c; an oscillation with frequency ω_c will start, and when the current becomes zero, T_c will discontinue conduction. The commutation cycle will repeat twice per rotor cycle. In the period from t_o to t_c the magnetic leakage energy is transferred to the power switch, the polarity of the voltage on the commutation capacitor having changed polarity. If some or other means is incorporated in the power switch for changing the polarity of this charge it may again be employed during the following commutation period. Some of this stored energy will then be transferred to the load, as the capacitor will discharge through the machine windings. The voltage on the capacitor will stabilize at the value where the energy dissipated in resistive elements and transferred to the mechanical load during the commutation cycle is equal to the energy added from the leakage inductance of the machine in the course of each complete cycle.

The commutation period will vary in length, depending on the current I_o at which the process is started. In order to keep the influence of the commutation process on the rotor current waveform small, the commutation period is chosen much smaller than a half rotor period if possible. At present it is not the intention to discuss this commutation process in all its details. It should be noted however, that the voltage on the capacitor at time t_c is strongly dependent on the magnitude of the current that has been switched off. This means that the commutation-process becomes load-dependent, with a reaction time of one half cycle of the rotor voltage. Especially in the commutation of large currents this is an important advantage.

When considering this circuit for practical application, it is evident that two drawbacks present themselves.

(a) The circuit needs two antiparallel switches per phase.
(b) Application to three-phase machines in practice necessitates the presence of a neutral conductor to switch the phase current.

Both of these drawbacks may be eliminated by first rectifying the rotor voltage before switching. This changes the maximum allowable current flow angle per phase, and consequently the maximum attainable torque. However, during the present investigations this has been kept to the value of π by rectifying each phase separately. A possible scheme that may be employed is suggested in fig. 5.10b. Let the capacitor again be charged by some or other means. An unwanted effect of introducing the rectifier is that during the commutation cycle the discharge current of the capacitor will flow through the diodes of the rectifying bridge in two components i_{d1} and i_{d2}.

This means that reverse voltage across the main thyristor T_m will never exceed the voltage across the conducting diodes, i.e.

$$\left.\begin{aligned} \bar{v}_{Tm} &= v_{D3} + v_{D4} = v_{D1} + v_{D2} \\ \text{further} \quad t'_{off} &= f \frac{1}{\bar{v}_{Tm}} \end{aligned}\right\} \quad 5.1$$

where t'_{off} is the turn-off time of the main thyristor.

When it is considered that the sum of the forward-voltage across the diodes should not be more than 4V, the equation 5.1 indicates that the turn-off time will become long. A further disadvantage of the circuit of fig. 5.10b is that the capacitor does not ring, but merely discharges, therefore wasting all the commutation energy in each cycle. The discharge time will be extremely short due to the low voltages across D3, D4 and T_c, causing a large current. In practice it may then be expected that the commutating thyristor, and diodes, may be destructed. Insertion of a commutating inductor L_c in series with the capacitor will build a resonant circuit. Now

$$\bar{v}_{Tm} = v_{D3} + v_{D4} + v_{Lc} \qquad 5.2$$

increasing the reverse voltage across the thyristor to the order of the capacitor voltage. The capacitive energy will be conserved to a large extent.

The actual circuit that may be employed is indicated in fig. 5.10c. Here an auxiliary circuit Ta-La has been added in order to assure that the charge on the commutating capacitor has the correct polarity at the start of each commutation cycle. After time t_c (end of commutation), the thyristor T_a is triggered and the charge rings round to polarity 2.

The functioning of the circuit is now changed to such an extent that it is worthwhile to consider it anew.

Assume the induced rotor e.m.f. constant during the short interval of commutation. The current at instant t_o through L_{re} is still I_o. Therefore, on starting commutation thryistor T_c it may be written that:

$$e_r + V_c \simeq (L_{re} + L_c) \frac{di_r}{dt} + I_o R_e \qquad 5.3$$

when the resistance of the commutation circuit is neglected. Therefore

$$v_{qp} \simeq V_c \cdot \left[\frac{L_{re}}{L_{re} + L_c}\right] \qquad 5.4$$

when $L_{re} >> L_c$, as is usually the case.

From examination of fig. 5.10c it is evident that the voltage of equation 5.4 will produce a free-wheeling effect with the diodes D_2 and D_3. On neglecting the voltage drop across the diodes the effect of the freewheeling diodes is to decouple the actual commutation circuit from the rotor circuit during the period in which the reverse voltage

of the capacitor C_c turns off thyristor T_m. Therefore the action of these diodes will be referred to as "decoupling" in the future.

It must be realized, on the other hand, that since the capacitor does not discharge through the machine windings any more, the opportunity has been lost to transfer the stored leakage inductance energy to the mechanical load. Either circuit $L_c T_c$ or $L_a R_a$ must be dimensioned in such a way as to handle the dissipation of this energy.

The current during the decoupling period now flows in the circuit $T_c L_c D_4 D_3 C_c$ and $T_c L_c D_2 D_1 C_c$. This reaches a maximum approximately when the voltage on C_c is zero, and then decreases. Somewhere in the cycle the decoupling current again becomes equal to the rotor current. At this instant the decoupling action is discontinued, the bridge assumes its normal function, and the commutation proceeds as described previously.

The basic changes in functioning of the power switch has now been described. The action may be divided into three parts:

(i) Conduction-cycle during which the switch performs its basic short circuit function with T_m conducting.

(ii) The turn-off cycle during which the thyristor T_m is turned off and the commutation circuit decoupled from the rotor.

(iii) The actual rotor current commutating process during which the rotor current is reduced to zero and the leakage energy stored in C_c.

A power switch with an auxiliary commutation circuit.

It has been stressed that the switch discussed previously presents the interesting characteristics that the commutation is current dependent. Whether this characteristic is considered an advantage or a disadvantage depends on the point of view, however. It is extremely valuable in case of commutating large currents. In the case of small currents being commutated the commutating voltage will become correspondingly small, and when the current becomes too small the unpleasant possibility exists of the commutating voltage disappearing. After this commutation cannot be obtained again. It is then necessary to supply an external energy source to ensure a minimum capacitor voltage. A further unpleasant consequence of employing the circuit shown(fig. 5.10c) is the series short circuit that may be formed by the thyristors T_a and T_c when triggered simultaneously by spurious voltages in the circuit. This is a configuration that is usually attempted to avoid in power switches if possible. Should such a coincidence of triggering pulses occur, the commutating voltage will also disappear, again enforcing the inclusion of an extra power supply to supply new charge in such cases.

Due to these and other practical factors it was considered to employ an auxiliary commutated power switch. This creates the possibility to isolate the commutation circuit from the rotor circuit, increasing the reliability. Since the auxiliary commutation circuit is fed from an external source it is alway possible to initiate a second commutation cycle when the first cycle fails. The auxiliary power supply may be considered a drawback, yet it is also necessary in the previously discussed switch if a reliable functioning is required.

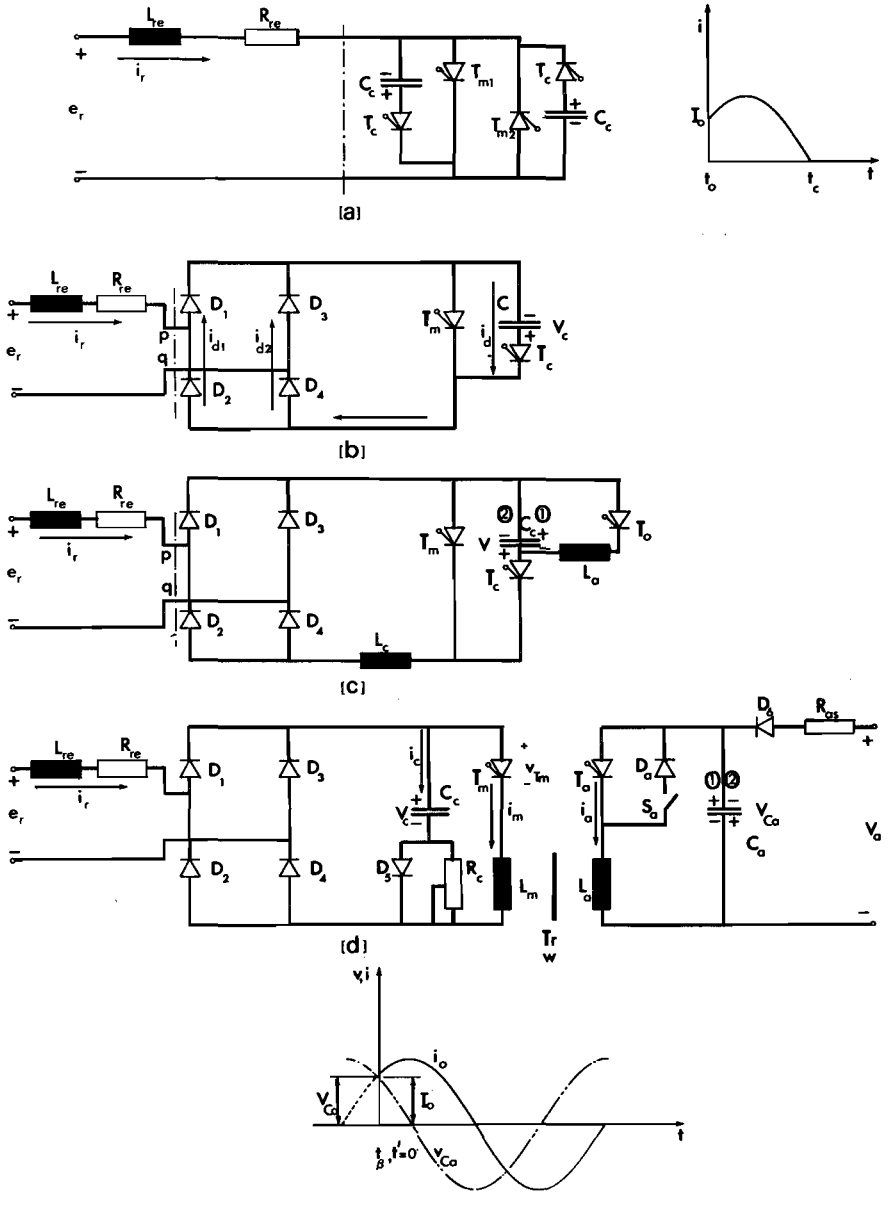

FIG. 5.10 CIRCUITS RELEVANT TO THE COMMUTATION OF THE ROTOR CURRENT OF AN INDUCTION MACHINE.

In the power electronics literature circuits employing auxiliary commutation are numerous, but relatively new. The switch employed at present may be considered to be related to the switch of Ohno[54] although it has been developed independently. The calculations are different, since the conception and use differ for the two examples. For the same reasons as pointed out previously, the power switch has been built up with a bridge rectifier. The general principle of the circuit will now be discussed:

Consider the main thyristor T_m to be conducting. The capacitor C_a is charged to condition 1, fig. 5.10(d), while T_a is blocking and switch S_a nonconducting. At the output of the rectifier bridge a higher voltage than in the case of the previously described switch will appear during conduction, caused by the inductance L_m of the secondary of the commutation transformer Tr during part of the cycle. On triggering thyristor T_a, C_a rings with L_a, the voltage on the capacitor appearing over the inductor L_a, causing a turn-off voltage to appear across L_m. At this instant the rotor current is commutated into the capacitor C_c, and the current flowing through L_m is commutated to L_a. The switch is so designed that the elements R_{re}, L_{re} and C_c form a resonant circuit. When the rotor commutation current i_c, reaches zero the circuit returns to its rest-state. The capacitor C_a has now been charged to state 2 during the ringing-process, and returns to the original state during the following cycle by charging over the source V_a, resistance R_a and diode D_6.

It has been remarked that the rotor current is commutated into C_c at the instant T_a is triggered. This then transfers the leakage energy of the machine to C_c, and at the end of the commutation cycle (t_c) the capacitor will have been charged up to a voltage V_{cc}. During the next conduction cycle this energy must be dissipated. The first possibility that presents itself is to dissipate the energy in a resistance R_c in series with the capacitor by dimensioning the circuit $R_c C_c L_m$ in such a way that it is overdamped when T_m is fired. This proposal has an unpleasant consequence. The rotor rectifier cannot conduct unless the voltage V_c falls beneath the value of the induced rotor voltage e_r, implying a long and slip-dependent delay of conduction, and a corresponding loss in maximum torque of the machine. To eliminate this drawback the circuit has been made oscillatory. On triggering T_m, the energy will be transferred in an extremely short time to the secondary inductance L_m of the turn-off transformer. At a time when the capacitor and inductor voltage approaches zero the rotor current will start to flow as D_1 and D_4 comes into conduction. When this occurs it is impossible for the two inductances to be connected in series, and L_m will cause a voltage to switch D_3 and D_2 into conduction, in order to decouple the power switch from the rotor as in the previous case. The original short circuit conditions has now been returned to the rotor, as long as the decoupling diodes conduct. It may be considered a less pleasant side effect that the energy will now be dissipated in the diodes. When the decoupling diodes cease to conduct, the cycle will be completed by the turn-off of the rotor circuit at time t_8 as already described. When it is desired to initiate the turn-off process before cut-off of the decoupling diodes, the energy contained in L_m will be transported to C_a via L_a.

Considering the action of the power switch with an auxiliary commutation circuit the processes may be represented schematically as in

fig. 5.11. The following particulars may be taken as characteristic of the investigated auxiliary commutated switching circuit.

(i) The functions of storage of the leakage energy and of supplying commutating voltage has been divided amongst the capacitors C_c and C_a respectively.

(ii) Galvanic isolation between commutation circuit and main circuit increases reliability.

(iii) The auxiliary supply ensures failsafe commutation as far as possible.

(iv) The auxiliary supply is required to supply the full commutation energy after each commutation cycle due to the resistive charging.

(v) The stored leakage energy is dissipated in the power circuit again, mainly in the diodes and the main conduction path during the decoupling period.

Similar to other electronic commutating circuits, the auxiliary commutation circuit suffers from the draw-back that with increasing circuit to be commutated, the available circuit turn-off time decreases. This is infortunate, since the necessary element-turn-off time increases with current. Study of the circuit has now indicated that by an extremely simple modification of the circuit the characteristics (iv) and (v) (more accurately they are drawbacks) may be eliminated. In the first circuit considered it was explained that the commutation is load-dependent. For the present circuit this may be established again by combining the functions C_c and C_a to a certain extent. This combination is executed by introducing the diode D_a shown in fig. 5.10(d). In this way the two elements remain separate, and only combine their functions for part of the period. In the next paragraph the functioning of the circuit will be traced.

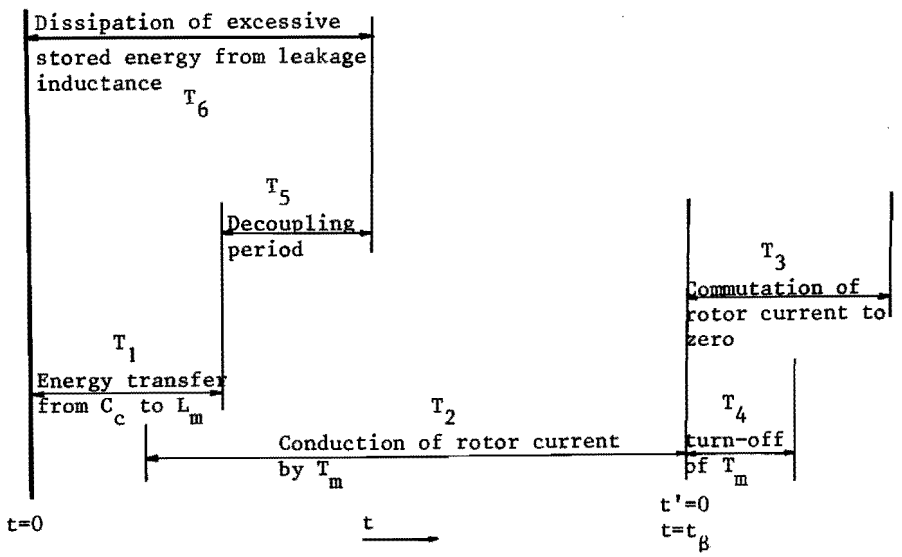

FIG. 5.11 THE DIFFERENT PARTS OF THE SWITCHING CYCLE OF AN AUXILIARY COMMUTATED SWITCH.

5.3.1.2 *Consideration of a modified auxiliary commutated power electronic switch.*

Let the switch S_a in fig. 5.10d be closed to connect D_a into the circuit. For the following discussion it will be taken that the conduction cycle starts at t=0 as indicated in fig. 5.11. It will be assumed that the initial conditions are:

$$\left.\begin{aligned} i_c \equiv 0 \equiv i_a \equiv i_m \equiv i_r \\ v_{C_a}\ (t=0) = V_{C_a} \\ v_{C_c}\ (t=0) = V_{C_c} \end{aligned}\right\} \qquad 5.5$$

When T_m is now triggered, two oscillations will start (the resistance R_c is in the zero position), assuming that the circuits are designed to be in the underdamped condition. As in the first version of the auxiliary commutated switch an oscillation between C_c and L_m is set up. Additionally an oscillation will start between C_c, C_a and Tr. Since the leakage inductance of the transformer is very much smaller than the main inductance L_m, the second oscillation will be of a much higher frequency, as will be proved experimentally. This will continue till the current through D_a tends to change its direction. As T_a is still non-conducting at this stage, this oscillation will then discontinue. The capacitor C_a has now attained a voltage V_{C_a}. The circuit can be dimensioned in such a way that the greater part of the stored leakage inductance energy of the rotor in C_c is transferred to C_a. The oscillation between C_c and L_m continues as before until the voltage on C_c becomes zero, and the decoupling period commences as predicted for the previous switch. However, since the larger part of the stored energy has been transferred to C_a, this dissipation-cycle (see fig. 5.11) is much shorter. The drawback of unnecessary energy dissipation in the bridge diodes has been largely alleviated. It should be noted that this energy transfer process only occurs when

$$V_{C_c} > w.V_{C_a} \qquad 5.6$$

where w is the turns ratio of the idealized transformer Tr. Once the freewheeling is initiated, the power switch short circuits the rotor during the conduction cycle in a way completely analogous to the action of the previously described version of the switch.

When the commutation cycle is now initiated to switch off the rotor current with triggering of T_a, an oscillation starts in the circuit C_a T_a L_a, again resulting in a turn-off voltage appearing across T_m, as the initial polarity on C_a is as given by condition 1 in fig. 5.10(d). Previously this oscillation discontinued when the capacitor C_a attained the polarity condition 2, since the current was then blocked by T_a. Due to D_a the oscillation now continues until polarity condition 1 has once more been attained. Because of the dissipation in the circuit this

voltage will be smaller than the initial voltage, but it represents an important improvement on the resistive charging of C_a. During the following conduction cycle the voltage of C_a will again be brought up to value V'_{C_a} by the energy transport from main to auxiliary circuit.

In the practical circuits this transport of energy proved so effective that the circuit functioned without any auxiliary source at all. Although it should be realised that the actual circuit phenomena are still more complicated than exposed here, the previous explanation gives an indication of what has been accomplished by the modification. It is important to realize that inclusion of D_a has now re-established the link between the two separate functions of C_c and C_a. This will be termed function coupling. When the condition of relation 5.6 is fulfilled , the initial conditions in the commutation circuit are a function of the current that has been commutated to zero during the previous cycle. Under steady state conditions this can have important consequences. Let this now be examined under simplified circumstances.

All resistances in main and commutation circuits are to be neglected to a first approximation. The initial conditions at time t_β ($t'=0$) are:

$$\left.\begin{aligned} i_r \quad (t'=0) &\simeq i_m \quad (t'=0) = I_o \\ v_{C_c} \quad (t'=0) &\simeq 0 \\ v_{C_a} \quad (t'=0) &= V'_{C_a} \end{aligned}\right\} \qquad 5.7$$

Let the turns ratio of the idealized transformer Tr be

$$w = \frac{i_a}{i_m}$$

The voltage on C_a, with reference to fig. 5.10(d), is:

$$v_{C_a} = \sqrt{(V'_{C_a})^2 + \left(\frac{I'_o}{\omega_a C_a}\right)^2} \cos(\omega_a t' + \phi_a) \qquad 5.8$$

with

$$\phi_a = \arctan\left(\frac{I'_o}{\omega_a C_a V_{C_a}}\right), \quad I'_o = w\, I_o, \quad \omega_a = \frac{1}{\sqrt{L_a C_a}}$$

As soon as the turn-off voltage appears on L_m, i_r is commutated into C_c. Assuming

$$\omega_c >> \omega_r \qquad 5.9$$

the voltage on C_c may be approximated by:

$$v_{C_c} = \sqrt{\frac{L_{re}}{C_c}}\, I_o \sin \omega_c t' \qquad \omega_c = \frac{1}{\sqrt{L_{re} C_c}} \qquad 5.10$$

The voltage across the main thyristor is given by:

$$v_{T_m} = v_{C_c} - v_{L_m} \qquad 5.11$$

If the available circuit turn-off time is now designated by t_{off}, the defining equation becomes:

$$\cos(\omega_a t_{off} + \phi_a) = \frac{\sqrt{\frac{L_{re}}{C_c}}\, I_o}{w\sqrt{(V'_{C_a})^2 + \left(\frac{wI_o}{\omega_a C_a}\right)^2}} \sin \omega_c t_{off} \qquad 5.12$$

If it is now considered in the first instance that the factor by which the harmonic function on the right hand side of rel. 5.12 is multiplied, tends to a constant value for large I_o, and in the second instance taken into account that

$$\omega_a >> \omega_c \qquad 5.13$$

as already stated in paragraph 5.3.1.1, it follows that

$$t_{off\ 1} \simeq \left\{ \frac{\pi}{2\omega_a} - \frac{1}{\omega_a} \arctan\left(\frac{w\, I_o}{\omega_a C_a V_a}\right) \right\} \qquad 5.14$$

when condition 5.6 is not fulfilled, and the voltage on the auxiliary capacitor is still constant and equal to the source voltage, i.e.

$$V'_{C_a} = V_a$$

This function is shown in curve 1, fig. 5.12. It should be noted how the available circuit turn-off time initially decreases sharply. Although many aspects have been neglected in this simplifed explanation, the results correspond well with practical observations, where it was noted that deterioration in circuit turn-off time is chiefly due to the phase-shift of the oscillation in the auxiliary circuit.

If condition 5.6 is now fulfilled, let

$$V'_{C_a} = y.V_{C_c} = y.\sqrt{\frac{L_{re}}{C_c}}\, I_o \qquad 5.15$$

The phase angle at which the oscillation starts will now become constant if the proportionality factor y empirically assumed in rel. 5.15 remains constant. In practice this is found to be the case. In this case it may be shown that under the same conditions cited previously

$$t_{off\ 2} = \left\{ \frac{\pi}{2\omega_a} - \frac{1}{\omega_a} \arctan \frac{w}{y}\sqrt{\frac{L_a C_c}{L_{re} C_a}} \right\} \qquad 5.16$$

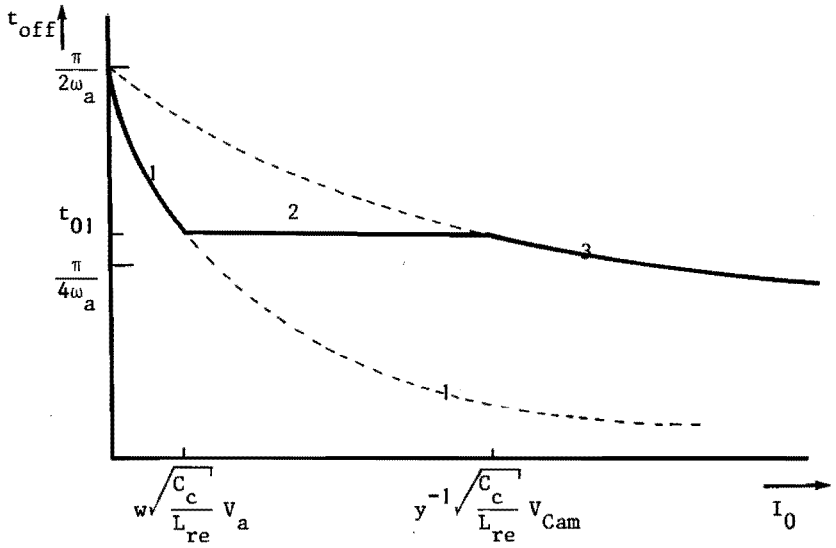

FIG. 5.12 ILLUSTRATION OF IMPROVEMENT OF CIRCUIT TURN-OFF TIME OF AN AUXILIARY COMMUTATED ELECTRONIC SWITCH BY ADDITION OF FUNCTION COUPLING.

The turn-off time has now become constant, as indicated by part 2 of the curve in fig. 5.12. It is of course now to be expected that the voltage in the auxiliary circuit will continue to increase, and due to the voltage rating of the semiconductor elements used, this voltage must be limited. If the voltage across C_a is now limited to

$$V'_{C_a} = V_{C_{am}} \qquad 5.17$$

by some or other clipping device, the circuit turn-off time is given by:

$$t_{off\ 3} = \left\{ \frac{\pi}{2\omega_a} - \frac{1}{\omega_a} \arctan\left(\frac{w\ I_o}{\omega_a C_a V_{C_{am}}} \right) \right\} \qquad 5.18$$

The turn-off time now decreases as if a higher auxiliary source voltage had been used.

As will subsequently be evident from the oscillograms, the electronic switch built according to the previously illustrated ideas functioned well and is an important improvement on a normal auxiliary commutated switch. The behaviour of these switches have been studied more extensively than reported here. Inclusion of resistances does not alter the behaviour fundamentally. Treatment of the effects of transformer leakage inductances and the influence of the auxiliary power source on the turn-off oscillation complicates the problem, but does not distract from the advantages that may be obtained from the proposed electronic switch configuration.

The solution suggested here is applicable to all auxiliary commutated electronic power switches. The circuit configuration will not

always be of such a nature that coupling of the function of commutating capacitor and auxiliary capacitor can be achieved by such a simple alteration as in the present case. Whenever this coupling is brought about, however, an improvement analogous to that depicted in fig. 5.12 will appear.

5.3.1.3 *Consideration of an electronic switching circuit for the low-high chopper used for rotor control.*

In the electronic chopper circuits LH1, LH2, LH3 of figures 5.5, 5.7, 5.9 an electronic switching circuit with forced commutation is used. With reference to the brief discussion of commutation in chapter 2, the circuit arrangement may be classed as parallel forced commutation, since the charged capacitor supplying the necessary commutation energy is ultimately connected in parallel to the main thyristor. Fig. 5.13 indicates a simplified schematic arrangement of the electronic chopper circuit as developed for application in the electronic Leblanc and in the compensated electronic Scherbius cascade. Consider the operation of this circuit.

Let the switch S_1 be nonconducting and the switch S_2 be in position 1. The electronic switching circuit will now operate as a resistively loaded chopper. The commutation capacitor C_c has a polarity as given by condition 1, fig. 5.13.

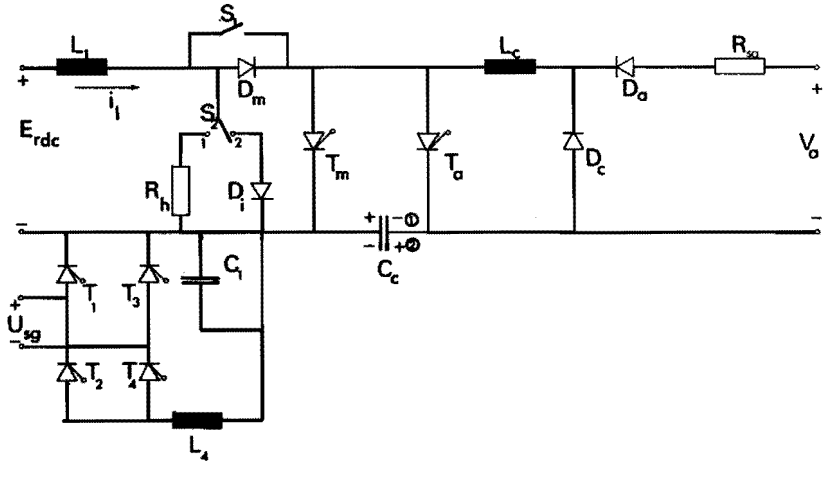

FIG. 5.13 PARALLEL-COMMUTATED CHOPPER CIRCUIT USED IN THE ELECTRONIC LEBLANC AND COMPENSATED ELECTRONIC SCHERBIUS CASCADES.

T_m conducts and T_a is blocking. Upon triggering T_a, the capacitor applies a large negative bias to T_m, and consequently C_c charges to polarity 2 according to an exponential function. It is now generally accepted that T_a turns off, current passes through R_h, and the circuit is in a new steady condition. This will subsequently be subjected to investigation. Upon now starting T_m again to initiate the following cycle, the capacitor C_c rings through the circuit $C_c D_c L_c T_m$ to attain charge polarity as given by state 1. The auxiliary power supply V_a in this case is intended to start up the system and to maintain the charge on C_c when T_m has been conducting for a long time.

This chopper circuit is a variation of the first high-low chopper circuits developed for control of direct current machines by *Jones* (33 and *Abraham Heumann and Koppelmann* (1 , as described in chapter 1. The variant for the resistive load has been described by *Golde* (22 , and the dimensioning investigated by *Cieszow* and *Kulka* (9 . Consequently these aspects will not be treated here.

The circuit of fig. 5.13 again contains some modifications and exhibits some commutation phenomena not previously described in the literature. These aspects will be briefly explained. Practical investigation of the developed circuits in the described systems indicated that when T_m has been turned off, and C_c charged through T_a to polarity 2, T_a may either turn off due to its holding current being reached, or remain conducting especially at high repetition frequencies. This may draw continuous current from the auxiliary supply V_a. This current may even prevent the holding current of T_a from being reached. T_a is then turned-off by the charge on C_c when T_m is fired in exactly the same way that it has turned off T_m in the previous cycle. Furthermore when the current has been commutated to R_h, the voltage on C_c after charging will be

$$v_{C_c} = i_1 . R_h \qquad 5.19$$

Especially at low repetition frequencies this is rather unfortunate, since i_1 may decrease to a low value (see chapter 4). Consequently C_c again partly discharges, impairing commutation. This has been alleviated by including D_m. Practical investigations have shown the expectations to be borne out.

When the circuit is used in a compensated electronic Scherbius cascade, the commutation action changes. Let S_2 be in position 2. The diode D_m may now be shorted out by S_1. A schematic representation of the inverter circuit to absorb the chopper output power (see chapter 4) is given by T_1 to T_4. The mean inverter back e.m.f. appears across C_1. The diode D_i is incorporated to retain the capacitor voltage and protect T_m from destruction. Upon triggering T_a, T_m is turned off, and the entire current i_1 commutated into C_c, since D_i will be reverse biased. In contrast to the turn-off cycle in the auxiliary commutated chopper and the parallel-commutated chopper, the voltage on C_c is a linear function of time, and has a maximum voltage V_i. The available circuit turn-off time is consequently again a function of the current to be commutated, since the inductive energy above a certain voltage level will always be stored in C_1. A situation analogous to the auxiliary commutated electronic switch without function coupling exists. An improvement with the same principles already described may be

obtained if necessary.

5.3.2 *TRANSMISSION OF TRIGGERING COMMANDS TO POWER ELECTRONIC SWITCHES.*

The problem of delivering the triggering commands to the power electronic switches in a suitable way is very important in power electronic and machine-electronic systems, since the correct and reliable functioning of the entire system ultimately depends on correct triggering. Since a great many types of circuits have been devised in the past, the problem will now be considered as general as possible. Some of the conditions imposed on the triggering circuits are the following:

1. In large systems the power switches operate at high power and voltage levels, necessitating isolation of the information-electronics from the power-electronics by a transformer. This is especially important in systems where the triggering circuits should be isolated from each other due to elements in series or antiparallel.
2. The operating frequency of the power converter may change, requiring corresponding changes in the frequency of operation of the gating circuit.
3. The duty cycle of the power switch may depart considerably from the value of 50% assumed for a normal square wave. (Especially in d.c. to d.c. converters)
4. In some applications, especially variable frequency inverters, the frequency of operation may decrease to values even low for power applications (The period may even exceed 1 sec.)
5. In many power applications, fast turn-on and turn-off of the current through the converter are necessary. This poses corresponding requirements for the gating signals to the semiconductor switches initiating conduction and commutation. (Especially with elements in series or in parallel)
6. There are different conditions demanding that the gating signal must be sustained for the full conduction period of the switching element. Thyristor-elements, although fundamentally only needing a short pulse to trigger into the conducting state, require sustained gating signals due to holding current requirements, and general circuit conditions such as lagging power factor and reactive filter elements (B4 . Transistors as power switches require a gating signal during the whole conduction-period.

An examination of these requirements indicates that when employing a magnetically cored transformer transmitting a gating signal having the same cycle-frequency as the power switching element, conditions 1 and 2 may be satisfied. However, unless special resetting precautions are taken, condition 3 will result in cumulative saturation of the core. It is evident that to satisfy 4, the cross section of the core will in the end become extremely large, influencing not only the transformer size, but also adversely the performance. Taking the fast rise-time into account (5), a compromise is necessary between the conflicting solutions regarding isolation (1), core size (4, 6) and close coupling (5). Economic questions add to the complication of the problem.

It has previously been treated extensively by *Turnbull* (73 why a carrier frequency gating system represents an optimum choice in such cases. Such a system may be considered to be defined by the schematic of fig. 5.14. The transmission of a square wave carrier frequency input

to the isolating transformer is gated. After transformation this on-off modulated carrier wave is rectified, and filtered if necessary, restoring the original gating function. The transformer, rated for the carrier frequency, is small. Considerable design freedom exists to obtain good isolation, good coupling, optimum component use etc. All types of duty cycles may be transmitted. *Turnbull* has given an excellent exposition of the utility of these systems, and therefore the attractive design possibilities will not be discussed further.

The present investigation is intended to extend the analysis of the carrier frequency gating technique in order to arrive at a system delivering a constant output signal during transmission, without using filters in the output circuit. The analysis indicates that the most important aspect is the philosophy of the arrangement of the magnetically-cored isolating transformer and the non-linear rectifier output circuit. This corresponds to experience in the field of high power mutators, where voltage drop due to leakage reactance in the rectifier transformers is a well-known phenomenon.

5.3.2.1 *Some problems concerning gating of static switches.*

During gating of these switches careful consideration must be given to the rise-time, the duration and the fall-time of the output signal. Some of the considerations of the previous paragraph will be recapitulated, and new considerations added.

(a) In high-performance power-electronic circuits triggering pulses with a short rise-time are mostly desired. Neglecting the effect of an output filter, the rise-time is limited by the leakage inductance of the isolation transformer. To reduce this effect the transformers may be kept small, which dictates shorter pulse duration, a given order of magnitude for the saturation flux of the possible core materials being assumed.

(b) The duration of the triggering signal cannot be chosen at will. The following factors determine the necessary duration:

(b) (i) The delay between current flow through the element to be triggered, and the voltage to which the derivation of the starting time of the command is related, is not known explicitly. Mostly this delay is determined by conditions in the power electronic circuit and the load, which may be dynamic.
Fortunately the range of variation is known. (An inverter with feedback rectifiers and inductive load for example). This poses the condition of extending the triggering signal over an appreciable part of the operation cycle.

(b) (ii) When highly inductive circuits are switched on, and the current builds up from zero, the signal must be sustained at least until the latching current of the device has been reached (if applicable).

(b) (iii) The type of power switch used. Transistors need a drive signal at least exceeding the saturation value over the whole conduction period when employed as power switches.

(c) In some applications the fall-time of the output signal after switch-off of transmission is critical. Again neglecting the effect of

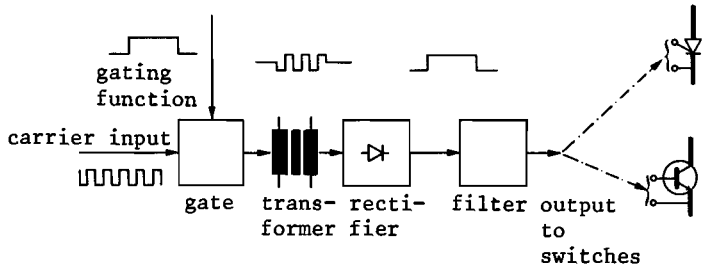

FIG. 5.14 SCHEMATIC OF A TYPICAL CARRIER FREQUENCY GATING SYSTEM FOR STATIC CONVERTERS.

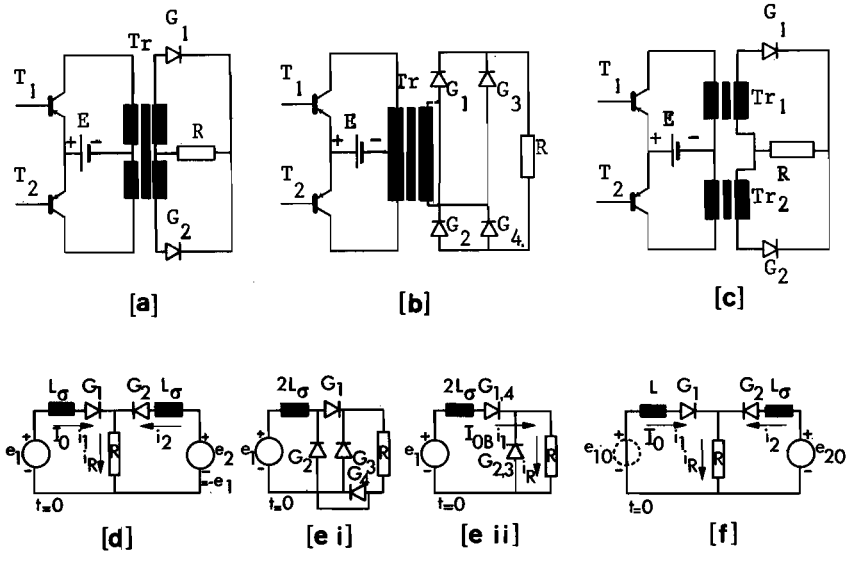

FIG. 5.15 MODELS ANALYSED.

a - c Three basic classes of carrier frequency gating systems.
d - f Corresponding equivalent circuits.

a filter in the output, this fall-time is determined by the arrangement of windings on the core and the magnetic energy contained in the transformer as a whole. Addition of a filter circuit makes the situation worse.

In circuits in the lower inductance range the state of the art is such that condition (b) (ii) can be fulfilled by a single pulse. For satisfying condition (b) (i) in this case it is then possible to employ either a pulse-burst technique or a carrier-frequency technique. When it is desired to have a constant output signal during transmission, (condition (b) (ii) and/or (b) (iii)) a carrier frequency solution is optimal. Unfortunately the output signal, after rectification, will not be absolutely constant, as is to be explained subsequently. This is due to:

a. The departure of the input waveform to the transformer from an ideal square wave.
b. The leakage inductance of the transformer.

This drawback is mostly alleviated by adding a small capacitive filter circuit in the output. In some applications this is allowable, although rise and fall-time deteriorate (a) and (c). Nevertheless this may not be desirable in some circuits employing forced commutation, as the energy stored in the filter tends to apply positive gate drive to the thyristor during part of the period of negative anode to cathode voltage applied by the forced commutation circuit to the thyristor. This increases the requirements for the commutation circuit, and the dissipation in the thyristor.

It is evident that the voltage drop caused in the output during commutation (see later) by leakage inductance is fundamental. Improvement of the input waveform to the transformer by cascading more amplifier stages and reducing the leakage reactance of the transformer both have a definite limit. In addition this approach requires small tolerances in components and manufacture. At it is known that leakage inductance of transformers provide certain effects in conjunction with rectifiers, it appears worthwhile to examine the commutation effects in order to arrive at a solution.

5.3.2.2 *Model to be analysed.*

In order to apply a simple analysis for comparison of all the systems, it will be assumed that the magnetic core operates in a linear region. The diodes to be used are ideal, and the loading of the circuit a resistor (highly doped gate-cathode junction of a thyristor). Neglecting magnetising losses and current, a linear equivalent circuit will be used.

Three alternatives will be distinguished, as shown in fig. 5.15a, b and c - to be referred to as type A, B and C. In the first type of configuration, the primary and secondary of the transformer T_r are both centre-tapped, the output being rectified as shown (fig. 5.15a). The switches T_1 and T_2 are assumed ideal so that the waveform on the transformer input becomes a perfect square wave when T_1 and T_2 are switched by identical signals being shifted with respect to each other by a half period. Equivalent leakage inductance per output halve is L_σ , and the

amplitude of the square wave at the input E. Configuration of type B is the same, save for the output rectifier being a bridge. The suggestion now offers itself to split the transformer Tr up into two, and by allowing an overlap time Δt between the driving function for T_1 and T_2 (waveform asymmetric) attempt to compensate for the leakage voltage drop during commutation in one branch by supplying voltage during the overlapping time from the other. This results in type C (fig. 5.15c). Taking all the previous particulars into consideration, the equivalent circuits are as shown in fig. 5.15d, e and f.

Employing an equivalent leakage inductance L_σ during commutation in all these cases does not imply that this quantity is determined magnetically in the same way in all the systems. It is the intention to illustrate the difference in characteristics by assuming a reactance effect of the same magnitude in the three systems. As the voltage level in type B is higher by a factor two, the same magnification has been given to the reactive effect. A practical determination of L_σ in type A for example, is not simply due to coupling between the four windings of the transformer during commutation.

Figures 5.15a, b and c are only intended as a schematic representation of the most outstanding features of the three types of output circuits that are discussed in relation to carrier frequency gating systems. These diagrams are not complete to obtain perfect working electronic systems, but need the addition of more components. As this will only tend to obscure the essential characteristics here under discussion, it has been decided not to present the electronic detail in this discussion.

The equivalent circuits are all specified at time t=0 (fig. 5.15d, e and f). Should one wish to employ these circuits for calculations in other than the commutation periods, it is possible that changes may be necessary in the circuit parameters. This is especially important in the case of type C overlapping arrangement (fig.15c and f). During overlapping action, both inductances have value L_σ . When either e_{10} or e_{20} becomes zero (initiation of commutation) the associated inductance changes from L_σ to L, the total equivalent inductance necessary to represent the magnetic energy in the transformer.

5.3.2.3 *Analysis during the commutation period.*

TYPE A (fig. 5.15a)

Input waveform symmetrical, with period T

$$\left.\begin{aligned} e_1 &= -E\ , \quad 0 < t < T/2 \qquad e_2 = -e_1 \\ e_1 &= E\ , \quad T/2 < t < T \end{aligned}\right\} \qquad 5.20$$

Between time 0 and t_1 both G_1 and G_2 may be taken to conduct, with initial value of i_1 equal to I_o. At t_1, i_1 will become zero, and i_2 will increase to complete the commutation process. Solution of the circuit equations yields:

$$0 < t < t_1 : i_1 = -\frac{E}{L_\sigma} t + \frac{I_o}{2}\left[1 + \exp -\left\{\frac{2t}{\tau}\right\}\right]$$

$$i_2 = \frac{E}{L_\sigma} t - \frac{I_o}{2}\left[1 - \exp -\left\{\frac{2t}{\tau}\right\}\right] \qquad 5.21$$

$$i_R = I_o \exp -\left\{\frac{2t}{\tau}\right\}$$

$$t = t_1, \quad i_1 = 0, \quad i_R = I_{min}$$

$$t > t_1 , \quad i_2 = i_R = I_o - \left[I_o - I_{min}\right] \exp -\left\{\frac{t-t_1}{\tau}\right\} \qquad 5.22$$

with τ the time constant of R and L_σ and $I_o = \frac{E}{R}$. The minimum value of the gate current

$$I_{min} = I_o \exp -\left\{\frac{2t_1}{\tau}\right\} \qquad 5.23$$

TYPE B (fig. 5.15 e(i) and (ii)):

During conduction of G_1 and G_4, G_2 and G_3 block, so that the equivalent circuit becomes that of (e(ii)).

$$\left.\begin{aligned} e_1 &= -2E \quad , \quad 0 < t < T/2 \\ &= 2E \quad , \quad T/2 < t < T \end{aligned}\right\} \qquad 5.24$$

It is now evident that commutation will not be complete before i_1 is zero. Solution of the circuit equations gives:

$$0 < t < t_1 : i_1 = i_R = I_{oB}\left[2 \exp -\left\{\frac{t}{2\tau}\right\} - 1\right] \qquad 5.25$$

$$t = t_1 : i_1 = i_R = 0 \qquad 5.26$$

$$t > t_1 : i_2 = I_R = I_{oB}\left[1 - \exp -\left\{\frac{t-t_1}{2\tau}\right\}\right] \qquad 5.27$$

with $I_{oB} = \frac{2E}{R}$.

TYPE C (fig. 5.15f):

The waveforms assumed for this circuit will be the following:

$$\left.\begin{array}{l|l} e_{10} = 0, \quad 0 < t < \frac{T}{2} - \Delta t & e_{20} = E, \quad -\Delta t < t < \frac{T}{2} \\ e_{10} = E, \quad \frac{T}{2} - \Delta t < t < T & e_{20} = 0, \quad \frac{T}{2} < t < T - \Delta t \end{array}\right\} \quad 5.28$$

An overlapping time Δt for the two waveforms therefore exists. Due to the fact that when T_1 in fig. 5.15c is opened, no coupling with any other circuit exists than through the output rectifier; the inductance of importance during commutation in this circuit is the total inductance L, and not merely the leakage inductance.
Solution between time zero and t_1, when $i_1 = 0$, yields

$$\left.\begin{array}{l} 0 < t < t_1 : i_1 = I_1 + I_2 \left[\exp - \left\{\frac{t}{\tau_e}\right\}\right] - \frac{E}{L_\Sigma} t \\ \qquad i_2 = \left[\frac{L_\Sigma}{L_\sigma} - 1\right] I_2 \exp - \left\{\frac{t}{\tau_e}\right\} + \frac{L}{L_\Sigma} I_o - I_1 + \frac{E}{L_\Sigma} t \end{array}\right\} 5.29$$

therefore

$$i_R = \frac{L_\Sigma}{L_\sigma} I_2 . \exp - \left\{\frac{t}{\tau_e}\right\} + \frac{L}{L_\Sigma} I_o$$

with

$$\tau_e = \frac{\tau_1 \tau}{\tau_1 + \tau} = \frac{L L_\sigma}{L_\Sigma R}, \quad L_\Sigma = L + L_\sigma, \quad \tau_1 = \frac{L}{R}$$

$$I_1 = I_o \left[1 - \frac{L_\sigma}{L_\Sigma} + \frac{L L_\sigma}{L_\Sigma^2}\right], \quad I_2 = I_o \left[\frac{L_\sigma}{L_\Sigma} - \frac{L L_\sigma}{L_\Sigma^2}\right], \quad I_o = \frac{E}{R}$$

The minimum value of i_R is attained at $t = t_1$

$$t = t_1 \quad i_R = I_R = \frac{\tau_1}{\tau_e} I_2 \left[\exp - \left\{\frac{t_1}{\tau_e}\right\}\right] + \frac{L}{L_\Sigma} I_o \qquad 5.30$$

for

$$t < t_1 : \quad i_R = I_o - \left[I_o - I_R\right] \exp - \left\{\frac{t - t_1}{\tau}\right\} \qquad 5.31$$

The analysis of these systems will not be carried further for non-ideal waveforms. The present analysis is sufficient to illustrate the superiority of type C arrangement. This only improves with deterioration of waveform. Equation 5.23 indicates that although the output current of type A contains a strong dip during commutation, it does not necessarily become zero. Under practical conditions this may become more pronounced due to rise-time of the input waveform. Type B results in a minimum output current zero, and is the least elegant of the systems

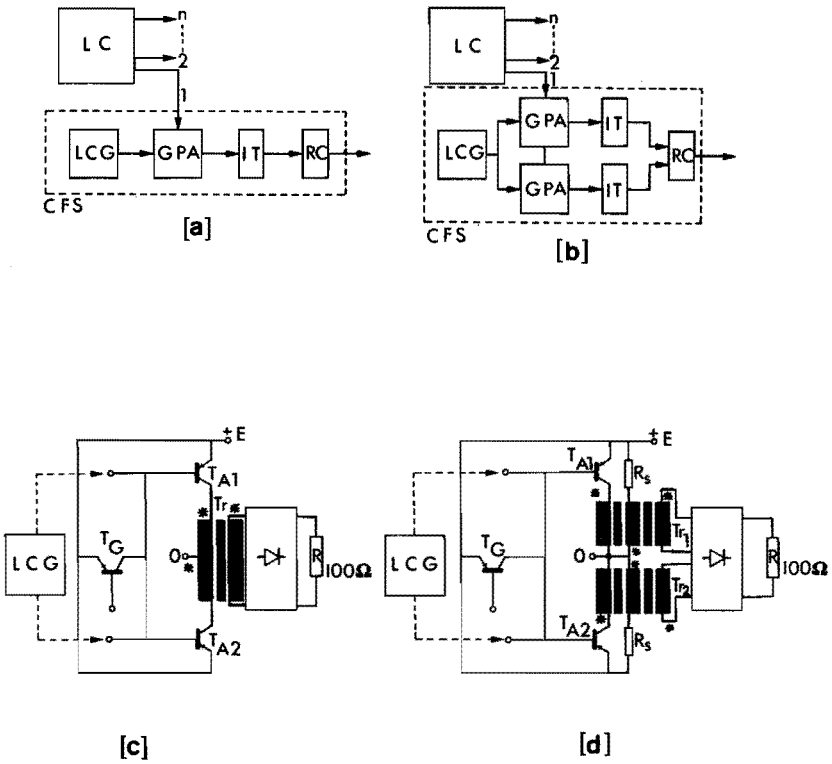

FIG. 5.16 BUILT-UP SYSTEMS.

a,b. Block diagrams of conventional (type B) and overlapping (type C) systems.
c,d. Schematic lay-out of corresponding output circuits.
L.C. : Logic circuitry
L.C.G.: Local carrier frequency generator
G.P.A.: Gated power amplifier
I.T. : Isolation transformer
R.C. : Rectifier circuit
C.F.S.: Carrier frequency triggering system.

analysed. Taking the rise-time of the input voltage into account, the current rise-time will decrease after $t=t_1$. Equation 5.30 indicates that in the system with overlap a constant current component exists in the output during commutation. From this simplified analysis it appears that it is not possible to compensate completely for the commutation effects. Further analysis and practical experiments indicate that in practice an apparent overcompensation may be found. This will be apparent from the oscillograms[80].

Experimental verification of the characteristics was found in the practical gating systems employed in the built-up systems already described. In contrast to previous solutions described in the literature [73], these systems have local carrier wave generation. Adaptability is higher with each unit having its own carrier supply, since units may be removed or added to a system at will, without the possibility of affecting each other through loading of a central carrier frequency supply. Circuit detail of the electronic system will not be presented.

Arrangement of a system to type B is shown in fig. 5.16a, the power amplifier being gated at its input by the logic circuitry. In the schematic lay-out of the gated power amplifier in fig. 5.16c T_G represents the gating circuit. The waveform of the local carrier frequency generator is symmetrical as already specified, having a rise-time of the order of a microsecond. The composition of an overlap-system is given in fig. 5.16b, while the schematic arrangement of the output is given in fig. 5.16d, the carrier wave being asymmetric (equation 5.28). As the output transistors in fig. 5.16c are in balanced arrangement, conditions for resetting the core of Tr are fulfilled. To obtain the same utilization of the material in Tr_1 and Tr_2 it is advisable to add the resetting winding shown (fig. 5.16d). In the balanced arrangement, all other parameters being equal, the switch-off time at the end of a transmission period will be longer, since with T_{A1} and T_{A2} nonconducting due to gating, the magnetic energy will decay through the load. In the overlap system the third winding enables the magnetic energy to be fed back against the constant supply voltage via R_s. This results in fast switch-off, an important advantage of this system, although not following strictly from the previous analysis. This switch-off action is also somewhat different from that assumed during commutation in the analysis.

It may therefore be concluded that (in conjunction with oscillograms to be presented subsequently) it has been demonstrated that during carrier wave transmission of gating signals for static switches it is impossible to deliver a constant output voltage during transmission due to commutation effects in the indispensible rectifiers. The situation may be improved by constructing transformers with very low leakage to precise tolerances, and by cascaded stages of amplification in an attempt to reduce the carrier-wave rise-time. These solutions are only partly effective without an output filter, and the feasibility disputable. In specialised applications necessitating such an output with fast switch-off times, (no filter) it has been demonstrated effective to employ an overlapping technique with an asymmetric waveform. In this system neither the rise- and fall-time of the input waveform, nor the leakage inductance of the transformer is critical. Their effect on the output may be compensated by a simple adjustment of the asymmetry of the carrier wave. The system retains all the inherent advantages of a carrier-frequency gating system as previously exposed in the

literature.

In the machine-electronic systems described in previous paragraphs it will be noted that other types of triggering units than the overlapping carrier frequency system explained have also been used. This has been done to investigate the characteristics of the other types. It has become clear that the blocking oscillator so often used in power electronic systems is the least suitable. As a matter of fact all the circuit configurations employing a self-oscillating output stage are less suitable. Considerations of switching transients, speed of response and reliability give rise to this conclusion.

5.3.3 *REGARDING THE APPLICATION OF SEMICONDUCTOR SWITCHING ELEMENTS IN POWER ELECTRONIC SWITCHING CIRCUITS.*

Semiconductor power switching elements, and in the present case specifically power diodes and thyristors, are well established in the field of power electronics. Yet their application still presents many problems in the case of well optimized, reliable design. When these elements are employed in laboratory systems such as used in the present instance they are often used to ultimate capacity regarding reverse and blocking voltages, current carrying capacity etc. If during operation the system functions unreliably it is also very important to know whether it is a fundamental system problem, or originates with the semiconductor switches. It has been found that for all the specialized applications described in this study the normally available particulars are not sufficient to be able to decide on these matters without doubt.

In order to be able to determine the characteristics of each element a semiconductor testing unit was constructed for performing a range of static and dynamic tests. The equipment has also been used to investigate the nature of some of the physical processes occurring during transients in the elements, although it would carry too far to report on those aspects in the present study. A schematic diagram of the main testing unit has been included in fig. 5.17, while the practical lay-out of the equipment is illustrated in fig. 5.19 (b).

The unit has been designed to be able to measure the following particulars of a thyristor or diode tablet:

(i) Static current-voltage characteristic - chiefly for an accurate determination of leakage currents up to 2 kV. The high voltage power supply (1) may be seen in fig. 5.19 (b). With reference to fig. 5.17 it can be seen that by closing S_4, S_7 and S_8 these characteristics are to be measured.

(ii) Voltage current characteristics at a sweep rate of 50 Hz, with and without triggering of the test specimen. These characteristics are displayed on X-Y oscilloscope (2) (fig. 5.19 (b)) and may be taken up for either blocking or reverse direction or both by respectively using D_bS_1, D_rS_3 or S_2. Latching current may be determined by variation of the current limiting resistor R_1, while the step-up transformer T_r enables the test to be carried out up to a peak value of 3 kV (fig. 5.17). DU4 is a delay unit to assure that TU21 excites the test thyristor at approximately 120 degrees after the zero voltage condition of the supply as

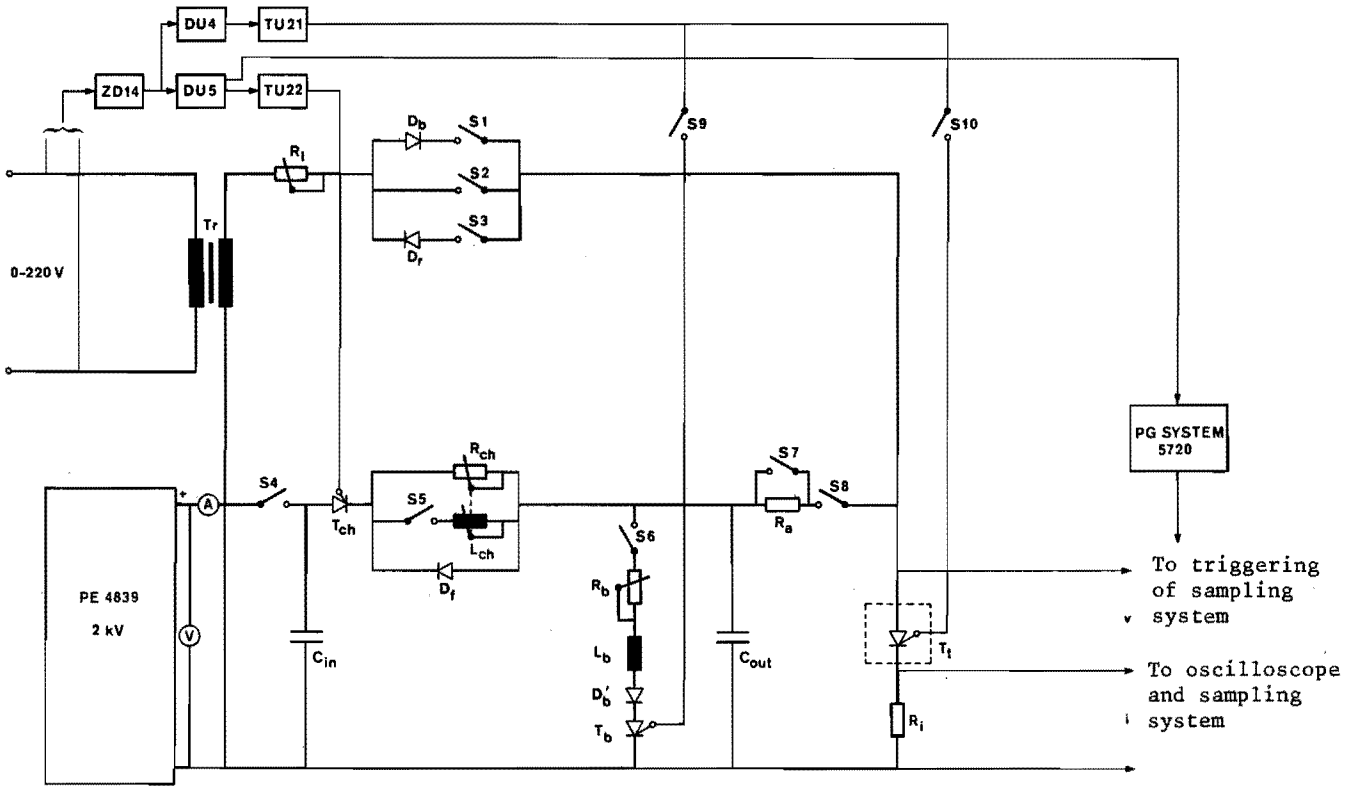

FIG. 5.17 SCHEMATIC OF DEVELOPED THYRISTOR TESTING EQUIPMENT.

detected by ZD14.

(iii) Voltage transient behaviour. During this test the maximum voltage-time gradient at rated voltage, that may be applied to the thyristor before it triggers into a conduction state, is determined. While most of these types of tests described in the literature seem to employ an exponential voltage transient (see for instance work by *Udvardi-Lakos* and *Surk* [74]), the equipment built up applies either an exponential transient or a linear transient by adaptation of a known circuit [B5]. An exponential transient is obtained by opening S_5, S_7 and closing S_8. By triggering T_{ch}, C_{in} is discharged via R_{ch} into C_{out}. R_{ch} automatically provides the maximum current-time gradient to which the specimen has been subjected. DU5 is a delay unit to ensure that the transient is repeated at 25 Hz by repetitive triggering of T_{ch} through TU22. Due to the fact that this thyristor operates in an extremely low inductance circuit with a very high di/dt the specifications regarding the output of TU22 are special. It has to deliver an output current pulse into the thyristor gate-cathode junction of amplitude at least 1 Ampere and a rise-time of not more than 40 n sec. at a voltage isolation level of 2 kV. This is achieved by a special triggering technique.
Closing S_5 results in a waveform on C_{out} that approaches a linear dV/dt. On triggering T_{ch} a resonant circuit is built up through C_{in}, L_{ch}/R_{ch}, C_{out}. When the voltage on C_{out} reaches a value equal to that on C_{in}, the freewheel diode D_f comes into action; consequently cutting the sine-wave off at half-amplitude. At present the equipment is capable of achieving a voltage time gradient of maximum 500 V/μsec. at voltages up to 1000 V.
A possibility to investigate the influence of a bias on the dV/dt characteristic has been incorporated in the circuit $R_b L_b T_b$. The charge remaining on C_{out} after each transient is removed through this circuit. Variation of the value of R_b then changes the bias conditions in a range having approximately twice the value of the rated voltage.

(iv) By opening S_6 and triggering the test specimen to discharge C_{out} it is possible to determine the value of the time of switching on of the test specimen. The holding current of the element may also be determined in this way.

During these transient tests the characteristics are read out by oscilloscope. Especially for the dV/dt tests a sampling system combined with a storage oscilloscope has been set up. This has been chosen for two reasons:

a) It has been found that during switching of the thyristors transients are set-up at frequencies in excess of the bandwidth of conventional equipment.

b) Due to the high voltages involved it is extremely difficult to repeat the transients at a high frequency. Using a sampling system simultaneously supplies a convenient output to drive a conventional X-Y recorder.

It is understandable that the use of the sampling system poses special problems as regards the reproducibility of the 25 Hz transients. (Low jitter and accurate triggering) It is believed that these problems have been solved satisfactorily. The power-electronic equipment is

contained in the unit 4 in fig. 5.19 (b), while all other electronic equipment are concentrated in 6. Sampling system and recorder are indicated by 7 and 8 respectively, while 3 indicates a constant temperature oven for more accurate investigation of especially the transient phenomena.

The described unit is not yet capable of providing a test for the element turn-off time at rated current. Such a unit is currently being developed.

PART II

EXPERIMENTAL INVESTIGATION OF THE CHARACTERISTICS OF SOME GROUP II AND GROUP IIA MACHINE-ELECTRONIC SYSTEMS.

5.4 A BRIEF REVIEW OF THE EXPERIMENTAL INVESTIGATIONS.

The problem of presenting the experimental investigations is again chiefly one of selection, since all observations cannot be presented in minute detail when one considers the range of systems investigated. Furthermore a large amount of experimental work was devoted to developing and setting up the machine-electronic systems, tracing all system faults and inaccuracies in order to be as sure as possible that the measurements will represent the specified conditions. This work is not regarded to be necessary to report upon in a study of the present type.

The investigations concern the electronic control of electromechanical energy conversion. Therefore the most important experimental results are those indicating the relationship between the electronic variable and the electromagnetic torque. These results are presented in the form of torque-speed curves with the electronic variable as parameter. The transfer function may be determined from these curves, while more information regarding the behaviour of the electromechanical converter (harmonic torques etc.) may also be deduced herefrom. In developing the theory presented in the previous chapters assumptions regarding the electrical wave forms were made. To judge the validity of these assumptions in the present situations oscillograms of the appropriate waveforms are to be presented and discussed.

During discussion of the development of the systems in this chapter some attention was devoted to functioning of parts of the power-electronics and information electronics, and to measurements on the semiconductor elements. In order to illustrate these aspects a series of oscillograms will be included and discussed. In the calculations of chapter 4 attention has also been given to some of the electrical characteristics of the systems, and by comparison with experimental measurements it will be investigated to what extent the assumptions has been fulfilled and whether the electrical characteristics measured are representative.

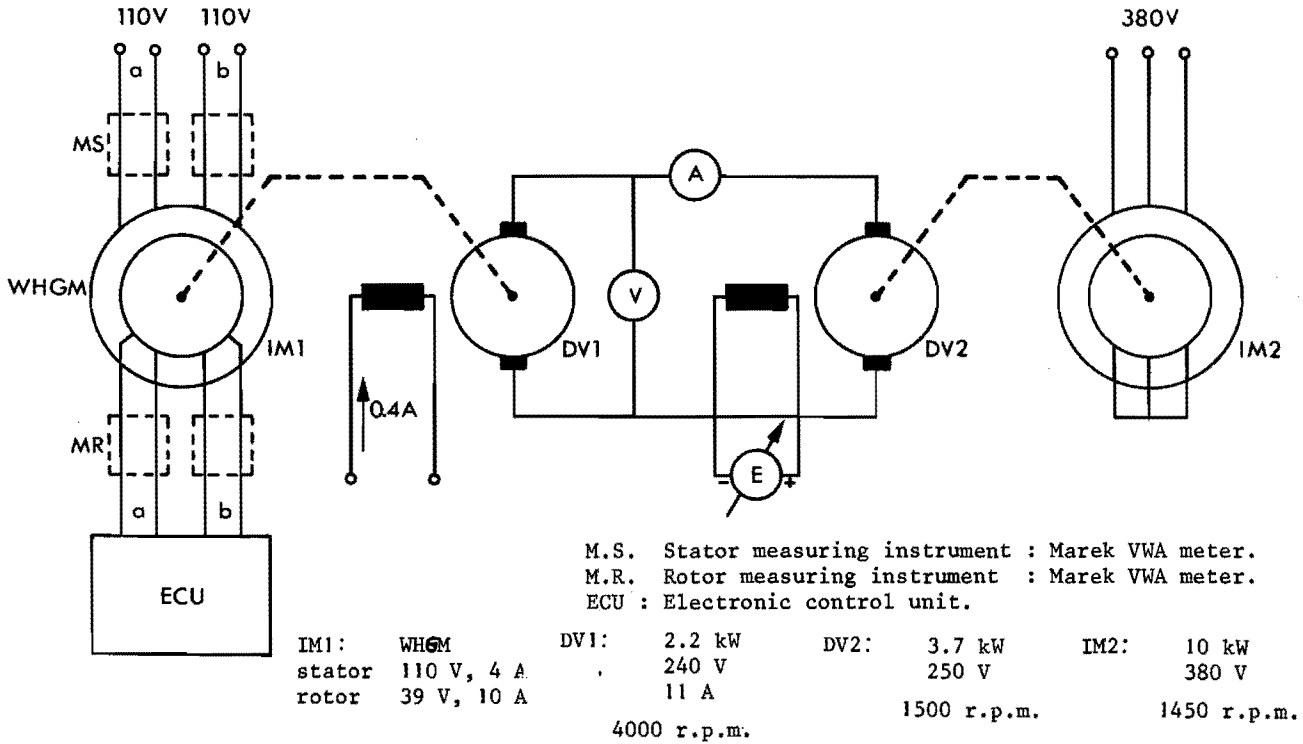

FIG. 5.18(a) DIAGRAM OF POWER CONNECTIONS FOR THE EXPERIMENTS ON THE WESTINGHOUSE GENERALIZED MACHINE.

5.5 CONCERNING THE ACTUAL EXPERIMENTAL SET-UP.

In previous paragraphs it has already been mentioned that the systems developed on the semi-four-phase machine as an electromechanical converter were tested on the Westinghouse Generalized Machine. All the information-electronic and power-electronic subsystems were built into one unit. This has been designed to be operated with the Generalized Machine as one complete set, and is indicated in fig. 5.19.

The particulars concerning the machine may be summed up as follows:

Stator resistance R_s = 2.86 Ω
Rotor resistance R_r = 0.75 Ω
Maximum mutual inductance between stator and rotor
M_{sr} = 170.50 mH
Stator inductance L_s = 472.00 mH
Rotor inductance L_r = 74.10 mH
Two pole machine, synchronous speed 3000 r.p.m.; Rotor voltage 30 V
Maximum allowable continuous stator current 4 A
Maximum allowable continuous rotor current 10 A.

The machine was operated at a stator voltage of 110 V to eliminate saturation of the magnetic circuit as much as possible. In some cases an external rotor resistance of 3Ω per phase was included to shift the speed of maximum torque to standstill.

In fig. 5.19(a) the different parts of the experimental system may be seen. The racks 1 to 4 contain all the information electronic subsystems necessary to operate the systems described schematically in figs. 5.1 to 5.7. The power electronic subsystems are contained in 5, 6, 7, 8 for the said systems. The Generalized Machine operated as an induction machine is shown by 9 and the complementary d.v. machine by 11. The torque-measuring equipment (10) and auxiliary machine (12) are also in evidence. The torque measuring equipment (Satiger Mohilo type 857) functions on the following principle: A high frequency generator feeds a measuring coil on the shaft of the machine via a transformer (10). The magnetic coupling of this coil with a second coil on the shaft is proportional to the torsion in the shaft, and consequently to the torque. The output of the second coil is coupled via a second transformer to the amplifier (13) where it is demodulated and amplified for recording.

The electrical measurements should be executed with some care since the use of conventional equipment may lead to introduction of appreciable errors ([17], especially with wattmeters. Special thermo-electrodynamometer instruments have been developed by *Marek* for our measurements (14). The instruments have an accuracy of 0.5% in the frequency range of 0 Hz to 10 kHz, and of 1.5% in the range 0 Hz to 20 kHz on current, voltage and wattmeter scales.

Experiments on the larger three-phase machine are only reported on briefly in this study, and therefore the experimental set-up will be described shortly. Fig. 5.19(c) depicts the systems. The three phase slip-ring induction machine has the following particulars:

Stator voltage 220/380 V
Stator current 17.8/10.2 A
Rotor voltage 92 V
Rotor current 20,5 A
Power rating 2,95 kW , 955 r.p.m. continuous.

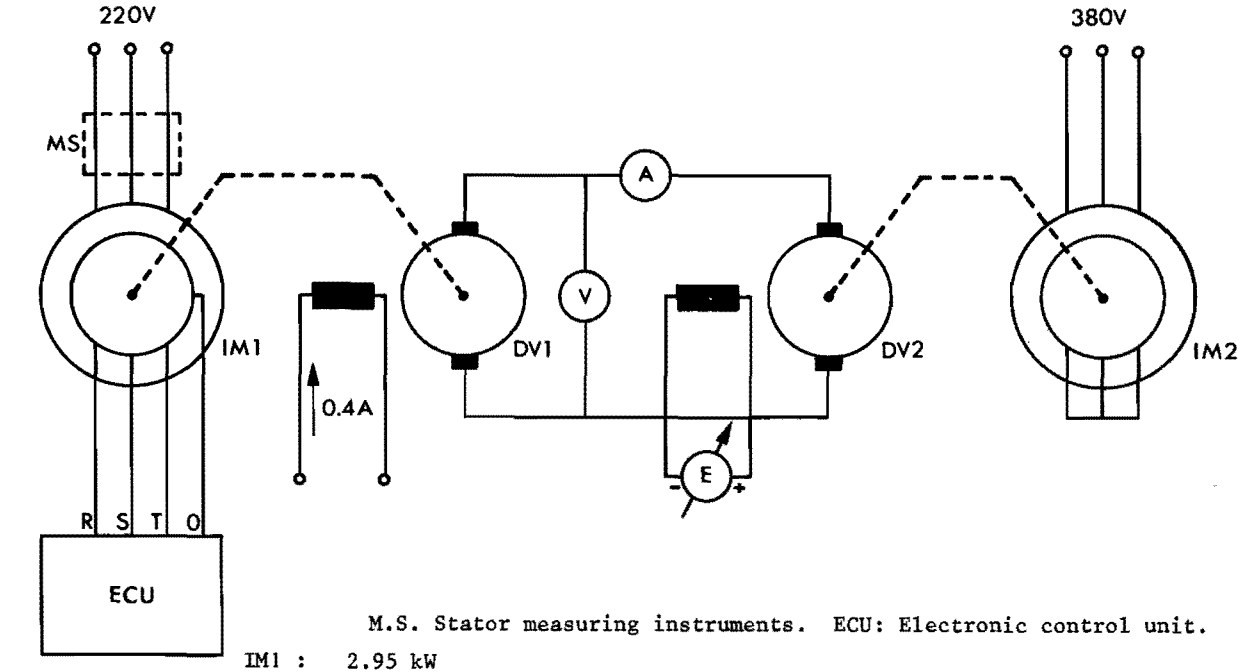

M.S. Stator measuring instruments. ECU: Electronic control unit.

DV1: 2.95 kW, 220 V, 16 A, 1450 r.p.m.

IM1 : 2.95 kW
stator 220/380 V, 17.8/10.2 A
rotor 92 V, 20.5 A
995 r.p.m.

DV2: 6 kW, 220 V, 27.5 A, 1450 r.p.m.

IM2 : 15 kW
stator 380 V, 30 A, 1440 r.p.m.

FIG. 5.18(b) DIAGRAM OF POWER CONNECTIONS FOR THE EXPERIMENTS ON THE THREE PHASE MACHINE.

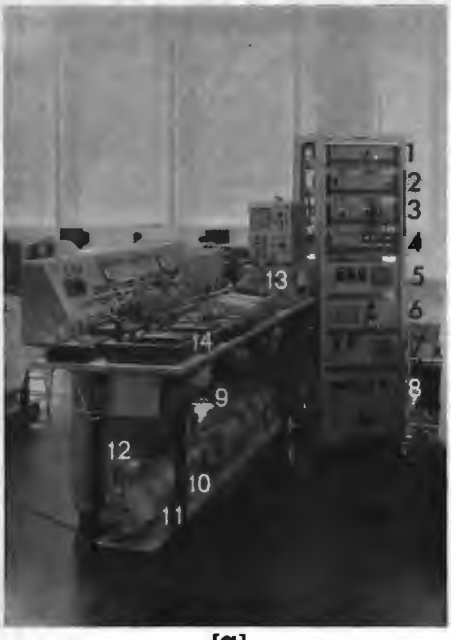

[a]

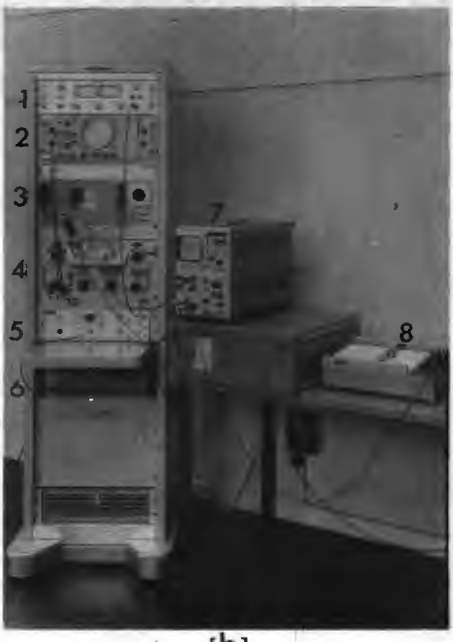

[b]

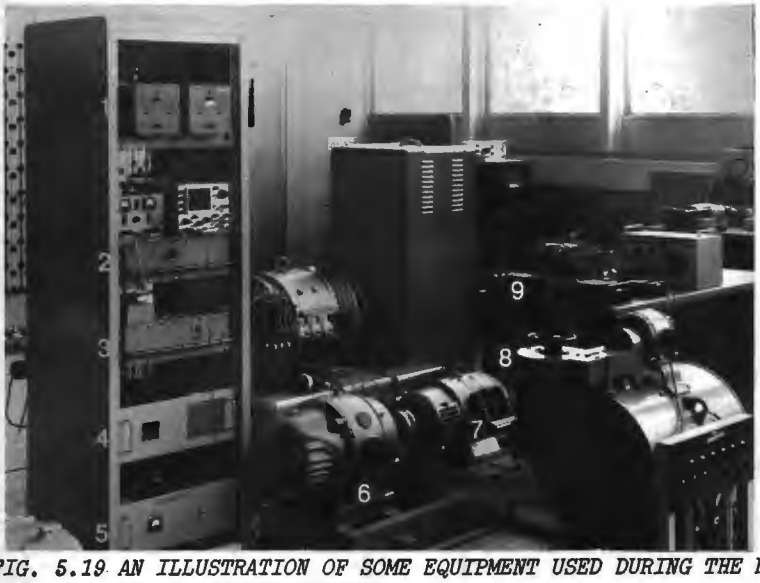

[c]

FIG. 5.19 AN ILLUSTRATION OF SOME EQUIPMENT USED DURING THE EXPERIMENTAL INVESTIGATIONS.

(a) Equipment for experiments on the semi-four-phase machine.

(b) Equipment for determining characteristics of power semiconductor switching elements.

(c) Equipment for experiments on the three-phase machine.

The stator and rotor was connected in star, and in the rotor the neutral point was made accessible through a fourth slip-ring. In order to avoid some of the saturation effects the machine was operated at 220 V line voltage in star, since its magnetizing characteristic indicated that at 380 V the magnetic circuit was already saturated to an appreciable degree.

The induction machine (6) was mounted on the same shaft with the d.v. generator (7) and the flywheel (8). The electronic chopper circuit for operation in electronic Leblanc cascade is incorporated in rack 5 and the information electronic part in 3, while the resistive load for the low-high chopper is indicated by 1. The system for constant α_r-control is comprised by the information-electronics (2) and power-electronics (4) as described.

5.6 SOME OF THE EXPERIMENTAL MEASUREMENTS CONDUCTED ON THE DESCRIBED SYSTEMS.

5.6.1 *TORQUE-SPEED CHARACTERISTICS OF THE SYSTEMS.*

In the previous paragraph the equipment for measuring the shaft torque of the controlled machine has been described. The results of measurements conducted on the machine-electronic systems operating with the Westinghouse Generalized Machine are shown in figures 5.20 to 5.25. During all these measurements the parameter that would be varied when the system is part of a controlled drive, was kept constant, and a torque speed curve recorded.

To obtain a measure of the true electromagnetic torque of the machine the loss torques were plotted in each case. Under these conditions the controlled machine was left unexcited, and the torque-speed curve recorded. This curve may then be taken as a reference line for obtaining the mean electromagnetic torque. As it was in the present case possible to measure the true shaft torque of the machine, it may be expected that the results will be more accurate than when they had been obtained by an indirect method with the complementary machine.

In fig. 5.26 some experimental results obtained on the larger three-phase machine are shown. These results have been obtained through power output of the d.v. generator of the Ward Leonard Ilgner set, and display the same parameter variation as in the case of the semi-four-phase machine. The electromagnetic torque is determined by again recording the system losses with the induction machine unexcited and the power electronic system passive.

5.6.2 *ELECTRICAL CHARACTERISTICS OF SOME SYSTEMS.*

For reasons already discussed, the electrical measurements presented here have been deliberately limited. In fig. 5.21 some examples of measurements on the machine electronic system with α_s-control are given. The measurements cover the case of a low resistance rotor. Effective stator current, power factor, effective rotor current and angle of current extinction is presented as a function of speed.

As will be evident from the calculated characteristics of chapter 4, and from the experimental results, the system for β_r-control or t_{β_r}-

control is able to deliver an electromagnetic torque in excess of the torque of the machine in an uncontrolled state at that specific speed. By choosing a certain value for the control parameter the same torque as in the uncontrolled state may be delivered (i.e. equal mechanical characteristics) and the electrical characteristics may be compared. This may be done from table 5.1 and 5.2.

In chapter 4 it was stated that a motivation for the investigations on the β_r-control (or t_{β_r}-control) is the possibility for power factor compensation. Since the rotor control systems with a switching frequency equal to the rotor frequency known in the past have all used some or other form of ignition delay, the β_r-control system is compared to the α_r-control in table 5.3. It has been assumed that the nominal torque at which the machine will be operated is equal to half the maximum torque for the purposes of this comparison.

Speed r.p.m.	Stator voltage V	Stator current A	Rotor current A	Power factor
0	110.5	4.2	9.8	0.306
300	110.5	4.14	9.7	0.319
2000	110.5	3.55	8.35	0.534

TABLE 5.1

WESTINGHOUSE GENERALIZED MACHINE AS INDUCTION MACHINE

Speed r.p.m.	Stator voltage V	Stator current A	Rotor current A	Power factor
0	109.75	1.22	3.3	0.748
300	109.50	1.24	3.35	0.752
2000	110.75	1.8	4.65	0.883

TABLE 5.2

WESTINGHOUSE GENERALIZED MACHINE WITH ROTOR CURRENT CONTROL BY VARIATION OF EXTINCTION ANGLE - MACHINE CONTROLLED TO GIVE SAME TORQUE AS IN UNCONTROLLED CASE.

	N = 1400 r.p.m. T_e = 0.5 p.u. = 0.25 $T_{max.}$			
	Stator voltage V	Stator current A	Rotor current A	Power factor
α_r-control	109.75	2.39	4.9	0.288 ind.
β_r-control	110	0.835	2.15	0.56 cap.

TABLE 5.3

WESTINGHOUSE GENERALIZED MACHINE. COMPARISON OF α_r-CONTROL AND β_r-CONTROL

5.6.3 *A GENERAL DISCUSSION OF THE EXPERIMENTAL RESULTS - THE ELECTRO-MECHANICAL CHARACTERISTICS.*

5.6.3.1 *Systems for stator control by delay of the triggering angle (α_s-control, $\Delta\alpha_s$-control)*

Consider the torque-speed curves for α_s-control represented in fig. 5.20(a) (no external resistance) and fig. 5.20(b) (for 3Ω external resistance). Examine the results for $\alpha_s = 90^o$ in comparison with the curves of chapter 4, fig. 4.3.2(a) and (b). In both cases it may be seen that the theoretical results depart more or less from experimental measurement. (Theoretical curve indicated by dotted line) Fig. 5.20(a) indicates that from standstill to the slip of maximum torque the theoretical and experimental results differ by a maximum of about 7% - the theoretically calculated torque being higher. As the calculated torque-slip characteristic at full conduction (fig. 5.20(c) also departs from the measured curved in the same sense in this region, it may be concluded that the effects causing this discrepancy are not associated with the control influences, but correspond to the specified values of the linearized machine parameters not describing the electromechanical converter adequately. It should furthermore be realized that the accuracy of torque measurement is judged at approximately 5%. In any event the difference between calculated and theoretical values at slip below the slip of maximum torque is of such an order that it may be concluded that the theory developed in chapter 4 for the stator controlled induction machine describes the machine adequately as far as the torque-speed characteristics (and consequently transfer function) in this region are concerned, when the influence of the "induced excitation components" are neglected. It is extremely significant that the sense in which the calculated torque departs from the measured torque changes in the region of maximum torque. With respect to relation 4.46d it may be seen that all terms of torque originating from the "induced excitation components" involve terms with $1-s$ or $1-s^2$, and consequently it may be expected that these terms will become more important with an increase in speed (or decrease in slip). It should also be remembered

LEGEND TO FIG. 5.20

Recorded on Westinghouse Generalized Machine as specified in the text.

(a) Stator α-control.
No external resistor.

1. Rotor short circuit.
2. $\alpha_s = 45^o$
3. $\alpha_s = 54^o$
4. $\alpha_s = 63^o$
5. $\alpha_s = 72^o$
6. $\alpha_s = 90^o$
7. $\alpha_s = 108^o$
8. $\alpha_s = 126^o$
9. $T_e^s = 0$

(b) Stator α-control.
External rotor resistor 3Ω/phase.

1. Rotor short circuit.
2. $\alpha_s = 54^o$
3. $\alpha_s = 63^o$
4. $\alpha_s = 72^o$
5. $\alpha_s = 90^o$
6. $\alpha_s = 108^o$
7. $\alpha_s = 126^o$
8. $T_e^s = 0$

(c) Stator Δα-control.
No external resistor.

1. Rotor short circuit.
2. $\Delta\alpha_s = 9^o$
3. $\Delta\alpha_s = 18^o$
4. $\Delta\alpha_s = 36^o$
5. $\Delta\alpha_s = 54^o$
6. $\Delta\alpha_s = 72^o$
7. $\Delta\alpha_s = 90^o$
8. $T_e^s = 0$

(d) Stator Δα -control.
External rotor resistor 3Ω/phase.

1. Rotor short circuit.
2. $\Delta\alpha_s = 9^o$
3. $\Delta\alpha_s = 18^o$
4. $\Delta\alpha_s = 36^o$
5. $\Delta\alpha_s = 54^o$
6. $\Delta\alpha_s = 72^o$
7. $\Delta\alpha_s = 90^o$
8. $T_e^s = 0$

(e) Comparison of steady state, uncontrolled electromagnetic torque to theoretically calculated values.

1. Measured torque-speed curve, rotor short circuited, no external resistor.
2. Calculated with values of (3), R_r compensated to

$$R_r = 0.83\ \Omega/\text{phase}$$

3. Calculated with $R_r = 0.75\Omega$
$R_r^s = 2.86\Omega$
$M_{sr}^s = 170.5$ mH
$L_s = 472$ mH
$L_s^r = 74.1$ mH
$U_{sg}^r = 110$ V

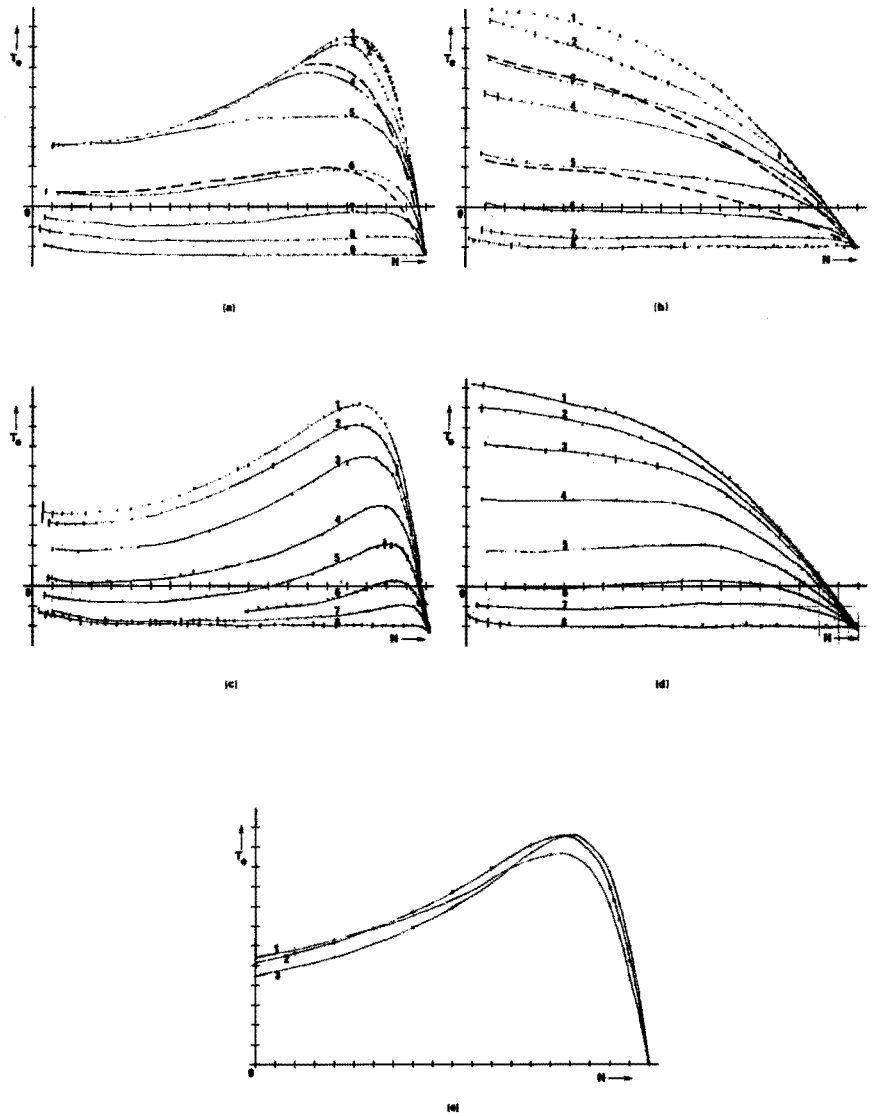

FIG. 5.20 EXPERIMENTAL TORQUE-SPEED CHARACTERISTICS OF SOME SYSTEMS WITH CONTROL OF THE INSTANT OF CURRENT IGNITION IN THE STATOR CIRCUIT OF AN INDUCTION MACHINE.

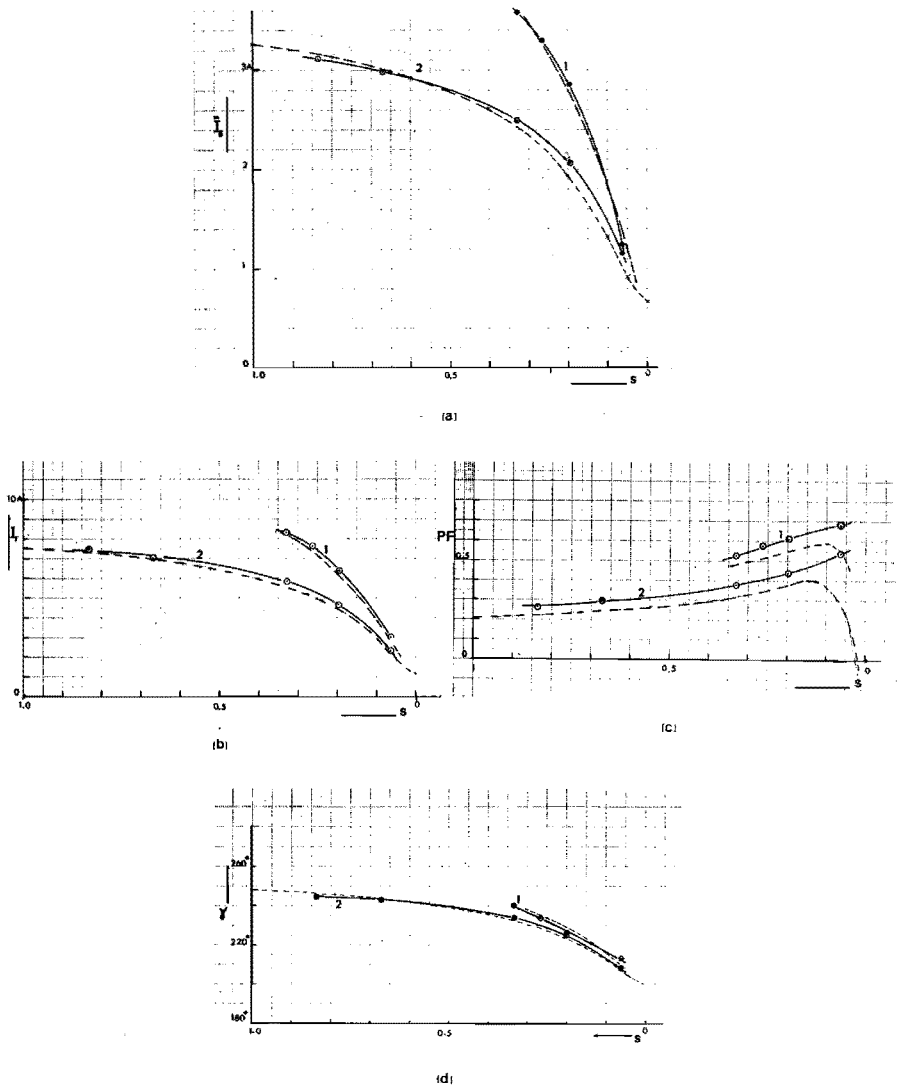

(a) Effective stator current as a function of slip.
(b) Effective rotor current as a function of slip.
(c) Power factor as a function of slip.
(d) Angle of natural commutation as a function of slip.
In all cases the curves indicated by a broken line represent calculated values.

FIG. 5.21 COMPARISON OF SOME MEASURED AND CALCULATED ELECTRICAL CHARACTERISTICS OF α_s-CONTROL.
1 : $\alpha_s = 63^o$; 2 : $\alpha_s = 90^o$.

that the amplitude of these components as well as the phase relationship show a complicated interdependence as a function of slip. All these effects combine to result in the difference between experimental and calculated results found in the region of low slip. From fig. 5.20(a) it may be seen that for small torques these results may depart by as much as 40% for $\alpha_s=90^o$. As shown by studying the results for $\alpha_s=63^o$ (which gives a torque of the order of the uncontrolled torque) this discrepancy becomes less with decreasing control angle. This may be expected, since the "induced excitation" then acts for a shorter time, and the influence of harmonic components reduces due to the currents approaching a sinusoidal waveform.

When the case of a high resistance rotor is now studied, the effects noted in the region above maximum torque should be much more in evidence, since this region is "expanded" from zero slip to standstill. The remarks made above may therefore be seen to hold for fig. 5.20(b). It may be seen clearly how the influence of the "induced excitation" components gradually increases with decreasing slip, to reduce again in the region near synchronous speed. At smaller control angles ($\alpha_s = 63^o$) it is evident how the discrepancy decreases. For $\alpha_s=63^o$ it is not more than 20%, which again makes the results quite useful. As pointed out in the discussion of the calculated characteristics in chapter 4, *Takeuchi*[9] has employed a method of calculation for the characteristics of a single phase induction machine that may be seen as another specialized case of the general theory developed in chapter 3. From the present observations it does not appear that one can support his view that the "induced excitation" components can be neglected, especially in the case of high-resistance rotors having a low speed at which maximum torque occurs. What has most probably made the results of Takeuchi, and the present results for a high resistance rotor, agree reasonably with the measured results is the influence of the rotor time constant on the induced e.m.f. as investigated extensively in appendix 4 and in chapter 4. The extent of all these influences unfortunately prohibit a minute experimental investigation for the present.

An examination of the experimental torque-speed curves of fig. 5.20 (c) and (d) indicates the important difference between α_s-control and $\Delta\alpha_s$-control, as pointed out theoretically in chapter 4. These two machine-electronic systems will have the same electrical characteristics when operated at the same mechanical conditions. Their transfer characteristics during application for control purposes may be seen to differ appreciably, however. The similarity between fig. 5.20(b) and (d) indicates that the difference again occurs chiefly at slips in excess of the slip of maximum torque. Relation 4.8b indicates that in this case the triggering angle α_s is a function of the extinction angle γ_s. Calculations and subsequent experimental results indicate that the extinction angle γ_s increases appreciably only for slips in excess of the slip of maximum torque, so that the difference between the characteristics of fig. 5.20 (a), (b) and (c), (d) may be considered to be explained. It has been stressed in chapter 4 that halfwaving instability can occur with α_s-control under some triggering conditions, but not with $\Delta\alpha_s$-control. As expected this was also found during the experimental recording of the characteristics of fig. 5.20. The halfwaving instability only occurs for the control angles obeying the condition that for some or other slip the angle becomes less than the

LEGEND TO FIG. 5.22

Recorded on Westinghouse Generalized Machine as specified in the text.

(a) α_r-control. No external rotor resistor.

1. Rotor short circuit
2. $\alpha_r = 45^o$
3. " $= 54^o$
4. " $= 63^o$
5. " $= 72^o$
6. " $= 85^o$
7. " $= 90^o$
8. " $= 99^o$
9. " $=120^o$
10. $T_e = 0$

(b) α_r-control. External resistor of 3 Ω/phase.

1. Rotor short circuit
2. $\alpha_r = 30$
3. " $= 54$
4. " $= 63$
5. " $= 72$
6. " $= 85$
7. " $= 90$
8. " $= 99$
9. " $=120$
10. $T_e = 0$

(c) Δt_{α_r}-control. No external rotor resistor. Triggering by pulse train.

1. Rotor short circuit
2. $\Delta t = 370$ µs
3. " $= 1$ ms
4. " $= 2$ ms
5. " $= 3$ ms
6. " $= 4$ ms
7. " $= 5$ ms
8. " $= 6$ ms
9. " $= 7$ ms
10. " $= 8$ ms
11. " $= 9$ ms
12. " $= 10$ ms
13. $T_e = 0$

(d) Δt_{α_r}-control. External resistor of 3Ω/phase. Triggering by pulse train.

1. Rotor short circuit
2. $\Delta t = 370$ µs
3. " $= 1$ ms
4. " $= 2$ ms
5. " $= 3$ ms
6. " $= 4$ ms
7. " $= 5$ ms
8. " $= 6$ ms
9. " $= 7$ ms
10. " $= 8$ ms
11. " $= 9$ ms
12. " $= 10$ ms
13. $T_e = 0$

(e) Δt_{α_r}-control, no external rotor resistor; monopulse triggering; 370 µs omitted, otherwise corresponding with (c).

(f) Δt_{α_r}-control. External resistor of 3Ω/phase; monopulse triggering; 370 µs omitted, otherwise corresponding with (d)

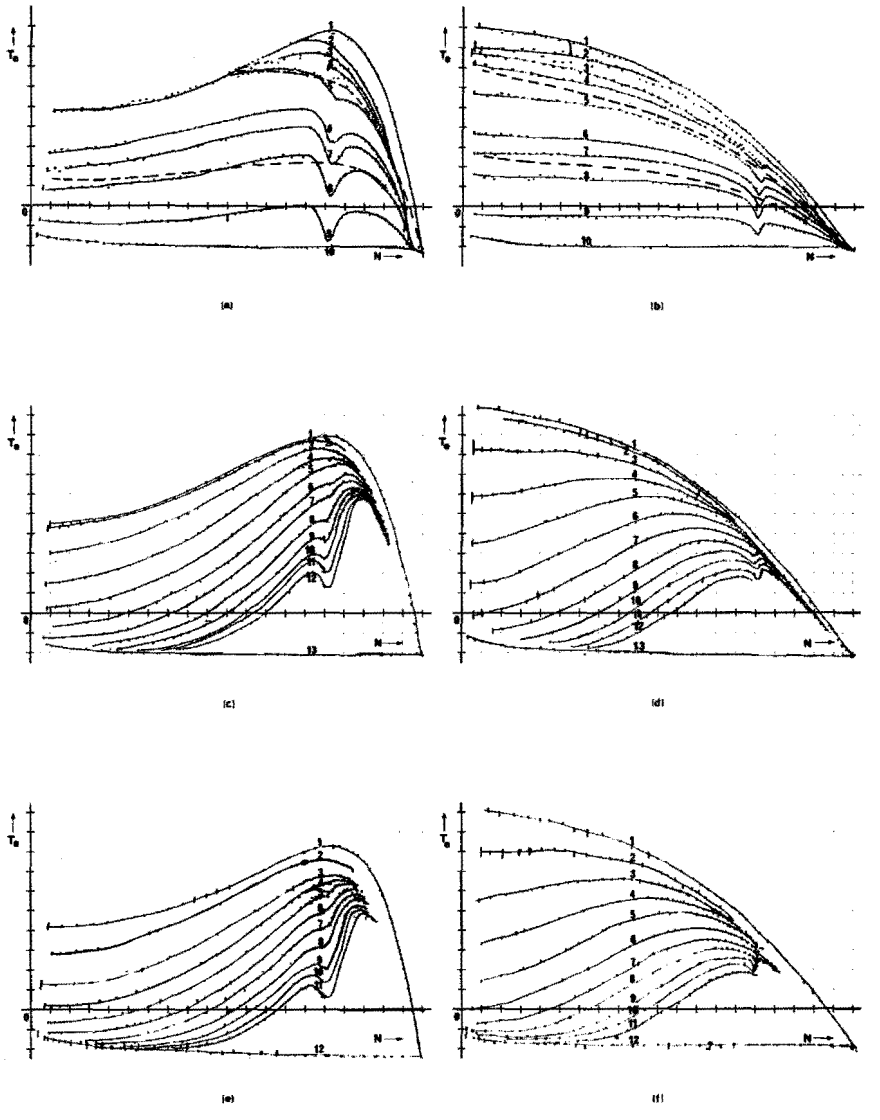

FIG. 5.22 EXPERIMENTAL TORQUE-SPEED CHARACTERISTICS OF SOME SYSTEMS WITH CONTROL OF THE INSTANT OF CURRENT IGNITION IN THE ROTOR CIRCUIT OF AN INDUCTION MACHINE.

steady-state phase angle of the machine. As these types of effects have been reported on elsewhere [80] they will not be discussed further at present.

5.6.3.2 *Systems for rotor control by delay of the triggering instant (α_r-control, Δt_{α_r}-control).*

For a comparison of the theoretical and experimental results one should refer to the figures 4.6 and 5.22. As in the previous case all experimental curves has again been recorded for the two cases of low (internal) rotor resistance and an external resistor of 3Ω per phase.

In chapters 3 and 4, where the methods for simplified calculation concerning these systems were developed, it was stressed that this type of model may only be used to obtain an approximate insight into the expected mechanical and electrical characteristics of the system. The experimental results bear out this presumption, since the torque-speed curves correspond in nature to the calculated curves in both cases. In fig. 5.22(a) and (b) the calculated results for $\alpha_r=63^o$ and $\alpha_r=90^o$ have again been represented by broken lines. From fig. 5.22(a) it follows that for $\alpha_r=90^o$ the agreement between theoretical and experimental results is always better than about 20% in the regions where the influence of the harmonic torque causing the "saddles" may be neglected. Seeing the simplified theory this agreement is good. In the present instance the correspondence between theoretical and experimental results need not necessarily decrease as the angle of control increases. Although it is true that the percentage of harmonics will increase in relation to the fundamental current, it should also be kept in mind that the currents decrease, and the departure of the induced rotor e.m.f. from the assumed simple harmonic time function need not become worse. The two effects are acting opposite to each other. This corresponds to the results of the measurements, since fig. 5.22(a) indicates that correspondence is the same for $\alpha_r=63^o$ and $\alpha_r=90^o$.

With a high rotor resistance calculations agree to within 10% for $\alpha_r=63^o$ and to within 15% for $\alpha_r=90^o$. This indicates that especially in the case of a high resistance rotor the developed methods of calculation may be used to good effect.

During the theoretical discussions of chapter 4 (paragraph 4.3.1.1) it was pointed out that when the voltage across the electronic switch is integrated to derive the switching commands (constant integral delay) a type of characteristic corresponding to the $\Delta\alpha_s$-control will be obtained. However, when the system has Δt_{α_r}-control the slip dependence of the triggering angle should impart unpleasant characteristics to the described system. From fig. 5.22(c) and (d) recorded for this type of system this is immediately evident. It may be seen that for an increasing delay time the slip of maximum torque increases, while the curve rises more steeply towards its maximum. This characteristic is more clearly evident from fig. 5.22(d), where the first part of the torque-slip curve is again "expanded". In control applications these types of characteristics will be a definite disadvantage as compared to the α_r-control or the integral-delay control.

In the practical system investigated the triggering instability was again found to be significant. As it concerns an effect not previously discussed, some attention will be devoted to its explanation.

From oscillogram OS2 it may be seen that at low slip the induced e.m.f. waveform of the rotor contains an important contribution of tooth harmonics. This is not an effect peculiar to the Westinghouse Generalized Machine, but common to induction machines with wound rotor. If the semiconductor switches (thyristors or triacs) are now excited by a short pulse (approximately 200 μsec), and the angle of ignition becomes small (low slip) the voltage may be negative for the duration of the triggering pulse due to the tooth harmonics, and the element will not conduct during the cycle (figure 5.22(e) and (f)). The extension of the range of operation obtained by addition of a pulse-train (or carrier-frequency) triggering unit may be seen from a comparison of figure 5.22 (c) with figure 5.22(e), or of figure 5.22(d) with figure 5.22(f). Oscillograms OS17 and OS18 display the pulse train used.

In the torque-speed curves of fig. 5.22 two peculiar effects may be noted. In the first instance a torque saddle at a slip between s=0.2 and s=0.3 is in evidence. Since the model for calculation of the torques has assumed zero stator resistance of the machine, harmonic torques cannot be predicted. It will later be shown that this torque is due to the third harmonic rotor current generated by switching. Such effects may be eliminated in three phase systems. Secondly it may be seen in fig. 5.22(a) and fig. 5.22(b) that the torque reduces to zero in all cases before synchronous speed is reached. This is due to the voltage drop of the semiconductor switches. In the present case the rotor voltage at zero speed is 39 V, and this effect is much more pronounced as compared to what may be expected in practical machines. Theoretical investigations of this effect not included in this thesis has indicated that the type of control and type of triggering unit also influence this characteristic.

5.6.3.3 *Systems for rotor control by delay of the instant of current extinction - a system for t_{β_r}-control.*

The different alternatives for deriving the switching commands for a system with current extinction control have been discussed in chapter 4. The experimental system having the characteristics of fig. 5.23(a) and (b) use control by constant time of current conduction since the angle of ignition is zero. Due to the slip-dependence of the conduction angle contained in equation 4.62 it was expected that the torque should decrease with decreasing slip. The experimental curves of fig. 5.23(a) and (b) indicate this to be true.

As in the case of the control by delay of the ignition instant it may be concluded that the assumed model describes the nature of the characteristics adequately. By a comparison of fig. 4.8 with the above-mentioned results the correspondence may be studied. The broken lines in fig. 5.23 (a) and (b) again represent the calculated results for t_β=10msec. in the present case. Experimental values for the torque prove to be about 30% higher than the calculated values for the same t_β in the case of a low rotor resistance. Correspondence is some 30% in the case of a high rotor resistance as depicted in fig. 5.23(b).

For this departure of the experimental values from those calculated by means of the proposed simplified model of chapter 4, a good reason may be advanced. It was already remarked previously that it is not possible to interrupt the rotor current in the inductive rotor circuit

LEGEND TO FIG. 5.23

Recorded on Westinghouse Generalized Machine as specified in the text.

(a) t_{β_r} -control. No external resistor.

1. t_{β_r} = 4 ms
2. " = 5 ms
3. " = 6 ms
4. " = 7 ms
5. " = 8 ms
6. " = 9 ms
7. " = 10 ms
8. " = 12 ms
9. " = 14 ms
10. " = 18 ms
11. " = 20 ms
12. " = 30 ms
13. " = 40 ms
14. Switch continuously conducting.
15. T_e = 0

(b) t_{β_r} -control. 3 external resistor/phase.

1. t_{β_r} = 4 ms
2. " = 5 ms
3. " = 6 ms
4. " = 7 ms
5. " = 8 ms
6. " = 9 ms
7. " = 10 ms
8. " = 12 ms
9. " = 14 ms
10. " = 20 ms
11. " = 40 ms
12. Switch continuously conducting.
13. T_e = 0

(c)
1. Rotor short circuit
2. Same, with resistance of power switch.
3. Previous with effect of semiconductor voltage drop.
4. Switch continuously conducting.
5. Same as 4, with capacitor C_c disconnected.
6. T_e = 0

(d)
1. Rotor short circuit.
2. Effect of voltage drop of bridge and main thyristor.
3. 2 Diodes in series with main thyristor (T_m).
4. 5 Diodes in series with main thyristor.
5. T_e = 0.

LEGEND TO FIG. 5.24

(a)
1. α_i = 12.1°
2. " = 48.6°
3. Inverter short circuited.
4. α_i = 72.4°
5. " = 90.0°
6. " = 104.6°
7. " = 110.4°
8. " = 115.8°
9. " = 122.4°
10. Limit of continuous current
11. T_e = 0

(b)
1. Rotor circuit shorted at output of rectifier.
2. Rectifier loaded with smoothing inductor, R=0.43Ω
3. Rectifier loaded with smoothing inductor, R=2.84Ω
4. T_e = 0

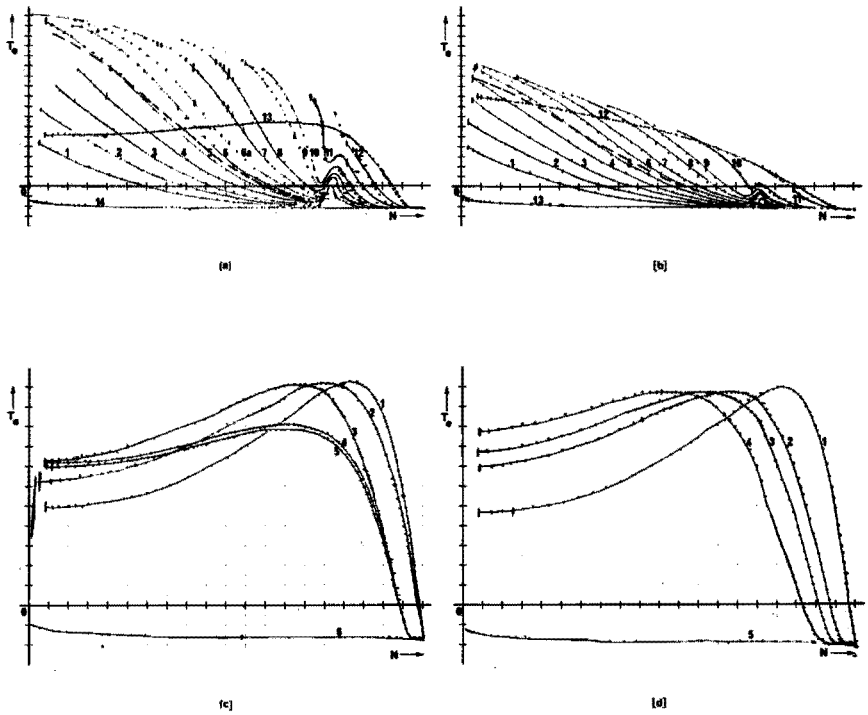

FIG. 5.23 EXPERIMENTAL TORQUE-SPEED CHARACTERISTICS OF SOME SYSTEMS WITH CONTROL OF THE INSTANT OF CURRENT EXTINCTION IN THE ROTOR CIRCUIT OF AN INDUCTION MACHINE.

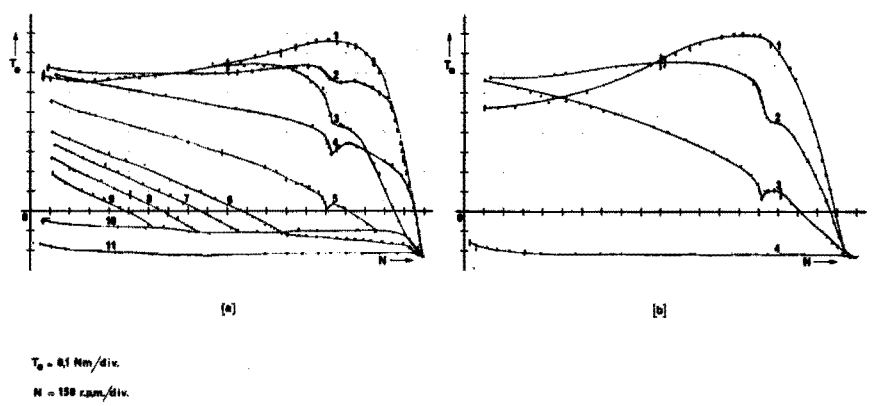

FIG. 5.24 EXPERIMENTAL TORQUE-SPEED CHARACTERISTICS CONCERNING AN ELECTRONIC SCHERBIUS CASCADE.

instantaneously. After a commutation command has been given to the rotor electronic switch a certain time elapses before the rotor current has been reduced to zero. This has been explained in Part I of the present chapter. The actual effective rotor current flowing in the case investigated will be larger than expected on theoretical grounds for a given angle at which commutation is commenced. The time during which the rotor current flows after commutation has been initiated will be termed "excess time".

It may now be shown theoretically - and proved experimentally - that this excess time increases as the angle of current extinction β_r is decreased. Decrease of β_r decreases the initial current at which the commutation process of the rotor current is started, and due to the phase considerations mentioned in Part I of this chapter as an explanation of the reduction of the circuit turn-off time of an electronic switch (paragraph 5.3), the excess time increases. It may therefore be expected that the model used for calculations will become less suitable as the angle of current control decreases. This proves to be the case in practice. Furthermore reference to the oscillograms OS21 and OS22 indicate an excess time from 1 to 2 msec. for $t_{\beta_r} \approx 8$ msec. Referring to fig. 5.23(a) and (b) it may be seen that the theoretical curve for $t_{\beta_r} = 10$ msec. corresponds much better to an experimental curve of $t_{\beta_r} = 8$ msec or $t_{\beta_r} = 9$ msec., as is to be expected from the preceding discussion.

Some interesting characteristics may be obtained from the system. As predicted theoretically the system can deliver a much higher torque than the uncontrolled machine. In the motoring region of the induction machine the maximum torque occurs at zero speed. This does not represent the maximum electromagnetic torque of the system - the torque increases with slip. If the torque at stalling be related to the maximum value of the torque of the uncontrolled machine, a ratio of 1.65 is obtained theoretically. Experimentally this ratio has been found to be 2.4 (fig. 5.23). The discrepancy between the two values may again be mainly ascribed to the excess time. As predicted in the discussion of the theoretical calculations the system is capable of delivering this torque because of the increased current flow possible through the "repetitive surge" nature of the current, and because of the improved-capacitive - power factor. This corresponds with the experimental results, since a higher rotor resistor results in lower torques in the motoring region, and a lower ratio of maximum torque at standstill to maximum torque in uncontrolled condition. Theoretical and experimental values for this ratio are 1.18 and 1.47 respectively.

In the forced commutation switch employed to switch off the rotor current semiconductor-elements and inductors are included in the main current path, as described in the first part of this chapter. This not only introduces an extra voltage drop into the rotor circuit, but also adds resistive and inductive effects to the rotor. Fig. 5.23(c) and (d) indicate these effects. In fig. 5.23(c) curve 1 represents the shorted rotor circuit, curve 2 the resistive effects of the power switch components without semiconductor-elements and inductive effects. Curve 3 indicates how the torque-speed relation is affected by the semiconductor voltage drops, while for curve 4 the inductive effects of the power switch are added. It should be kept in mind that these inductive influences will be somewhat different from the present steady state influence with the electronic switch operating - as follows from

the discussion of the operation of the switch presented previously. Fig. 5.23(d) represents the influence of adding several semiconductor elements in series.

From fig. 5.23(a) and (b) the influence of harmonic torques due to the rotor switching may be seen to be very pronounced between s=0.2 and s=0.3. This will be discussed subsequently.

5.6.3.4 *Systems for rotor control by a low-high chopper circuit with resistive load (electronic Leblanc cascade) and with inverter load (compensated electronic Scherbius cascade).*

In the discussion of the systems with rotor chopper control presented in chapter 4 it was pointed out that under certain assumptions one may expect to find the torque to be only a function of the rotor current. These assumptions were:

(i) rectifier output current approaches a perfect d.c.
(ii) commutation effects in the rotor rectifier neglected.

It will now be investigated how these predictions of the simple model corresponds with the practical results, since it may not reasonably be expected that the assumed conditions will always be fulfilled.

During theoretical investigation of these systems it was assumed that the input current to the electronic chopper circuit (output current of the rotor rectifier) will be varied by changing the current ratio k_R at a constant current difference, or by changing the current difference Δi at a constant current ratio. Let the experimental torque-speed curves of fig. 5.25(c) and (e) be examined. The first has been recorded with constant current ratio, the second with constant current difference. If harmonic torques are neglected, the torque remains constant to within about 5% over the whole control range. The small change experienced may be ascribed to the neglected commutation effects in the rotor rectifier and the departure of the chopper current from a constant mean value with fixed current levels, as shown in figures 4.13(a) and 4.13(b). In these cases the current difference was approximately 1 A in fig. 5.25(e). For these values of Δi the assumptions of the simplified model are still valid.

According to fig. 4.13(d) the most linear relationship between control parameter (Δi in this case) and the torque may be expected when Δi is varied at a constant current ratio k_R. A study of the experimental results of fig. 5.25(d) indicates that this can have unpleasant consequences due to harmonic torques and unbalanced currents. In the first instance Δi increases with increasing current, causing an increased content of harmonic torques upsetting the linear relation between rotor current and torque. Secondly, at large Δi interference between the chopper switching and rotor-synchronous rectifier switching gives rise to asymmetrical rotor currents, causing large torque saddles at s=0.5 (fig. 5.25(d)). The unbalance effect is further illustrated by fig. 5.25(b) for a constant value of Δi, where it may be clearly seen that the unbalanced torque does not decrease with decreasing rotor current, due to the constant value of Δi (Δi = 4.6 A). In all the curves the influence of the harmonic torque between s=0.2 and s=0.3 may again be seen.

LEGEND TO FIG. 5.25

Recorded on Westinghouse Generalized Machine as specified in the text $R_h = 11.5\ \Omega$.

(a) Electronic Leblanc cascade. Δi constant, k_R variable.

1. Chopper continuously conducting.
2. i_{01} = 9.0 A , i_{02} = 6.6 A
3. " 8.0 " 5.6
4. " 7.2 " 4.8
5. " 6.4 " 3.8
6. " 5.4 " 3.0
7. " 4.6 " 2.1
8. " 3.6 " 1.0
9. R_h-line
10. $T_e^h = 0$

(b) Electronic Leblanc cascade. Δi constant, k_R variable.

1. Continuous conduction.
2. i_{01} = 9.0 A , i_{02} = 4.4 A
3. " 8.0 " 3.4
4. " 7.2 " 2.8
5. " 6.2 " 1.6
6. R_h-line
7. $T_e^h = 0$

(c) Electronic Leblanc cascade. k_R = constant, Δi variable.

1. Chopper continuously conducting.
2. i_{01} = 8.9 A , i_{02} = 6.5 A
3. " 6.9 " 5.0
4. " 5.8 " 3.9
5. " 4.9 " 3.1
6. " 4.2 " 2.9
7. " 3.5 " 2.2
8. R_h-line
9. $T_e^h = 0$

(d) Electronic Leblanc cascade. k_R = constant, Δi variable.

1. Continuous conduction.
2. i_{01} = 12.4 A , i_{02} = 6.0 A
3. " 9.0 " 4.2
4. " 7.0 " 3.2
5. " 5.8 " 2.6
6. " 4.9 " 2.1
7. " 4.3 " 1.8
8. " 3.7 " 1.5
9. " 3.4 " 1.3
10. R_h-line
11. $T_e^h = 0$

(e) Electronic Leblanc cascade. Δi=constant, k_R variable.

1. Continuous conduction.
2. i_{01} = 8.4 A , i_{02} = 7.8 A
3. " 8.0 " 7.0
4. " 7.0 " 6.1
5. " 6.2 " 5.2
6. " 5.4 " 4.4
7. " 4.7 " 3.5
8. " 3.6 " 2.6
9. " 2.7 " 1.5
10. " 1.8 " 0.6
11. R_h-line
12. $T_e^h = 0$

(f) Compensated electronic Scherbius cascade. Δi= constant, k_R variable.

1. Continuous conduction.
2. i_{01} = 8.4 A , i_{02} = 7.8 A
3. " 8.0 " 7.0
4. " 7.0 " 6.1
5. " 6.2 " 5.2
6. " 5.4 " 4.4
7. " 4.7 " 3.5
8. " 3.6 " 2.6
9. " 2.7 " 1.5
10. " 1.8 " 0.6
11. $T_e = 0$

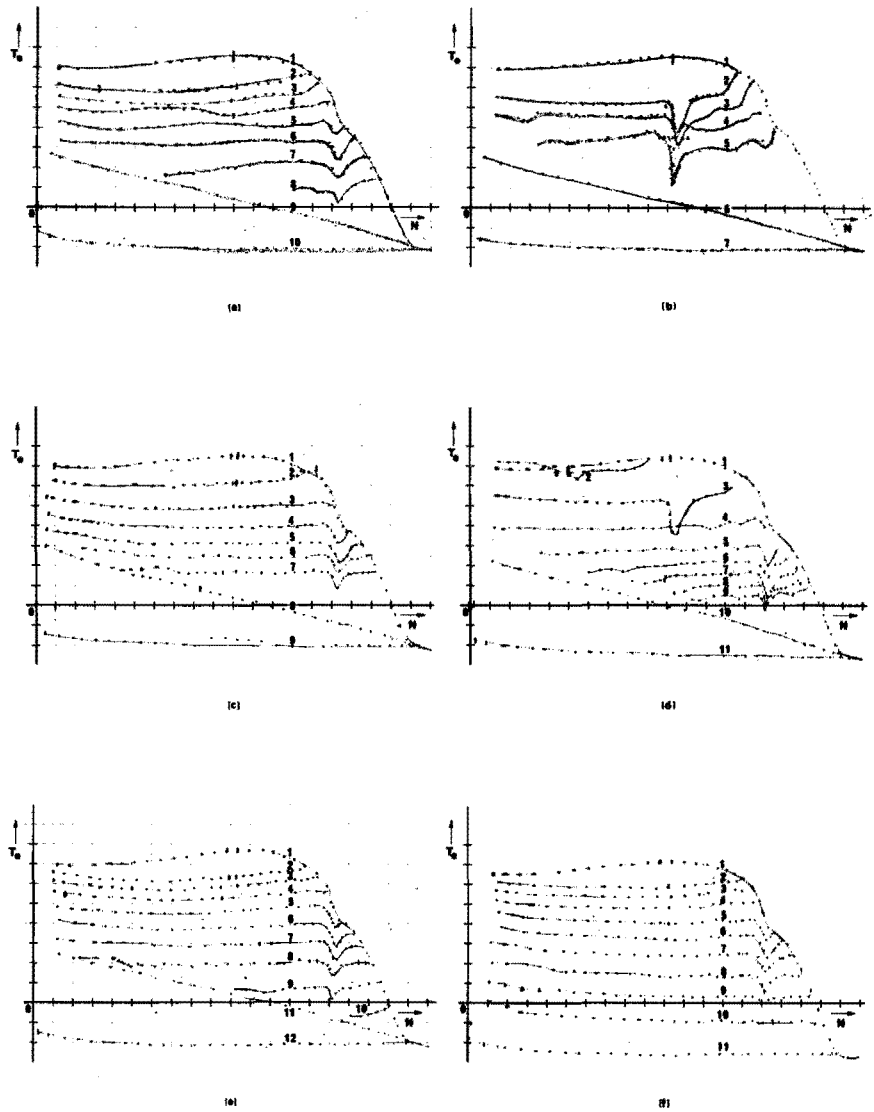

FIG. 5.25 EXPERIMENTAL TORQUE-SPEED CHARACTERISTICS CONCERNING AN ELECTRONIC LEBLANC CASCADE AND A COMPENSATED ELECTRONIC SCHERBIUS CASCADE.

It may therefore be concluded from the above observations that although fig. 4.13(c) indicates that variation of k_R at a constant Δi results in a relationship between control parameter and torque that departs more from linearity than the variation of Δi at constant k_R does, the practical effects in the machine pose directly opposing requirements, tending to restrict the range of application of Δi-control very much. This will be discussed further with the aid of some included oscillograms later.

In all the torque-speed curves presented in fig. 5.25(a) to 5.25(e) it may be seen that the torque-speed curve with the resistive load of the chopper as a rotor resistor forms the limit of the control range. Let the experimental results for the compensated electronic Scherbius cascade as represented in fig. 5.25(f) now be regarded.The different curves have been recorded with the parameter settings as used for the constant Δi curves of fig. 5.25(e), and it may be seen that there is a negligible difference between the curves. As expected in the course of the simplified theoretical investigations the influence of the chopper/rectifier combination should be identical on the machine in both cases when the assumptions of chapter 4 hold. This appears to be the case from 5.25(f). The only differences between the electronic Leblanc and compensated electronic Scherbius cascades are electrical, and this cannot be presented in the torque-speed curves.

It may furthermore be noted that for the lower rotor currents where chopper operation was limited by the rotor resistance line in the case of the electronic Leblanc cascade, the operation as a compensated electronic Scherbius cascade allows control over the entire torque and speed range.

All experimental torque-speed relations of fig. 5.25 display the same influence of semiconductor voltage drop and inductive effects of the power switch experienced previously for other systems.

5.6.3.5 *An electronic Scherbius cascade (Westinghouse Generalized Machine).*

Fig. 5.24(a) and (b) show some results obtained on an electronic Scherbius cascade system as described. In the theoretical discussion of chapter 4 certain assumptions regarding output current of the rotor-rectifier and commutation effects in the rectifier had been made. Fig. 5.24(b) now indicates the influence of two different smoothing inductors in the rectifier output. In both these cases the inverter for feeding back the slip power was short-circuited, while curve 1 represents the torque-speed curve with a short circuit across the output of the rectifier. In all these curves the influence of the semiconductor voltage drop may be observed.A comparison of the curves indicates how the inclusion of the inductor in the rectifier output, and the consequent change in input current waveform, changes the phase-dependence of the active power in the rotor circuit. The resistance of the inductor employed for recording curve 3 was the higher of the two.

In fig. 5.24(a) the curve for a shorted inverter circuit (curve 3) is again reproduced. With reference to relation 4.86 it may be concluded that the system functioned as follows. Let curve 6 be considered. If the resistive voltage drop is small in comparison with the back-e.m.f. of the inverter, the torque will be proportional to the rotor

where $\frac{d\theta_r}{dt}$ gives the speed of rotation of a specific harmonic field with respect to the rotor body. This field may arise due to interaction of time-harmonic currents with space-harmonics of the MMF distribution. An investigation of the possible interactions between space and time harmonics that could give rise to the observed distortion now results in the following comparative table.

Order of space harmonic	Order of time harmonic	$\left(\frac{d\theta_r}{dt}\right)$	$s_o^{\nu_{sr}}$
1	3	-3	0.25
3	5	-5/3	0.375
3	9	-3	0.25
5	11	-11/5	0.31
7	13	-13/7	0.35

TABLE 5.4

REGARDING HARMONIC TORQUES DUE TO ROTOR CONTROL OF THE SEMI-FOUR-PHASE MACHINE.

When it is now considered that the armature winding of the rotor of the Westinghouse Generalized Machine is of such a nature that approximately 9% of third space harmonic may be expected, a consideration of the torque distortion in the said figures results in the identification of the harmonic fields.

It may be concluded that the distortion is due to rotor-stator asynchronous torques arising from third order harmonics of the rotor current. Interaction between space harmonics of order three and time harmonics of order nine also seems possible, since this field has a synchronous speed fitting the experimental measurements. However, as the amplitude of the 9th harmonic will be negligible in comparison to the third, this interaction should in any case be responsible for a much smaller contribution to the distortion than that contributed by the third harmonic. From the torque-speed curves it may additionally be concluded that the α_r-control and t_{β_r}-control systems result in an appreciable third order time harmonic current content in the rotor of the Westinghouse Generalized Machine.

5.6.3.7 α_r *Control and electronic Leblanc cascade with a three-phase machine.*

In the description of the experimental equipment it was mentioned

current. For a given value of α_i the mean back-e.m.f. will be constant ($\alpha_i = 104.6^{o}$) in this case. Assuming that the d.c. in the intermediary rectifier circuit (and consequently the effective rotor current I_r) is determined by the difference between mean rectified rotor e.m.f. and mean inverter back e.m.f., it follows that this current will reduce linearly with decreasing slip. This results in a linearly decreasing torque with decreasing slip (curves 4, 5, 6, 7, 8, 9).

When the control angle of the feed-back inverter is reduced below the value at which the electronic circuit absorbs power from the rotor circuit, the power flow is reversed. However, as soon as the reversed direct output voltage of the inverter circuit exceeds the sum of the resistive voltage drop in the intermediary circuit and the semiconductor voltage drop in the rotor rectifier bridge circuit, a current will be circulated through the rotor rectifier bridge, and the induction machine will experience this as a shorted rotor circuit, as exemplified by curves 1 and 2.

In the discussion in chapter 4 it was stated clearly that the current through the intermediary d.c. circuit of the electronic frequency changer should be continuous. When this is not the case, the operating mode of the inverter will change (B15 - with various consequences. While it is not the intention to examine these consequences in detail - they have also not been investigated in the text - it is still interesting to note the change taking place in the characteristics in fig. 5.24(a) at this"discontinuous current limit". Refer to curve 6, where it may be seen that as soon as it crosses curve 10 which marks this limit, the relationship changes.

5.6.3.6 *Considerations concerning harmonic torques in the systems employing the semi-four-phase machine.*

In the model of the electromechanical converter as used throughout chapters 2, 3 and 4, and stated explicitly in chapter 3, no consideration has been given to space harmonics of the current distribution on stator or rotor. Now it has been observed that all the torque-speed curves recorded in figures 5.22, 5.23, 5.24 and 5.25 for machine-electronic systems with rotor control of the semi-four-phase machine indicate a distortion of the "fundamental" torque-speed relation in the slip region:

$$0.2 < s < 0.3 \qquad 5.32a$$

The distortion resulting from operating the electronic chopper circuit in the electronic Leblanc cascade or in the compensated electronic Scherbius cascade in a mode with large Δi is excluded from the following consideration.

In the course of the power flow discussions of chapter 2 the harmonic torques resulting from switching action in the rotor circuit were considered. From relation 2.14e it may be noted that

$$s_0^{\nu sr} = \frac{1}{\left(1 - \frac{d\theta_r}{dt}\right)} \qquad 5.32b$$

RESULTS RECORDED ON A 3 kW three-phase slip-ring induction machine for 380 V operated at 220 V as specified in the text.

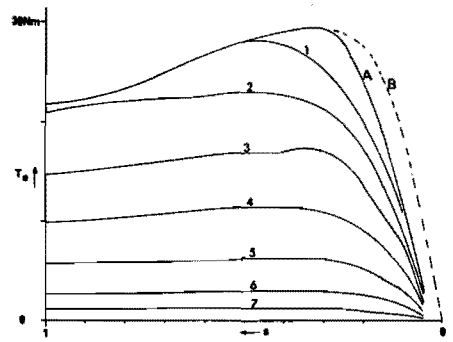

(a) α_r-control. No external resistor.

1. α_r = 45°
2. " = 60°
3. " = 75°
4. " = 90°
5. " = 105°
6. " = 120°
7. " = 135°

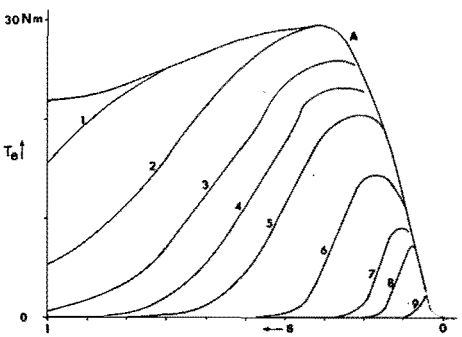

(b) t_{α_r}-control.

1. t_{α_r} = 4 ms
2. " = 6 ms
3. " = 8 ms
4. " = 10 ms
5. " = 12.5 ms
6. " = 20 ms
7. " = 35 ms
8. " = 50 ms
9. " = 100 ms

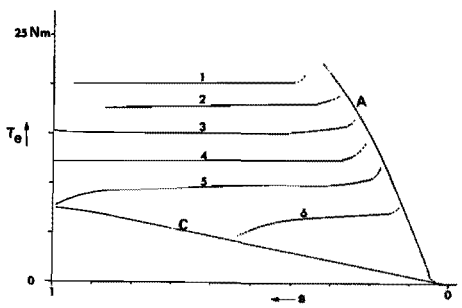

(c) Electronic Leblanc cascade, R_h = 5.75Ω , Δi = 10 A.

1. i_{01} = 40 A
2. " = 35 A
3. " = 30 A
4. " = 25 A
5. " = 20 A
6. " = 15 A

FIG. 5.26 EXPERIMENTAL TORQUE-SPEED CHARACTERISTICS OF SOME SYSTEMS TESTED ON A THREE-PHASE MACHINE.

that the three-phase controlled induction machine was intended as a prime mover in a Ward Leonard Ilgner set. The only aspect important as far as the present study is concerned is whether this three-phase machine has shown any effects not found on the semi-four-phase machine, since it was in a way intended as a check on the work at lower power levels.

Fig. 5.26(a) indicates that the torque-speed curves obtained for the α_r-control are analogous to the results obtained for the smaller semi-four-phase machine. As shown by the system diagram in fig. 5.8 the star-point of the rotor was connected in order to allow currents of all orders to flow. No distortion was observed.

In discussion of the results of fig. 5.22 reference was made to the characteristics of Δt_{α_r}-control. Fig. 5.26(b) displays the characteristics of t_{α_r}-control (see relation 5.64(b)) and again it must be remarked that these characteristics will be unsuitable for most applications, and certainly for current limitation in a Ward Leonard Ilgner set.

The torque-speed curves for the control of the three phase machine by an electronic Leblanc cascade (presented in fig. 5.26(c))are exactly analogous to the results presented in fig. 5.25 for the semi-four-phase machine. The current difference Δi was kept constant, and as long as the conditions set out in chapter 4 (paragraph 4.3.3.2, chiefly relation 4.78) were fulfilled, no detrimental effects were observed.

5.6.4 *A GENERAL DISCUSSION OF THE EXPERIMENTAL RESULTS - THE ELECTRICAL CHARACTERISTICS.*

In the first instance attention will be given to the correspondence of the calculated results with some measured characteristics as shown for the α_s-control in fig. 5.21(a) to (d). For the effective stator current (fig. 5.21(a)) and effective rotor current (fig. 5.21(b)) it may be seen that a correspondence within 5% has been obtained for the greater part of the slip range. Since the terms due to the induced excitation components of the total excitation have been neglected, it may be expected that the correspondence will deteriorate at higher speeds. Reference to relations 4.44c and 4.45(c) indicates that these terms again occur in the expressions multiplied by a factor $1-s$. As pointed out previously the harmonic impedances of the instantaneous symmetrical component equivalent circuit (fig. 4.4) are also a function of slip and all these influences combine to result in the difference evident in fig. 5.21 (a) and (b). It should be noted that at low slip the stator effective current for $\alpha_s=90^o$ departs appreciably from the calculated value. This increases with decrease of conduction angle, as the difference between the calculated/measured discrepancy for $\alpha_s=63^o$ and $\alpha_s=90^o$ illustrates. Correspondence between calculated values and experimental values are better for rotor currents than for stator currents.

In the expressions for the effective currents no phase angles appear, and since these values are therefore not phase sensitive, the correspondence between experimental and theoretical results is as yet no absolute test for the model over the whole speed range. The torque expression contains the difference of two phase angles for each pair of stator/rotor current components, and although the correspondence is

good in some parts of the slip region - as already seen previously - even this does not impart enough information concerning the correctness of the applied model. The extinction angle and power-factor will now be examined.

Fig. 5.21(d) indicates that although correspondence between calculated and measured values for γ_e is well within 5% for the high slips, it decreases rapidly above s=0.1. The departure of the measured phase angle from the calculated values is even more clear from fig. 5.21(c). The curves have the same tendency up to a slip of s=0.1, and then it may be seen how the application of the model without taking the induced voltage components into account departs totally from the practical situation, as was expected in the discussion of chapter 4. The test of the power-factor appears to be the most sensitive indication as to the correctness of the model.

In the second instance some attention will be given to certain electrical characteristics of the t_{β_r}-control, as represented in tables 5.1, 5.2 and 5.3. Let the β_r electrical characteristics of the Westinghouse Generalized Machine in uncontrolled condition be compared to the electrical characteristics of the t_{β_r}-control system. In both cases the same mechanical characteristics β_r are specified (tables 5.1 and 5.2). From table 5.5 it may be seen how the controlled machine draws a much smaller current at a much better power factor.

Reference to table 5.3 suffices for a comparison of the electrical characteristics of the systems for control of extinction angle or ignition angle of the rotor current. One should not only note the fact that the currents are again lower and the power factor more favourable, but that in the case of the extinction-angle control the induction machine operates with a capacitive power factor.

Speed	Ratio of effective stator voltages	Ratio of effective currents		Ratio of mean torques	Ratio of power factors
		stator	rotor		
0	1	0.29	0.34	1	2.45
300	1	0.30	0.34	1	2.36
2000	1	0.51	0.56	1	1.65

TABLE 5.5

COMPARISON OF UNCONTROLLED INDUCTION MACHINE WITH INDUCTION MACHINE WITH t_{β_r}-CONTROL IN TERMS OF CHARACTERISTICS OF UNCONTROLLED MACHINE.

5.6.5 *A GENERAL DISCUSSION OF THE EXPERIMENTAL RESULTS - THE PRESENTED OSCILLOGRAMS.*

(It is to be noted that all the oscillograms presented in this section of the characteristics of the semi-four-phase machine have been recorded for the case of zero external rotor resistance, i.e. $R_{re} = 0$).

Oscillograms OS1, OS2, OS3 indicate some machine characteristics of the Westinghouse Machine. In succession it may be seen what the rotor current is at a speed of 2200 r.p.m. with a short circuited rotor, what the open circuit induced rotor e.m.f. is at a speed of 2800 r.p.m. and what the rotor current is at a speed of 2200 r.p.m. when the rotor rectifier has the smoothing inductor used with the electronic Leblanc cascade as a load. The harmonic content of both induced voltage and rotor current is in evidence. OS2 also contains output pulses u_{ZD} from a zero detector unit on the simulation principle to indicate the amount of drift with speed, as the unit is usually calibrated at standstill. OS4 presents the zero detector output pulses and the simulated rotor e.m.f. at standstill.

Oscillograms OS5 to OS12 represent effects to be seen at the stator input terminals of a system with α_s-control. It is evident that the angle of current extinction is in excess of 180^o as calculated in chapter 4. As may be seen from OS5 the induced voltage is negligible in comparison to the supply voltage during the period that the electronic switch blocks. OS6 indicates how current decreases and γ_s^a decreases with increasing speed and increasing induced e.m.f. It should be noted how the induced e.m.f. can become negative at $(\gamma_s^a - \pi)$. From OS7 it may be seen that the induced e.m.f. continues to rise with increasing speed, while the frequency approaches the supply frequency, as predicted in chapter 4. OS8 indicates the conditions at synchronous speed. The induced e.m.f. is approximately in phase with the supply voltage and higher than in all previous cases. The oscillograms appear to support the approximations developed in chapter 4 for the induced e.m.f. No sudden change in e_s^a is apparent when the other phase starts or stops conduction. Refer to OS7 for instance. OS9 indicates the increased inductive power that will be drawn from the supply as calculated and measured.

In the discussion of the possible information-electronic input units that may be used for control of the ignition angle in 4.2.1 it was suggested that the voltage across the electronic switch may be used. This results in $\Delta\alpha_s$-control as recorded in fig. 5.20. That the capacitive filter elements necessary to protect the semiconductor switches against transients can be troublesome in this respect can be deduced from OS10, OS11 and OS12, where the distortion of the voltage across the machine windings, when the power-electronic switch is nonconducting, is evident. OS5 to OS8 were recorded with the filter circuit omitted. This of course tends to have destructive effects on the semiconductor switches. The decrease of the current with speed, and the change in the steady state phase angle of the machine for $\alpha_s = 90^o$ may clearly be seen in OS11 and OS12.

Oscillograms OS13 to OS18 indicate some characteristics of ignition-angle control of the rotor current. The output pulses u_{ZD} of the zero detector as obtained from a simulation of the induced rotor voltage is presented as a reference in all oscillograms on the rotor control systems. OS13 indicates that an analogous current flow as compared to the α_s-control is obtained, while OS14 indicates other influences on the current waveform than those assumed for the simplified model treated during analysis. Harmonic frequencies arising from the nonsinusoidal current distribution in space on the rotor and the tooth-harmonics have an important influence, as shown by OS1. At higher speeds the tooth harmonics are also found in the voltage across the electronic

switch u_e^a, as a comparison of OS15 and OS16 illustrates. Seeing the waveform of OS2 this may be expected. As stated in the previous discussion of this type of system, this influence of the tooth harmonics becomes amplified to such an extent that triggering by a pulse-train as shown in OS17 and OS18 becomes necessary.

Characteristics of extinction-angle control are indicated in the oscillograms OS19 to OS24. Comparing the current flow angle in this case to that of the ignition angle control illustrates the difference in power factor characteristics. It will be evident that the rotor current does not start to flow at $\alpha = 0$, due to the characteristics of the power switch. OS21 and OS22 indicates current flow resulting in torques far in excess of the maximum torque under uncontrolled conditions at the particular speed. Space harmonic influences are again evident at the higher speed in OS22. The "excess time" necessary for the rotor current to be reduced to zero is in evidence in all the oscillograms.

Consider the electronic switch voltage u_e^a in OS23. As explained in part I of this chapter time is necessary to transport the energy contained in storage capacitor C_c away (see fig. 5.10(d)). The time during which the rotor is decoupled may also be clearly seen, while the rise in the input voltage to the electronic switch, on initiation of commutation, is due to the leakage inductance energy in the rotor windings being stored in C_c. After completion of the commutation cycle the induced rotor voltage appears across the electronic switch. With reference to fig. 5.23, OS24 indicates instability occurring due to the harmonic distortion caused by the harmonics of order three, and their multiples in the rotor at $s \simeq 0.25$.

Current waveforms in the electronic Scherbius cascade are shown by OS25 and OS26. It should be noted that the commutation influences tend to cause an inductive phase shift for the fundamental current harmonic as compared to the assumptions of chapter 4. OS26 indicates the phase angle between inverter current i_i and supply voltage u_{sg}. From these figures it may also be concluded that the current in the d.c. intermediary circuit will be approximately constant. This corresponds to the assumptions of the simplified theory. Some conditions in the *electronic Leblanc cascade are indicated by OS27 to OS36*, and are related to the waveforms for the electronic Scherbius cascade. In OS27 it may be seen that the rotor current approaches the 90^o conduction angle assumed for a full four phase bridge in chapter 4. The chopper circuit is nonconducting, and the rectifier output consequently loaded by the smoothing inductor and rotor resistor R_h. When the chopper operates, the d.c. at the rectifier output is shown in OS28, with rotor current in OS29. The current waveforms are similar to those of OS25, with the higher frequency effects superposed, as already stressed several times in the text. The limit of chopper operation at low speed is represented by OS31, while the same at high speed may be seen in OS30. Chopper current at the rectifier output, and the two rotor currents during interference of chopper and rotor frequency, are depicted succesively in OS32, OS33 and OS34. Current through the resistive load of the low-high chopper and the main conduction branch of the electronic switch (OS35 and OS36) concludes the series.

It has been found that for the *compensated electronic Scherbius cascade* the waveforms on the machine side do not differ from those of the electronic Leblanc cascade, while at the inverter side they

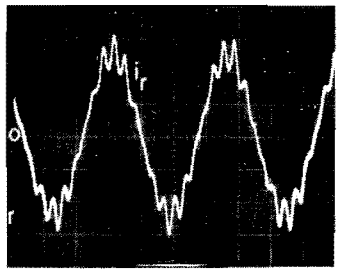

OS1 N=2200 rpm 3A/div.
20ms/div.

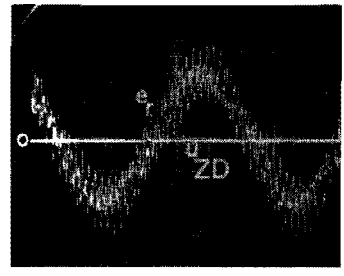

OS2 N=2800 rpm e_r : 2V/div.
50ms/div. u_{ZD}:20V/div.

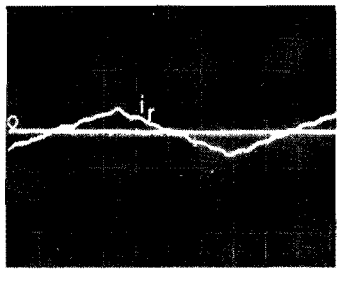

OS3 N=2200 rpm 6A/div.
10ms/div.

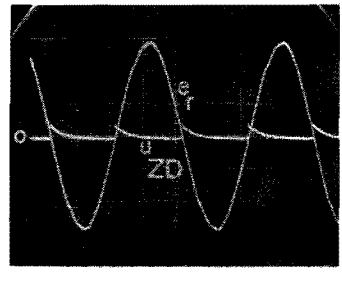

OS4 N=0 e_r :20V/div.
5ms/div. u_{ZD}:20V/div.

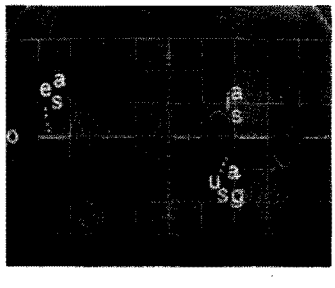

OS5 N=800 rpm e_s^a, u_{sg}^a :50V/div.
$\alpha_s = 126^o$; i_s^a : 2,5A/div.
5ms/div.

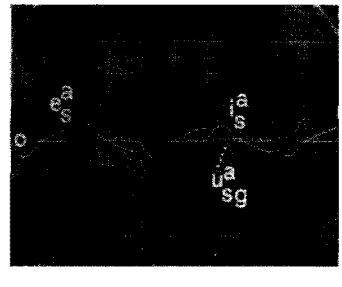

OS6 N=2800 rpm
scales OS5

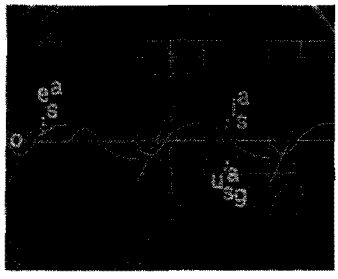

OS7 N=2920 rpm
scales OS5

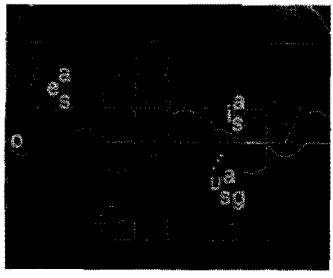

OS8 N=3000 rpm
scales OS5

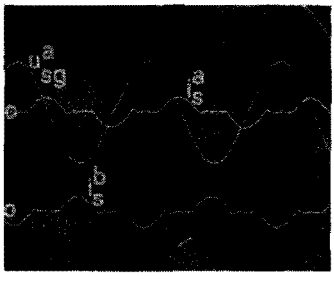

OS9 N=800 rpm u^a_{sg} :100V/div.
$\alpha_s=126^o$; i_s : 5A/div.
5ms/div.

OS10 N=800 rpm
scales OS9

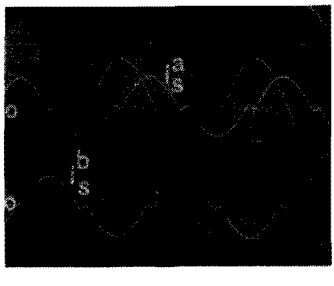

OS11 N=800 rpm
$\alpha_s=90^o$ scales OS9

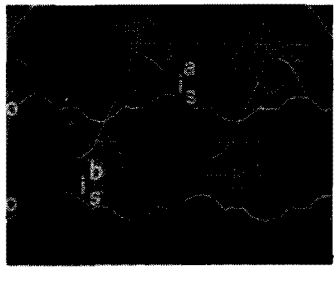

OS12 N=2800 rpm
scales OS9

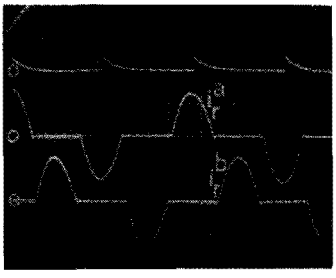

OS13 N=800 rpm i_r:2,5A/div.
$\alpha_r=124^o$;
5ms/div.

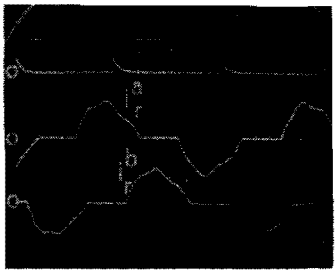

OS14 N=2000 rpm i_r:5A/div.
$\alpha_r=110^o$;
10ms/div.

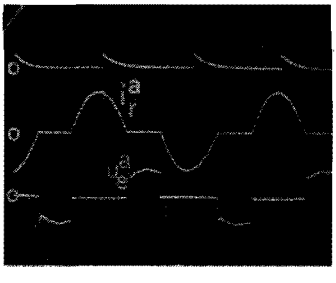

OS15 N=800 rpm i_r^a: 5A/div.
$\alpha_r=106^o$; u_e^a:50V/div.
5ms/div.

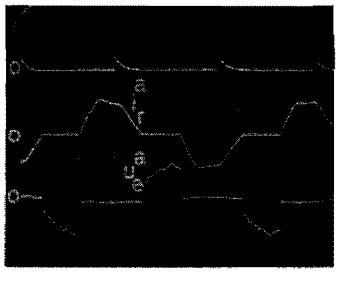

OS16 N=2000 rpm i_r^a: 5A/div.
$\alpha_r=115^o$; u_e^a:20V/div.
10ms/div.

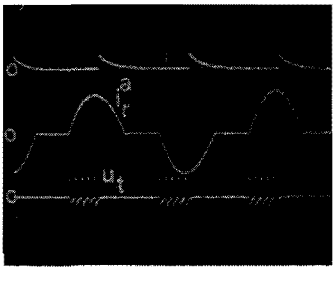

OS17 N=800 rpm i_r^a: 5A/div.
$\alpha_r=106^o$; u_t:20V/div.
5ms/div.

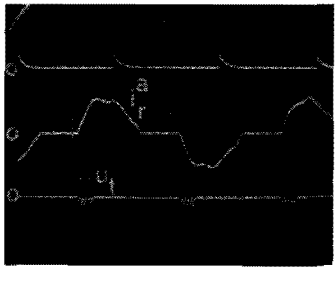

OS18 N=2000 rpm i_r^a: 5A/div.
$\alpha_r=115^o$; u_t:20V/div.
10ms/div.

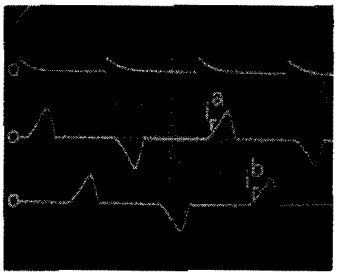

OS19 N=800 rpm i_r: 5A/div.
$\beta_r = 60^o$;
5ms/div.

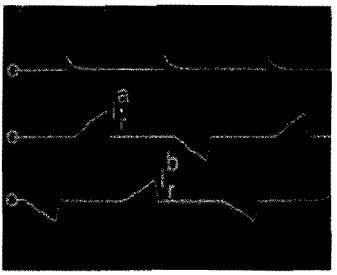

OS20 N=2000 rpm i_r: 5A/div.
$\beta_r = 74^o$;
10ms/div.

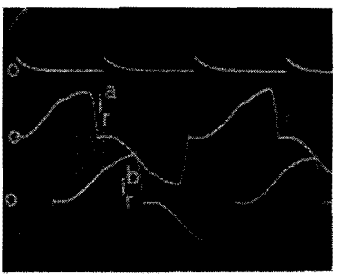

OS21 N=800 rpm i_r:10A/div.
$\beta_r = 150^o$;
5ms/div.

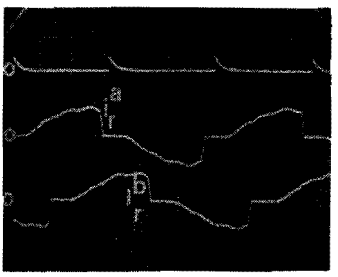

OS22 N=2000 rpm i_r:10A/div.
$\beta_r = 150^o$;
10ms/div.

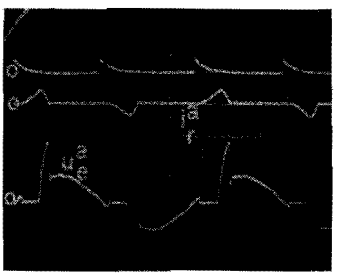

OS23 N=800 rpm i_r^a:10A/div.
$\beta_r = 50^o$; u_e^a:50V/div.
5ms/div.

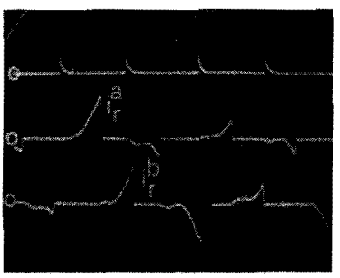

OS24 N=2280 rpm i_r:10A/div.
20ms/div.

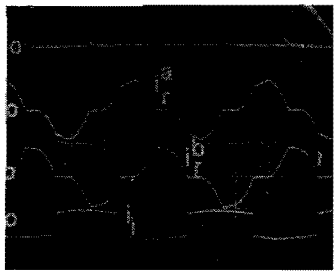

OS25 N=0 i_r: 5A/div.
$\alpha_i=110^o$ i_i:10A/div.
5ms/div.

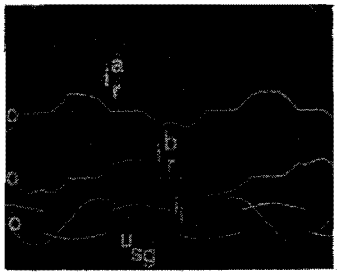

OS26 N=800 rpm i :5A/div.
$\alpha_i=110^o$;
5ms/div.

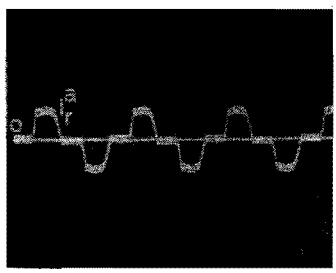

OS27 N=1000 rpm i_r:1.5A/div.
10ms/div.

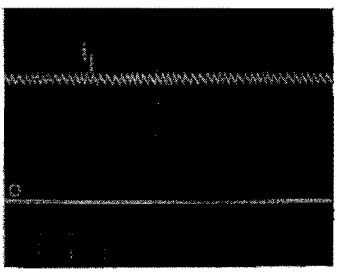

OS28 N=850 rpm i_1:2A/div.
5ms/div.
$i_{01}=8A$
$i_{02}=7A$

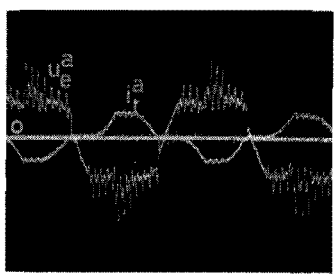

OS29 N=850 rpm i_r^a: 6A/div.
5ms/div. u_e^a:20V/div.
$i_{01}=8A$
$i_{02}=7A$

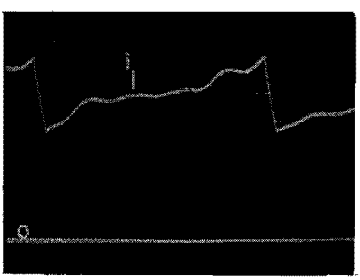

OS30 N=2400 rpm i_1:1A/div.
5ms/div.
$i_{01}=5A$
$i_{02}=3A$

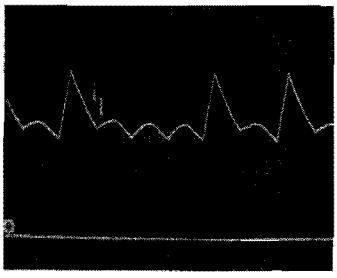

OS31 N=225 rpm i_1=1A/div.
5ms/div.
i_{01}=5A
i_{02}=3A

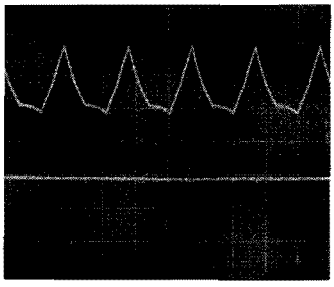

OS32 N=0 i_1:2A/div.
5ms/div.
i_{01}=8A
i_{02}=4A

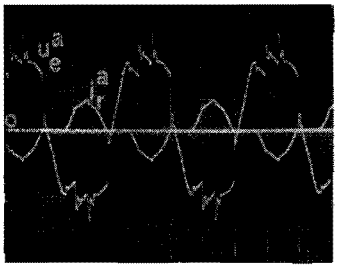

OS33 N=0 i_r^a: 6A/div.
5ms/div. u_e^a:20V/div.

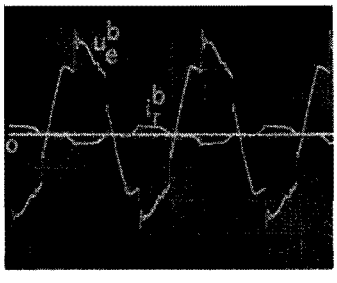

OS34 N=0 i_r^b: 6A/div.
5ms/div. u_e^b:20V/div.

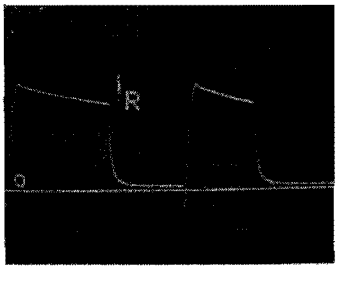

OS35 i_R: 1.4A/div.
500µs/div.

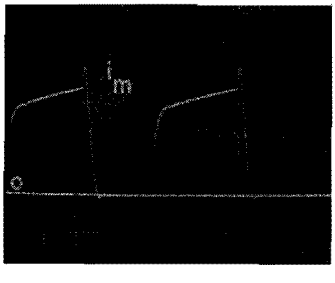

OS36 i_m: 1.4A/div.
500µs/div.

OS37 8A/div.
2ms/div.

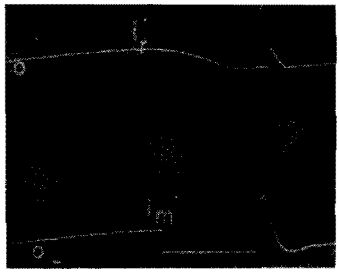

OS38 16A/div.
1ms/div.

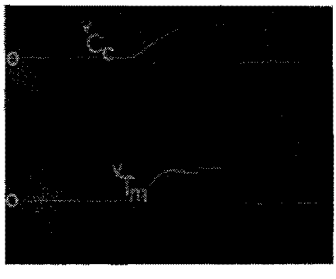

OS39 100V/div.
1ms/div.

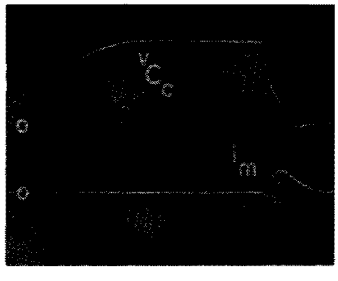

OS40 50V/div.
500µs/div. 32A/div.

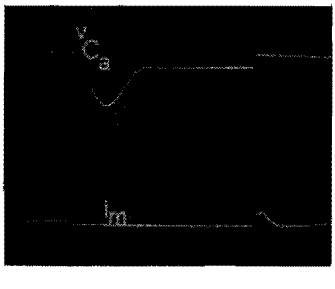

OS41 100V/div.
1ms/div.

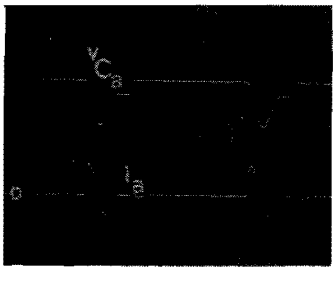

OS42 100V/div.
2ms/div. 8A/div.

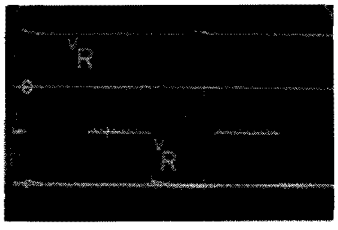

OS43 V_R:5V/div. 20µs/div.
V_R:5V/div. 500µs/div.

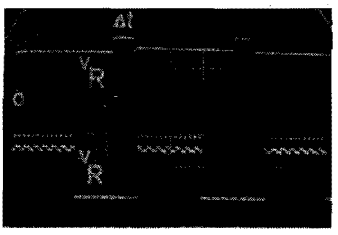

OS44 V_R:2V/div. 20µs/div.
V_R:2V/div. 500µs/div.

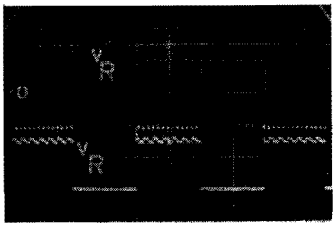

OS45 V_R:2V/div. 2µs/div.
V_R:2V/div. 500µs/div.

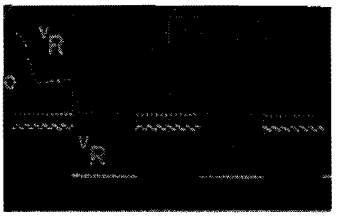

OS46 V_R:2V/div. 200ns/div.
V_R:2V/div. 500µs/div.

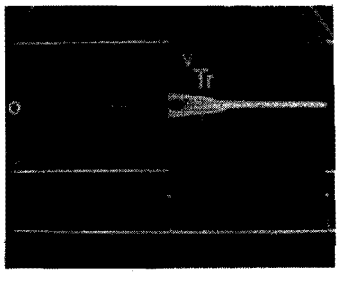

OS47 V_{Tr}: 10V/div.
200µs/div.

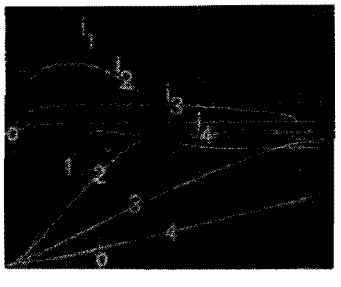

OS48 i_1-i_4: 10mA/div.
1µs/div. 1-4 100V/div.

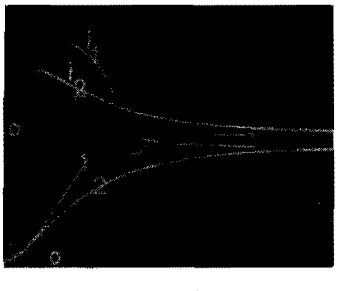

OS49 (Scales OS48)

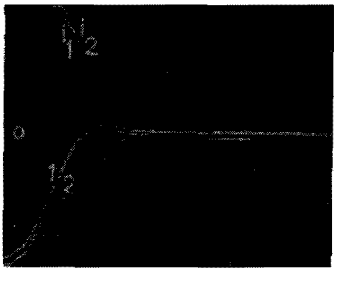

OS50 (Scales OS48)
1 starts from -170V
2 starts from 0V

correspond to those for the classical electronic Scherbius cascade, with a high frequency switching effect superposed.

The auxiliary commutated electronic switch functions as explained by the series of oscillograms OS37 to OS42. Since this has been discussed at some length in part I, it will not be repeated here. It may clearly be seen how the current commutates from the main thyristor T_m into C_c at initiation of commutation, and furthermore how the voltage on C_a is increased by the transport of energy from C_c at the beginning of a new conduction cycle.

Some characteristics of the *carrier-frequency triggering systems* discussed in part I of this chapter *are shown in OS43 - OS47.*

In OS43 and OS44 the output voltage V_R across 100 ohm is displayed for both systems, type B and C respectively. (transmission period approx. 500 Hz as prescribed by the logic circuitry). OS43 indicates clearly that the rectifier output becomes zero as found in equation 5.26. For the practical unit shown it even becomes negative, an observation that may be attributed to the finite rise and fall times of the input waveform, and charge-storage in the rectifiers.

OS44 indicates clearly that the output voltage of the overlap-unit never becomes negative or zero during a transmission period. Due to the departure of the practically constructed circuit from the idealized model one may even mention an overcompensation during commutation ([78]. It may also be observed that the two output transformers Tr_1 and Tr_2 are not precisely identical. The approximate time of overlap Δt may be observed. OS46 and OS47 demonstrate the difference in switch-off times for the two systems clearly. In OS47 the voltage on the primary of the carrier frequency transformer is shown. OS45 shows the fast switch-on time of the developed system.

A brief example of some results obtained on the *thyristor testing system* is formed by *OS48, OS49 and OS50.* OS48 represents a family of dV/dt curves with the corresponding capacitive currents for a BTY95 thyristor tablet, while OS49 illustrates the important difference between capacitive current into the device when an exponential or linear dV/dt transient is applied in the blocking direction. Although it is sometimes claimed that bias conditions contribute very much to the amplitude of the capacitive current ([B5] , investigations on commercial devices of the type mentioned have failed to prove this. In curve 1 the transient started at -170V and continued to +200V, while for curve 2 the transient started at zero volt. It may be seen that a negligible difference exists in capacitive current. Characteristics such as these are recorded for thyristors before use in a power electronic switching circuit.

5.7 CONCLUSION.

In this chapter a limited amount of experimental work on the variable slip group (or Group II) of the machine-electronic systems has been presented. This experimental work may be divided into the development of the machine-electronic systems and the measurement of the mechanical and electrical characteristics of the developed systems.

In the course of this development investigations had been done on force commutated electronic power switches. A solution combining the disadvantages of a current-dependent circuit turn-off time and a

current-dependent leakage energy in the supply to be switched was suggested, worked out and tested. It was shown that the method to obtain current-independent circuit turn-off time has general validity and may be applied in other power-electronic switches as well. During development and operation of the machine-electronics it was further noted that triggering problems sometimes lead to instabilities in the machine-electronic systems. The problem of transmission of triggering signals was investigated generally, and it was shown that the carrier frequency gating system with overlap as suggested presented an important advance over existing systems. Attention paid to other problems in power electronics and the application of power semiconductors was only pointed out very briefly.

In chapter 3 calculation of the characteristics of a general n-m phase switched electromechanical transducer was examined. The variable slip systems were selected from amongst the different groups for investigations. In chapter 4 the induction machine with stator control by variation of the delay of the ignition angle was investigated extensively with the aid of the theory of chapter 3. For the purpose of this investigation the excitation function of the machine was divided into components derived from the switched voltage and components derived from the "induced excitation function". The experimental results of this chapter has shown that under some circumstances the "induced excitation" components may be neglected when calculating the electromagnetic torque, the effective stator current, the effective rotor current and the angle of natural current commutation. At low speeds good correspondence between calculated and measured characteristics is obtained for mechanical and electrical characteristics. This correspondence is the better for low resistance rotors, since the experimental results has proven that when the "induced excitation" components are neglected, the largest discrepancy with the theoretical calculations occur at slips lower than the slip of maximum torque. It was shown theoretically and experimentally that the most sensitive test for the applicability of the model is the power factor of the system. This illustrates the difference between the model with the "induced excitation" components taken into account and with these components neglected. Experimental results of this chapter has also indicated that the simplified power flow models developed in chapter 3 from the power flow considerations of chapter 2 may be employed to obtain a qualitative analysis of variable slip systems with rotor control. A study of the oscillograms has indicated that under operating conditions in the motoring region that was investigated, the assumptions necessary to arrive at the simplified model are mostly fulfilled. In cases where they are not valid the unbalanced and harmonic torques arising due to the switching are of such a nature that the system becomes useless as a controlled electrical drive.

The experimental results obtained on the semi-four-phase machine indicated the influence of the generated rotor current harmonics due to switching. As these influences can be detrimental in practical applications, it was important to investigate some systems on a practically scaled three-phase system. No such effects were observed, and in general the results corresponded well with the results obtained on the semi-four-phase systems.

1. Abraham, L., Heumann, K., Koppelmann, F. Anfahren, Regeln und Nutzbremsen von Gleichstromfahrzeugen mit steuerbaren Siliziumzellen. VDE Fachber., 22, 89-100, 1962.

2. Abraham, L., Patzschke, U. Pulstechnik für die Drehzahlsteuerung von Asynchronmotoren. AEG-Mitt., 54, 133-140, 1964.

3. Abraham, L., Koppelmann, F. Die Zwangskommutierung: ein neuer Zweig der Stromrichtertechnik ETZ-A, 87, 649-658, 1966.

4. Alexanderson, E.F.W., Edwards, M.A., Willis, C.H. Electronic speed control of motors. Discussion of this paper by Alexanderson. Trans. A.I.E.E., 57, 343-352, 1938.

5. Bauerlein, G. Brushless dc motor uses hall-effect devices. Electronics, April 6, 58, 1962.

6. Bayha, H. Regelantriebe mit Stromrichtern. Siemens Zeitschrift, 13, 303, 1933.

7. Beiler, A.H. Thyratron motor at the logan plant. Trans. A.I.E.E., 57, 19-24, 1938.

8. Blaufuss, K. Drehzahlregelung von Gleichstrommotoren durch Stromstösse. Arch. Elektrotechn., 34, 581-590, 1940.

9. Cieszow, G., Kulka, S. Die Anwendung von pulsgesteuerten Widerständen bei Gleichstrom-Reihenschluszmotoren und Drehstrom-Schleifringläufermotoren. AEG-Mitt., 55, 123-129, 1965.

10. Cooper-Hewitt, P. U.S.A. Patent application 1,007,694, 20th March 1908.

11. Cordier, J.-P. Regulation de la vitesse d'un moteur asynchrone au moyen de semi-conducteurs. Revue E, 5 (10), 327-346, 1968.

12. Dällenbach, W., Gerecke, E. Die Strom- und Spannungsverhältnisse der Groszgleichrichter. Arch.Elektrotechn.14, 171-246, 1924.

13. Davis, R.M., Barwell, F.T. The commutatorless diesel-electric locomotive. Proc.I.E.E. Conf. 10-11 Nov., 126-133, 1965.

14. Dolaberidze, G.P. The conversion of d.c. into a.c. at variable frequency for electric traction. Elektrotekhnika, no.4 (April), 58-62, 1965.

15. Dunoyer, L., Toulon, P. Sur une propriété remarquable de la colonne positive de l'arc au mercure-relais a arc de grande puissance. Le Journal de Physique et le Radium, 5, 257-266, 289-303, 1924.

16. Erlicki, M.S. Inverter rotor drive of an induction motor. I.E.E.E. Trans. Power Apparatus Syst. PAS-84, (11), 1011-1016, 1965.

17. Erlicki, M.S., Ben-Uri, J., Schieber, D. Power measurement errors in controlled rectifier circuits. I.E.E.E. Trans. Indust. Gen. Applic. IGA-2, 309-310, 1966.

18. Editorial in ETZ, 24 (10), 187-188, 1903.

19. Gentry, F.E., Scace, R.I., Flowers, J. A three terminal a.c. switch. I.E.E.E. Electron Device Conference, Washington Oct.31, 1963.

20. Gerecke, E., Badr. H. Asynchronmaschinen mit primärseitig eingebauten steuerbaren Ventilen. Neue Technik, 4, 125-143, 1962.

21. Gerecke, E., Terens, U. Mittels eines rotorseitigen Stromrichters regelbarer Asynchronmotor. Neue Technik, 3, 110-124, 1961.

22. Golde, E. Asynchronmotor mit elektronischer Schlupfregelung. AEG-Mitt., 54 (11/12), 666-671.

23. Griffith, R.C. Thyratron control equipment for high speed resistance welding. G.E. Rev., 33, 511, 1930.

24. Grondahl, L.O. Theories of a new solid junction rectifier. Science 64, 306-308, 1926.

25. Hamudhanov, M.Z."Variable frequency operation of asynchronous motors using electronic frequency changers" in: Technical Problems of electric drives. Moscow, U.S.S.R. Academy of Science, 1957.

26. Heumann, K. Elektrotechnische Grundlagen der Zwangskommutierung. Neue Möglichkeiten der Stromrichtertechnik. E.und M.,84, 99-112, 1967.

27. Hölters, F. Schaltung und Steuerung von Stromrichtermotoren. E.u.M.,61, 221-228, 1943.

28. Hori, T. Secondary excitation of induction motors using rectifier circuits. Elect.Engng. Japan, 87 (a), 55-65, 1967.

29. Hull, A.W. Gas-filled thermionic tubes. Trans-A.I.E.E., 47, 753-763, 1928.

30. Hull, A.W., Hot-cathode thyratrons. G.E.Rev., 32 (7), 390-399, 1929.

31. Ivakhenko, A.G. Regulation of the speed of a three phase asynchronous motor with the aid of thyratrons and series transformers. Elektrichestvo, no.9, (Sept) 57-59, 1948.

32. Jain, G.C. The effect of voltage waveshape on the performance of a 3-phase induction motor. I.E.E.E. Trans. Power Apparatus Syst. PAS 83, 561-566, 1964.

33. Jones, D. Variable pulse width inverter. Electronic Equipment Engineering (Nov), 29-30, 1961.

34. Kern, E. Der kommutatorlose Einphasen-Lokomotivmotor 40 bis 60 Hz. Elektr.Bahnen, 7, 313-321, 1931.

35. Kesselring, F. Theoretische und experimentelle Untersuchung über den rotierenden Gleichrichter. Diss. E.T.H. Zurich, 1923.

36. Koch, F. Über ein neues System der Entnahme von Gleichstrom aus Wechselstromnetzen. ETZ, 22, 853-854, 1901.

37. Koppelmann, F. Der Kontaktumformer. ETZ 62, 3-16, 1941.

38. Korb, F. Einstellung der Drehzahl von Induktionsmotoren durch antiparallele Ventile auf der Netzseite. ETZ-A, 86 (8), 275-279, 1965.

39. Kovács, K.P.Über die genaue und vollständige Simulation des am Ständer mit steuerbaren Siliziumtrioden geregelten Drehstrom-Asynchronmotors. Acta Techn.Hung. 48, 445-458, 1964.

40. Krost, H., Moczala, H. Elektronische Drehzahlregelung bürstenloser Gleichstrom-Kleinstmotoren. ETZ-A, 86 (19), 628-632, 1965.

41. Laithwaite, E.R. Electrical variable speed drives. Engineer's Digest, 25, 115-165, 1964.

42. Lavi, A., Polge, R.J. Induction motor speed control with static inverter in the rotor. I.E.E.E. Trans. Power Apparatus Syst. PAS-85 (1), 76-84, 1966.

43. Lemmrich, J. Der synchronisierte Induktionsmotor. ETZ-A, 85 (22), 724-726, 1964.

44. Lenz, P. Gittergesteuerte Gasentladung als regelbarer Wechselstromwiderstand. Arch.Elektrotechn. 27, 497-504, 1933.

45. Libesny, A. Stromwandlung durch Quecksilber-Vakuum-Apparate. E.und M., 24, 799-802, 1906.

46. Löbl, O. Bahnumrichtersystem Löbl/RWE. Elektr.Bahnen, 8, 65-69, 1932.

47. Marti, O.K. The mercury-arc rectifier applied to a.c. railway electrification. A.I.E.E. Trans., 51, 659-668, 1932.

48. Merrit, H.E. Exact solutions for cubic and quartic equations Control Engineering 8 (3), 145, 1961.

49. Meyer, M. Ueber die untersynchrone Stromrichterkaskade. ETZ-A, 82, 589-596, 1961.

50. Moll, J.L., Tannenbaum, M., Goldey, I.M., Holonyak, N. p-n-p-n transistor switches. Proc. I.R.E., 44 (9), 1174 - 82.1956.

51. Niesten, J.G. Toepassingsmogelijkheden voor halfgeleiderschakel-elementen bij roterende elektromechanische omzetters, bezien tegen de achtergrond van de frekwentie-voorwaarde. De Ingenieur, 77, E43-E52, 1965.

52. Nishida, F., Mizuno, S. Speed control of wound rotor induction motor by Scherbius system. Elect. Engng. Japan, 84 (9), 53-62, 1964.

53. Novotny, D.W., Fath, A.F. The analysis of induction machines controlled by series connected semiconductor switches. Paper presented to the I.E.E.E. Feb.24, 1967. 19 p.

54. Ohno, E. Commutation characteristics of a thyristor inverter with an auxiliory commutation circuit. Elect.Engng. Japan, 86 (8), 101-112, 1966.

55. Petersen, W.,Diskussion zu M. Schenkel: Technische Grundlagen und Anwendungen gesteuerter Gleichrichter und Umrichter. ETZ 53, 761-770, 1932. Diskussion: 771-773.

56. Presser, E. Der Selengleichrichter. ETZ, 53, 339-341, 1932.

57. Prince, D.C. The direct current transformer utilizing thyratron tubes. G.E. Rev., 31, 347-350, 1928.

58. Prince, D.C. The inverter. G.E. Rev., 28, 676-681, 1925.

59. Recklinghausen, M. von. Die Quecksilberlampe und sonstige Quecksilber-vakuumapparate. ETZ, 25 (51), 1102-1107, 1904.

60. Reichel, W. Diskussionsbeitrag. ETZ, 53, 778-779, 1932.

61. Schäfer, B. Ein neuer Quecksilberdampfgleichrichter für grosze Leistungen. ETZ, 32 (1), 2, 1911.

62. Schenkel, M. Eine unmittelbare asynchrone Umrichtung für niederfrequente Bahnnetze. Elektr.Bahnen, 8, 69-73, 1932.

63. Schilling, W. Zur Regelung von Gleichstrommotoren über gitter-gesteuerte Gleichrichter. Arch. Elektrotechn. 29, 622-631, 1935.

64. Shockley, W., Sparks, M., Teal, G.K. p-n Junction transistors. Phys. Rev. 83 (1), 151-162, 1951.

65. Sequenz, H. Die Verwendung von Entladungsgefässen bei elektrischen Maschinen. E.und M. 55, 274-280, 1937.

66. Shepherd, W., Stanway, J. The polyphase induction motor controlled by firing angle adjustment of silicon controlled rectifiers. I.E.E.E. Internat. Conv.Rec., Pt4, 135-154, 1964.

67. Stöhr, M. Lokomotivsysteme für hochgespannten Gleichstrom. E.u.M., 58, 381-389, 1940.

68. Stöhr, M. Stromrichterkaskade für Doppelzonenregelung. E.u.M., 58, 177-186, 1940.

69. Stöhr, M. Vergleich zwischen Stromrichtermotor und untersynchroner Stromrichterkaskade. E.u.M., 57, 581-591, 1939.

70. Takeuchi, T.J. Characteristics of single phase induction motor controlled by single-phase back-to-back SCR. Elect.Engng.Japan, 86 (11), 14-23, 1966.

71. Tirrill, A.A. Regulators for alternating current work. Electrical Journal, 8, 502-509, 1908.

72. Tompkins, F.N. The parallel type inverter. A.I.E.E. Trans. 51, 707-714, 1932.

73. Turnbull, F.G. A carrier frequency gating circuit for static inverters converters and cycloconverters. I.E.E.E. Trans. Magnetics, MAG-2, 14-17, 1966.

74. Udvardi-Lakos, J., Surk, R. Prüfgerät zur Bestimmung der kritischen Spannungs-steilheit von Thyristoren. BBC-Nachrichten, 49, 17-20, 1967.

75. Voorhoeve, N.A.J. Ein für praktische Verwendung geeignetes Verfahren für Spannungsregelung an Generatoren mit Hilfen von Hochvakuumröhren. Arch. Elektrotechn., 21, 228-243, 1929.

76. Voorhoeve, N.A.J. Spanningsregeling van elektrische machines door ontladingsbuizen. Dissertatie TH-Delft, 1930.

77. Walraven, A. Regeling van het toerental van kleine induktie-motoren door middel van thyristors. Philips Technisch Tijd-schrift 28 (1), 1-13, 1967.

78. Wyk, J.D. van. On carrier frequency gating systems for static switching circuits. I.E.E.E. Trans. Magnetics, June 1969.

79. Wyk , J.D. van. Power and machine-electronics I. 1914-1966. A selected bibliography. South African Institute of Electrical Engineers 1969 (to be publ.).

80. Wyk, J.D. van. Symmetrical and asymmetrical stable modes in systems for electronic stator control of asynchronous machines by semiconductor switches. Electronics Letters, 4 (21) 453-455, 1968.

LITERATURE : BOOKS

B1 Bedford, B.D. , Hoft, R.G.
Principles of inverter circuits.
New York, Wiley, 1964.

B2 Bijl, H.J. van der
The thermionic vacuum tube and its applications.
New York, Mc Graw-Hill, 1920.

B3 Bolliger, A.
Die Hochspannungs-Gleichstrommaschine.
Berlin, Springer, 1921.

B4 Gentry, F.E., Holonyak, N., Zastrow, E.E. von, Gutzwiller, F.W.
Semiconductor controlled rectifiers.
New Yersey, Prentice-Hall, 1964.

B5 Hoffmann, A., Stocker, K.
Thyristor Handbuch: Der Thyristor als Bauelement der Leistungselektronik.
Berlin, Siemens, 1965.

B6 Langsdorf, A.S.
Theory of alternating current machinery. Second edition.
New York, Mc Graw-Hill, 1955.

B7 Marti, O.K., Winograd, H.
Stromrichter (Unter besonderer Berücksichtigung der Quecksilberdampf-Groszgleichrichter).
Deutsche Bearbeitung von O. Gramisch.
München, Oldenbourg, 1933.

B8 Meyer, M.
Stromrichter mit erzwungener Kommutierung.
Erlangen, Siemens, 1967.
(Thyristoren in der technischen Anwendung Band 2).

B9 Niesten, J.G.
Elektromechanika II. Bewerkt door E.M.H. Kamerbeek.
Eindhoven, Technische Hogeschool, 1968.

B10 Rissik, H.
Fundamental theory of the arc converter.
London, Chapman and Hall, 1939.

B11 Rissik, H.
Mercury-arc currents converters.
London, Pitman, 1935.

B12 Say M.G.
The performance and design of alternating current machines.
Third edition.
London, Pitman, 1958.

B13 Schuisky, W.
Induktionsmaschinen.
Wien, Springer, 1957.

B14 Takeuchi, T.J.
Theory of SCR circuit and application to motor control.
Tokyo, Electrical Engineering College Press, 1968.

B15 Wasserab, Th.
Schaltungslehre der Stromrichtertechnik.
Berlin, Springer, 1962.

B16 White, D.C., Woodson, H.H.
Electromechanical energy conversion.
New York, Wiley, 1959.

A2.1 CONCERNING THE TORQUES AND POWER RELATIONS FOR THE SYSTEMATIC MODEL.

The model for analysis is accepted as proposed in the text. Let the stator current be as given in relation 2.5. Every stator harmonic current is coupled with a magnetic field of the same order. Whether this is a rotating field and what the direction of rotation is, depends on the multiphase balanced system that feeds the transducer, and may only be determined for the specific case that is investigated.

Stator currents of angular frequency $\nu_s.2\pi f_s$ set up rotating fields in the air gap with an angular speed with respect to the stator body:

$$\frac{d\theta_s}{dt} = \frac{(-1)^{c_s}.\nu_s\omega_s}{p} \qquad c_s = 1 \text{ or } 2 \qquad \text{A2.1}$$

where θ_s is the stator circumferential coordinate (see fig. 1.1) and $\omega_{s/p}$ the angular speed of the fundamental field with $\left|\frac{\omega_s}{p}\right| = 2\pi f_s$. The assumption that the machine windings are sinusoidally distributed is still valid.

Correspondingly rotor currents of frequency $\nu_r 2\pi f_r$ set up fields with speed:

$$\frac{d\theta_r}{dt} = \frac{(-1)^{c_r}.\nu_r\omega_r}{p} \qquad c_r = 1,2 \text{ or } -\infty \qquad \text{A2.2}$$

with respect to the rotor body, with $\left|\frac{\omega_r}{p}\right| = 2\pi f_r$.

When both the rotor windings and the stator windings are fed by current sources, with the fundamental frequencies corresponding to the general frequency relation, as the definitions of chapter 1 have considered, synchronous torques will occur at speeds given by:

$$2\pi f_m = \left|\frac{\nu_s.2\pi f_s \pm \nu_r.2\pi f_r}{p}\right| \qquad \text{A2.3a}$$

where f_m is the mechanical frequency related to the speed by $2\pi f_m = |\omega_m|$.

Now consider the situation where the rotor or stator is not fed by a current source, and therefore the stator resp. rotor harmonic fields will form asynchronous torques with the rotor resp. stator induced currents.

From rel. A.2.1 for harmonics of order ν_s in the stator setting up rotating fields, the angular speed with respect to the rotor of these fields will be:

$$= (-1)^{c_s}\nu_s.\frac{\omega_s}{p} - \omega_m, \qquad \text{A2.4a}$$

where $\frac{\omega_s}{p}$ is the angular speed of the fundamental stator rotating field. The frequency of the induced rotor currents corresponding to the stator harmonic current of order ν_s. becomes

$$\nu_{rs}.2\pi f_r = p.\left|(-1)^{c_s}\nu_s.\frac{\omega_s}{p} - \omega_m\right| \qquad \text{A2.4b}$$

Taking into account that:

$$s = \frac{\frac{\omega_s}{p} - \omega_m}{\frac{\omega_s}{p}} = \frac{\omega_r}{\omega_s} \quad \text{or} \quad p\omega_m = \omega_s(1-s)$$

$$\nu_{rs} f_r = \frac{1}{2\pi} \left| \omega_r \left\{ \frac{(-1)^{c_s} \nu_s}{s} - \frac{1-s}{s} \right\} \right| \qquad \text{A2.4c}$$

The order ν_{rs} will not in general be a whole number.

Similarly, for the action of the harmonics of order ν_r in the rotor causing a rotating field it is found that this rotating field has a speed of rotation with respect of the stator of:

$$\frac{(-1)^{c_r} \nu_r \cdot \omega_r}{p} + \omega_m \qquad \text{A2.4d}$$

resulting in stator currents with frequencies:

$$\nu_{sr} f_s = \frac{1}{2\pi} \left| \omega_s \left\{ 1 + \left[(-1)^{c_r} \nu_r - 1 \right] \cdot s \right\} \right| \qquad \text{A2.4e}$$

the same criteria being valid for ν_{sr}.

If the total electromagnetic air gap torque is $\overline{T}_e$, the above reasoning indicates in general for the model under discussion this torque will be composed of a sum of torques due to a synchronous interaction between stator and rotor, a sum of torques due to an asynchronous interaction between stator and rotor and finally a sum of torques due to an asynchronous interaction between rotor and stator. The components are to be indicated respectively by:

$$\overline{T}_e^{syn.} = \sum_{\nu_s, \nu_r} \overline{T}_{e(\nu_s, \nu_r)} \qquad \nu_s, \nu_r \geq 1$$

$$\overline{T}_e^{asyn.sr} = \sum_{\nu_{rs}} \overline{T}_{e(\nu_{rs})} \qquad \nu_{rs} > 0$$

$$\overline{T}_e^{asyn.rs} = \sum_{\nu_{sr}} \overline{T}_{e(\nu_{sr})} \qquad \nu_{sr} > 0$$

Taking the sum:

$$\overline{T}_e = \sum_{\nu_s, \nu_r} \overline{T}_{e(\nu_s, \nu_r)} + \sum_{\nu_{rs}, \nu_{sr}} \overline{T}_{e(\nu_{sr}, \nu_{rs})} \qquad \text{A2.5a}$$

Extracting the fundamental torque:

$$\overline{T}_e = \overline{T}_{e(1)} + \sum_{\nu_s, \nu_r} \overline{T}_{e(\nu_s, \nu_r)} + \sum_{\nu_{rs}, \nu_{sr}} \overline{T}_{e(\nu_{sr}, \nu_{rs})} \qquad \text{A2.5b}$$

$$\nu_{sr}, \nu_{rs} > 0$$

$$\nu_s, \nu_r \geq 2, \text{ whole}$$

The extracted fundamental torque $\overline{T}_{e(1)}$ will now be defined. If the fundamental angular frequency of stator and rotor is fixed at $2\pi f_s$ and $2\pi f_r$ respectively, they will interact at one speed given by

$$\omega_m = \frac{\omega_s}{p} - \frac{\omega_r}{p} \qquad \text{A2.6a}$$

where $\frac{\omega_s}{p}$ and $\frac{\omega_r}{p}$ are again the speed of rotation of stator/rotor fundamental magnetic fields. This synchronous interaction produces the component $\overline{T}^{syn.}_{e(1)}$ of $\overline{T}_{e(1)}$. At any arbitrary mechanical speed ω_m the fundamental currents in the stator winding set up a rotating field resulting in current with frequency:

$$f_{rs} = \frac{1}{2\pi}\left|\omega_s - p\omega_m\right| \quad \text{in general} \neq \frac{1}{2\pi}\left|\omega_r\right| \qquad \text{A2.6b}$$

in the rotor. As these currents arise by induction, they satisfy the frequency condition and give rise to an asynchronous stator-rotor component $\overline{T}^{asyn.sr}_{e(1)}$ of $\overline{T}_{e(1)}$.

Exactly in the same way currents are induced by the fundamental rotor field in the stator at frequency

$$f_{sr} = \frac{1}{2\pi}\left|\omega_r + p\omega_m\right| \quad \text{in general} \neq \frac{1}{2\pi}\left|\omega_s\right| \qquad \text{A2.6c}$$

giving rise to the torque component $\overline{T}^{asyn.rs}_{e(1)}$ of $\overline{T}_{e(1)}$.

The components of the harmonic torques may be defined identically.

If the general power balance for the electromechanical transducer in the steady state is now taken into account, (eq. 2.4 and A2.5b substituted), it is obtained as:

$$P^s_{in} - P^s_{de} = P^r_{de} - P^r_{in} + \overline{T}_{e(1)}\omega_m + \omega_m\left\{\sum_{\nu_s,\nu_r} \overline{T}_{e(\nu_s,\nu_r)}\right\} + \left\{\sum_{\nu_{rs},\nu_{sr}} \overline{T}_{e(\nu_{rs},\nu_{sr})}\right\}\omega_m \qquad \text{A2.7a}$$

Extracting the fundamental powers:

$$\left\{P^s_{in(1)} - P^s_{de(1)}\right\} + \left\{\sum_{\nu_s} P^s_{in(\nu_s)} - \sum_{\nu_s,\nu_{sr}} P^s_{de(\nu_s,\nu_{sr})}\right\} =$$

$$\left\{P^r_{de(1)} - P^r_{in(1)}\right\} + \left\{\sum_{\nu_r,\nu_{rs}} P^r_{de(\nu_r,\nu_{rs})} - \sum_{\nu_r} P^r_{in(\nu_r)}\right\}$$

$$+ \overline{T}_{e(1)}\omega_m + \left\{\sum_{\nu_s\nu_r} \overline{T}_{e(\nu_s,\nu_r)}\right\}\omega_m + \left\{\sum_{\nu_{rs},\nu_{sr}} \overline{T}_{e(\nu_{rs},\nu_{sr})}\right\}\omega_m \qquad \text{A2.7b}$$

where it has been assumed that the stator and rotor electrical input power and the dissipation consist of the following components:

$$P^s_{in} = P^s_{in(1)} + \sum_{\nu_s} P^s_{in(\nu_s)} \; ; \; P^s_{de} = P^s_{de(1)} + \sum_{\nu_s,\nu_{sr}} P^s_{de(\nu_s,\nu_{sr})}$$

$$P^r_{in} = P^r_{in(1)} + \sum_{\nu_r} P^r_{in(\nu_r)} \quad ; \quad P^r_{de} = P^r_{de(1)} + \sum_{\nu_r,\nu_{rs}} P^r_{de(\nu_r,\nu_{rs})}$$

$$\nu_r,\nu_s \geqslant 2 \text{ , whole; } \nu_{sr},\nu_{rs} > 0$$

as it may be assumed that the stator or rotor voltage sources contain harmonics of order ν_s,ν_r respectively.

With reference to the systematic investigation of machine-electronics systems, some special cases of the above power balance are to be investigated.

A2.1.1 *SYNCHRONOUS TRANSDUCERS. ROTOR CONNECTED TO A DIRECT VOLTAGE SUPPLY (f_r=0). THE STATOR CONNECTED TO A CURRENT SOURCE CONTAINING HARMONICS OF ORDER ν_s.*

Under these circumstances, the following simplifications are possible:

$$\sum_{\nu_{sr}} P^s_{de(\nu_{sr})} \equiv 0 \quad ; \quad \sum_{\nu_r} P^r_{in(\nu_r)} \equiv 0$$

$$\sum_{\nu_r} P^r_{de(\nu_r)} \equiv 0 \quad ; \quad \sum_{\nu_s,\nu_r} \overline{T}_{e(\nu_s,\nu_r)} \equiv 0$$

Consequently the power balance becomes:

$$\left\{P^s_{in(1)} - P^s_{de(1)}\right\} + \left\{\sum_{\nu_s} P^s_{in(\nu_s)} - \sum_{\nu_s} P^s_{de(\nu_s)}\right\} = \left\{P^r_{de(1)} - P^r_{in(1)}\right\} + \sum_{\nu_{rs}} P^r_{de(\nu_{rs})} + \overline{T}_{e(1)}\omega_m + \left\{\sum_{\nu_{rs}} \overline{T}_{e(\nu_{rs})}\right\}\omega_m \qquad \text{A2.8a}$$

The fundamental torque $\overline{T}_{e(1)}$ will only contain the synchronous component in this case, as the fundamental stator field is stationary with respect to the rotor, the transducer operating at

$$\omega_m = \frac{\omega_s}{p}$$

Equating $\left\{P^s_{in(1)} - P^s_{de(1)}\right\} = P^s_{g(1)} = \overline{T}_{e(1)} \cdot \frac{\omega_s}{p}$ A2.8b

and $\sum_{\nu_s} \left\{P^s_{in(\nu_s)} - P^s_{de(\nu_s)}\right\} = \sum_{\nu_s} P^s_{g(\nu_s)}$ A2.8c

where

$$P^{s}_{g(\nu_s)} = \overline{T}_{e(\nu_{rs})} \cdot \omega^{syn}_{m_{\nu rs}}$$

with the harmonic synchronous speed of the fundamental machine

$$\omega^{syn}_{m_{\nu rs}} = \frac{(-1)^{c_{s_{\nu_s}}} \omega_s}{p} \qquad \text{A2.8d}$$

it is found that

$$\overline{T}_{e(1)} \cdot \frac{\omega_s}{p} + \sum_{\nu_s} \overline{T}_{e(\nu_{rs})} \frac{(-1)^{c_{s_{\nu_s}}} \omega_s}{p} = \overline{T}_{e(1)} \cdot \omega_m + \sum_{\nu_s} \overline{T}_{e(\nu_{rs})} \cdot \frac{s_{\nu rs}(-1)^{c_{s_{\nu_s}}} \omega_s}{p}$$

$$+ \left\{ \sum_{\nu_{rs}} \overline{T}_{e(\nu_{rs})} \right\} \omega_m \qquad \text{A2.8e}$$

since

$$P^{r}_{de(1)} - P^{r}_{in(1)} = 0$$

and the harmonic torques all have an asynchronous character and originate from the stator. The rotor harmonic copper loss is represented by

$$\sum_{\nu_{rs}} P^{r}_{de(\nu_{rs})} = \sum_{\nu_{rs}} \overline{T}_{e(\nu_{rs})} \cdot \frac{s_{\nu rs}(-1)^{c_{s_{\nu_s}}} \omega_s}{p}$$

with

$$s_{\nu rs} = \frac{(-1)^{c_{s_{\nu_s}}} \omega_s - p\omega_m}{(-1)^{c_{s_{\nu_s}}} \omega_s} \qquad \text{A2.8f}$$

representing the harmonic slip.

A2.1.2 *ASYNCHRONOUS TRANSDUCER. POWER INPUT TO THE ROTOR ZERO, STATOR SUPPLY CONTAINING HARMONICS OF ORDER* ν_s.

The rotor electrical port is terminated by a short-circuit. Let the stator supply voltage, and consequently the stator current, contain harmonics of order ν_s.
The following may now be taken into account:

$$\sum_{\nu_{sr}} P^{s}_{de(\nu_{sr})} \equiv 0 \quad ; \quad P^{r}_{in(1)} \equiv 0 \quad ; \quad \sum_{\nu_r} P^{r}_{in(\nu_r)} \equiv 0$$

$$\sum_{\nu_s, \nu_r} \overline{T}_{e(\nu_s, \nu_r)} \equiv 0 \quad ; \quad \sum_{\nu_r} P^{r}_{de(\nu_r)} \equiv 0$$

The power balance is:

$$\left\{P^s_{in(1)} - P^s_{de(1)}\right\} + \left\{\sum_{\nu_s} P^s_{in(\nu_s)} - \sum_{\nu_s} P^s_{de(\nu_s)}\right\} = P^r_{de(1)} + \sum_{\nu_{rs}} P^r_{de(\nu_{rs})}$$

$$+ \overline{T}_{e(1)}\omega_m + \omega_m \left\{\sum_{\nu_{rs}} \overline{T}_{e(\nu_{rs})}\right\} \qquad \text{A2.9a}$$

The fundamental torque $\overline{T}_{e(1)}$ contains only a stator - rotor asynchronous component, and all the harmonic torques also have the same character. Taking into account that in the case of operation as induction machine

$$P^r_{de(1)} = \overline{T}_{e(1)} \cdot \frac{s\omega_s}{p} \qquad \text{A2.9b}$$

and observing the relations used to simplify A2.8:

$$\overline{T}_{e(1)} \cdot \frac{\omega_s}{p} + \sum_{\nu_s} \overline{T}_{e(\nu_{rs})} \frac{(-1)^{c_{s\nu_s}} \omega_s}{p} = \overline{T}_{e(1)} \cdot \frac{s\omega_s}{p} + \overline{T}_{e(1)} \cdot \omega_m$$

$$+ \sum_{\nu_s} \overline{T}_{e(\nu_{rs})} \cdot \frac{{}_{s\nu_{rs}} \cdot (-1)^{c_{s\nu_s}} \omega_s}{p} + \sum_{\nu_{rs}} \overline{T}_{e(\nu_{rs})} \cdot \omega_m \qquad \text{A2.9c}$$

A2.1.3 *ASYNCHRONOUS TRANSDUCER, POWER INPUT TO THE ROTOR ZERO, ROTOR CURRENT CONTAINING HARMONICS OF ORDER ν_r DUE TO SWITCHING.*

The rotor electrical port is again terminated by a short circuit. Switching action takes place in the rotor, and the rotor current contains harmonics of order ν_r, while the stator supply voltage obeys a simple harmonic time function of frequency f_s.

The conditions simplifying the general power relation A2.7b in this case are:

$$\sum_{\nu_s} P^s_{in(\nu_s)} \equiv 0 \quad ; \quad P^r_{in(1)} \equiv 0 \quad ; \quad \sum_{\nu_r} P^r_{in(\nu_r)} \equiv 0$$

$$\sum_{\nu_s} P^s_{de(\nu_s)} \equiv 0 \quad ; \quad \sum_{\nu_{rs}} P^r_{de(\nu_{rs})} \equiv 0 \quad ; \quad \sum_{\nu_s, \nu_r} \overline{T}_{e(\nu_s, \nu_r)} \equiv 0$$

In this case the general power balance given in equation A2.7 becomes:

$$\left\{P^s_{in(1)} - P^s_{de(1)}\right\} - \sum_{\nu_{sr}} P^s_{de(\nu_{sr})} = P^r_{de(1)} + \sum_{\nu_r} P^r_{de(\nu_r)} + \overline{T}_{e(1)}\omega_m + \sum_{\nu_{sr}} \left\{\overline{T}_{e(\nu_{sr})}\right\}\omega_m \qquad \text{A2.10a}$$

The speeds of rotation of the rotor fields are given in rel. A2.2 and the speed of rotation with respect to the stator in A2.4d. The speed of rotation with respect to the stator is zero at the harmonic synchronous speed of the "fundamental machine"

$$\omega^{syn}_{m_{\nu sr}} = -\frac{(-1)^{c_r}\nu_r\omega_r}{p} = \frac{(-1)^{\overline{c_r+1}}\nu_r\omega_r}{p} \qquad \text{A2.10b}$$

c_r=1, or 2 depending on the order of the harmonic field.
The harmonic slip is defined as:

$$s_{\nu sr} = \frac{\omega^{syn}_{m_{\nu sr}} - \omega_m}{\omega^{syn}_{m_{\nu sr}}} = \frac{(-1)^{c_r}\nu_r\omega_r + p\omega_m}{(-1)^{c_r}\nu_r\omega_r} \qquad \text{A2.10c}$$

The additional copper loss in the stator circuit is due to the induction from the rotor, and is equal to the harmonic slip loss.
These losses are:

$$\sum_{\nu_{sr}} P^s_{de(\nu_{sr})} = \sum_{\nu_r} \overline{T}_{e(\nu_{sr})} \cdot s_{\nu sr} \frac{(-1)^{\overline{c_r+1}}\nu_r\omega_r}{p} = \sum_{\nu_{sr}} \overline{T}_{e(\nu_{sr})} \cdot s_{\nu sr} \cdot \omega^{syn}_{m_{\nu sr}} \qquad \text{A2.10d}$$

The equation for power flow is now rearranged, resulting in:

$$P^s_{in(1)} = P^s_{de(1)} + P^r_{de(1)} + \overline{T}_{e(1)} \cdot \omega_m + \sum_{\nu_r} P^r_{de(\nu_r)} + \sum_{\nu_{sr}} P^s_{de(\nu_{sr})} + \left[\sum_{\nu_{sr}} \overline{T}_{e(\nu_{sr})}\right]\omega_m$$

The fundamental air gap power in the present situation will be:

$$P^r_{de(1)} + \overline{T}_{e(1)} \cdot \omega_m = \overline{T}_{e(1)} \cdot \frac{\omega_s}{p} = P^s_{g(1)} \neq \left[P^s_{in(1)} - P^s_{de(1)}\right] \qquad \text{A2.10e}$$

In analogy a "harmonic air gap power" is to be defined for the harmonic fields as:

$$\sum_{\nu_{sr}} P^s_{de(\nu_{sr})} + \left[\sum_{\nu_{sr}} \overline{T}_{e(\nu_{sr})}\right] \cdot \omega_m = \sum_{\nu_r} \overline{T}_{e(\nu_{sr})} \cdot \frac{(-1)^{c_r+1}\nu_r\omega_r}{p} = \sum_{\nu_r} P^r_{g(\nu_r)} \qquad \text{A2.10e}$$

It can now be seen that the fundamental input power may be divided into two components:

$$P^s_{in(1)} = P^s_{in(1,1)} + P^s_{in(1,\nu)} \qquad \text{A2.10f}$$

where

$$P^s_{in(1,1)} = P^s_{de(1)} + \overline{T}_{e(1)} \cdot \frac{\omega_s}{p}$$

and

$$P^s_{in(1,\nu)} = \sum_{\nu_r} P^r_{de(\nu_r)} + \sum_{\nu_r} \overline{T}_{e(\nu_{sr})} \frac{(-1)^{\overline{c_r+1}} \nu_r \omega_r}{p}$$

The implication of this division of the input power may be seen as follows. The power input at fundamental frequency has a component supplying the power associated with the stator and rotor currents causing the fundamental component of the torque, and a component that is converted into harmonic power by the action of the non-linear element in the rotor. The fundamental dissipation loss $P^s_{de(1)}$ in the stator may be termed a "non-conversion" loss, since it is in principle unnecessary for the electromechanical conversion of power by asynchronous interaction. Identical considerations are valid for the harmonic dissipation loss $\sum_{\nu_r} P^r_{de(\nu_r)}$ in the rotor windings.

A rearrangement of the power flow equation taking rel. A2.10d and rel. A2.10f into account now results in:

$$P^s_{in(1,1)} - P^s_{de(1)} + P^s_{in(1,\nu)} - \sum_{\nu_r} P_{de(\nu_r)} = \overline{T}_{e(1)} \cdot \frac{s\omega_s}{p} + \overline{T}_{e(1)} \cdot \omega_m$$

$$+ \sum_{\nu_r} \overline{T}_{e(\nu_{sr})} \cdot s_{\nu sr} \frac{(-1)^{\overline{c_r+1}} \nu_r \omega_r}{p} + \left[\sum_{\nu_{sr}} \overline{T}_{e(\nu_{sr})} \right] \cdot \omega_m \qquad \text{A2.10g}$$

Up to the present the only particulars considered known for the model were powers and frequencies. To calculate the value of the above two components of the fundamental input power it is also necessary to take phase relationships between the different components of current and voltage into account. As attention will be devoted in subsequent chapters to solutions for the current components caused by the different voltage components due to switching, the above relation will be left in its present form for the purposes of chapter 2.

A2.1.4 *STATOR AND ROTOR CONNECTED TO SINUSOIDAL VOLTAGE SUPPLY OF RESPECTIVELY STATOR AND ROTOR FREQUENCY, ROTOR HARMONICS DUE TO SWITCHING IN THE ROTOR CIRCUIT.*

In the case now to be investigated it will be assumed that switching action takes place in the rotor circuit. Rotor current harmonics of order ν_r therefore exist causing stator currents of order ν_{sr} by induction as in the previous case. The following conditions hold:

$$\sum_{\nu_s} P^s_{in(\nu_s)} \equiv 0 \; ; \; \sum_{\nu_{rs}} P^r_{de(\nu_{rs})} \equiv 0 \quad \sum_{\nu_r, \nu_s} \overline{T}_{e(\nu_r, \nu_s)} \equiv 0$$

$$\sum_{\nu_r} P^r_{in(\nu_r)} \equiv 0 \quad \sum_{\nu_s} P^s_{de(\nu_s)} \equiv 0$$

Thus:

$$P^s_{in} - P^s_{de(1)} - \sum_{\nu_{sr}} P^s_{de(\nu_{sr})} = P^r_{de(1)} - P^r_{in(1)} + \sum_{\nu_r} P^r_{de(\nu_r)}$$

$$+ \overline{T}_{e(1)}\omega_m + \left[\sum_{\nu_{sr}} \overline{T}_{e(\nu_{sr})}\right] \omega_m \qquad \text{A2.11a}$$

Only fundamental power can be delivered by both the stator and rotor sources, while a certain amount of this power from each source should contribute to the harmonic losses and harmonic power output. In analogy to A2.10e:

$$P^r_{in(1)} = P^r_{in(1,1)} + P^r_{in(1,\nu)} \qquad \text{A2.11b}$$

Rewriting the power balance of A2.11a by using A2.10e and A2.11b:

$$P^s_{in(1,1)} - P^s_{de(1)} + P^s_{in(1,\nu)} + P^r_{in(1,\nu)} - \sum_{\nu_r} P^r_{de(\nu_r)} =$$

$$= P^r_{de(1)} - P^r_{in(1,1)} + \overline{T}_{e(1)}\cdot\omega_m + \sum_{\nu_{sr}} P^s_{de(\nu_{sr})} + \left[\sum_{\nu_{sr}} \overline{T}_{e(\nu_{sr})}\right] \omega_m \qquad \text{A2.11c}$$

If it is now substituted in this relation that the fundamental air gap power is given by

$$P^s_{g(1)} = P^s_{in(1,1)} - P^s_{de(1)} = P^r_{de(1)} - P^r_{in(1,1)} + \overline{T}_{e(1)}\cdot\omega_m,$$

it follows that:

$$P^s_{in(1,\nu)} + P^r_{in(1,\nu)} - \sum_{\nu_r} P^r_{de(\nu_r)} = \sum_{\nu_{sr}} P^s_{de(\nu_{sr})} + \left[\sum_{\nu_{sr}} \overline{T}_{e(\nu_{sr})}\right] \omega_m$$

In the case of the rotor source voltage zero a harmonic air gap power was defined (see rel.A2.10f). Application to the above relations results in the following expression for the harmonic air gap power:

$$\sum_{\nu_r} P^r_{g(\nu_r)} = P^s_{in(1,\nu)} + P^r_{in(1,\nu)} - \sum_{\nu_r} P^r_{de(\nu_r)}$$

The power flow relation A2.11c is now expressed in terms of the different torque components as:

$$\overline{T}_{e(1)}\cdot\frac{\omega_s}{p} + \sum_{\nu_r} \overline{T}_{e(\nu_{sr})} \frac{(-1)^{\overline{c_r+1}}\nu_r\omega_r}{p} = \overline{T}_{e(1)}\cdot\frac{s\omega_s}{p} + \overline{T}_{e(1)}\cdot\omega_m +$$

$$+ \sum_{\nu_r} \overline{T}_{e(\nu_{sr})}\cdot s_{\nu sr} \frac{(-1)^{\overline{c_r+1}}\nu_r\omega_r}{p} + \left[\sum_{\nu_{sr}} \overline{T}_{e(\nu_{sr})}\right]\cdot\omega_m \qquad \text{A2.11d}$$

Regarding the relation A2.11d it may be remarked that by taking the expressions for fundamental and harmonic air gap power into account as stated in equations A2.10f for the case of app.A2.1.3, the same type of expression may be obtained in lieu of equation A2.10g, as used in the text in relation 2.14a. The only difference existing between the cases of A2.1.3 and A2.1.4 is located in the division of the stator resp. stator and rotor fundamental input power into fundamental power and harmonic power due to the switching action in the rotor. In the situation where the rotor voltage sources were zero it was remarked that it is not possible to calculate the division of the fundamental power with the particulars known at present. The same conclusion is reached for the present case where the rotor is fed from voltage sources of fundamental rotor frequency. Relation A2.11c (or A2.11d) will be left in its present form for the purposes of chapter 2.

A2.1.5 *CONCERNING A SIMPLIFIED POWER FLOW MODEL FOR THE SYSTEMS WITH ROTOR HARMONICS OF ORDER* ν_r.

In the last two instances investigated it proved impossible to specify the power flow explicitly, although it was still possible to express the power flow equation in terms of the fundamental and harmonic torques and their respective synchronous speeds and slips. This will enable these relations to be subjected to investigation in the present chapter. When it is to be attempted in later chapters to calculate the currents and torques in the machine, it will become evident that there is a need for a more simplified model for the systems represented in appendix A2.1.3 and A2.1.4. It will now be investigated to what extent a valid simplified power flow model may be used in these two situations.

In the first instance it may be considered that the stator resistance is zero. With zero rotor voltage, consider that the following conditions now hold:

$$P^s_{de(1)} \equiv 0 \equiv \sum_{\nu_{sr}} P^s_{de(\nu_{sr})} \; ; \; \sum_{\nu_{sr}} \overline{T}_{e(\nu_{sr})} \equiv 0$$

The power balance of A2.10a now becomes:

$$P^s_{in(1)} = P^r_{de(1)} + \sum_{\nu_r} P^r_{de(\nu_r)} + \overline{T}_{e(1)} \cdot \omega_m \qquad \text{A2.12a}$$

Since the possibility of harmonic torques due to rotor-stator interaction has now been eliminated, the only active power delivered to the rotor will be of fundamental frequency. The harmonic power exchange between rotor and stator is constrained to reactive power. Expressing relation A2.12 in terms of the fundamental torque it is found that:

$$\overline{T}_{e(1)} \cdot \frac{\omega_s}{p} = P^r_{de(1)} + \sum_{\nu_r} P^r_{de(\nu_r)} + \overline{T}_{e(1)} \cdot \omega_m, \qquad \text{A2.12b}$$

This implies that the relation between the rotor dissipation and synchronous fundamental power will be given by:

$$P^r_{de(1)} + \sum_{\nu_r} P^r_{de(\nu_r)} = \overline{T}_{e(1)} \cdot \frac{s\omega_s}{p} \qquad \text{A2.12c}$$

This explicit relation existing between the rotor dissipation and the electromagnetic torque due to the fundamental frequency will enable the calculation of the torque when the dissipation is known.

Let the constraint that the rotor source voltage is zero now be relaxed, and consequently assume the rotor electrical ports to be fed by an ideal voltage supply system of fundamental rotor frequency. The harmonic currents due to the switching action still circulate in the rotor circuits. Consequently the following power balance may be derived from rel. A2.11a:

$$P^{s}_{in(1)} = P^{r}_{de(1)} - P^{r}_{in(1)} + \sum_{\nu_r} P^{r}_{de(\nu_r)} + \overline{T}_{e(1)} \cdot \omega_m \qquad \text{A2.12d}$$

As in the previous case the stator dissipation is zero, and the active input power at the stator electrical ports must equal the active air gap power. Therefore:

$$\overline{T}_{e(1)} \cdot \frac{\omega_s}{p} = P^{r}_{de(1)} - P^{r}_{in(1)} + \sum_{\nu_r} P^{r}_{de(\nu_r)} + \overline{T}_{e(1)} \cdot \omega_m \qquad \text{A2.12e}$$

The relation between the synchronous air gap active power and the rotor active power now becomes:

$$P^{r}_{de(1)} - P^{r}_{in(1)} + \sum_{\nu_r} P^{r}_{de(\nu_r)} = \overline{T}_{e(1)} \cdot \frac{s\omega_s}{p} \qquad \text{A2.12f}$$

In the previous arguments of this paragraph no restriction has been placed upon the existence of harmonic fields (as described by equation A2.2). If these harmonic fields still exist in the air gap of the machine, inducing circulating currents in the stator, it is not to be expected that the induced e.m.f.'s in the rotor circuits will be simple harmonic functions of time. As will be evident in subsequent chapters, calculation of the currents in the rotor windings is considerably simplified when it is known that the induced e.m.f.'s are simple harmonic functions of time. Once the rotor currents are known, the dissipation is known and the appropriate relation can be selected from the relations A2.12c or A2.12f to calculate the electromagnetic torque.

Therefore, in order to be able to use the power flow relations developed in this chapter and this appendix in subsequent work, it will be stated that the induced e.m.f.'s are simple harmonic time functions. This is assumed by postulating the existence of a "field source". This "field source" feeds the stator electrical ports, and acts in such a way that under all conditions the rotating magnetic field in the air gap of the machine remains constant.

A3.1 CONCERNING THE CALCULATION OF THE EXPRESSIONS FOR THE CONVERSION CURRENTS IN STATOR AND ROTOR CONTROLLED ELECTROMECHANICAL TRANSDUCERS.

A3.1.1 *STATOR-CONTROLLED TRANSDUCERS: CALCULATION OF CURRENTS.*

In the text the expressions for the excitation functions concerned with the instantaneous symmetrical component currents involved in the energy conversion process have been given. To exploit the complex conjugate relationship it is substituted in the stator-conversion voltages that:

$$\left.\begin{aligned}
\underset{s\ \overline{2h+1}}{\dot{\bar{V}}^{xp} } &= \left\{ (z_s)^{\overline{x-1}} \right\}^{1-\overline{2h+1}} \underset{s\ \overline{2h+1}}{\dot{\bar{U}}^{x}} \\
\underset{s\ \overline{2h+1}}{\dot{\bar{V}}^{xn*} } &= \left\{ (z_s)^{\overline{x-1}} \right\}^{1+\overline{2h+1}} \underset{s\ \overline{2h+1}}{\dot{\bar{U}}^{x*}} \\
\underset{s\ \overline{2h+1}}{\dot{\bar{V}}^{xn} } &= \left\{ (z_s)^{\overline{x-1}} \right\}^{\overline{n-1}-\overline{2h+1}} \underset{s\ \overline{2h+1}}{\dot{\bar{U}}^{x}} \\
\underset{s\ \overline{2h+1}}{\dot{\bar{V}}^{xp*} } &= \left\{ (z_s)^{\overline{x-1}} \right\}^{\overline{n-1}+\overline{2h+1}} \underset{s\ \overline{2h+1}}{\dot{\bar{U}}^{x*}}
\end{aligned}\right\} \quad \text{A 3.1a}$$

and in the rotor conversion voltages that:

$$\left.\begin{aligned}
\dot{V}_r^{xp} &= \dot{U}_r^{x} \\
\dot{V}_r^{xn*} &= (z_r)^{2\overline{x-1}} \dot{U}_r^{x*} \\
\dot{V}_r^{xn} &= \left\{ (z_r)^{\overline{m-2}-\overline{x-1}} \right\} \dot{U}_r^{x} \\
\dot{V}_r^{xp*} &= \left\{ (z_r)^{m.\overline{x-1}} \right\} \dot{U}_r^{x*}
\end{aligned}\right\} \quad \text{A 3.1b}$$

Under the Ku-transformation from rotor to stator, the rotor instantaneous symmetrical conversion voltages then become:

$$\begin{bmatrix} \dot{u}_r^{2,t} . \exp j(p\overline{\omega_m t+\theta_o}) \\ \dot{u}_r^{m,t} \exp -j(p\overline{\omega_m t+\theta_o}) \end{bmatrix} = \frac{1}{\sqrt{2m}} \begin{bmatrix} (\dot{V}_r^{xp} \exp j\omega_r t + \dot{V}_r^{xn*} \exp -j\omega_r t) \exp j(p\overline{\omega_m t+\theta_o}) \\ (\dot{V}_r^{xn} \exp j\omega_r t + \dot{V}_r^{xp*} \exp -j\omega_r t) \exp -j(p\overline{\omega_m t+\theta_o}) \end{bmatrix} \quad \text{A 3.2a}$$

Observing all the above relations, the instantaneous symmetrical component voltages concerned with the energy conversion under the Ku rotor stator transformation become:

$$\begin{bmatrix} \dot{\bar{u}}_s^{2,t} \\ \dot{\bar{u}}_s^{n,t} \end{bmatrix} = \frac{1}{\sqrt{2n}} \sum_{x=1}^{n} \sum_{h=0}^{\infty} \begin{bmatrix} \dot{\bar{V}}_{s\ \overline{2h+1}}^{xp} \exp j(\overline{2h+1}\omega_s t) + \dot{\bar{V}}_{s\ \overline{2h+1}}^{xn*} \exp -j(\overline{2h+1}\omega_s t) \\ \dot{\bar{V}}_{s\ \overline{2h+1}}^{xn} \exp j(\overline{2h+1}\omega_s t) + \dot{\bar{V}}_{s\ \overline{2h+1}}^{xp*} \exp -j(\overline{2h+1}\omega_s t) \end{bmatrix} \qquad \text{A 3.2b}$$

and

$$\begin{bmatrix} \dot{u}_r^{2,t} \exp j(p\overline{\omega_m t+\theta_o}) \\ \dot{u}_r^{m,t} \exp -j(p\overline{\omega_m t+\theta_o}) \end{bmatrix} = \frac{1}{\sqrt{2m}} \begin{bmatrix} \dot{V}_r^{xp} \exp j(\omega_s t+p\theta_o) + \dot{V}_r^{xn*} \exp -j(\overline{\omega_s -2p\omega_m} t-p\theta_o) \\ \dot{V}_r^{xn} \exp j(\overline{\omega_s -2p\omega_m} t-p\theta_o) + \dot{V}_r^{xp*} \exp -j(\omega_s t+p\theta_o) \end{bmatrix} \qquad \text{A 3.2c}$$

From relations 3.36a, 3.42a and the above voltage components the stator "positive" sequence component follows as:

$$\dot{\bar{I}}_s^{2,t} = \frac{1}{\sqrt{2n}} \sum_{x=1}^{n} \sum_{h=0}^{\infty} \left\{ \frac{\dot{\bar{V}}_{s\ \overline{2h+1}}^{xp} \exp j(\overline{2h+1}\omega_s t)}{\left[Z_{sD} - \frac{\frac{nm}{4} M_{sr}^2 D(D-jp\omega_m)}{Z_{rD}^-} \right]} + \frac{\dot{\bar{V}}_{s\ \overline{2h+1}}^{xn*} \exp -j(\overline{2h+1}\omega_s t)}{\left[Z_{sD} - \frac{\frac{nm}{4} M_{sr}^2 D(D-jp\omega_m)}{Z_{rD}^-} \right]} \right\} +$$

$$- \frac{1}{\sqrt{2m}} \sum_{x=1}^{m} \left\{ \frac{\sqrt{\frac{nm}{4}} M_{sr} D\dot{V}_r^{xp} \exp j(\omega_s t+p\theta_o)}{\left[Z_{rD}^- Z_{sD} - \frac{nm}{4} M_{sr}^2 D(D-jp\omega_m) \right]} + \frac{\sqrt{\frac{nm}{4}} M_{sr} D\dot{V}_r^{xp*} \exp -j(\overline{\omega_s -2p\omega_m} t-p\theta_o)}{\left[Z_{rD}^- Z_{sD} - \frac{nm}{4} M_{sr}^2 D(D-jp\omega_m) \right]} \right\} \qquad \text{A3.3a}$$

Similarly it is found that the "negative" sequence component is represented by:

$$\dot{\bar{I}}_s^{n,t} = \frac{1}{\sqrt{2n}} \sum_{x=1}^{n} \sum_{h=0}^{\infty} \left\{ \frac{\dot{\bar{V}}_{s\ \overline{2h+1}}^{xn} \exp j(\overline{2h+1}\omega_s t)}{\left[Z_{sD} - \frac{\frac{nm}{4} M_{sr}^2 D(D+jp\omega_m)}{Z_{rD}^+} \right]} + \frac{\dot{\bar{V}}_{s\ \overline{2h+1}}^{xp*} \exp -j(\overline{2h+1}\omega_s t)}{\left[Z_{sD} - \frac{\frac{nm}{4} M_{sr}^2 D(D+jp\omega_m)}{Z_{rD}^+} \right]} \right\} +$$

$$- \frac{1}{\sqrt{2m}} \sum_{x=1}^{m} \left\{ \frac{\sqrt{\frac{nm}{4}} M_{sr} D\dot{V}_r^{xn} \exp j(\overline{\omega_s -2p\omega_m} t-p\theta_o)}{\left[Z_{rD}^+ Z_{sD} - \frac{nm}{4} M_{sr}^2 D(D+jp\omega_m) \right]} + \frac{\sqrt{\frac{nm}{4}} M_{sr} D\dot{V}_r^{xp*} \exp -j(\omega_s t+p\theta_o)}{\left[Z_{rD}^+ Z_{sD} - \frac{nm}{4} M_{sr}^2 D(D+jp\omega_m) \right]} \right\} \qquad \text{A 3.3b}$$

By selective comparison of relations 3.42b, A3.3a and A3.3b the four unknown general complex amplitudes $\dot{\bar{I}}_{s\ \overline{2h+1}}^{xp}$; $\dot{\bar{I}}_{s\ \overline{2h+1}}^{xn}$; $\dot{I}_{sr}^{xp}$; $\dot{I}_{sr}^{xn}$, are determined as given in relations 3.42c and 3.42d.

In order to be able to calculate the electromagnetic torque of the transducer, it is still necessary to obtain explicit expressions for the instantaneous symmetrical components of the rotor currents under the Ku rotor-stator transformation. With reference to relations 3.36b, 3.43b

and the above voltage components the "positive" sequence component of the rotor current follows:

$$\dot{i}^{2,t\ ks}_{r} = -\frac{1}{\sqrt{2n}} \sum_{x=1}^{n} \sum_{h=0}^{\infty} \left\{ \frac{\sqrt{\frac{nm}{4}} M_{sr}(D-jp\omega_m)\ \dot{\bar{V}}^{xp}_{s\ \overline{2h+1}}\ \mathrm{expj}(\overline{2h+1}\omega_s t)}{\left[Z^{-}_{rD} Z_{sD} - \frac{nm}{4} M^{2}_{sr} D(D-jp\omega_m) \right]} \right.$$

$$\left. + \frac{\sqrt{\frac{nm}{4}} M_{sr}(D-jp\omega_m)\ \dot{\bar{V}}^{xn*}_{s\ \overline{2h+1}}\ \mathrm{exp-j}(\overline{2h+1}\omega_s t)}{\left[Z^{-}_{rD} Z_{sD} - \frac{nm}{4} M^{2}_{sr} D(D-jp\omega_m) \right]} \right\}$$

$$+ \frac{1}{\sqrt{2m}} \sum_{x=1}^{m} \left\{ \frac{Z_{sD} \dot{V}^{xp}_{r} \mathrm{expj}(\omega_s t + p\theta_o)}{\left[Z^{-}_{rD} Z_{sD} - \frac{nm}{4} M^{2}_{sr} D(D-jp\omega_m) \right]} + \frac{Z_{sD} \dot{V}^{xn*}_{r} \mathrm{exp-j}(\overline{\omega_s - 2p\omega_m} t - p\theta_o)}{\left[Z^{-}_{rD} Z_{sD} - \frac{nm}{4} M^{2}_{sr} D(D-jp\omega_m) \right]} \right\} \qquad \text{A 4.3a}$$

The "negative" sequence component consequently is:

$$\dot{i}^{m,t\ ks}_{r} = -\frac{1}{\sqrt{2n}} \sum_{x=1}^{n} \sum_{h=0}^{\infty} \left\{ \frac{\sqrt{\frac{nm}{4}} M_{sr}(D+jp\omega_m)\ \dot{\bar{V}}^{xn}_{s\ \overline{2h+1}}\ \mathrm{expj}(\overline{2h+1}\omega_s t)}{\left[Z^{+}_{rD} Z_{sD} - \frac{nm}{4} M^{2}_{sr} D(D-jp\omega_m) \right]} \right.$$

$$\left. + \frac{\sqrt{\frac{nm}{4}} M_{sr}(D+jp\omega_m)\ \dot{\bar{V}}^{xp*}_{s\ \overline{2h+1}}\ \mathrm{exp-j}(\overline{2h+1}\omega_s t)}{\left[Z^{+}_{rD} Z_{sD} - \frac{nm}{4} M^{2}_{sr} D(D+jp\omega_m) \right]} \right\}$$

$$+ \frac{1}{\sqrt{2m}} \sum_{x=1}^{m} \left\{ \frac{Z_{sD} \dot{V}^{xn}_{r} \mathrm{expj}(\overline{\omega_s - 2p\omega_m} t - p\theta_o)}{\left[Z^{+}_{rD} Z_{sD} - \frac{nm}{4} M^{2}_{sr} D(D+jp\omega_m) \right]} + \frac{Z_{sD} \dot{V}^{xp*}_{r} \mathrm{exp-j}(\omega_s t + p\theta_o)}{\left[Z^{+}_{rD} Z_{sD} - \frac{nm}{4} M^{2}_{sr} D(D+jp\omega_m) \right]} \right\} \qquad \text{A 4.3b}$$

Comparing relations 3.43b, A4.3a and A4.3b it is possible to calculate the unknown general complex amplitudes $\dot{I}^{xp}_{r\ \overline{2h+1}}$; $\dot{I}^{xn}_{r\ \overline{2h+1}}$; $\dot{I}^{xp}_{rr}$; $\dot{I}^{xn}_{rr}$ as given in relations 3.43c and 3.43d.

A3.1.2 *STATOR-CONTROLLED TRANSDUCERS: CALCULATION OF ELECTROMAGNETIC TORQUE.*

When the expressions 3.42 and 3.43 for the instantaneous symmetrical component currents under the rotor-stator Ku-transformation are substituted into torque-relations 3.14 or 3.17, it is obtained that:

$$T_e = jp\sqrt{\frac{mn}{4}}M_{sr}\left\{\left(\frac{1}{\sqrt{2n}}\sum_{x=1}^{n}\sum_{h=0}^{\infty}\left[\dot{\bar{I}}_{s}^{xn}\,\overline{2h+1}\,\exp j\,\overline{2h+1}\omega_s t + \dot{\bar{I}}_{s}^{xp*}\,\overline{2h+1}\,\exp -j\,\overline{2h+1}\omega_s t\right]\right.\right.$$

$$\left.\left. + \frac{1}{\sqrt{2m}}\sum_{x=1}^{m}\left[\dot{I}_{sr}^{xn}\exp j(\overline{2s-1}\omega_s t) + \dot{I}_{sr}^{xp*}\exp -j\omega_s t\right]\right)\right.$$

$$\times\left(\frac{1}{\sqrt{2n}}\sum_{x=1}^{n}\sum_{h=0}^{\infty}\left[\dot{I}_{r}^{xp}\,\overline{2h+1}\,\exp j\,\overline{2h+1}\omega_s t + \dot{I}_{r}^{xn*}\,\overline{2h+1}\,\exp -j\,\overline{2h+1}\omega_s t\right]\right.$$

$$\left. + \frac{1}{\sqrt{2m}}\sum_{x=1}^{m}\left[\dot{I}_{rr}^{xp}\exp j\omega_s t + \dot{I}_{rr}^{xn*}\exp -j(\overline{2s-1}\omega_s t)\right]\right)$$

$$-\left(\frac{1}{\sqrt{2n}}\sum_{x=1}^{n}\sum_{h=0}^{\infty}\left[\dot{\bar{I}}_{s}^{xp}\,\overline{2h+1}\,\exp j\,\overline{2h+1}\omega_s t + \dot{\bar{I}}_{s}^{xn*}\,\overline{2h+1}\,\exp -j\,\overline{2h+1}\omega_s t\right]\right.$$

$$\left. + \frac{1}{\sqrt{2m}}\sum_{x=1}^{m}\left[\dot{I}_{sr}^{xp}\exp j\omega_s t + \dot{I}_{sr}^{xn*}\exp -j(\overline{2s-1}\omega_s t)\right]\right)$$

$$\times\left(\frac{1}{\sqrt{2n}}\sum_{x=1}^{n}\sum_{h=0}^{\infty}\left[\dot{I}_{r}^{xn}\,\overline{2h+1}\,\exp j\,\overline{2h+1}\omega_s t + \dot{I}_{r}^{xp*}\,\overline{2h+1}\,\exp -j\,\overline{2h+1}\omega_s t\right]\right.$$

$$\left.\left. + \frac{1}{\sqrt{2m}}\sum_{x=1}^{m}\left[\dot{I}_{rr}^{xn}\exp j(\overline{2s-1}\omega_s t) + \dot{I}_{rr}^{xp*}\exp -j\omega_s t\right]\right)\right\}$$

Evaluating all the products for this expression, and simplifying, gives the general electromagnetic torque equation 3.44a in the text. By rearranging the expression, and changing the order of appropriate summations, it is possible to express the equations in a form containing complex conjugate pairs as follows:

$$T_e = jp\sqrt{\frac{nm}{4}}M_{sr} \cdot \left\{ \frac{1}{2n} \sum_{y=1}^{n} \sum_{x=1}^{n} \sum_{h=0}^{\infty} \left(\left[\underline{\dot{\bar{I}}}^{yn}_{s\ \overline{2h+1}} \cdot \dot{I}^{xp}_{r\ \overline{2h+1}} - \underline{\dot{\bar{I}}}^{yp}_{s\ \overline{2h+1}} \cdot \dot{I}^{xn}_{r\ \overline{2h+1}} \right] \exp j2(\overline{2h+1}\omega_s t) \right.\right.$$

$$- \left[\underline{\dot{\bar{I}}}^{yn*}_{s\ \overline{2h+1}} \cdot \dot{I}^{xp*}_{r\ \overline{2h+1}} - \underline{\dot{\bar{I}}}^{yp*}_{s\ \overline{2h+1}} \cdot \dot{I}^{xn*}_{r\ \overline{2h+1}} \right] \exp -j2(\overline{2h+1}\omega_s t)$$

$$\left. + \left[\left(\underline{\dot{\bar{I}}}^{yn}_{s\ \overline{2h+1}} \cdot \dot{I}^{xn*}_{r\ \overline{2h+1}} - \underline{\dot{\bar{I}}}^{yn*}_{s\ \overline{2h+1}} \cdot \dot{I}^{xn}_{r\ \overline{2h+1}} \right) + \left(\underline{\dot{\bar{I}}}^{yp*}_{s\ \overline{2h+1}} \cdot \dot{I}^{xp}_{r\ \overline{2h+1}} - \underline{\dot{\bar{I}}}^{yp}_{s\ \overline{2h+1}} \cdot \dot{I}^{xp*}_{r\ \overline{2h+1}} \right) \right] \right)$$

$$+ \frac{1}{2\sqrt{nm}} \sum_{y=1}^{n} \sum_{x=1}^{m} \sum_{h=0}^{\infty} \left(\left[\underline{\dot{\bar{I}}}^{yn}_{s\ \overline{2h+1}} \cdot \dot{I}^{xp}_{rr} - \dot{I}^{yn}_{r\ \overline{2h+1}} \cdot \dot{I}^{xp}_{sr} \right] \exp j2(\overline{h+1}\omega_s t) \right.$$

$$- \left[\underline{\dot{\bar{I}}}^{yn*}_{s\ \overline{2h+1}} \cdot \dot{I}^{xp*}_{rr} - \dot{I}^{yn*}_{r\ \overline{2h+1}} \cdot \dot{I}^{xp*}_{sr} \right] \exp -j2(\overline{h+1}\omega_s t)$$

$$+ \left[\underline{\dot{\bar{I}}}^{yn}_{s\ \overline{2h+1}} \cdot \dot{I}^{xn*}_{rr} - \dot{I}^{yn}_{r\ \overline{2h+1}} \cdot \dot{I}^{xn*}_{sr} \right] \exp j2(\overline{h+1-s}\omega_s t)$$

$$- \left[\underline{\dot{\bar{I}}}^{yn*}_{s\ \overline{2h+1}} \cdot \dot{I}^{xn}_{rr} - \dot{I}^{yn*}_{r\ \overline{2h+1}} \cdot \dot{I}^{xn}_{rr} \right] \exp -j2(\overline{h+1-s}\omega_s t)$$

$$+ \left[\underline{\dot{\bar{I}}}^{yp*}_{s\ \overline{2h+1}} \cdot \dot{I}^{xp}_{rr} - \dot{I}^{yp*}_{r\ \overline{2h+1}} \cdot \dot{I}^{xp}_{sr} \right] \exp -j2h\omega_s t$$

$$- \left[\underline{\dot{\bar{I}}}^{yp}_{s\ \overline{2h+1}} \cdot \dot{I}^{xp*}_{rr} - \dot{I}^{yp}_{r\ \overline{2h+1}} \cdot \dot{I}^{xp*}_{sr} \right] \exp j2h\omega_s t$$

$$\left. + \left[\underline{\dot{\bar{I}}}^{yp*}_{s\ \overline{2h+1}} \cdot \dot{I}^{xn*}_{rr} - \dot{I}^{yp*}_{r\ \overline{2h+1}} \cdot \dot{I}^{xn*}_{sr} \right] \exp -j2(\overline{h+s}\omega_s t) \right)$$

$$- \left[\underline{\underline{\dot{I}}}^{yp}_{s\ \overline{2h+1}} . \dot{I}^{xn}_{rr} - \dot{I}^{yp}_{r\ \overline{2h+1}} . \dot{I}^{xn}_{sr} \right] \exp j2(\overline{h+s}\omega_s t) \Bigg)$$

$$+ \frac{1}{2m} \sum_{y=1}^{m} \sum_{x=1}^{m} \Bigg(\left[\dot{I}^{yn}_{sr} . \dot{I}^{xp}_{rr} - \dot{I}^{yp}_{sr} . \dot{I}^{xn}_{rr} \right] \exp j2s\omega_s t$$

$$- \left[\dot{I}^{yn*}_{sr} . \dot{I}^{xp*}_{rr} - \dot{I}^{yp*}_{sr} . \dot{I}^{xn*}_{rr} \right] \exp -j2s\omega_s t$$

$$+ \left[\left\{ \dot{I}^{yn}_{sr} . \dot{I}^{xn*}_{rr} - \dot{I}^{yn*}_{sr} . \dot{I}^{xn}_{rr} \right\} + \left\{ \dot{I}^{yp*}_{sr} . \dot{I}^{xp}_{rr} - \dot{I}^{yp}_{sr} . \dot{I}^{xp*}_{rr} \right\} \right] \Bigg) \Bigg\}$$

By observing the rule for the subtraction of two complex numbers the relation may be rewritten in a simplified form as given in 3.44b. Splitting this relation up into its different components as indicated in the text will result in the following torque components:

$$\sum_{h=0}^{\infty} T^{puls.sr}_{e(2h+1)}(2\ \overline{2h+1}\omega_s t) = - \frac{p}{2} \sqrt{\frac{m}{n}} M_{sr} \sum_{y=1}^{n} \sum_{x=1}^{n} \sum_{h=0}^{\infty} \Bigg(Im \left\{ \left[\underline{\underline{\dot{I}}}^{yn}_{s\ \overline{2h+1}} . \dot{I}^{xp}_{r\ \overline{2h+1}} - \underline{\underline{\dot{I}}}^{yp}_{s\ \overline{2h+1}} . \dot{I}^{xn}_{r\ \overline{2h+1}} \right] . \exp j2(\overline{2h+1}\omega_s t) \right\} \Bigg)$$

$$\sum_{h=0}^{\infty} T^{asyn.sr}_{e(2h+1)} = - \frac{p}{2} \sqrt{\frac{m}{n}} M_{sr} \sum_{y=1}^{n} \sum_{x=1}^{n} \sum_{h=0}^{\infty} \Bigg(Im \left\{ \dot{I}^{yn}_{s\ \overline{2h+1}} . \dot{I}^{xn*}_{r\ \overline{2h+1}} \right\} + Im \left\{ \underline{\underline{\dot{I}}}^{yp*}_{s\ \overline{2h+1}} . \dot{I}^{xp}_{r\ \overline{2h+1}} \right\} \Bigg)$$

$$\sum_{h=0}^{\infty} T^{puls.rs}_{e(2h+1)}(\overline{2h+1}\omega_s t) = - \frac{pM_{sr}}{2} \sum_{y=1}^{n} \sum_{x=1}^{m} \sum_{h=0}^{\infty} \Bigg(Im \left\{ \left[\underline{\underline{\dot{I}}}^{yn}_{s\ \overline{2h+1}} . \dot{I}^{xp}_{rr} - \dot{I}^{yn}_{r\ \overline{2h+1}} . \dot{I}^{xp}_{sr} \right] . \exp j2(\overline{h+1}\omega_s t) \right\} \Bigg)$$

$$\sum_{h=0}^{\infty} T^{syn}_{e(2h+1)}(\overline{2h+1-s}\omega_s t) = -\frac{pM_{sr}}{2}\sum_{y=1}^{n}\sum_{x=1}^{m}\sum_{h=0}^{\infty}\left(Im\left\{\left[\underline{\dot{I}}^{yn}_{s\ \overline{2h+1}}.\dot{I}^{xn*}_{rr} - \dot{I}^{yn}_{r\ \overline{2h+1}}.\dot{I}^{xn*}_{sr}\right].\right.\right.$$

$$\left.\left.\exp j2(\overline{h+1-s}\omega_s t)\right\}\right)$$

$$\sum_{h=1}^{\infty} T^{puls.rs}_{e(\overline{2h+1})}(2h\omega_s t) = -\frac{pM_{sr}}{2}\sum_{y=1}^{n}\sum_{x=1}^{m}\sum_{h=1}^{\infty}\left(Im\left\{\left[\underline{\dot{I}}^{yp*}_{s\ \overline{2h+1}}.\dot{I}^{xp}_{rr} - \dot{I}^{yp*}_{r\ \overline{2h+1}}.\dot{I}^{xp}_{sr}\right].\right.\right.$$

$$\left.\left.\exp -j2h\omega_s t\right\}\right)$$

$$T^{asyn.}_{e(1)h=0} = -\frac{pM_{sr}}{2}\sum_{y=1}^{n}\sum_{x=1}^{m}\left(Im\left\{\left[\underline{\dot{I}}^{yp*}_{s1}.\dot{I}^{xp}_{rr} - \dot{I}^{yp*}_{r1}.\dot{I}^{xp}_{sr}\right]\right\}\right)$$

$$\sum_{h=0}^{\infty} T^{syn.}_{e(2h+1)}(\overline{2h+s}\omega_s t) = -\frac{pM_{sr}}{2}\sum_{y=1}^{n}\sum_{x=1}^{m}\sum_{h=0}^{\infty}\left(Im\left\{\left[\underline{\dot{I}}^{yp*}_{s\ \overline{2h+1}}.\dot{I}^{xn*}_{rr} - \dot{I}^{yp*}_{r\ \overline{2h+1}}.\dot{I}^{xn*}_{sr}\right].\right.\right.$$

$$\left.\left.\exp -j2(\overline{h+s}\omega_s t)\right\}\right)$$

$$T^{syn}_{e(1)}(2s\omega_s t) = -\frac{p}{2}\sqrt{\frac{L}{m}}_{sr}\sum_{y=1}^{n}\sum_{x=1}^{m}\left(Im\left\{\left[\dot{I}^{yn}_{sr}.\dot{I}^{xp}_{rr} - \dot{I}^{yp}_{sr}.\dot{I}^{xn}_{rr}\right]\ \exp j2s\omega_s t\right\}\right)$$

$$T^{asyn.rs}_{e(1)} = -\frac{p}{2}\sqrt{\frac{m}{L}}_{sr}\sum_{y=1}^{n}\sum_{x=1}^{m}\left(Im\left\{\dot{I}^{yn}_{sr}.\dot{I}^{xn*}_{rr}\right\} + Im\left\{\dot{I}^{yp*}_{sr}.\dot{I}^{xp}_{rr}\right\}\right)$$

as given in equation 3.44c.

A.3.3 CALCULATIONS CONCERNING A SIMPLIFIED MODEL FOR MACHINE-ELECTRONIC SYSTEMS OF GROUP II WITH ROTOR CONTROL.

Calculation of the torque and the different current components for a machine-electronic system of Group II, class 2, with control of the conduction angle of the rotor current is to be undertaken. As explained in the text of chapter 3, and in appendix A2.1.5, the conditions in the present model has been chosen so that the induced e.m.f. in the x th rotor phase will be sinusoidal, i.e.

$$e_r^x = s\sqrt{2}\, E_{ro} \sin(\omega_r t - \overline{x-1}\,\Delta_r) \qquad \Delta_r = \frac{2\pi}{m} \qquad \text{A3.6}$$

Consider the first phase, $\Delta_r = 0$.

The total input power per phase is represented by:

$$\sum_{h=0}^{\infty} \frac{p^r \text{ phase}}{de(2h+1)} = sE_{ro}\bar{\bar{I}}_{r1} \cos\psi_{re_ri_{r1}} \qquad \text{A3.7}$$

where $\psi_{re_ri_{r1}}$ is the phase angle by which the fundamental current is lagging on the induced voltage. It may be calculated from the current equation 3.52 that:

$$\bar{\bar{I}}_{r\ \overline{2h+1}} = I_r\left\{\left(A^i_{r\ \overline{2h+1}}\right)^2 + \left(B^i_{r\ \overline{2h+1}}\right)^2\right\}^{\frac{1}{2}} \exp -j\psi_{r\ \overline{2h+1}}$$

$$\psi_{r\ \overline{2h+1}} = \arctan\left(\frac{B^i_{r\ \overline{2h+1}}}{A^i_{r\ \overline{2h+1}}}\right) \qquad I_r = \frac{E_{ro}}{\sqrt{\frac{R_r^2}{s^2} + \omega_s^2 L_{r\sigma}^2}}$$

$$A^i_{r\ \overline{2h+1}} = \frac{1}{\pi}\left\{\frac{\cos(2h\alpha - \psi_r) - \cos(2h\beta - \psi_r)}{2h} + \frac{\cos(2\overline{h+1}\alpha - \psi_r) - \cos(2\overline{h+1}\beta - \psi_r)}{2\overline{h+1}} + \right.$$

$$+ \frac{2\sin(\alpha - \psi_r)}{\cot^2\psi_r + \overline{2h+1}^2}\left[(\cot\psi_r \cos\overline{2h+1}\beta - \overline{2h+1}\sin\overline{2h+1}\beta)\exp -\xi\cot\psi_r + \right.$$

$$\left.\left. + \overline{2h+1}\sin\overline{2h+1}\alpha - \cot\psi_r \cos\overline{2h+1}\alpha\right]\right\} \qquad \text{A3.8a}$$

$$B^i_{r\ \overline{2h+1}} = \frac{1}{\pi}\left\{\frac{\sin(2h\beta - \psi_r) - \sin(2h\alpha - \psi_r)}{2h} - \frac{\sin(2\overline{h+1}\beta - \psi_r) - \sin(2\overline{h+1}\alpha - \psi_r)}{2\overline{h+1}}\right.$$

$$+ \frac{2\sin(\alpha - \psi_r)}{\cot^2\psi_r + \overline{2h+1}^2}\left[(\cot\psi_r \sin\overline{2h+1}\beta + \overline{2h+1}\cos\overline{2h+1}\beta)\exp -\xi\cot\psi_r + \right.$$

$$\left.\left. - \left(\cot\psi_r \sin\overline{2h+1}\alpha + \overline{2h+1}\cos\overline{2h+1}\alpha\right)\right]\right\} \qquad \text{A3.8b}$$

Taking into consideration that the fundamental current is:

$$\bar{\bar{I}}_{r1} = E_{ro}\left(\frac{R_r^2}{s^2} + \omega_s^2 L_{r\sigma}^2\right)^{-\frac{1}{2}}\left\{\left(A_{r1}^i\right)^2 + \left(B_{r1}^i\right)^2\right\}^{\frac{1}{2}}$$

it is found from rel. A3.7 that the total rotor electrical power is:

$$\sum_{h=0}^{\infty} \frac{P^r}{de(2h+1)} = 2.s\, E_{ro}^2\left(\frac{R_r^r}{s^2} + \omega_s^2 L_{r\sigma}^2\right)^{-\frac{1}{2}} \cdot \left(B_{r1}^i\right) \qquad \text{A3.8c}$$

with

$$B_{r1}^i = \lim_{h\to 0}\left(\frac{B^i}{r\ \sqrt{2h+1}}\right)$$

$$= \frac{1}{\pi}\left\{\xi\cos\psi_r - \frac{\sin(2\beta - \psi_r) - \sin(2\alpha - \psi_r)}{2} + \right.$$

$$\left. + \frac{2\sin(\alpha - \psi_r)}{\operatorname{cosec}^2\psi_r}\left[(\cot\psi_r \sin\beta + \cos\beta)\exp - \xi\cot\psi_r - (\cot\psi_r \sin\alpha + \cos\alpha)\right]\right.$$

and

$$A_{r1}^i = \lim_{h\to 0}\left(\frac{A^i}{r\ \sqrt{2h+1}}\right)$$

$$= \frac{1}{\pi}\left\{\frac{\cos(2\alpha - \psi_r) - \cos(2\beta - \psi_r)}{2} - \xi \sin\psi_r\right.$$

$$\left. + \frac{2\sin(\alpha - \psi_r)}{\operatorname{cosec}^2\psi_r}\left[(\cot\psi_r\cos\beta - \sin\beta)\exp - \xi\cot\psi_r + \sin\alpha - \cot\psi_r\cos\alpha\right]\right\}$$

Substitution of rel. A3.8c into relation 3.51b results in the expression 3.53 for the torque.

APPENDIX 4

A4.1 THE EXPRESSIONS FOR THE SWITCHED SUPPLY VOLTAGES IN THE CASE OF STATOR CONTROL BY DELAY OF THE IGNITION ANGLE.

If $\bar{\bar{u}}^{x}_{sg}(t)$ represent the switched part of the supply waveform applied to each phase, and this is expressed as

$$\bar{\bar{u}}^{x}_{sg}(t) = \frac{1}{\sqrt{2}} \sum_{h=0}^{\infty} \left\{ \dot{\bar{\bar{U}}}^{x}_{sg\ \overline{2h+1}} \exp j(\overline{2h+1}\omega_s t) + \dot{\bar{\bar{U}}}^{x*}_{sg\ \overline{2h+1}} \exp -j(\overline{2h+1}\omega_s t) \right\} \qquad A4.1$$

with $\dot{\bar{\bar{U}}}^{x}_{sg\overline{2h+1}}$ the effective value of the (2h+1)th harmonic voltage, these harmonic components will be represented by

$$\dot{\bar{\bar{U}}}^{x}_{sg\ \overline{2h+1}} = \frac{\sqrt{2}}{\pi} \int_{0}^{\pi} \left\{ \bar{\bar{u}}^{x}_{sg}(\omega_s t) \exp -j(\overline{2h+1}\omega_s t) \right\} d(\omega_s t)$$

The two phases are assumed balanced in all respects. Therefore:

$$\dot{\bar{\bar{U}}}_{sg\ \overline{2h+1}} = \frac{\sqrt{2}}{\pi} \int_{0}^{(\gamma_s - \pi)} \left\{ \frac{\sqrt{2}U_{sg}}{2j} (\exp j\omega_s t - \exp -j\omega_s t) \exp -j\overline{2h+1}\omega_s t \right\} d(\omega_s t)$$

$$+ \frac{\sqrt{2}}{\pi} \int_{\alpha_s}^{\pi} \left\{ \frac{\sqrt{2}U_{sg}}{2j} (\exp j\omega_s t - \exp -j\omega_s t) \exp -j\overline{2h+1}\omega_s t \right\} d(\omega_s t)$$

for $h \neq 0$

$$= \frac{U_{sg}}{\pi} \left\{ (2h)^{-1} (\exp -j2h\gamma_s - \exp -j2h\alpha_s) - (\overline{2h+1})^{-1} (\exp -j\overline{2h+1}\gamma_s - \exp -j\overline{2h+1}\alpha_s) \right\} \qquad A4.2a$$

for $h = 0$

$$\dot{\bar{\bar{U}}}_{sg1} = \frac{U_{sg}}{\pi} \left\{ \lim_{h \to 0} (2h)^{-1} (\exp -j2h\gamma_s - \exp -j2h\alpha_s) - \tfrac{1}{2} (\exp -j2\gamma_s - \exp -j2\alpha_s) \right\}$$

$$\therefore \quad \dot{\bar{\bar{U}}}_{sg1} = \frac{U_{sg}}{\pi} \left\{ -j(\gamma_s - \alpha_s) - \tfrac{1}{2} (\exp -j2\gamma_s - \exp -j2\alpha_s) \right\} \qquad A4.2b$$

with $\gamma_s - \alpha_s = \xi_s$

Since the two supply voltages may be written as:

$$\left.\begin{aligned} u^{a}_{sg}(t) &= \sqrt{2}U_{sg}\sin(\omega_s t + \pi/2) \\ u^{b}_{sg}(t) &= \sqrt{2}U_{sg}\sin(\omega_s t) \end{aligned}\right\} \qquad \text{A4.3}$$

the forward and backward harmonic components of u^{a}_{sg} will be shifted by $(j)^{\overline{2h+1}}$ and $(-j)^{\overline{2h+1}}$ with respect to those of u^{b}_{sg}, leading to the expressions 4.19.

With regard to other considerations it is also useful to express these voltages in trigonometric form as

$$\begin{bmatrix} \bar{\bar{u}}^{a}_{sg}(t) \\ \bar{\bar{u}}^{b}_{sg}(t) \end{bmatrix} = \sqrt{2}\sum_{h=0}^{\infty} \bar{\bar{U}}_{sg\ \overline{2h+1}} \begin{bmatrix} \cos\{\overline{2h+1}(\omega_s t + \frac{\pi}{2}) - \phi_{s\ \overline{2h+1}}\} \\ \cos\{\overline{2h+1}\omega_s t - \phi_{s\ \overline{2h+1}}\} \end{bmatrix} \qquad \text{A4.4a}$$

with:

$$\bar{\bar{U}}_{sg\ \overline{2h+1}} = U_{sg}\left\{(A^{u}_{s\ \overline{2h+1}})^2 + (B^{u}_{s\ \overline{2h+1}})^2\right\}^{\frac{1}{2}}; \quad \phi_{s\ 2h+1} = \tan^{-1}\left(\frac{B^{u}_{s\ \overline{2h+1}}}{A^{u}_{s\ \overline{2h+1}}}\right) \qquad \text{A4.4b}$$

and for $h \neq 0$

$$\left.\begin{aligned} A^{u}_{s\ \overline{2h+1}} &= \frac{1}{\pi}\left\{\frac{\cos 2h\gamma_s - \cos 2h\alpha_s}{2h} - \frac{\cos 2(h+1)\gamma_s - \cos 2(h+1)\alpha_s}{2(h+1)}\right\} \\ B^{s}_{s\ \overline{2h+1}} &= \frac{1}{\pi}\left\{\frac{\sin 2h\gamma_s - \sin 2h\alpha_s}{2h} - \frac{\sin 2(h+1)\gamma_s - \sin 2(h+1)\alpha_s}{2(h+1)}\right\} \end{aligned}\right\} \qquad \text{A4.4c}$$

For $h = 0$

$$\left.\begin{aligned} A^{u}_{s1} &= \frac{1}{\pi}\left\{-\frac{\cos 2\gamma_s - \cos 2\alpha_s}{2}\right\} \\ B^{u}_{s1} &= \frac{1}{\pi}\left\{(\gamma_s - \alpha_s) - \frac{\sin 2\gamma_s - \sin 2\alpha_s}{2}\right\} \end{aligned}\right\} \qquad \text{A4.4d}$$

A4.2 AN EXAMINATION OF THE CONDITIONS LEADING TO THE PRESENCE OF AN INDUCED VOLTAGE ACROSS THE WINDINGS IN THE NON-CONDUCTING STATE OF THE ELECTRONIC SWITCHING CIRCUITS.

As the problem of knowing the induced voltages across the windings of a two-phase machine (fig. 4.2a) has a much more general implication than the case of stator voltage control by ignition delay treated at present, it will be considered in some more detail in this appendix. As mentioned in the text phase "b" will be taken as normative, and phase "a" as complementary. Consideration will be given to mode I. Taking into account relations 4.20:

$$t_1 < t < t_2 \qquad \begin{bmatrix} e^a_{s1} \\ e^b_{s1} \\ 0 \\ 0 \end{bmatrix} = \begin{bmatrix} D(M_{sr}\cos p\omega_m t) & -D(M_{sr}\sin p\omega_m t) \\ D(M_{sr}\sin p\omega_m t) & D(M_{sr}\cos p\omega_m t) \\ R_r + DL_r & 0 \\ 0 & R_r + DL_r \end{bmatrix} \cdot \begin{bmatrix} i^a_{r1} \\ i^b_{r1} \end{bmatrix} \qquad \text{A4.5}$$

with e^a_{s1} and e^b_{s1} the corresponding induced voltages in the phases.

If the Park-transformation is employed to obtain the system of fig. 4.2b from the previous system, the relations are:

$$\begin{bmatrix} i^d_r \\ i^q_r \end{bmatrix} = \begin{bmatrix} \cos p\omega_m t & -\sin p\omega_m t \\ \sin p\omega_m t & \cos p\omega_m t \end{bmatrix} \cdot \begin{bmatrix} i^a_r \\ i^b_r \end{bmatrix}; \quad \begin{bmatrix} i^a_r \\ - \\ i^b_r \end{bmatrix} = \begin{bmatrix} \cos p\omega_m t & \sin p\omega_m t \\ -\sin p\omega_m t & \cos p\omega_m t \end{bmatrix} \cdot \begin{bmatrix} i^d_r \\ i^q_r \end{bmatrix} \qquad \text{A4.6}$$

and it is immediately obvious that:

$$\begin{bmatrix} e^a_{s1} \\ e^b_{s1} \end{bmatrix} = \begin{bmatrix} DM_{sr} & 0 \\ 0 & DM_{sr} \end{bmatrix} \cdot \begin{bmatrix} i^d_{r1} \\ i^q_{r1} \end{bmatrix} \qquad \text{A4.7}$$

From rel. A4.5 also

$$\begin{bmatrix} i^a_{r1} \\ i^b_{r1} \end{bmatrix} = \begin{bmatrix} I^a_r(t_1) \\ I^b_r(t_1) \end{bmatrix} \exp - (t - \tfrac{\gamma - \pi}{\omega_s})\tau_r^{-1} \qquad \text{A4.8a}$$

with τ_r the rotor time constant $L_r.R_r^{-1}$

Substitution in rel. A4.6 then results in the final expressions for the direct axis and quadrature axis currents during the time interval t_1 to t_2:

$$\begin{bmatrix} i_{r1}^{di} \\ i_{r1}^{qi} \end{bmatrix} = \begin{bmatrix} \cos\sqrt{1-s}\omega_s t & -\sin\sqrt{1-s}\omega_s t \\ \sin\sqrt{1-s}\omega_s t & \cos\sqrt{1-s}\omega_s t \end{bmatrix} \cdot \begin{bmatrix} I_r^a(t_1) & \exp -t'\tau_r^{-1} \\ I_r^b(t_1) & \exp -t'\tau_r^{-1} \end{bmatrix} \qquad \text{A4.8b}$$

The expression for the induced e.m.f. in phase b under these conditions now becomes

$$e_{s1}^{bi} = DM_{sr}\left\{ I_r^a(t_1)\exp-\tau_r^{-1}t' \sin p\omega_m t + I_r^b(t_1)\exp-\tau_r^{-1}t' \cos p\omega_m t \right\}$$

or

$$e_{s1}^{bi} = M_{sr}\exp-t'.\tau_r^{-1}\left\{\left(p\omega_m I_r^a(t_1) - I_r^b(t_1).\tau_r^{-1}\right)\cos p\omega_m t - \left(p\omega_m I_r^b(t_1) + I_r^a(t_1)\,\tau_r^{-1}\right)\sin p\omega_m t\right\} \qquad \text{A4.9}$$

where $t' = (t - t_1) = (t - \frac{\chi - \pi}{\omega_s})$

and $I_r^a(t_1)$ and $I_r^b(t_1)$ are the as yet unknown values of i_{r1}^a and i_{r1}^b at time $t' = 0$.
Now consider the interval with the complementary phase "a" conducting. The equations are:

$t_2 < t < t_3$

$$\begin{bmatrix} u_{s2}^a \\ e_{s2}^b \\ 0 \\ 0 \end{bmatrix} = \begin{bmatrix} R_s + DL_s & D\{M_{sr}\cos p\omega_m t\} & -D\{M_{sr}\sin p\omega_m t\} \\ 0 & D\{M_{sr}\sin p\omega_m t\} & D\{M_{sr}\cos p\omega_m t\} \\ D\{M_{sr}\cos p\omega_m t\} & R_r + DL_r & 0 \\ -D\{M_{sr}\sin p\omega_m t\} & 0 & R_r + DL_r \end{bmatrix} \cdot \begin{bmatrix} i_{s2}^a \\ i_{r2}^a \\ i_{r2}^b \end{bmatrix} \qquad \text{A4.10}$$

When relations A4.6 are taken into account, these equations are simplified, and as e_{s2}^b are related to i_{r2}^q by a similar relation as A4.7, the following treatment will refer to fig. 4.2b in order to calculate e_{s2}^b.

From the above therefore:

$$\begin{bmatrix} u^a_{s2} \\ e^b_{s2} \\ 0 \\ 0 \end{bmatrix} = \begin{bmatrix} R_s + L_s D & M_{sr} D & 0 \\ 0 & 0 & M_{sr} D \\ M_{sr} D & R_r + L_r D & p\omega_m L_r \\ -p\omega_m M_{sr} & -p\omega_m L_r & R_r + L_r D \end{bmatrix} * \begin{bmatrix} i^a_{s2} \\ i^d_{r2} \\ i^q_{r2} \end{bmatrix} \qquad \text{A4.11}$$

To determine i^q_{r2}, the currents i^a_{s2} and i^d_{r2} are eliminated from the set of equations composed by the first and last two of the set A4.11. Writing the coefficients in terms of the rotor and stator electrical time constants the equation for i^q_r will be:

$$D^3 i^q_{r2} + \left\{ \frac{\tau_s^{-1} + \tau_r^{-1}}{\sigma} + \tau_r^{-1} \right\} D^2 i^q_{r2} + \left\{ \frac{\tau_r^{-1} + 2\tau_s^{-1}}{\tau_r \sigma} + p^2 \omega_m^2 \right\} D i^q_{r2}$$

$$+ \left\{ \frac{\tau_r^{-2} + p^2 \omega_m^2}{\tau_s \sigma} \right\} i^q_{r2} = \frac{p\omega_m M_{sr}}{\sigma \tau_r L_s L_r} \cdot u^a_{s2} \quad . \qquad \text{A4.12a}$$

By introducing some reduced parameters, the equation may be written in the following form:

$$\underline{D}^3 \underline{i}^q_{r2} + \left\{ \frac{r_s + r_r}{\sigma} + r_r \right\} \underline{D}^2 \underline{i}^q_{r2} + \left\{ r_r \frac{r_r + 2r_s}{\sigma} + \overline{1-s}^2 \right\} \underline{D} \underline{i}^q_{r2}$$

$$+ \left\{ r_s \cdot \frac{r_r^2 + \overline{1-s}^2}{\sigma} \right\} \underline{i}^{q2}_r = \frac{r_r (1-s)}{\sigma} \underline{u}^a_{s2} \qquad \text{A4.12b}$$

with

$$\left.\begin{aligned} &\underline{D} = \frac{1}{\omega_s} D, \quad \underline{t} = \omega_s t \\ &r_r = \frac{R_r}{\omega_s L_r} \; ; \; r_s = \frac{R_s}{\omega_s L_s} \\ &\underline{u}^a_{s2} = u^a_{s2} \left\{ \frac{M_{sr} U^s_N}{L_r \omega_s L_s} \right\}^{-1} \; ; \; \underline{i}^q_{r2} = i^q_{r2} \left\{ \frac{M_{sr} U^N_s}{L_r \omega_s L_s} \right\}^{-1} \end{aligned}\right\} \qquad \text{A4.12c}$$

and U^s_N the normal voltage that may be chosen to suit the system. The third order homogeneous equation of the above relation A4.12b may be solved exactly numerically. As the coefficients are dependent on the slip of the machine, however, this will only supply a solution at one particular speed of the machine. The algebraic expressions for the accurate roots of the characteristic equation[48] when using the above coefficients do not allow any significant interpretation, and

therefore the problem will be approximated in the different slip ranges. Consider relation A4.12a, written in terms of the slip:

$$D^3 i^q_{r2} + \left\{ \frac{\tau_s^{-1} + \tau_r^{-1}}{\sigma} + \tau_r^{-1} \right\} D^2 i^q_{r2} + \left\{ \frac{\tau_r^{-1} + 2\tau_s^{-1}}{\tau_r \sigma} + \overline{1-s}^2 \omega_s^2 \right\} Di^q_{r2}$$

$$+ \left\{ \frac{\tau_r^{-2} + \overline{1-s}^2 \omega_s^2}{\tau_s \sigma} \right\} i^q_{r2} = \frac{\overline{1-s}.\omega_s.M_{sr}}{\sigma_r L_s L_r \tau_r} \cdot u^a_{s2} \qquad \text{A4.12d}$$

In the slip region where

$$\sigma^{-1} \omega_s^{-2} (\tau_r^{-2} + 2\tau_s^{-1}\tau_r^{-1}) << \overline{1-s}^2 \qquad \text{A4.13a}$$

it is also valid that

$$\tau_r^{-2} \omega_s^{-2} << \overline{1-s}^2 \qquad \text{A4.13b}$$

and the equation may consequently be approximated by:

$$D^3 i^q_{r2} + \left\{ \frac{\tau_s^{-1} + \tau_r^{-1}}{\sigma} + \tau_r^{-1} \right\} D^2 i^q_{r2} + \overline{1-s}^2 \omega_s^2 Di^q_{r2} + \left\{ \frac{\overline{1-s}^2 \omega_s^2}{\tau_s \sigma} \right\} i^q_{r2} = \frac{\overline{1-s} \omega_s M_{sr}}{\sigma \tau_r L_s L_r} \cdot u^a_{s2} \qquad \text{A4.13c}$$

This will be a good approximation in the speed ranges where the slip is either appreciably larger or appreciably smaller than unity.
The break-even slips will be defined as:

$$s_{fa} = 1 \pm \left\{ \sigma^{-1} \omega_s^{-2} (\tau_r^{-2} + 2\tau_s^{-1}\tau_r^{-1}) \right\}^{\frac{1}{2}} \qquad \text{A4.13d}$$

giving the validity range as

$$\left.\begin{aligned} s &<< 1 - \left\{ \sigma^{-1} \omega_s^{-2} (\tau_r^{-2} + 2\tau_s^{-1}\tau_r^{-1}) \right\}^{\frac{1}{2}} \\ s &>> 1 + \left\{ \sigma^{-1} \omega_s^{-1} (\tau_r^{-2} + 2\tau_s^{-1}\tau_r^{-1}) \right\}^{\frac{1}{2}} \end{aligned}\right\} \qquad \text{A4.13e}$$

This is illustrated by the division of the slip scale into several regions according to the above criteria, i.e.:

region of high slip;
region of low slip;
region of excessive slip.

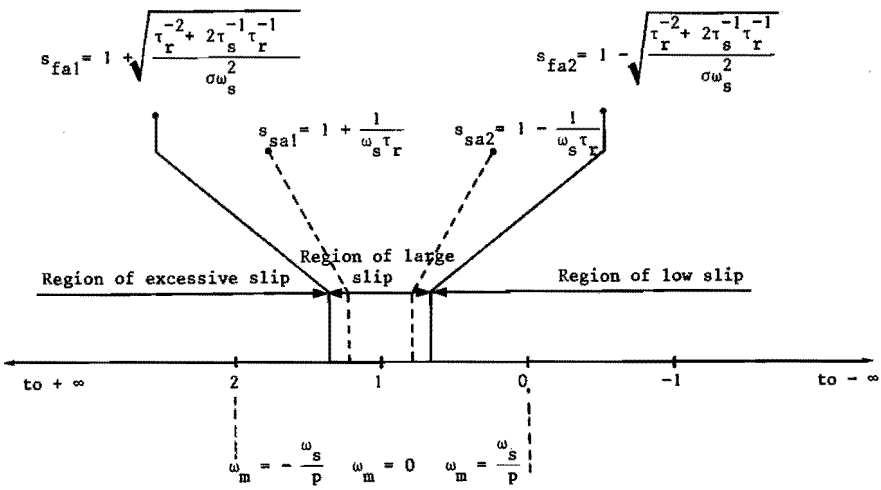

Complementary to the previous regions the following situation may arise:

$$\sigma^{-1}\omega^{-2}(\tau_r^{-2} + 2\tau_s^{-1}\tau_r^{-1}) >> \overline{1-s}^2 \qquad \text{A4.14a}$$

and also

$$\tau_r^{-2}\omega_s^{-2} >> \overline{1-s}^2 \qquad \text{A4.14b}$$

the last being the more stringent condition, as may be deduced from the slip diagram. Under these conditions the equation will become:

$$D^3 i^q_{r2} + \left\{\frac{\tau_s^{-1} + \tau_r^{-1}}{\sigma} + \tau_r^{-1}\right\} D^2 i^q_{r2} + \left\{\frac{\tau_r^{-1} + 2\tau_s^{-1}}{\tau_r\sigma}\right\} Di^q_{r2} + \frac{1}{\tau_s\tau_r^2\sigma} = \frac{\overline{1-s}\omega_s M_{sr}}{\sigma\tau_r\tau_s L_r} \cdot u^a_{s2} \qquad \text{A4.14c}$$

By definition the break-even slips of this approximation will be:

$$s_{sa} = 1 \pm \omega_s^{-1}\tau_r^{-1} \qquad \text{A4.14d}$$

In the subsequent work the two approximations represented by relations A4.13c and A4.14 will be referred to as the first and the second approximation respectively. It is to be noted that due to the different definitions given to the boundary slips for the first approximation and the second approximation in relations A4.13d and A4.14d, the transition region where neither of these approximations may be used is somewhat extended.

In the design of induction machines an attempt is usually made to keep the stator resistance as low as possible, and for the larger machine sizes[812] it is an allowable simplification to take the stator time constant as long compared to the rotor time constant. This simplification becomes even more allowable in machines used in Group II machine-electronic systems, as external rotor resistance is customarily introduced to cope with large dissipation at low speeds. The equations for the first and second approximation, with

$$\tau_s^{-1} << \tau_r$$

become

$$D^3 i_{r2}^q + (\frac{1+\sigma}{\sigma\tau_r}) D^2 i_{r2}^q + \overline{1-s}^2 \omega_s^2 D i_{r2}^q = \frac{\overline{1-s}\omega_s M_{sr}}{\sigma\tau_r L_s L_r} \cdot u_{s2}^a \qquad \text{A4.15a}$$

and

$$D^3 i_{r2}^q + (\frac{1+\sigma}{\sigma\tau_r}) D^2 i_{r2}^q + \frac{1}{\sigma\tau_r} D i_{r2}^q = \frac{\overline{1-s}\omega_s M_{sr}}{\sigma\tau_r L_s L_r} \cdot u_{s2}^a \qquad \text{A4.15b}$$

First approximation (low and excessive slip)

Attempting a solution of relation A4.15a as being the resulting equation for the first approximation, the roots of the characteristic equation are

$$\lambda_1 = 0; \quad \lambda_{2,3} = -(\frac{1+\sigma}{2\sigma\tau_r}) \pm (\frac{\overline{1+\sigma}^2}{4\sigma^2\tau_r^2} - \overline{1-s}^2\omega_s^2)^{\frac{1}{2}}$$

From relation A4.13a:

$$\frac{1}{\sigma\tau_r^2} + \frac{2}{\sigma\tau_s\tau_r} << \overline{1-s}^2\omega_s^2$$

under the present approximation. Depending on the magnitude of the leakage coefficient of the machine

$$(\frac{\overline{1+\sigma}^2}{4\sigma}) \frac{1}{\sigma\tau_r^2} < \overline{1-s}^2\omega_s^2 \qquad \text{A4.16a}$$

and the characteristic roots will be

$$\lambda_{2,3} = -\tau_e^{-1} \pm j\omega_e$$

where the effective damping coefficient and the eigenfrequency will be given by:

$$\tau_e = (\frac{2\sigma}{1+\sigma})\tau_r \qquad \text{A4.16b}$$

$$\omega_e = (\overline{1-s}^2\omega_s^2 - \frac{\overline{1+\sigma}^2}{4\sigma^2\tau_r^2})^{\frac{1}{2}} \qquad \text{A4.16c}$$

This enables the current under the first approximation to be expressed as

$$i_{r2}^{qi} = I_{ri}^{qi} + \exp{-t''}\tau_e^{-1}(I_{rii}^{qi}\cos\omega_e t'' + I_{riii}^{qi}\sin\omega_e t'') + i_{r2}^{qi}(t = \infty) \qquad \text{A4.16d}$$

with $t'' = (t-t_2) = (t - \frac{2\alpha-\pi}{2\omega_s})$

In relation to this solution for the current in the q-axis some important observations can be made. Obviously at slips far removed from s_{fa1} and s_{fa2} in the excessive slip and low slip regions with (relations A4.14a and A4.16a valid) the eigenfrequency of the transient induced voltage in the b-phase, found from:

$$\begin{bmatrix} e_{s2}^{a} \\ e_{s2}^{b} \end{bmatrix} = \begin{bmatrix} M_{sr}D & 0 \\ 0 & M_{sr}D \end{bmatrix} \cdot \begin{bmatrix} i_{r2}^{d} \\ i_{r2}^{q} \end{bmatrix} \qquad \text{A4.17}$$

will approach the frequency of mechanical rotation of the rotor of the machine, times the number of pairs of poles. This component will be damped out at a time constant somewhat smaller than the time constant of the rotor, depending on the leakage coefficient of the machine. For larger machines it may be expected that this time constant will decrease, seeing that one may expect the leakage coefficient to decrease somewhat.

As may be expected, the induced e.m.f. in phase "b" also contains a term with the supply frequency during the time that phase "a" conducts. It will be shown subsequently, however, that this term is proportional to the speed of rotation, and a function of the rotor time constant, decreasing with decreasing speed, and with increasing time constant.

It is now extremely interesting to note that the eigenfrequency of the induced voltage starts to depart significantly from the proportionality to the speed of rotation as the break-even slips s_{fa1} and s_{fa2} are approached on the slip scale. The break-even slips defined by the approximation used for the eigenfrequency are:

$$1-s^2 = (\frac{\overline{1+\sigma}^2}{4\sigma})\sigma^{-1}\tau_r^{-2}\omega_s^{-2} \qquad \text{A4.18a}$$

$$s'_{1,2} = 1 \pm \frac{\overline{1+\sigma}}{2\sigma}\cdot\tau_r^{-1}\omega_s^{-1} \qquad \text{A4.18b}$$

Especially for larger machines where both the leakage coefficient and the rotor resistance tend to decrease, a comparison of rel. 4.18 and 4.13 indicate that when

$$\tfrac{1}{2}(1-\sigma)\,\sigma^{-\frac{1}{2}} > \underline{1} \qquad \text{A4.18c}$$

the eigenfrequency will decrease more rapidly than the slip will approach the boundary slip for the first approximation. In an extreme case the eigenfrequency will become zero, the nature of solution A4.16 will change, and an extra damping term be introduced.

The solution of i_{r2}^{qi} $(t = \infty)$ will now be considered:

$$u^a_{s2} = \sqrt{2}U_{sg}\cos(\omega_s t' + \psi_1) = \sqrt{2}U_{sg}\cos\omega_s t$$

Let $$i^{qi}_{r2}(t = \infty) = \sqrt{2}I^{qi}_{r2}\cos(\omega_s t + \psi^{qi}_2) \qquad \text{A4.19a}$$

Finding $$D^3 i^{qi}_{r2}(t = \infty),\ D^2 i^{qi}_{r2}(t = \infty) \text{ and } Di^{qi}_{r2}(t = \infty)$$

it is found by substitution into A4.15a by the method of undetermined coefficients that:

$$i^{qi}_{r2}(t = \infty) = \sqrt{2}\,\frac{\sqrt{1-s}\,M_{sr}U_{sg}}{\omega_s L_s L_r\left\{\omega_s^2\sigma^2\tau_r^2(1-1-s^2)^2 + (1+\sigma)^2\right\}^{\frac{1}{2}}}\cos(\omega_s t + \psi^{qi}_2) \qquad \text{A4.19b}$$

and $$\psi^{qi}_2 = \left\{\pi - \tan^{-1}\left(\frac{\sigma\tau_r\omega_s(1-\sqrt{1-s}^2)}{1+\sigma}\right)\right\} \qquad \text{A4.19c}$$

The constants I^{qi}_{ri}, I^{qi}_{rii} and I^{qi}_{riii} still have to be determined in order to specify the transient solution. These will be determined from

$$i^{qi}_{r2}(t = t_2)\ ;\ Di^{qi}_{r2}(t = t_2)\ ,\ D^2 i^{qi}_{r2}(t = t_2)$$

From considerations that it is impossible for i^q_r to change instantaneously in amplitude,

$$i^{qi}_{r2}(t = t_2) = i^{qi}_{r1}(t = t_2)$$

Using A4.6 and A4.8 this results in

$$i^{qi}_{r2}(t = t_2) = i^a_{r1}(t = t_2)\sin p\omega_m t_2 + i^b_{r1}(t = t_2)\cos p\omega_m t_2$$

or

$$i^{qi}_{r2}(t = t_2) = I^a_r(t_1)\exp-\tau_r^{-1}\left(\frac{2\alpha_s - 2\gamma_s + \pi}{2\omega_s}\right)\sin\left(\frac{\sqrt{1-s}\,.\,2\alpha_s - \pi}{2}\right) +$$

$$+ I^b_r(t_1)\exp-\tau_r^{-1}\left(\frac{2\alpha_s - 2\gamma_s + \pi}{2\omega_s}\right)\cos\left(\frac{\sqrt{1-s}\,.\,2\alpha_s - \pi}{2}\right) \qquad \text{A4.20a}$$

Similarly it is stated that $i^{di}_{r2}(t = t_2)$ is continuous, and it is found that:

$$i^{di}_{r2}(t = t_2) = I^a_r(t_1)\exp-\tau_r^{-1}\left(\frac{2\alpha_s - 2\gamma_s + \pi}{2\omega_s}\right)\cos\left(\frac{\sqrt{1-s}\,.\,2\alpha_s - \pi}{2}\right) +$$

$$- I^b_r(t_1)\exp-\tau_r^{-1}\left(\frac{2\alpha_s - 2\gamma_s + \pi}{2\omega_s}\right)\sin\left(\frac{\sqrt{1-s}\,.\,2\alpha_s - \pi}{2}\right) \qquad \text{A4.20b}$$

From relation A4.11, by elimination of i^{a}_{s2} which is still zero at $t = t_2$

$$Di^{qi}_{r2}(t = t_2) = \overline{1-s}\omega_s\, i^{di}_{r2}(t = t_2) - \tau_r^{-1} i^{qi}_{r2}(t = t_2) \qquad \text{A4.20c}$$

and

$$D^2 i^{qi}_{r2}(t = t_2) = \tau_r^{-2} i^{qi}_{r2}(t = t_2) - \overline{1-s}^2\omega_s^2\, i^{qi}_{r2}(t = t_2) +$$

$$- 2\,\overline{1-s}\omega_s\, \tau_r^{-1} i^{di}_{r2}(t = t_2) \qquad \text{A4.20d}$$

By finding the corresponding expressions from A4.16d, and solving the following equations, the constants are found

$$\begin{bmatrix} 0 & 1 & -\cos(\omega_s t_2 + \psi^{qi}_2) \\ \overline{1-s}\omega_s & -\frac{1}{\tau_r} & \omega_s \sin(\omega_s t_2 + \psi^{qi}_2) \\ -\frac{2\,\overline{1-s}\omega_s}{\tau_r} & (\frac{1}{\tau_r^2} - \overline{1-s}^2\omega_s^2 & \omega_s^2 \cos(\omega_s t_2 + \psi^{qi}_r) \end{bmatrix} \begin{bmatrix} i^{di}_{r2}(t = t_2) \\ i^{qi}_{r2}(t = t_2) \\ \sqrt{2}\, I^{qi}_{r2} \end{bmatrix}$$

$$= \begin{bmatrix} 1 & 1 & 0 \\ 0 & -\frac{1}{\tau_e} & \omega_e \\ 0 & (\frac{1}{\tau_e^2} - \omega_e^2) & -\frac{2\omega_e}{\tau_e} \end{bmatrix} \cdot \begin{bmatrix} I^{qi}_{ri} \\ I^{qi}_{rii} \\ I^{qi}_{riii} \end{bmatrix} \qquad \text{A4.20e}$$

Therefore:

$$I^{qi}_{rii} = \frac{2\,\overline{1-s}\omega_s}{\tau_r}\left(\frac{\tau_e^2 - \tau_r\tau_e}{1+\omega_e^2\tau_e^2}\right) i^{di}_{r2}(t = t_2) - \left(\frac{\tau_e^2 - 2\tau_r\tau_e - \tau_r^2\tau_e^2.\overline{1-s}^2\omega_s^2}{\tau_r^2(1+\omega_e^2\tau_e^2)}\right) i^{qi}_{r2}(t = t_2) +$$

$$- \tau_e \left(\frac{2\omega_s \sin(\omega_s t_2 + \psi^{qi}_2) + \omega_s^2\tau_e \cos(\omega_s t_2 + \psi^{qi}_2)}{1+\omega_e^2\tau_e^2}\right)\sqrt{2}\, I^{qi}_{r2} \qquad \text{A4.20f}$$

$$I_{ri}^{qi} = \left\{1 + \left(\frac{\tau_e^2 - 2\tau_r\tau_e - \tau_r^2\tau_e^2\,\overline{1-s}^2\omega_s^2}{\tau_r^2(1+\omega_e^2\tau_e^2)}\right)\right\} i_{r2}^{qi}(t = t_2) - 2.\frac{\overline{1-s}\omega_s}{\tau_r}\left(\frac{\tau_e^2 - \tau_r\tau_e}{1+\omega_e^2\tau_e^2}\right) i_{r2}^{di}(t = t_2)$$

$$+\left\{\left(\frac{\omega_s^2\tau_e}{1+\omega_e^2\tau_e^2}\right) - 1\right\} \sqrt{2}I_{r2}^{qi}\cos(\omega_s t_2 + \psi_2^{qi}) + \left(\frac{2\omega_s\tau_e}{1+\omega_e^2\tau_e^2}\right) \sqrt{2}I_{r2}^{qi}\sin(\omega_s t_2 + \psi_2^{qi}) \qquad \text{A4.20g}$$

and

$$I_{riii}^{qi} = \frac{\overline{1-s}\omega_s}{\omega_e}\left\{1 + \frac{2}{\tau_r}\left(\frac{\tau_e - \tau_r}{1+\omega_e^2\tau_e^2}\right)\right\} i_{r2}^{di}(t = t_2) - \frac{1}{\tau_r\omega_e}\left\{1 + \left(\frac{\tau_e - 2\tau_r - \tau_r^2\tau_e\,\overline{1-s}^2\omega_s^2}{\tau_r(1+\omega_e^2\tau_e^2)}\right)\right\} i_{r2}^{qi}(t = t_2)$$

$$+\frac{\omega_s}{\omega_e}\left\{\left(1 - \frac{2}{1+\omega_e^2\tau_e^2}\right)\sin(\omega_s t_2 + \psi_2^{qi}) - \left(\frac{\omega_s\tau_e}{1+\omega_e^2\tau_e^2}\right)\cos(\omega_s t_2 + \psi_2^{qi})\right\} \sqrt{2}I_{r2}^{qi} \qquad \text{A4.20h}$$

with

$$\cos\psi_2^{qi} = -\frac{(1+\sigma)}{\left\{(1+\sigma)^2 + \sigma^2\tau_r^2\omega_s^2(1-\overline{1-s}^2)^2\right\}^{\frac{1}{2}}} \qquad \text{A4.20i}$$

$$\sin\psi_2^{qi} = -\frac{\sigma\tau_r\omega_s(1-\overline{1-s}^2)}{(1+\sigma)}\cos\psi_2^{qi}$$

By using relations A4.17 and A4.16d the induced e.m.f. is obtained as:

$$e_{s2}^{bi} = M_{sr}D\left\{\exp-\frac{t''}{\tau_e}\left(I_{rii}^{qi}\cos\omega_e t'' + I_{riii}^{qi}\sin\omega_e t''\right) + \sqrt{2}I_{r2}^{qi}\cos(\omega_s t + \psi_2^{qi})\right\}$$

$$e_{s2}^{bi} = M_{sr}\left\{\exp-\frac{t''}{\tau_e}\left[\left(\omega_e I_{riii}^{qi} - \frac{1}{\tau_e}I_{rii}^{qi}\right)\cos\omega_e t'' - \left(\omega_e I_{riii}^{qi} + \frac{1}{\tau_e}I_{rii}^{qi}\right)\sin\omega_e t''\right] + \right.$$

$$\left. - \omega_s\sqrt{2}I_{r2}^{qi}\sin(\omega_s t + \psi_2^{qi})\right\} \qquad \text{A4.21}$$

This first approximation for the induced e.m.f. in phase "b" will then be valid in the low and excessive slip regions, with characteristics as previously discussed.

Second approximation (large slip)

Relation A4.15b represents the approximate equation. Attempting a solution, the roots of the characteristic equation become

$$\lambda_1 = 0, \quad \lambda_{2,3} = -\left(\frac{1+\sigma}{2\sigma}\right)\tau_r^{-1} \pm \left\{\left(\frac{1+\sigma}{4\sigma}\right)^2\tau_r^{-2} - \sigma^{-1}\tau_r^{-2}\right\}^{\frac{1}{2}}$$

or rewriting:

$$\lambda_{2,3} = -\tau_r^{-1}\left\{\left(\frac{1+\sigma}{2\sigma}\right) \mp \left(\frac{\overline{1+\sigma}^2}{\overline{2\sigma}^2} - \sigma^{-1}\right)^{\frac{1}{2}}\right\} \qquad \text{A4.22a}$$

Seeing that the square-root term will have a positive value less than the first term for all values of the leakage coefficient physically realisable, the equation for the current can be expressed as:

$$i_{r2}^{qii} = I_{ri}^{qii} + I_{rii}^{qii}\exp{-t''}\tau_{e-}^{-1} + I_{riii}^{qii}\exp{-t''}\tau_{e+}^{-1} + i_{r2}^{qii} \quad (t = \infty) \qquad \text{A4.22b}$$

with t" as defined for i_{r2}^{qi} and

$$\tau_{e-}^{-1} = \tau_r^{-1}\left\{\left(\frac{1+\sigma}{2\sigma}\right) - \left(\frac{\overline{1+\sigma}^2}{\overline{2\sigma}^2} - \sigma^{-1}\right)^{\frac{1}{2}}\right\} \qquad \text{A4.22c}$$

$$\tau_{e+}^{-1} = \tau_r^{-1}\left\{\left(\frac{1+\sigma}{2\sigma}\right) + \left(\frac{\overline{1+\sigma}^2}{\overline{2\sigma}^2} - \sigma^{-1}\right)^{\frac{1}{2}}\right\}$$

This indicates that the decrease in the eigenfrequency of the induced e.m.f. observed with the slip approaching the region defined as "large" slip from the approximation theory developed here, corresponds with the behaviour found by the second approximation. On the basis of A4.18 it was remarked that in an extreme case the eigenoscillation of the induced e.m.f. may even disappear, and an extra damping term be introduced. However, care must be taken, since in the end the validity of the approximation is of course doubtful.

The above relations indicate that it is indeed permissible to expect the eigenoscillation to disappear as the machine decreases its speed, in the end only retaining the rotor time constant dependent supply frequency term at very low speeds. Attention will now be devoted to determining the steady state term of the quadrature-axis current responsible for this component of the induced e.m.f. By using relations A4.19a and A4.15b:

$$i_{r2}^{qii}(t = \infty) = \frac{\overline{1-s}\omega_s M_{sr}\sqrt{2}U_{sg}}{\sigma\tau_r L_s L_r}\left(\frac{1}{F(D)} \cdot R_e\left\{\exp j\omega_s t\right\}\right)$$

with

$$F(D) = \left\{D^3 + \sigma^{-1}\tau_r^{-1}(1+\sigma)D^2 + \sigma^{-1}\tau_r^{-2}D\right\}$$

Therefore

$$i_{r2}^{qii}(t = \infty) = \sqrt{2}\,\frac{\overline{1-s}\omega_s M_{sr}U_{sg}}{\sigma\tau_r L_s L_r}\left(R_e\left\{\frac{\exp j\omega_s t}{F(j\omega_s)}\right\}\right)$$

which becomes, after rearrangement:

$$i_{r2}^{qii}(t = \infty) = \sqrt{2}\,\frac{\tau_r\overline{1-s}M_{sr}U_{sg}}{L_s L_r\left\{(1+\sigma)^2\omega_s^2\tau_r^2 + (\sigma\omega_s^2\tau_r^2 - 1)^2\right\}^{\frac{1}{2}}}\cos(\omega_s t + \psi_2^{qii}) \qquad \text{A4.23a}$$

$$= \sqrt{2} I_{r2}^{qii} \cos(\omega_s t + \psi_2^{qii}) \qquad \text{A4.23b}$$

with

$$\psi_2^{qii} = \left\{ \pi - \tan^{-1} \left(\frac{\sigma \omega_s^2 \tau_r^2 - 1}{\overline{1+\sigma} \omega_s \tau_r} \right) \right\} \qquad \text{A4.23c}$$

The constants I_{ri}^{qii}, I_{rii}^{qii} and I_{riii}^{qii} of relation A4.22b still have to be determined in order to be able to specify the current completely. By again stating that it is impossible for either i_r^q or i_r^d to suffer an instantaneous change in amplitude, it is obtained that:

$$i_{r2}^{qii}(t = t_2) = i_{r1}^{qi}(t = t_2)$$

and

$$i_{r2}^{dii}(t = t_2) = i_{r1}^{di}(t = t_2)$$

The expressions obtained in relations A4.20a to A4.20d may be employed to solve for these constants. By finding the corresponding expressions from A4.22b the following equations are found:

$$\begin{bmatrix} 0 & 1 & -\cos(\omega_s t_2 + \psi_2^{qii}) \\ \overline{1-s}\omega_s & -\frac{1}{\tau_r} & \omega_s \sin(\omega_s t_2 + \psi_2^{qii}) \\ \frac{-2\overline{1-s}\omega_s}{\tau_r} & \left(\frac{1}{\tau_r^2} - \overline{1-s}^2 \omega_s^2\right) & \omega_s^2 \cos(\omega_s t_2 + \psi_2^{qii}) \end{bmatrix} \cdot \begin{bmatrix} i_{r2}^{dii}(t = t_2) \\ i_{r2}^{qii}(t = t_2) \\ \sqrt{2} I_{r2}^{qii} \end{bmatrix}$$

$$= \begin{bmatrix} 1 & 1 & 1 \\ 0 & -\frac{1}{\tau_{e-}} & -\frac{1}{\tau_{e+}} \\ 0 & \frac{1}{\tau_{e-}^2} & \frac{1}{\tau_{e+}^2} \end{bmatrix} \cdot \begin{bmatrix} I_{ri}^{qii} \\ I_{rii}^{qii} \\ I_{riii}^{qii} \end{bmatrix} \qquad \text{A4.24}$$

Solution yields the following three constants:

$$I_{ri}^{qii} = \overline{1-s}\omega_s \tau_{e-} \left\{ 1 + \frac{\tau_{e+}(\tau_r - 2\tau_{e-})}{\tau_{e-} - \tau_r} \right\} i_{r2}^{dii}(t = t_2) +$$

$$+\left\{1-\frac{\tau_{e-}}{\tau_r}+\frac{\tau_{e+}(\tau_{e-}-\overline{1-s}^2\omega_s^2\tau_r^2\tau_{e-}-\tau_r)}{\tau_r^2}\right\}i_{r2}^{qii}(t=t_2)+$$

$$+\left\{\omega_s^2\tau_{e-}\tau_{e+}-1\right\}\sqrt{2}I_{r2}^{qii}\cos(\omega_s t_2+\psi_2^{qii})+\omega_s\left\{\tau_{e-}+\tau_{e+}\right\}\sqrt{2}I_{r2}^{qii}\sin(\omega_s t_2+\psi_2^{qii}) \qquad \text{A4.24a}$$

$$I_{rii}^{qii}=-\overline{1-s}\omega_s\tau_e\left\{1+\frac{\tau_{e+}(\tau_r-2\tau_{e-})}{\tau_r(\tau_{e-}-\tau_{e+})}\right\}i_{r2}^{dii}(t=t_2)+$$

$$+\frac{\tau_{e-}}{\tau_r}\left\{1-\frac{\tau_{e+}(\tau_{e-}-\overline{1-s}^2\omega_s^2\tau_r^2\tau_{e-}-\tau_r)}{\tau_r(\tau_{e-}-\tau_{e+})}\right\}i_{r2}^{qii}(t=t_2)+$$

$$-\tau_{e-}\omega_s\left\{1+\frac{\tau_{e+}}{(\tau_{e-}-\tau_{e+})}\right\}\sqrt{2}I_{r2}^{qii}\sin(\omega_s t_2+\psi_2^{qii})-\left\{\frac{\omega_s^2\tau_{e-}\tau_{e+}}{\tau_{e-}-\tau_{e+}}\right\}\cos(\omega_s t_2+\psi_2^{qii}) \qquad \text{A4.24b}$$

$$I_{riii}^{qii}=\left\{\frac{\overline{1-s}\omega_s\tau_{e+}^2(\tau_r-2\tau_{e-})}{\tau_r(\tau_{e-}-\tau_{e+})}\right\}i_{r2}^{dii}(t=t_2)+\left\{\frac{\tau_{e+}^2(\tau_{e-}-\overline{1-s}^2\omega_s^2\tau_r^2\tau_{e-}-\tau_r)}{\tau_r^2(\tau_{e-}-\tau_{e+})}\right\}i_{r2}^{qii}(t=t_2)$$

$$+\left\{\frac{\omega_s^2\tau_{e+}^2\tau_{e-}}{\tau_{e-}-\tau_{e+}}\right\}\sqrt{2}I_{r2}^{qii}\cos(\omega_s t_2+\psi_2^{qii})+\left\{\frac{\omega_s\tau_{e+}^2}{\tau_{e-}-\tau_{e+}}\right\}\sqrt{2}I_{r2}^{qii}\sin(\omega_s t_2+\psi_2^{qii}) \qquad \text{A4.24c}$$

with

$$\left.\begin{aligned}\cos\psi_2^{qii}&=-\frac{\overline{1+\sigma}\omega_s\tau_r}{\left\{\overline{1+\sigma}^2\omega_s^2\tau_r^2+(\sigma\omega_s^2\tau_r^2-1)^2\right\}^{\frac{1}{2}}}\\ \text{and}\quad\sin\psi_2^{qii}&=-\frac{(\sigma\omega_s^2\tau_r^2-1)}{(\overline{1+\sigma}\omega_s\tau_r)}\cos\psi_2^{qii}\end{aligned}\right\} \qquad \text{A4.24d}$$

Now that the constants are known, and consequently the quadrature axis current specified by the second approximation, the induced e.m.f. in the normative phase (phase "b") may be found from relation A4.17 and the expression for the current A4.22b as:

$$e_{s2}^{bii}=M_{sr}D\left\{I_{rii}^{qii}\exp{-t''}\tau_{e-}^{-1}+I_{riii}^{qii}\exp{-t''}\tau_{e+}^{-1}+\sqrt{2}I_{r2}^{qii}\cos(\omega_s t+\psi_2^{qii})\right\}$$

$$e_{s2}^{bii}=-M_{sr}\left\{\frac{1}{\tau_{e-}}I_{rii}^{qii}\exp{-t''}\tau_{e-}^{-1}+\frac{1}{\tau_{e+}}I_{riii}^{qii}\exp{-t''}\tau_{e+}^{-1}+\omega_s\sqrt{2}I_{r2}^{qii}\sin(\omega_s t+\psi_2^{qii})\right\} \qquad \text{A4.25}$$

This indicates that in the high slip region the induced e.m.f. in the normative and complementary phase will contain no eigenfrequency term, but will correspond to the supply frequency plus an exponential decay. In order to be able to determine the initial conditions for the direct axis and quadrature axis currents during the third period of time (i.e. $t_3 < t < t_4$) when the complementary phase will be nonconducting, the current in the direct axis during the presently investigated time interval must be known. From the simultaneous set A4.11 it may be deduced that

$$i^d_{r2} = -\frac{\tau_r}{p\omega_m} D^2 i^q_{r2} - \frac{1}{p\omega_m} D i^q_{r2} - \tau_r . p\omega_m i^q_{r2}$$

or

$$\overline{1-s}\,\omega_s i^d_{r2} = -\tau_r D^2 i^q_{r2} - D i^q_{r2} - \tau_r \overline{1-s}^2 \omega_s^2 i^q_{r2} \qquad \text{A4.26}$$

By now stating that the direct axis current will have a functional construction similar to the quadrature axis current, the expressions may be written down in analogy to the approximations used in A4.16d and A4.22b. Therefore:

$$i^{di}_{r2} = I^{di}_{ri} + \exp -t''\tau_e^{-1} \left\{ I^{di}_{rii} \cos\omega_e t'' + I^{di}_{riii} \sin\omega_e t \right\} + \sqrt{2} I^{di}_{r2} \cos(\omega_s t + \psi^{di}_2) \qquad \text{A4.27a}$$

By using A4.26 the relations with the constants found for i^{qi}_{r2} under the first approximation are:

$$I^{di}_{ri} = -\tau_r \overline{1-s}\,\omega_s I^{qi}_{ri}$$

$$I^{di}_{r2} = \frac{\left\{ 1 + \omega_s^2 \tau_r^2 (1-\overline{1-s}^2)^2 \right\}^{\frac{1}{2}}}{(1-s)} I^{qi}_{r2}$$

$$\psi^{di}_2 = \left\{ \psi^{qi}_2 - \tan^{-1}\left(\frac{1}{\tau_r \omega_s (1-\overline{1-s}^2)} \right) \right\}$$

$$\begin{bmatrix} I^{di}_{rii} \\ I^{di}_{riii} \end{bmatrix} = \begin{bmatrix} \left\{ \frac{\tau_e - \tau_r}{\overline{1-s}\,\omega_s \tau_e^2} + \frac{\tau_r \omega_e^2}{\overline{1-s}\,\omega_s} - \tau_r \overline{1-s}\,\omega_s \right\} & \left\{ \frac{\omega_e (2\tau_r - \tau_e)}{\overline{1-s}\,\omega_s \tau_e} \right\} \\ \left\{ \frac{\omega_e (\tau_e - 2\tau_r)}{\overline{1-s}\,\omega_s \tau_e} \right\} & \left\{ \frac{\tau_e - \tau_r}{\overline{1-s}\,\omega_s \tau_e^2} + \frac{\tau_r \omega_e^2}{\overline{1-s}\,\omega_s} - \tau_r \overline{1-s}\,\omega_s \right\} \end{bmatrix} \cdot \begin{bmatrix} I^{qi}_{rii} \\ I^{qi}_{riii} \end{bmatrix} \qquad \text{A4.27b}$$

Similarly it may be found that for the second approximation the following holds true:

$$i^{dii}_{r2} = I^{dii}_{ri} + I^{dii}_{rii} \exp -t''\tau_{e-}^{-1} + I^{dii}_{riii} \exp -t''\tau_{e+}^{-1} + \sqrt{2} I^{dii}_{r2} \cos(\omega_s t + \psi^{dii}_2) \qquad \text{A4.28a}$$

with

$$I_{ri}^{dii} = -\tau_r \overline{1-s}\omega_s I_{ri}^{qii}$$

$$I_{rii}^{dii} = \left\{ \frac{\tau_{e-} - \tau_r}{\overline{1-s}\omega_s \tau_{e-}^2} - \tau_r \overline{1-s}\omega_s \right\} I_{rii}^{qii}$$

$$I_{riii}^{dii} = \left\{ \frac{\tau_{e+} - \tau_r}{\overline{1-s}\omega_s \tau_{e+}^2} - \tau_r \overline{1-s}\omega_s \right\} I_{riii}^{qii} \qquad \text{A4.28b}$$

$$I_{r2}^{dii} = \frac{\left\{ 1 + \omega_s^2 \tau_r^2 (1-\overline{1-s}^2)^2 \right\}^{\frac{1}{2}}}{(1-s)} I_{r2}^{qii}$$

and

$$\psi_2^{dii} = \left\{ \psi_2^{qii} - \tan^{-1} \left(\frac{1}{\tau_r \omega_s (1-\overline{1-s}^2)} \right) \right\}$$

The behaviour of the induced voltage in the normative phase will now be investigated during the time after the current in the complementary phase has become zero, i.e. during the time between t_3 and t_4 as defined in fig. 4.3(b).

$$t_3 < t < t_3$$

From relations A4.11, with $i_s^a \equiv 0$, the equations for the transformed rotor phases become

$$\begin{bmatrix} 0 \\ \\ 0 \end{bmatrix} = \begin{bmatrix} (R_r + L_r D) & p\omega_m L_r \\ \\ -p\omega_m L_r & (R_r + L_r D) \end{bmatrix} \cdot \begin{bmatrix} i_{r3}^d \\ \\ i_{r3}^q \end{bmatrix} \qquad \text{A4.29a}$$

Solving for the quadrature-axis currents from

$$D^2 i_{r3}^q + 2\tau_r^{-1} D i_{r3}^q + (\tau_r^{-2} + p^2 \omega_m^2) i_{r3}^q = 0 \qquad \text{A4.29b}$$

the characteristic roots will be:

$$\lambda_{1,2} = -\tau_r^{-1} \pm j\overline{1-s}\omega_s \qquad \text{A4.29c}$$

Consequently the solution is

$$i_{r3}^{qi} = \exp -t'''\tau_r^{-1} (I_{ri}^{qi} \cos \overline{1-s}\omega_s t''' + I_{rii}^{qi} \sin \overline{1-s}\omega_s t''')$$

Similarly $$i_{r3}^{di} = \exp -t'''\tau_r^{-1}(I_{ri}^{dI}\sin\sqrt{1-s}\omega_s t''' + I_{rii}^{dI}\cos\sqrt{1-s}\omega_s t''') \qquad \text{A4.29d}$$

with only I_{ri}^{qI} and I_{rii}^{qI} as arbitrary constants, the relation between the currents from A4.26a being

$$i_{r3}^{di} = \frac{1}{p\omega_m\tau_r} \cdot i_{r3}^{qi} + \frac{1}{p\omega_m} Di_{r3}^{qi} \qquad \text{A4.29e}$$

with $t''' = (t - t_3)$. The following conditions are known:

$$i_{r3}^{qi}(t = t_3) = i_{r2}^{qi,ii}(t = t_3)$$

$$Di_{r3}^{qi}(t = t_3) = p\omega_m . i_{r2}^{di,ii}(t = t_3) - \tau_r^{-1} . i_{r2}^{qi,iii}(t = t_3)$$

the actual expressions depending on the slip range the machine is operating in. Examining the relations giving the constants for i_{r2}^{q} and i_{r2}^{d}, it will be obvious that the algebraic expressions for the present case will become even more elaborate. As it serves no purpose, they will not be reproduced at present.

The solutions of A4.29 indicate that the quadrature and direct axis currents execute a damped oscillation at the mechanical frequency of the machine. The induced e.m.f. in phase b is:

$$e_{s3}^{bi} = M_{sr} D\left\{\exp -t'''\tau_r^{-1}(I_{ri}^{qI}\cos\sqrt{1-s}\omega_s t''' + I_{rii}^{qI}\sin\sqrt{1-s}\omega_s t''')\right\}$$

or

$$e_{s3}^{bi} = M_{sr}\exp -t'''\tau_r^{-1}\left\{(\sqrt{1-s}\omega_s I_{rii}^{qI} - \frac{I_{ri}^{qI}}{\tau_r})\cos\sqrt{1-s}\omega_s t''' - (\sqrt{1-s}\omega_s I_{ri}^{qI} + \frac{I_{rii}^{qI}}{\tau_r})\sin\sqrt{1-s}\omega_s t'''\right\} \qquad \text{A4.30}$$

which is seen to be quite analogous to the expression for the induced e.m.f. during the first part of the cycle as given in expression A4.9

Investigation of the induced voltage when stator and rotor time constants tend to a large value: a third approximation.

As explained in the text, a definite case is to be presented for examining the nature of the induced voltage when all stator and rotor resistances are neglected, especially to gain insight into the phenomena, as the expressions presented in the previous section are mostly of considerable complexity, and interdependent.
As before, the period that the electronic switch of phase "b" blocks will be divided into three periods, i.e. both stator phases nonconducting (t_1 to t_2), phase 'b' nonconducting and phase 'a' conducting (t_2 to t_3) and again both phases nonconducting (t_3 to t_4).

$$t_1 < t < t_2 \ , \ R_s = 0 = R_r$$

$$\begin{bmatrix} e^{a}_{sl} \\ e^{b}_{sl} \\ 0 \\ 0 \end{bmatrix} = \begin{bmatrix} M_{sr}D & 0 \\ 0 & M_{sr}D \\ L_{r}D & p\omega_{m}L_{r} \\ -p\omega_{m}L_{r} & L_{r}D \end{bmatrix} \cdot \begin{bmatrix} i^{d}_{rl} \\ i^{q}_{rl} \end{bmatrix} \qquad \text{A4.31a}$$

resulting in the homogeneous equations

$$D^{2}i^{q}_{rl} + p^{2}\omega_{m}^{2}i^{q}_{rl} = 0 = p^{2}\omega_{m}^{2}i^{d}_{rl} + D^{2}i^{d}_{rl}$$

Solving the quadrature current

$$i^{qii}_{rl} = I^{qa}_{ri}\cos p\omega_{m}t' + I^{qb}_{ri}\sin p\omega_{m}t' \qquad \text{A4.31b}$$

with t' as already specified.
It is known that for $t = t_1$

$$\left.\begin{aligned} i^{qii}_{rl}(t = t_1) &= I^{a}_{r}(t_1)\sin p\omega_{m}t_1 + I^{b}_{r}(t_1)\cos p\omega_{m}t_1 \\ i^{dii}_{rl}(t = t_1) &= I^{a}_{r}(t_1)\cos p\omega_{m}t_1 - I^{b}_{r}(t_1)\sin p\omega_{m}t_1 \end{aligned}\right\} \qquad \text{A4.31c}$$

From A4.31 $Di^{qii}_{rl} = p\omega_{m}i^{dii}_{rl}$, so that by determining

$i^{qii}_{rl}(t = t_1)$ and $Di^{qii}_{rl}(t = t_1)$ from A4.31b and substituting from A4.31c, the quadrature-axis current is

$$t_1 < t < t_2 : i^{qii}_{rl} = I^{a}_{r}(t_1)\sin p\omega_{m}t + I^{b}_{r}(t_1)\cos p\omega_{m}t \qquad \text{A4.31d}$$

similarly

$$t_1 < t < t_2 : i^{dii}_{rl} = I^{a}_{r}(t_1)\cos p\omega_{m}t - I^{b}_{r}(t_1)\sin p\omega_{m}t \qquad \text{A4.31e}$$

Thus from relation A4.17 with the necessary simplifications:

$$t_1 < t < t_2 : e^{bii}_{sl} = \overline{1-s}\omega_{s}M_{sr}\left\{I^{a}_{r}(t_1)\cos \overline{1-s}\omega_{s}t - I^{b}_{r}(t_1)\sin \overline{1-s}\omega_{s}t\right\} \qquad \text{A4.31f}$$

$$t_2 < t < t_3 \ , \ R_s \equiv 0 \equiv R_r$$

The voltage-current relationships are:

$$\begin{bmatrix} u^a_{s2} \\ e^b_{s2} \\ 0 \\ 0 \end{bmatrix} = \begin{bmatrix} L_s D & M_{sr} D & 0 \\ 0 & 0 & M_{sr} D \\ M_{sr} D & L_r D & p\omega_m L_r \\ -p\omega_m M_{sr} & -p\omega_m L_r & L_r D \end{bmatrix} \cdot \begin{bmatrix} i^a_{s2} \\ i^d_{r2} \\ i^q_{r2} \end{bmatrix} \qquad \text{A4.32a}$$

The homogeneous equation for i^q_r is found from this set as:

$$D^2 i^q_r + p^2\omega^2_m = 0 \qquad \text{A4.32b}$$

again resulting in a solution

$$t_2 < t < t_3 \; i^{qiii}_{r2} = I^{qiii}_{ri} \cos p\omega_m t'' + I^{qiii}_{rii} \sin p\omega_m t'' \qquad \text{A4.32c}$$

Actually the set of equations for the "a"-phase, rotor direct axis and rotor quadrature axis result in a characteristic equation of the third order, as follows:

$$\lambda^3 + p^2\omega^2_m\lambda = 0$$

as may also be deduced form the general relations A4.12a and 4.12b by setting either $\tau_s^{-1} \equiv 0 \equiv \tau_r^{-1}$ or $r_s \equiv 0 \equiv r_r$. The corresponding equations for the "a" phase and quadrature rotor axis are:

$$(D^3 + p^2\omega^2_m D) i^d_{r2} = -\frac{M_{sr}}{\sigma L_r L_s} (D^2 + p^2\omega^2_m) u^a_{s2} \qquad \text{A4.32d}$$

and

$$(D^3 + p^2\omega^2_m D) i^a_{s2} = \frac{1}{\sigma L_s} (D^2 + p^2\omega^2_m) u^a_{s2} \qquad \text{A4.32e}$$

The equation for the quadrature axis current simplifies due to the absence of any direct current component when the rotor resistance is reduced to zero. The quadrature-current also does not have a sustained or steady state component of supply frequency under these conditions. These remarks will be proved subsequently, when it will be shown that in the limit the approximate equations set up in the first part of this appendix regarding the induced stator winding e.m.f. during switching, reduce to the equations now to be derived.

In order to determine the constants in A4.32c, the direct an quadrature axis currents are again taken to be continuous at the switching instant t_2. Therefore:

$$\left.\begin{aligned} & i^{qiii}_{r2}(t''= +0) = i^{qiii}_{r1}(t'''= -0) = i^{qii}_{r1}(t = t_2) = I^a_r(t_1)\sin p\omega_m t_2 + I^b_r(t_1)\cos p\omega_m t_2 \\ & \text{identically:} \\ & i^{diii}_{r2}(t''= +0) = i^{diii}_{r1}(t'''= -0) = i^{dii}_{r1}(t = t_2) = I^a_r(t_1)\cos p\omega_m t_2 - I^b_r(t_1)\sin p\omega_m t_2 \end{aligned}\right\} \qquad \text{A4.33a}$$

The condition for the first time derivative of i_r^q is:

$$Di_{r2}^{qiii} = p\omega_m i_{r2}^{diii} + p\omega_m \frac{M_{sr}}{L_r} i_{s2}^{aiii} \qquad \text{A4.33b}$$

Taking into account that the current in stator phase "a" is zero at the switching instant t_2, and equating A4.33 with A4.32c, it is again found that:

$$t_2 < t < t_3: \; i_{r2}^{qiii} = I_r^a(t_1)\sin p\omega_m t + I_r^b(t_1)\cos p\omega_m t \qquad \text{A4.34b}$$

It is to be remarked that in spite of the fact that the complementary phase "a" has been switched in, the quadrature-axis current continues its oscillation at the mechanical frequency started in the previous period.

From A4.32a it may now be found:

$$\begin{bmatrix} \frac{u_{s2}^a}{L_s} \\ 0 \end{bmatrix} = \begin{bmatrix} D & \frac{M_{sr}}{L_s} D & 0 \\ D & \frac{L_r}{M_{sr}} D & \frac{p\omega_m L_r}{M_{sr}} \end{bmatrix} \cdot \begin{bmatrix} i_{s2}^a \\ i_{r2}^d \\ i_{r2}^q \end{bmatrix} \qquad \text{A4.35a}$$

By elimination of i_s^a:

$$Di_{r2}^{diii} = -\frac{M_{sr}}{\sigma L_r L_s} u_{s2}^a - \frac{p\omega_m}{\sigma} i_{r2}^{qiii}$$

Therefore:

$$i_{r2}^{diii} = -\int \frac{M_{sr}\sqrt{2}U_{sg}\cos\omega_s t}{\sigma L_r L_s} dt - \int \frac{p\omega_m}{\sigma} \left\{ I_r^a(t_1)\sin p\omega_m t + I_r^b(t_1)\cos p\omega_m t \right\} dt + K$$

From A4.33a $i_{r2}^{diii}(t = t_2)$ is known, so that the constant of integration is easily evaluated, representing the corresponding d.c. component of the direct-axis rotor current, i.e.:

$$K = I_{ri}^{diii} = \frac{M_{sr}}{\omega_s \sigma L_r L_s} \cdot \sqrt{2}U_{sg}\sin\omega_s t_2 + \left(\frac{\sigma-1}{\sigma}\right) I_r^a(t_1)\cos p\omega_m t_2 - \left(\frac{\sigma-1}{\sigma}\right) I_r^b(t_1)\sin p\omega_m t_2 \qquad \text{A4.35b}$$

$$\therefore \; i_{r2}^{diii} = \frac{M_{sr}}{\omega_s \sigma L_r L_s} \sqrt{2}U_{sg} \left\{ \sin\omega_s t_2 - \sin\omega_s t \right\} + \frac{I_r^a(t_1)}{\sigma} \left\{ \overline{\sigma-1} \cos p\omega_m t_2 + \cos p\omega_m t \right\}$$

$$- \frac{I_r^b(t_1)}{\sigma} \left\{ \overline{\sigma-1} \sin p\omega_m t_2 + \sin p\omega_m t \right\} \qquad \text{A4.35c}$$

From the same set A4.35a it now follows directly that:

$$Di_{s2}^{aiii} = \frac{u_{s2}^{a}}{L_s} - \frac{M_{sr}}{L_s} Di_{r2}^{diii}$$

or

$$i_{s2}^{aiii} = \int \left(\frac{u_{s2}^{a}}{L_s} - \frac{M_{sr}}{L_s} Di_{r2}^{diii}\right) dt + I_{si}^{aiii}$$

Evaluating I_{si}^{aiii} from the condition that the phase current is still zero at the instant of switching in (in the ideal case), an expression is found for i_s^a that indicates the mutual coupling of the a-phase and the direct axis, in contrast to its rotational relation to the quadrature-axis

$$i_{s2}^{aiii} = \frac{\sqrt{2}U_{sg}}{\sigma\omega_s L_s}\left\{\sin\omega_s t - \sin\omega_s t_2\right\} + \frac{M_{sr}}{\sigma L_s} I_r^a(t_1)\left\{\cos p\omega_m t_2 - \cos p\omega_m t\right\}$$

$$- \frac{M_{sr}}{\sigma L_s} I_r^b(t_1)\left\{\sin p\omega_m t_2 - \sin p\omega_m t\right\} \qquad \text{A4.35d}$$

The currents in the period t_2 to t_3 are now completely specified.
From A4.32a the induced e.m.f. in phase b is:

$$e_{s2}^{biii} = M_{sr} Di_{r2}^{qiii} = \overline{1-s}\omega_s M_{sr}\left\{I_r^a(t_1)\cos\overline{1-s}\omega_s t + I_r^b(t_1)\sin\overline{1-s}\omega_s t\right\} \qquad \text{A4.36}$$

$$t_3 < t < t_4 \;,\; R_s \equiv 0 \equiv R_r$$

It is again found that:

$$\begin{bmatrix} e_{s3}^{a} \\ e_{s3}^{b} \\ 0 \\ 0 \end{bmatrix} = \begin{bmatrix} M_{sr}D & 0 \\ 0 & M_{sr}D \\ L_r D & p\omega_m L_r \\ -p\omega_m L_r & L_r D \end{bmatrix} \cdot \begin{bmatrix} i_{r3}^{d} \\ i_{r3}^{q} \end{bmatrix} \qquad \text{A4.37a}$$

with homogeneous equations

$$D^2 i_{r3}^{q} + p^2\omega_m^2 i_{r3}^{q} \equiv 0 \equiv p^2\omega_m^2 i_{r3}^{q} + D^2 i_{r3}^{q}$$

so that the same solutions as in the first time interval from t_1 to t_2 are found, i.e.

$$t_3 < t < t_4 \quad i_{r3}^{qiii} = I_{ri}^{qiv} \cos p\omega_m t''' + I_{rii}^{qiv} \sin p\omega_m t''' \qquad \text{A4.37b}$$

Since both i_{r3}^{d} and i_{r3}^{q} are again constrained to be continuous, the first derivative of i_{r3}^{q} will also be continuous, as it is determined by the magnitude of i_r^d (from relation A4.37a). Care must now be taken with the initial conditions, however, as the functional expression for i_r^d changes at the switching instant t_3

$$i_{r3}^{qiii}(t''' = +0) = i_{r2}^{qiii}(t''' = -0) = i_{r2}^{qiii}(t = t_3)$$

$$Di_{r3}^{qiii}(t''' = +0) = Di_{r2}^{qiii}(t''' = -0) = Di_{r2}^{qiii}(t = t_3)$$

Determining these values from A4.43b and A4.37b and substituting in the above relations results in exactly the same expression for i_r^q as previously:

$$t_3 < t < t_4: \quad i_{r3}^{qiii} = I_r^a(t_1)\sin p\omega_m t + I_r^b(t_1)\cos p\omega_m t \qquad \text{A4.37c}$$

Employing the relation A4.37a, the equation for i_r^d is:

$$t_3 < t < t_4: \quad i_{r3}^{diii} = I_r^a(t_1)\cos p\omega_m t - I_r^b(t_1)\sin p\omega_m t \qquad \text{A4.37d}$$

The resulting induced e.m.f. is:

$$e_{s3}^{biii} = \overline{1-s}\omega_s M_{sr} \left\{ I_r^a(t_1)\cos \overline{1-s}\omega_s t + I_r^b(t_1)\sin \overline{1-s}\omega_s t \right\} \qquad \text{A4.38}$$

A DISCUSSION OF THE LIMITING CONDITIONS

In conclusion to this appendix some attention will be devoted to a discussion of the different aspects of the equations developed.

By taking the stator time constant into account in the equations one introduces a damping into the d.c. components of the stator phase currents and the rotor direct and quadrature currents. This is analogous to the results found in the studies of short circuiting of a synchronous machine ([89], a problem reminiscent of the present investigation in some respects. This time constant was therefore neglected during the present investigations, as it was felt that it will not alter the problem fundamentally.

The rotor time constant is important as far as the eigenfrequency of the induced e.m.f., damping and d.c. components of the quadrature axis rotor current are concerned. In the case of a stator time constant it may be argued that the tendency is to keep this as low as possible in an induction machine. In the case of the rotor time constant this is not a priori true. Due to the inclusion of external rotor resistances to keep the excessive dissipation out of the machine during low speed operation of these variable-slip systems, the electrical rotor time constant may be influenced to such an extent that it is no longer permissible to disregard its influence.

Comparison of the direct and quadrature axis rotor currents during the time intervals, t_1 to t_2 and t_3 to t_4, (the stator phases do not conduct) with and without rotor resistances, indicates that the only difference found here is the damping of the oscillation of both currents at the mechanical frequency. Consequently the only influence of a decreasing rotor time constant on the induced e.m.f. during these periods will be a change in amplitude of the undamped oscillation, and further damping of this oscillation.

Due to the complexity of the equations the influence of the time constant of the rotor is not so obvious on the quadrature current- and correspondingly the induced e.m.f. - in the normative phase, when the complementary phase is conducting, i.e. in time interval t_2 to t_3. Only the first approximation for the equations describing this interval are considered, as this covers the usual range of operating speeds of a variable slip drive.

Consider the effective time constant and the eigenfrequency from relations A4.16b and c.

$$\lim_{\tau_r \to \infty} \tau_e = \lim_{\tau_r \to \infty} \left(\frac{2\sigma}{1+\sigma}\right)\tau_r = \infty$$

$$\lim_{\tau_r \to \infty} \omega_e = \lim_{\tau_r \to \infty} \left(\overline{1-s}^2\omega_s^2 - \frac{\overline{1+\sigma}^2}{4\sigma^2\tau_r^2}\right)^{\frac{1}{2}} = \overline{1-s}\omega_s$$

This is borne out by the equations developed directly for i_r^q from A4.32a.

Let the d.c. component of i_{r2}^{qi} be examined. From A4.20g let

$$I_{ri}^{qi} = K_1 i_{r2}^{qi}(t = t_2) + K_2 i_{r2}^{di}(t = t_2) + K_3 I_{r2}^{qi}\cos(\omega_s t_2 + \psi_2^{qi}) + K_4 I_{r2}^{qi}\sin(\omega_s t_2 + \psi_2^{qi}) \qquad \text{A4.40a}$$

with the constants as defined by comparison of A4.40a and A4.20g

$$\lim_{\tau_r \to \infty} K_1 = \lim_{\tau_r \to \infty} \left\{1 + \frac{\tau_e^2 - 2\tau_r\tau_e - \tau_r^2\tau_e^2\,\overline{1-s}^2\omega_s^2}{\tau_r^2(1+\omega_e^2\tau_e^2)}\right\}$$

or

$$\lim_{\tau_r \to \infty} K_1 = \lim_{\tau_r \to \infty} \left\{1 + \frac{\tau_r^{-2} - 2\tau_r^{-1}\tau_e^{-1} - \overline{1-s}^2\omega_s^2}{(\tau_e^{-2} + \omega_e^2)}\right\} = 0$$

Furthermore

$$\lim_{\tau_r \to \infty} K_2 = \lim_{\tau_r \to \infty} -\left\{2\,\overline{1-s}\omega_s \cdot \left(\frac{\tau_r^{-1} - \tau_e^{-1}}{\tau_e^{-2} + \omega_e^2}\right)\right\} = 0$$

also

$$\lim_{\tau_r \to \infty} K_3 = -1 \quad \text{and} \quad \lim_{\tau_r \to \infty} K_4 = 0$$

These two constants are both multiplied by I_{r2}^{q1}. Let the limit of I_{r2}^{q1} be investigated:

$$\lim_{\tau_r \to \infty} I_{r2}^{qi} = \lim_{\tau_r \to \infty} \left\{\tau_r^{-1}\,\frac{\overline{1-s}M_{sr}U_{sg}}{\omega_s L_s L_r(\omega_s\sigma^2(1-\overline{1-s}^2)^2 + \overline{1+\sigma}^2\tau_r^{-2})^{\frac{1}{2}}}\right\} = 0$$

It may therefore be stated that

$$\lim_{\tau_r \to \infty} I_{ri}^{qi} = 0$$

This has been borne out by the solution developed directly from the simplified equations A4.32a, where it was already pointed out that the characteristic equation for the quadrature-axis current simplifies to a second order form due to the absence of a direct current component. These observations correspond with the results obtained on the problem of short circuiting the a.c. windings of a synchronous generator without resistance[89].

Examine the first transient term I^{qi}_{rii}:

Use expression A4.20f, and note

$$I^{qi}_{rii} = - K_2 i^{di}_{r2}(t = t_2) + K_5 i^{qi}_{r2}(t = t_2) + K_6 I^{qi}_{r2} \qquad \text{A4.40b}$$

It has already been proven that

$$\lim_{\tau_r \to \infty} -K_2 = 0$$

$$\lim_{\tau_r \to \infty} K_5 = \lim_{\tau_r \to \infty} -\left\{\frac{\tau_r^{-2} - 2\tau_r^{-1}\tau_e^{-1} - \overline{1-s}^2\omega_s^2}{\tau_e^{-2} + \omega_e^2}\right\} = 1$$

$$\lim_{\tau_r \to \infty} K_6 = \lim_{\tau_r \to \infty} -\sqrt{2}\left\{\frac{2\tau_e^{-1}\omega_s \sin(\omega_s t_2 + \psi_2^{qi}) + \omega_s^2 \cos(\omega_s t_2 + \psi_2^{qi})}{(\tau_e^{-2} + \omega_e^2)}\right\}$$

$$= -\sqrt{2}\left\{\frac{\cos(\omega_s t_2 + \psi_2^{qi})}{\overline{1-s}^2}\right\}$$

Seeing that $\lim_{\tau_r \to \infty} (I^{qi}_{r2}) = 0$, it may be concluded that

$$\lim_{\tau_r \to \infty} I^{qi}_{rii} = i^{qi}_{r2}(t = t_2)$$

The second transient term I^{qi}_{riii}

Relation A4.20h results in:

$$I^{qi}_{riii} = K_7 i^{di}_{r2}(t = t_2) + K_8 i^{qi}_{r2}(t = t_2) + K_9 I^{qi}_{r2} \qquad \text{A4.40c}$$

Determining the limits:

$$\lim_{\tau_r \to \infty} K_7 = \lim_{\tau_r \to \infty} \left\{\frac{\overline{1-s}\omega_s}{\omega_e}\left(1 + \frac{2\tau_e^{-1}\tau_r^{-1} - 2\tau_e^{-2}}{\tau_e^{-2} + \omega_e^2}\right)\right\} = 1$$

and

$$\lim_{\tau_r \to \infty} K_8 = \lim_{\tau_r \to \infty} -\left\{\omega_e^{-1}\tau_r^{-1} + \frac{\tau_r^{-2} - 2\tau_e^{-1}\tau_r^{-1} - \overline{1-s}^2\omega_s^2}{\omega_e \tau_e(\tau_e^{-2} + \omega_e^2)}\right\} = 0$$

$$\lim_{\tau_r \to \infty} K_9 = \lim_{\tau_r \to \infty} \sqrt{2}.\frac{\omega_s}{\omega_e}\left\{(1-\frac{2}{\tau_e^2(\tau_e^{-2}+\omega_e^2)})\sin(\omega_s t_2+\psi_2^{qi})-(\frac{\omega_s}{\tau_e(\tau_e^{-2}+\omega_e^2)})\cos(\omega_s t_2+\psi_2^{qi})\right\}$$

$$= \sqrt{2}\left\{\frac{\sin(\omega_s t_2+\psi_2^{qi})}{1-s}\right\}$$

Since the limit of I_{r2}^{qi} is known to be zero,

$$\lim_{\tau_r \to \infty} I_{riii}^{qi} = i_{r2}^{di}(t = t_2)$$

Substitution of these expressions into A4.16d, taking into account that $\lim_{\tau_r \to \infty} i_{r2}^{qi}(t = \infty) = 0$ as may be shown from $\lim_{\tau_r \to \infty} I_{r2}^{qi}$, indicates that:

$$\lim_{\tau_r \to \infty} i_{r2}^{qi}(t) = \lim_{\tau_r \to \infty} \exp-\frac{t''}{\tau_e}\left\{i_{r2}^{qi}(t = t_2)\cos\omega_e t''+ i_{r2}^{di}(t = t_2)\sin\omega_e t''\right\}$$

Calculating the limits from A4.20a and b the result is:

$$\lim_{\tau_r \to \infty} i_{r2}^{qi}(t) = I_r^a(t_1)\sin\sqrt{1-s}\omega_s t+ I_r^b(t_1)\cos\sqrt{1-s}\omega_s t = i_{r2}^{qiii}(t)$$

as determined in relation A4.34b by neglecting all rotor and stator resistances.

The first approximation used for the period when the normative phase blocks, and the complementary phase conducts, has in the preceding been demonstrated equivalent to the third approximation in the limit when the rotor time constant becomes very large. This limiting process indicates that it is the rotor time constant that appear in all the terms coupling the quadrature current, and consequently the induced voltage in the normative phase ("b"), to the influence of the supply through conduction of the complementary phase.

A4.3 THE EXPRESSIONS FOR THE SWITCHED VOLTAGES IN THE STATOR CIRCUIT (IN THE CASE OF STATOR CONTROL BY DELAY OF IGNITION ANGLE) AND INSTANTANEOUS SYMMETRICAL COMPONENT TRANSFORMS OF THESE VOLTAGES.

In the previous appendix the induced voltage was derived by an approximation neglecting resistance effects in rotor and stator.
Let therefore:

$$\bar{e}_s^b(t) \simeq \sqrt{1-s}\omega_s M_{sr}\left\{I_r^a(t_1)\cos\sqrt{1-s}\omega_s t - I_r^b(t_1)\sin\sqrt{1-s}\omega_s t\right\}$$

$$\therefore \bar{e}_s^b(t) \propto \sqrt{1-s}\,\sqrt{2}\,E_{sr}^{ba}\cos\sqrt{1-s}\omega_s t - \sqrt{1-s}\,\sqrt{2}\,E_{sr}^{bb}\sin\sqrt{1-s}\omega_s t \qquad \text{A4.41a}$$

where

$$\left.\begin{aligned}\sqrt{2}\,E_{sr}^{ba} &= \omega_s M_{sr} I_r^a(t_1)\\ \sqrt{2}\,E_{sr}^{bb} &= \omega_s M_{sr} I_r^b(t_1)\end{aligned}\right\} \qquad \text{A4.41b}$$

Alternatively:

$$\bar{\bar{e}}_s^b(t) \quad \frac{\overline{1-s}}{j\sqrt{2}} \left\{ (jE_{sr}^{ba} - E_{sr}^{bb}) \exp j\,\overline{1-s}\omega_s t + (jE_{sr}^{ba} + E_{sr}^{bb}) \exp -j\,\overline{1-s}\omega_s t \right\} \qquad \text{A4.41c}$$

Writing

$$\bar{\bar{e}}_s^b(t) = \frac{\overline{1-s}}{\sqrt{2}} \sum_{h=0}^{\infty} \left\{ \dot{\bar{\bar{E}}}_{s\ \overline{2h+1}} \exp j(\overline{2h+1}\omega_s t) + \dot{\bar{\bar{E}}}^{*}_{s\ \overline{2h+1}} \exp -j(\overline{2h+1}\omega_s t) \right\} \qquad \text{A4.41d}$$

it is implied that:

$$\sqrt{2}.\overline{1-s}\ \dot{\bar{\bar{E}}}^b_{s\ \overline{2h+1}} = \frac{2}{\pi} \int_0^{\pi} \left\{ \bar{\bar{e}}_s^b(\omega_s t) \exp -j\ \overline{2h+1}\omega_s t \right\} d\omega_s t = \sqrt{2}\ \overline{1-s}\ \dot{\bar{\bar{E}}}_{s\ \overline{2h+1}}$$

as the two phases are assumed identical. Ultimately it is obtained that

$$\dot{\bar{\bar{E}}}_{s\ \overline{2h+1}} = \frac{1}{j\pi} (jE_{sr}^{ba} - E_{sr}^{bb}) \int_{\gamma_s - \pi}^{\alpha_s} \exp j(\overline{1-s} - \overline{2h+1})\omega_s t\, d\omega_s t$$

$$+ \frac{1}{j\pi} (jE_{sr}^{ba} + E_{sr}^{bb}) \int_{\gamma_s - \pi}^{\alpha_s} \exp -j(\overline{1-s} + \overline{2h+1})\omega_s t\, d\omega_s t$$

$$\therefore \dot{\bar{\bar{E}}}_{s\ \overline{2h+1}} = \frac{jE_{sr}^{ba}}{\pi} \left\{ \frac{\exp -j(2h+2-s)\alpha_s - \exp -j(2h+2-s)(\gamma_s - \pi)}{2h+2-s} + \frac{\exp -j(2h+s)\alpha_s - \exp -j(2h+s)(\gamma_s - \pi)}{2h+s} \right\}$$

$$+ \frac{E_{sr}^{bb}}{\pi} \left\{ \frac{\exp -j(2h+2-s)\alpha_s - \exp -j(2h+2-s)(\gamma_s - \pi)}{2h+2-s} - \frac{\exp -j(2h+s)\alpha_s - \exp -j(2h+s)(\gamma_s - \pi)}{(2h+s)} \right\} \qquad \text{A4.41e}$$

As has been stated previously, the harmonic components of the waveforms of phase "a" will be shifted with respect to those of phase "b" with $\pi/2$, so that

$$\exp \pm j(\overline{2h+1}\omega_s t) \rightarrow (\pm j)^{\overline{2h+1}} \exp \pm j(\overline{2h+1}\omega_s t)$$

giving an expression for $e_s^a(t)$ from the above. The expressions for $e_s^a(t)$ and $e_s^b(t)$ are then found as given in relation 4.37a. For calculations concerning power and torque it is sometimes useful to have the relation in the alternative trigonometric form:

$$\begin{bmatrix} \bar{\bar{e}}_s^a(t) \\ \bar{\bar{e}}_s^b(t) \end{bmatrix} = \sqrt{2}\ \overline{1-s} \sum_{h=0}^{\infty} E^{ba}_{s\ \overline{2h+1}} \begin{bmatrix} \cos\left\{ \overline{2h+1}\left(\omega_s t + \frac{\pi}{2}\right) - \phi^{ea}_{\overline{2h+1}} \right\} \\ \cos\left\{ \overline{2h+1}\omega_s t - \phi^{ea}_{\overline{2h+1}} \right\} \end{bmatrix} +$$

$$+\sqrt{2}\sqrt{1-s}\sum_{h=0}^{\infty} E^{bb}_{s\ \overline{2h+1}} \begin{bmatrix} \cos\left\{\overline{2h+1}\,(\omega_s t+\frac{\pi}{2})-\phi^{eb}_{\overline{2h+1}}\right\} \\ \cos\left\{\overline{2h+1}\,\omega_s t-\phi^{eb}_{\overline{2h+1}}\right\} \end{bmatrix} \qquad \text{A4.42a}$$

the coefficients being

$$E^{ba}_{s\ \overline{2h+1}} = E^{ba}_{sr}\left\{(A^{Ea}_{s\ \overline{2h+1}})^2+(B^{Ea}_{s\ \overline{2h+1}})^2\right\}^{\frac{1}{2}} ;\ \phi^{Ea}_{\overline{2h+1}} = \tan^{-1}\left(\frac{B^{Ea}_{s\ \overline{2h+1}}}{A^{Ea}_{s\ \overline{2h+1}}}\right) \qquad \text{A4.42b}$$

$$E^{bb}_{s\ \overline{2h+1}} = E^{bb}_{sr}\left\{(A^{Eb}_{s\ \overline{2h+1}})^2+(B^{Eb}_{s\ \overline{2h+1}})^2\right\}^{\frac{1}{2}} ;\ \phi^{Eb}_{\overline{2h+1}} = \tan^{-1}\left(\frac{B^{Eb}_{s\ \overline{2h+1}}}{A^{Eb}_{s\ \overline{2h+1}}}\right)$$

with

$$\left.\begin{aligned} A^{Ea}_{s\ \overline{2h+1}} &= \frac{1}{\pi}\left\{\frac{\sin(2h+2-s)\alpha_s-\sin(2h+2-s)(\gamma_s-\pi)}{2h+2-s}+\frac{\sin(2h+s)\alpha_s-\sin(2h+s)(\gamma_s-\pi)}{2h+s}\right\} \\ B^{Ea}_{s\ \overline{2h+1}} &= \frac{1}{\pi}\left\{\frac{\cos(2h+2-s)(\gamma_s-\pi)-\cos(2h+2-s)\alpha_s}{2h+2-s}+\frac{\cos(2h+s)(\gamma_s-\pi)-\cos(2h+s)\alpha_s}{2h+s}\right\} \\ A^{Eb}_{s\ \overline{2h+1}} &= \frac{1}{\pi}\left\{\frac{\cos(2h+2-s)\alpha_s-\cos(2h+2-s)(\gamma_s-\pi)}{2h+2-s}-\frac{\cos(2h+s)\alpha_s-\cos(2h+s)(\gamma_s-\pi)}{2h+s}\right\} \\ B^{Eb}_{s\ \overline{2h+1}} &= \frac{1}{\pi}\left\{\frac{\sin(2h+2-s)\alpha_s-\sin(2h+2-s)(\gamma_s-\pi)}{2h+2-s}-\frac{\sin(2h+s)\alpha_s-\sin(2h+s)(\gamma_s-\pi)}{2h+s}\right\} \end{aligned}\right\} \qquad \text{A4.42c}$$

It is to be noted that in the above coefficients, and the coefficients of the exponential series A4.41e the following slips result in limiting situations:

$$\left.\begin{aligned} s_1 &= 2h+2 \\ s_2 &= -\ 2h \end{aligned}\right\} \qquad \text{A4.42d}$$

The only slip in the normal range of operation answering to this condition is zero slip. Seeing that the rotor currents are also zero at synchronous speed this point is excluded from consideration.

Now taking into account the instantaneous symmetrical component transformation (as used in the text, paragraph 4.2.2.5) for the semi-four-phase system under investigation, the following is obtained for the stator voltages- the rotor voltages being zero:

$$\begin{bmatrix} \underline{\dot{u}}^{+}_{s} \\ \underline{\dot{u}}^{-}_{s} \end{bmatrix} = \frac{1}{\sqrt{2}} \begin{bmatrix} \underline{u}^{a}_{sg}(t) + j\underline{u}^{b}_{sg}(t) + \underline{e}^{a}_{s}(t) + j\underline{e}^{b}_{s}(t) \\ \underline{u}^{a}_{sg}(t) - j\underline{u}^{b}_{sg}(t) + \underline{e}^{a}_{s}(t) - j\underline{e}^{b}_{s}(t) \end{bmatrix}$$

Substituting the derived expressions from relations A4.1 and A4.41d

$$\begin{bmatrix} \dot{\bar{\bar{U}}}_s^+ \\ \dot{\bar{\bar{U}}}_s^- \end{bmatrix} = \frac{1}{2} \sum_{h=0}^{\infty} \begin{bmatrix} (j)^{\overline{2h+1}+j} \\ (j)^{\overline{2h+1}-j} \end{bmatrix} \left\{ \dot{\bar{\bar{U}}}_{sg\ \overline{2h+1}} + \overline{1-s}\ \dot{\bar{\bar{E}}}_{s\ \overline{2h+1}} \right\} \exp j(\overline{2h+1}\omega_s t)$$

$$+ \begin{bmatrix} (-j)^{\overline{2h+1}+j} \\ (-j)^{\overline{2h+1}-j} \end{bmatrix} \left\{ \dot{\bar{\bar{U}}}^*_{sg\ \overline{2h+1}} + \overline{1-s}\ \dot{\bar{\bar{E}}}^*_{s\ \overline{2h+1}} \right\} \exp -j(\overline{2h+1}\omega_s t) \qquad \text{A4.43}$$

It may now be shown that the forward and backward components of the "positive sequence" voltage exists only for the

$$(4h+1)\text{st and } (4h+3)\text{rd}$$

harmonics respectively.

In the same way it may be proved that the converse is true for the forward and backward of the "negative sequence" voltage. The final expressions obtained for the coefficients will then be the following for the grid voltage:

$$\dot{\bar{\bar{U}}}_{sg\ \overline{4h+1}} = \frac{U_{sg}}{\pi} \left\{ \frac{\exp -j4h\gamma_s - \exp -j4h\alpha_s}{4h} - \frac{\exp -j\overline{4h+2}\gamma_s - \exp -j\overline{4h+2}\alpha_s}{4h+2} \right\} \qquad \text{A4.44a}$$

$$\dot{\bar{\bar{U}}}_{sg\ \overline{4h+3}} = \frac{U_{sg}}{\pi} \left\{ \frac{\exp -j\overline{4h+2}\gamma_s - \exp -j\overline{4h+2}\alpha_s}{4h+2} - \frac{\exp -j\overline{4h+4}\gamma_s - \exp -j\overline{4h+4}\alpha_s}{4h+4} \right\} \qquad \text{A4.44b}$$

For the induced voltage it is obtained that:

$$\dot{\bar{\bar{E}}}_{s\ \overline{4h+1}} = \frac{jE^{ba}_{sr}}{\pi} \left\{ \frac{\exp -j(\overline{4h+2-s}\alpha_s) - \exp -j(\overline{4h+2-s}.\gamma_s - \pi)}{4h+2-s} \right.$$

$$\left. + \frac{\exp -j(\overline{4h+s}\alpha_s) - \exp -j(\overline{4h+s}.\gamma_s - \pi)}{4h+s} \right\}$$

$$+ \frac{E^{bb}_{sr}}{\pi} \left\{ \frac{\exp -j(\overline{4h+2-s}\alpha_s) - \exp -j(\overline{4h+2-s}.\gamma_s - \pi)}{4h+2-s} + \right.$$

$$\left. - \frac{\exp -j(\overline{4h+s}\alpha_s) - \exp -j(\overline{4h+s}.\gamma_s - \pi)}{4h+s} \right\} \qquad \text{A4.44c}$$

$$\dot{\underline{\underline{E}}}_{s\ \overline{4h+3}} = \frac{jE^{ba}_{sr}}{\pi}\left\{\frac{\exp-j(\overline{4h+4-s}\alpha_s) - \exp-j(\overline{4h+4-s}.\overline{\gamma_s-\pi})}{4h+4-s}\right.$$

$$\left. + \frac{\exp-j(\overline{4h+2+s}\alpha_s) - \exp-j(\overline{4h+2+s}.\overline{\gamma_s-\pi})}{4h+2+s}\right\}$$

$$+ \frac{E^{bb}_{sr}}{\pi}\left\{\frac{\exp-j(\overline{4h+4-s}\alpha_s) - \exp-j(\overline{4h+4-s}.\overline{\gamma_s-\pi})}{4h+4-s}\right.$$

$$\left. - \frac{\exp j(\overline{4h+2+s}\alpha_s) - \exp-j(\overline{4h+2+s}.\overline{\gamma_s-\pi})}{4h+2+s}\right\} \qquad \text{A4.44d}$$

From the relation A4.43 and the coefficients of relations A4.44a to d it is now possible to develop the expressions for the instantaneous symmetrical component transforms of the switched terminal excitation functions of 4.19a. These expressions are given in relations 4.38 in the text.

A4.4 CONCERNING THE CALCULATION OF THE ANGLE OF NATURAL COMMUTATION AND THE INITIAL CONDITIONS FOR THE INDUCED STATOR VOLTAGE.

As shown in the text, it is possible to find an equation containing the current ignition angle α_s, the commutation angle γ_s and the slip as variables from the equation for the stator current when one neglects that part of the stator current due to the "induced excitation" part of the input voltage. To obtain this equation use is made of the knowledge that the phase current in the normative phase b is zero at $\omega_s t = \gamma_s$.

Taking the complete excitation function into account implies as variables α_s, γ_s, s and the two rotor currents $I^a_r(t_1)$ and $I^b_r(t_1)$ at $\omega_s t = (\gamma_s - \pi)$ (see paragraph 4.2.2.4).

Taking relation 4.37c, and the stator current in phase b, it may be stated that:

$$\left.\begin{aligned} X_M.i^a_r(\omega_s t = \overline{\gamma_s-\pi}) - \sqrt{2}\ E^{ba}_{sr} &\equiv 0 \\ X_M.i^b_r(\omega_s t = \overline{\gamma_s-\pi}) - \sqrt{2}\ E^{bb}_{sr} &\equiv 0 \\ i^b_s(\omega_s t = \overline{\gamma_s-\pi}) &\equiv 0 \end{aligned}\right\} \qquad \text{A4.45a}$$

Relations 4.44c and 4.45c express the currents in terms of coefficients

$$\underline{\underline{I}}^E_{s\ \overline{4h+1}},\ \underline{\underline{I}}^E_{s\ 4h+3},\ I^E_{r\ \overline{4h+1}},\ I^E_{r\ \overline{4h+3}}$$

and phase angles

$$\psi^E_{s\ \overline{4h+1}},\ \psi^E_{s\ \overline{4h+3}},\ \psi^E_{sr\ \overline{4h+1}},\ \psi^E_{sr\ \overline{4h+3}}$$

that are dependent on the already previously used harmonic coefficients

$$\dot{\underline{\underline{E}}}_{s\ \overline{4h+1}} \quad \text{and} \quad \dot{\underline{\underline{E}}}_{s\ \overline{4h+3}}$$

In order to obtain expressions containing the separated initial conditions E^{ba}_{sr} and E^{bb}_{sr} these

coefficients from 4.38c and 4.38d will be noted, in analogy to rel. 4.41e and A4.42a, as:

$$\underline{\underline{E}}_{sr\ \overline{4h+1}} = E^{ba}_{sr}\, C^{Ea}_{s\ \overline{4h+1}} \exp -j\phi^{Ea}_{s\ \overline{4h+1}} + E^{bb}_{sr}\, C^{Eb}_{s\ \overline{4h+1}} \exp -j\phi^{Eb}_{s\ \overline{4h+1}}$$

$$\underline{\underline{E}}_{sr\ \overline{4h+3}} = E^{ba}_{sr}\, C^{Ea}_{s\ \overline{4h+3}} \exp -j\phi^{Ea}_{s\ \overline{4h+3}} + E^{bb}_{sr}\, C^{Eb}_{s\ \overline{4h+3}} \exp -j\phi^{Eb}_{s\ \overline{4h+3}}$$

with

$$C^{E(^a_b)}_{s\ \overline{4h+1}} = \left\{ \left(A^{E(^a_b)}_{s\ \overline{4h+1}}\right)^2 + \left(B^{E(^a_b)}_{s\ \overline{4h+1}}\right)^2 \right\}^{\frac{1}{2}}; \quad \phi^{E(^a_b)}_{s\ \overline{4h+1}} = \arctan \left\{ \frac{B^{E(^a_b)}_{s\ \overline{4h+1}}}{A^{E(^a_b)}_{s\ \overline{4h+1}}} \right\}$$

where for instance $C^{E(^a_b)}_{s\ \overline{4h+1}} \rightarrow C^{Ea}_{s\ \overline{4h+1}}$ or $C^{Eb}_{s\ \overline{4h+1}}$

$$C^{E(^a_b)}_{s\ \overline{4h+3}} = \left\{ \left(A^{E(^a_b)}_{s\ \overline{4h+3}}\right)^2 + \left(B^{E(^a_b)}_{s\ \overline{4h+3}}\right)^2 \right\}^{\frac{1}{2}}; \quad \phi^{E(^a_b)}_{s\ \overline{4h+3}} = \arctan \left\{ \frac{B^{E(^a_b)}_{s\ \overline{4h+3}}}{A^{E(^a_b)}_{s\ \overline{4h+1}}} \right\} \qquad \text{A4.45b}$$

where the coefficients A,B have been defined in relations 4.38c and 4.38d. By substituting these expressions into the exponential form of the stator currents of relation 4.44b and expanding into a trigonometric expression, the stator current in phase b is found to be given at $\omega_s t = \gamma_s - \pi$ by:

$$\begin{aligned} i^b_s(\omega_s t=\gamma_s-\pi) = \sqrt{2} \sum_{h=0}^{\infty} \Bigg\{ & \underline{\underline{I}}^u_{s\ \overline{4h+1}}(\alpha_s,\gamma_s,s)\cos\left[\overline{4h+1}(\gamma_s-\pi)-\psi^u_{s\ \overline{4h+1}}(\alpha_s,\gamma_s,s)\right] + \\ & + \underline{\underline{I}}^u_{s\ \overline{4h+3}}(\alpha_s,\gamma_s,s)\cos\left[\overline{4h+3}(\gamma_s-\pi)-\psi^u_{s\ \overline{4h+3}}(\alpha_s,\gamma_s,s)\right] \Bigg\} + \\ + \overline{1-s}E^{ba}_{sr}\sqrt{2} \sum_{h=0}^{\infty} \Bigg\{ & Y^{Ea}_{s\ \overline{4h+1}}(\alpha_s,\gamma_s,s)\cos\left[\overline{4h+1}(\gamma_s-\pi)-\phi^{YEa}_{s\ \overline{4h+1}}(\alpha_s,\gamma_s,s)\right] + \\ & + Y^{Ea}_{s\ \overline{4h+3}}(\alpha_s,\gamma_s,s)\cos\left[\overline{4h+3}(\gamma_s-\pi)-\phi^{YEa}_{s\ \overline{4h+3}}(\alpha_s,\gamma_s,s)\right] \Bigg\} + \\ + \overline{1-s}E^{bb}_{sr}\sqrt{2} \sum_{h=0}^{\infty} \Bigg\{ & Y^{Eb}_{s\ \overline{4h+1}}(\alpha_s,\gamma_s,s)\cos\left[\overline{4h+1}(\gamma_s-\pi)-\phi^{YEb}_{s\ \overline{4h+1}}(\alpha_s,\gamma_s,s)\right] + \\ & + Y^{Eb}_{s\ \overline{4h+3}}(\alpha_s,\gamma_s,s)\cos\left[\overline{4h+3}(\gamma_s-\pi)-\phi^{YEb}_{s\ \overline{4h+3}}(\alpha_s,\gamma_s,s)\right] \Bigg\} = 0 \end{aligned} \qquad \text{A4.45c}$$

In this expression the newly introduced elements are

$$Y^{E(\frac{a}{b})}_{s\ \overline{4h+1}}(\alpha_s,\gamma_s s) = \frac{C^{E(\frac{a}{b})}_{s\ \overline{4h+1}}}{Z_{s\ \overline{4h+1}}} \quad ; \quad Y^{E(\frac{a}{b})}_{s\ \overline{4h+3}}(\alpha_s,\gamma_s s) = \frac{C^{E(\frac{a}{b})}_{s\ \overline{4h+3}}}{Z_{s\ \overline{4h+3}}}$$

$$\phi^{YE(\frac{a}{b})}_{s\ \overline{4h+1}} = \left(\phi^{E(\frac{a}{b})}_{s\ \overline{4h+1}} + \phi^{Z}_{\overline{4h+1}}\right) \quad ; \quad \phi^{YE(\frac{a}{b})}_{s\ \overline{4h+3}} = \left(\phi^{E(\frac{a}{b})}_{s\ \overline{4h+3}} + \phi^{Z}_{\overline{4h+3}}\right) \qquad \text{A4.45d}$$

In an exactly similar way it is possible to modify the expressions for the rotor currents given in relation 4.45c to obtain at $\omega_s t = (\gamma_s - \pi)$ that:

$$i^a_r(\omega_s t=\gamma_s-\pi) = \sqrt{2}\sum_{h=0}^{\infty}\left\{I^u_{r\ \overline{4h+1}}(\alpha_s,\gamma_s s)\sin\left[\overline{4h+s}(\gamma_s-\pi)-\phi^u_{sr\ \overline{4h+1}}(\alpha_s,\gamma_s s)\right] + \right.$$

$$\left. - I^u_{r\ \overline{4h+3}}(\alpha_s,\gamma_s s)\sin\left[\overline{4h+4-s}(\gamma_s-\pi)-\phi^u_{sr\ \overline{4h+3}}(\alpha_s,\gamma_s s)\right]\right\} +$$

$$+ \overline{1-s}E^{ba}_{sr}\sqrt{2}\sum_{h=0}^{\infty}\left\{Y^{Ea}_{sr\ \overline{4h+1}}(\alpha_s,\gamma_s s)\sin\left[\overline{4h+s}(\gamma_s-\pi)-\phi^{YEa}_{sr\ \overline{4h+1}}(\alpha_s,\gamma_s s)\right] + \right.$$

$$\left. - Y^{Ea}_{sr\ \overline{4h+3}}(\alpha_s,\gamma_s s)\sin\left[\overline{4h+4-s}(\gamma_s-\pi)-\phi^{YEa}_{sr\ \overline{4h+3}}(\alpha_s,\gamma_s s)\right]\right\} +$$

$$+ \overline{1-s}E^{bb}_{sr}\sqrt{2}\sum_{h=0}^{\infty}\left\{Y^{Eb}_{sr\ \overline{4h+1}}(\alpha_s,\gamma_s s)\sin\left[\overline{4h+s}(\gamma_s-\pi)-\phi^{YEb}_{sr\ \overline{4h+1}}(\alpha_s,\gamma_s s)\right] + \right.$$

$$\left. - Y^{Eb}_{sr\ \overline{4h+3}}(\alpha_s,\gamma_s s)\sin\left[\overline{4h+4-s}(\gamma_s-\pi)-\phi^{YEb}_{sr\ \overline{4h+3}}(\alpha_s,\gamma_s s)\right]\right\} =$$

$$= 0 \qquad \text{A4.45e}$$

and

$$i^b_r(\omega_s t=\overline{\gamma_s-\pi}) = -\sqrt{2}\sum_{h=0}^{\infty}\left\{I^u_{r\ \overline{4h+1}}(\alpha_s,\gamma_s s)\cos\left[\overline{4h+s}(\gamma_s-\pi)-\psi^u_{sr\ \overline{4h+1}}(\alpha_s,\gamma_s s)\right] + \right.$$

$$\left. + I^u_{r\ \overline{4h+3}}(\alpha_s,\gamma_s s)\cos\left[\overline{4h+4-s}(\gamma_s-\pi)-\psi^u_{sr\ \overline{4h+3}}(\alpha_s,\gamma_s s)\right]\right\} +$$

$$- \overline{1-s}E^{ba}_{sr}\sqrt{2}\sum_{h=0}^{\infty}\left\{Y^{Ea}_{sr\ \overline{4h+1}}(\alpha_s,\gamma_s s)\cos\left[\overline{4h+s}(\gamma_s-\pi)-\phi^{YEa}_{sr\ \overline{4h+1}}(\alpha_s,\gamma_s s)\right] + \right.$$

$$+ Y^{Ea}_{sr\ \overline{4h+3}}(\alpha_s,\gamma_s s)\cos\left[\overline{4h+4-s}(\gamma_s-\pi)-\phi^{YEa}_{sr\ \overline{4h+3}}(\alpha_s,\gamma_s s)\right]\Bigg\} +$$

$$- \overline{1-s}\,E^{bb}_{sr}\sqrt{2}\sum_{h=0}^{\infty}\left\{Y^{Eb}_{sr\ \overline{4h+1}}(\alpha_s,\gamma_s s)\cos\left[\overline{4h+s}(\gamma_s-\pi)-\phi^{YEb}_{sr\ \overline{4h+1}}(\alpha_s,\gamma_s s)\right] +\right.$$

$$\left. + Y^{Eb}_{sr\ \overline{4h+3}}(\alpha_s,\gamma_s s)\cos\left[\overline{4h+4-s}(\gamma_s-\pi)-\phi^{YEb}_{sr\ \overline{4h+3}}(\alpha_s,\gamma_s s)\right]\right\} =$$

$$= 0 \qquad \text{A4.45f}$$

In these expressions the parameters that have as yet not been defined are:

$$Y^{E(^a_b)}_{sr\ \overline{4h+1}}(\alpha_s,\gamma_s,s) = \frac{C^{E(^a_b)}_{s\ \overline{4h+1}}}{Z_{sr\ \overline{4h+1}}} \quad ; \quad Y^{E(^a_b)}_{sr\ \overline{4h+3}}(\alpha_s,\gamma_s,s) = \frac{C^{E(^a_b)}_{s\ \overline{4h+3}}}{Z_{sr\ \overline{4h+3}}}$$

$$\phi^{YE(^a_b)}_{sr\ \overline{4h+1}} = \left[\phi^{E(^a_b)}_{sr\ \overline{4h+1}} + \phi^{Z}_{sr\ \overline{4h+1}}\right]; \quad \phi^{YE(^a_b)}_{sr\ \overline{4h+3}} = \left[\phi^{E(^a_b)}_{sr\ \overline{4h+3}} + \phi^{Z}_{sr\ \overline{4h+3}}\right] \qquad \text{A4.45g}$$

By a comparison of the relations A4.45a, A4.45c, A4.45e and A4.45f with the set of equations 4.48c given in the text for $\omega_s t = \gamma - \pi$ the parameters defined as infinite series in this last equation may be found as follows:

$$I^{au}_r(\alpha_s,\gamma_s,s)\sqrt{2}\sum_{h=0}^{\infty}\left\{I^{u}_{r\ \overline{4h+1}}(\alpha_s,\gamma_s s)\sin\left[\overline{4h+s}(\gamma_s-\pi)-\psi^{u}_{sr\ \overline{4h+1}}(\alpha_s,\gamma_s s)\right]\right.$$

$$\left. - I^{u}_{r\ \overline{4h+3}}(\alpha_s,\gamma_s s)\sin\left[\overline{4h+4-s}(\gamma_s-\pi)-\psi^{u}_{sr\ \overline{4h+3}}(\alpha_s,\gamma_s s)\right]\right\}$$

$$I^{bu}_r(\alpha_s,\gamma_s s) = -\sqrt{2}\sum_{h=0}^{\infty}\left\{I^{u}_{r\ \overline{4h+1}}(\alpha_s,\gamma_s s)\cos\left[\overline{4h+s}(\gamma_s-\pi)-\psi^{u}_{sr\ \overline{4h+1}}(\alpha_s,\gamma_s s)\right]\right.$$

$$\left. + I^{u}_{r\ \overline{4h+3}}(\alpha_s,\gamma_s s)\cos\left[\overline{4h+4-s}(\gamma_s-\pi)-\psi^{u}_{sr\ \overline{4h+3}}(\alpha_s,\gamma_s s)\right]\right\}$$

$$I^{bu}_s(\alpha_s,\gamma_s s) = \sqrt{2}\sum_{h=0}^{\infty}\left\{\bar{\bar{I}}^{u}_{s\ \overline{4h+1}}(\alpha_s,\gamma_s s)\cos\left[\overline{4h+1}(\gamma_s-\pi)-\psi^{u}_{s\ \overline{4h+1}}(\alpha_s,\gamma_s s)\right]\right.$$

$$+ \left.\left. \bar{\bar{I}}^{u}_{s\ \overline{4h+3}}(\alpha_s,\gamma_s,s)\cos\left[\overline{4h+3}(\gamma_s-\pi)-\psi^{u}_{s\ \overline{4h+3}}(\alpha_s,\gamma_s,s)\right]\right\}\right.$$

$$Y^{aEa}_{r}(\alpha_s,\gamma_s,s)= \sqrt{2}\sum_{h=0}^{\infty}\left\{ Y^{Ea}_{sr\ \overline{4h+1}}(\alpha_s,\gamma_s,s)\sin\left[\overline{4h+s}(\gamma_s-\pi)-\phi^{YEa}_{sr\ \overline{4h+1}}(\alpha_s,\gamma_s,s)\right] + \right.$$

$$\left. - Y^{Ea}_{sr\ \overline{4h+3}}(\alpha_s,\gamma_s,s)\sin\left[\overline{4h+4-s}(\gamma_s-\pi)-\phi^{YEa}_{sr\ \overline{4h+3}}(\alpha_s,\gamma_s,s)\right]\right\}$$

$$Y^{aEb}_{r}(\alpha_s,\gamma_s,s)= \sqrt{2}\sum_{h=0}^{\infty}\left\{ Y^{Eb}_{sr\ \overline{4h+1}}(\alpha_s,\gamma_s,s)\sin\left[\overline{4h+s}(\gamma_s-\pi)-\phi^{YEb}_{sr\ \overline{4h+1}}(\alpha_s,\gamma_s,s)\right] + \right.$$

$$\left. - Y^{Eb}_{sr\ \overline{4h+3}}(\alpha_s,\gamma_s,s)\sin\left[\overline{4h+4-s}(\gamma_s-\pi)-\phi^{YEb}_{sr\ \overline{4h+3}}(\alpha_s,\gamma_s,s)\right]\right\}$$

$$Y^{bEa}_{r}(\alpha_s,\gamma_s,s)= -\sqrt{2}\sum_{h=0}^{\infty}\left\{ Y^{Ea}_{sr\ \overline{4h+1}}(\alpha_s,\gamma_s,s)\cos\left[\overline{4h+s}(\gamma_s-\pi)-\phi^{YEa}_{sr\ \overline{4h+1}}(\alpha_s,\gamma_s,s)\right] + \right.$$

$$\left. + Y^{Ea}_{sr\ \overline{4h+3}}(\alpha_s,\gamma_s,s)\cos\left[\overline{4h+4-s}(\gamma_s-\pi)-\phi^{YEa}_{sr\ \overline{4h+3}}(\alpha_s,\gamma_s,s)\right]\right\}$$

$$Y^{bEb}_{r}(\alpha_s,\gamma_s,s)= -\sqrt{2}\sum_{h=0}^{\infty}\left\{ Y^{Eb}_{sr\ \overline{4h+1}}(\alpha_s,\gamma_s,s)\cos\left[\overline{4h+s}(\gamma_s-\pi)-\phi^{YEb}_{sr\ \overline{4h+1}}(\alpha_s,\gamma_s,s)\right] + \right.$$

$$\left. + Y^{Eb}_{sr\ \overline{4h+3}}(\alpha_s,\gamma_s,s)\cos\left[\overline{4h+4}-s(\gamma_s-\pi)-\phi^{YEb}_{sr\ \overline{4h+3}}(\alpha_s,\gamma_s,s)\right]\right\}$$

$$Y^{bEa}_{s}(\alpha_s,\gamma_s,s)= \sqrt{2}\sum_{h=0}^{\infty}\left\{ Y^{Ea}_{s\ \overline{4h+1}}(\alpha_s,\gamma_s,s)\cos\left[\overline{4h+1}(\gamma_s-\pi)-\phi^{YEa}_{s\ \overline{4h+1}}(\alpha_s,\gamma_s,s)\right] + \right.$$

$$\left. + Y^{Ea}_{s\ \overline{4h+3}}(\alpha_s,\gamma_s,s)\cos\left[\overline{4h+3}(\gamma_s-\pi)-\phi^{YEa}_{s\ \overline{4h+3}}(\alpha_s,\gamma_s,s)\right]\right\}$$

$$Y^{bEb}_{s}(\alpha_s,\gamma_s,s)= \sqrt{2}\sum_{h=0}^{\infty}\left\{ Y^{Ea}_{s\ \overline{4h+1}}(\alpha_s,\gamma_s,s)\cos\left[\overline{4h+1}(\gamma_s-\pi)-\phi^{YEb}_{s\ \overline{4h+1}}(\alpha_s,\gamma_s,s)\right] + \right.$$

$$\left. + Y^{Eb}_{s\ \overline{4h+3}}(\alpha_s,\gamma_s,s)\cos\left[\overline{4h+3}(\gamma_s-\pi)-\phi^{YEb}_{s\ \overline{4h+3}}(\alpha_s,\gamma_s,s)\right]\right\} \qquad \text{A4.45h}$$

A4.5 CONCERNING A MACHINE-ELECTRONIC SYSTEM WITH ROTOR CONTROL HAVING A MINIMUM FUNDAMENTAL PHASE SHIFT.

Consider a system where the instant of triggering is variable, and forced commutation is used to reduce the current to zero. Since the current flow angle may now be shifted at will as explained in the text, it will be attempted to minimize the fundamental phase shift between current and induced voltage.

Let

$$\beta_r - \alpha_r = \xi_{ro}, \quad \text{or} \quad \beta_r = (\xi_{ro} + \alpha_r) \qquad \text{A4.46a}$$

To minimize the phase angle between the fundamental current component and the induced sinusoidal rotor voltage,

$$\frac{d}{d\alpha_r}(\cos\psi_{r1}) = 0 = \frac{d}{d\alpha_r}\left\{\frac{B^i_{r1}(\alpha_r)}{\overline{A^i_{r1}(\alpha_r)}^2 + \overline{B^i_{r1}(\alpha_r)}^2}\right\}$$

$$\therefore \left\{(A^i_{r1})^2 \frac{dB^i_{r1}}{d\alpha_r} - (A^i_{r1})(B^i_{r1})\frac{dA^i_{r1}}{d\alpha_r}\right\}\left[(A^i_{r1})^2 + (B^i_{r1})^2\right]^{-3/2} = 0$$

As specified in the text the current flow angle is to be kept constant. The expressions for the coefficients are then modified into (see appendix A3.3):

$$A^i_{r1} = \frac{1}{\pi}\left\{\sin\xi_{ro}\sin(2\alpha_r+\xi_{ro}-\psi_r) - \xi_{ro}\sin\psi_r + \frac{2\sin(\alpha_r-\psi_r)}{\operatorname{cosec}^2\psi_r}\left[(\cot\psi_r\cos\overline{\xi_{ro}+\alpha_r} - \sin\overline{\alpha_r+\xi_{ro}})\exp-\xi_{ro}\cot\psi_r + \sin\alpha_r - \cot\psi_r\cos\alpha_r\right]\right\} \qquad \text{A4.46b}$$

$$B^i_{r1} = \frac{1}{\pi}\left\{\xi_{ro}\cos\psi_r - \sin\xi_{ro}\cos(2\alpha_r+\xi_{ro}-\psi_r) + \frac{2\sin(\alpha_r-\psi_r)}{\operatorname{cosec}^2\psi_r}\left[(\cot\psi_r\sin\overline{\xi_{ro}+\alpha_r} + \cos\overline{\alpha_r+\xi_{ro}})\exp-\xi_{ro}\cot\psi_r - \cot\psi_r\sin\alpha_r - \cos\alpha_r\right]\right\} \qquad \text{A4.46c}$$

It may now be determined that:

$$\frac{dA^i_{r1}}{d\alpha_r} = \frac{1}{\pi}\left\{2\sin\xi_{ro}\cos(2\alpha_r+\xi_{ro}-\psi_r) + \frac{2\sin(\alpha_r-\psi_r)}{\operatorname{cosec}^2\psi_r}\left[\cos\alpha_r + \cot\psi_r\sin\alpha_r - (\cot\psi_r\sin\overline{\xi_{ro}+\alpha_r} + \cos\overline{\alpha_r+\xi_{ro}})\exp-\xi\cot\psi_r\right]\right.$$

$$+\frac{2\cos(\alpha_r-\psi_r)}{\mathrm{cosec}^2\psi_r}\left[(\cot\psi_r\cos\overline{\alpha_r+\xi_{ro}}-\sin\overline{\alpha_r+\xi_{ro}})\exp-\xi_{ro}\cot\psi_r+\sin\alpha_r-\cot\psi_r\cos\alpha_r\right]\Bigg\} \quad \text{A4.47a}$$

$$\frac{dB^{i}_{r1}}{d\alpha}=\frac{1}{\pi}\Bigg\{2\sin\xi_{ro}\sin(2\alpha_r+\xi_{ro}-\psi_r)$$

$$+\frac{2\cos(\alpha_r-\psi_r)}{\mathrm{cosec}^2\psi_r}\left[(\cot\psi_r\sin\overline{\xi_{ro}+\alpha_r}+\cos\overline{\alpha_r+\xi_{ro}})\exp-\xi_{ro}\cot\psi_r-\cot\psi_r\sin\alpha_r-\cos\alpha_r\right]$$

$$+\frac{2\sin(\alpha_r-\psi_r)}{\mathrm{cosec}^2\psi_r}\left[(\cot\psi_r\cos\overline{\xi_{ro}+\alpha_r}-\sin\overline{\alpha_r+\xi_{ro}})\exp-\xi_{ro}\cot\psi_r-\cot\psi_r\cos\alpha_r+\sin\alpha_r\right]\Bigg\} \quad \text{A4.47b}$$

A4.6 CONCERNING THE OPERATION OF A LOW-HIGH CHOPPER CIRCUIT.

A4.6.1 *LOW-HIGH CHOPPER WITH RESISTIVE LOAD.*

For the low-high chopper circuit (see fig.4.11(b)) the following differential equations are valid when rel. 4.66 is taken into account:

$$\left.\begin{aligned} &0<t<\tau_t: \frac{di_t}{dt}+i_t\cdot\frac{R_h}{L}=-\frac{E_1}{L}\\ &\tau_t<t<(\tau_t+\tau_z): \frac{di_z}{dt'}=-\frac{E_1}{L},\ t'=t-\tau_t \end{aligned}\right\} \quad \text{A4.48a}$$

Taking the initial conditions as shown in fig.4.11(c) into account, the currents under conditions of two level current control are:

$$\left.\begin{aligned} i_t &= (i_{01}-I_2)\exp-\frac{t}{\tau_h}+I_2\\ i_z &= -\frac{E_1}{L}t'+i_{02} \end{aligned}\right\} \quad \text{A4.48b}$$

since in the present case $I_2=-(\frac{E_1}{R_h})$ and $\tau_h=\frac{L}{R_h}$.
Relation between the two currents i_{01} and i_{02} are given by:

$$\left.\begin{aligned} i_{02} &= (i_{01}-I_2)\exp-\frac{\tau_t}{\tau_h}+I_2\\ i_{01} &= -\frac{E_1}{L}\cdot\tau_z+i_{02} \end{aligned}\right\} \quad \text{A4.48c}$$

With reference to the above relations the times of power transport and zero power transport may be found as:

$$\tau_t = \tau_h \ln\left(\frac{i_{01} - I_2}{i_{02} - I_2}\right)$$

$$\tau_z = (i_{02} - i_{01}).\frac{L}{E_1} \qquad \text{A4.48d}$$

For characteristics of the power transport the following currents are calculated:

$$I_{1\ mean} = \frac{\left[\frac{E_1}{L} I_2 \ln\left(\frac{i_{01} - I_2}{i_{02} - I_2}\right) - \frac{1}{2\tau_h}(i_{01}^2 - i_{02}^2) - \frac{E_1}{L}(i_{01} - I_2)\right]}{\left[\frac{E_1}{L}\ln\left(\frac{i_{01} - I_2}{i_{02} - I_2}\right) - \frac{1}{\tau_h}(i_{01} - i_{02})\right]}$$

$$I_{h\ mean} = -\frac{E_1}{L} \cdot \left[\frac{I_2 \ln\left(\frac{i_{01} - I_2}{i_{02} - I_2}\right) - \overline{i_{01} - i_{02}}}{\frac{E_1}{L}\ln\left(\frac{i_{01} - I_2}{i_{02} - I_2}\right) - \frac{1}{\tau_h}(i_{01} - i_{02})}\right]$$

$$I_1^2 = \frac{\left\{\frac{E_1}{L} I_2^2 \ln\left(\frac{i_{01} - I_2}{i_{02} - I_2}\right) + (i_{01} - i_{02})\left[\frac{E_1}{2L}(i_{01} + i_{02} + 2I_2) - \frac{1}{3\tau_h}(3 i_{01} i_{02} + \overline{i_{01} - i_{02}}^2)\right]\right\}}{\left[\frac{E_1}{L}\ln\left(\frac{i_{01} - I_2}{i_{02} - I_2}\right) - \frac{1}{\tau_h}(i_{01} - i_{02})\right]}$$

$$I_h^2 = \frac{\left[\frac{E_1}{L} . I_2^2 \ln\left(\frac{i_{01} - I_2}{i_{02} - I_2}\right) + \frac{E_1}{2L}(i_{01} - i_{02})(i_{02} + i_{01} + 2I_2)\right]}{\left[\frac{E_1}{L}\ln\left(\frac{i_{01} - I_2}{i_{02} - I_2}\right) - \frac{1}{\tau_h}(i_{01} - i_{02})\right]} \qquad \text{A4.49a}$$

These expressions for the currents may be written in more universal and compact form when the following parameters are defined:

$$k_R = \frac{i_{02}}{i_{01}} \quad ; \quad n_R = \frac{I_2}{i_{01}} = -\frac{E_1}{i_{01} . R_h} \qquad \text{A4.50}$$

The expressions A4.47 consequently reduce to:

$$I_{1\ mean} = i_{01} \cdot \left[\frac{n_R^2 \ln\left(\frac{1 - n_R}{k_R - n_R}\right) + \frac{1}{2}(1 - k_R^2) + (1 - k_R) n_R}{n_R \ln\left(\frac{1 - n_R}{k_R - n_R}\right) + \overline{1 - k_R}}\right]$$

$$I_{h\ mean} = i_{01}\left[\frac{n_R^2 \ln\left(\frac{1-n_R}{k_R-n_R}\right) + (1-k_R)n_R}{n_R \ln\left(\frac{1-n_R}{k_R-n_R}\right) + \sqrt{1-k_R}}\right]$$

$$I_i^2 = i_{01}^2 \cdot \left\{\frac{n_R^3 \ln\left(\frac{1-n_R}{k_R-n_R}\right) + (1-k_R)\left[\frac{n_R}{2}(2n_R+1+k_R) + \frac{1}{3}(3k_R+\sqrt{1-k_R^2})\right]}{n_R \ln\left(\frac{1-n_R}{k_R-n_R}\right) + \sqrt{1-k_R}}\right\}$$

$$I_h^2 = i_{01}^2 \cdot \left[\frac{n_R^3 \ln\left(\frac{1-n_R}{k_R-n_R}\right) + \frac{n_R}{2}(1-k_R)(2n_R+1+k_R}{n_R \ln\left(\frac{1-n_R}{k_R-n_R}\right) + \sqrt{1-k_R}}\right]$$

When one considers the different periods of rel. A4.48 the expressions become:

$$\tau_t = \tau_h \cdot \ln\left(\frac{1-n_R}{k_R-n_R}\right)$$

A4.52a

$$\tau_z = \tau_h \cdot \left(\frac{1-k_R}{n_R}\right)$$

The repetition frequency will consequently be:

$$f_{chop} = \frac{1}{\tau_h}\left\{\frac{1}{\ln\left(\frac{1-n_R}{k_R-n_R}\right) + \frac{1-k_R}{n_R}}\right\}$$

A4.52b

A4.6.2 *LOW-HIGH CHOPPER BETWEEN TWO VOLTAGE SOURCES.*

In the previous paragraph attention was devoted to a chopper with resistive load. If the resistive load of the electronic Leblanc cascade is replaced by a supply synchronous inverter to absorb the chopper output power and feed it back to the supply system, the relations previously determined will be modified. It will be assumed that both the low voltage rectified rotor e.m.f. and the inverter back e.m.f. present ideal voltage sources.

For the low-high chopper circuit as given in fig. 4.11 the following differential equations are valid:

$$0 < t < \tau_t : \frac{di_t}{dt} + i_t \cdot \frac{(R_l + R_h)}{L} = \frac{E_h - E_l}{L}$$

A4.53a

with $i_t = i_l$.

$\tau_t < t < (\tau_t + \tau_z)$:

$$\frac{di_z}{dt'} + i_z \cdot \frac{R_1}{L} = -\frac{E_1}{L} \quad , \qquad \text{A4.53b}$$

with $i_z = i_1$

$t' = \tau - \tau_t$

Taking the initial values into account, the currents may be found as:

$$i_t = (i_{01} - I_2') \exp -\frac{t}{\tau_\Sigma} + I_2' \qquad \text{A4.54a}$$

$$i_z = (i_{02} - I_1) \exp -\frac{t'}{\tau_1} + I_1 \qquad \text{A4.54b}$$

with $$\tau_\Sigma = \frac{L}{R_1 + R_h} \; ; \; \tau_1 = \frac{L}{R_1} \; ; \; I_2' = \frac{E_h - E_1}{R_h + R_1} \; ; \; I_1 = \frac{-E_1}{R_1} \qquad \text{A4.54c}$$

The relations between the current levels, or equivalently between the power transport time and zero transport time, are consequently expressed as:

$$i_{02} = (i_{01} - I_2') \exp -\frac{\tau_t}{\tau_\Sigma} + I_2' \qquad \text{A4.55a}$$

$$i_{01} = (i_{02} - I_1) \exp -\frac{\tau_z}{\tau_1} + I_1 \qquad \text{A4.55b}$$

$$\tau_t = \tau_\Sigma \ln\left(\frac{i_{01} - I_2'}{i_{02} - I_2'}\right) \qquad \text{A4.55c}$$

$$\tau_z = \tau_1 \ln\left(\frac{i_{02} - I_1}{i_{01} - I_1}\right) \qquad \text{A4.55d}$$

Since consideration will be given to a two level current control in the present case, the current expression will be left in the formsof rel. A4.54. In order to characterise the power transport it will again be necessary to know the following currents:
(i) The mean input current at the low voltage terminals
(ii) The r.m.s. input current at the low voltage terminals
(iii) The mean output current at the high voltage terminals.
(iv) The r.m.s. output current at the high voltage terminals.
From relations A4.54a and A4.54b these values may be calculated as:

$$I_{1\ mean} = \left[\frac{I_2'\tau_\Sigma \ln\left(\frac{i_{02} - I_2'}{i_{01} - I_2'}\right) + I_1\tau_1 \ln\left(\frac{i_{01} - I_1}{i_{02} - I_1}\right) + (i_{01} - i_{02})(\tau_1 - \tau_\Sigma)}{\tau_1 \ln\left(\frac{i_{01} - I_1}{i_{02} - I_1}\right) + \tau_\Sigma \ln\left(\frac{i_{02} - I_2'}{i_{01} - I_2'}\right)} \right] \qquad \text{A4.56a}$$

$$I_{h\ mean} = \left[\frac{I_2'\tau_\Sigma \ln\left(\frac{i_{02} - I_2'}{i_{01} - I_2'}\right) - (i_{01} - i_{02})\tau_\Sigma}{\tau_1 \ln\left(\frac{i_{01} - I_1}{i_{02} - I_1}\right) + \tau_\Sigma \ln\left(\frac{i_{02} - I_2'}{i_{02} - I_2'}\right)} \right] \qquad \text{A4.56b}$$

The r.m.s. currents are given by:

$$I_1^2 = \left[\frac{I_2'^2\tau_\Sigma \ln\left(\frac{i_{02} - I_2'}{i_{01} - I_2'}\right) + I_1^2\tau_1 \ln\left(\frac{i_{01} - I_1}{i_{02} - I_1}\right) + 2(i_{01} - i_{02})(I_1\tau_1 - I_2'\tau_\Sigma)}{\tau_1 \ln\left(\frac{i_{01} - I_1}{i_{02} - I_1}\right) + \tau_\Sigma \ln\left(\frac{i_{02} - I_2'}{i_{01} - I_2'}\right)} \right.$$

$$\left. + \frac{\frac{1}{2}\left\{\tau_1(\overline{i_{01} - I_1}^2 - \overline{i_{02} - I_1}^2) + \tau_\Sigma(\overline{i_{02} - I_2'}^2 - \overline{i_{01} - I_2'}^2)\right\}}{\tau_1 \ln\left(\frac{i_{01} - I_1}{i_{02} - I_1}\right) + \tau_\Sigma \ln\left(\frac{i_{02} - I_2'}{i_{01} - I_2'}\right)} \right] \qquad \text{A4.56c}$$

$$I_h^2 = \left[\frac{I_2'^2\tau_\Sigma \ln\left(\frac{i_{02} - I_2'}{i_{01} - I_2'}\right) - 2(i_{01} - i_{02})I_2'\tau_\Sigma + \frac{1}{2}\tau_\Sigma\left\{(i_{02} - I_2')^2 - (i_{01} - I_2')^2\right\}}{\tau_1 \ln\left(\frac{i_{01} - I_1}{i_{02} - I_1}\right) + \tau_\Sigma \ln\left(\frac{i_{02} - I_2'}{i_{01} - I_2'}\right)} \right] \qquad \text{A4.56d}$$

Up to the present the equations have been derived for the circuit as shown in fig.4.11(a). The chopper circuit will be used in an electronic Scherbius cascade, and as explained in the text this means that the rotor resistance may be added to the resistance of the low voltage source. The resistance at the high-voltage side is kept as low as possible with a view to the recuperation. In the following expressions it will be assumed that:

$$\left.\begin{aligned} & R_h \simeq 0 \\ \text{therefore} \quad & \tau_\Sigma \simeq \tau_1 \end{aligned}\right\} \qquad \text{A4.57a}$$

and to express the currents in a more compact form corresponding with the intended two-level current control the following parameters are introduced:

$$k_E = \frac{i_{01}}{i_{02}} \quad , \quad q = \frac{E_1}{E_h} \quad , \quad n_E = \frac{i_{02} \cdot R_1}{E_h} \qquad \text{A4.57b}$$

In terms of these parameters the expressions become:

$$I_{l\ mean} = \frac{i_{02}}{n_E}\left[\frac{(1-q)\ln\left(\frac{n_E+q-1}{k_E n_E+q-1}\right) - q\ln\left(\frac{k_E n_E+q}{n_E+q}\right)}{\ln\left(\frac{k_E n_E+q}{n_E+q}\right) + \ln\left(\frac{n_E+q-1}{k_E n_E+q-1}\right)}\right] \qquad \text{A4.58a}$$

$$I_{h\ mean} = \frac{i_{02}}{n_E}\left[\frac{(1-q)\ln\left(\frac{n_E+q-1}{k_E n_E+q-1}\right) - n_E(k_E-1)}{\ln\left(\frac{k_E n_E+q}{n_E+q}\right) + \ln\left(\frac{n_E+q-1}{k_E n_E+q-1}\right)}\right] \qquad \text{A4.58b}$$

$$I_l^2 = \frac{i_{02}^2}{n_E^2}\left[\frac{(q-1)^2\ln\left(\frac{n_E+q-1}{k_E n_E+q-1}\right) - n_E(k_E-1) + q^2\ln\left(\frac{k_E n_E+q}{n_E+q}\right)}{\ln\left(\frac{k_E n_E+q}{n_E+q}\right) + \ln\left(\frac{n_E+q-1}{k_E n_E+q-1}\right)}\right] \qquad \text{A4.58c}$$

$$I_h^2 = \frac{i_{02}^2}{n_E^2}\left[\frac{(q-1)^2\ln\left(\frac{n_E+q-1}{k_E n_E+q-1}\right) - n_E(1-q)(k_E-1) + \tfrac{1}{2}n_E^2(1-k_E^2)}{\ln\left(\frac{k_E n_E+q}{n_E+q}\right) + \ln\left(\frac{n_E+q-1}{k_E n_E+q-1}\right)}\right] \qquad \text{A4.58d}$$

The two parts τ_t and τ_z of the switching cycle and the chopping frequency may be expressed in terms of the normalized parameters as:

$$\tau_t = \tau_1 . \ln\left(\frac{k_E n_E+q-1}{n_E+q-1}\right) \qquad \text{A4.58e}$$

$$\tau_z = \tau_1 . \ln\left(\frac{n_E+q}{k_E n_E+q}\right) \qquad \text{A4.58f}$$

$$f_{chop} = \tau_1^{-1}\left[\ln\left(\frac{k_E n_E+q-1}{n_E+q-1}\right) + \ln\left(\frac{n_E+q}{k_E n_E+q}\right)\right]^{-1} \qquad \text{A4.58g}$$

O P S O M M I N G

In hierdie proefskrif word aandag gegee aan die elektroniese beheer van die elektromeganiese energieomsetting in elektriese masjiene. Daar is al baie werk op hierdie gebied gedoen, maar die aard van die werk is in die meeste gevalle baie gespesialiseerd. Dit veroorsaak natuurlik dat 'n mens langsamerhand nie meer die basies verbindingslyne tussen al die verskillende aspekte van die probleem kan sien nie. Die navorsingswerk wat in hierdie studie beskryf word is eintlik bedoel om 'n meer algemene benadering van die masjien-elektronika aan te voor. Daar dit egter by die eksperimente nie moontlik is om alle bestaande en nuwe sisteme te toets nie, moet 'n mens tog maar 'n keuse maak. 'n Poging is aangewend om 'n hele groep van sisteme te ontwikkel ten einde op hierdie manier ook 'n praktiese vergelykende studie te kan uitvoer. Verder word werk in die masjien-elektronika - soos hierdie vakgebied hier genoem word - meestal oorheers deur die aspekte van die drywingselektronika wat daarby gebruik word. Ofskoon die drywingselektronika nodig is om so'n sisteem te laat werk, is dit nie in die eerste instansie nodig vir begripsvorming omtrent die basiese beginsels nie. Deur die hele werk is daar gevolglik 'n poging aangewend om hierdie vertroebeling te vermy.

Alhoewel die gedagte dat masjien-elektronika eintlik sy ontstaan te danke het aan die halfgeleierskakelaars, dikwels voorkom, is dit nie waar nie. Hoofstuk 1 bied dan ook, naas 'n algemene beskouing oor die omvang en aard van die masjien-elektronika, 'n groot hoeveelheid geskiedkundige materiaal. Hierdie geskiedkundige materiaal bied in baie opsigte nuwe feite aan wat nie vantevore algemeen bekend was nie.

In Hoofstuk 2 word aandag gegee aan die sistematiek van die masjien-elektronika-sisteme. Voordat 'n algemene studie aangepak kan word, moet 'n mens eers 'n goeie ordening in die veelhied van sisteme aanbring. Om hierdie doel te bereik word aan die hand van die drywingsvloei van die grondfrekewensie in die sisteme 'n klassifikasiesisteem ontwikkel. Drie hoofgroepe met uiteenlopende karakteristieke word aangedui (Groep I, Groep II, en Groep III). Deur 'n verdere bespreking word daarop gewys dat masjien-elektronika-sisteme met 'n meer ingewikkelde struktuur as daardie sisteme wat die drie hoofgroepe vorm, altyd saamgestel kan word uit elemente van die verskillende groepe, en dus gemengde-sisteme genoem kan word. Aangesien in masjien-elektronika-sisteme altyd baie bofrekwensies voorkom, word die invloed van die bofrekwensies op die drywingsvloei ondersoek. Hierdie algemene indeling word nou verder uitgewerk vir praktiese masjien-elektronika-sisteme. Die verdere indeling van die sisteme berus nou op die struktuur van die drywingselektronikabaan wat by die beheer gebruik word, en op die verskillende skakelmodes daarvan.

In hoofstuk 3 word gestel dat 'n mens altyd die effek van die opwekkingsfunksie, wat op die wikkelings van die masjien te staan kom as gevolg van die werking van die skakelaars wat die drywingsvloei moet beheer, kan simuleer met 'n serie- en parallelskakelaar in daardie fase, gekombineer met 'n veelfasige opwekking. Die spannings van die veelfasige opwekking hoef nie enkelvoudig harmonies te wees nie. Deur hierdie model te gebruik word die werking van 'n n-m fase elektromeganiese omsetter ondersoek onder die gestelde opwekking wat in eerste benadering as willekeurig ongebalanseer veronderstel word. Die stelle differensiaalvergelykings wat die sisteem beskryf word eers vereenvoudig

deur gebruik te maak van 'n oomblikswaarde-simmetriese-komponente-transformasie en in die geval van statorbeheer of rotorbeheer respektiewelik van 'n kompleksedraaitransformasie van rotor na stator of van stator na rotor. Die oplossing van al die strome, na bepaling van die verskillende getransformeerde dryffunksies, gee die moontlikheid om al die komponente van die oomblikswaarde en die gemiddelde waarde van die elektromagnetiese draaimoment te bepaal. Hierdie komponente word dan ingedeel in pulserende draaimomente, sinchrone draaimomente en asinchrone draaimomente. Die ontwikkeling van hierdie algemene teorie vir masjien-elektronika word dan afgesluit met 'n beskouing oor die voorstelling van die berekende strome in 'n reeks van ekwivalente bane. Die invloed van 'n simmetriese geskakelde opwekkingsfunksie op al die fases word ondersoek op die strome, ekwivalente bane en die elektromagnetiese draaimoment.

Dit sal later duidelik word dat die toepassing van die algemene teorie wat ontwikkel is, baie en lang berekenings inhou. Om in staat te wees om meer insig te kry in die eienskappe van sisteme met so'n eenvoudige model as moontlik, word hoofstuk 3 afgesluit met die teorie van sisteme met beheer in die rotorbaan van 'n induksiemasjien. Hierdie teorie is 'n voortbouing op party van die drywingsvloeibeskouings wat in hoofstuk 2 aandag ontvang het.

Hoofstuk 4 gee nou aandag aan die verdere uitwerking van die teorie van hoofstuk 3 vir 'n bepaalde geval. Dit is vanwee die baie omvangryke werk nodig om maar 'n sisteem te kies, en daardie sisteem dan te behandel. Soos in die inleiding opgemerk is, sal dit dan weer 'n stuk gespesialiseerde werk word. Om hierdie beswaar so goed as moontlik uit die weg te ruim, word in hoofstuk 4 ook aandag gegee aan 'n hele groep van sisteme, nl. Groep II en Groep IIA. By hierdie sisteme is die glip altyd veranderlik, en daarom ook die rotordrywing.

'n Sisteem met statorbeheer deur verandering van die vertraging van die ontsteekhoek word ondersoek met behulp van die algemene teorie van hoofstuk 3. Aangesien dit vir die oordragsfunksie baie belangrik is op watter manier die skakelopdrag afgelei word van die strome of spannings van die sisteme, word aandag gegee aan die verskillende moontlikhede om hierdie funksie uitte voer. Die belang daarvan kom later in die eksperimentele werk weer te voorskyn. Nadat die manier waarop geskakel word vastgestel is, moet die dryffunksie gesoek word. Hiervoor is dit baie belangrik om te weet wat die verloop van die geïnduseerde spanning op die statorwikkelings is, as die elektroniese skakelaars nie gelei nie. Hierdie probleem word grondig ondersoek en 'n benaderingsteorie word ontwikkel. Die dryffunksie word nou in twee verdeel: 'n voedingsverwante dryffunksie en 'n geïnduseerde spannings-verwante dryffunksie. Eersgenoemde werk op die fase as die elektroniese skakelaar gelei, en laasgenoemde as die skakelaar nie gelei nie. Deur hiervan gebruik te maak word die strome, en ook die elektromagnetiese draaimoment en ander groothede, in twee reekse van bofrekwensiekomponente verdeel. Elke reeks is 'n gevolg van een van die dele van die dryffunksie. Algemene berekenings word dan uitgevoer om die verskillende karakteristieke eienskappe te bepaal. Die numeriese berekenings vir die masjien wat in die eksperimente gebruik word, word uitgevoer met 'n syferrekenaar ten einde 'n hele reeks eienskappe te kan bepaal. Die werk is van so 'n omvang dat die nie sonder die gebruik van 'n syferrekenaar moontlik is nie.

Die ander sisteme van Groep II en Groep IIA wat ondersoek word, word met behulp van die vereenvoudigde modelle ontleed. Hierdie sisteme om-

vat rotorbeheer van 'n induksiemasjien deur verandering van die vertraging van die inskakeloomblik van die rotorstroom, deur verandering van die vertraging van die uitskakeloomblik van die rotorstroom, deur belasting van die rotor met 'n hoëfrekwensiekapper wat 'n weerstands belasting het (elektroniese Leblanckaskade), deur 'n elektroniese Scherbiuskaskade en deur 'n elektroniese Scherbiuskaskade met reaktiewe drywingskompensasie. Om soos in die vorige geval ook weer die invloed van die manier waarop die skakelopdrag afgelei word, aan te toon, word vir elke sisteem die verskillende moontlikhede ondersoek. Dit is nie moontlik om alle karakteristieke te ondersoek nie, of selfs nie om al die ondersoekte eienskappe weer te gee nie. Dit word alleen gedoen in so 'n mate as wat nodig is om nuwe aspekte aan die lig te bring. Om numeriese berekenings uit te voer met behulp van die vereenvoudigde modelle is weer 'n syferrekenaar gebruik. Al hierdie berekenings word in die eksperimentele werk getoets.

Die sisteme wat in hoofstuk 4 aan 'n teoretiese ontleding onderwerp is, word in hoofstuk 5 aan 'n eksperimentele toets onderwerp. Aangesien die meetfasiliteite by so 'n omvangryke studie belangrik is, is 'n eenheid ontwikkel waarin al die sisteme saamgebou is vir gebruik saam met 'n Westinghouse Universele Masjien. Hierdie masjien is semi-vierfasig, en aangesien die drywing ook laag is, is dit verstandig om enkele eksperimente te herhaal met sisteme wat ontwikkel is vir 'n driefasige masjien met groter drywing. Op hierdie masjien word dan 'n rotorbeheersisteem met verandering van die inskakeloomblik van die rotorstroom en 'n elektroniese Leblanckaskade getoets.

Die ontwerp en ontwikkeling van die eksperimentele masjien-elektronika sisteme omvat 'n veld wat nie binne die raamwerk van die huidige proefskrif val nie. Daarom word van die eksperimentele sisteme alleen maar 'n kort beskrywing met behulp van vereenvoudigde blokdiagramme gegee. Tog is enkele van die probleme wat gedurende hierdie fase van die werk opgelos is, van so 'n algemene aard dat dit vir die hele gebied van die masjien-elektronika geld. Aan hierdie probleme word kortliks aandag gegee. Die toepassing van elektroniese skakelaars met gedwonge kommutasie om induktiewe strome te onderbreek word ondersoek en 'n algemene oplossing aanbeveel vir die eiesoortige probleme van hierdie gebied. Transmissie van ontsteekseine na drywingselektroniese skakelaars word grondig ondersoek, die gebreke van bestaande sisteme bepaal, en 'n voorstel om die tekortkomings op te hef gedoen. Die toepassing van drywingshalfgeleiers bring baie probleme mee. Daar word kortliks beskryf hoe 'n spesiale apparaat ontwikkel is vir metinge en studie hieraan.

Van alle sisteme wat in hoofstuk 4 behandel is, is draaimomentkrommes geregistreer as funksie van die beheerparameter en die glip. Hierdie resultate is die belangrikste vir die bepaling van die oordragsfunksie en die elektromeganiese energieomsettingseienskappe. Daar is nog baie meer kombinasies van elektriese eienskappe, maar dis nie moontlik om hulle almal aan te bied nie. Vir die inskakelhoekbeheer in die stator word die statorstroom, rotorstroom, natuurlike kommutasiehoek en die arbeidsfaktor vir 'n paar parameterwaardes gegee. By die rotorbeheersisteme is dit ook nie moontlik om alle elektriese eienskappe aan te bied nie. Daar word volstaan deur aan te toon hoe die rotorbeheer deur uitskakeling van die rotorstroom kan lei tot heeltemaal niekonvensionele eienskappe van 'n induksiemasjien. Die voordele hiervan kom duidelik na vore as 'n mens dit vergelyk met 'n induksiemasjien

sonder beheer of met beheer van die inskakelhoek van die rotorstroom. Aandag word kortliks geskenk aan sekere bofrekwensiedraaimomente wat gedurende die eksperimentele werk waargeneem is, asook aan die resultate verkry vir die driefasige sisteme. Ossillogramme word aangebied ten einde metinge te ondersteun, te illustreer hoe die eksperimentele toestande met die aannames ooreenkom en om die werking van sommige sisteme 'n bietjie op te helder.

Die eksperimentele werk toon aan dat die algemene teorie wat in hoofstuk 3 aangebied is, die gedrag van 'n masjien-elektronika-sisteem baie goed beskryf. Indien die komponente as gevolg van die geïnduseerde spanningsverwante dryffunksie nagelaat word, moet verwag word dat by klein glip aansienlike afwykings sal optree. Die vereenvoudigde modelle gee 'n goeie kwantatiewe aanduiding van die eienskappe van die rotorbeheersisteme, en vestig die aandag op verskeie interessante punte.

NAWOORD BY DIE AFSLUITING VAN HIERDIE WERK.

Die vyf jaar wat ek aan die Technische Hogeschool te Eindhoven as gas kon vertoef, het 'n besondere geleentheid tot navorsing gebied, waarvoor ek baie dankbaar is. Ek wil ook graag my waardering betuig teenoor die hele Groep Elektromechanika vir alle hulp en bystand by die navorsingswerk en die totstandkoming van hierdie proefskrif. Dit is nie moontlik om alles op te noem wat elke persoon bygedra het nie.

Die groepsleier, prof.dr.ir. J.G. Niesten het steeds maar belangstelling in my werk gehad, en ek wil graag my dank betuig vir al sy tyd wat hy beskikbaar gestel het om hierdie werk te kon bespreek. Vir gesprekke wat baie probleme vir my opgehelder het, moet ek Ir. W.J. de Zeeuw, Ir. E.M.H. Kamerbeek en Ir. J.A. Schot baie bedank.

Die totstandkoming van so'n werk is eintlik spanwerk, en daarom my erkentlikheid teenoor die lede van die navorsingspan wat saam met my aan al hierdie probleme gewerk het. Aangesien die samestelling van die span steeds gewissel het, is dit moeilik om almal by naam te noem. Ek dink hier aan die baie T.H. "stage-studente" en HTS-praktikante wat saamgewerk het. Wat die studente betref geld verder my waardering teenoor Ir. H.J.M. Henkelman en Ir. J. Roede, wat aan deelgebiede gewerk het as 'n vervulling van 'n deel van die vereistes vir hulle doktorale eksamen in die elektrotegniek aan die T.H.E. By die totstandkoming van die eksperimentele sisteme en die metinge was die hulp van Mnre W.A.M. van den Boom, J.G.M. van de Laak en J.H. Wouterse onmisbaar. Ek kon dit onmoontlik alles self gedoen het. Ook by die totstandkoming van hierdie manuskrip het hulle 'n groot bydrae gelewer, en was sonder uitsondering selfs bereid om vir berekeninge en metinge van hulle eie tyd op te offer. Mnr. van de Laak het 'n groot bydrae gelewer deur byna al die tekeninge te maak. My eggenote is ek baie dankbaar vir al die tikwerk aan hierdie en vorige manuskripte. Die uitgebreide bibliografiese werk was alleen moontlik deur die biblioteekkundige hulp wat sy kon bied, die katalogi wat sy saamgestel het en die raad wat sy gegee het.

Vir die voorbereiding van die finale manuskrip gaan my dank aan Mev. E.M.A.B.M. Groenenberg, Mev. M.J.C.P.M. Kanters, Mej. E.C.B.M. Luijbrechts en my eggenote.

Ek wil graag my erkentlikheid betuig teenoor die Suid-Afrikaanse Yster en Staal Industriële Korporasie vir studieverlof en studiefasiliteite gedurende die afgelope jare.

Op aanbeveling van die senaat van die T.H. Eindhoven volg hier 'n kort lewensbeskrywing van die skrywer.

Jacobus Daniel van Wyk is gebore op 19 November 1939 in Fauresmith. Geniet laerskoolopleiding te Kuruman en Kimberley, en hoërskoolopleiding te Kimberley en Bronkhorstspruit en lê in 1957 die eindeksamen af. Besoek vanaf 1958 tot 1961 die Universiteit van Pretoria en behaal in 1962 'n eerste graad in elektriese ingenieurswese. Tree in 1962 in diens van die Suid-Afrikaanse Yster en Staal Industriële Korporasie (Yskor) te Pretoria as ingenieurskwekeling. Was vanaf 1963 tot Junie 1964 verbonde aan die Departement Elektrotegniese Ingenieurswese van die Universiteit van Pretoria in 'n tydelike pos as lektor. Vertoef daarna enkele maande by die Departement Navorsing en Prosesontwikkeling van Yskor, en is vanaf die einde van 1964 verbonde aan die Groep

Elektromechanika van die Technische Hogeschool te Eindhoven, eers as tegniese amptenaar, en sedert 1966 as wetenskaplike medewerker in tydelike diens. Behaal in 1966 'n meestersgraad in die ingenieurswese aan die Universiteit van Pretoria.

S T E L L I N G E N

1. Bij voeding van de stator van een induktiemachine uit een elektronische frekwentie-omzetter, waarvan de uitgangsspanning naast de grondgolf ook nog bovenharmonische komponenten bevat, kan het door Abraham en Patzschke voorgestelde hybride machine-elektronika systeem aanleiding geven tot ernstige problemen bij de aanloop van de machine ten gevolge van het feit, dat alle mogelijke synchrone kleefkoppels dan bij stilstand optreden.
(Abraham, L.; Patzschke, U. AEG "75 Jahre Käfigläufermotoren. Berlin, 133-140, 1964).

2. Bij de analyse van de wijze, waarop het gedrag van een elektromechanische energie-omzetter door het opnemen van elektronische schakelaars in zijn stator- of rotorcircuits tijdens kwasi-stationair bedrijf wordt beïnvloed, is het gebruik van een analoge rekenmachine geen conditio sine qua non.
Zulks is in tegenspraak met het onder meer door Gerecke en Badr ingenomen standpunt terzake.
(Gerecke, E.; Badr, H. Neue Technik, 4, 125-134, 1962).

3. Door de samenhang tussen de machinespanning (in hoofdstuk 3 en 4 van dit proefschrift aangeduid met "excitation function") en het van de bedrijfstoestand van de machine afhankelijke schakelspel van de elektronische schakelaars, moet de methode van analyse welke gebruik maakt van de ontbinding van de machinestromen in Fourier-komponenten - zoals vooral gebruikt in de analyse van frekwentie-gestuurde machines - met grote voorzichtigheid worden gehanteerd.
(Zie b.v. Heumann, K.; Jordan, K.G. AEG: 75 Jahre Käfigläufer-motoren, Berlin, 1964, 107-116, 117-122.
Klingshirn, E.A.; Jordan, H.E.; IEEE Trans.Power Apparatus Syst., PAS-87, 624-631, 1968.
Jain, G.C.; IEEE Trans.Power Apparatus Syst., PAS-83, 561-566, 1964).

4. In de machine-elektronika dient men zich te hoeden voor een onverantwoord ingewikkelde analyse van de schakelelektronika naast een onverantwoorde vereenvoudiging van de elektrische machine, zoals bijvoorbeeld bij de studie van een elektronische Scherbius-kaskade uit de vakliteratuur naar voren treedt.
(Meyer, M. ETZ-A, 82, 589-596, 1961.
Nishida, F.; Mizuno, S., Elect.Engng.Japan, 84(9), 53-62, 1964.
Erlicki, M.S., IEEE Trans.Power Apparatus Syst., PAS-84, 1011-1016, 1965.
Hori, T., Elect.Engng.Japan, 87(9), 55-65, 1967).

5. Bij de huidige stand van de techniek van de machine-elektronika is fundamentele studie van een funktionerend systeem van veel groter belang dan de verbetering van een detail van de schakeling of de optimalisering van een deelsysteem.

6. Toekomstig onderzoek in de vermogenselektronika dient zich meer dan tot dusver te richten op het kompenseren van blindvermogen en van bovenharmonischen door het gebruik van "komplementaire" vermogenselektronische schakelingen.

7. Bestudering van de historische ontwikkeling van de machine-elektronika vanaf het tijdperk van het kwikdampvat bevestigt de verwachting ten aanzien van schaalvergroting en versnelde ontwikkeling bij de komst van de halfgeleidertechniek. Voor de toekomst zal deze tendens zich alléén bij de vermogenselektronika voortzetten (Hoofdstuk 1 van dit proefschrift).

8. De volumeverhouding van halfgeleiderschakelelementen en kwikdampvaten houdt een goede belofte in voor een magnetisch uitschakelbare halfgeleider-schakelaar voor groot vermogen.

9. Waarnemingen van de elektroluminescentie tijdens spanningstransiënten in de blokkeerrichting aan thyristoren kunnen leiden tot een beter begrip van het instabiliteitsfenomeen dat optreedt bij het overschrijden van een kritieke waarde van de spanningsfluxie.

10. De waargenomen zichtbare straling vanuit het gebied rond de emitter periferie van silicium planaire transistoren - werkende in het avalanche-gebied van de stroomspanningskarakteristieken van de kollektor-basis-junktie - kan ten dele worden verklaard met behulp van het "emitter-push-in" effekt.
Wyk, J.D.van, Proc. IEEE, 53, 307-308, 1965.
Wyk, J.D.van, Solid-State Electronics, 8, 803-805, 1965.
Loro, A. Solid-State Electronics, 9, 904-905, 1966.

11. Tegen het antwoord van Tunmer op de diskussie-bijdrage van Heymann betreffende rekombinatiestraling uit transistorstrukturen vallen belangrijke argumenten in te brengen.
Heymann, F.G., discussion to Tunmer, H. Trans. SAIEE, 57, 105-111, (discussion p.113), 1966.

12. Het verdient aanbeveling om een direkte koppeling aan te brengen tussen het voor een bepaald onderzoekprojekt bestemde budget en het bedrag, beschikbaar voor vorming van een literatuurkollektie op dat gebied.

13. Bij gebruikmaking van het klassifikatiesysteem hetwelk wordt toegepast in de bibliotheek van de T.H. Eindhoven is de mogelijkheid tot ontsluiting van alle informatie welke dit proefschrift bevat twijfelachtig.

14. Rendement van speurwerk kan belangrijk worden vergroot door het toevoegen van een "information-scientist" aan elk "research team" dat met een nieuw onderzoekprojekt begint.

15. De in Zuid-Afrika door de industrie gevolgde methode voor het verstrekken van studiebeurzen aan studenten in de techniek is zeer schadelijk voor 's lands ekonomie.

Eindhoven, 19 augustus 1969 J.D. van Wyk.